Universitat
de les Illes Balears

DOCTORAL THESIS

2021

RESPONSE OF NITROGEN FIXERS ASSOCIATED WITH *POSIDONIA OCEANICA* TO ENVIRONMENTAL FACTORS AND EMERGING POLLUTANTS

Víctor Fernández Juárez

Universitat de les Illes Balears

DOCTORAL THESIS
2021

DOCTORAL PROGRAM OF MARINE ECOLOGY

RESPONSE OF NITROGEN FIXERS ASSOCIATED WITH *POSIDONIA OCEANICA* TO ENVIRONMENTAL FACTORS AND EMERGING POLLUTANTS

Víctor Fernández Juárez

Supervisor: Dr. Nona Sheila Agawin Romualdo

Supervisor: Dr. Antoni Bennasar Figueras

Tutor: Dr. Nona Sheila Agawin Romualdo

Doctor by the Universitat de les Illes Balears

Universitat de les Illes Balears

Dr. Nona Sheila Agawin Romualdo and Dr. Antoni Bennasar Figueras, of the University of the Balearic Islands

We DECLARE:

That the thesis entitled "Response of nitrogen fixers associated with *Posidonia oceanica* to environmental factors and emerging pollutants", presented by Víctor Fernández Juárez to obtain a doctoral degree, has been completed under our supervision.

For all intents and purposes, we hereby sign this document.

Signatures:

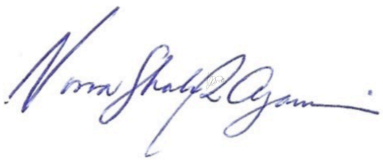

Nona Sheila Agawin Romualdo Antoni Bennasar Figueras

Palma de Mallorca, 1st April 2021

A mi madre

THESIS BY COMPENDIUM OF PUBLICATIONS

The doctoral thesis is structured as a compilation of five original scientific research articles published in peer-reviewed international journals or in the review process, namely:

1- **Fernández-Juárez V, Bennasar-Figueras A, Tovar-Sanchez A and Agawin N.S.R (2019).** The role of iron in the P-acquisition mechanisms of the unicellular N_2-fixing cyanobacteria *Halothece* sp., found in association with the Mediterranean Seagrass *Posidonia oceanica*. *Front. Microbiol*. 10:1903. doi: 10.3389/fmicb.2019.01903. ***Chapter 1.***

*Journal impact factor: 4.236, JCR impact 2019-2020: Q1 in Microbiology.

Republication: Alexandre Morrot, editor. Prime Archives in Microbiology. Hyderabad, India: Vide Leaf. 2020. ***Chapter 1.***

2- **Fernández-Juárez V, Bennasar-Figueras A, Sureda-Gomila A, Ramis-Munar G and Agawin N.S.R (2020).** Differential effects of varying concentrations of phosphorus, iron and nitrogen in N_2-fixing cyanobacteria. *Front. Microbiol. 11:541558.* doi: 10.3389/fmicb.2020.541558. ***Chapter 2.***

*Journal impact factor: 4.236, JCR impact 2019-2020: Q1 in Microbiology.

3- **Fernández-Juárez V, Jaén-Luchoro D, Bryto-Echeverria J, Agawin N. S. R, Bennasar-Figueras A, and Echeveste P (2021)**. Everything is everywhere: physiological responses of the Mediterranean Sea and Eastern Pacific Ocean epiphyte *Cobetia* sp. to varying nutrient concentration. *Microb Ecol.* 1-18. *http/doi.org/10.1007/s00248-021-01766-z.* ***Chapter 3.***

*Journal impact factor: 3.356, JCR impact 2019-2020: Q1 in Marine & Fresh Water Biology.

4- **Fernández-Juárez V, Zech E.H, Pol-Pol E, and Agawin N.S.R (2021)** Dependence of the effects of pH changes, temperature and elevated levels of CO_2 on the nutrient status of N_2-fixing bacteria. Submitted to *Limnology and Oceanography*. ***Chapter 4.***

*Journal impact factor 2019-2020: 3.778, JCR impact 2019-2020: Q1 in Limnology.

5- **Fernández-Juárez V, López-Alforja X, Frank-Comas A, Echeveste P, Bennasar-Figueras A, Ramis-Munar G, Gomila R.M, and Agawin N. S. R (2021).** The "good, the bad and the double-sword" effects of exposure to MPs and their organic additives on marine bacteria. *Front. Microbiol.* doi*:* 10.3389/fmicb.2020.581118. ***Chapter 5.***

*Journal impact factor: 4.236, JCR impact 2019-2020: Q1 in Microbiology.

*Source of quality indices: InCites Journal Citation Reports published on 29 June 2020.

CONTENTS

ACKNOWLEGMENTS/AGRADECIMIENTOS

Una etapa acaba y otra empieza… Han sido los tres años y medio más intensos de mi vida, plenamente dedicados a lo que amo, que es la ciencia. Durante esta etapa han sido muchos los altibajos, cabreos y bajos estados de ánimo, donde los buenos momentos han superado con creces a los malos. No tengo palabra para describir mi satisfacción personal de llegar a mi objetivo que es dedicarme a la ciencia. Este periodo de mi vida, no solo me ha permitido formarme a nivel profesional, sino también a nivel personal.

La primera persona a la que quiero agradecer y dedicar esta tesis es a mi madre, la persona que me ha tenido que aguantar mi mal humor, cabreos y desánimos, y la que me ha apoyado des del primer momento en esta gran aventura. Quiero darte las gracias por todo, ya que no hubiera llegado tan lejos sin tu cariño y apoyo.

Quiero hacer mención especial a mi mentora y "jefa" durante estos años, que es la Dra. Nona Sheila Agawin Romualdo. Sé Nona que no ha sido fácil trabajar conmigo, debido al trabajo extra que ha conllevado, y verdaderamente valoro las horas que has invertido en mí. No sabes lo que te agradezco la oportunidad que me brindaste cuando hace ya casi cuatro años entre a tu despacho temeroso y sin saber muy bien que estaba haciendo. Nunca podré agradecerte lo suficiente toda la confianza que me diste y la libertad que he tenido estos años para poder desarrollar mi investigación, y sobre todo por confiar en mí y de mi potencial, cuando nadie lo había hecho hasta ese momento. Gracias a ti he podido tener una de mis etapas más felices de mi vida. De verdad y de corazón, ¡GRACIAS!

Dar las gracias a mi otro mentor, el Dr. Antoni Bennasar Figuras, la primera persona que me introdujo en la investigación, y que sino fuera por él no estaría donde estoy hoy en día. De verdad, GRACIAS, por darme la oportunidad de dar mis primeros pasitos en este mundillo.

No me puedo olvidar de mi amigo y "consultor oficial de dudas" el Dr. Daniel Jaén Luchoro, vía conexión Suecia. No puedo agradecerte lo suficiente tus enseñanzas Dani. Para mí eres mi gran mentor a nivel laboratorio, con el que aprendí las primeras buenas prácticas de laboratorio, y donde pude darme cuenta de que definitivamente la "ciencia" era mi lugar. Solo espero que en futuro sigamos colaborando tal y como lo hacemos en el presente.

Como no mencionar al Dr. Pedro Echeveste. No puedo estar más agradecido y contento del networking y colaboraciones que hemos realizado durante esta etapa. GRACIAS, por darme la oportunidad de estar viajar a Chile y trabajar junto a ti en Antofagasta, uno de los dos meses más emocionantes que recuerdo, y que añoro con gran nostalgia. Tengo que agradecerte especialmente todos tus consejos tanto profesionales como personales, que me han servido para tenerte como referente científico y personal, y en especial al tiempo invertido, como si hubieras sido mi tercer director de tesis. ¡Gracias amigo, y espero que nos veamos pronto!

El Dr. Antoni Busquets Bisbal es uno de los "imprescindibles" que no puede faltar en los agradecimientos. Nunca olvidaré el día que me comentaste que necesitaban a una persona para el departamento de Ecología y que subiese a preguntar. Gracias a ti, estoy donde hoy en día me encuentro. Quiero agradecerte todo el tiempo que le has dedicado a mis interminables dudas, y que sin dudarlo dejabas lo que estuvieras haciendo para asesorarme en todo lo que podías. Has sido unas de las personas que más me ha ayudado, a sabiendas de que durante esta etapa me he encontrado falto de referentes en el laboratorio con los que poder aprender. Sin ninguna duda puedo decir que para mí eres un referente como profesional, y que nunca olvidaré todas tus enseñanzas.

Tengo que mencionar y agradecer a todos los estudiantes que han pasado por mi laboratorio y que en la medida de lo posible he intentado enseñarles todo lo que he podido. Mención especial a Xabier López-Alforja y Carlos Enrique Payá, amigos y compañeros, con los que he disfrutado cada día que he ido al laboratorio. De corazón os deseo la mejor suerte en este mundo que es la ciencia. Acordarme de la Dra. Elena Bazara Ruíz, por lo pesado que he sido con la estadística, y por asesorarme en todo lo que ha podido.

Seguro que me dejo a muchas más personas que en menor o mayor parte han contribuido durante este periodo, a todas y cada una de ellas,

MUCHAS GRACIAS

FUNDING

This thesis has been conducted within the framework of the project entitled “Controles biológicos y ambientales de la fijación de nitrógeno en praderas de *Posidonia oceanica*” (CTM2016-75457-P), led by Dr. Nona Sheila Agawin Romualdo (University of the Balearic Islands, Spain). A two month stay at the University of Antofagasta (Chile) was funded by the Santander Ibero-America scholarship 2019-2020 and Cátedra del Mar 2019, supervised by Dr. Pedro Echeveste (University of Antofagasta, Antofagasta, Chile).

ACRONYMS AND ABBREVIATIONS

ADH: alcohol dehydrogenase

APA: alkaline phosphatase activity

APase: alkaline phosphatase

ASW: artificial seawater

ARA: acetylene reduction assay

AU: arbitrary units

BNF: biological N_2-fixation

C4-ABCS: 4-dicarboxylate ABC transporter substrate-binding protein

DCFH-DA: 2′,7′-dichlorofluorescein diacetate

DCF: 2′,7′-dichlorofluorescein

DEHP: dioctyl-phthalate

DIP: dissolved inorganic phosphorus

DIN: dissolved inorganic nitrogen

DOC: dissolved organic carbon

DOP: dissolved organic phosphorus

DSMZ: German Collection of Microorganisms and Cell Cultures GmbH

Fe: iron

FID: flame ionization detector

FITC: fluorescein isothiocyanate

FSC: forward scatter

FUR: ferric uptake regulator

HBCD: 1,2,5,6,9,10-hexabromocyclododecane

HCS: Humboldt Current System

IPCC: Intergovernmental Panel on Climate Change

MB: marine broth

MPs: microplastics

MS: Mediterranean Sea

MUF: 4-methylumbelliferyl

MUF-P: 4-methylumbelliferyl phosphate

NtcA: global nitrogen regulator

OD: optical density

P: phosphorus

PC: phycocyanin

PCC: Pasteur Collection Culture

PDB: Protein Data Bank

PE: polyethylene

PE: phycoerythrin

PFM: position frequency matrix

PhoA: alkaline phosphatase type A

PhoD: alkaline phosphatase type D

PhoX: alkaline phosphatase type X

PP: polypropylene

PPM: particle per million

PPT: particle per thousand

PS: polystyrene

PVC: polyvinyl chloride

ROS: reactive oxygen species

SSC: side scatter

TBDTs: TonB-dependent transporters

TBS: transcriptional binding sites

TDP: total dissolved phosphorus

TFs: transcriptional factors

Tux4: turks island salts

ABSTRACT

N_2-fixers bacteria or diazotrophs reduce atmospheric nitrogen (N_2) into ammonia (NH_3) and play a significant role in the ocean's N-cycles by providing new inorganic nitrogen to planktonic and benthic primary producers. The epiphytic and endophytic N_2-fixing population found in association with the endemic Mediterranean seagrass *Posidonia oceanica* can potentially provide the entire N-demand to this seagrass. The Mediterranean Sea is one of the most oligotrophic seas in the world and at the same time subject to global climate change factors (e.g., ocean acidification and warming) and emerging pollutants (e.g., plastic pollution). Considering the importance of N_2-fixers in the health and functioning of seagrasses, nothing is known about the effects of current environmental challenges in these microorganisms. From a physiological and molecular point of view, this thesis investigates the role of nutrient availability, climate change factors (i.e., temperature, pH and CO_2) and emerging pollutants (i.e., plastics) through pioneering multifactorial experiments. Different species of N_2-fixing phototrophic and heterotrophic bacteria found in association with *P. oceanica* were used as model test species. The thesis is divided into two main sections, revealing the role of (**I**) nutrient availability [phosphorus (P), iron (Fe) and nitrogen (N)] and (**II**) anthropogenic factors (CO_2 and its concomitant effect on ocean acidification and warming, and microplastics and their organic additives) in regulating the functioning of N_2-fixers associated with *P. oceanica*. The results show that the responses of the N_2-fixing bacteria to environmental factors and emerging pollutants tested are species-specific, suggesting that the N_2-fixing community structure associated with *Posidonia oceanica* will change in response to these factors.

RESUMEN

Las bacterias fijadoras de N_2 o diazótrofos reducen el nitrógeno atmosférico (N_2) en amoníaco (NH_3) y desempeñan un papel esencial en los ciclos del N del océano, al proporcionar nuevo nitrógeno inorgánico a los productores primarios planctónicos y bentónicos. La población fijadora de N_2 epífita y endofítica que se encuentra en asociación a *Posidonia oceanica*, planta endémica del Mar Mediterráneo, puede potencialmente proporcionar de toda la demanda de N a esta fanerógama marina. El mar Mediterráneo es uno de los mares más oligotróficos del mundo y, al mismo tiempo, está sujeto a factores del cambio climático (p. ej., acidificación y calentamiento de los océanos) y contaminantes emergentes (p. ej., plásticos). Por tanto, los fijadores de N_2 deben hacer frente a la oligotrofia y los factores antropogénicos. Considerando la importancia de estas poblaciones microbianas en la salud de la planta, no se sabe nada sobre los efectos de los actuales desafíos ambientales en estas poblaciones microbianas. Desde un punto de vista fisiológico y molecular, esta tesis investiga el papel de la disponibilidad de nutrientes, los factores del cambio climático (temperatura, pH y CO_2) y los contaminantes emergentes (polución por plásticos), a través de pioneros experimentos multifactoriales. Durante esta tesis, se utilizaron como especies modelo diferentes bacterias fototróficas y heterótrofas fijadoras de N_2 asociadas a *P. oceanica*. La tesis se divide en dos secciones principales, revelando el papel de (**I**) la disponibilidad de nutrientes [fósforo (P), hierro (Fe) y nitrógeno (N)] y (**II**) de los factores antropogénicos (CO_2 y su efecto concomitante en la acidificación del océano y calentamiento, y microplásticos y sus aditivos orgánicos asociados) en la regulación del funcionamiento de fijadores de N_2 asociados a *P. oceanica*. Los resultados muestran que las respuestas de las bacterias fijadoras de N_2 a los factores ambientales y los contaminantes emergentes analizados son específicas de la especie, lo que sugiere que la estructura de la comunidad fijadora de N_2 asociada a *P. oceanica* cambiará en respuesta a estos factores.

RESUM

Els bacteris fixadors de N_2 o diazòtrofs redueixen el nitrogen atmosfèric (N_2) en amoníac (NH_3) i tenen un paper important en els cicles del N en l'oceà, al proporcionar nou nitrogen inorgànic als productors primaris planctònics i bentònics. La població fixadora de N_2 epífita i endofítica que es troba en associació amb *Posidonia oceanica*, planta endèmica del Mar Mediterrani, pot potencialment proporcionar tota la demanda de N a aquesta planta. El mar Mediterrani és un dels mars més oligotròfics del món i, a el mateix temps, està subjecte a factors de canvi climàtic (p. ex., acidificació i escalfament dels oceans) i contaminants emergents (p. ex., plàstics). Per tant, els fixadors de N_2 han de fer front a la oligotròfia i els factors antropogènics. Atesa la importància d'aquestes poblacions microbianes en la salut de la planta, no se sap res sobre els efectes dels actuals desafiaments ambientals. Des d'un punt de vista fisiològic i molecular, aquesta tesi investiga el paper de la disponibilitat de nutrients, els factors del canvi climàtic (temperatura, pH i CO_2) i els contaminants emergents (pol·lució plàstica) a través de pioners experiments multifactorials. Durant aquesta tesis, es van utilitzar com a espècies model diferents bacteris fototròfics i heteròtrofs fixadores de N_2 associades amb *P. oceanica*. La tesi es divideix en dues seccions principals, revelant el paper de (**I**) la disponibilitat de nutrients [fòsfor (P), ferro (Fe) i nitrogen (N)] i (**II**) del factors antropogènics (CO_2 i el seu efecte concomitant a la acidificació de l'oceà i escalfament, microplàstics i els seus additius orgànics associats) en la regulació del funcionament de fixadors de N_2 associats amb *P. oceanica*. Els resultats mostren que les respostes dels bacteris fixadors de N_2 als factors ambientals i els contaminants emergents analitzats són específiques de l'espècie, el que suggereix que l'estructura de la comunitat fixadora de N_2 associada a *P. oceanica* canviarà en resposta a aquests factors.

1. GENERAL INTRODUCTION

GENERAL INTRODUCTION

1.1 The Mediterranean Sea

The Mediterranean Sea is a semi-enclosed sea, with an extension of 2.96 x10^6 Km^2 (i.e., representing 0.82% of the world's oceans), surrounded by the continents of Europe, Africa and Asia and connected to the Atlantic Ocean by the Strait of Gibraltar (**Figure 1.1**). It is a hot spot of biodiversity, harboring and giving shelter to more than 17000 species (Coll et al., 2010). There is also a high number of endemic species, one of which is the seagrass *Posidonia oceanica*. This seagrass offers valuable ecological functions in the Mediterranean regions. Despite being a hotspot of biodiversity and home to endemic species, the Mediterranean Sea is oligotrophic and at the same time subject to intense anthropogenic pressure.

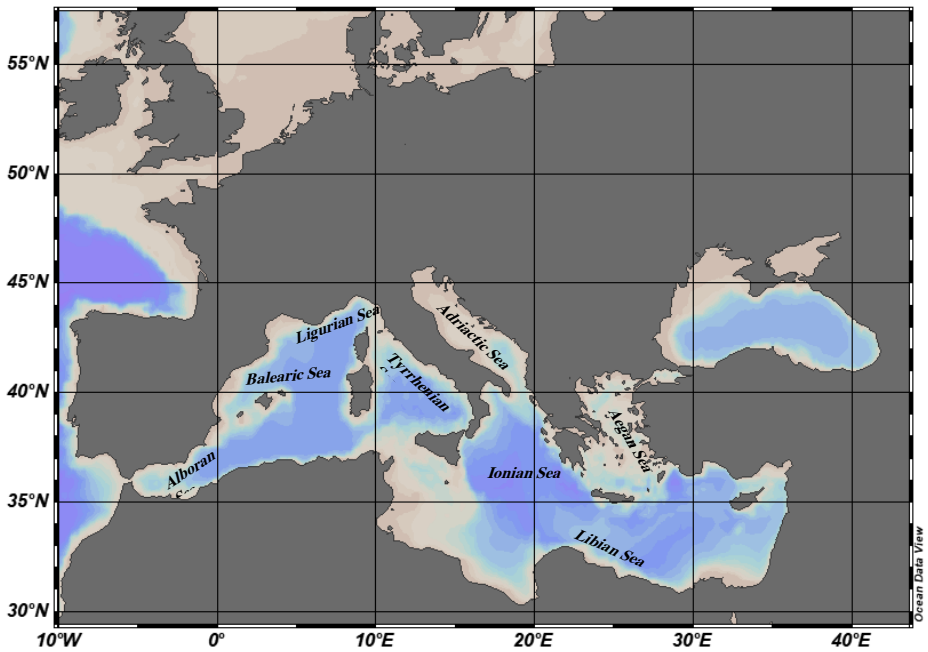

Figure 1.1. The Mediterranean Sea is subdivided into different littles seas, among which stand out the Alboran Sea, the Balearic Sea, the Ligurian Sea, the Tyrrhenian Sea, the Ionian Sea, the Adriatic Sea, the Aegean Sea, and the Libyan Sea. **Source**: Own production via Open Data View (ODV).

Nutrient regimes in the Mediterranean Sea

The Mediterranean Sea is considered one of the most oligotrophic seas in the world, chronically limited by phosphorus (P), with a decreasing gradient of dissolved inorganic P (DIP) concentrations from west to east basins (Tanhua et al., 2013) **(Figures 1.2A** and **1.2B**). For the surface layers, the average concentration of DIP in the Mediterranean Sea is 0.4 µM. For deep waters, the typical DIP concentration in the Western and Eastern

Mediterranean waters is 0.4 µM and 0.25 µM, respectively (Lazzari et al., 2016; Powley et al., 2017ab) (**Figure 1.2A** and **1B**). Dissolved inorganic nitrogen (DIN) can also be at limiting concentrations in the water column. The (NO_3^-) concentration average in the surface layers is 4.75 µM, while for deep waters in the Western and Eastern Mediterranean Sea is 9 µM and 6 µM, respectively. These DIN values are lower than in the North Atlantic Ocean and North West Pacific Ocean, where NO_3^- levels are found around 16 µM and 50 µM, respectively (Powley et al., 2017ab). Nitrogen (N) and P concentrations in the water column of the Mediterranean waters (20-28:1) do not follow the N:P Redfield ratio (16:1), suggesting an enrichment by N over the P (**Figure 1.2B**). The combination of external N inputs from N-deposition and atmospheric nitrogen (N_2) fixation may explain this high Redfield ratio (Kim et al., 2010; Ridame et al., 2011). In this region, iron (Fe) may come from the surrounding land and airborne dust from the Sahara Desert (Statham and Hart, 2005). However, Fe can be a seasonal limiting factor (i.e., minimum levels in the winter months and maximum levels in the spring and summer months), controlling phytoplankton growth (Sarthou and Jeandel, 2001; Statham and Hart, 2005). Their concentrations can vary spatially near the coasts at a range of 2.4-3.6 nM, while in the open sea, Fe is found at the range of 1 nM (Statham and Hart., 2005). The temporal and spatial fluctuations in nutrient concentrations in the Mediterranean Sea suggest that the Mediterranean macro- and microorganisms must have mechanisms to cope with these changes to maintain their growth and productivity.

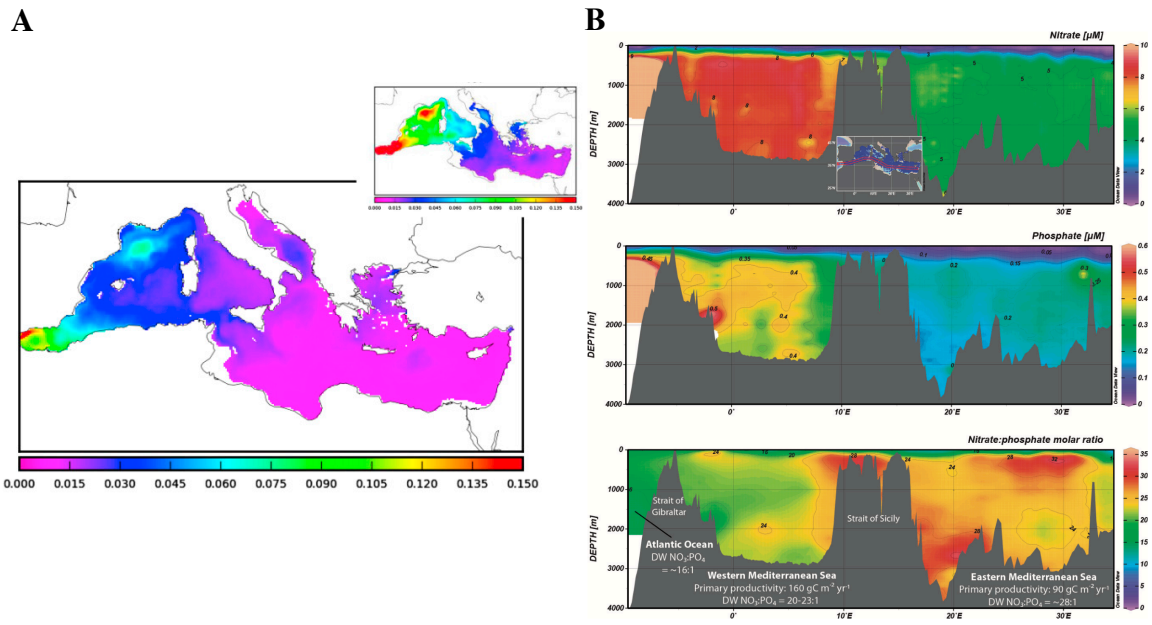

Figure 1.2. Oligotrophy of the Mediterranean Sea. **A)** P-oligotrophy from west to eastward basins. **B)** Phosphorus (P) and N concentration in the Mediterranean Sea, together with the Redfield ratio of NO_3^-: PO_4^{3-}. **Source**: **A)** Lazzari et al. (2016) and **B)** Powley et al. (2017a).

Anthropogenic threats in the Mediterranean Sea

Ocean acidification and warming

Carbon dioxide (CO_2) emissions have been increasing since the start of the industrial revolution in 1750 (Etheridge et al., 1996), reaching 410 particles per million (ppm) (**Figures 1.3A** and **1.3B).** One of the most impacted areas by human action is the Mediterranean Sea. This region is usually used as a miniature model of the world's oceans for predicting the changes derived from the increase in CO_2 emissions (Lejeusne et al., 2010). During the last decades, CO_2 storage has increased in the Mediterranean Sea since it can absorb more anthropogenic CO_2 per unit area than other marine environments (Palmiéri et al., 2015). At the end of this century, it is predicted that atmospheric CO_2 will reach 750 ppm or beyond 1000 ppm (Raupach et al., 2007). The increasing CO_2 levels have clear consequences on the chemistry of marine environments (Dutkiewicz et al., 2015). According to the Global Carbon Project (2020), approximately one-third of anthropogenic emissions are accumulated in the oceans, being one of the largest carbon sinks, aside from the soil and forests (Sabine et al., 2004). The CO_2 molecules can react chemically with seawater forming carbonic acid (H_2CO_3) and then bicarbonate (HCO_3^-), whose dissociation releases carbonate (CO_3^{2-}) and protons (H^+), resulting in seawater acidification. Increasing CO_2 emissions also causes changes in the Earth's energy heat balance, leading to an increase in air and seawater temperature. In the Mediterranean Sea, the pH is decreasing -0.0044 ± 0.00006 annually (Flecha et al., 2015), while seawater surface temperature has increased by an average of 1 ºC in the past two decades (**Figure 1.4**). Hence, it is expected that the waters in the Mediterranean Sea will reach a pH of 7.7 and an increase from 2 to 6 °C by 2100 (IPCC, 2014). In the special case of the Spanish Mediterranean coast, the sea surface temperature is increasing by 0.026-0.035 ºC per year (López-García, 2015). Although the role of ocean acidification and warming has been investigated in planktonic communities (i.e., from prokaryotes to eukaryotes) (Brierley and Kingsford, 2009; Cavicchioli et al., 2019), little is known about the effect of global climate change factors (i.e., the increasing CO_2 levels and its concomitant effect in pH decrease and temperature increase), especially in combination with other abiotic factors (e.g., nutrient concentration), in the N_2-fixers found in association with benthic systems.

Emerging pollutants: plastics

The Mediterranean Sea is one of the most polluted seas in the world, in which 95% of the waste is made of plastic (Alessi and Di Carlo, 2018). Depending on the plastic size,

they are classified into macroplastics (> 250 mm), mesoplastics (1-25 mm), microplastics (MPs) (1-1000 µm) and nanoplastics (NPs) (< 1 µm) (Hartmann et al., 2019). Bigger-sized plastic debris are dangerous for marine fauna due to ingestion or entanglement, and more than 557 species of marine life have been listed to be affected by plastics (Kühn et al., 2015). The plastic degradation by abiotic (e.g., ultraviolet rays) or biotic factors (e.g., degradation by microorganisms) to smaller plastics (MPs and NPs) may end up in lower trophic chains (i.e., planktonic and benthic microorganisms). Besides MPs can enter into higher trophic chains, finally be consumed by humans, with potentially adverse effects (Rubio et al., 2020). The plastic concentrations (sometimes termed as "soup") in the Mediterranean Sea are extremely high, reaching $1.94 \times 10^6 \pm 5.64 \times 10^5$ MPs Km^{-2} floating on the surface, with the Adriatic Sea the most affected area **(Figure 1.5A)**. The most abundant polymers in the Mediterranean Sea are polyethylene (PE) followed by polypropylene (PP), both representing 68% of the total plastic waste. Other MPs like polyvinyl chloride (PVC) are also detected in the water column (**Figures 1.5B** and **1.5C**) (Suaria et al., 2016). Due to their densities and sizes, MPs can end up and accumulate in the sediments (Reisser et al., 2015). The Mediterranean seafloor can be accumulating up to 191 pieces of MPs per 50 g of sediment (Kane et al., 2020). This suggests the susceptibility of the benthic system (e.g., *P. oceanica* meadows) to plastic pollution. Plastics are polymers constituted by long carbon chains that may contain other substances, e.g., associated chemical additives [e.g., fluoranthene, 1,2,5,6,9,10-hexabromocyclododecane (HBCD) and dioctyl-phthalate (DEHP)]. These additives are used to improve the plastic chemical properties. However, due to their low molecular weights, additives can be liberated from plastic polymers and are extremely harmful to marine ecosystems. Moreover, MPs can be sources and vectors for organic pollutants since they may be sorbed onto them and affect marine biota (Bakir et al., 2014).

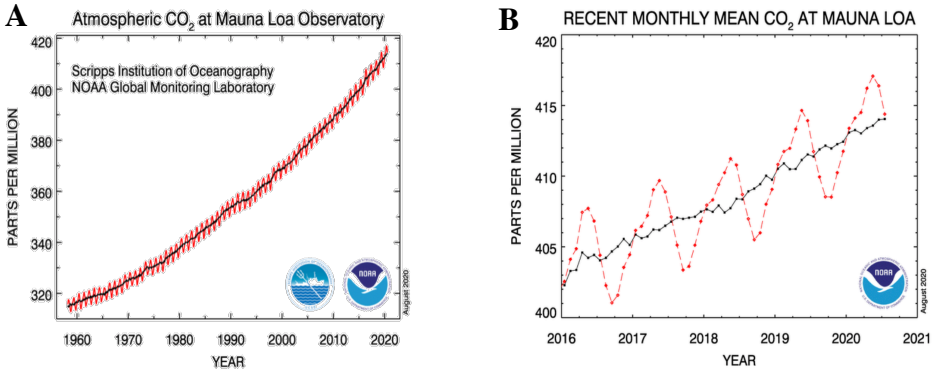

Figure 1.3. The full record of the global mean of CO_2 atmospheric concentration from **A)** 1960 and **B)** 2016 to 2020-2021. **Source:** https://www.esrl.noaa.gov/gmd/ccgg/trends/, retrieved January 2021.

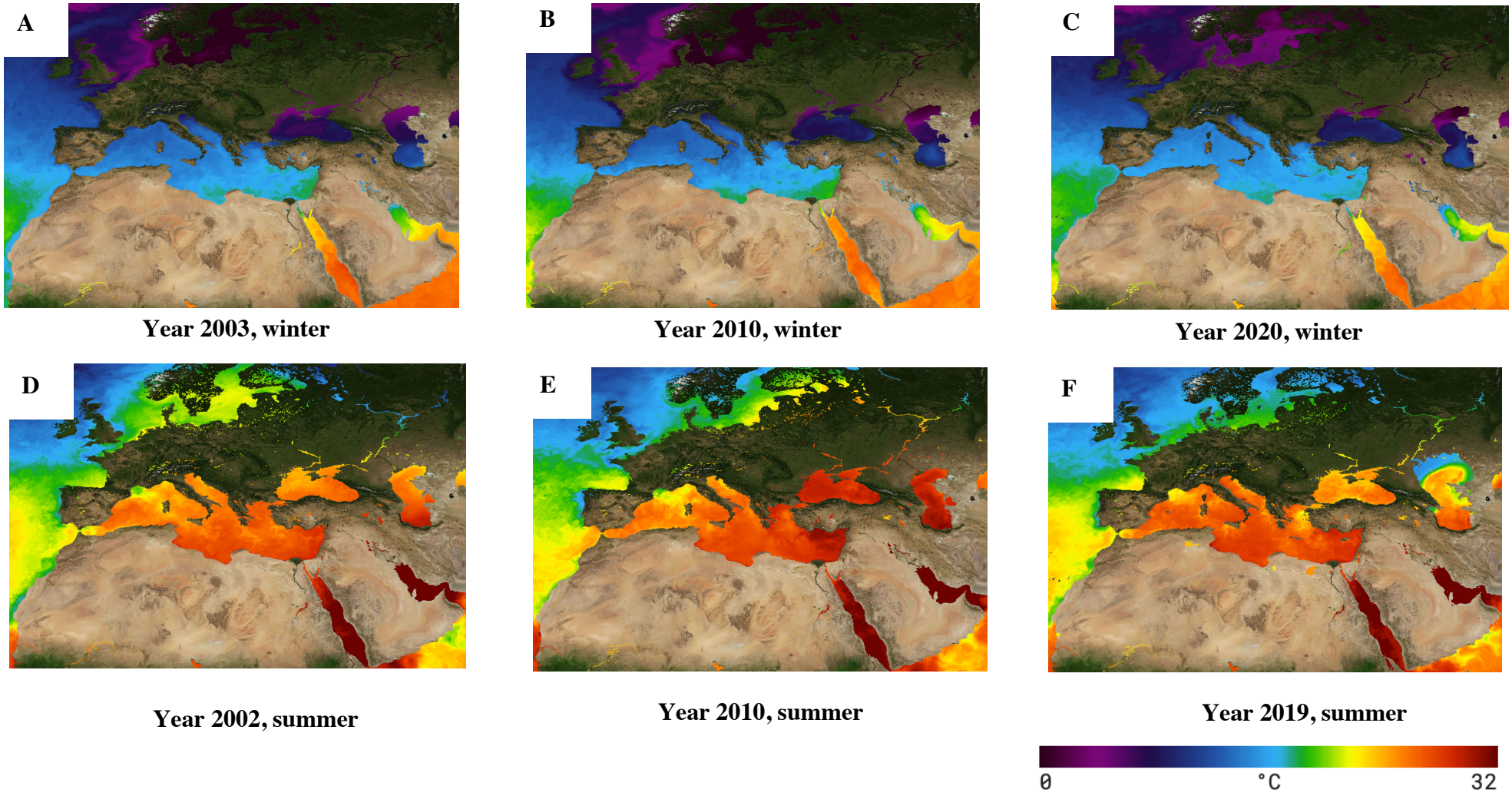

Figure 1.4. Changes in seawater temperature of the Mediterranean Sea from 2002 to 2020 in **A-C)** winter and **D-F)** summer. The data extracted show that seawater surface temperature of the Mediterranean Sea has been increased by an average of 1 ºC in the past two decades. **Source**: data extracted from NASA tool, State Of the Ocean [SOTO],https://podaac-tools.jpl.nasa.gov/soto/#b=BlueMarble_ShadedRelief_Bathymetry&l=GHRSST_L4_MUR_Sea_Surface_Temperature(la=true),GHRSST_L4_MUR_Sea_Surface_Temperature_Anomalies,MODIS_Aqua_CorrectedReflectance_TrueColor,MODIS_Aqua_Chlorophyll_A&ve=-224.67570589722152,-89.36205278230554,160.1850746018103,129.79478055742092&pl=false&pb=false&d=2021-02-17&ao=false&as=2021-02-08&ae=2021-02-15&asz=1/day&afr=500&tlr=days, retrieved Summer 2020.

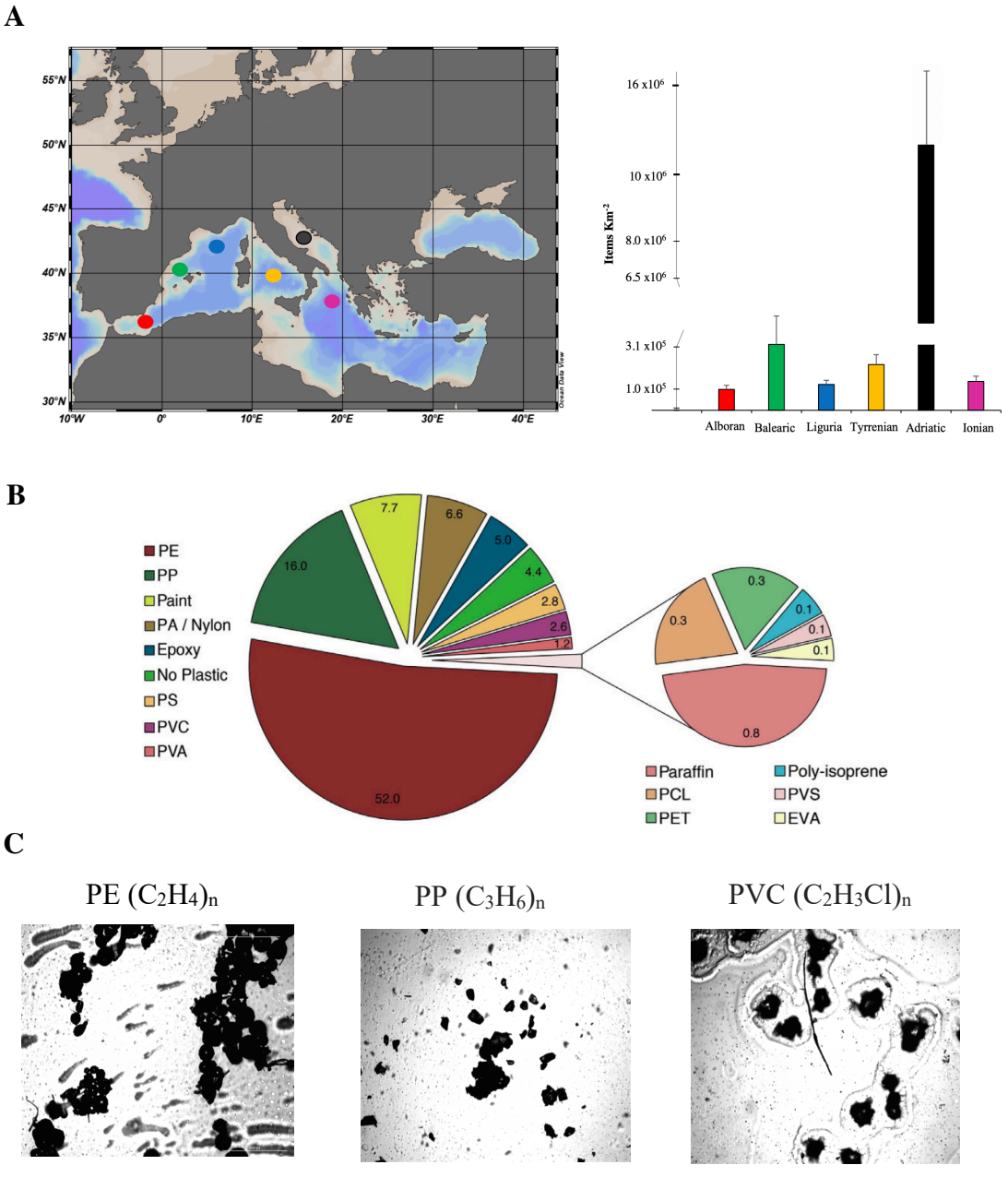

Figure 1.5. Most abundant MPs in the Mediterranean Sea. **A)** Items by Km^{-2} are represented in the different seas of the Mediterranean Sea: the Alboran Sea, the Balearic Sea, the Liguria Sea, the Tyrrhenian Sea, the Adriatic Sea, and the Ionian Sea, represented by different colors. There was no data available for the Aegean Sea. Data was extracted from https://litterbase.awi.de/litter from studies published between 2010 and 2019. **B)** Distribution of MPs in the Mediterranean Sea. **C)** Chemical structure and morphology of the most common MPs found in the Mediterranean Sea. Images were taken with confocal microscopy. **Source**: **A)** Own production using Ocean Data View, **B)** Suaria et al. (2016), and **C)** images were taken by confocal microscopy.

1.2 *Posidonia oceanica*

Posidonia oceanica (L.) Delile is an endemic marine phanerogam occupying 50 x10^3 km^2 in the coastline of the Mediterranean Sea. This long-living plant, cataloged as the longest living being on the planet (can reach more than 100000 years old) (Arnaud-Haond et al., 2012), is a slow-growing plant and found between 0-50 meters (m) deep. *Posidonia oceanica* is composed of roots, rhizome, and leaves (**Figures 1.6A** and **1.6B**). It reproduces sexually since it is a flowering plant, but it can also reproduce asexually (i.e., a clone is capable of reproducing itself).

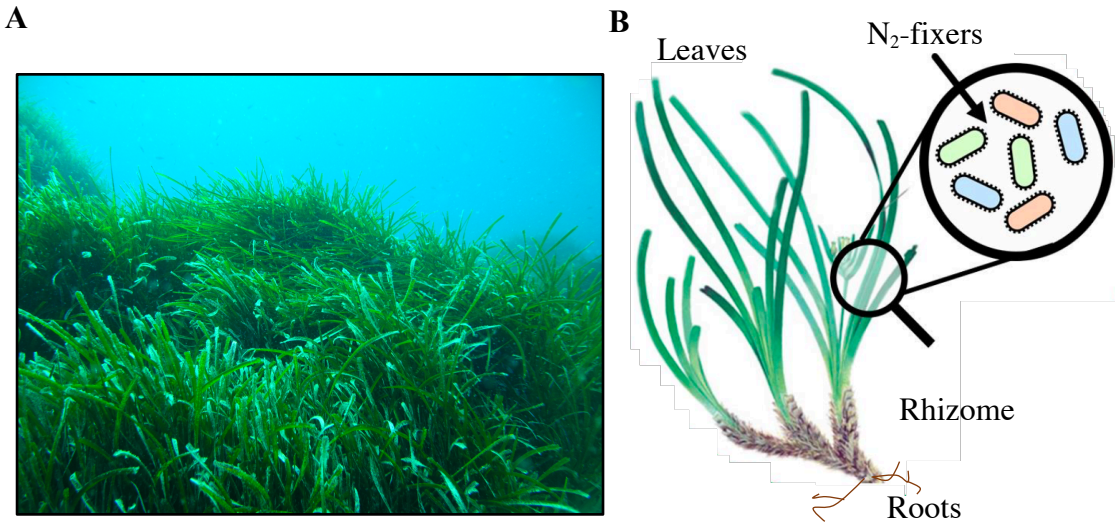

Figure 1.6. *Posidonia oceanica*. **A)** *Posidonia oceanica* meadow. **B)** *Posidonia oceanica* is constituted by leaves, roots and rhizome. **Source**: **A)** Photo took by Ivan Ruiz Llobera and **B)** book "Praderas y Bosques Marinos de Andalucía and modified by Xabier López-Alforja.

Posidonia oceanica meadows offer valuable ecological functions involved in the productivity, sustenance, and quality of coastal Mediterranean marine ecosystems. They maintain clear and oxygenate the seawater (e.g., producing 14 L of O_2 per day), and remove CO_2 from the water column, acting as carbon sinks and buffers for ocean acidification (Vassallo et al., 2013). Seagrasses take part in various biogeochemical processes such as nutrient recycling and mixing, sediment stabilization and shoreline protection, mitigating the impact of waves. *Posidonia oceanica* beds harbor a high diversity of macro-and microorganisms, i.e., with up to 400 flora and 1000 animal species (Gutiérrez et al., 2012; Campagne et al., 2015; Agawin et al., 2016). Microorganisms associated with *P. oceanica* are found as epiphytic or endophytic populations in the leaves, roots and rhizomes, forming what is known as the holobiont, i.e., a biological unit between the microorganisms and the plant (Ugarelli et al., 2017). The microbial

populations, from bacteria to eukaryotic microorganisms, are essential for the maintenance and survival of the plant. The associated microorganisms can provide nutrients (e.g., P, Fe and N), vitamins and secondary metabolites to the plant, and *P. oceanica*, in turn, can provide dissolved organic carbon (and nutrients) to the bacteria from exudates of the leaves and roots (Ugarelli et al., 2017). Yet, the role of the associated microorganisms in the maintenance and survival of the plant is still poorly understood. Among these microbial populations, N_2-fixers or diazotrophs can potentially provide the total N-demand for *P. oceanica* (Agawin et al., 2016 and 2017). Through the analysis of *nifH* gene (i.e., which codify the Fe-protein of the nitrogenase), it was revealed the high diversity of N_2-fixing microorganisms associated with *P. oceanica* [*Cyanobacteria*, (α-, β-, δ- and γ-) *Proteobacteria*, *Firmicutes*, *Bacteroidetes* and *Archaea*] (Agawin et al., 2017) (**Figure 1.7**). These N_2-fixers may have different growth and nutrients requirements and may have different responses to the environmental challenges, e.g., different nutrient concentrations of P, Fe and N, the increase of CO_2 levels (and its concomitant effects in seawater pH and temperature) or emergent pollutants (e.g., plastic contamination). The responses of these N_2-fixers to these environmental factors and emergent pollutants have not been studied, and nothing is known about the consequences to the plant itself.

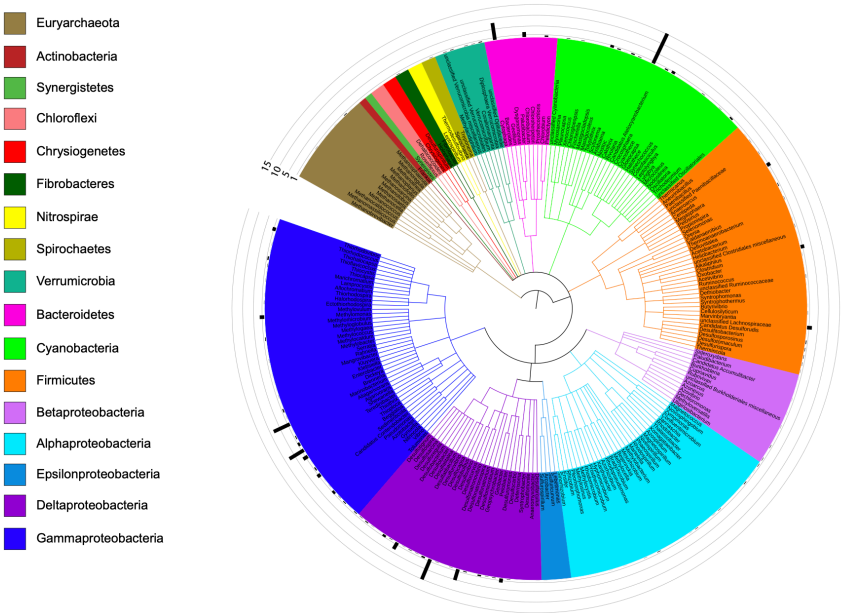

Figure 1.7. N_2-fixing bacterial distribution in *P. oceanica* (phylogenetic tree), based on the *nifH* analysis. **Source:** Supplementary material Agawin et al. (2017).

1.3 N_2-fixation and diazotrophs

N_2-fixation

Biological N_2-fixation (BNF) carried out by microbial communities is an essential process in the marine N-cycle, providing new N to the marine systems and compensating the loss of N due to ocean denitrification and anaerobic ammonium oxidation (anammox). The BNF has direct relevance in the biological pump of organic components to deep waters (Sohm et al., 2011; Zehr and Capone, 2020), and it is an energy costly redox process in which atmospheric di-nitrogen gas (N_2) is reduced to ammonium and needs the hydrolysis of 16 ATP (**eq. 1.1**). This reaction is catalyzed by an enzymatic complex called nitrogenase, which is formed by NifH, NifD and NifK proteins (Hoffman et al., 2014). The nitrogenase complex is composed of a homodimeric NifH component (Fe protein) and heterotetrameric NifDK component (MoFe protein), which contains iron-molybdenum cofactor (FeMo-co), forming the Mo-nitrogenase (**Figure 1.8A**) (Hoffman et al., 2014). The Mo-nitrogenases are the most widespread nitrogenases, although alternative forms exist, e.g., vanadium nitrogenases (V-nitrogenases, **Figure 1.8B**) and iron-only nitrogenases (Fe-only nitrogenases) (Mus et al., 2018). Generally, nitrogenases are extremely sensitive to molecular oxygen (O_2), and diazotrophs must develop strategies to avoid nitrogen inhibition, explained below.

$$N_2 + 8e^- + 16ATP + 8H^+ \rightarrow 2NH_3 + H_2 + 16ADP + 16PO_4^{3-} \quad \textbf{(eq. 1.1)}$$

N_2-fixation through the Mo-nitrogenase is a well-regulated process in which several genes participate. Besides the structural components, i.e., *nifH*, *nifD* and *nifK*, there are genes involved to assemble the FeMo-cofactor, i.e., *nifE*, *nifN* and *nifB*; involved in the synthesis and insertion of the FeMo-protein cofactor, i.e., *nifX*, *nifQ*, *nifV* and *nifY*; for the synthesis of the metallocluster, i.e., *nifU*, *nifS* and *nifZ*; for the correct folding of the nitrogenase, i.e., *nifM* and *nifW*; and a whole group of accessories genes as *iscAnif*, *orf8*, *nifZ*, *clpX* and *nifF* (Mus et al., 2018). The exact molecular mechanism behind N_2-fixation remains unknown, but the N_2-fixation can be controlled by C/N ratio, O_2 concentration, light: dark photoperiod, or metal availability (i.e., Fe, Mo or V) (Mus et al., 2018). Dissolved inorganic nitrogen (DIN, e.g., NH_4^+, NH_3 and NO_3^-) is one of the main regulators of the BNF (Knapp, 2012) since nitrogenase is highly inhibited by increasing levels of DIN. Studies in cultivable N_2-fixers showed that elevated DIN concentrations from 30 µM of NO_3^- and 200 µM of NH_4^+ can strongly decrease N_2-fixation rates (Knapp,

2012). When inorganic nitrogen is available, N_2-fixers prefer inorganic forms of nitrogen over fixing N_2 considering that BNF is an energy-expensive process that requires 16 ATP and 25% more energy than taking up DIN from the media (Manhart and Wong, 1980; Nelson et al., 1982; Knapp, 2012). However, nothing is known about the effect of different concentrations of DIN on diazotrophs associated with benthic systems.

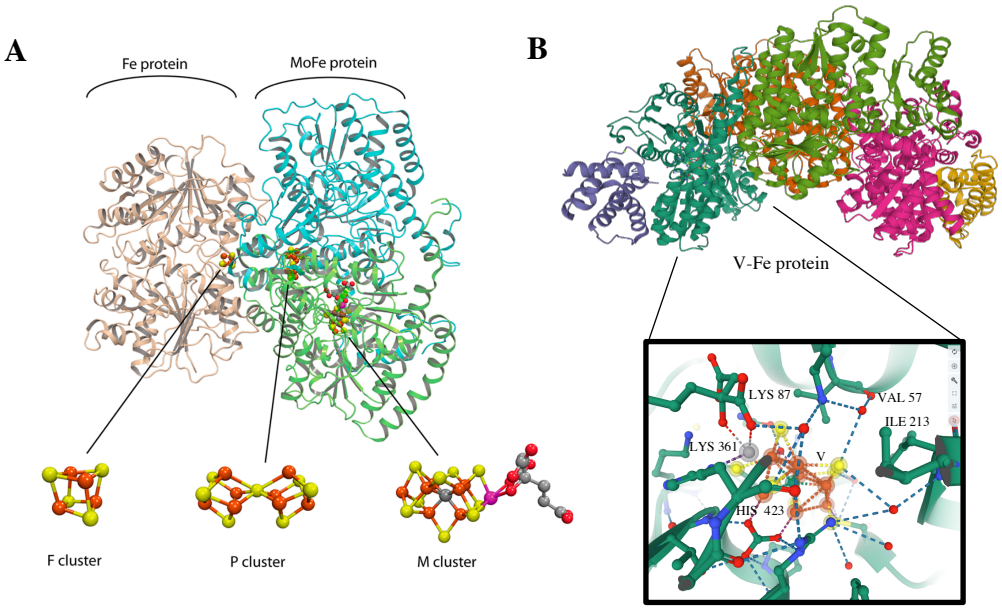

Figure 1.8. Nitrogenase complex. **A)** Mo-Fe nitrogenase structure. **B)** V-Fe nitrogenase. **Source**: **A)** Hoffman et al. (2014) and **B)** own production from protein data bank (PDB: 7ADY).

Marine diazotrophs

In the open sea, BNF is carried out by a small group of bacterial and archaeal species. Cyanobacteria, which are oxygenic photosynthetic bacteria are the main N_2-fixers in the marine water column, supporting 25-50% of global N_2-fixation (Sohm et al., 2011; Zehr and Capone, 2020). They can be classified as (**I**) unicellular (e.g., *Cyanothece*, *Crocosphaera* or *Cyanothece*-like organisms) (**Figure 1.9A**), (**II**) filamentous heterocyst-forming (e.g., *Richelia*, *Calothrix* and relatives) **(Figure 1.9B**) and (**III**) filamentous non-heterocyst-forming cyanobacteria (i.e., *Trichodesmium*) (Zehr, 2011). Although cyanobacteria can be considered obligatory autotrophs, i.e., they synthesize organic compounds from inorganic ones, most of them can take up organic carbon sources and oxidize them as mixotrophs (Rippka et al., 1979). The major groups of N_2-fixers are *Trichodesmium*, *Richelia*/*Calothrix*, UCYN-A and *Crocosphaera* (UCYN-B) (Zehr, 2011). Since the N_2-fixation is highly sensitive to redox processes (Zehr, 2011), these cyanobacterial diazotrophs must develop strategies to avoid N_2-fixation inhibition by

molecular oxygen liberated from photosynthesis. Unicellular cyanobacterial cells (e.g., UCYN-B) may separate temporarily two incompatible processes: N_2-fixation (at night) and photosynthesis (at day) in the same cells. Because of that, these two processes must be tightly controlled through well-regulated circadian clocks (Toepel et al., 2008). On the contrary, filamentous heterocyst-forming cyanobacteria have specialized cells (i.e., heterocyst) in which N_2-fixation takes place in anoxic conditions and under light photoperiod. Unlike the unicellular cyanobacteria, this does not have an add-on cost of temporally separating N_2-fixation and photosynthetic processes. In the case of filamentous non-heterocyst-forming cells (e.g., *Trichodesmium*), they can fix N_2 aerobically under the light photoperiod and are capable of combined a spatial and temporal separation between the photosynthetic process and N_2-fixation (Zehr, 2011). However, the exact mechanism of action behind this is still unknown (Zehr, 2011), and some reports suggest that *Trichodesmium* can differentiate in vegetative cells (diazocyte) in which nitrogenase can accumulate (Fredriksson and Bergman, 1997; Sandh et al., 2012).

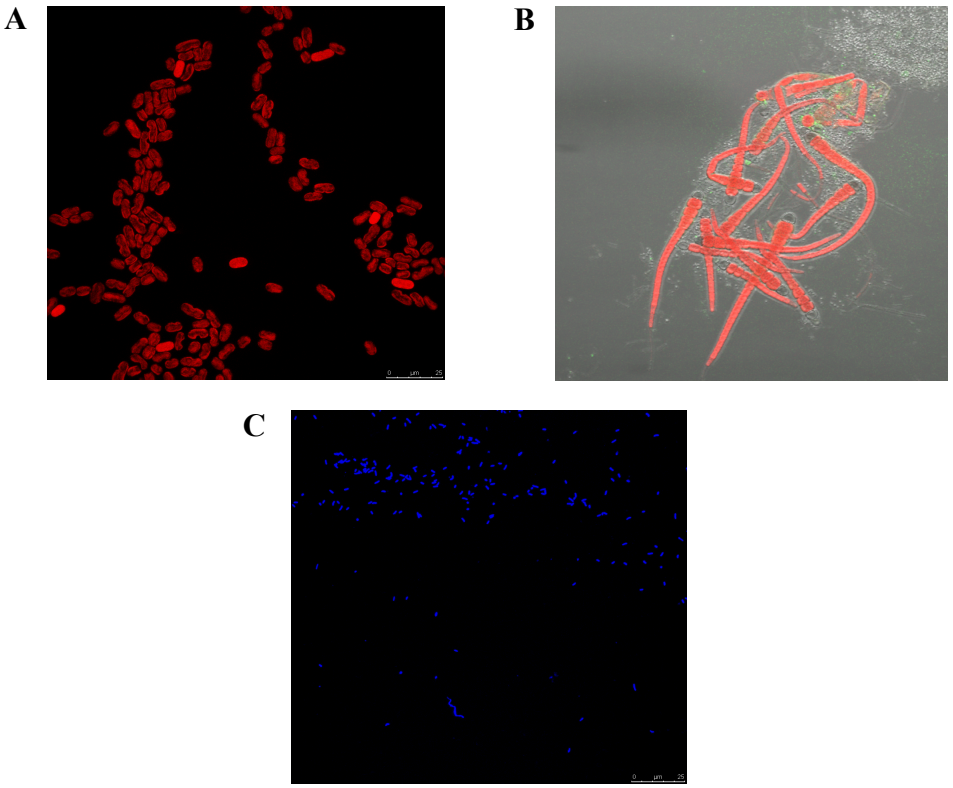

Figure 1.9. Confocal microscopical images of N_2-fixing bacteria. **A)** Unicellular cyanobacteria, *Halothece* sp. PCC 7418. **B)** Filamentous heterocyst-forming, *Calothrix* sp. PCC 7103. **C)** Heterotrophic bacteria, *Marinobacterium litorale* DSM 23545, visualized with DAPI. **Source: A-C)** images taken by confocal microscopy.

Although cyanobacteria are considered the major N_2-fixing diazotrophs in the oceans, studies on the role of the heterotrophic bacteria in the BNF is recently increasing (Zehr and Capone, 2020). In the euphotic zone of the Indian Ocean, heterotrophic bacteria can be the majors N_2-fixers (Shiozaki et al., 2014), suggesting their importance in the N cycles. Heterotrophic bacteria are considered the central axis of microbial food webs, which require organic matter for growth, and they are usually smaller than phototrophic bacteria (Sarmento et al., 2010; Anderson, 2018).

Role of environmental factors and emerging pollutants in N_2-fixation

Ocean nutrient concentrations can control diazotrophic activity. Phosphorus (P) and Fe are considered the main limiting nutrients for N_2-fixation in the world's oceans (Sañudo-Wilhelmy et al., 2001; Mills et al., 2004; Moore et al., 2009; Moore et al., 2013; Browning et al., 2017; Zehr and Capone, 2020). N_2-fixers require a higher demand for P and Fe than non-diazotrophic bacteria (Falkowski, 1997; Ward et al., 2013). N_2-fixation reaction is energetically costly, requiring 16 ATPs (**eq. 1.1**), and this P-dependence of N_2-fixation is well illustrated for *Trichodesmium*, in which there is a linear correlation between the P cellular content of the cells and its N_2-fixation rates (Sañudo-Wilhelmy et al., 2001). As a consequence of the low P concentrations in the Mediterranean Sea, P may be the main limiting factor controlling N_2-fixing activities in the region (Sohm et al., 2011). Iron (Fe) availability can control the diazotrophic activities since nitrogenase contains 38 Fe atoms per holoenzyme. Moreover, Fe can be a cofactor of the alkaline phosphatases (APases) which release DIP from dissolved organic phosphorus (DOP), fueling N_2-fixing activities (Browning et al., 2017; Hoffman et al., 2014). Since Fe availability may change seasonally in the Mediterranean Sea (Statham and Hart, 2005), Fe can also limit the N_2-fixation activities of diazotrophs in the region.

Diazotrophic activities of phototrophic and heterotrophic bacteria can also be controlled by CO_2 concentrations in the oceans. Increasing CO_2 levels can decrease the activity of the carbon concentration mechanisms (CCMs) in carboxysomes, saving energy which can be used to catalyze the N_2-fixation process, and thus, increasing the N_2-fixing rates (and diazotrophic growth) (Eichner et al., 2014a). Several heterotrophic bacteria can fix and assimilate CO_2 through different carboxylation reactions via phosphoenolpyruvate (PEP) carboxylase and pyruvate carboxylase, producing oxaloacetate that is incorporated into the Krebs cycle (Santruckova et al., 2005). This process can contribute 2-8% of the cellular carbon abundance (Spona-Friedl et al., 2020).

Presumably, the increase of CO_2 levels could raise the ATP synthesis, in both in cyanobacteria and heterotrophic bacteria, which can be used for the N_2-fixation process. The effect of increased CO_2 levels in marine N_2-fixers is described in several reports, although they focus on few model test species, e.g., on the filamentous cyanobacterium *Trichodesmium* (Barcelos e Ramos et al., 2007; Breitbarth et al., 2007; Fu et al., 2007, 2008; Hutchins et al., 2007; Levitan et al., 2007; Czerny et al., 2009; Garcia et al., 2011, 2013ab; Shi et al., 2012; Eichner et al., 2014ab; Boatman et al., 2017). Even though they show inconsistent and contradictory results, increasing CO_2 concentrations can increase growth and N_2-fixation rates. However, nothing is known on the effect of CO_2 in heterotrophic N_2-fixing bacteria. Increasing CO_2 concentrations have concomitant effects of decreasing pH and increasing temperature levels, which can also affect N_2-fixers. However, there are no reports about the effect of lowering pH in marine diazotrophs. *In vivo* studies in soil samples suggest that nitrogenase is active in a range of pH 4.7-7, reaching its maximum activity at pH 6-7 (Schubert et al., 1990). Some reports indicate that increasing temperature levels of the water column will increase N_2-fixation rates by up to 22-27% by the end of this century (Boyd and Doney, 2002; Fu et al., 2014; Jiang et al., 2018), while others predict a decrease in the N_2-fixation rates when the interaction with other environmental factors (e.g., pH, nutrients regimes and competition between cells) are considered (Wrightson and Tagliabue, 2020). Only a few studies consider the interactive effect of CO_2 with other environmental variables, particularly nutrient availabilities (e.g., P and Fe) in marine bacteria, suggesting that the effect of global climate factors (i.e., CO_2, pH and temperature) may be controlled by the nutrient status of the microorganisms.

The effects of other anthropogenic factors, e.g., plastic pollution, are poorly understood in N_2-fixers. Marine plastics debris are associated with a high diversity of bacteria, forming a community known as the plastisphere (Zettler et al., 2013). These systems may be a hot-spot for N_2-fixers since *nifH, nifD,* and *nifK* genes have been detected on the plastic surfaces (Bryant et al., 2016). Although several reports have studied the effect of plastics and/or MPs in the bacterial populations, these reports are focused on plastic degradation and biofilm formation (Harrison, 2011; Bryant et al., 2016; Romera-Castillo et al., 2018; Tetu et al., 2019; Machado et al., 2020; Piccardo et al., 2020; Sarker et al., 2020; Seeley et al., 2020), and very little is known about the physiological responses of marine bacteria with exposure to plastics (e.g., MPs) and their organic additives. There is no information on the effects of plastics in the N_2-fixation

process, and further studies on the effects of plastics and their organic additives on diazotrophs associated with seagrasses should be evaluated (Maity and Pramanick, 2020), considering the susceptibility of benthic systems to plastic accumulation. The size and chemical composition of plastics are characteristics that must be taken into account when evaluating plastic contamination in diazotrophs (Paul-Pont et al., 2018).

Adaptative mechanisms for marine diazotrophs

Phosphorus (P), especially DIP, is extremely limited in the Mediterranean marine waters (Lazzari et al., 2016). The DIP is necessary for adenosine triphosphate (ATP) and nucleic acids (DNA/RNA) synthesis. In most bacteria, it is a key structural component of cell membranes (Santos-Beneit, 2015). ATP-dependent reactions, e.g., N_2-fixation, have a strong P-dependence (Sañudo-Wilhelmy et al., 2001), and diazotrophs usually have to cope with changes in P-concentration, developing strategies to obtain it. P-limitation triggers the activation of the APases, which are capable of hydrolyzing dissolved organic P (DOP) from the water column (**Figure 1.10**). The activity of these enzymes is controlled by metal cofactors, e.g., Ca, Mg, Fe and/or Zn. According to this, APases can be classified into three families: PhoA (with two Zn^{2+} and one magnesium Mg^{2+} ions), PhoD (e.g., PhoD from *Bacillus subtilis* model has an active site formed with one Fe^{3+} and two Ca^{2+} ions) and PhoX (with three Ca^{2+} and one/two Fe^{3+} ions) (Rodriguez et al., 2014; Yong et al., 2014). PhoX is the family most distributed in marine environments (Sebastian and Ammerman, 2009). Hence, it is hypothesized that metals (e.g., Fe), which regulate N_2-fixation rates, may provide the necessary DIP for fueling the BNF, controlling the alkaline phosphatase activity (APA).

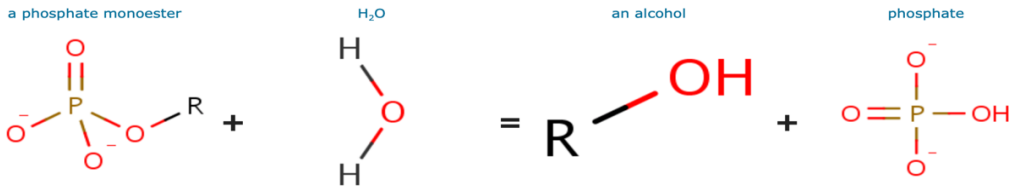

Figure 1.10. Mechanism of action of APases. **Source**: UniProt.

Alkaline phosphatases (APases) are part of what is known as the Pho regulon, a group of genes involved in the adaptation and survival under P-limiting conditions (Santos-Beneit, 2015). Aside from APases, which are usually found in the periplasm (i.e., in the

gram-negative bacteria), the "classical" Pho regulon also contains high-affinity (e.g., PstS, PstC, PstA and PstB) and low-affinity phosphate transporters, and proteins involved in the P reservoir (e.g., PpK, PpX and PpA). Other elements with unknown functions, as PhoU, can play a key role in regulating the PhoR and Pst system activity **(Figure 1.11**). The expression of these genes is mainly controlled by a two-component system, PhoR-PhoB. Phosphorus limitation causes the autophosphorylation of the PhoR, which phosphorylates and activates PhoB (**Figure 1.11**). PhoR is an inner-membrane histidine kinase, while PhoB is a transcriptional factor (TF) that recognizes and binds to a consensus DNA sequence (i.e., PHO box) through its DNA-binding motif. In cyanobacteria, the PHO box is formed by three tandem repeats of 8 bp separated by 3 bp, unlike the PHO Box from *Escherichia coli* which is formed by two direct repeats of 7 bp separated by 5 bp (Yuan et al., 2006; Su et al., 2007; Tiwari et al., 2015). Investigating what genes form part of the Pho regulon (e.g., using bioinformatic tools) can shed light on the adaptation and survival of marine diazotrophs living in continuous changes of nutrient concentrations.

Iron (Fe) is a micronutrient that requires tight regulation and homeostasis, found as Fe (II) and Fe (III) in the water column. To fulfill the Fe requirements of the nitrogenase, N_2-fixers need from 5 to 100-fold more Fe than non-N_2-fixers (Kustka et al., 2004). The dominant Fe species under aerobic and low pH conditions is Fe (II), which can diffuse across the outer membrane of the gram-negative bacteria into the periplasm. From the periplasm, the Fe (II) is transported to the cytoplasm by specific transporters (e.g., FutABC and FeoAB) (Lau et al., 2016). The dominant form in the oxygenated water column is Fe (III), which is insoluble and must be chelated with organic molecules, i.e., siderophores. Siderophores are transported into the cells by specific transporters, e.g., TonB-dependent transporters (TBDTs) (Noinaj et al., 2010). Seasonal patterns, which control windborne desert dust (i.e., rich in Fe), and environmental factors, e.g., increasing CO_2 levels and its concomitant effect in pH and temperature, can limit Fe in the oceans. Thereby, ocean acidification and warming might trigger changes in the Fe-chemistry which makes Fe (III) less available to organic chelators (e.g., siderophores), while Fe (II) can be oxidized into non-bioassimilable forms. This can reduce Fe-uptake, limiting the diazotrophic activities (Shi et al., 2010; Samperio-Ramos et al., 2016). Therefore, N_2-fixers must adapt to varying Fe levels by triggering molecular responses through the Fur regulator, which controls the Fur regulon, i.e., genes involved in the Fe-metabolism (Fillat, 2014).

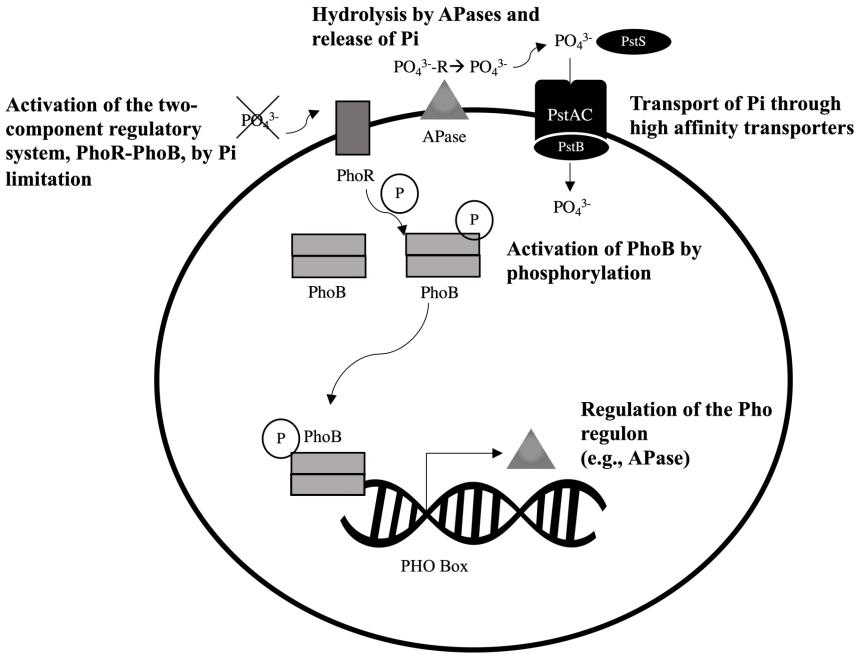

Figure 1.11. Pho regulon regulation. Under Pi limitation, the two-component system PhoR-PhoB is activated, through the autophosphorylation of PhoR, which phosphorylates PhoB. PhoB (phosphorylated), which binds to the PHO box (a transcriptional binding site), is a transcriptional factor that modulates and controls the expression of genes related to P limitation, which is known as the Pho regulon, e.g., APases. Hence, cells can respond to P-limitation, e.g., releasing Pi from organic sources that can be transported across high-affinity transporters. **Source**: own production.

Elevated Fe-intracellular concentrations might enhance oxidative stress via Fenton and Haber-Weiss reactions, generating reactive oxygen species (ROS) (Kranzler et al., 2013) (**eq. 1.2** and **1.3**). The ROS, e.g., superoxide oxygen ($O_2^{-\cdot}$), hydrogen peroxide (H_2O_2) or the hydroxyl radical ($OH\cdot$), are highly reactive molecules that are extremely toxic at DNA, protein and lipid levels, ultimately causing cell death (Cabiscol et al., 2000). In cyanobacteria, another target of ROS can be the phycobilisomes, downregulating the photosynthetic activities (Latifi et al., 2009). Due to aerobic metabolisms, cells must develop strategies to maintain ROS levels to avoid a ROS imbalance that leads to oxidative stress. Moreover, marine bacteria are exposed to environmental and anthropogenic factors that may enhance ROS production (Lesser, 2006). Like other microorganisms or higher organisms, marine bacteria have different strategies to avoid oxidative stress via the so-called antioxidants, i.e., non-enzymatic or enzymatic defenses. Non-enzymatic defenses are composed of small organic molecules that can reduce ROS, e.g., glutathione or carotenoids (found in cyanobacteria). Antioxidant enzymes, essential for detoxifying ROS, are metal-dependent enzymes (e.g., Mn, Cu or Fe) which include

the superoxide dismutase (SOD), catalase (CAT), glutathione peroxidase (GPx) and glutathione reductase (GR). These parameters can be used as cell biomarkers for evaluating cell health (Ferrat et al., 2003; Benedetti et al., 2015). For N_2-fixers, high ROS levels are correlated with the inhibition of the nitrogenase activity since N_2-fixation is very sensitive to the redox processes (Alquéres et al., 2010). Only a few studies consider the role of oxidative stress in diazotrophs, and more studies should evaluate the role of environmental factors (e.g., nutrient concentration or anthropogenic factors) and emerging pollutants in the oxidative processes in N_2-fixers.

$$Fe + H_2O_2 \longrightarrow Fe\ (III) + HO^- + HO\cdot \text{ (Fenton reaction) (\textbf{eq. 1.2})}$$

$$H_2O_2 + O_2^{-\cdot} \xrightarrow[Fe\ (II)/\ Fe\ (III)]{} HO^- + HO\cdot \text{ (Haber-Weiss net reaction) (\textbf{eq. 1.3})}$$

In summary, considering the valuable ecological functions that the Mediterranean *P. oceanica* seagrass offers and the importance of N_2-fixers in the maintenance of this plant, this work seeks the investigation of the role of abiotic factors in the diazotrophs from a physiological and molecular point of view. For this general purpose, different species (i.e., phototrophic and heterotrophic N_2-fixing bacteria) found in association with *P. oceanica* were used as model test species. This thesis is divided into two main sections describing, (**1**) the effect of nutrient availabilities (P, Fe and N) and (**2**) the effect of anthropogenic factors [i.e., global climate change factors (CO_2, pH and temperature), and emerging pollutants (i.e., MPs and their most common associated additives)] in diazotrophs (**Figure 2.1**).

2. OBJECTIVES

OBJECTIVES

2.1 General hypothesis

Marine coastal environments such as seagrass meadows (e.g., the endemic Mediterranean *Posidonia oceanica*) experience fluctuations of environmental factors (e.g., changes in nutrient concentration) due to natural biogeochemical processes. *Posidonia oceanica* meadows are also subject to anthropogenic action, e.g., increasing CO_2 levels and emerging pollutants (e.g., plastic pollution) (**Figure 2.1**). Nothing is known about the effects of environmental factors and emerging pollutants in N_2-fixers found in association with *P. oceanica*, and how N_2-fixing bacteria respond to the changing environment at the physiological and molecular level. *Posidonia oceanica* harbors a high diversity of N_2-fixing phototrophic and heterotrophic bacteria and these N_2-fixers may have different growth requirements and sensitivity to the environmental factors and emerging pollutants, and their responses may be species-specific. Considering the importance of N_2-fixers in supplying inorganic N to the plant, studies on these populations must be conducted to predict future changes in the health of the plant.

The general hypothesis of this work is that diazotrophs found in association with seagrass meadows will be controlled by relevant environmental factors and emergent pollutants, affecting and limiting physiological and biochemical parameters, and N_2-fixation rates, according to the bacterial nature (i.e., phototrophs or heterotrophs).

2.2 General objectives

1. To investigate how relevant abiotic factors (i.e., environmental factors and emerging pollutants) affect the growth and N_2-fixation activities of N_2-fixing microorganisms through pioneering multi-factorial laboratory experiments.
2. To investigate the molecular mechanisms behind the responses to environmental factors and emerging pollutants to understand how these N_2-fixers can adapt and survive in a changing environment. These analyses aim to investigate molecular biomarkers [e.g., alkaline phosphatase activity (APA) or reactive oxygen species (ROS)], which can be used as a diagnostic tool to assess the health status of the N_2-fixers.

2.3 Specific objectives

1. General *objective 1* is achieved following these specific activities:

The investigation of the responses of N_2-fixers (i.e., phototrophs and heterotrophs) in terms of growth and N_2-fixation activities by flow cytometry and acetylene reduction assay (ARA), respectively, in multi-factorial *in-vitro* controlled laboratory experiments at:

(**I**) Different nutrient concentrations [phosphorus (P), iron (Fe) and nitrogen (N)] (**Chapters 1-3**).

(**II**) Different CO_2 concentrations (i.e., environmental, 410 ppm and expected CO_2 at the end of the century, 1000 ppm), pH and temperature levels (**Chapter 4**).

(**III**) Different concentrations and types of emerging pollutants [microplastics (MPs) and their associated additives] (**Chapter 5**).

2. The general *objective 2* is achieved following the specific activities:

The investigation of the molecular responses of N_2-fixers to environmental factors and emerging pollutants to seek biomarkers which can be used as a diagnostic tool to assess the health status of the N_2-fixers, through:

(**I**) Laboratory experiments:

- **a.** Investigating the P-acquisition mechanisms, e.g., the alkaline phosphatase activity (APA) and P-uptake through fluorometric and spectrometric assays, respectively, and studying the role of Fe in these mechanisms.
- **b.** Investigating the production of reactive oxygen species (ROS) as a cell stress biomarker, using fluorometric methods.
- **c.** Revealing changes in cell morphology and apoptotic processes, using microscopical analyses.
- **d.** Investigating protein overexpression, using MALDI-TOF analyses.

(**II**) *In-silico* analyses:

- **a.** Investigating the genomic features through the isolation, sequencing and identification of potential N_2-fixers through genomic comparative analyses.
- **b.** Describing the Pho, Fur and NtcA regulon through the design of position frequency matrix (PFM) and algorithms, and predicting the elements behind the P, Fe and N-limitation.

c. Predicting the tridimensional structure of proteins directly related to the adaptation to the global stressors (e.g., PhoD) on phototrophic and heterotrophic bacteria.

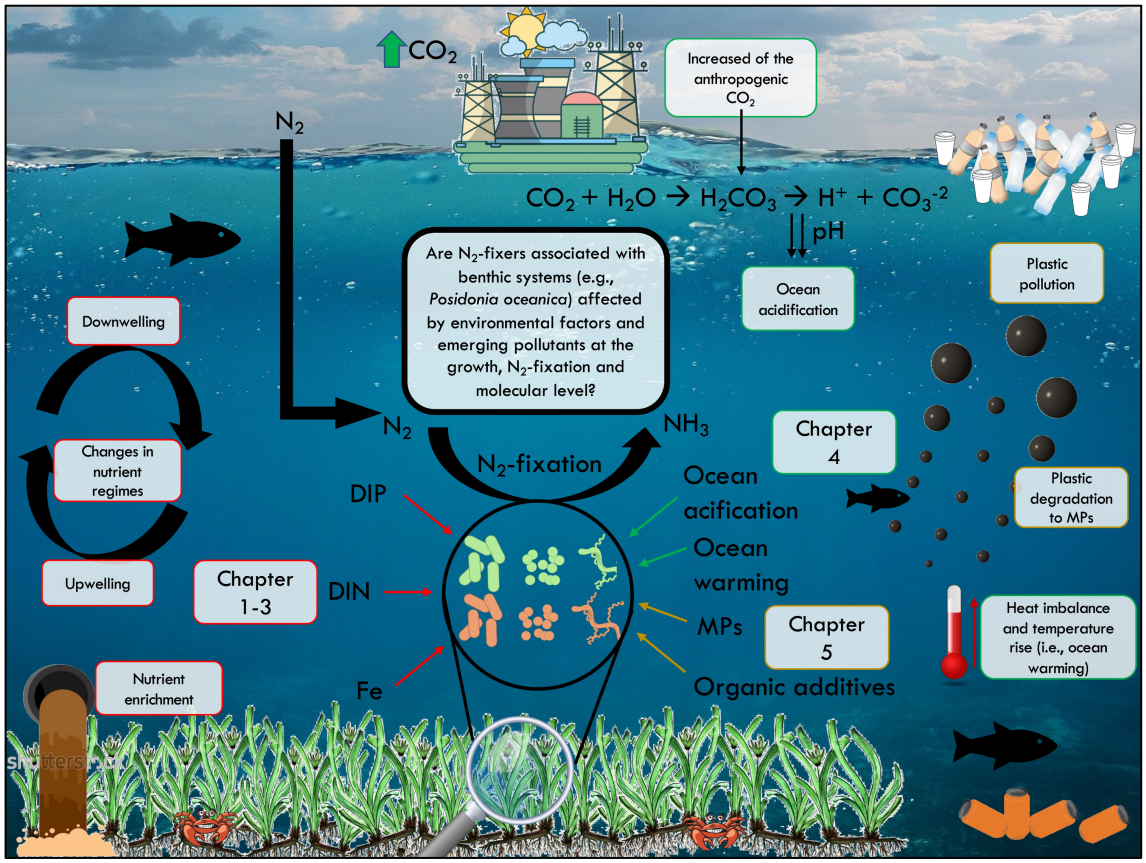

Figure 2.1. Environmental factors and emerging pollutants threaten *Posidonia oceanica*. Summary of all the abiotic factors (i.e., different nutrient regimes in red, anthropogenic CO_2 and its concomitant effect in ocean acidification and warming in green, and plastic pollution and their organic additives associated in yellow) that might affect the diazotrophic population found in association with benthic systems, e.g., *P. oceanica* meadows. The main aim of this thesis was to evaluate the role of the global stressors at the physiological and molecular level, showing if N_2-fixing communities are affected according to their nature (e.g., phototrophic and heterotrophic). **Source:** own production.

3. RESEARCH ARTICLES BY CHAPTERS

SECTION I: EFFECT OF NUTRIENT REGIMES IN PHOTOTROPHIC AND HETEROTROPHIC BACTERIA

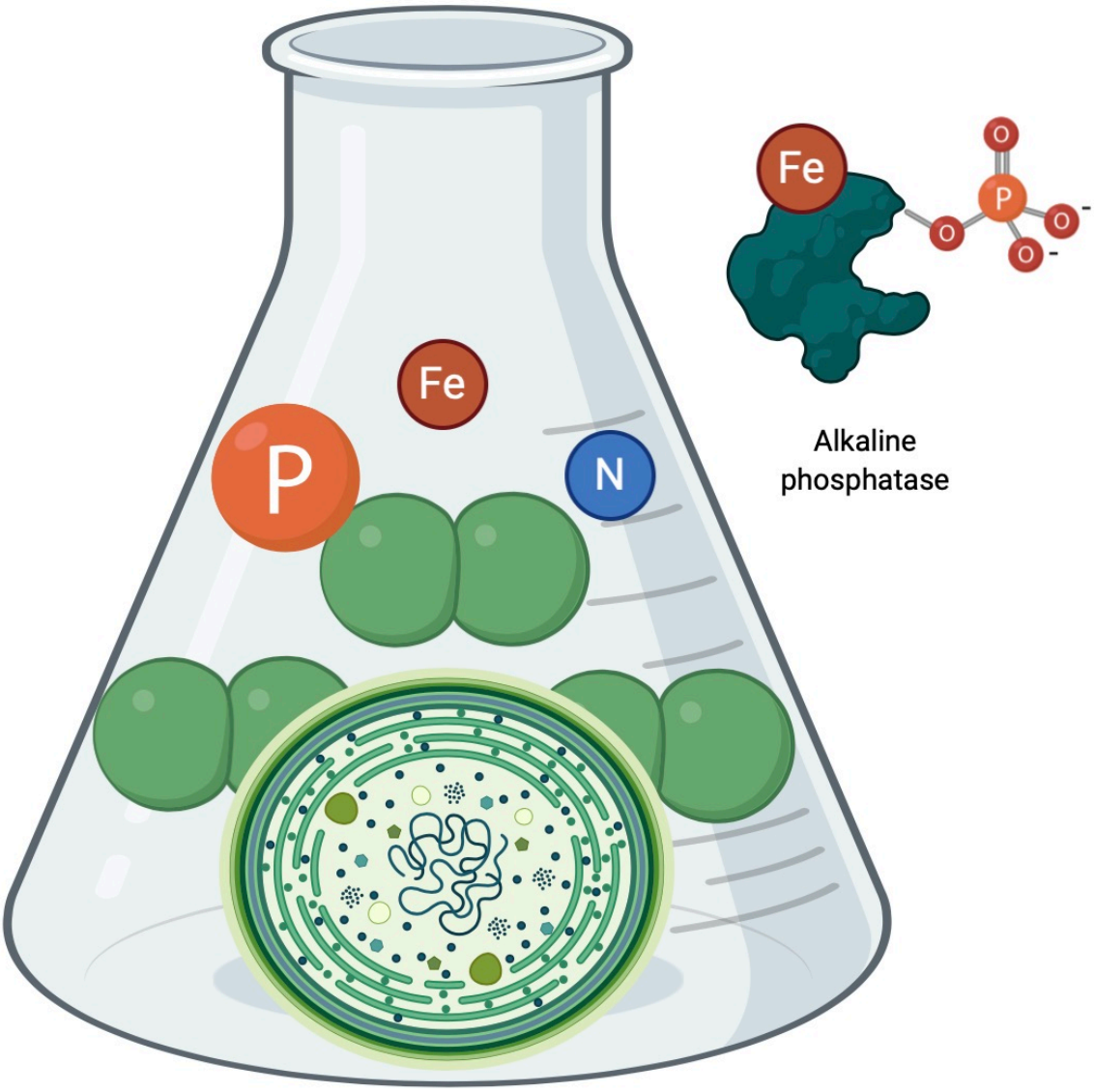

3.1 Chapter 1

frontiers in Microbiology

ORIGINAL RESEARCH
published: 22 August 2019
doi: 10.3389/fmicb.2019.01903

The Role of Iron in the P-Acquisition Mechanisms of the Unicellular N_2-Fixing Cyanobacteria *Halothece* sp., Found in Association With the Mediterranean Seagrass *Posidonia oceanica*

Víctor Fernández-Juárez[1], Antoni Bennasar-Figueras[2], Antonio Tovar-Sanchez[3] and Nona Sheila R. Agawin[1]*

[1]Marine Ecology and Systematics (MarEs), Department of Biology, Universitat de les Illes Balears (UIB), Palma, Spain, [2]Grup de Recerca en Microbiologia, Departament de Biologia, Universitat de les Illes Balears (UIB), Palma, Spain, [3]Department of Ecology and Coastal Management, Andalusian Institute for Marine Sciences, ICMAN (CSIC), Cádiz, Spain

OPEN ACCESS

Edited by:
Pia H. Moisander, University of Massachusetts Dartmouth, United States

Reviewed by:
Frédéric Partensky, Centre National de la Recherche Scientifique (CNRS), France
Thomas Browning, GEOMAR Helmholtz Center for Ocean Research Kiel, Germany

***Correspondence:**
Víctor Fernández-Juárez
victor.fernandez@uib.es

Specialty section:
This article was submitted to Aquatic Microbiology, a section of the journal Frontiers in Microbiology

Received: *20 May 2019*
Accepted: *02 August 2019*
Published: *22 August 2019*

Citation:
Fernández-Juárez V, Bennasar-Figueras A, Tovar-Sanchez A and Agawin NSR (2019) The Role of Iron in the P-Acquisition Mechanisms of the Unicellular N_2-Fixing Cyanobacteria Halothece sp., Found in Association With the Mediterranean Seagrass Posidonia oceanica. Front. Microbiol. 10:1903. doi: 10.3389/fmicb.2019.01903

Posidonia oceanica, an endemic seagrass of the Mediterranean Sea harbors a high diversity of N_2-fixing prokaryotes. One of these is *Halothece* sp., a unicellular N_2-fixing cyanobacteria detected through *nifH* analysis from the epiphytes of *P. oceanica*. The most related strain in culture is *Halothece* sp. PCC 7418 and this was used as the test organism in this study. In the Mediterranean Sea, phosphorus (P) and iron (Fe) can be the major limiting nutrients for N_2 fixation. However, information about the mechanisms of P-acquisition and the role of metals (i.e., Fe) in these processes for N_2-fixing bacteria is scarce. From our genomic analyses of the test organism and other phylogenetically related N_2-fixing strains, *Halothece* sp. PCC 7418 is one of the strains with the greatest number of gene copies (eight copies) of alkaline phosphatases (APases). Our structural analysis of PhoD (alkaline phosphatase type D) and PhoU (phosphate acquisition regulator) of *Halothece* sp. PCC 7418 showed the connection among metals (Ca^{2+} and Fe^{3+}), and the P-acquisition mechanisms. Here, we measured the rates of alkaline phosphatase activity (APA) through MUF-P hydrolysis under different combinations of concentrations of inorganic P (PO_4^{3-}) and Fe in experiments under N_2-fixing (low NO_3^- availability) and non-N_2 fixing (high NO_3^- availability) conditions. Our results showed that APA rates were enhanced by the increase in Fe availability under low levels of PO_4^{3-}, especially under N_2-fixing conditions. Moreover, the increased PO_4^{3-}-uptake was reflected in the increased of the P-cellular content of the cells under N_2 fixation conditions. We also found a positive significant relationship between cellular P and cellular Fe content of the cells ($r^2 = 0.71$, $p < 0.05$). Our results also indicated that Fe-uptake in *Halothece* sp. PCC 7418 was P and Fe-dependent. This study gives first insights of P-acquisition mechanisms in the N_2-fixing cyanobacteria (*Halothece* sp.) found in *P. oceanica* and highlights the role of Fe in these processes.

Keywords: *Halothece* sp. PCC 7418, *Posidonia oceanica*, alkaline phosphatase, N_2 fixation, PO_4^{3-}-Fe uptake, iron, PhoD, PhoU

INTRODUCTION

Posidonia oceanica is an endemic seagrass in the Mediterranean Sea, forming extensive meadows with valuable established key ecological services: high primary productivity, as a carbon sink, as a habitat and nursery for a variety of micro- and macro-organisms, as sediment stabilizers, as buffers for ocean acidification, and as an important site for biogeochemical processes (e.g., nitrogen cycles) (Gutiérrez et al., 2012; Campagne et al., 2015; Agawin et al., 2016). Atmospheric nitrogen (N_2) fixation associated with *P. oceanica* meadows are similar in rates or even higher than tropical seagrasses and may play a key role in maintaining the high productivity of the *P. oceanica* in oligotrophic waters (Agawin et al., 2016, 2017). N_2 fixation in *P. oceanica* is carried out by microorganisms called diazotrophs that can be found on the surface of the leaves, roots, and rhizomes (epiphytic population) or even on the inside of the roots (endophytic population) (Sohm et al., 2011; Agawin et al., 2019). Among the diazotrophic prokaryotes, a huge variety of diazotrophic cyanobacteria have been detected based on the sequence analysis of *nifH* gene (gene coding for the nitrogenase enzyme responsible for the N_2 fixation) on the leaves of *P. oceanica* (Agawin et al., 2016, 2017).

In general, cyanobacteria are key components in the marine food web, contributing significantly to primary production in oligotrophic oceans (Agawin et al., 2000; Herrero and Flores, 2008). Compared with other phytoplankton taxa, cyanobacteria have elevated ratio of nitrogen (N):phosphorus (P) (a molar ratio above 25 compared with the general Redfield ratio of 16 in marine phytoplankton) and can be a consequence of having two light-harvesting complexes (Redfield, 1934; Geider and La Roche, 2002; Quigg et al., 2011). Changes affecting the N:P ratios in their environment by limiting concentration of N or P, could change their N:P tissue composition and may have consequences in their adaptation and survival and possibly the N_2 fixation activities of diazotrophic cyanobacteria (Sañudo-Wilhelmy et al., 2001; Sohm et al., 2011). Nonetheless, these versatile microorganisms may have several adaptive mechanisms to changes in their dynamic marine environment (e.g., nutrient availability) (Tandeau de Marsac and Houmard, 1993; Schwarz and Forchhammer, 2005; Herrero and Flores, 2008).

Phosphorus, (i.e., inorganic phosphorus, PO_4^{3-}), together with iron (Fe) are hypothesized to be the major limiting nutrients for N_2 fixation (Mills et al., 2004; Moore et al., 2009, 2013). Phosphorus is vital for the storage and retrieval system of genetic information (DNA/RNA), for the energy metabolism through ATP dependence (Kornberg, 1995; Santos-Beneit, 2015; Tiwari et al., 2015), and in most bacteria, it is important for the structure of the cell membrane. During P-starvation, microorganisms produce enzymes that are hydrolyze P-esters contained in dissolved organic phosphorus (DOP) releasing dissolved inorganic phosphorus (DIP), that the cells can utilize. These enzymes are called alkaline phosphatases (APases) and in marine bacteria they are included in three main families: PhoA, PhoX, and PhoD. APases are metalloenzymes that require metal co-factors. PhoA forms a coordinate with two zinc (Zn^{2+}) and one magnesium (Mg^{2+}) ions; PhoX forms a coordinate with three calcium (Ca^{2+}) and one/two Fe^{3+} ions (Yong et al., 2014); and PhoD coordinates with an unknown number of Ca^{2+} ions. In *Bacillus subtilis* model, PhoD has an active site formed with one Fe^{3+} and two Ca^{2+} ions (Rodriguez et al., 2014). This information suggests the possible interaction between metals (e.g., Fe^{3+}, Ca^{2+}, Mg^{2+}, and Zn^{2+}) in the mechanisms of P-acquisition involving APases. In *Halothece* sp. PCC 7418, two types of APases have been reported: PhoA (two copies) and PhoD (one copy). Calcium dependence was proven in PhoD in *Halothece* sp. PCC 7418 (Kageyama et al., 2011). However, Fe dependence of PhoD and the relative importance between these two types of APases (PhoA and PhoD) have not been demonstrated in *Halothece* sp. PCC 7418.

APases are included in what is known as the Pho regulon. It is a huge regulatory group of genes that control P-acquisition. Pho regulon is composed of elements related with (1) high-affinity phosphate transport (PstS, PstC, PstA, and PstB) and low-affinity phosphate transport, (2) extracellular enzymes capable of obtaining PO_4^{3-} from organic phosphates (APases), and (3) polyphosphate metabolism (PpK, PpX, and PpA) as P reservoir or elements with unknown functions (PhoU) (Blanco et al., 2002; Yuan et al., 2006; Santos-Beneit, 2015). PhoU coordinates with metal cluster (Zn^{2+} or Fe^{3+}), and may have a role in the control of autokinase activity of the PhoR and Pst systems (Gardner et al., 2014). The Pho regulon is mainly controlled by PhoR-PhoB, a two-component regulatory system (Santos-Beneit, 2015). PhoR is an inner-membrane histidine kinase, while PhoB is a transcriptional factor that recognizes and binds to consensus sequence named PHO box. In cyanobacteria, PHO box is formed by three tandem repeats of 8 bp separated by 5 bp, unlike PHO Box from *Escherichia coli*, formed by two direct repeats of 7 bp separated by 5 bp (Yuan et al., 2006; Su et al., 2007; Tiwari et al., 2015).

The P-acquisition mechanisms in bacteria are well studied in the Atlantic ocean, where Fe is shown to enhance the P-acquisition mechanisms in N_2-fixing cyanobacterial species, *Trichodesmium* spp. and *Crocosphaera watsonii* (Fu et al., 2005; Dyhrman and Haley, 2006; Browning et al., 2017). However, there is scarcely any information about the relation between metals (e.g., Fe) and P-acquisition mechanisms in N_2-fixing cyanobacteria found in association with the Mediterranean seagrass, *P. oceanica*, taking into account the multiple ecological benefits of this seagrass in the region. The Mediterranean Sea is oligotrophic, characterized by low water column PO_4^{3-} concentrations and a decreasing gradient of PO_4^{3-} concentrations from west to east basins (Tanhua et al., 2013). Knowledge on the P-acquisition mechanisms of N_2-fixing organisms in an environment with limiting levels of PO_4^{3-} is particularly important. Moreover, the Mediterranean Sea is subject to Saharan atmospheric dust deposition containing Fe (Statham and Hart, 2005), which can play a role in the P-acquisition mechanisms of the organisms.

To study, for the first time, the P-acquisition mechanisms in N_2-fixing cyanobacteria associated with the dominant coastal ecosystem in the region (*P. oceanica* seagrass beds), we selected a diazotrophic unicellular cyanobacteria, *Halothece* sp. found on the leaves of *P. oceanica* (Agawin et al., 2017) as our test species.

The most related culturable strain is *Halothece* sp. PCC 7418, and this was used as the test organism in this study. The halotolerant *Halothece* sp. PCC 7418 (originally called *Synechococcus* PCC 7418), also known as *Aphanothece halophytica*, was originally isolated from Solar Lake on the eastern shore of the Sinai Peninsula in 1972 (UniProt source). First, we made a genomic analyses of the Pho regulon to check the regulatory group of genes that control the P-acquisition mechanisms and then a structural analysis of PhoD (alkaline phosphatase type D) and PhoU (phosphate acquisition regulator) of *Halothece* sp. PCC 7418 to investigate the connection among metals (e.g., Ca^{2+} and Fe^{3+}) and the P-acquisition mechanisms of this species. Second, we experimentally investigated how the availability of Fe affects the alkaline phosphatase activity (APA), their PO_4^{3-}-uptake rates, and the magnitude of the effect under different levels of PO_4^{3-} and NO_3^- availability, and how the availability of PO_4^{3-} and Fe affect Fe-uptake rates of the cells.

MATERIALS AND METHODS

Genome Analysis

With the goal of comparing *Halothece* sp. PCC 7418 Pho regulon with its closest genomes (Luo et al., 2009), the distribution of the number of copies of Pho regulon components in selected strains was analyzed. The genome from *Halothece* sp. PCC 7418 (GenBank: NC_019779.1) and genomes from other closely related microorganisms were compared using the dedicated bacterial information system Pathosystems Resource Integration Center (PATRIC). This database, and the analysis tools included, offers an easy interface in which annotated genes that are included in different subsystems can be searched (Wattam et al., 2017).

Three-Dimensional Predicted Structures

Sequences of PhoD and PhoU in FASTA format were sent to the I-Tasser server for protein 3D-structure prediction (Zhang, 2008), with their domains previously checked in Pfam 32.0 (Finn et al., 2016). The predicted structures for PhoD and PhoU of *Halothece* sp. PCC 7418 were sent to POSA (Li et al., 2014) for a structural alignment against PhoD of *B. subtilis* (PDB: 2YEQ) and PhoU of *Pseudomonas aeruginosa* (PDB: 4Q25), respectively; the two more evolutionarily related homologous proteins available to date in databases (i.e., that have both similar sequences and 3D models). To describe the Fe coordination positions of these proteins, residues from both (i.e., PhoD and PhoU of *Halothece* sp. PCC 7418 against 2YEQ and 4Q25, respectively) were mapped through alignment with Uniprot Clustal Omega (The UniProt Consortium, 2014). The predicted structures and the corresponding structural alignments were visualized with Pymol (DeLano, 2002).

Strain and Culture Conditions

Halothece sp. PCC 7418, was obtained from the Pasteur Culture Collection of Cyanobacteria (PCC) and maintained in 250 ml acid-cleaned Quartz Erlenmeyer flasks containing 150 ml of ASNIII + Tu4X medium (initial pH 7.5) (Stanier et al., 1979). The medium was supplemented with 0.1–0.3% (w/v) of glucose and grown in a rotary shaker (120 r.p.m.) with a photoperiod of 12 h light:12 h dark under low intensity fluorescent light (30 μE m^{-2} s^{-1}) at 25°C. Three conditions were established for inorganic phosphorus (PO_4^{3-}) concentrations: [Low PO_4^{3-}] (0.1 μM), [Medium PO_4^{3-}] (1 μM), and [High PO_4^{3-}] (45 μM). Furthermore, three conditions for Fe were established: [Low Fe] (2 nM), [Medium Fe] (20 nM), and [High Fe] (7.5 μM). These PO_4^{3-} and Fe concentration were combined in nine conditions ([Low PO_4^{3-}–Low Fe], [Low PO_4^{3-}–Medium Fe], [Low PO_4^{3-}–High Fe], [Medium PO_4^{3-}–Low Fe], [Medium PO_4^{3-}–Medium Fe], [Medium PO_4^{3-}–High Fe], [High PO_4^{3-}–Low Fe], [High PO_4^{3-}–Medium Fe], and [High PO_4^{3-}–High Fe]), and these treatments were tested in two sets of experiments: growth under 4.4 mM of NO_3^- (optimal concentration) and 0.15 mM of NO_3^- (low concentration, and referred from now on as [Low NO_3^-]) (**Table 1**). The solutions of PO_4^{3-}, Fe, and NO_3^- were prepared from K_2HPO_4, ferric citrate, and $NaNO_3$, respectively. The batch cultures were maintained for over 10 days for each experiment and the initial inoculum of cells was added at exponential phase ($O.D_{750\ nm} \cong 0.2$) from their original ASNIII + Tu4X medium.

Selected treatments ([Low PO_4^{3-}–Low Fe], [Low PO_4^{3-}–High Fe], [High PO_4^{3-}–Low Fe], and [High PO_4^{3-}–High Fe]), were also used to compare the results under NO_3^- starvation (6.66 nM) and optimal NO_3^- conditions. Cultures were maintained at the same conditions as described above for over 12 days. During the last day, PO_4^{3-}, Fe, and/or NO_3^- were added to the different treatments to achieve optimal concentrations of PO_4^{3-} (45 μM), Fe (7.5 μM), and NO_3^- (4.4 mM) to evaluate the changes in the APA rates, and the new conditions were maintained for over 4 days. The different conditions of the experiments are shown in **Table 1**.

The importance of PhoD in *Halothece* sp. PCC 7418 was investigated by changing the availability of the metal co-factors for PhoA (Zn^{2+} and Mg^{2+}). The method used was as described above in the initial main experiments except that the medium was depleted with Mg and Zn and the condition of PO_4^{3-} and Fe was: [Medium PO_4^{3-}–High Fe] under optimal NO_3^-.

All cultures were performed in duplicate, and the study parameters (APA, N_2 fixation, uptake rates of PO_4^{3-} and Fe, TDP and/or P/Fe/Mn cellular content) were evaluated during the different phases of the culture ($O.D_{750\ nm} \cong 0.01–0.2$). A subsample of the cells (1.5 ml) was taken from the culture flasks during the experiment and were counted through flow cytometric analysis (as described below) to normalize the results per cell. All samples were manipulated in a class-100 clean hood, to avoid Fe contamination.

Flow Cytometry Analysis

Cells were fixed with glutaraldehyde 25% (v/v) in H_2O (Sigma-Aldrich) [final concentration 0.05% (v/v)] and were counted with a Becton Dickinson FACS-Verse cytometer (Beckton & Dickinson, Franklin Lakes, New Jersey, USA). Fluorescent beads, BD FACSuite™ CS&T research beads (Beckton & Dickinson and Company BD Biosciences, San Jose, USA), were used as internal standard to calibrate the instrument. The cytometer

TABLE 1 | List of all experimental treatments conducted in this study.

Experiments			
Condition (optimal and low NO_3^-)			Description
[Low PO_4^{3-} –Low Fe]	[Medium PO_4^{3-} –Low Fe]	[High PO_4^{3-} –Low Fe]	First experiment – optimal NO_3^- (4.4 mM)
[Low PO_4^{3-} –Medium Fe]	[Medium PO_4^{3-} –Medium Fe]	[High PO_4^{3-} –Medium Fe]	Second experiment – low NO_3^- (0.15 mM)
[Low PO_4^{3-} –High Fe]	[Medium PO_4^{3-} –High Fe]	[High PO_4^{3-} –High Fe]	Third experiment – NO_3^- starvation (6 nM), comparing with optimal NO_3^- in selected treatments
Recovery experiments			
Initial treatment	**Condition of NO_3^-**	**Nutrient added (at day 12)**	**Resulting treatment (maintained for 4 days)**
[Low PO_4^{3-} –Low Fe]	Optimal NO_3^- (4.4 mM)	PO_4^{3-} and Fe	[High PO_4^{3-} –High Fe] in optimal NO_3^- treatment.
[Low PO_4^{3-} –Low Fe]	NO_3^- starvation (6.66 nM)	PO_4^{3-}, Fe, and NO_3^-	[High PO_4^{3-} –High Fe] in optimal NO_3^- treatment.

In the recovery experiments, PO_4^{3-}, Fe, and/or NO_3^- were added to the different initial treatments to achieve optimal conditions to evaluate the changes in APA rates.

shows fluorescence patterns for FITC, PE, PerCP-CyTM5.5 and APC. To count the *Halothece* sp. PCC 7418 cells, we selected FITC (488 nm excitation, 530/30 nm emission) and PE (488 nm excitation, 576/26 nm emission) combination fluorescence signals which show clearly the population of the cells. A total of 10,000 cells were counted in each sample and the counted cells were expressed as cells μl^{-1}.

Alkaline Phosphatase Activity

Alkaline phosphatase activity (APA) was evaluated through a fluorometric assay, in which the hydrolysis of the fluorogenic substrate (S) 4-methylumbelliferyl phosphate (MUF-P, Sigma-Aldrich) to 4-methylumbelliferyl (MUF) was measured. Generally, an end point enzymatic assay was conducted with a concentration of 2 µM MUF-P during the exponential phase of the culture ($O.D_{750\ nm} \cong 0.1$). After 1 h incubation in darkness at room temperature, APA was measured in a microtiter plate that contained borate buffer at pH 10 (3:1 of sample:buffer). The MUF production (fmole MUF $cell^{-1}$ h^{-1}) was measured with a Cary Eclipse spectrofluorometer (FL0902M009, Agilent Technologies) at 359 nm (excitation) and 449 nm (emission) and using a calibration standard curve with commercial MUF (Sigma-Aldrich).

Saturation curves of velocity (V, fmole MUF $cell^{-1}$ h^{-1}) vs. substrate (S, µM) were made under [Low NO_3^-] condition during the final exponential phase of the culture ($O.D_{750\ nm} \cong 0.2$), using different concentrations of MUF-P: 0, 0.05, 0.1, 0.5, 2, and 5 µM. The maximum velocity (Vmax) at saturating substrate concentrations was obtained from each plot of V vs. S. The Michaelis–Menten constant, Km (µM), which represents the substrate concentration at half Vmax was calculated using de Hill plot equation (Ascenzi and Amiconi, 1987). The evolution of MUF-P hydrolysis rates (fmole MUF $cell^{-1}$) with time (h) was recorded over 1 h in the treatments under [Low PO_4^{3-} –Low Fe], [Low PO_4^{3-} –High Fe], and [High PO_4^{3-} –High Fe] at the last day of the experiment with 5 µM of MUF-P under NO_3^- starvation and NO_3^- optimal conditions and the APA rate (fmole MUF $cell^{-1}$ h^{-1}) was calculated as the slope of the fitted line.

PO_4^{3-} Uptake Rates, Nutrient Concentrations in the Culture Medium and in the Cells

Samples for the determination of PO_4^{3-} and total dissolved P (TDP) were centrifuged for 15 min at 16,000 ×*g* under 4°C. The supernatant was collected from the centrifuged tubes and used for PO_4^{3-} determinations following standard spectrophotometric methods (Hansen and Koroleff, 2007). TDP concentrations were also analyzed using the latter method after persulfate digestion. Samples for Fe analyses of culture media were filtered through sterile 0.2 µm filters (MFV5-025, FilterLab) at different times (initial and final) during the experiments. The metal (Fe) concentrations of culture medium were measured by inductively coupled plasma mass spectrometry (ICP-MS; iCap, Thermo Scientific), following the trace-metal clean techniques described in Tovar-Sanchez et al. (2006) and Tovar-Sanchez and Sañudo-Wilhelmy (2011).

The PO_4^{3-} concentrations in the culture medium were determined at different times: 0, 1, 4, and 10 days in the experimental treatment of [High PO_4^{3-}]: [Low Fe], [Medium Fe], and [High Fe]), and under [Low NO_3^-] and optimal NO_3^- conditions. Specific PO_4^{3-} uptake rates (pmole PO_4^{3-} $cell^{-1}$ day^{-1}) were calculated as described in (Ghaffar et al., 2017). Briefly, specific PO_4^{3-} uptake rates were calculated as the mass balance of PO_4^{3-} over the multiple days by taking the differences of PO_4^{3-} concentrations at two different times (T_0–T_1, T_0–T_4, and T_0–T_{10}) and normalized by the number of cells counted at different time points (0, 1, 4, and 10) through the following equation:

$$PO_4^{3-}\text{ – uptake}\left(\text{pmole } PO_4^{3-}\text{ cell}^{-1}\text{ day}^{-1}\right)=\frac{A-B}{Ti-Tf} \quad (1)$$

A is μmole PO_4^{3-} cell^{-1} at the initial time (*Ti*) and *B* is the μmole PO_4^{3-} cell^{-1} at the final time (*Tf*).

TDP concentrations were also measured at different times: 0, 4, 8, and 12 days in the experiments under NO_3^- starvation at [Low PO_4^{3-}] and [High PO_4^{3-}] conditions. Fe-uptake rates were measured under N_2-fixing conditions (i.e., [Low NO_3^-] conditions). Initial and final Fe concentrations of the culture media were measured, and the difference between time = 0 and time = 10 (T_0–T_{10}) was used to determine the Fe-uptake during the 10 days of the experiment. Specific Fe-uptake (fmole Fe cell^{-1} day^{-1}) was calculated the same way as the specific PO_4^{3-}-uptake rates described above.

Cellular contents of phosphorus (P), Fe, and other metals (i.e., Mn, V, Co, Ni, or Zn) were also determined by collecting the cells under [Low NO_3^-] treatment conditions through filtration of a known volume of culture (20 ml) with 0.2-μm acid-cleaned polycarbonate filters (Merck-Millipore). Elemental concentrations of P and Fe in the cyanobacterial samples were determined by inductively coupled plasma mass spectrometry (ICP-MS; iCap, Thermo Scientific), after microwave acid digestion (CEM, Mars 5) using nitric acid (high purity Suprapur®, Merck) (Tovar-Sanchez et al., 2006; Tovar-Sanchez and Sañudo-Wilhelmy, 2011).

Acetylene Reduction Assay

N_2-fixing activities were measured with the acetylene reduction assay (ARA) method under known N_2-fixing conditions for unicellular cyanobacteria (i.e., low NO_3^- concentrations, anaerobic environment, dark phase of the photoperiod, Reddy et al., 1993), and under low-medium levels of Fe and in low-medium-high levels of PO_4^{3-}. A volume of 50 ml from treatments with [Low NO_3^-] condition at day 8 of the experiment was transferred to anaerobic tubes for cultivation for 2 days, and after which, ARA measurements were done following the method described in Agawin et al. (2014). Duplicate 10 ml samples of culture from each experimental tube, were filtered through 0.45 μm GF/F filters (MFV5-025, FilterLab). The filters were deposited in hermetic vials containing 1 ml of the corresponding culture medium. Acetylene (C_2H_2) was added at 20% (v/v) final concentration in each vial using gas-tight Hamilton syringes. The filters were incubated in the vials for 3 h at room temperature in the dark. After 3 h incubation time, 10 ml of headspace gas were removed with a gas-tight Hamilton syringe from the incubation vials or tubes, transferred and stored in Hungate tubes and sealed with hot melt adhesive glue (SALKI, ref. 0430308) to minimize gas losses (Agawin et al., 2014). Ethylene and acetylene were determined using a GC (model HP-5890, Agilent Technologies) equipped with a flame ionization detector (FID). The column was a Varian wide-bore column (ref. CP7584) packed with CP-PoraPLOT U (27.5 m length, 0.53 mm inside diameter, 0.70 mm outside diameter, and 20 μm film thickness). Helium was used as carrier gas at a flow rate of 30 ml min^{-1}. Hydrogen and airflow rates were set at 30 and 365 ml min^{-1}, respectively. The split flow was used so that the carrier gas flow through the column was 4 ml min^{-1} at a pressure of 5 psi. Oven, injection, and detector temperatures were set at 52, 120, and 170°C, respectively. Ethylene produced was calculated using the equations in Stal (1988). The acetylene reduction rates were converted to N_2 fixation rates (pmole N_2 ml^{-1} h^{-1}) using a factor of 4:1 (Jensen and Cox, 1983).

Statistical Analyses

Univariate Analysis of variance (ANOVA) factor analyses and *post-hoc* (Bonferroni) was used to study the effect of the nutrient treatment conditions to APA rates, P-cellular content and specific PO_4^{3-}, and Fe uptake rates. In other cases, where we want to highlight a specific point, we use individual *t* tests. Regression analyses were used to determine the relationships between P-cellular content vs. N_2 rates fixation, P-cellular content vs. Fe-cellular content and P/Fe-cellular content vs. other metals (i.e., Mn). The statistical analyses were performed using the SPSS program version 21 (IBM Corp year 2012).

RESULTS

Pho Regulon of *Halothece* sp. PCC 7418

The distribution of the number of copies of Pho regulon components of *Halothece* sp. PCC 7418 and its closest genomes (Luo et al., 2009) are shown in **Figure 1** and **Supplementary Table S1**. The *Gloeocapsa* sp. PCC 7428 genome had the highest number of copies detected (up to 45), suggesting that this species is one of the better adapted species to P-limitation. On the other hand, *Nostoc punctiforme* PCC 73102 and *Chroococcidiopsis thermalis* PCC 7203 genomes had the lowest number of copies of the Pho regulon components. Our test microorganism *Halothece* sp. PCC 7418 genome was the fourth cyanobacterium containing more copies of the Pho regulon (26): 1 for *phoU*, 4 for *pstS*, 3 for *pstC*, 2 for *pstA*, 3 for *pstB*, 1 for *phoR-phoB*, 8 for APases, 1 for *ppK*, 1 for *ppX,* and 1 for *ppA*. With eight copies of APases, it was the second cyanobacterium containing more APases (8), only surpassed by *Gloeocapsa* sp. PCC 7428 (19), suggesting a key role of the APases in *Halothece* sp. PCC 7418. Annotation in PATRIC did not annotate any specific APase, except for a PhoD. No low-affinity phosphate transporters were detected.

Structural Analysis of PhoD and PhoU of *Halothece* sp. PCC 7418

Three-Dimensional Structure of PhoD and Its Implication in Alkaline Phosphatase Activity

The annotated PhoD of *Halothece* sp. PCC 7418 displayed 511 amino acids (aa) with two domains i.e., PhoD-like phosphatase N-terminal domain and PhoD-like phosphatase domain. Predicted structure of PhoD (C-score = 0.00, estimated TM-score = 0.71 ± 0.11, estimated RMSD = 7.4 ± 4.3 Å) had 10 α-helix and 21 β-chains. PhoD of *Halothece* sp. PCC 7418 was homologue to the crystal structure of PhoD of *B. subtilis* (2YEQ) of 522 aa, with an identity of 47.5% and coverage of 91.6%. **Figure 2A** shows the structural alignment between PhoD of *Halothece* sp. PCC 7418 and 2YEQ. The sequence

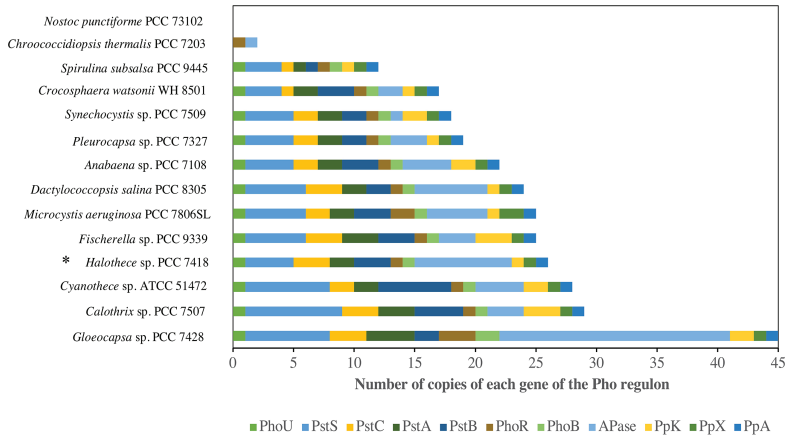

FIGURE 1 | Distribution of the Pho regulon in *Halothece* sp. PCC 7418 (*) and genomes of its closest cyanobacterial relatives. Annotated genes were identified in PATRIC.

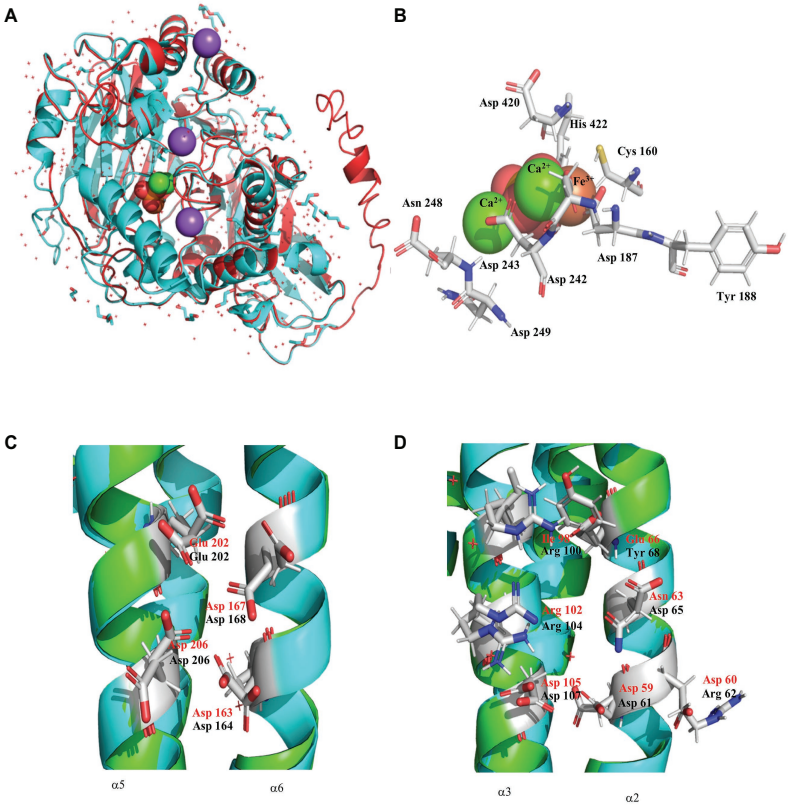

FIGURE 2 | Structural analysis of PhoD and PhoU of *Halothece* sp. PCC 7418. **(A)** Predicted structure of PhoD of *Halothece* sp. PCC 7418 is represented in red and aligned with the crystal structure 2YEQ that is displayed in blue cyan. **(B)** Active center of PhoD of the test bacterium showing all the aminoacids involved in coordination with two Ca^{2+} and Fe^{3+} ions. **(C)** Cluster 1 of PhoU, trinuclear metal site with Fe, between α5 and α6. **(D)** Cluster 2 of PhoU, tetranuclear metal site with three Fe and one Ni, between α2 and α3. Black amino acids are from predicted PhoU and red amino acids are from 4Q25. All the structures were represented with Pymol.

alignment displayed up to 40.11% similarity and was used with the intention to describe the hypothetical catalytic center. The catalytic center for PhoD of *Halothece* sp. PCC 7418, using the catalytic center of 2YEQ (in parenthesis) as a template, consisted of Cys 160 (Cys 124), Asp 187 (Asp 151), Tyr 188 (Tyr 152), Asp 242 (Asp 209), Asp 243 (Asp 210), Asn 248 (Asn 215), Asp 249 (Asn 216), Asp 420 (Asp 380), and His 422 (His 382) (**Figure 2B**). All these amino acids are described in 2YEQ as the active site and coordinate with two Ca^{2+} and one Fe^{3+} ions (Rodriguez et al., 2014). Only one substitution was detected in Asp 249, where in 2YEQ is Asn 216.

The *in-silico* results described above of PhoD and how it coordinates with Ca^{2+} and Fe^{3+} ions in its active site in *Halothece* sp. PCC 7418 corroborates with the results of the experiment testing the relative importance of PhoD and PhoA in *Halothece* sp. PCC 7418, showing that the APA rates, with the depletion of Mg^{2+} and Zn^{2+} which are the metal co-factors of PhoA, did not differ considerably with sufficient availability of Mg^{2+} and Zn^{2+} (**Figure 3**). This suggests that PhoD (and not PhoA) is the more active APase in *Halothece* sp. PCC 7418.

Three-Dimensional Structure of PhoU

Annotated PhoU had 224 amino acids (aa) and presented two PhoU domains. The predicted structure of PhoU (C-score = 0.55, estimated TM-score = 0.79 ± 0.09, estimated RMSD = 4.5 ± 2.9 Å) had seven α-helix without β-chains. The protein with more structure homology was PhoU of *P. aeruginosa* (4Q25) of 250 aa with an identity of 32.5% and coverage of 93.3%. Sequence alignment with 4Q25 showed 27.45% of identity and we used this alignment to describe its metal clusters (**Figures 2C,D**). Results showed that *Halothece* sp. PCC 7418 using 4Q25 as a template displayed at least one metal cluster, and possibly a second one, forming a trinuclear metal site with three Fe and tetranuclear metal site with three Fe and one nickel (Ni). The first cluster was complete and had the same aa as *P. aeruginosa* (in parenthesis) and was formed by Asp 164 (Asp 163), Asp 168 (Asp 167), Glu 202 (Glu 202), and Asp 206 (Asp 206), between α-helixes 5 and 6 (**Figure 2C**). The second cluster was incomplete and did not have all the aa that are present in *P. aeruginosa*. Only three aa of seven aa in *P. aeruginosa* (in parenthesis) coincide with *Halothece* sp. PCC 7418, and this cluster consisted of Asp 61 (Asp 59), Arg 62 (Asp 60), Asp 65 (Asn 63), Tyr 68 (Glu 66), Arg 100 (Ile 98), Arg 104 (Arg 102), and Asp 107 (Asp 105) between α-helix 2 and 3 (**Figure 2D**; Lee et al., 2014).

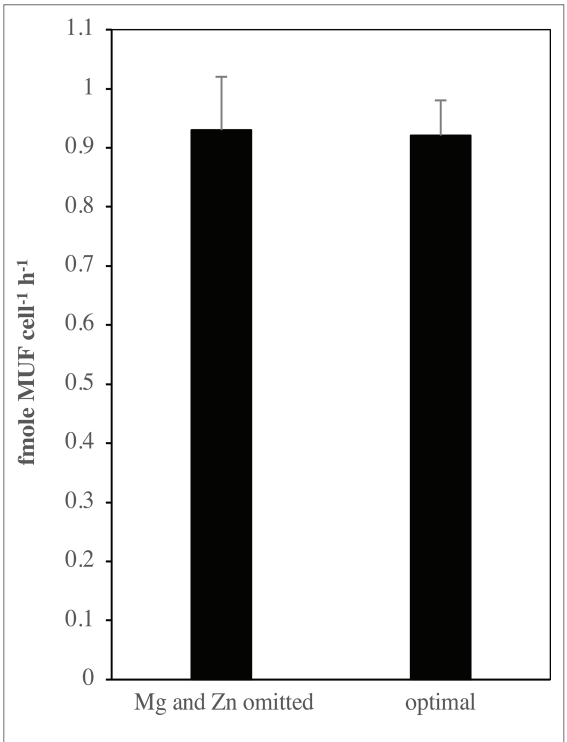

FIGURE 3 | End point assay measurement of alkaline phosphatase activity (APA) under Mg/Zn omission compared with optimal condition. Values are the mean, and the error bar is the spanning range between the two duplicate measurements.

Alkaline Phosphatase Activity in *Halothece* sp. PCC 7418

Generally, APA rates were significantly higher ($p < 0.05$) in [Low NO_3^-] conditions compared with optimal NO_3^- conditions (**Figure 4A**). Under [Low NO_3^-] APA rates were ≈ 7 times higher in [Low–Medium PO_4^{3-}] and ≈ 77 times higher in [High PO_4^{3-}] compared with their rates under optimal NO_3^- conditions. Moreover, under optimal NO_3^- conditions, APA rates did not have significant differences among the treatments (**Figure 4A**). Under [Low NO_3^-], treatment combinations of PO_4^{3-} and Fe levels had a significant effect on APA rates (ANOVA, $p < 0.05$), where the rates were significant higher ($p < 0.05$) at the highest Fe levels and at low to medium PO_4^{3-} levels, compared with other treatment combinations (**Figure 4A**). **Figure 4B** shows the differences in the kinetics of APA for treatments under [Low NO_3^-] at low and medium PO_4^{3-} levels and low and high Fe levels. At high Fe levels with low to medium PO_4^{3-} levels, the V vs. S curve did not reach saturation levels with the maximum S added (5 μM MUF-P). The Vmax and Km, calculated using the available data for these treatments, were: Vmax, 4.92 ± 0.56 fmole $cell^{-1}$ h^{-1}; Km of 3.47 ± 0.94 μM at [Low PO_4^{3-}–High Fe] and Vmax, 4.26 ± 0.43 fmole $cell^{-1}$ h^{-1}; Km of 7.24 ± 0.57 μM at [Medium PO_4^{3-}–High Fe]. On the contrary to high Fe levels, APase kinetics reached saturation levels with the maximum S added (**Figure 4B**) at low Fe levels with Vmax, 1.55 ± 0.19 fmole $cell^{-1}$ h^{-1}; Km of 1.53 ± 0.31 μM at [Low PO_4^{3-}–Low Fe] and Vmax, 1.88 ± 0.06 fmole $cell^{-1}$ h^{-1}; Km of 2.02 ± 0.94 μM at [Medium PO_4^{3-}–Low Fe].

The APA rates calculated were considerable higher (up to 6-fold) under NO_3^- starvation compared with under NO_3^- optimal conditions (**Figure 5A**). Treatments with [High Fe] in [Low PO_4^{3-}] reached the maximum rates at 0.21 ± 0.07 fmole $cell^{-1}$ h^{-1} under NO_3^- starvation condition, and at 0.03 ± 0.01 fmole $cell^{-1}$ h^{-1} under NO_3^- optimal condition (**Figure 5A**). Additions of PO_4^{3-}, Fe, and/or NO_3^- to obtain

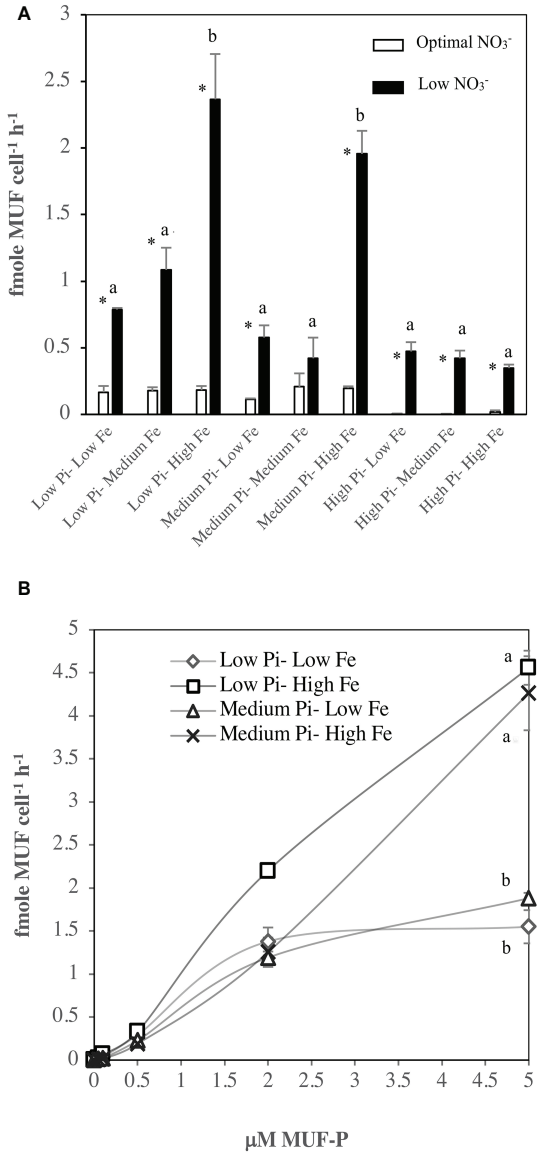

FIGURE 4 | Rates of alkaline phosphatase activity (APA) in *Halothece* sp. PCC 7418 under optimal NO_3^- and [Low NO_3^-] conditions. **(A)** End point assay of APA under optimal and [Low NO_3^-] conditions with 2 µM of MUF-P. **(B)** Saturation curve, velocity (V, fmole MUF $cell^{-1}$ h^{-1}) vs. substrate (S, µM) under [Low NO_3^-] in [Low PO_4^{3-} –Low Fe], [Low PO_4^{3-} –High Fe], [Medium PO_4^{3-} –Medium Fe], and [Medium PO_4^{3-} –High Fe], up to 5 µM of MUF-P. PO_4^{3-} is represented as Pi. In **(A,B)**, values are the mean and the error bar is the spanning range between the duplicate measurements. Asterisks (*) indicate significant differences ($p < 0.05$) between NO_3^- optimal and [Low NO_3^-] conditions of the same PO_4^{3-} and Fe combination treatments, by individual *t* student test. Different letters indicate pairwise significant differences ($p < 0.05$) among treatments in [Low NO_3^-] using a *post-hoc* test (Bonferroni) after ANOVA over the whole dataset was done.

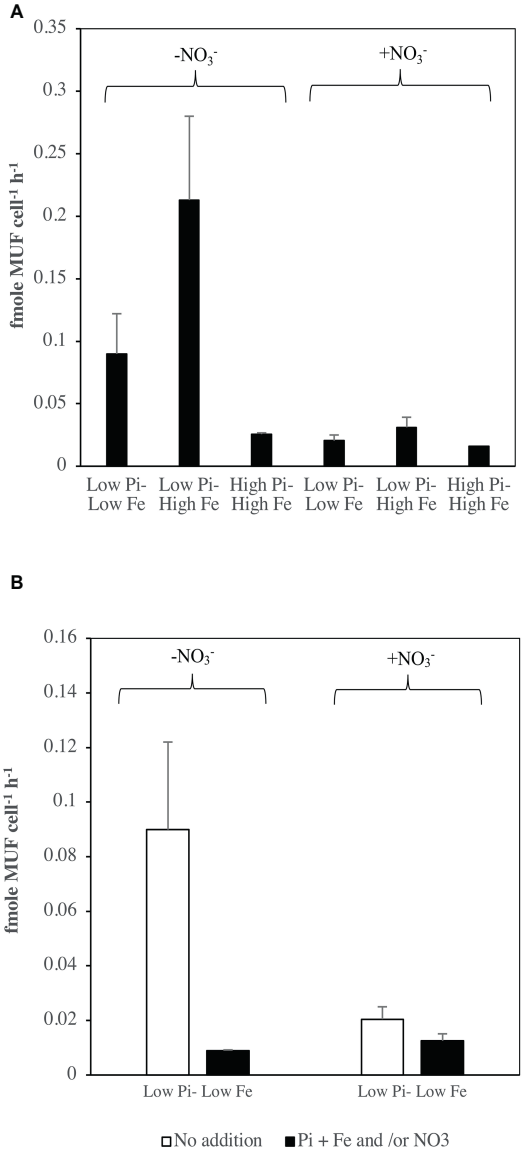

FIGURE 5 | Rates of alkaline phosphatase activity (APA, fmole MUF $cell^{-1}$ h^{-1}) in *Halothece* sp. PCC 7418 under NO_3^- starvation conditions compared with the optimal NO_3^- treatments under **(A)** treatment conditions: [Low PO_4^{3-} –Low Fe], [Low PO_4^{3-} –High Fe], and [High PO_4^{3-} –High Fe] and **(B)** under re-inoculum of nutrients in treatment conditions: [Low PO_4^{3-} –Low Fe, + PO_4^{3-} + Fe + NO_3^-] and [Low PO_4^{3-} –Low Fe + PO_4^{3-} + Fe]. PO_4^{3-} is represented as Pi. Values are the mean, and the error bar is the spanning range between the duplicate measurements.

optimum concentration of PO_4^{3-}, Fe, and/or NO_3^- resulted in reduced APA rates particularly under the initial NO_3^- starvation conditions (**Figure 5B**).

Phosphorus-Uptake at Different Levels of Iron Availability and Iron-Uptake at Different Levels of PO_4^{3-} Availability

Generally, P-cellular content varied significantly (ANOVA, $p < 0.05$) under N_2-fixing conditions [Low NO_3^-] among treatment combinations with significantly higher values at [High PO_4^{3-}–High Fe] treatment compared with other treatment combinations (**Figure 6A**). On the other hand, specific PO_4^{3-}-uptake rates under N_2-fixing conditions [Low NO_3^-] and optimal NO_3^- conditions generally did not vary significantly (ANOVA, $p > 0.05$) among treatment combinations (**Figure 6B**). However, specific *t*-tests conducted under [Low NO_3^-] conditions, showed PO_4^{3-}-uptake rates to be on average 200 times significantly higher ($p < 0.05$) than the rates under optimal conditions of NO_3^- in T_0–T_4 and T_0–T_{10} in low to medium Fe levels (**Figure 6B**). Different concentrations of Fe in [High PO_4^{3-}] did not show significant differences in PO_4^{3-}-uptake rates ($p > 0.05$) (**Figure 6B**).

The time course of depletion of total dissolved phosphate (TDP) in the culture media showed that under optimal NO_3^- conditions, the media were depleted with TDP while under NO_3^- starvation conditions, the cells were not capable in

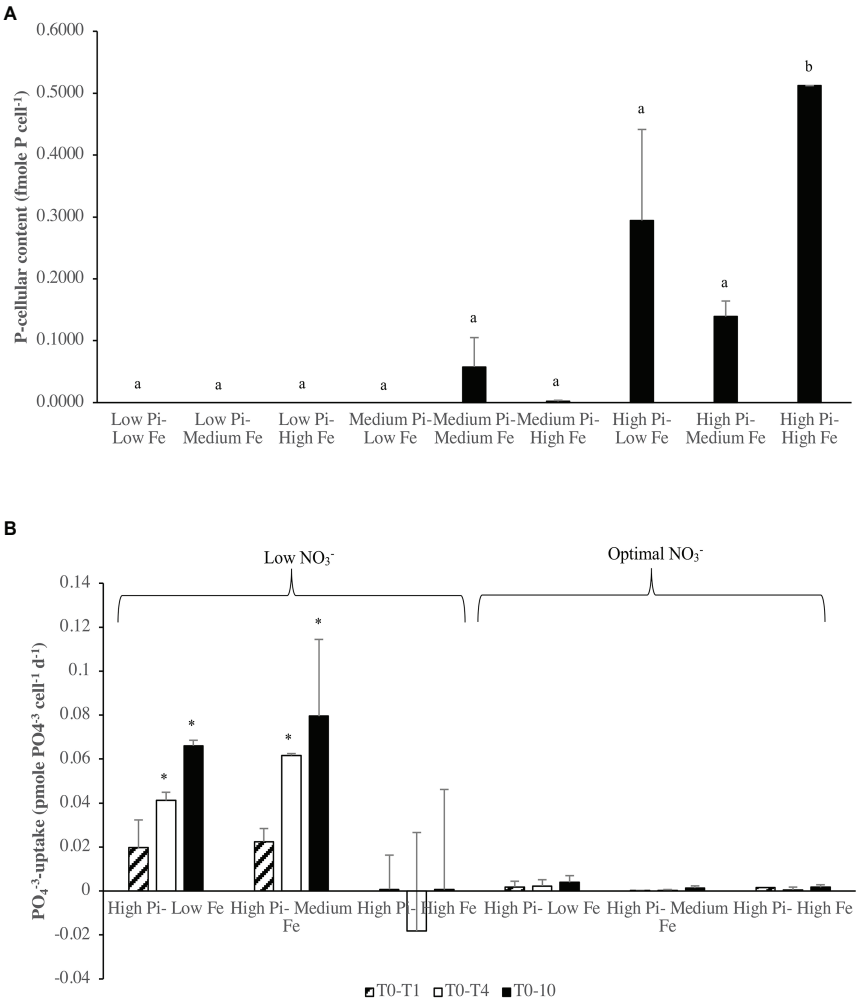

FIGURE 6 | (A) P-cellular content (fmole P cell⁻1) under N_2-fixing conditions in *Halothece* sp. PCC 7418, at different PO_4^{3-} and Fe levels. **(B)** Specific net PO_4^{3-}-uptake rates (pmole PO_4^{3-}-uptake cell^{-1} day^{-1}) in *Halothece* sp. PCC 7418 under [Low NO_3^-] and optimal NO_3^- conditions at three different periods (T_0–T_1, T_0–T_4, and T_4–T_{10}). PO_4^{3-} is represented as Pi. Values are the mean, and the error bar is the spanning range between the duplicate measurements. Different letters indicate pairwise significant differences ($p < 0.05$) among treatments using a *post-hoc* test (Bonferroni) after ANOVA over the whole dataset was done, and asterisks (*) indicate significant differences ($p < 0.05$) between [Low NO_3^-] and NO_3^- optimal conditions by individual *t* student tests for each treatment combination of PO_4^{3-} and Fe.

depleting TDP from the media (**Figure 7A**). Fe did not have a significant effect in TDP depletion ($p > 0.05$). The time course of depletion of TDP in the re-inoculum conditions at [Low PO_4^{3-} –Low Fe] (under NO_3^- starvation and NO_3^- optimal conditions), showed the same tendency, in which under NO_3^- starvation conditions, TDP was not depleted (**Figure 7B**).

Figure 8 shows the specific Fe-uptake rates at different levels of PO_4^{3-} and Fe under N_2-fixing conditions. Results showed that generally, specific Fe-uptake rates varied significantly at different treatment combinations of PO_4^{3-} and Fe (ANOVA, $p < 0.05$). Fe-uptake rates were significantly higher ($p < 0.05$) at [High PO_4^{3-}] conditions compared to [Low PO_4^{3-}] and [Medium PO_4^{3-}] conditions. There were also significant differences ($p < 0.05$) of increased Fe-uptake with increasing availability of Fe.

Phosphorus-Cellular Content and Its Relationship With N_2 Fixation and Iron-Cellular Content

Phosphorus cellular content of *Halothece* sp. PCC 7418 showed significant positive linear correlation with N_2 fixation rates ($p < 0.05$, $r^2 = 0.86$, $n = 12$) (**Figure 9A**). Moreover, the P-cellular content of the cells showed significant positive linear correlation with their Fe contents ($p < 0.05$, $r^2 = 0.71$, $n = 18$) (**Figure 9B**). The P and Fe-cellular contents of the cells did not show significant correlations with other metals (i.e., Mn).

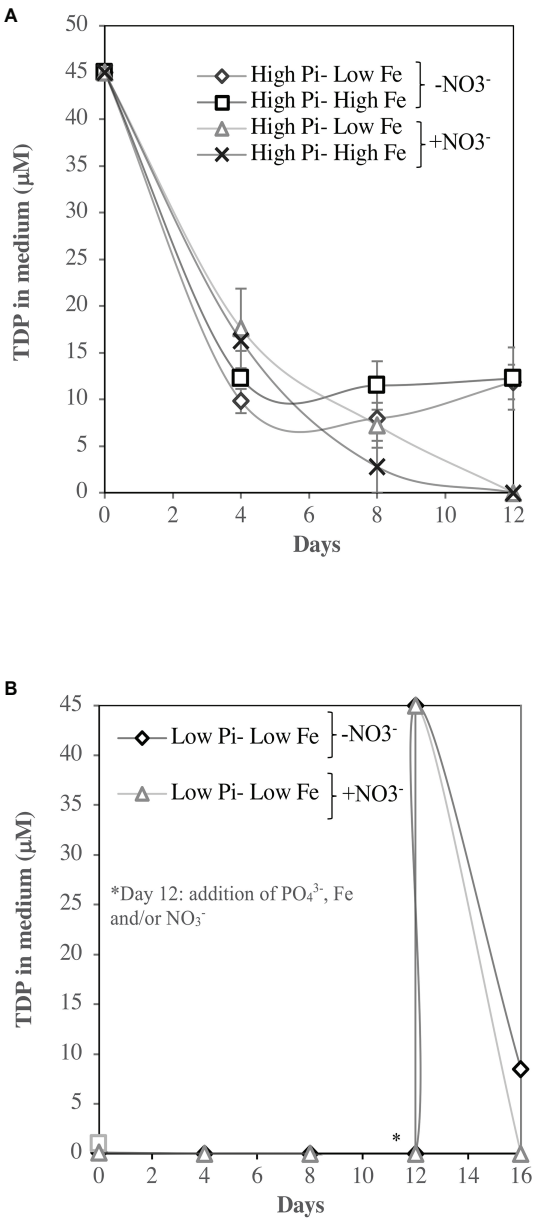

FIGURE 7 | TDP (µM) under NO_3^- starvation and optimal NO_3^- conditions. **(A)** TDP consumption (µM) under NO_3^- starvation and NO_3^- optimal conditions. **(B)** TDP consumption in the re-inoculated conditions in [Low PO_4^{3-} –Low Fe] (under NO_3^- starvation and NO_3^- optimal conditions). PO_4^{3-} is represented as Pi. Values are the mean, and the error bar is the spanning range between the duplicate measurements. In **(A)**, letters indicate significant differences ($p < 0.05$) by *t* student test.

DISCUSSION

Pho Regulon and the Three-Dimensional Structure of PhoD and PhoU of *Halothece* sp. PCC 7418: Elucidating the Role of Iron as Co-factor

The Pho regulon of *Halothece* sp. PCC 7418 is composed of genes whose protein products are involved in different functions: autokinase activity of PhoR and phosphate transport (PhoU); high-affinity phosphate transport (PstS, PstC, PstA, and PstB), in a two-component regulatory system (PhoR-PhoB); extracellular enzymes capable of obtaining PO_4^{3-} from organic phosphates (Alkaline Phosphatases, APases); and polyphosphate metabolism (PpK, PpX, and PpA) (Santos-Beneit, 2015). However, no low-affinity transporters were annotated while some studies demonstrated that this strain exhibited low-affinities transporters (Tripathi et al., 2013). *Halothece* sp. PCC 7418 contains a Pho regulon with 11 distinct genes in single or multiple copies altogether accounting 26 distinct loci in the whole genome, suggesting that *Halothece* sp. PCC 7418 is well adapted to survive to P-limiting conditions. In model strains whose P-acquisition mechanisms are well studied such as *Trichodesmium* spp. and *Crocosphaera watsonii* they only have 15 copies and 19 copies respectively in their Pho regulon (Fu et al., 2005; Dyhrman and Haley, 2006).

Genome analysis indicated that *Halothece* sp. PCC 7418 and *Gloeocapsa* sp. PCC 7428 were the strains with more copies of Alkaline Phosphatases (APase), 8 and 19, respectively (**Figure 1**). These two cyanobacteria are halotolerant species, and there are studies that suggest that salt stress enhance APA in halophytic strains (Kageyama et al., 2011). In a previous study (Kageyama et al., 2011), *Halothece* sp. PCC 7418 only showed

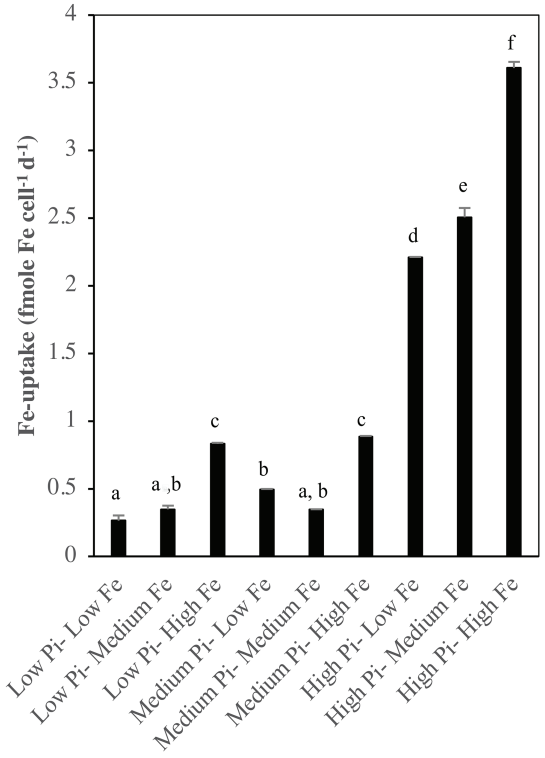

FIGURE 8 | Fe-uptake in *Halothece* sp. PCC 7418 (fmole Fe cell^{-1} day^{-1}) measured as the difference of the initial Fe concentration and the final Fe concentration at day 10 day of the experiment under [Low NO_3^-]. PO_4^{3-} is represented as Pi. Values are the mean, and the error bar is the spanning range between the duplicate measurements, and letters indicate significant differences ($p < 0.05$) between treatments using a *post-hoc* test (Bonferroni) after ANOVA over the whole dataset was done.

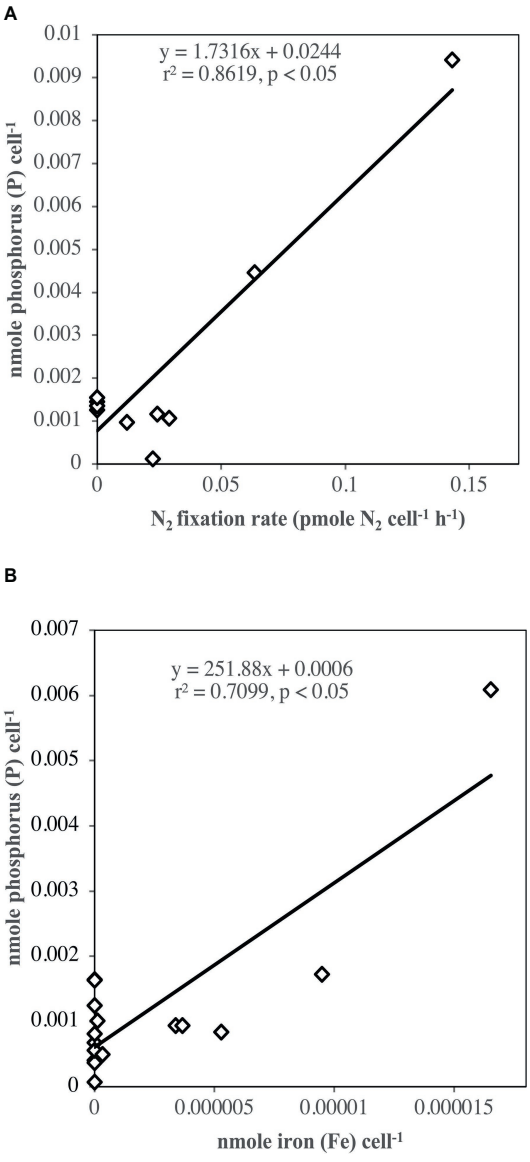

FIGURE 9 | Linear regression analyses **(A)** between P-cellular content and N_2 fixation and **(B)** between P and Fe-cellular content. Cellular content was measured in [Low NO_3^-] using pooled data from all PO_4^{3-} and Fe combination treatments.

three APases: two PhoA and one PhoD. Of the eight APases found in our study for the same species, one of them is also annotated as PhoD and the rest are not annotated to a specific type of APase. PhoD, together with PhoX, is one of the most abundant APases in marine habitats and its activity may be controlled by availability of its metal co-factor(s) (e.g., Fe^{3+}, Ca^{2+}, Mg^{2+}, and Zn^{2+}) (Luo et al., 2009; Zeng et al., 2011).

Three-dimensional analyses with PhoD of *Halothece* sp. PCC 7418 revealed its active site as a homologue to the crystal structure of PhoD of *B. subtilis* with two Ca^{2+} and one Fe^{3+} ions as co-factors (**Figure 2B**; Rodriguez et al., 2014). Previous studies on APase activity in *Halothece* sp. PCC 7418 indicated Ca^{2+} dependence of PhoD (Kageyama et al., 2011) but the Fe^{3+} dependence was not investigated. The experiment conducted here wherein the omission of Mg^{2+} and Zn^{2+} (but not Fe^{3+} in the culture medium) did not result in any significant changes in APase activity (**Figure 3**), suggesting that the APases of *Halothece* sp. PCC 7418 (i.e., PhoD) do not require these metals (Mg^{2+} and Zn^{2+}) as co-factors as in the case of PhoA (Kageyama et al., 2011), and the most active APase could be PhoD.

Iron is not only important as a co-factor for the activities of APase but can be essential in other components of Pho regulon like PhoU in which the results of the 3D-dimensional analyses in this study showed PhoU of *Halothece* sp. PCC 7418 forming at least one Fe-containing metal cluster, and possible a second cluster (**Figures 2C,D**), using as a model, the PhoU of *P. aeruginosa* (4Q25). PhoU can participate in the PO_4^{3-} transport across the cell membranes of bacteria in

the regulation of the phosphate-specific transport systems (Santos-Beneit, 2015) and in controlling cellular phosphate metabolism (Lubin et al., 2015). The specific role of PhoU in *Halothece* sp. PCC 7418, however, remains to be investigated.

Alkaline Phosphatase Activity in *Halothece* sp. PCC 7418: Experimental Analysis of Regulation by Iron, NO_3^-, and Phosphorous Availabilities

Experimental measurements of APA in *Halothece* sp. PCC 7418 under different levels in Fe availability revealed higher activities with higher levels of Fe (**Figures 4A,B** and **Figure 5A**), confirming the regulatory role of Fe in the APase (i.e., PhoD) in this species as we predicted in our 3D-structural analyses of its PhoD (**Figure 2B**). However, the effect of Fe availability on the rates of APA in *Halothece* sp. PCC 7418 depends on the availability of inorganic sources of nitrogen (i.e., NO_3^-) wherein at low NO_3^- concentrations, increasing Fe availability enhanced the APA rates (**Figures 4A,B**). We showed that under [Low NO_3^-] and at high Fe levels, APA was not saturated (**Figure 4B**). We hypothesized that under these conditions, the Vmax of APases from *Halothece* sp. PCC 7418 is so high that increasing MUF-P concentrations, up to 10 μM (in the other assays that were additionally conducted),was not high enough to saturate the enzyme because of the enhancement of APA by high levels of the Fe co-factor.

At high or optimal NO_3^- concentrations, APA rates in general are lower than in NO_3^- starvation conditions (**Figure 5A**) and even lower than in [Low NO_3^-] treatments (**Figure 4A**). These results can be due to peculiar characteristics of the N_2 fixation process. High concentrations of readily assimilable forms of dissolved inorganic nitrogen (DIN, i.e., NH_4, NO_3^-) are known to inhibit N_2 fixation as evidenced by DIN inhibition studies (Knapp, 2012). The N_2 fixation process ($N_2 + 8e^- + 16ATP + 8H^+ \rightarrow 2NH_3 + H_2 + 16ADP + 16\,PO_4^{3-}$) is an energetically costly processes requiring 16 ATPs and 25% more energy is needed to reduce N_2 than to reduce NO_3^- to NH_4. A N_2-fixing cell such as *Halothece* sp. PCC 7418 would rather reduce first the available NO_3^- than to fix N_2. Conversely, the N_2-fixing process is stimulated with low NO_3^- availability (Manhart and Wong, 1980; Nelson et al., 1982). Since the energy (ATP) to fuel N_2 fixation is dependent on PO_4^{3-}, the demand for PO_4^{3-} is theoretically enhanced when the cells are doing N_2 fixation (in conditions under low NO_3^- availability). Thus, APase activities are expected to be stimulated under low NO_3^- conditions, and consequently depend on the availability of Fe because APases such as PhoD may have Fe as co-factor. Moreover, Fe is an important structural component of the nitrogenase enzyme catalyzing the N_2 fixation process. Nitrogenase contains 38 Fe atoms per holoenzyme since nitrogenase is characterized by slow reaction rates the N_2-fixers need a large cellular pool of this enzyme, and thus more Fe is needed (Hoffman et al., 2014). The enhanced rates of APase under N_2-fixing conditions (low NO_3^- availability) and high Fe availability with low PO_4^{3-} levels is expected as APases activities are induced with low PO_4^{3-} levels in the medium (Romano et al., 2017). The control of NO_3^- and PO_4^{3-} availabilities in APase activities for N_2-fixing cells such as *Halothece* sp. PCC 7418 is further supported here with the results of decreased APA rates when NO_3^-, PO_4^{3-} and Fe were added to cells growing previously with low PO_4^{3-}, low Fe and/or low NO_3^- levels (**Figure 5B**).

Phosphorus and Iron-Uptake and Cellular Contents in *Halothece* sp. PCC 7418

The PO_4^{3-}-uptake measurements in *Halothece* sp. PCC 7418 were done in the experimental units with high PO_4^{3-} levels because (1) the method used for PO_4^{3-} analyses was not sensitive enough to measure very low levels of PO_4^{3-} (≤ 0.1 μM), and (2) APase activities are not induced at high PO_4^{3-} levels allowing us to evaluate if Fe is also important in PO_4^{3-} transport mechanisms and not only in APase activities. PO_4^{3-}-uptake rates of *Halothece* sp. PCC 7418 was significantly higher under N_2-fixing conditions ([Low NO_3^-]) than in non-N_2 fixing conditions due to the high demand of P for the energy costly N_2 fixation (**Figure 6B**). The dependence of N_2 fixation on P in *Halothece* sp. PCC 7418 is evidenced here with the significant linear correlation between cellular P content of the cells and their rates of N_2 fixation (**Figure 9A**), consistent with studies carried out in *Trichodesmium* spp. in the Atlantic (Sañudo-Wilhelmy et al., 2001). In addition, not only N_2-fixing conditions can enhance the P-requirements of cyanobacteria. It is also reported that under nitrogen limitation, phytoplankton can accumulate carbohydrates and phospholipids, increasing their P-cellular content (Liefer et al., 2019). Different concentrations of Fe, however, did not show significant differences in PO_4^{3-}-uptake at high levels of PO_4^{3-} availability. This suggests that PO_4^{3-}-uptake mechanisms in this case are not dependent on Fe levels or the Fe present in all treatments (from low to high Fe concentrations) are sufficient for the cells (**Figure 6B**). The latter case may be most likely since we found significant correlations between the P-cellular and Fe-cellular content of the cells (**Figure 9B**). These results are also consistent with our data that the highest P-cellular content was found at high Fe levels (**Figure 6A**), suggesting the narrow connection between P and Fe. The relation between P and Fe cellular contents is also supported by evidences that high concentrations of elemental P are found associated (or co-localized spatially) with Fe within the cells of phytoplankton [*Chlorella* sp. and *Chlamydomonas* sp. (Diaz et al., 2009)]. The Fe-uptake measurements in *Halothece* sp. PCC 7418 in N_2-fixing conditions revealed that Fe-uptake was correlated with P with high Fe-uptake rates at higher PO_4^{3-} levels (**Figure 8**). This may be due to the P-dependence (ATP) of Fe transporters (Noinaj et al., 2010; Kranzler et al., 2013). Results also show the tendency of higher Fe-uptake rates in higher concentrations of Fe in the media, suggesting a passive transport of this metal in *Halothece* sp. PCC 7418. However, this needs to be further investigated.

The time course of depletion of total dissolved phosphate (TDP) in the media (**Figure 7A**), showed that under NO_3^- starvation conditions, cells did not deplete TDP, and even increased at the final stage of the experiment suggesting a liberation of cellular TDP of dying cells. Extreme NO_3^- starvation conditions

are suggested here to be detrimental to the growth of *Halothece* sp. PCC 7418 and may have consequences on their P-uptake mechanisms, explaining why APA rates were lower than in [Low NO_3^-] conditions. Even when the nutrients (PO_4^{3-}, Fe and/or NO_3^-) were re-inoculated in the cultures that were previously starved with NO_3^-, the cells did not acclimate and were not capable of depleting TDP from the media (**Figure 7B**). Whereas, much of the previous research has focused on the inhibition or sensitivity of N_2 fixation to increased availability of dissolved inorganic nitrogen (e.g., NO_3^-, NH_4^+) (Knapp, 2012), investigations on the physiological conditions for growth of N_2-fixers are few. Spiller and Shanmugam (1987), gave some evidences that a unicellular species of marine N_2-fixer *Synechococcus* sp. strain SF1 (isolated from macroalgae, *Sargassum fluitans*) is dependent on the presence and type of carbon (C) source to support its growth with N_2 as the sole nitrogen source. Their results showed, for example, that without the addition of C source (e.g., HCO_3^-), there was no growth of the species tested with N_2 as the sole source. Moreover, some studies have reported less cell yield of unicellular N_2 fixers when grown with N_2 as sole N source compared with addition of NO_3^- since N_2 fixation is an energetically costly process (Spiller and Shanmugam, 1987; Agawin et al., 2007). Our result that extreme NO_3^- starvation condition (at nM levels close to N_2 as sole source) is suggested to be detrimental to the growth of *Halothece* sp. PCC 7418 may be due to the type of C source (glucose and citrate) in our treatments which may not be the optimum for growth of this species with N_2 as sole N source. This hypothesis however needs more investigations.

In summary, this is the first study investigating the interaction between PO_4^{3-}, Fe, and NO_3^- availabilities in the P-acquisition mechanisms of a unicellular N_2-fixing bacteria found in association with the Mediterranean seagrass *P. oceanica*. The results suggest that APase activities under inorganic P-limited conditions are enhanced by increased Fe availabilities. The PO_4^{3-} and Fe dependence of *Halothece* sp. PCC 7418 depends whether they are grown in N_2-fixing conditions (i.e., low NO_3^- levels) or not. Genomic and structural analyses have also shown the tight association between P-acquisition mechanisms and Fe in *Halothece* sp. PCC 7418. Studies combining genomic and protein structural analyses and experimental approaches are important to investigate in detail the control of environmental factors (e.g., availability of metals and nutrients) to the functioning of N_2-fixing organisms found in important species of seagrasses.

DATA AVAILABILITY

The raw data supporting the conclusions of this manuscript will be made available by the authors, without undue reservation, to any qualified researcher.

AUTHOR CONTRIBUTIONS

VF-J and NA designed the experiments. VF-J conducted all experiments and led the writing of the paper. All authors contributed to the writing and review of the manuscript, and NA is the supervisor of the laboratory.

FUNDING

This work was supported by funding to NA through the Agencia Estatal de Investigación and the European Regional Development Funds project (CTM2016-75457-P).

ACKNOWLEDGMENTS

We acknowledge the support and help of Scientific Technical Service (Dr. Guillem Ramis Munar and Maria Trinidad Garcia Barceló) of the University of the Balearic Islands for cytometry and gas-chromatography analyses, respectively. We also thank Pere Ferriol Buñola and Alba Coma Ninot for the help in the acquisition of the cultures.

SUPPLEMENTARY MATERIAL

The Supplementary Material for this article can be found online at: https://www.frontiersin.org/articles/10.3389/fmicb.2019.01903/full#supplementary-material

REFERENCES

Agawin, N. S. R., Duarte, C. M., and Agusti, S. (2000). Nutrient and temperature control of the contribution of picoplankton to phytoplankton biomass and production. *Am. Soc. Limnol. Oceanogr.* 45, 591–600. doi: 10.4319/lo.2000.45.3.0591

Agawin, N. S. R., Rabouille, S., Veldhuis, M. J. W., Servatius, L., Hol, S., Van Overzee, M. J., et al. (2007). Competition and facilitation between unicellular nitrogen-fixing cyanobacteria and non – nitrogen-fixing phytoplankton species. *Limonol. Oceanogr.* 52, 2233–2248. doi: 10.4319/lo.2007.52.5.2233

Agawin, N. S. R., Benavides, M., Busquets, A., Ferriol, P., Stal, L. J., and Arístegui, J. (2014). Dominance of unicellular cyanobacteria in the diazotrophic community in the Atlantic Ocean. *Limnol. Oceanogr.* 59, 623–637. doi: 10.4319/lo.2014.59.2.0623

Agawin, N. S. R., Ferriol, P., Cryer, C., Alcon, E., Busquets, A., Sintes, E., et al. (2016). Significant nitrogen fixation activity associated with the phyllosphere of Mediterranean seagrass *Posidonia oceanica*: first report. *Mar. Ecol. Prog. Ser.* 551, 53–62. doi: 10.3354/meps11755

Agawin, N. S. R., Ferriol, P., Sintes, E., and Moyà, G. (2017). Temporal and spatial variability of in situ nitrogen fixation activities associated with the Mediterranean seagrass *Posidonia oceanica* meadows. *Limnol. Oceanogr.* 62, 2575–2592. doi: 10.1002/lno.10591

Agawin, N. S. R., Ferriol, P., and Sintes, E. (2019). Simultaneous measurements of nitrogen fixation activities associated with different plant tissues of the seagrass *Posidonia oceanica*. *Mar. Ecol. Prog. Ser.* 611, 111–127. doi: 10.3354/meps12854

Ascenzi, P., and Amiconi, G. (1987). Logarithmic plots in enzymology. Representation of the Michaelis-Menten equation. *Biochem. Educ.* 15, 83–84. doi: 10.1016/0307-4412(87)90093-8

Blanco, A. G., Sola, M., Gomis-Rüth, F. X., and Coll, M. (2002). Tandem DNA recognition by PhoB, a two-component signal transduction transcriptional activator. *Structure* 10, 701–713. doi: 10.1016/S0969-2126(02)00761-X

Browning, T. J., Achterberg, E. P., Yong, J. C., Rapp, I., Utermann, C., Engel, A., et al. (2017). Iron limitation of microbial phosphorus acquisition in the tropical North Atlantic. *Nat. Commun.* 8, 1–7. doi: 10.1038/ncomms15465

Campagne, C. S., Salles, J. M., Boissery, P., and Deter, J. (2015). The seagrass *Posidonia oceanica*: ecosystem services identification and economic evaluation of goods and benefits. *Mar. Pollut. Bull.* 97, 391–400. doi: 10.1016/j.marpolbul.2015.05.061

DeLano, W. (2002). The PyMOL Molecular Graphics System. *Schrödinger*, *LLC*. Available at: http://www.pymol.org

Diaz, J., Ingall, E., Vogt, S., de Jonge, M. D., Paterson, D., Rau, C., et al. (2009). Characterization of phosphorus, calcium, iron, and other elements in organisms at sub-micron resolution using X-ray fluorescence spectromicroscopy. *Limnol. Oceanogr. Methods* 7, 42–51. doi: 10.4319/lom.2009.7.42

Dyhrman, S. T., and Haley, S. T. (2006). Phosphorus scavenging in the unicellular marine diazotroph *Crocosphaera watsonii*. *Appl. Environ. Microbiol.* 72, 1452–1458. doi: 10.1128/AEM.72.2.1452-1458.2006

Finn, R. D., Coggill, P., Eberhardt, R. Y., Eddy, S. R., Mistry, J., Mitchell, A. L., et al. (2016). The Pfam protein families database: towards a more sustainable future. *Nucleic Acids Res.* 44, D279–D285. doi: 10.1093/nar/gkv1344

Fu, F. X., Zhang, Y., Bell, P. R. F., and Hutchins, D. A. (2005). Phosphate uptake and growth kinetics of *Trichodesmium* (Cyanobacteria) isolates from the North Atlantic Ocean and the Great Barrier Reef, Australia. *J. Phycol.* 41, 62–73. doi: 10.1111/j.1529-8817.2005.04063.x

Gardner, S. G., Johns, K. D., Tanner, R., and McCleary, W. R. (2014). The PhoU protein from *Escherichia coli* interacts with PhoR, PstB, and metals to form a phosphate-signaling complex at the membrane. *J. Bacteriol.* 196, 1741–1752. doi: 10.1128/JB.00029-14

Geider, R. J., and La Roche, J. (2002). Redfield revisited: variability of C:N:P in marine microalgae and its biochemical basis. *Eur. J. Phycol.* 37, 1–17. doi: 10.1017/S0967026201003456

Ghaffar, S., Stevenson, R. J., and Khan, Z. (2017). Effect of phosphorus stress on *Microcystis aeruginosa* growth and phosphorus uptake. *PLoS One* 12:e0174349. doi: 10.1371/journal.pone.0174349

Gutiérrez, J. L., Jones, C. G., Byers, J. E., Arkema, K. K., Berkenbusch, K., Commito, A., et al. (2012). Physical ecosystem engineers and the functioning of estuaries and coasts. *Treatise Estuar. Coast. Sci.* 7, 58–81. doi: 10.1016/B978-0-12-374711-2.00705-1

Hansen, H. P., and Koroleff, F. (2007). "Determination of nutrients" in *Method of seawater analysis*. eds. K. Grasshoff, K. Kremling, and M. Ehrhardt. doi: 10.1002/9783527613984.ch10

Herrero, A., and Flores, E. (2008). *The cyanobacteria: Molecular biology, genomics, and evolution*. Wymondham, UK: Caister Academic Press.

Hoffman, B. M., Lukoyanov, D., Yang, Z. Y., Dean, D. R., and Seefeldt, L. C. (2014). Mechanism of nitrogen fixation by nitrogenase: the next stage. *Chem. Rev.* 114, 4041–4062. doi: 10.1021/cr400641x

Jensen, B. B., and Cox, R. P. (1983). Direct measurements of steady-state kinetics of cyanobacterial N_2 uptake by membrane-leak mass spectrometry and comparisons between nitrogen fixation and acetylene reduction. *Appl. Environ. Microbiol.* 45, 1331–1337.

Kageyama, H., Tripathi, K., Rai, A. K., Cha-Um, S., Waditee-Sirisattha, R., and Takabe, T. (2011). An alkaline phosphatase/phosphodiesterase, PhoD, induced by salt stress and secreted out of the cells of *Aphanothece halophytica*, a halotolerant cyanobacterium. *Appl. Environ. Microbiol.* 77, 5178–5183. doi: 10.1128/AEM.00667-11

Knapp, A. N. (2012). The sensitivity of marine N_2 fixation to dissolved inorganic nitrogen. *Front. Microbiol.* 3, 1–14. doi: 10.3389/fmicb.2012.00374

Kornberg, A. (1995). Inorganic polyphosphate: toward making a forgotten polymer unforgettable. *J. Bacteriol.* 177, 491–496. doi: 10.1128/jb.177.3.491-496.1995

Kranzler, C., Rudolf, M., Keren, N., and Schleiff, E. (2013). Iron in cyanobacteria. *Adv. Bot. Res.* 65, 57–105. doi: 10.1016/B978-0-123-94313-2.00003-2

Lee, S. J., Park, Y. S., Kim, S. J., Lee, B. J., and Suh, S. W. (2014). Crystal structure of PhoU from *Pseudomonas aeruginosa*, a negative regulator of the Pho regulon. *J. Struct. Biol.* 188, 22–29. doi: 10.1016/j.jsb.2014.08.010

Li, Z., Natarajan, P., Ye, Y., Hrabe, T., and Godzik, A. (2014). POSA: a user-driven, interactive multiple protein structure alignment server. *Nucleic Acids Res.* 42, W240–W245. doi: 10.1093/nar/gku394

Liefer, J. D., Garg, A., Fyfe, M. H., Irwin, A. J., Benner, I., Brown, C. M., et al. (2019). The macromolecular basis of phytoplankton C:N:P under nitrogen starvation. *Front. Microbiol.* 10, 1–16. doi: 10.3389/fmicb.2019.00763

Lubin, E. A., Fiebig, A., Laub, M. T., Henry, J. T., and Crosson, S. (2015). Identification of the PhoB regulon and role of PhoU in the phosphate starvation response of *Caulobacter crescentus*. *J. Bacteriol.* 198, 187–200. doi: 10.1128/jb.00658-15

Luo, H., Benner, R., Long, R. A., and Hu, J. (2009). Subcellular localization of marine bacterial alkaline phosphatases. *Proc. Natl. Acad. Sci. USA* 106, 21219–21223. doi: 10.1073/pnas.0907586106

Manhart, J. R., and Wong, P. P. (1980). Nitrate Effect on Nitrogen Fixation (Acetylene Reduction): Activities of legume root nodules induced by rhizobia with varied nitrate reductase activities. *Plant Physiol.* 65, 502–505. doi: 10.1104/pp.65.3.502

Mills, M. M., Ridame, C., Davey, M., La Roche, J., and Geider, R. J. (2004). Iron and phosphorus co-limit nitrogen fixation in the eastern tropical North Atlantic. *Nature* 429, 232–294. doi: 10.1038/nature02550

Moore, C., Mills, M. M., Achterberg, E. P., Geider, R. J., Laroche, J., Lucas, M. I., et al. (2009). Large-scale distribution of Atlantic nitrogen fixation controlled by iron availability. *Nat. Geosci.* 2, 867–871. doi: 10.1038/ngeo667

Moore, C., Mills, M. M., Arrigo, K. R., Berman-Frank, I., Bopp, L., Boyd, P. W., et al. (2013). Processes and patterns of oceanic nutrient limitation. *Nat. Geosci.* 6, 701–710. doi: 10.1038/ngeo1765

Nelson, D. C., Waterbury, J. B., and Jannasch, H. W. (1982). Nitrogen fixation and nitrate utilization by marine and freshwater Beggiatoa. *Arch. Microbiol.* 133:172. doi: 10.1007/BF00414997

Noinaj, N., Guillier, M., Barnard, T. J., and Buchanan, S. K. (2010). TonB-dependent transporters: regulation, structure, and function. *Annu. Rev. Microbiol.* 64, 43–60. doi: 10.1146/annurev.micro.112408.134247

Quigg, A., Irwin, A. J., and Finkel, Z. V. (2011). Evolutionary inheritance of elemental stoichiometry in phytoplankton. *Proc. R. Soc. B Biol. Sci.* 278, 526–534. doi: 10.1098/rspb.2010.1356

Reddy, K. J., Haskell, J. B., Sherman, D. M., and Sherman, L. A. (1993). Unicellular, aerobic nitrogen-fixing cyanobacteria of the genus *Cyanothece*. *J. Bacteriol.* 175, 1284–1292. doi: 10.1128/jb.175.5.1284-1292.1993

Redfield, A. C. (1934). *On the proportions of organic derivatives in sea water and their relation to the composition of plankton*. James Johnstone Memorial Volume: Liverpool UK: University Press of Liverpool, 176–192.

Rodriguez, F., Lillington, J., Johnson, S., Timmel, C. R., Lea, S. M., and Berks, B. C. (2014). Crystal structure of the *Bacillus subtilis* phosphodiesterase PhoD reveals an iron and calcium-containing active site. *J. Biol. Chem.* 289, 308893–308899. doi: 10.1074/jbc.M114.604892

Romano, S., Bondarev, V., Kölling, M., Dittmar, T., and Schulz-Vogt, H. N. (2017). Phosphate limitation triggers the dissolution of precipitated iron by the marine bacterium *Pseudovibrio* sp. FO-BEG1. *Front. Microbiol.* 8, 1–11. doi: 10.3389/fmicb.2017.00364

Santos-Beneit, F. (2015). The Pho regulon: a huge regulatory network in bacteria. *Front. Microbiol.* 6. doi: 10.3389/fmicb.2015.00402

Sañudo-Wilhelmy, S. A., Kustka, A. B., Gobler, C. J., Hutchins, D. A., Yang, M., Lwiza, K., et al. (2001). Phosphorus limitation of nitrogen fixation by *Trichodesmium* in the central Atlantic Ocean. *Nature* 411, 66–69. doi: 10.1038/35075041

Schwarz, R., and Forchhammer, K. (2005). Acclimation of unicellular cyanobacteria to macronutrient deficiency: emergence of a complex network of cellular responses. *Microbiology* 151, 2503–2514. doi: 10.1099/mic.0.27883-0

Sohm, J. A., Webb, E. A., and Capone, D. G. (2011). Emerging patterns of marine nitrogen fixation. *Nat. Rev. Microbiol.* 9, 499–508. doi: 10.1038/nrmicro2594

Spiller, H., and Shanmugam, K. T. (1987). Physiological conditions for nitrogen fixation in a unicellular marine cyanobacterium, *Synechococcus* sp. strain SF1. *J. Bacteriol.* 169, 5379–5384. doi: 10.1128/jb.169.12.5379-5384.1987

Stal, L. J. (1988). Acetylene reduction technique for assay of nitrogenase. *Methods Enzymol.* 167, 474–484.

Stanier, R. Y., Deruelles, J., Rippka, R., Herdman, M., and Waterbury, J. B. (1979). Generic assignments, strain histories and properties of pure cultures of cyanobacteria. *Microbiology* 111, 1–61. doi: 10.1099/00221287-111-1-1

Statham, P. J., and Hart, V. (2005). Dissolved iron in the Cretan Sea (eastern Mediterranean). *Limnol. Oceanogr.* 50, 1142–1148. doi: 10.4319/lo.2005.50.4.1142

Su, Z., Olman, V., and Xu, Y. (2007). Computational prediction of Pho regulons in cyanobacteria. *BMC Genomics* 8, 1–12. doi: 10.1186/1471-2164-8-156

Tandeau de Marsac, N., and Houmard, J. (1993). Adaptation of cyanobacteria to environmental stimuli: new steps towards molecular mechanisms. *FEMS Microbiol. Lett.* 104, 119–189. doi: 10.1111/j.1574-6968.1993.tb05866.x

Tanhua, T., Hainbucher, D., Schroeder, K., Cardin, V., Álvarez, M., and Civitarese, G. (2013). The Mediterranean Sea system: a review and an introduction to the special issue. *Ocean Sci.* 9, 789–803. doi: 10.5194/os-9-789-2013

The UniProt Consortium (2014). UniProt: a hub for protein information. *Nucleic Acids Res.* 43, D204–D212. doi: 10.1093/nar/gku989

Tiwari, B., Singh, S., Kaushik, M. S., and Mishra, A. K. (2015). Regulation of organophosphate metabolism in cyanobacteria. A review. *Microbiology* 84, 2913–2902. doi: 10.1134/S0026261715030200

Tovar-Sanchez, A., and Sañudo-Wilhelmy, S. A. (2011). Influence of the Amazon River on dissolved and intra-cellular metal concentrations in *Trichodesmium* colonies along the western boundary of the sub-tropical North Atlantic Ocean. *Biogeosciences* 8, 217–225. doi: 10.5194/bg-8-217-2011

Tovar-Sanchez, A., Sañudo-Wilhelmy, S. A., Kustka, A. B., Agustí, S., Dachs, J., Hutchins, D. A., et al. (2006). Effects of dust deposition and river discharges on trace metal composition of *Trichodesmium* spp. in the tropical and subtropical North Atlantic Ocean. *Limnol. Oceanogr.* 51, 1755–1761. doi: 10.4319/lo.2006.51.4.1755

Tripathi, K., Sharma, N. K., Kageyama, H., Takabe, T., and Rai, A. K. (2013). Physiological, biochemical and molecular responses of the halophilic cyanobacterium *Aphanothece halophytica* to Pi-deficiency. *Eur. J. Phycol.* 48, 461–473. doi: 10.1080/09670262.2013.859303

Wattam, A. R., Davis, J. J., Assaf, R., Boisvert, S., Brettin, T., Bun, C., et al. (2017). Improvements to PATRIC, the all-bacterial bioinformatics database and analysis resource center. *Nucleic Acids Res.* 45, D535–D542. doi: 10.1093/nar/gkw1017

Yong, S. C., Roversi, P., Lillington, J., Rodriguez, F., Krehenbrink, M., Zeldin, O. B., et al. (2014). A complex iron-calcium cofactor catalyzing phosphotransfer chemistry. *Science* 345, 1170–1173. doi: 10.1126/science.1254237

Yuan, Z. C., Zaheer, R., Morton, R., and Finan, T. M. (2006). Genome prediction of PhoB regulated promoters in *Sinorhizobium meliloti* and twelve proteobacteria. *Nucleic Acids Res.* 34, 2686–2697. doi: 10.1093/nar/gkl365

Zeng, Y. F., Ko, T. P., Lai, H. L., Cheng, Y. S., Wu, T. H., Ma, Y., et al. (2011). Crystal structures of *Bacillus* alkaline phytase in complex with divalent metal ions and inositol hexasulfate. *J. Mol. Biol.* 409, 214–224. doi: 10.1016/j.jmb.2011.03.063

Zhang, Y. (2008). I-TASSER server for protein 3D structure prediction. *BMC Bioinformatics* 9:40. doi: 10.1186/1471-2105-9-40

Conflict of Interest Statement: The authors declare that the research was conducted in the absence of any commercial or financial relationships that could be construed as a potential conflict of interest.

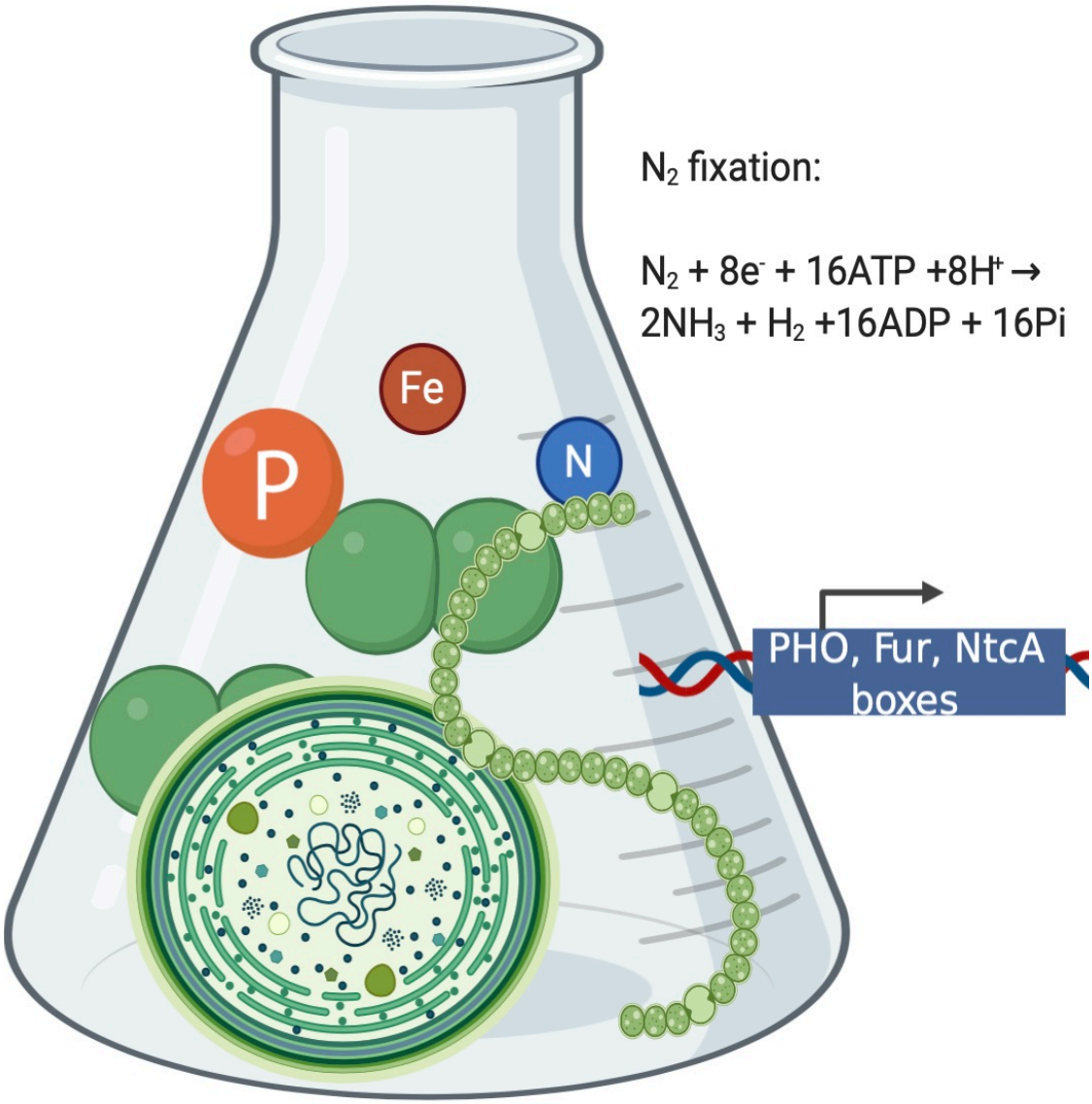
N_2 fixation:
$N_2 + 8e^- + 16ATP + 8H^+ \rightarrow$
$2NH_3 + H_2 + 16ADP + 16Pi$
Fe
P
N
PHO, Fur, NtcA boxes

3.2 Chapter 2

frontiers in Microbiology

ORIGINAL RESEARCH
published: 25 September 2020
doi: 10.3389/fmicb.2020.541558

Differential Effects of Varying Concentrations of Phosphorus, Iron, and Nitrogen in N_2-Fixing Cyanobacteria

Víctor Fernández-Juárez[1], Antoni Bennasar-Figueras[2], Antoni Sureda-Gomila[3], Guillem Ramis-Munar[4] and Nona S. R. Agawin[1]**

[1] Marine Ecology and Systematics (MarES), Department of Biology, University of the Balearic Islands, Palma, Spain, [2] Grup de Microbiologia, Department of Biology, University of the Balearic Islands, Palma, Spain, [3] Research Group on Community Nutrition and Oxidative Stress, University of the Balearic Islands and CIBEROBN (Fisiopatología de la Obesidad y la Nutrición), Palma, Spain, [4] Cellomic Unit of University Institute of Research in Health Sciences of the Balearic Islands, Palma, Spain

OPEN ACCESS

Edited by:
Mar Benavides, Institut de Recherche Pour le Développement (IRD), France

Reviewed by:
Ulisse Cardini, University of Naples Federico II, Italy
Douglas G. Capone, University of Southern California, United States
Francisco M. Cornejo-Castillo, University of California, Santa Cruz, United States

***Correspondence:**
Víctor Fernández-Juárez
victor.fernandez@uib.es
Nona S. R. Agawin
nona.agawin@uib.es

Specialty section:
This article was submitted to Aquatic Microbiology, a section of the journal Frontiers in Microbiology

Received: *09 March 2020*
Accepted: *18 August 2020*
Published: *25 September 2020*

Citation:
Fernández-Juárez V, Bennasar-Figueras A, Sureda-Gomila A, Ramis-Munar G and Agawin NSR (2020) Differential Effects of Varying Concentrations of Phosphorus, Iron, and Nitrogen in N_2-Fixing Cyanobacteria. Front. Microbiol. 11:541558. doi: 10.3389/fmicb.2020.541558

Diazotrophs or N_2-fixers are one of the most ecologically significant groups in marine ecosystems (pelagic and benthic). Inorganic phosphorus (PO_4^{3-}) and iron (Fe) can limit the growth and N_2-fixing capacities of cyanobacteria. However, studies investigating co-limitation of these factors are lacking. Here, we added different concentrations of PO_4^{3-} and Fe in two cyanobacterial species whose relatives can be found in seagrass habitats: the unicellular *Halothece* sp. (PCC 7418) and the filamentous *Fischerella muscicola* (PCC 73103), grown under different nitrate (NO_3^-) concentrations and under N_2 as sole N source, respectively. Their growth, pigment content, N_2-fixation rates, oxidative stress responses, and morphological and cellular changes were investigated. Our results show a serial limitation of NO_3^- and PO_4^{3-} (with NO_3^- as the primary limiting nutrient) for *Halothece* sp. Simultaneous co-limitation of PO_4^{3-} and Fe was found for both species tested, and high levels of Fe (especially when added with high PO_4^{3-} levels) inhibited the growth of *Halothece* sp. Nutrient limitation (PO_4^{3-}, Fe, and/or NO_3^-) enhanced oxidative stress responses, morphological changes, and apoptosis. Furthermore, an extensive bio-informatic analysis describing the predicted Pho, Fur, and NtcA regulons (involved in the survival of cells to P, Fe, and N limitation) was made using the complete genome of *Halothece* sp. as a model, showing the potential of this strain to adapt to different nutrient regimes (P, Fe, or N).

Keywords: *Halothece* sp. PCC 7418, *Fischerella muscicola* PCC 73103, phosphorus, iron, nitrogen, N_2-fixation, reactive oxygen species production, Pho–Fur–NtcA regulon

INTRODUCTION

Diazotrophs or N_2-fixers, one of the most important ecological groups, are microorganisms capable of converting atmospheric dinitrogen gas (N_2) into a readily usable form of dissolved inorganic nitrogen, i.e., ammonia (NH_3). This process is carried out through the nitrogenase protein complex (encoded by *nifH*, *nifD*, and *nifK*) by nitrogenase-containing autotrophic and heterotrophic bacteria (Hoffman et al., 2014). Biological N_2-fixation is an essential process in the marine N-cycle, providing new N to the oceans and compensating ocean denitrification (Sohm et al., 2011). In coastal benthic communities (e.g., Mediterranean seagrass

Posidonia oceanica communities), N_2-fixers are also important sources of new N, potentially supplying the entire demand of N of the associated plants (Agawin et al., 2016, 2017). These benthic communities can harbor a high diversity of N_2-fixing cyanobacteria among which are different groups of cyanobacteria that can be classified as unicellular, filamentous heterocyst forming, and filamentous non-heterocyst forming (Zehr, 2011).

Factors affecting the growth and abundance of cyanobacteria include both abiotic [e.g., macronutrients (e.g., phosphorus, P, and nitrogen, N), micronutrients (e.g., iron, Fe), light, and temperature] and biotic factors (e.g., viral cell lysis or grazing) (Sohm et al., 2011; Zehr, 2011). The nutrients P, N, and Fe are suggested to be the most important liming nutrients for cyanobacterial growth (Mills et al., 2004; Browning et al., 2017). Phosphorus (P) has key structural (i.e., for nucleic acids and for the cell membranes of most bacteria) and functional roles in various metabolic processes and limiting concentrations of P affect photosynthesis, respiration, and activities of ATP-dependent enzymes (Tripathi et al., 2013; Santos-Beneit, 2015). Nitrogen is essential for protein synthesis, and limiting concentrations of N can reduce cellular growth rates and contribute to the phenomenon called chlorosis, which causes degradation of phycobiliproteins and can lead to posterior downregulation of photosynthesis (Richaud et al., 2001; Klotz et al., 2015). Iron (Fe) is also important for photosynthesis and growth (Sunda and Huntsman, 2015); however, cells must maintain a state of homeostasis since elevated Fe-intracellular concentrations can enhance oxidative stress via Fenton and Haber–Weiss reactions (Kranzler et al., 2013). Under Fe limitation, cyanobacteria can import Fe into the cells through various high-affinity Fe transporters (Kranzler et al., 2014) or through the liberation of low-molecular-weight Fe chelators (e.g., siderophores) (Kranzler et al., 2013). In order to survive and adapt in limiting nutrient conditions, cyanobacteria must trigger molecular mechanisms by transcription factors (TFs). The most well-studied TFs in marine bacteria are PhoB, ferric uptake (Fur), and global nitrogen (NtcA) regulators involved in the acquisition of P, Fe, and N, respectively (Baichoo and Helmann, 2002; Yuan et al., 2006; Llacer et al., 2010). The PhoB, together with PhoR, an inner-membrane histidine kinase, forms a two-component regulatory system (Santos-Beneit, 2015). These TFs are activated or repressed to adapt to a changing environment (e.g., changes in nutrient concentrations) and recognize consensus sequences called transcriptional binding sites (TBS), namely, the PHO box, Fur, and NtcA boxes (Baichoo and Helmann, 2002; Yuan et al., 2006; Llacer et al., 2010), which control the expression of specific genes. The genes controlled by these TFs (PhoB, Fur, or NtcA) are part of what is known as the Pho, Fur, and NtcA regulons, and their prediction can help us understand how cells may adapt and survive under limiting concentrations of P, Fe, and N, respectively.

The demand for P, Fe, and N for N_2-fixing cyanobacteria may be different from that for non-N_2-fixing bacteria. Generally, cyanobacteria have elevated ratio of nitrogen (N):phosphorus (P) (a molar ratio above 25 compared with the general Redfield ratio of 16 in marine phytoplankton) (Redfield, 1934; Geider and La Roche, 2002; Quigg et al., 2011). For cyanobacteria, Fe requirements are 10-fold higher than in non-photosynthetic bacteria (Kranzler et al., 2013). For cyanobacterial N_2-fixers, Fe is even more important, as Fe is an important structural component of the nitrogenase complex (i.e., *nifH*) (Hoffman et al., 2014). N_2-fixation also requires a large amount of photosynthetically derived energy, which in turn is P-dependent (Sañudo-Wilhelmy et al., 2001). While non-N_2-fixing cyanobacteria are usually limited by N, N_2-fixing cyanobacteria can use ubiquitous atmospheric N_2, conferring them a competitive advantage over non-N_2-fixing cyanobacteria in N-limited waters (Sohm et al., 2011). Usually, under limiting concentrations of inorganic N (e.g., NH_3 and NO_3^-), N_2-fixation is stimulated, while high concentrations of inorganic N inhibit N_2-fixation (Manhart and Wong, 1980; Nelson et al., 1982; Knapp, 2012). In a previous study, the P-requirements of *Halothece* sp. PCC 7418 increased in N-limited conditions (i.e., when N_2-fixation was stimulated), consequently activating their P-acquisition mechanisms [i.e., alkaline phosphatase activity (APA) and P-uptake], which were in turn controlled by Fe availability (Fernández-Juárez et al., 2019). How the concentrations of P and Fe (and their interacting effects) affect the different groups of N_2-fixing cyanobacteria grown in differing N conditions remains to be investigated.

Here, we investigated the response to different concentrations of PO_4^{3-} and Fe, in a multi-factorial design, of two species of N_2-fixing cyanobacteria: the unicellular *Halothece* sp. PCC 7418 and the filamentous heterocyst-forming *Fischerella muscicola* PCC 73103, grown under different nitrate (NO_3^-) concentrations and under N_2 as sole N source, respectively. Relatives of these two cyanobacteria have been previously found in association with the seagrass *P. oceanica* (**Supplementary Material**, **Supplementary Figure S1**, Agawin et al., 2017). The responses were measured in terms of physiological and molecular parameters (growth, pigment content, N_2-fixation rates, oxidative stress, morphology, and apoptosis). To understand how *Halothece* sp. (PCC 7418) adapts in nutrient limiting environments, an extensive *in silico* analysis was done, taking as a model the complete genome of *Halothece* sp. to predict the Pho, Fur, and NtcA boxes, and the Pho, Fur, and NtcA regulons, respectively.

MATERIALS AND METHODS

Strains and Growth Conditions

N_2-fixing bacterial strains (*Halothece* sp. PCC 7418 and *F. muscicola* sp. PCC 73103) were obtained from Pasteur Culture Collection of Cyanobacteria (PCC). Experiments were conducted in 250-ml acid-clean quartz Erlenmeyer flasks filled with 150 ml of their corresponding culture media. We used ASN-III + Turks Island salts 4× medium and $BG11_0$ culture medium for *Halothece* sp. and *F. muscicola*, respectively (Stanier et al., 1979). These media were supplemented with 0.1–0.3% (p/v) glucose, and cells were cultivated under aerobic condition in 12:12-h light–dark cycle at 25°C and under continuous low-intensity fluorescent light (≅30 $\mu E\ m^{-2}\ s^{-1}$) in a rotatory shaker (120 rpm). The batch cultures were maintained for over 10–14 days for each experiment, and the initial inoculum of cells was added

at the exponential phase [O.D.$_{750\ nm/975\ nm} \cong 0.2$ (*Halothece* sp.)/1.0 (*F. muscicola*)] from their original culture medium. All samples were manipulated in a class-100 clean hood to avoid Fe contamination. The subcultures for seeding were centrifuged and washed with their corresponding medium without PO_4^{3-}, Fe, and NO_3^-.

For *Halothece* sp., three conditions were established for PO_4^{3-} concentrations: [Low PO_4^{3-}] (0.1 μM), [Medium PO_4^{3-}] (1 μM), and [High PO_4^{3-}] (45 μM). Furthermore, three conditions for Fe were also established: [Low Fe] (2 nM), [Medium Fe] (20 nM), and [High Fe] (7.5 μM). These PO_4^{3-} and Fe concentrations were combined in nine experimental conditions ([Low PO_4^{3-}–Low Fe], [Low PO_4^{3-}–Medium Fe], [Low PO_4^{3-}–High Fe], [Medium PO_4^{3-}–Low Fe], [Medium PO_4^{3-}–Medium Fe], [Medium PO_4^{3-}–High Fe], [High PO_4^{3-}–Low Fe], [High PO_4^{3-}–Medium Fe], and [High PO_4^{3-}–High Fe]) (**Supplementary Table S1**). The solutions of PO_4^{3-}, Fe, and NO_3^- were prepared from dipotassium phosphate (K_2HPO_4), ferric citrate ($C_6H_5FeO_7$), and sodium nitrate ($NaNO_3$), respectively. As reference for the nutrient concentrations for [Low PO_4^{3-}] and [Low Fe], we followed the surface water concentrations of the Mediterranean Sea (Statham and Hart, 2005; Powley et al., 2017), while for [High PO_4^{3-}] and [High Fe], we followed the optimal concentrations of ASN-III + Turks Island salts 4× medium. We performed two sets of experiments following Fernández-Juárez et al. (2019): under 4.4 mM of NO_3^- (optimal concentration) and 0.15 mM of NO_3^- (referred to from now on as [Low NO_3^-] and represents the minimum amount of NO_3^- in which *Halothece* sp. grew with maximal N_2-fixation rates). The cells were incubated for 10 days in these experiments (**Supplementary Table S1**). After these experiments, we selected the experimental conditions – [Low PO_4^{3-}–Low Fe], [Low PO_4^{3-}–High Fe], [High PO_4^{3-}–Low Fe], and [High PO_4^{3-}–High Fe] – in which *Halothece* sp. cells were grown under extremely limiting NO_3^- concentrations (6.66 nM), following NO_3^- concentrations in the Mediterranean Sea as reference (Powley et al., 2017; **Supplementary Table S1**). The cultures were maintained over 12 days. To check the reversibility of the phenotypic characteristics of the cells, we re-inoculated with PO_4^{3-}, Fe, and/or NO_3^- in optimal concentrations (PO_4^{3-}: 45 μM, Fe: 7.5 μM, and NO_3^-: 4.4 mM) at day 12. Inorganic phosphorus (PO_4^{3-}) was added to [Low PO_4^{3-}–Low Fe], and NO_3^- was added to [High PO_4^{3-}–High Fe] in extremely limiting NO_3^- treatments; and PO_4^{3-} and Fe were added to [Low PO_4^{3-}–Low Fe] in optimal NO_3^- treatments. These cultures were maintained for over 4 days more (**Supplementary Table S1**).

For *F. muscicola*, PO_4^{3-} and Fe were added in nine combination treatments as previously described for *Halothece* sp. but using 180 μM for [High PO_4^{3-}] and 30 μM for [High Fe]. These optimal concentrations for PO_4^{3-} and Fe are recommended for $BG11_0$ medium (Stanier et al., 1979). These PO_4^{3-} and Fe combinations were performed without any combined N source, and cultures were maintained over 14 days.

All cultures with their respective treatment conditions were performed in duplicate, and growth, pigment content, N_2-fixation rates, reactive oxygen species (ROS) production and morphological and/or cellular response (e.g., apoptosis) were measured. For *Halothece* sp., subsamples of the culture (1.5 ml) were taken from the culture flasks at the final stage of the experiment and were counted through flow cytometric analysis to normalize the results per cell and for the phenotype recovery experiments. For *F. muscicola*, results were normalized per total chlorophyll (Chl).

Growth Measurement

The growth of *Halothece* sp. and *F. muscicola* was measured by optical density (O.D.) using a quartz cuvette and read in Cary Eclipse spectrometer. Growth measurements were measured in *Halothece* sp. every 2 days at 750 nm. In *F. muscicola*, we measured O.D. at 975 nm (maximum O.D. of the cells), and this was measured every 2–4 days. Growth rate (μ, day^{-1}) and generation time (T_g, days) were calculated following the formula described in Widdel (2010) and Ng et al. (2015):

$$\mu = \frac{Ln\ (O.D.f) - Ln\ (O.D.i)}{Tf - Ti} \quad (1)$$

$$T_g = \frac{Ln\ (2)}{\mu} \quad (2)$$

where $O.D._f$ is the O.D. at the final time (Tf) and $O.D._i$ is the O.D. at the initial time (T_i) of the exponential phase of the growth curve.

To evaluate the type of co-limitation of the growth response of N and P (simultaneous co-limitation, independent co-limitation, or serial limitation), we followed the log ratio effect-size criteria based on the mean treatment and control response in Harpole et al. (2011) and Hedges et al. (1999). We calculated the following log growth response ratios as follows:

$$\text{Nitrogen (N) response}: \ln(N_1P_0/N_0P_0) \quad (3)$$

$$\text{Phosphorus (P) response}: \ln(N_0P_1/N_0P_0) \quad (4)$$

$$N + P \text{ response}: \ln(N_1P_1/N_0P_0) \quad (5)$$

For *Halothece* sp., N_0P_0 represents the growth rate under extremely limiting NO_3^- conditions at [Low PO_4^{3-}], N_1P_0 is the growth rate under [Low NO_3^-] or optimal NO_3^- at [Low PO_4^{3-}] conditions, N_0P_1 is the growth rate under extremely limiting NO_3^- conditions at [High PO_4^{3-}], and N_1P_1 is the growth rate under combinations of under [Low NO_3^-] or optimal NO_3^- at [High PO_4^{3-}] conditions. Responses = 0 are responses identical to control values (no response), >0 are positive responses, and <0 are negative responses. The critical threshold value, representing the minimum significant treatment responses at $p = 0.05$ relative to N_0P_0, was calculated to graphically determine the nature of co-limitation. To choose this critical threshold value, we used the T-score criteria, in which those values that surpass the critical T-score were considered statistically significant (**Supplementary Material**, Harpole et al., 2011). We also evaluated the type of co-limitation growth response of PO_4^{3-} and Fe under NO_3^- optimal and [Low NO_3^-]

conditions, substituting Fe for N in the eqs. 3–5 above, with Fe_0P_0 representing the growth rate under [Low Fe] at [Low PO_4^{3-}] conditions. For *F. muscicola*, we could only evaluate the nature of P and Fe co-limitation because all the treatments were incubated with no added combined N source.

Monod kinetic models were performed with data of the initial concentrations of PO_4^{3-}, Fe, and NO_3^- (Monod, 1949). The Monod growth curves for *Halothece* sp. were plotted against different concentrations of NO_3^- and PO_4^{3-} incubated at different PO_4^{3-} ([Low PO_4^{3-}], [Medium PO_4^{3-}], and [High PO_4^{3-}]) and Fe ([Low–Medium Fe] and [High Fe]) concentrations, respectively. The Monod growth curves for *F. muscicola* incubated at different Fe concentrations ([Low–Medium Fe] and [High Fe]) were also plotted against different concentrations of PO_4^{3-}. Monod kinetic parameters were calculated from plotted hyperbolic functions of the Monod equation:

$$\mu = \frac{\mu' max\ (Q - Qmin)}{Q} \quad (6)$$

where Q is the concentration of NO_3^- or PO_4^{3-}, Q_{min} is the minimal concentration of NO_3^- or PO_4^{3-} for growth, and μ'_{max} is the maximum specific growth rate. Half-velocity constant (K_μ) was calculated as the concentration at half of the μ'_{max} (Monod, 1949).

Abundance Measurement of *Halothece* sp. Using Flow Cytometry

Halothece sp. cells at the end of the different experiments were fixed with glutaraldehyde 25% (v/v) in H_2O (Sigma-Aldrich) [final concentration 0.05% (v/v)] and were counted in a Becton Dickinson FACSVerse cytometer (Becton and Dickinson, Franklin Lakes, NJ, United States). Fluorescent beads, BD FACSuite™ CS&T research beads (Becton and Dickinson and Company BD Biosciences, San Jose, CA, United States), were used as internal standard to calibrate the instrument. To count *Halothece* sp. cells, we selected fluorescein isothiocyanate (FITC) (488-nm excitation, 530/30-nm emission) and phycoerythrin (PE) (488-nm excitation, 576/26-nm emission) combination fluorescence signals, which show clearly the population of the cells, recording for each sample a total of 10×10^3 cells.

Pigment Measurement in *Fischerella muscicola*

Chlorophyll (Chla, Chlb, and total Chl) and phycobiliprotein [R-PE and R-phycocyanin (R-PC)] content for *F. muscicola* were measured and calculated following Porra et al. (1989) and Sobiechowska-Sasim et al. (2014). Briefly, for chlorophyll measurements, 5-ml samples of the cultures were filtered through MFV5-025 glass microfiber filters (MFV5-025, FilterLab), grounded, and extracted with 4 ml of acetone 80% for 2 h. After extraction, cells and filter debris were discarded by centrifugation, and the supernatant was read at 647 and 664 nm in quartz cuvette in a Cary Eclipse spectrometer. For phycobiliproteins, 5-ml samples of the culture were filtered as described above, grounded, and extracted in a buffer medium composed of 0.25 M of Trizma base, 10 mM of disodium EDTA, and 2 mg ml^{-1} of lysozyme. After extraction, cells and filter debris were centrifuged, and supernatants were read at 564, 618, and 750 nm in quartz cuvette in a Cary Eclipse spectrometer.

N_2-Fixation Rate Measurement by Acetylene Reduction Assay

N_2-fixation rates of *Halothece* sp. (pmol N_2-fixed $cell^{-1}$ h^{-1}) and *F. muscicola* (nmol N_2-fixed nmol total Chl^{-1} h^{-1}) were measured through acetylene reduction assay (ARA) at the end of the experiments, following the method of Agawin et al. (2014). *Halothece* sp. N_2-fixing activities were measured under known N_2-fixing conditions (i.e., anaerobic condition and during the dark photoperiod and in [Low NO_3^-]) (Reddy et al., 1993). For *F. muscicola*, measurements of N_2-fixation rates were performed under aerobic conditions during both light and dark photoperiods. Samples of known volume of the cultures (10 ml) were filtered through 0.45-μm GF/F filters (MFV5-025, FilterLab), these filters were incubated with acetylene at 20% (v/v) final concentration injected in each vial using gas-tight Hamilton syringes, and ethylene production was measured (after 3 h of incubation) by gas chromatographic (GC) methods. Ethylene and acetylene were determined using a GC (model HP-5890, Agilent Technologies) equipped with a flame ionization detector (FID). The column was a Varian wide-bore column (ref. CP7584) packed with CP-PoraPLOT U (27.5-m length, 0.53-mm inside diameter, 0.70-mm outside diameter, 20-μm film thickness). Helium was used as carrier gas at a flow rate of 30 ml min^{-1}. Hydrogen and airflow rates were set at 30 and 365 ml min^{-1}, respectively. The split flow was used so that the carrier gas flow through the column was 4 ml min^{-1} at a pressure of 5 psi. Oven, injection, and detector temperatures were set at 52, 120, and 170°C, respectively. Before passing the samples in the GC, standard ethylene and acetylene were ran, and their retention times noted. Ethylene produced was calculated using the equations in Stal (1988). The acetylene reduction rates were converted to N_2-fixation rates (nmol ml^{-1} h^{-1}) using a factor of 4:1 (Jensen and Cox, 1983).

Measurement of Reactive Oxygen Species Production

The ROS production was measured using the molecular probe 2′,7′-dichlorofluorescein diacetate (DCFH-DA; Sigma) in culture media (ASN-III + Turks Island salts 4× or $BG11_0$), which was added to a 96-well microplate (Thermo Scientific) containing cyanobacterial samples (final concentration of probe at 15 μg ml^{-1}). Within the cells, H_2O_2 production oxidizes DCFH-DA to 2′,7′-dichlorofluorescein (DCF) whose green fluorescence can be measured at 25°C in a FLx800 Microplate Fluorescence Reader (BioTek Instruments, Inc.) for 1 h with an excitation of 480 nm and emission of 530 nm. The measurements (the slope of the linear regression obtained) were expressed as arbitrary units (AU) per $cell^{-1}$. DCFH-DA was added in ASN-III + Turks Island salts 4× or $BG11_0$ without cells as blanks under the same conditions as above.

Microscopy and Morphological Studies

Autofluorescence, morphological changes, and DCF oxidized by ROS were observed with a confocal microscope (Leica TCS SPE, Leica Microsystems). Samples were placed onto a clean glass microscope slide, and 40× and 100× objective lens were used to visualize the cells. Images were processed using the software Leica application suite (Leica Microsystems). Autofluorescence was detected with an excitation of 532 nm and an emission of 555- to 619-nm wavelengths. For visualization of DCF oxidized by ROS, we used excitation of 488 nm and emission of 493- to 562-nm wavelengths. Cell apoptosis for *F. muscicola* was observed with Alexa Fluor 488 annexin V/Dead Cell Apoptosis Kit (Thermo Fisher), in which apoptotic cells were detected when the exposed phosphatidylserine of these cells conjugates with annexin. Annexin was detected and visualized at excitation of 530–570 nm and emission of 488-nm wavelengths.

Bio-Informatic *in silico* Analysis

The TBSs (PHO box, Fur, and NtcA boxes) for SphR (i.e., PhoB), ferric uptake regulator (Fur), and global nitrogen regulator (NtcA) already described in cyanobacteria were explored and downloaded from RegPrecise (May, 2020), a web resource for collection, visualization, and analysis of transcriptional regulons reconstructed by comparative genomics (Novichkov et al., 2013). From this database, multifasta files were generated for each TBS, including several genera of cyanobacteria (*Cyanothece*, *Gloeobacter*, *Microcystis*, *Nostoc*, *Prochlorococcus*, *Synechococcus*, *Synechocystis*, *Thermosynechococcus*, and *Trichodesmium*). We obtained three separated multifasta files (one for each TBS type) that contained 77 sequences for PHO box, 167 sequences for Fur boxes, and 228 sequences for NtcA boxes (**Supplementary Material**). For the prediction of the TBS (PHO box, Fur, and NtcA boxes) for *Halothece* sp., we used a user-friendly web interface for prediction of prokaryote promoter elements and regulons, PePPER, using the DNA motif build and search platform[1] (de Jong et al., 2012). Position frequency matrices (PFMs; using MEME and subsequently transposed to a MOODS compatible PWM format) were made from each multifasta file (**Supplementary Material**). The PFMs generated were searched in the whole genome of *Halothece* sp. PCC 7418 (GenkBank: NC_019779.1), obtaining 804 hits for SphR (PhoB), 822 hits for Fur, and 238 hits for NtcA. The corresponding hits were manually explored with UGENE (Golosova et al., 2014). We selected the potential TBS on the basis of their relative positions to the genes (a maximum of −800 bp upstream or +40 bp downstream). DNA sequence logos were generated with WebLogo (Crooks et al., 2004) to graphically indicate the relative frequency of each amino at each position, i.e., predicting the consensus sequences for Pho, Fur, and NtcA boxes. Finally, the genes detected as associated to PHO box, Fur, and NtcA boxes were annotated and submitted to EggNOG v5.0 for further identification of orthology relationships and for functional analysis to describe the Pho, Fur, and NtcA regulons, respectively (Huerta-Cepas et al., 2018).

[1]http://genome2d.molgenrug.nl/g2d_pepper_motifs.php

Statistical Analysis

Non-parametric test, Kruskal–Wallis analysis followed by an unpaired two-samples Wilcoxon test was used to study the effect of the nutrient treatment conditions to growth, pigment concentrations, N_2-fixation rates, and ROS production. Spearman's correlation was used to determine the relationships between growth and N_2-fixation rates. The statistical analyses were performed using the SPSS program version 21 (IBM Corp year 2012).

RESULTS

Effect of Varying Nutrient Concentrations (P, Fe, and/or N) on *Halothece* sp. and *Fischerella muscicola*

Growth of *Halothece* sp. Under Different Concentrations of NO_3^-

The decreasing concentrations of inorganic nitrogen (i.e., NO_3^-) negatively affected the growth of *Halothece* sp. PCC 7418 (Kruskal–Wallis, H = 24.55, 2 d.f., p = 0.045, **Table 1**). Average growth rates (μ, of all the combinations of different PO_4^{3-} and Fe concentrations) under optimal, low, and extremely limiting NO_3^- conditions were 0.33 ± 0.017 day^{-1} (T_g, 2.18 days), 0.24 ± 0.023 day^{-1} (T_g, 3.37 days), and 0.046 ± 0.0075 day^{-1} (T_g, 16.52 days), respectively. Under extremely limiting NO_3^- conditions, the growth of the unicellular cyanobacteria dramatically decreased with rates eight times lower than in optimal NO_3^- conditions, and cells were not able to overcome the latent growth phase in the cultures (**Table 1**).

Growth of *Halothece* sp. Under Different PO_4^{3-} and Fe Concentrations

No significant differences in growth of *Halothece* sp. were observed among different combination conditions of PO_4^{3-} and Fe under optimal NO_3^- (Kruskal–Wallis, H = 7.21, 8 d.f., p = 0.51, **Table 1**; and H = 9.02, 8 d.f., p = 0.34, **Figure 1A**). On the contrary, under [Low NO_3^-] conditions, significant differences were found (Kruskal–Wallis, H = 15.83, 8 d.f., p = 0.045, **Figure 1B**). Under [Low NO_3^-], at high concentrations of PO_4^{3-}, μ was generally higher than at medium and low concentrations (**Table 1** and **Figure 1B**) except when it was combined with high Fe levels (**Table 1** and **Figure 1B**), showing that high Fe levels had a negative impact on their growth at [High PO_4^{3-}] (**Figure 1B**).

Recovery of *Halothece* sp. After Nutrient Re-inoculation

The recovery of *Halothece* sp. cells from low PO_4^{3-} and low Fe (and/or under extremely limiting NO_3^-) to high PO_4^{3-} and high Fe concentrations with re-inoculation of the nutrients (PO_4^{3-}, Fe, and/or NO_3^-) in the medium was dependent on the initial conditions of PO_4^{3-}, Fe, and NO_3^- concentrations in the culture medium (**Figure 1C**). In the [Low PO_4^{3-}–Low Fe] condition under extremely limiting NO_3^- conditions, the cells exhibited total chlorosis, and the addition of PO_4^{3-}, Fe,

TABLE 1 | Growth rate (μ) and generation time (T_g) for *Halothece* sp. (at different NO_3^- concentrations) and *Fischerella muscicola* at different combinations of PO_4^{3-} and Fe concentrations.

Treatments/ parameters	*Halothece* sp.						*Fischerella muscicola*	
	Optimal NO_3^- (4.4 mM)		Low NO_3^- (0.15 mM)		Under extremely limiting NO_3^- (6.66 nM)		N_2 as only source of N	
	μ ± SR (d^{-1})	T_g ± SR (d)	μ ± SR (d^{-1})	T_g ± SR (d)	μ ± SR (d^{-1})	T_g ± SR (d)	μ ± SR (d^{-1})	T_g ± SR (d)
[Low PO_4^{3-}- Low Fe]	0.31 ± 0.06	2.33 ± 0.01	0.19 ± 0.01	3.74 ± 0.26	0.05 ± 0.00	12.91 ± 0.77	0.30 ± 0.03	2.32 ± 0.22
[Low PO_4^{3-}- Medium Fe]	0.31 ± 0.06	2.36 ± 0.02	0.13 ± 0.02	5.29 ± 0.65	*	*	0.26 ± 0.06	2.81 ± 0.62
[Low PO_4^{3-}- High Fe]	0.35 ± 0.08	2.08 ± 0.01	0.13 ± 0.01	5.56 ± 0.65	0.03 ± 0.00	20.87 ± 0.00	0.43 ± 0.26	2.53 ± 0.88
[Medium PO_4^{3-}- Low Fe]	0.33 ± 0.09	2.24 ± 0.03	0.25 ± 0.03	2.82 ± 0.30	*	*	0.42 ± 0.12	1.79 ± 0.52
[Medium PO_4^{3-}- Medium Fe]	0.27 ± 0.01	2.60 ± 0.05	0.29 ± 0.05	2.49 ± 0.41	*	*	0.22 ± 0.04	3.28 ± 0.58
[Medium PO_4^{3-}- High Fe]	0.42 ± 0.00	1.63 ± 0.03	0.20 ± 0.03	3.47 ± 0.53	*	*	0.25 ± 0.10	3.25 ± 1.29
[High PO_4^{3-}- Low Fe]	0.28 ± 0.05	2.56 ± 0.02	0.40 ± 0.02	1.75 ± 0.10	0.07 ± 0.02	10.84 ± 2.84	0.45 ± 0.23	2.06 ± 1.05
[High PO_4^{3-}- Medium Fe]	0.35 ± 0.04	2.04 ± 0.01	0.39 ± 0.01	1.77 ± 0.04	*	*	0.50 ± 0.09	1.44 ± 0.25
[High PO_4^{3-}- High Fe]	0.34 ± 0.03	2.04 ± 0.03	0.20 ± 0.03	3.54 ± 0.54	0.03 ± 0.01	21.36 ± 3.49	0.74 ± 0.00	0.94 ± 0.00

Values are the mean with their spanning range (SR) between the duplicate measurements. Asterisks (*) are conditions in which μ and T_g were not measured.

and NO_3^- (at final concentrations of 45 μM, 7.5 μM, and 4.4 mM, respectively) was not sufficient to restore their original phenotype. However, in [High PO_4^{3-}–High Fe] treatments under extremely limiting NO_3^- conditions, re-inoculation of NO_3^- exhibited slight recovery (recovering their greenish color; data not shown). In addition, in [Low PO_4^{3-}–Low Fe] treatment under optimal NO_3^-, which was re-inoculated with PO_4^{3-} and Fe, the cells responded with higher growth and recovered their greenish color (**Figure 1C**).

Growth of *Fischerella muscicola* Under Different PO_4^{3-} and Fe Concentrations

Unlike what was observed for *Halothece* sp., decreasing concentration of NO_3^- did not affect the μ of *F. muscicola* PCC 73103 (data not shown). With N_2 as sole N source, *F. muscicola* reached the maximum μ of 0.74 day^{-1} (T_g, 0.94 days) at the highest concentrations of PO_4^{3-} and Fe, and it was higher than the rest of the treatments (Kruskal–Wallis, H = 16.03, 8 d.f., p = 0.042, **Figure 2A**). The cells under [High PO_4^{3-}–High Fe] conditions also showed the highest average content of Chla, Chlb, and total chlorophyll (total Chl) (**Figure 2B**) and phycobiliprotein (R-PC and R-PE) content (**Figure 2C**).

Nature of Limitation of PO_4^{3-}, Fe, and/or NO_3^- in *Halothece* sp. and/or *Fischerella muscicola*

The evaluation of the limitation of NO_3^- and PO_4^{3-} in *Halothece* sp. under extremely limiting NO_3^- conditions concentrations revealed that cells were serially limited, i.e., first with NO_3^- and then with PO_4^{3-} (N response > 0, P response = 0 and N + P response > 0) (**Figure 3A**). PO_4^{3-} did not have any effect on the growth of cells when they were extremely N limited. Evaluating the effects of the addition of PO_4^{3-} and Fe with increased N supply, we showed that under optimal NO_3^-, *Halothece* sp. did not respond significantly to any addition of PO_4^{3-} and Fe ($p < 0.05$, **Figure 3B**). Under sufficient N supply (i.e., at [Low NO_3^-] when maximum rates of N_2-fixation were measured), PO_4^{3-} was the main limiting nutrient and Fe had a negative effect on the growth of *Halothece* sp. at high Fe levels (Fe response < 0, P response > 0, and P + Fe response > 0) (**Figure 3C**). However, we also found a simultaneous co-limitation of PO_4^{3-} and Fe (Fe response = 0, P response = 0, and P + Fe response > 0) when both elements were added at medium PO_4^{3-} and medium–high Fe concentrations for *Halothece* sp. (**Figure 3C**). For *F. muscicola*, a simultaneous co-limitation of PO_4^{3-} and Fe was also observed (Fe response = 0, P response = 0, and P + Fe response > 0) when both elements were added at high PO_4^{3-} and Fe concentrations (**Figure 3C**).

Monod Growth Kinetics of *Halothece* sp. and *Fischerella muscicola*

The N-dependent Monod growth kinetics of *Halothece* sp. incubated at different PO_4^{3-} concentrations showed P dependence (**Figure 4A**). *Halothece* sp. had higher maximum growth at high and medium PO_4^{3-} levels (μ'_{max} = 0.50 day^{-1}) compared with low PO_4^{3-} levels

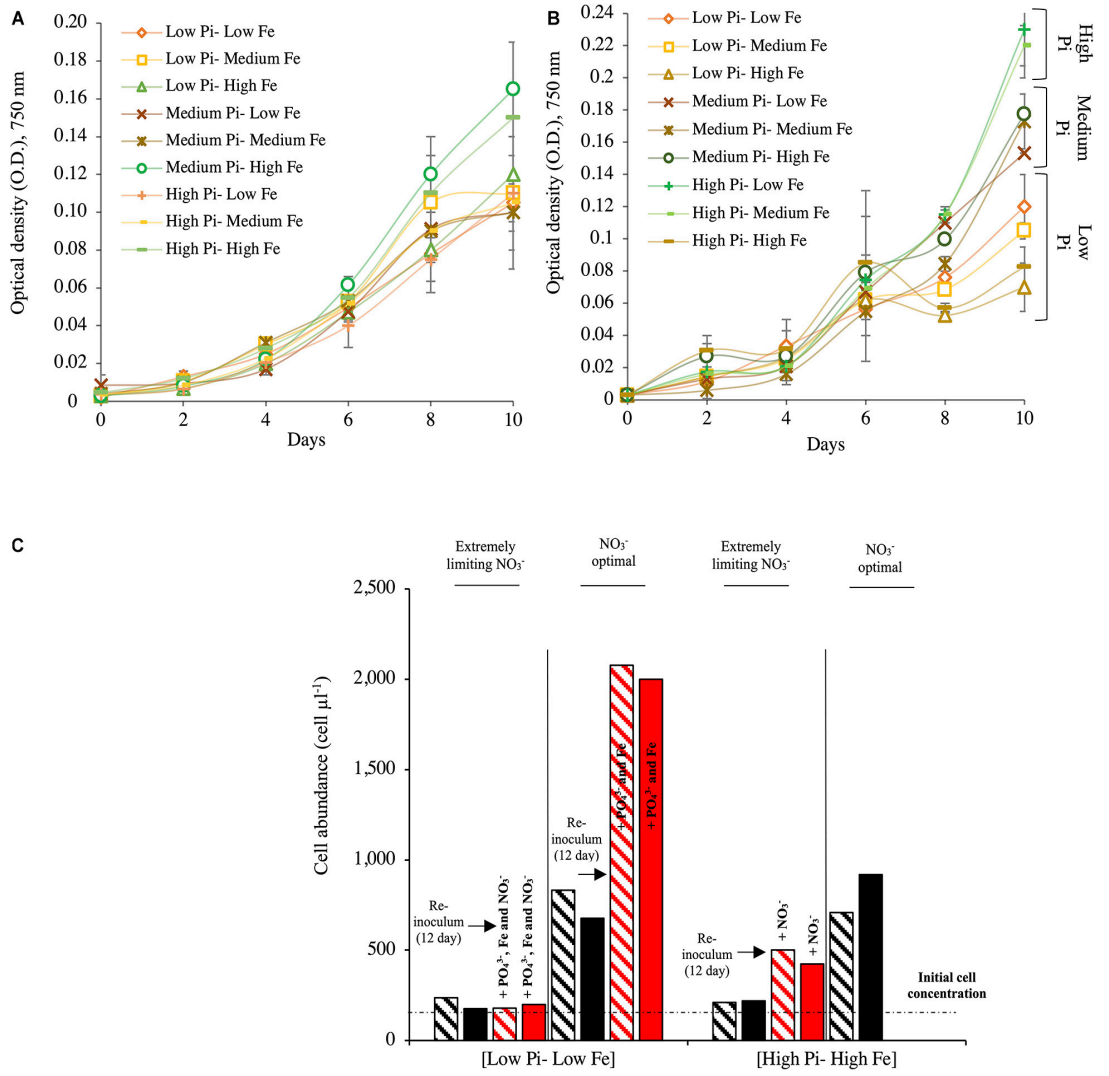

FIGURE 1 | Growth of *Halothece* sp. at different combinations of nutrient concentrations (PO_4^{3-}, Fe, and NO_3^-). **(A)** Growth for *Halothece* sp. under NO_3^- optimal conditions. **(B)** Growth for *Halothece* sp. under [Low NO_3^-] conditions. **(C)** Cell concentration after 12 days of incubation and recovery of *Halothece* sp. under different NO_3^- concentrations with the re-inoculum (black arrow) of PO_4^{3-}, Fe, and/or NO_3^- and incubated 4 days more (red bars). The initial cell concentration is referenced with the black dashed line. PO_4^{3-} is represented as Pi. In panels **(A,B)**, values are the mean with their spanning range (SR) between the duplicate measurements. In panel **(C)**, data presented are actual values of the duplicates (striped and solid bars).

(μ'_{max} = 0.44 day^{-1}). However, the half-velocity constant at [High PO_4^{3-}] (K_μ = 0.217 mM, with a Q_{min} = 1.55 mM) was the lowest compared with that at [Medium PO_4^{3-}] (K_μ = 0.45 mM, with a Q_{min} = 1.19 mM) and [Low PO_4^{3-}] (K_μ = 0.53 mM, with a Q_{min} = 1.22 mM) (**Figure 4A**). The P-dependent growth kinetics of *Halothece* sp. incubated at different Fe concentrations showed μ'_{max} (0.25 day^{-1}) and Q_{min} (5.37 µM) at high Fe levels that were lower and higher, respectively, than at low to medium Fe levels (μ'_{max} = 0.43 day^{-1}, Q_{min} = 3.13 µM); but K_μ was lower at [High Fe] (K_μ = 0.01 µM) than in [Low–Medium Fe] (K_μ = 0.35 µM) (**Figure 4B**). On the other hand, *F. muscicola* generally had higher values of the P-dependent kinetic parameters than *Halothece* sp. when incubated at different Fe concentrations (**Figure 4B**). *F. muscicola* had the higher maximum growth (μ'_{max} = 0.83 day^{-1}), half-velocity constant (K_μ = 1.85 µM), and higher minimal cell quota (Q_{min} = 12.58 µM) at high Fe treatments as compared with cells at low to medium levels of Fe (μ'_{max} = 0.62 day^{-1}, K_μ = 0.03 µM, Q_{min} = 12.33 µM) (**Figure 4B**).

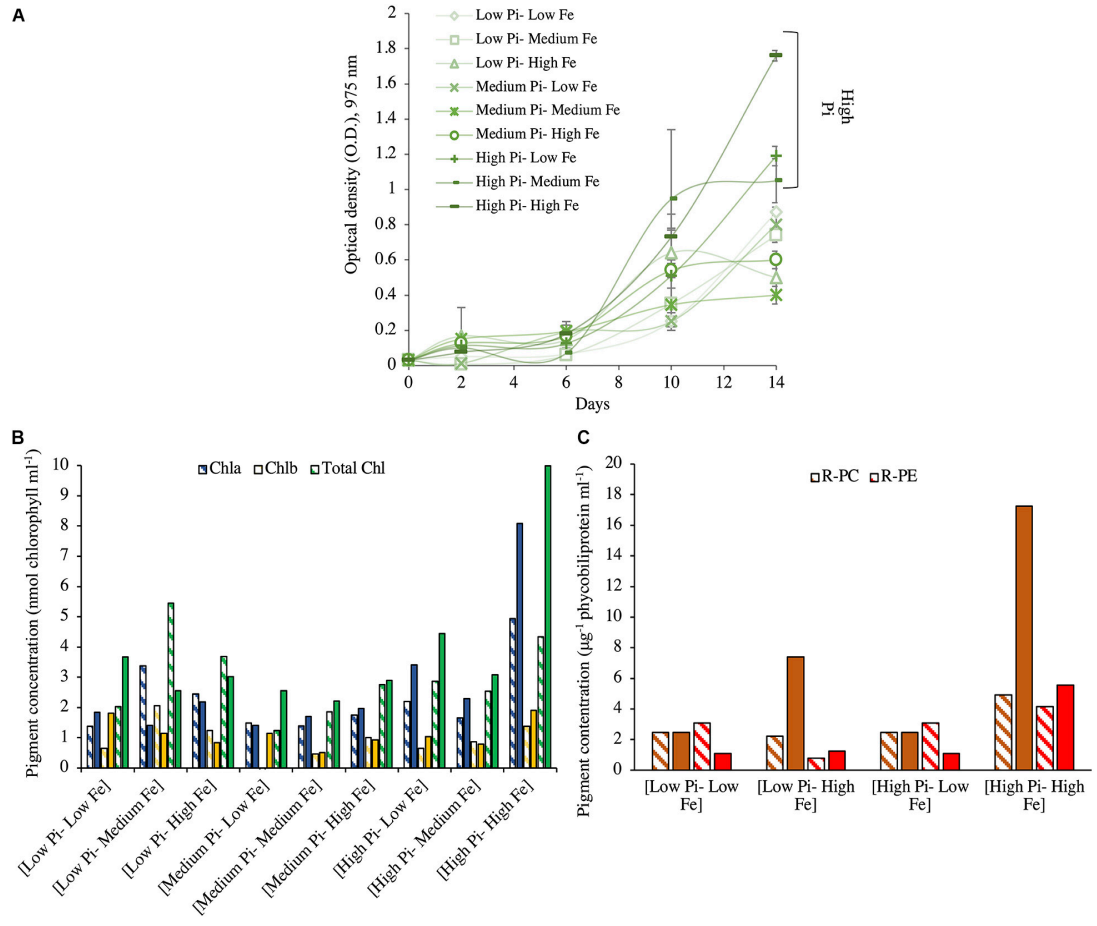

FIGURE 2 | Growth and pigment content for *Fischerella muscicola* at different concentrations of PO_4^{3-} and Fe after 14 days of incubation. **(A)** Growth for *F. muscicola* at different combinations of PO_4^{3-} and Fe where values are the mean with their spanning range (SR) between the duplicate measurements. **(B)** Chlorophyll (Chla, Chlb, and total Chl) and **(C)** phycobiliproteins (R-PC and R-PE) concentrations at different combinations of PO_4^{3-} and Fe concentrations. PO_4^{3-} is represented as Pi. In panels **(B,C)**, data presented are actual values of the duplicates (striped and solid bars).

Effect of Varying Concentrations of P and Fe on N_2-Fixation Rates of *Halothece* sp. and *Fischerella muscicola*

Halothece sp.-specific N_2-fixation rates under [Low NO_3^-] at different treatment combinations of PO_4^{3-} and Fe were significantly linearly correlated with cell concentrations (Spearman's correlation, $r = 0.7$, $p < 0.05$, $n = 18$). N_2-fixation rates at [Low PO_4^{3-}] conditions were undetectable and generally increased at medium PO_4^{3-} and at increasing Fe concentrations (**Figure 5A**). However, at the highest PO_4^{3-} and Fe concentrations, N_2-fixation was again undetectable (**Figure 5A**). For *F. muscicola*, where specific N_2-fixation rates were measured during the light and dark photoperiods, there were no significant differences among the treatments during the light and dark phase (Kruskal–Wallis, $H = 15.45$, 8 d.f., $p = 0.051$; data not shown). Higher N_2-fixation rates under high PO_4^{3-} levels were detected, especially when combined with high Fe concentrations (**Figure 5B**).

Effect of Varying Concentrations of P and Fe on the Production of Reactive Oxygen Species of *Halothece* sp. and *Fischerella muscicola*

Reactive oxygen species production for *Halothece* sp. was measured under optimal NO_3^- and [Low NO_3^-] conditions (**Figures 6A,B**). Under optimal NO_3^-, there were significant differences among the treatments (Kruskal–Wallis, $H = 15.67$, 8 d.f., $p = 0.047$, **Figure 6A**). ROS production was higher at [Low PO_4^{3-}–Low Fe] conditions compared with increasing concentrations of PO_4^{3-} at the same [Low Fe] conditions (**Figure 6A**). At [Low PO_4^{3-}] conditions, increasing Fe concentration reduced the ROS production (**Figure 6A**). On the

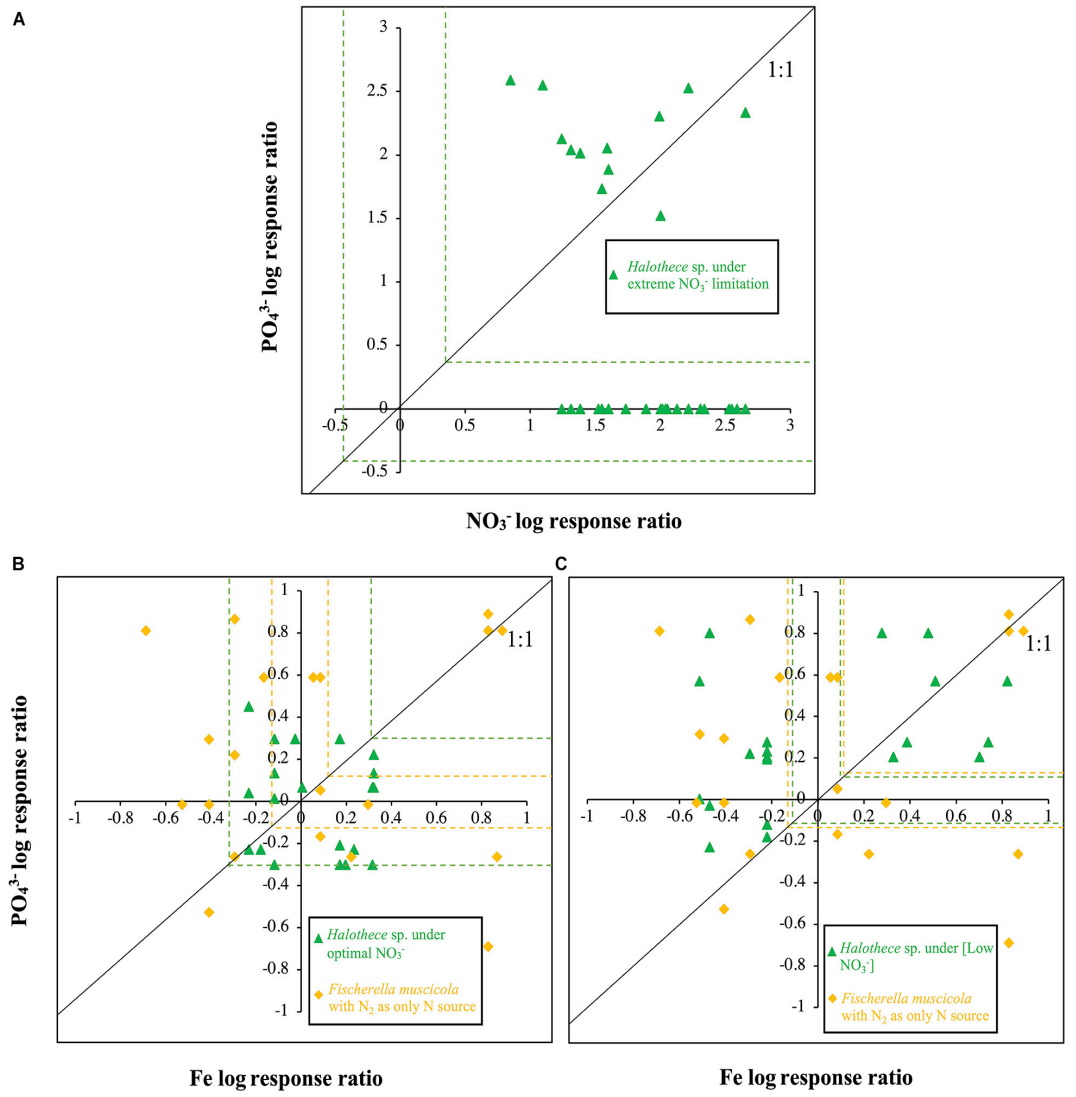

FIGURE 3 | Log nutrient responses for *Halothece* sp. and *Fischerella muscicola*. **(A)** PO_4^{3-} and NO_3^- log response ratios for *Halothece* sp. **(B)** and **(C)** PO_4^{3-} and Fe log response ratios for *Halothece* sp. **(B)** under optimal NO_3^- and **(C)** under [Low NO_3^-] conditions and *F. muscicola* with N_2 as sole N source. Each data point represents each replicate in which *X*-axis is the NO_3^- or Fe log response and *Y*-axis is the PO_4^{3-} log response. Dashed green (for *Halothece* sp.) and yellow lines (for *F. muscicola*) represent the critical threshold values [data points outside the critical values are significantly different (at $p = 0.05$) from N_0P_0 or Fe_0P_0]. PO_4^{3-} is represented as Pi.

other hand, cells under PO_4^{3-} and Fe limitation ([Low PO_4^{3-}–Low Fe]) and optimal NO_3^- showed higher ROS production, as observed with the greener color (oxidized DCF) of cells, compared with the red color of cells that were not producing ROS in [High PO_4^{3-}–High Fe] (**Figures 7A,B**). On the other hand, under [Low NO_3^-] conditions, we did not detect significant differences in ROS production (Kruskal–Wallis, $H = 13.80$, 8 d.f., $p = 0.087$, **Figure 6B**). Nonetheless, we observed ROS production under [Low NO_3^-] conditions to be higher at [Low PO_4^{3-}–Medium/High Fe] than the rest of the treatments except at [High PO_4^{3-}–High Fe] and [Low PO_4^{3-}–Low Fe] (**Figure 6B**). At [Medium Fe] conditions, increasing PO_4^{3-} concentrations reduced ROS production (**Figure 6B**).

The ROS production of *F. muscicola* did not vary among the different treatment combinations of PO_4^{3-} and Fe (Kruskal–Wallis, $H = 12.30$, 8 d.f., $p = 0.14$, **Figure 6C**). Nonetheless, there was a tendency of higher ROS production at [Low PO_4^{3-}–Low Fe] compared with [High PO_4^{3-}–High Fe] conditions, consistent

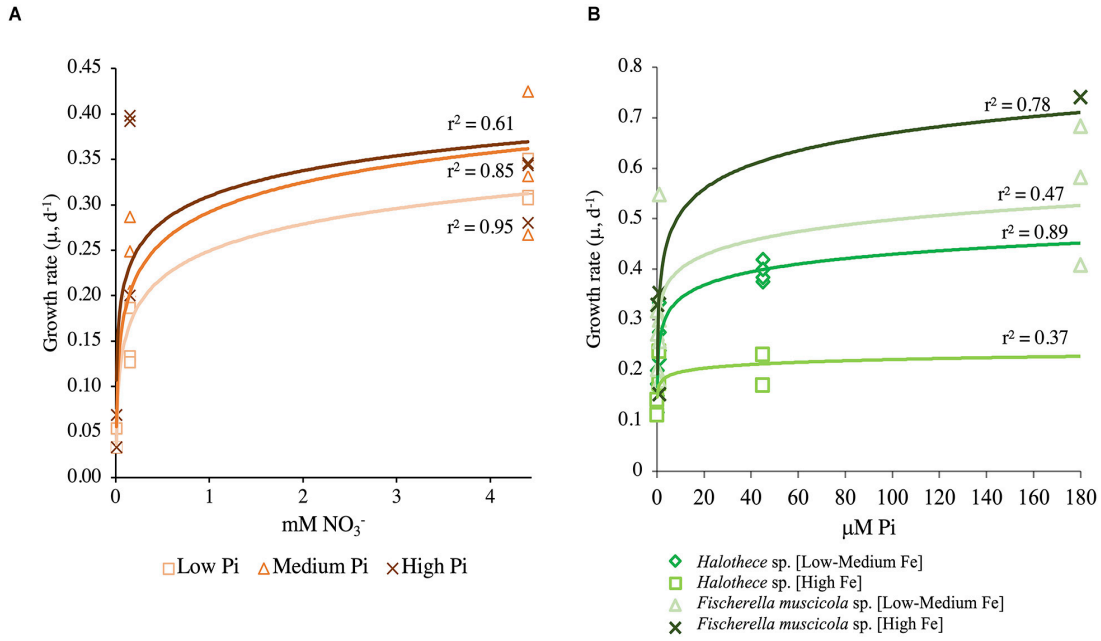

FIGURE 4 | Monod curves **(A)** at different PO_4^{3-} concentrations for *Halothece* sp. and *Fischerella muscicola* in function of NO_3^- initial levels and **(B)** at different Fe concentrations for *Halothece* sp. (under [Low NO_3^-]) and *F. muscicola* in function of PO_4^{3-} initial levels. PO_4^{3-} is represented as Pi.

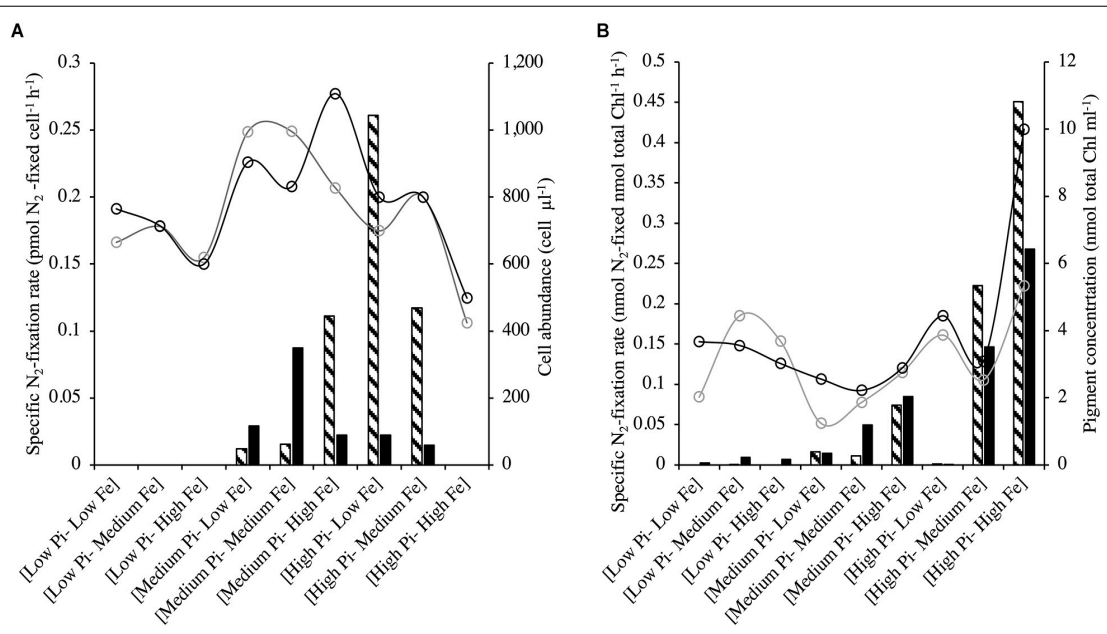

FIGURE 5 | N_2-fixation rates for **(A)** *Halothece* sp. and **(B)** *Fischerella muscicola* at different combinations of PO_4^{3-} and Fe concentrations. *Halothece* sp. were grown under [Low NO_3^-] to promote N_2-fixation. Bar graphics indicate N_2-fixation, while empty circles indicate cell abundance (cell μl^{-1}) for *Halothece* sp. and chlorophyll concentrations (nmol total Chl ml^{-1}) for *F. muscicola*. Data presented are actual values of the duplicates (striped and solid bars or light and heavy lined circles). PO_4^{3-} is represented as Pi.

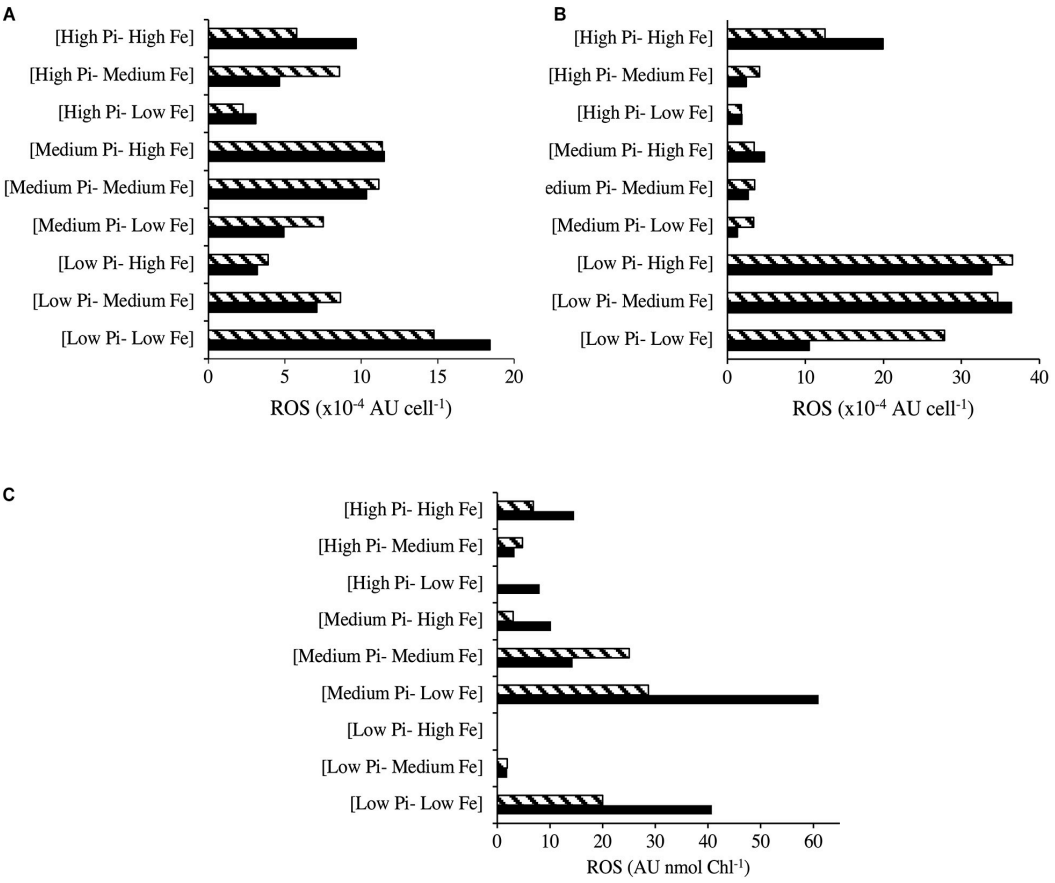

FIGURE 6 | Radical oxygen species (ROS) production at different combinations of PO_4^{3-} and Fe concentrations for *Halothece* sp. under **(A)** NO_3^- optimal and **(B)** [Low NO_3^-] conditions and **(C)** for *F. muscicola*. PO_4^{3-} is represented as Pi. Data presented are actual values of the duplicates (striped and solid bars).

with the confocal images showing oxidative stress, observing more green-yellowish color cells (indicative of ROS production) in [Low PO_4^{3-}–Low Fe] treatments (**Figure 7C**) than in [High PO_4^{3-}–High Fe] conditions (**Figure 7D**).

Effect of Varying Concentrations of P and Fe on the Morphology and Physiology of *Halothece* sp. and *Fischerella muscicola*

Halothece sp. cells under optimal nutrient conditions (PO_4^{3-}, Fe, and/or NO_3^-) exhibited sizes between 4 and 7 μm. Limitation of PO_4^{3-} and Fe under NO_3^- optimal and [Low NO_3^-] conditions did not cause changes in sizes. However, extremely limiting NO_3^- conditions caused an increase in size of the cells (up to two-fold with respect to the normal size), reaching an average size of 12.7 ± 0.74 μm. Under extremely limiting NO_3^- conditions together with PO_4^{3-} and Fe limitation, cells experience vacuole production together with modification of shape and breakage of the cells (**Figure 7E**). In addition, we also observed that under these same conditions, cells experience total chlorosis (dramatic loss of phycobiliproteins), and cells were barely visible under confocal microscopy compared with cells under optimal nutrient conditions.

Programmed cell death for *F. muscicola* was studied through apoptosis assay to detect mortality in four treatments: [Low PO_4^{3-}–Low Fe] (**Figure 7F**), [Low PO_4^{3-}–High Fe] (**Figure 7G**), [High PO_4^{3-}–Low Fe] (**Figure 7H**), and [High PO_4^{3-}–High Fe] (**Figure 7I**). Results showed that PO_4^{3-} and Fe limitation caused increased mortality. At [High PO_4^{3-}–High Fe], there was no signal of annexin V in conjugation with phosphatidylserine detected, indicating the good status of the cells in this treatment.

Prediction of Genes Involved in P, Fe, and N Adaptation and Survival in *Halothece* sp.

We predicted the consensus sequences for TBSs for SphR-PhoB (PHO box), Fur regulator (Fur Box), and NtcA protein (NtcA box) for *Halothece* sp. For PHO box, we

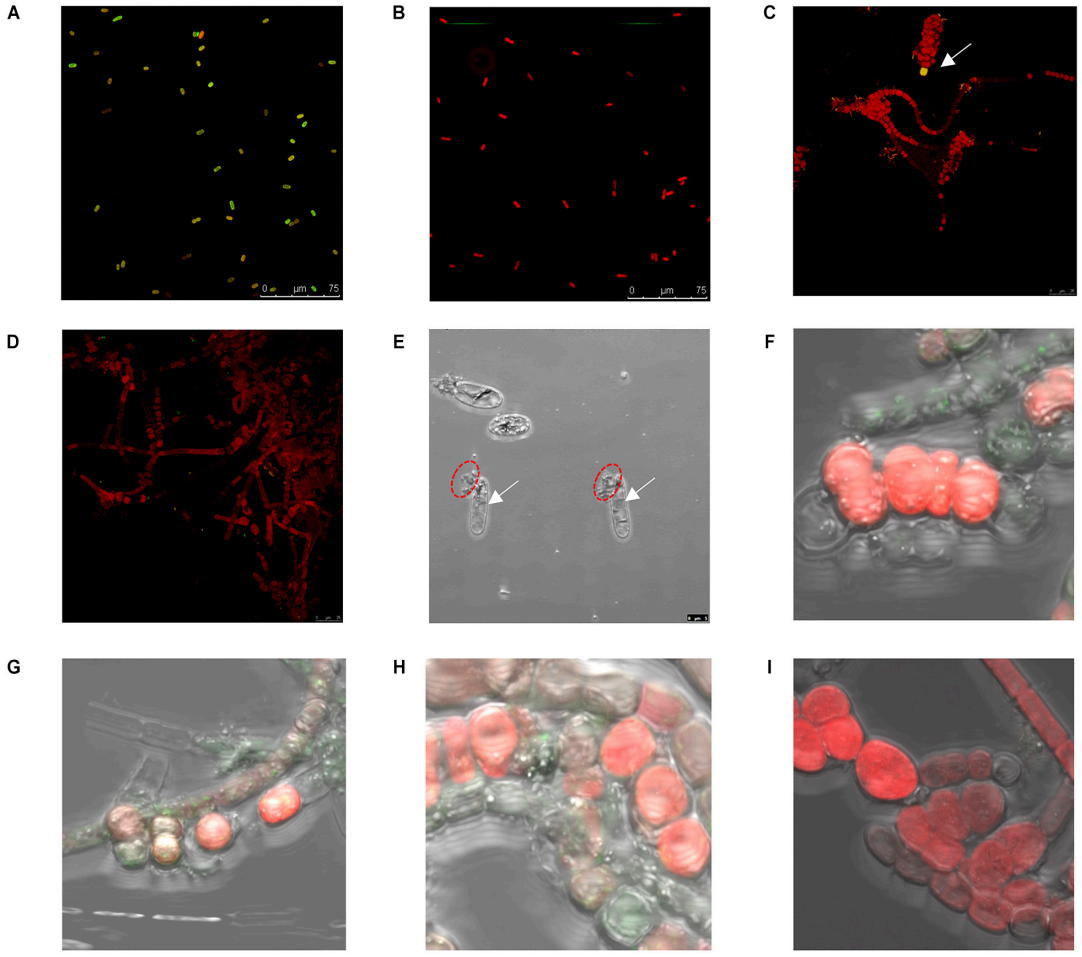

FIGURE 7 | Biochemical [e.g., reactive oxygen species (ROS) production], morphological, and physiological changes for *Halothece* sp. and *Fischerella muscicola*. **(A–D)** Confocal images of ROS production (green-yellow color) for *Halothece* sp. at panel **(A)** [Low PO_4^{3-}–Low Fe] and panel **(B)** [High PO_4^{3-}–High Fe] conditions and for *F. muscicola* at panel **(C)** [Low PO_4^{3-}–Low Fe] (in which the white arrow indicates the ROS production) and panel **(D)** [High PO_4^{3-}–High Fe] conditions. Images were taken at 400×. Panel **(E)** [Low PO_4^{3-}–Low Fe] condition under extremely limiting NO_3^- conditions under the bright field (arrows indicate vacuole formation, and red dashed circles indicate cell breaks). **(F–I)** Apoptosis assay results for *F. muscicola* under confocal microscopy. Panel **(F)** [Low PO_4^{3-}–Low Fe], panel **(G)** [Low PO_4^{3-}–High Fe], panel **(H)** [High PO_4^{3-}–Low Fe], and panel **(I)** [High PO_4^{3-}–High Fe]. In panels **(F–I)**, the green color resulted from the binding of annexin with the phosphatidylserines that were exposed in apoptotic cells, and images **(E–I)** were taken at 1,000× with zoom. PO_4^{3-} is represented as Pi.

established that consensus sequence was formed by three tandem repeats of 8 bp ($[ATTTAAAT]_3$) separated by 3 bp (**Figure 8A**). Fur Box was formed by 19 bp inverted repeats (ATTGAAAATTATTTT[T/C]AAT) (**Figure 8B**). Finally, NtcA box was constituted by $TGTAN_8TACA$ in which GTA at positions 2–4 and TAC at positions 13–15 were well conserved (**Figure 8C**). From the prediction of these boxes, we described what potential genes are implicated in Pho, Fur, and NtcA regulons (**Supplementary Tables S2–S4**).

Pho regulon (**Figure 8D**) was mainly constituted by genes involved in inorganic ion transport and metabolism (P) (10%), replication, recombination and repair (L) (10%), and cell wall/membrane/envelope biogenesis (M) (8%), detecting 218 genes (**Supplementary Table S2**). Among them, we detected genes that are part of the "classical" Pho regulon (e.g., some of them found in the same operon): PstS family phosphate ABC transporter substrate-binding protein-phosphate (*pstS*), ABC transporter permease subunit PstC-phosphate (*pstC*), ABC transporter permease PstA-phosphate (*pstA*), ABC transporter ATP-binding protein PstB (*pstB*), PhoQ sensor (*phoQ*), or alkaline phosphatase (*phoA*). In addition, we detected other genes under the control of PhoB such as *nblA* (involved in chlorosis processes); *gvpA*, *gvpN*, *gvpL*, and *gvpF* (involved in gas vesicles); *cas* genes (involved in CRISPR-Cas systems); and a

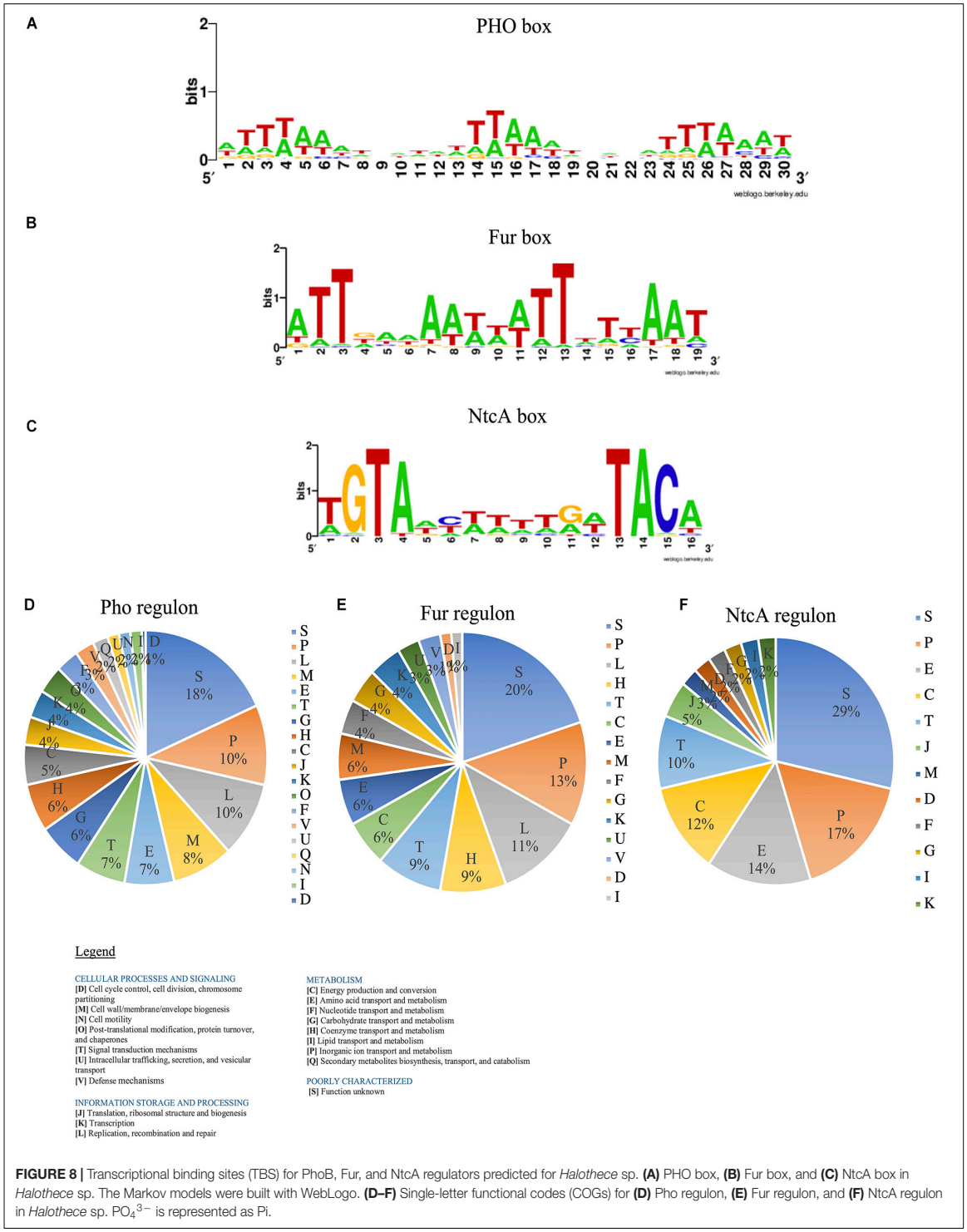

FIGURE 8 | Transcriptional binding sites (TBS) for PhoB, Fur, and NtcA regulators predicted for *Halothece* sp. **(A)** PHO box, **(B)** Fur box, and **(C)** NtcA box in *Halothece* sp. The Markov models were built with WebLogo. **(D–F)** Single-letter functional codes (COGs) for **(D)** Pho regulon, **(E)** Fur regulon, and **(F)** NtcA regulon in *Halothece* sp. PO_4^{3-} is represented as Pi.

whole group of genes that codify for transferases, endonucleases, ABC transporters, or transposases (**Supplementary Table S2**).

Fur regulon (**Figure 8E**) mostly was distributed in P (13%), L (11%), coenzyme transport and metabolism (H) (9%), and signal transduction mechanisms (T) (9%), detecting 73 genes (**Supplementary Table S3**). We detected genes under the control of Fur box directly involved in Fe acquisition, such as energy transducer TonB (*tonB*), MotA/TolQ/ExbB proton channel family protein, and three operons of transporter permease subunit (*feoA–feoB*). Fur boxes were detected upstream of genes related in photosynthesis and respiration [e.g., photosystem II reaction center protein X (*psbX*)], in the pathway of chlorophyll biosynthesis [glutamate-1-semialdehyde-2,1-aminomutase (*gsaI*)], and in bacteriochlorophyll biosynthesis [magnesium-protoporphyrin IX monomethyl ester anaerobic oxidative cyclase/DNA-binding response regulator (*bchE*)].

Finally, NtcA regulon (**Figure 8F**) was constituted by genes mostly involved in P (17%), amino acid transport and metabolism (E) (14%), and energy production and conversion (C) (12%), detecting 40 genes (**Supplementary Table S4**). We detected genes involved in N_2-fixation processes: FeMo cofactor biosynthesis protein (*nifB*) and molybdate ABC transporter substrate-binding protein (*modA*); in nitrogen assimilation: ferredoxin–nitrite reductase (*nirA*); in glutamine/glutamate assimilation: glutamate synthase [NADPH] large chain (*gltB*), type I glutamate-ammonia ligase (*glnN*) and sodium:glutamate symporter (*gltS*); and in ammonium assimilation: ammonium transporter (*amt*). In addition, Fur regulator itself potentially has a NtcA box.

DISCUSSION

Effect of Varying N Concentrations on *Halothece* sp. Compared With *Fischerella muscicola*

In this study, the dependence on the concentration of combined N sources such as NO_3^- for growth of diazotrophic cyanobacterial cultures differed between the unicellular *Halothece* sp. and the filamentous heterocyst-forming *F. muscicola* (**Table 1** and **Figures 1A–C**, **2A**, **3A**, **4A**). Theoretically, N_2-fixers are independent of inorganic N source (e.g., *F. muscicola*) because of their capability of fixing N_2 (Knapp, 2012). However, at extremely limiting NO_3^- conditions (i.e., 6.66 nM), almost having N_2 as sole N source, *Halothece* sp. were barely growing (**Table 1** and **Figures 1C**, **4A**), and their morphology (increased size) and physiology (i.e., exhibiting extreme chlorosis) changed. Chlorosis can result from the deprivation of NO_3^-, which promotes the degradation of phycobilisomes through the protein NblA (Klotz et al., 2015), which was detected here under the PhoB control (**Supplementary Table S2**). The observed increases in cell size, possibly, is a result of cell division cessation (Klotz et al., 2016). Moreover, vacuole formation was observed possibly due to the storage of compounds in response to severe N limitation (**Figure 7E**). Our results indicate that in some N_2-fixing species, e.g., *Halothece* sp., a minimum amount of combined N sources is necessary for the proper functioning of the cells (Q_{min} ranging from 1.19 to 1.51 mM of NO_3^-, **Figure 4A**). However, it remains to be investigated whether these cells in the natural environment, indeed, require a combined source of inorganic nitrogen and if this requirement can be supplied by other diazotrophs in N-limited waters.

Contrary with *Halothece* sp., *F. muscicola* cells were totally independent of combined N source and were able to grow with N_2 as the sole N source. The viability of unicellular N_2-fixers to grow under N_2 as sole N source may be dependent on the presence and type of additional carbon (C) source to support their growth as shown with *Synechococcus* sp. strain SF1 (isolated from macroalgae, *Sargassum fluitans*), which was not able to grow with HCO_3^- as sole C source (Spiller and Shanmugam, 1987). Here, *Halothece* sp. were cultured with glucose and citrate, and these may not be the optimal C source for their growth when grown at almost having N_2 as sole N source. Unicellular N_2-fixers also have been shown to grow more when NO_3^- is added compared when grown with only N_2 as sole N source (Agawin et al., 2007), since a larger energetic cost is associated with assimilating N_2 versus NO_3^- assimilation. Since N_2-fixation is sensitive to oxygen (O_2), cyanobacteria must develop strategies to avoid N_2-fixation inhibition by the O_2 liberated from photosynthesis. Unicellular cyanobacterial cells are able to separate temporarily two incompatible processes: N_2-fixation (at night) and photosynthesis (at day) in the same cell (De Bruijn, 2015). These two processes have to be tightly controlled to avoid inhibition of N_2-fixation through well-regulated circadian clocks (Toepel et al., 2008), and these strategies can be energy consuming. Aside therefore of the energy cost of assimilating N_2, *Halothece* sp. may have an add-on cost of temporally separating N_2-fixation and photosynthetic process, and thus they cannot be totally independent of combined sources of inorganic N. On the contrary, filamentous heterocyst-forming cells have specialized cells (heterocyst) in which N_2-fixation takes place in anoxic conditions and may not have an add-on cost of temporally separating N_2-fixation and photosynthetic processes and thus are better adapted to growing with N_2 as sole N source (De Bruijn, 2015; **Figure 5B**).

Effect of Varying Concentrations of P and Fe on *Halothece* sp. and *Fischerella muscicola*

Concentration of P and Fe in *Halothece* sp. and *Fischerella muscicola*

Phosphorus (P) is needed for many cellular components, such as cellular membranes, nucleic acids, and ATP-dependent reactions such as N_2-fixation, which is energetically costly, requiring 16 ATPs ($N_2 + 8e^- + 16ATP + 8H^+ \rightarrow 2NH_3 + H_2 + 16ADP + 16PO_4^{3-}$) (Hoffman et al., 2014). Under optimum conditions for N_2-fixation (at low [Low NO_3^-] for *Halothece* sp. and without any combined N source in the case of *F. muscicola*), increasing concentrations of PO_4^{3-} generally increased the growth of both species, suggesting that PO_4^{3-} was an important limiting factor for both species and affected their N_2-fixation rates (**Figures 1–5**). These results are consistent with the previous study of Fernández-Juárez et al. (2019) reporting

the increased rates of P-acquisition mechanisms (PO_4^{3-}-uptake rates and APAs) at [Low NO_3^-] for *Halothece* sp. At high concentrations of NO_3^- where N_2-fixation rates were lower (and thus this P-requirement can be lower), growth of *Halothece* sp. was independent of varying concentrations of PO_4^{3-}. It is well described that in some cyanobacteria, e.g., *Trichodesmium* sp., one of the major N_2-fixers in the Atlantic, P is the main element regulating N_2-fixation (Sañudo-Wilhelmy et al., 2001). Under P-limiting environments (e.g., the Mediterranean Sea), N_2-fixers must therefore depend on external P sources (such as Saharan dust deposition, Tanhua et al., 2013), and cells have to be well adapted to P limitation with mechanisms for phosphorus scavenging (Dyhrman and Haley, 2006; Fernández-Juárez et al., 2019).

Iron (Fe) had differing effects for *Halothece* sp. (i.e., toxic effect under high Fe levels under [Low NO_3^-]) and for *F. muscicola* (i.e., limiting growth under low Fe levels) (**Table 1** and **Figures 1B**, **2A**, **3B,C**, **4**, **5**). The results for *F. muscicola* were consistent with studies on *Crocosphaera watsonii* in which severe Fe limitation (3 nM) showed strong negative changes in growth and N_2-fixation, limiting both processes, while higher Fe levels (up to 400 nM) increased these two parameters (Jacq et al., 2014). N_2-fixation is an Fe-dependent process, since nitrogenase complex contains 38 Fe atoms per holoenzyme (Hoffman et al., 2014). This Fe dependence was observed for *F. muscicola* at high PO_4^{3-} levels (**Figure 5B**). However, in *Halothece* sp., high amounts of Fe (7.5 μM) inhibited N_2-fixation but only under high PO_4^{3-} levels, suggesting toxicity at these levels of PO_4^{3-} and Fe for this species (**Figures 3C**, **4B**, **5A**). Nonetheless, Fe can control N_2-fixation in *Halothece* sp. cells, considering the Fe dependence of their alkaline phosphatase D (PhoD), which releases PO_4^{3-} from organic sources to fuel N_2-fixation (Fernández-Juárez et al., 2019). Further studies must be conducted especially in *Halothece* sp. to determine which threshold of Fe concentrations can Fe inhibit/enhance growth and N_2-fixation rates.

Interaction Between P and Fe Under Different Nitrogen Concentrations

Cell Recovery Under P, Fe, and N Limitation in Halothece sp.

It is well documented how unicellular cyanobacteria cells are able to recover their phenotype by a genetically determined program (Klotz et al., 2016). Re-inoculum of PO_4^{3-} and Fe in [Low PO_4^{3-}-Low Fe] under NO_3^- optimal conditions and even in [High PO_4^{3-}–High Fe] under extremely limiting NO_3^- conditions with the addition of NO_3^- had as a consequence the partial or complete recovery of the green natural color and growth of the cells (**Figure 1C**). However, here, we observed that for *Halothece* sp., this program is "canceled" under extreme NO_3^- limitation and co-limitation of PO_4^{3-} and Fe. Under extremely limiting NO_3^- and [Low PO_4^{3-}–Low Fe] conditions, addition of PO_4^{3-} and Fe did not result in growth recovery of the cells, suggesting that nutrient co-limitation (PO_4^{3-}, Fe, and NO_3^-) could kill cells irreversibly by breakage of cells (**Figures 1C**, **7E**).

Nature of Nutrient Co-Limitation (P, Fe, and N) in Halothece sp. and Fischerella muscicola

In oligotrophic areas, e.g., the tropical North Atlantic, bacterial productivity and biomass are usually co-limited with N, P, and/or Fe (Mills et al., 2004; Arrigo, 2005; Moore et al., 2008). The interactions between these limiting nutrients can trigger different types of limitation: simultaneous co-limitation (nutrient limitation of, e.g., N, P, and/or Fe have collective responses), independent co-limitation (nutrient limitation of, e.g., N, P, and/or Fe have different responses), and serial limitation wherein the response of a second limiting nutrient is appreciable after the previous addition of the primary limiting nutrient (Harpole et al., 2011). To our knowledge, this study is the first to show evidences of serial limitation of N (NO_3^-) and P (PO_4^{3-}) in diazotrophs with combined N as the primary limiting nutrient as suggested by the results for *Halothece* sp. (**Figure 3A**). This suggests that in extremely N-limited waters, diazotrophs like *Halothece* sp. are not competitive enough to compensate for N-deficits of the system through their N_2-fixation activities and cannot deplete the P concentration enough for the other co-occurring diazotrophic or non-diazotrophic species in the community to become P-limited. The reverse would follow for *F. muscicola*, which was independent of combined N source. The simultaneous co-limitation of PO_4^{3-} and Fe observed in **Figure 3C** for *Halothece* sp. and *F. muscicola* may be due to the nature of the process of N_2-fixation, which is ATP dependent, and Fe is a structural component of the nitrogenase enzyme (Hoffman et al., 2014). Iron (Fe) is also a co-factor of alkaline phosphatases, which is one of the P-acquisition mechanisms of diazotrophs when P is in short supply (Santos-Beneit, 2015; Fernández-Juárez et al., 2019). However, the mechanisms behind the simultaneous limitation of PO_4^{3-} and Fe have to be further investigated as we also observed deleterious effects depending on the concentrations of these nutrients.

Differences in Nutrient Kinetics in Diazotrophs at Different P and Fe Concentrations

Of the two species of cyanobacteria tested, the one that can most probably adapt to low levels of PO_4^{3-} is the unicellular cyanobacterium *Halothece* sp. based on their nutrient kinetics (**Figure 4B**). Based on the Monod curves, the unicellular strain had the lowest K_μ and Q_{min}, indicating a better adaptation to PO_4^{3-} than the filamentous diazotroph (**Figure 4B**), albeit the K_μ measured in *Halothece* sp. under [High Fe] (i.e., 10 nM) shows lower affinity for PO_4^{3-} than that reported in the marine picophytoplankton *Synechococcus* (1 nM) (Kretz et al., 2015). In addition, its Q_{min} (2.27 μM) was much higher than that of the marine *Synechococcus* (3 nM) (Kretz et al., 2015), indicating that *Halothece* sp. is well adapted to P limitation but not at the level of *Synechococcus*. Unicellular cyanobacteria with smaller sizes are more efficient in acquiring nutrients in nutrient-limited waters because of their high surface: area ratios, while heterocyst-forming bacteria, which are generally bigger in size, need higher nutrient requirements (Haramaty et al., 2007). This is clearly shown in the Monod plot (**Figure 4B**), in which *F. muscicola* needs high amounts of Fe to growth, on the contrary of

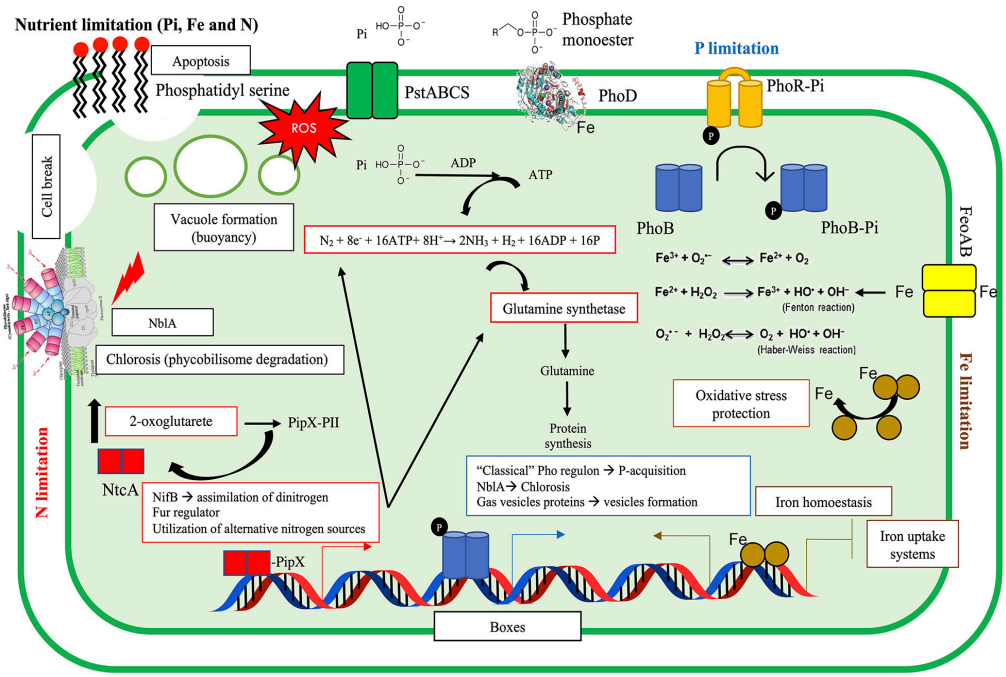

FIGURE 9 | Summary of PO_4^{3-}, Fe, and NO_3^- interactions and the physiological and molecular responses of the cyanobacteria tested. Nutrient limitation can result in chlorosis, apoptosis, vacuole formation, reactive oxygen species (ROS) production, and growth inhibition. In such situations, cells may activate different molecular mechanisms. Under PO_4^{3-} limitation (blue), the autophosphorylation of PhoR allows the phosphorylation of PhoB, regulating the P-response (i.e., expression of the "classical" Pho regulon, e.g., alkaline phosphatase, PhoD). Fur is a repressor (although it can play as activator) that responds to Fe limitation (brown) and inhibits/allows the transcription of the Fur regulon, through the association with divalent metal (i.e., Fe). Nitrogen limitation (red) triggers different responses through NtcA regulator. When N abundance is low, 2-oxoglutarate (2-OG) may increase, and this could bind to a complex called PII–PipX and breaks this association, allowing the disassociation of PipX, and the formation of PipX–NtcA. PipX is a coactivator of NtcA, and it is suggested that it can stabilize NtcA and would help to recruit RNA polymerase (Tiwari et al., 2015; Kaushik et al., 2016; Giner-Lamia et al., 2017). PO_4^{3-} is represented as Pi.

Halothece sp. in which high Fe levels inhibited cell abundance (**Figures 3C**, **4B**).

Reactive Oxygen Species Production and Apoptotic Changes Derived From P, Fe, and N Limitation

Nutrient limitation (i.e., PO_4^{3-}, Fe, and/or NO_3^-) increased ROS in both species, *Halothece* sp. and *F. muscicola* (**Figures 6A–C**, **7A–D**). Iron (Fe) had a key role in regulating ROS production. Increasing Fe levels can have different responses as shown in **Figures 6A–C**: (1) beneficial through increase activity of enzymatic antioxidant defenses or (2) extremely toxic through increase in Fenton and Haber–Weiss reaction (Latifi et al., 2009; Diaz and Plummer, 2018). The second case is suggested in **Figure 6B**, in which under [Low NO_3^-] and [High PO_4^{3-}], Fe increased ROS production and in turn can inhibit N_2-fixation (Alquéres et al., 2010). This could explain why *Halothece* sp. under [High PO_4^{3-}–High Fe] had lower growth and N_2-fixation rates than the other treatments with high levels of PO_4^{3-} (**Figure 5A**). On the contrary, in *F. muscicola*, Fe generally reduced ROS production (**Figure 6C**). The reduction of ROS production with Fe addition is consistent with a study on *Anabaena* PCC 7120, in which ROS increased up to 10-fold when the cells were starved with Fe (Latifi et al., 2005). The results of our apoptosis tests (normally applied to eukaryotic cells) for *F. muscicola* when cells were limited by PO_4^{3-} and/or Fe are first evidences of programmed cell death in cyanobacteria by nutrient limitation (**Figures 7F–I**). Further investigations have to be performed to figure out the molecular mechanisms behind this.

Prediction of Genes Involved in P, Fe, and N Limitation in *Halothece* sp.

We predicted the Pho, Fur, and NtcA boxes in the unicellular cyanobacterium *Halothece* sp. (PCC 7418), controlled by the master regulators in P, Fe, and N metabolism (PhoB, Fur, and NtcA, respectively), showing well-conserved sequences in this bacteria (**Figures 8A–C**), consistent with several studies (Tiwari et al., 2015; Kaushik et al., 2016; Giner-Lamia et al., 2017). A large majority of these genes associated to these boxes were involved in inorganic ion transport and metabolism (P) (**Figures 8D–F** and **Supplementary Tables S2–S4**), providing key information of how cyanobacteria respond to P, Fe, and N limitation (**Figure 9**). We detected genes involved in typical transporters in P, Fe, and N metabolism, in Fe storage, cell wall biosynthesis, amino acid metabolism,

photosynthesis, chlorosis, chlorophylls and PC biosynthesis, anti-phage systems (e.g., *cas* genes, implicated in the CRISPR-Cas systems), or even virulence (**Supplementary Tables S2–S4**). Through the created algorithms, we were able to detect elements from the "classical" Pho regulon (e.g., transporters, *pstABCS*, enzymes through which PO_4^{3-} is obtained from dissolved organic phosphorus, APases or stored phosphate, *ppK*), Fe transporters (e.g., *feoA* and *feoB*), and a whole group of genes involved in N metabolism (e.g., *gltBNS*, *amt*, and *nifB*) and thus being the most probable genes controlled by these TFs as is already described in *Cyanothece*, *Gloeobacter*, *Microcystis*, *Nostoc*, *Prochlorococcus*, *Synechococcus*, *Synechocystis*, *Thermosynechococcus*, and *Trichodesmium* (**Supplementary Material** [Multifasta] and **Supplementary Tables S2–S4**). A N_2-fixation regulator, *nifB*, was predicted under the control of NtcA, whose product is crucial in iron–molybdenum biosynthesis (**Supplementary Table S4**). Downstream of this gene, we localized an entire cluster of genes related to N_2-fixation: Fd III 4Fe-4S, *nifS*, *nifU*, *nifH*, *nifD*, *nifK*, *nifZ*, *nifE*, *nifN*, *nifX*, DUF683, and *nifW*. In addition, some reports affirm that NtcA binds and controls Fur protein (López-Gomollón et al., 2007), as we predicted in this study, showing that N limitation can increase Fur protein levels and suggesting the narrow connection between N and Fe metabolism.

In summary, we show that two species of N_2-fixing cyanobacteria potentially associated with seagrasses have differing sensibilities to PO_4^{3-}, Fe, and NO_3^- concentrations, showing that these nutrients interact with each other based on our experimental and bio-informatic analysis. Despite the low number replications (being conscious that some results cannot be generalized), the growth responses reported here at varying concentrations of PO_4^{3-} and Fe at different NO_3^- conditions must be taken with precaution since the internal storage of these nutrients could affect these results considering that the cells were inoculated from optimal nutrients conditions. This is a pilot study in which insights on nutrient limitation in N_2-fixers are reported. Nonetheless, our study of a multifactorial design provides useful data and important findings of nutrient limitation in marine diazotrophs (at physiological, biochemical, and genetic levels). Deeper molecular assays (i.e., transcriptomic or proteomic assays) are recommended to investigate all the predicted genes involved in P, Fe, and N metabolism.

DATA AVAILABILITY STATEMENT

The raw data supporting the article of this manuscript will be made available by the authors, without undue reservation, to any qualified researcher.

AUTHOR CONTRIBUTIONS

VF-J and NA designed the experiments. VF-J conducted all experiments. All authors led the writing of the manuscript, reviewed, and supervised by NA.

FUNDING

This work was supported by funding to NA through the Ministerio de Economía, Industria y Competitividad-Agencia Estatal de Investigación, and the European Regional Development Funds project (CTM2016-75457-P). AS-G was supported by the Spanish Ministry of Economy and Competitiveness, Instituto de Salud Carlos III (CIBEROBN CB12/03/30038).

ACKNOWLEDGMENTS

We acknowledge the support and help of Scientific Technical Service (Maria Trinidad Garcia Barceló) of the University of the Balearic Islands for gas chromatography analyses. We also thank Pere Ferriol Buñola and Alba Coma Ninot for the help in the acquisition of the cultures.

SUPPLEMENTARY MATERIAL

The Supplementary Material for this article can be found online at: https://www.frontiersin.org/articles/10.3389/fmicb.2020.541558/full#supplementary-material

Supplementary Table 1 | List of all experimental treatments conducted in this study.

Supplementary Table 2 | Pho regulon prediction. PHO boxes sequences, their position in the genome, orientation, the genes that are controlling (the Pho regulon), locus tag from these genes, the distance of the box from the gene and the gen function from single-letter of functional (COGs) are presented.

Supplementary Table 3 | Fur regulon prediction. Fur boxes sequences, their position in the genome, orientation, the genes that are controlling (the Fur regulon), locus tag from these genes, the distance of the box from the gene and the gen function from single-letter of functional (COGs) are presented.

Supplementary Table 4 | NtcA regulon prediction. NtcA boxes sequences, their position in the genome, orientation, the genes that are controlling (the NtcA regulon), locus tag from these genes, the distance of the box from the gene and the gen function from single-letter of functional (COGs) are presented.

REFERENCES

Agawin, N. S. R., Benavides, M., Busquets, A., Ferriol, P., Stal, L. J., and Arístegui, J. (2014). Dominance of unicellular *Cyanobacteria* in the diazotrophic community in the Atlantic Ocean. *Limnol. Oceanogr.* 59, 623–637. doi: 10.4319/lo.2014.59.2.0623

Agawin, N. S. R., Ferriol, P., Cryer, C., Alcon, E., Busquets, A., Sintes, E., et al. (2016). Significant nitrogen fixation activity associated with the phyllosphere of Mediterranean seagrass *Posidonia oceanica*: first report. *Mar. Ecol. Prog. Ser.* 551, 53–62. doi: 10.3354/meps11755

Agawin, N. S. R., Ferriol, P., Sintes, E., and Moyà, G. (2017). Temporal and spatial variability of in situ nitrogen fixation activities associated with the

Mediterranean sseagrass *Posidonia oceanica* meadows. *Limnol. Oceanogr.* 62, 2575–2592. doi: 10.1002/lno.10591

Agawin, N. S. R., Rabouille, S., Veldhuis, M. J. W., Servatius, L., Hol, S., Van Overzee, M. J., et al. (2007). Competition and facilitation between unicellular nitrogen-fixing *Cyanobacteria* and non – nitrogen-fixing phytoplankton species. *Limonol. Oceanogr.* 52, 2233–2248. doi: 10.4319/lo.2007.52.5.2233

Alquéres, S. M. C., Oliveira, J. H. M., Nogueira, E. M., Guedes, H. V., Oliveira, P. L., Câmara, F., et al. (2010). Antioxidant pathways are up-regulated during biological nitrogen fixation to prevent ROS-induced nitrogenase inhibition in *Gluconacetobacter diazotrophicus*. *Arch. Microbiol.* 192, 835–841. doi: 10.1007/s00203-010-0609-1

Arrigo, R. K. (2005). Marine microorganisms and global nutrient cycles. *Nature* 437, 343–348. doi: 10.1038/nature04158

Baichoo, N., and Helmann, J. D. (2002). Recognition of DNA by Fur: a reinterpretation of the Fur box consensus sequence recognition of DNA by Fur: a reinterpretation of the fur box consensus sequence. *J. Bacteriol.* 184, 5826–5832. doi: 10.1128/JB.184.21.5826

Browning, T. J., Achterberg, E. P., Yong, J. C., Rapp, I., Utermann, C., Engel, A., et al. (2017). Iron limitation of microbial phosphorus acquisition in the tropical North Atlantic. *Nat. Commun.* 8, 1–7. doi: 10.1038/ncomms15465

Crooks, G. E., Hon, G., Chandonia, J. M., and Brenner, S. E. (2004). WebLogo: a sequence logo generator. *Genome Res.* 14, 1188–1190. doi: 10.1101/gr.849004

De Bruijn, F. J. (2015). *Biological Nitrogen Fixation*. Amsterdam: Elsevier Inc, doi: 10.1002/9781119053095

de Jong, A., Pietersma, H., Cordes, M., Kuipers, O. P., and Kok, J. (2012). PePPER: a webserver for prediction of prokaryote promoter elements and regulons. *BMC Genomics* 13:299. doi: 10.1186/1471-2164-13-299

Diaz, J. M., and Plummer, S. (2018). Production of extracellular reactive oxygen species by phytoplankton: past and future directions. *J. Plankton Res.* 40, 655–666. doi: 10.1093/plankt/fby039

Dyhrman, S. T., and Haley, S. T. (2006). Phosphorus scavenging in the unicellular marine diazotroph *Crocosphaera watsonii*. *Appl. Environ. Microbiol.* 72, 1452–1458. doi: 10.1128/AEM.72.2.1452-1458.2006

Fernández-Juárez, V., Bennasar-Figueras, A., Tovar-Sanchez, A., and Agawin, N. S. R. (2019). The role of iron in the P-acquisition mechanisms of the unicellular N2-fixing *Cyanobacteria halothece* sp ., found in association with the Mediterranean seagrass *Posidonia oceanica*. *Front. Microbiol.* 10:1903. doi: 10.3389/fmicb.2019.01903

Geider, R. J., and La Roche, J. (2002). Redfield revisited: variability of C:N:P in marine microalgae and its biochemical basis. *Eur. J. Phycol.* 37, 1–17. doi: 10.1017/S0967026201003456

Giner-Lamia, J., Robles-Rengel, R., Hernández-Prieto, M. A., Isabel Muro-Pastor, M., Florencio, F. J., and Futschik, M. E. (2017). Identification of the direct regulon of NtcA during early acclimation to nitrogen starvation in the cyanobacterium *Synechocystis* sp. PCC 6803. *Nucleic Acids Res.* 45, 11800–11820. doi: 10.1093/nar/gkx860

Golosova, O., Henderson, R., Vaskin, Y., Gabrielian, A., Grekhov, G., Nagarajan, V., et al. (2014). Unipro UGENE NGS pipelines and components for variant calling. RNA-seq and ChIP-seq data analyses. *PeerJ* 2:e644. doi: 10.7717/peerj.644

Haramaty, L., Quigg, A., Berman-Frank, I., Finkel, Z. V., and Irwin, A. J. (2007). Nitrogen-fixation strategies and Fe requirements in *Cyanobacteria*. *Limnol. Oceanogr.* 52, 2260–2269. doi: 10.4319/lo.2007.52.5.2260

Harpole, W. S., Ngai, J. T., Cleland, E. E., Seabloom, E. W., Borer, E. T., Bracken, M. E. S., et al. (2011). Nutrient co-limitation of primary producer communities. *Ecol. Lett.* 14, 852–862. doi: 10.1111/j.1461-0248.2011.01651.x

Hedges, L. V., Gurevitch, J., and Curtis, P. S. (1999). The meta-analysis of response ratios in experimental ecology. *Ecology* 80, 1150–1156. doi: 10.1890/0012-9658(1999)080[1150:tmaorr]2.0.co;2

Hoffman, B. M., Lukoyanov, D., Yang, Z.-Y., Dean, D. R., and Seefeldt, L. C. (2014). Mechanism of nitrogen fixation by nitrogenase: the next stage. *Chem. Rev.* 114, 4041–4062. doi: 10.1021/cr400641x

Huerta-Cepas, J., Szklarczyk, D., Heller, D., Hernández-Plaza, A., Forslund, S. K., Cook, H., et al. (2018). eggNOG 5.0: a hierarchical, functionally and phylogenetically annotated orthology resource based on 5090 organisms and 2502 viruses. *Nucleic Acids Res.* 47, 309–314. doi: 10.1093/nar/gky1085

Jacq, V., Ridame, C., L'Helguen, S., Kaczmar, F., and Saliot, A. (2014). Response of the unicellular diazotrophic cyanobacterium *Crocosphaera watsonii* to iron limitation. *PLoS One* 9:e0086749. doi: 10.1371/journal.pone.0086749

Jensen, B. B., and Cox, R. P. (1983). Direct measurements of steady-state kinetics of *Cyanobacterial* N2 uptake by membrane-leak mass spectrometry and comparisons between nitrogen fixation and acetylene reduction. *Appl. Environ. Microbiol.* 45, 1331–1337. doi: 10.1128/aem.45.4.1331-1337.1983

Kaushik, M. S., Singh, P., Tiwari, B., and Mishra, A. K. (2016). Ferric Uptake Regulator (FUR) protein: properties and implications in *Cyanobacteria*. *Ann. Microbiol.* 66, 61–75. doi: 10.1007/s13213-015-1134-x

Klotz, A., Georg, J., Bučinská, L., Watanabe, S., Reimann, V., Januszewski, W., et al. (2016). Awakening of a dormant cyanobacterium from nitrogen chlorosis reveals a genetically determined program. *Cell Press* 26, 2862–2872. doi: 10.1016/j.cub.2016.08.054

Klotz, A., Reinhold, E., Doello, S., and Forchhammer, K. (2015). Nitrogen starvation acclimation in *Synechococcus elongatus*: redox-control and the role of nitrate reduction as an electron sink. *Life* 5, 888–904. doi: 10.3390/life5010888

Knapp, A. N. (2012). The sensitivity of marine N2 fixation to dissolved inorganic nitrogen. *Front. Microbiol.* 3:374. doi: 10.3389/fmicb.2012.00374

Kranzler, C., Lis, H., Finkel, O. M., Schmetterer, G., Shaked, Y., and Keren, N. (2014). Coordinated transporter activity shapes high-affinity iron acquisition in *Cyanobacteria*. *ISME J.* 8, 409–417. doi: 10.1038/ismej.2013.161

Kranzler, C., Rudolf, M., Keren, N., and Schleiff, E. (2013). Iron in *Cyanobacteria*. *Adv. Bot. Res.* 65, 57–105. doi: 10.1016/B978-0-12-394313-2.00003-2

Kretz, C. B., Bell, D. W., Lomas, D. A., Lomas, M. W., and Martiny, A. C. (2015). Influence of growth rate on the physiological response of marine *Synechococcus* to phosphate limitation. *Front. Microbiol.* 6:85. doi: 10.3389/fmicb.2015.00085

Latifi, A., Jeanjean, R., Lemeille, S., Havaux, M., and Zhang, C. C. (2005). Iron starvation leads to oxidative stress in *Anabaena* sp. *strain PCC* 7120. *J. Bacteriol.* 187, 6596–6598. doi: 10.1128/JB.187.18.6596-6598.2005

Latifi, A., Ruiz, M., and Zhang, C. C. (2009). Oxidative stress in *Cyanobacteria*. *FEMS Microbiol. Rev.* 33, 258–278. doi: 10.1111/j.1574-6976.2008.00134.x

Llacer, J. L., Espinosa, J., Castells, M. A., Contreras, A., Forchhammer, K., and Rubio, V. (2010). Structural basis for the regulation of NtcA-dependent transcription by proteins PipX and PII. *Proc. Natl. Acad. Sci. U.S.A.* 107, 15397–15402. doi: 10.1073/pnas.1007015107

López-Gomollón, S., Hernández, J. A., Wolk, C. P., Peleato, M. L., and Fillat, M. F. (2007). Expression of FurA is modulated by NtcA and strongly enhanced in heterocysts of *Anabaena* sp. PCC 7120. *Microbiology* 153, 42–50. doi: 10.1099/mic.0.2006/000091-0

Manhart, J. R., and Wong, P. P. (1980). Nitrate effect on nitrogen fixation (acetylene reduction): activities of legume root nodules induced by rhizobia with varied nitrate reductase activities. *Plant Physiol.* 65, 502–505. doi: 10.1104/pp.65.3.502

Mills, M. M., Ridame, C., Davey, M., La Roche, J., and Geider, R. J. (2004). Iron and phosphorus co-limit nitrogen fixation in the eastern tropical North Atlantic. *Nature* 429, 232–294. doi: 10.1038/nature02550

Monod, J. (1949). The growth of bacterial cultures. *Annu. Rev. Microbiol.* 3, 371–394. doi: 10.1146/annurev.mi.03.100149.002103

Moore, C. M., Mills, M. M., Langlois, R., Milne, A., Achterberg, E. P., La Roche, J., et al. (2008). Relative influence of nitrogen and phosphorus availability on phytoplankton physiology and productivity in the oligotrophic sub-tropical North Atlantic Ocean. *Limnol. Oceanogr.* 53, 291–305. doi: 10.4319/lo.2008.53.1.0291

Nelson, D. C., Waterbury, J. B., and Jannasch, H. W. (1982). Nitrogen fixation and nitrate utilization by marien and freshwater *Beggiatoa*. *Arch. Microbiol* 133, 172–177. doi: 10.1007/BF00414997

Ng, T. S., Chew, S. Y., Rangasamy, P., Mohd Desa, M. N., Sandai, D., Chong, P. P., et al. (2015). SNF3 as high affinity glucose sensor and its function in supporting the viability of *Candida glabrata* under glucose-limited environment. *Front. Microbiol.* 6:1334. doi: 10.3389/fmicb.2015.01334

Novichkov, P. S., Kazakov, A. E., Ravcheev, D. A., Leyn, S. A., Kovaleva, G. Y., Sutormin, R. A., et al. (2013). RegPrecise 3.0 - A resource for genome-scale exploration of transcriptional regulation in bacteria. *BMC Genomics* 14:745. doi: 10.1186/1471-2164-14-745

Porra, R. J., Thompson, W. A., and Kriedemann, P. E. (1989). Determination of accurate extinction coefficients and simultaneous equations for assayin chlorophylls a and b extracted with four different solvents. *Biochim. Biophys. Acta* 975, 384–394. doi: 10.1016/s0005-2728(89)80347-0

Powley, H. R., Krom, M. D., and Van Cappellen, P. (2017). Understanding the unique biogeochemistry of the Mediterranean Sea: insights from a coupled

phosphorus and nitrogen model. *Global Biogeochem. Cycles* 31, 1010–1031. doi: 10.1002/2017GB005648

Quigg, A., Irwin, A. J., and Finkel, Z. V. (2011). Evolutionary inheritance of elemental stoichiometry in phytoplankton. *Proc. R. Soc. BBiol. Sci.* 278, 526–534. doi: 10.1098/rspb.2010.1356

Reddy, K. J., Haskell, J. B., Sherman, D. M., and Sherman, L. A. (1993). Unicellular, aerobic nitrogen-fixing *Cyanobacteria* of the genus *Cyanothece*. *J. Bacteriol.* 175, 1284–1292. doi: 10.1128/jb.175.5.1284-1292.1993

Redfield, A. C. (1934). "On the proportions of organic derivatives in sea water and their relation to the composition of plankton," in *James Johnstone Meml*, ed. R. J. Daniel (Liverpool: Univ. Press Liverpool), 176–192.

Richaud, C., Zabulon, G., Joder, A., Thomas, J., and Zabulon, R. (2001). Nitrogen or sulfur starvation differentially affects phycobilisome degradation and expression of the *nblA* gene in *Synechocystis* strain PCC 6803. *J. Bacteriol.* 183, 2989–2994. doi: 10.1128/JB.183.10.2989

Santos-Beneit, F. (2015). The Pho regulon: a huge regulatory network in bacteria. *Front. Microbiol.* 6:402. doi: 10.3389/fmicb.2015.00402

Sañudo-Wilhelmy, S. A., Kustka, A. B., Gobler, C. J., Hutchins, D. A., Yang, M., Lwiza, K., et al. (2001). Phosphorus limitation of nitrogen fixation by *Trichodesmium* in the central Atlantic Ocean. *Nature* 411, 66–69. doi: 10.1038/35075041

Sobiechowska-Sasim, M., Stoń-Egiert, J., and Kosakowska, A. (2014). Quantitative analysis of extracted phycobilin pigments in *Cyanobacteria*—an assessment of spectrophotometric and spectrofluorometric methods. *J. Appl. Phycol.* 26, 2065–2074. doi: 10.1007/s10811-014-0244-3

Sohm, J. A., Webb, E. A., and Capone, D. G. (2011). Emerging patterns of marine nitrogen fixation. *Nat. Rev. Microbiol.* 9, 499–508. doi: 10.1038/nrmicro2594

Spiller, H., and Shanmugam, K. T. (1987). Physiological conditions for nitrogen fixation in a unicellular marine cyanobacterium, *Synechococcus* sp. strain SF1. *J. Bacteriol.* 169, 5379–5384. doi: 10.1128/jb.169.12.5379-5384.1987

Stal, L. J. (1988). Acetylene reduction technique for assay of nitrogenase. *Methods Enzymol.* 167, 474–484.

Stanier, R. Y., Deruelles, J., Rippka, R., Herdman, M., and Waterbury, J. B. (1979). Generic assignments, strain histories and properties of pure cultures of *Cyanobacteria*. *Microbiology* 111, 1–61. doi: 10.1099/00221287-111-1-1

Statham, P. J., and Hart, V. (2005). Dissolved iron in the Cretan Sea (eastern Mediterranean). *Limnol. Oceanogr.* 50, 1142–1148. doi: 10.4319/lo.2005.50.4.1142

Sunda, W., and Huntsman, S. (2015). High iron requirement for growth, photosynthesis, and low-light acclimation in the coastal cyanobacterium *Synechococcus bacillaris*. *Front. Microbiol.* 6:561. doi: 10.3389/fmicb.2015.00561

Tanhua, T., Hainbucher, D., Schroeder, K., Cardin, V., Álvarez, M., and Civitarese, G. (2013). The mediterranean Sea system: a review and an introduction to the special issue. *Ocean Sci.* 9, 789–803. doi: 10.5194/os-9-789-2013

Tiwari, B., Singh, S., Kaushik, M. S., and Mishra, A. K. (2015). Regulation of organophosphate metabolism in *Cyanobacteria*. A review. *Microbiology* 84, 291–302. doi: 10.1134/S0026261715030200

Toepel, J., Welsh, E., Summerfield, T. C., Pakrasi, H. B., and Sherman, L. A. (2008). Differential transcriptional analysis of the cyanobacterium *Cyanothece* sp. strain ATCC 51142 during light-dark and continuous-light growth. *J. Bacteriol.* 190, 3904–3913. doi: 10.1128/JB.00206-08

Tripathi, K., Sharma, N. K., Kageyama, H., Takabe, T., and Rai, A. K. (2013). Physiological, biochemical and molecular responses of the halophilic cyanobacterium *Aphanothece halophytica* to Pi-deficiency. *Eur. J. Phycol.* 48, 461–473. doi: 10.1080/09670262.2013.859303

Widdel, F. (2010). *Theory and Measurement of Bacterial Growth*. Bremen: University Bremen.

Yuan, Z. C., Zaheer, R., Morton, R., and Finan, T. M. (2006). Genome prediction of PhoB regulated promoters in *Sinorhizobium meliloti* and twelve *proteobacteria*. *Nucleic Acids Res.* 34, 2686–2697. doi: 10.1093/nar/gkl365

Zehr, J. P. (2011). Nitrogen fixation by marine *Cyanobacteria*. *Trends Microbiol.* 19, 162–173. doi: 10.1016/j.tim.2010.12.004

Conflict of Interest: The authors declare that the research was conducted in the absence of any commercial or financial relationships that could be construed as a potential conflict of interest.

3.3 Chapter 3

Microbial Ecology
https://doi.org/10.1007/s00248-021-01766-z

ENVIRONMENTAL MICROBIOLOGY

Everything Is Everywhere: Physiological Responses of the Mediterranean Sea and Eastern Pacific Ocean Epiphyte *Cobetia* Sp. to Varying Nutrient Concentration

Víctor Fernández-Juárez[1] · Daniel Jaén-Luchoro[2,3] · Jocelyn Brito-Echeverría[4] · Nona S. R. Agawin[1] · Antoni Bennasar-Figueras[5] · Pedro Echeveste[4,6]

Received: 24 October 2020 / Accepted: 22 April 2021

Abstract
Bacteria are essential in the maintenance and sustainment of marine environments (e.g., benthic systems), playing a key role in marine food webs and nutrient cycling. These microorganisms can live associated as epiphytic or endophytic populations with superior organisms with valuable ecological functions, e.g., seagrasses. Here, we isolated, identified, sequenced, and exposed two strains of the same species (i.e., identified as *Cobetia* sp.) from two different marine environments to different nutrient regimes using batch cultures: (1) *Cobetia* sp. UIB 001 from the endemic Mediterranean seagrass *Posidonia oceanica* and (2) *Cobetia* sp. 4B UA from the endemic Humboldt Current System (HCS) seagrass *Heterozostera chilensis*. From our physiological studies, both strains behaved as bacteria capable to cope with different nutrient and pH regimes, i.e., N, P, and Fe combined with different pH levels, both in long-term (12 days (d)) and short-term studies (4 d/96 h (h)). We showed that the isolated strains were sensitive to the N source (inorganic and organic) at low and high concentrations and low pH levels. Low availability of phosphorus (P) and Fe had a negative independent effect on growth, especially in the long-term studies. The strain UIB 001 showed a better adaptation to low nutrient concentrations, being a potential N_2-fixer, reaching higher growth rates (μ) than the HCS strain. P-acquisition mechanisms were deeply investigated at the enzymatic (i.e., alkaline phosphatase activity, APA) and structural level (e.g., alkaline phosphatase D, PhoD). Finally, these results were complemented with the study of biochemical markers, i.e., reactive oxygen species (ROS). In short, we present how ecological niches (i.e., MS and HCS) might determine, select, and modify the genomic and phenotypic features of the same bacterial species (i.e., *Cobetia* spp.) found in different marine environments, pointing to a direct correlation between adaptability and oligotrophy of seawater.

Keywords *Posidonia oceanica* · *Heterozostera chilensis* · Mediterranean Sea · Humboldt Current System · *Cobetia* sp. (UIB 001 and 4B UA) and nitrogen (N)-phosphorus (P)-iron (Fe) regimes

✉ Víctor Fernández-Juárez
victorfj@hotmail.es

[1] Marine Ecology and Systematics (MarES), Department of Biology, University of the Balearic Islands, Palma, Spain

[2] Department of Infectious Diseases, Sahlgrenska Academy, University of Gothenburg, Gothenburg, Sweden

[3] Culture Collection University of Gothenburg (CCUG), Sahlgrenska Academy of the University of Gothenburg, Gothenburg, Sweden

[4] Instituto de Ciencias Naturales Alexander von Humboldt, Universidad de Antofagasta, Antofagasta, Chile

[5] Grup de Microbiologia, Department of Biology, University of the Balearic Islands, Palma, Spain

[6] Instituto Milenio de Oceanografía, Concepción, Chile

Introduction

Seagrasses are one of the most productive ecosystems, placed in continental seashores of all continents but Antarctica [1], providing key ecological services. As relevant coastal primary producers, seagrasses fix atmospheric CO_2, acting as carbon sinks and O_2 releasers. They also sustain secondary production, trap particles, stabilize sediments, are key actors of biogeochemical processes (e.g., nitrogen cycles), and form the habitat and nursery for several micro- and macro-organisms [2]. Their associated microbiome takes part in the major ocean's biogeochemical cycles (e.g., nutrient cycling of nitrogen (N), phosphorus (P), and/or iron (Fe)) and microbial food webs [3–5], essential for the livelihood of seagrasses. Within the bacterial consortia, primary producers (e.g.,

Published online: 05 May 2021

Prochlorococcus and *Synechococcus*) play a critical role through their CO_2-fixing capacity [6], together with other bacteria in sulfide detoxification (which is highly toxic for plant growth [7]), and biological N_2-fixation (BNF) which compensates denitrification, converting dinitrogen gas (N_2) to inorganic N (i.e., ammonia, NH_3) [8]. The role of environmental factors (e.g., nutrient availability) modulating bacterial community composition, diversity, functioning, and, thus, the health and productivity of the seagrasses, remains to be investigated.

The implication of the microbial communities associated with seagrasses, which can be found as epiphytic or endophytic, has been profusely illustrated on the Mediterranean endemic seagrass *Posidonia oceanica* (L.) Delile [9–11]. N_2-fixers or diazotrophs can supply the entire N-demand of the plant, having a key role in nutrient cycling [12], considering the Mediterranean Sea (MS) oligotrophy. The MS is a semi-enclosed sea chronically limited by P [13], where P and N concentrations do not obey the Redfield ratio (i.e., 23–28:1) [14, 15]. Besides, Mediterranean waters are subjected to Saharan atmospheric dust deposition, which controls Fe concentrations in the water column [16]. On the other hand, the Humboldt Current System (HCS), which extends from the west coast of South America (Southern Chile) up to Ecuador and the Galapagos Islands, is one of the most productive marine ecosystems as a result of the transport of sub-Antarctic-enriched nutrient waters and often poor in Fe [17–19]. There, the endemic *Heterozostera chilensis* J. Kou seagrass thrives settled after long-distance dispersion of its ancestor, i.e., *Heterozostera nigricaulis*, from temperate waters of Australia across the Pacific Ocean [20, 21]. Noteworthy, it is intriguing how *H. chilensis* (former *H. nigricaulis*) was capable to settle in the cold waters of the HCS, concretely in Puerto Aldea, Bahia Chascos, and Isla Damas [21], where historically seaweeds have proliferated, but no seagrasses [22]. Among the many intrinsic characteristics that may have allowed *H. chilensis* to survive, the role of its associated microbiota in its maintenance and sustenance remains unclear.

Elucidating the nutrient regimes of N, P, and Fe of these microbial communities is of especial relevance as they limit microbial growth and activity [17], usually controlled by upwelling/downwelling processes or by atmospheric dust deposition [23]. The average ratio of N/P/Fe in microbial communities obeys to Redfield ratio, 16 (N):1 (P):0.0075 (Fe), and hence N and P are the major elements needed for microbial biomass, constituting around 7% and 1% of cell biomass, respectively [24, 25]. In P-limited waters, bacteria are capable of hydrolyzing P-esters contained in dissolved organic phosphorus (DOP) releasing dissolved inorganic phosphorus (DIP), through the so-called alkaline phosphatases (APases). Bacterial APases can be classified into three main families depending on the associated co-factor (i.e., Mg^{2+}, Zn^{2+}, Fe^{3+}, and/or Ca^{2+}): PhoA, PhoX, and PhoD [26]. Thus, metals, as Fe, are essential for enzyme activity as structural components. Nonetheless, Fe homeostasis has to be tightly regulated since it can promote oxidative stress by the generation of reactive oxygen species (ROS) through Fenton and Haber-Weiss reactions [27].

Multifactorial studies investigating the interactive effects of N, P, and Fe in marine microorganisms are very scarce [28–31]. Low dissolved inorganic N (DIN, e.g., NO_3^-), inorganic P (PO_4^{3-}), and Fe concentrations can impair growth, enhancing oxidative stress, morphological changes, and apoptosis processes, as well as limiting N_2-fixation rates [31]. In oligotrophic waters (e.g., North Atlantic Ocean or the MS), Fe can limit P-mechanisms as the alkaline phosphatase activity (APA) [32], and APA can be subjected to DIN concentration [30]. In the global ocean, microbial communities are faced with a wide range of nutrient regimes (e.g., from oligotrophy to eutrophic) and abiotic scenarios, selecting the best-adapted species worldwide [33]. Analyzing the biogeographic patterns of cosmopolitan species is of special relevance to better address the success of these species in adapting and surviving to a wide range of scenarios, an issue poorly studied with bacteria associated with seagrasses.

Gammaproteobacteria is one of the most distributed marine heterotrophic bacteria in the oceans [34]. Among them, the *Halomonadaceae* family (which include *Modicisalibacter*, *Halotalea*, *Zymobacter*, *Carnimonas*, *Cobetia*, *Kushneria*, and *Salinicola*) is found in almost any saline environment, being moderate halophilic bacteria and exopolysaccharides producers [35, 36]. As a result of the re-classification of the *Halomonas marina*, Arahal et al. (2002) described the genus *Cobetia* as a member of the *Halomonadaceae* [20], which comprises five species (i.e., *C. amphilecti*, *C. crustatorum*, *C. lioralis*, *C. marina*, and *C. pacifica*) [37–39]. *Cobetia* spp. are isolated as hydrocarbon-degrading, biosurfactants-producing, which display a nutritional versatility and different metabolic profiles (e.g., sugar utilization and assimilation), being sources of psychrophile enzymes. Besides, some strains have a key role in improving the water quality [40–43]. Although the ecophysiology and adaptation responses of *Cobetia* spp. remains poorly explored, the genus *Cobetia* is well distributed throughout the world oceans having been isolated from different marine ecological niches, pointing to their high adaptability.

Our genomic analysis proved that we isolated two strains that belong to the same species, inside the genus *Cobetia*, placed in geographically unrelated endemic seagrasses: *P. oceanica* from the MS and *H. chilensis* from the HCS. Based on our previous studies in which we described the sensitivity of the diazotrophic bacteria to different nutrient regimes and emerging pollutants [30, 31, 44], the aim of this study, considering the contrasting features of the MS and HCS at nutrient level, was to evaluate the physiological responses of the *Cobetia* spp. isolated, using batch cultures. For this

purpose, we conducted long-term (i.e., 12 days (d)) and short-term experiments (i.e., 4 d/96 h) towards different nutrient regimes (i.e., N, P, and Fe) and pH levels, measuring their physiological and biochemical responses.

Materials and Methods

Isolation, Sequencing, Identification, and Genomic Features of UIB 001 and 4B UA Strains

Isolation of the Strains

The strains UIB 001 and 4B UA were isolated from the roots of *P. oceanica* and leaves of *H. chilensis*, respectively. *Posidonia oceanica* roots were collected from Cala Nova (Mallorca) in Balearic Islands, Spain (39° 33′ 02.3″ N 2° 36′ 02.1″ E), while *H. chilensis* leaves were collected from the seashore of Puerto Aldea (Coquimbo), Chile (30° 17′ 37.83″ S–71° 36′ 24.55″ O). *Posidonia oceanica* roots were triturated in Tris-EDTA 1 mM pH 7.5, whereas *H. chilensis* leaves were rasped to gather the epiphytic community, which was maintained in sterile seawater. In both cases, the microbial consortia were cultured in modified artificial seawater (ASW) medium (L^{-1}: 25.0 g NaCl, 1.0 g $MgCl_2{\cdot}6H_2O$, 5.0 g $MgSO_4{\cdot}7H_2O$, 0.7 g KCl, 0.15 g $CaCl_2{\cdot}2H_2O$, 0.1 g KBr, 0.04 g $SrCl_2{\cdot}6H2O$, and 0.025 g H_3BO_3), with 1 ml L^{-1} trace metal [L^{-1}: 2.86 g H_3BO_3, 1.81 g $MnCl_2{\cdot}4\ H_2O$, 0.22 g $ZnSO_4{\cdot}7H_2O$, 0.39 g $NaMoO_4{\cdot}2H_2O$, 0.079 g $CuSO_4{\cdot}5H_2O$, and 0.049 g $Co(NO_3)_2{\cdot}6H2O$], glucose/citrate (final concentration 0.1% (v/v)), and with agarose (1.5% (p/v)). Cultures had N_2 as sole N source (with low P and Fe concentrations) and were incubated at 20 °C. The resulting colonies were subcultured in marine agar (MA) to obtain pure cultures.

Genome Sequencing

Total genomic DNA of the strains UIB 001 and 4B UA were extracted using the optimized version of Salvà Serra et al. (2018) [45]. Illumina whole-genome sequencing was performed (Eurofins Scientific, Luxemburg). Briefly, the DNA libraries were prepared following an optimized protocol and standard Illumina adapter sequences. Paired-end sequences were determined using the Illumina HiSeq platform (read mode, 2 × 150 bp). Additionally, DNAs were sequenced with a MinION Mk101B sequencer (Oxford Nanopore Technologies, Oxford, UK) for the generation of long-read sequences. The DNA library was prepared, using the rapid barcoding sequencing kit vR9 (SKQ-RBK004) and loaded into a FLO-MIN106 vR9.4 flow cell. The sequencing process was performed for 48 h (h) on MinKNOWN software v1.4.2 (Oxford Nanopore Technologies). The raw reads obtained were base called using Guppy software v3.5.1 (Oxford Nanopore Technologies). Quality of Illumina and nanopore reads were determined using fastQC (https://www.bioinformatics.babraham.ac.uk/projects/fastqc/) and NanoPlot software (https://github.com/wdecoster/NanoPlot), respectively. A hybrid assembly was done using Unicycler v0.4.7 [46] combining the Illumina and nanopore reads. The qualities of the genome sequences obtained were assessed using the Quality Assessment Tool for Genome Assemblies (QUAST) v4.5 [47]. For submission to GenBank, the whole-genome sequences were annotated with the Prokaryotic Genome Annotation Pipeline (PGAP) [48, 49].

Strain Identification

Complete 16s rRNA gene sequences were extracted from the obtained genomes and analyzed using EzBioCloud to determine the closely related species [50]. Afterward, the genome sequences or the strains UIB 001 and 4B UA were compared with the genomes of the closely related species, which were obtained from NCBI. Comparative 16S rRNA gene sequence analyses were done using the Kimura two-parameter model to calculate evolutionary distances. Cluster analyses and phylogenetic trees were built by Neighbor-Joining, using the MEGA7 software [51]. Bootstrap values were determined for 1000 replications. Average nucleotide identities by BLAST (ANIb) were determined using the JSpeciesWS tool [52]. The digital DNA–DNA hybridization (dDDH) similarity values were determined with the Genome-to-Genome Distance Calculator (GGDC) [53]. Only results of the recommended formula 2 (sum of all identities found in high-scoring segment pairs (HSPs) divided by the overall HSP length) in the GGDC analyses were considered.

Genomic Difference Detection Through Pan-Genome Analysis and Single Nucleotide Polymorphisms (SNPs)

Pan-genome analysis was performed following an already described procedure [54]. Briefly, homologous determinations were performed using the software Get_Homologues [55], based on two different algorithms: Cluster of Orthologous Genes Triangle (COGT) and Orthologous Markov Cluster (OMCL). The total number of clusters conforming the pan-genome was determined with the consensus of COGT and OMCL. Exclusive proteins of each strain, extracted from the pan-genome determination, were assigned to a functional category using the eggNOG-mapper v2 online tool [56]. Single nucleotide polymorphism (SNPs) analyses were done using Snippy (https://github.com/tseemann/snippy), using the default parameters and the genome of strain UIB 001 as a reference.

Experimental Design

Prior to the experiments, temperature (4–42 °C) and NaCl tolerance (0–20% (p/v)) were tested. Besides, biochemical tests were carried out in the Spanish Type Culture Collection (CECT) using API 20NE and API ZYM test kits (Biomerieux), following the manufacturer's instructions and adding Marine Cations Supplement in a 1/10 ratio, and incubated at 30 °C. To evaluate their ability to cope with different nutrient regimes and changes in cell morphology, bacterial cells were grown in ASW with agarose (1.5% (p/v)), containing optimal nutrients (+N, +P, +Fe, and +carbon source (C)), N_2 as sole N source (−N, +P, +Fe, and +C), without P and Fe (+N, −P, −Fe, and +C), without N, P, and Fe (−N, −P, −Fe, and +C), with N, P, Fe, and not C (+N, +P, +Fe, and −C), and without N, P, Fe, and C (−N, −P, −Fe, and −C).

Cobetia sp. isolates were cultured and acclimatized in marine broth (MB) at 20 °C and 150 r.p.m. The subcultures for seeding were centrifuged and washed with their corresponding medium without N, P, and Fe. All the experiments were performed in triplicate in sterile 50 mL Falcon tubes and/or 2 mL microplates in modified ASW culture media (without agarose), in batch cultures. We inoculated 7×10^5 cell mL^{-1} in each treatment. Samples were manipulated in a glass-clean hood to avoid Fe contamination, and cultures were maintained over 4–12 d, at 20 °C and 120 r.p.m.

Different inorganic/organic N (i.e., NH_3 from NH_4Cl and/or $C_4H_{11}NO_3$ [Tris]), inorganic P (i.e., PO_4^{3-} from K_2HPO_4), and Fe (from ferric citrate [$C_6H_5FeO_7$]) concentrations were tested at different pH (6–8), as shown in the Supplementary Table S1, based in previous works [30, 31]. Briefly, for N, four levels of inorganic (NH_3) and/or organic N (Tris) were tested: Non-N [0 mM], 0.8 mM NH_3, 1 mM Tris, and 1 mM Tris +0.8 mM NH_3; for PO_4^{3-}, two levels were tested: [Low PO_4^{3-}, 0.005 μM] and [High PO_4^{3-}, 50 μM], as well as for Fe, [Low Fe, 1 nM] and [High Fe, 1 μM]. All these concentrations were combined in three different experimental designs: (**I**) long-term studies (12 days) performing growth curves (where growth rates (μ) and duplication times (*Tg*) were measured) at pH 8 and (**II**) and (**III**) short-term studies (96 h), testing N, and PO_4^{3-} concentration effects at different pH levels, respectively. During the experiment, subsamples were taken to measure growth, alkaline phosphatase activity (APA), and reactive oxygen species (ROS). Besides, (**IV**) we measured APA under different levels of PO_4^{3-} (0.005–100 μM) and Fe (1 nm and 1 μM) at pH 8 after 96 h (Supplementary Table S1).

Flow Cytometry and Growth Responses

Flow cytometry was used to assess changes in cell abundances. For long-term studies, subsamples of the culture (1.5 mL) were daily sampled, fixed with 36% (p/v) of formalin and froze at −20 °C until reading at the end of the experiments. For the rest of the experiments, measurements were performed without freezing nor fixing. The cytometer used was the BD FACSJazz™, previously calibrated with the SPHEROTM Ultra Rainbow Fluorescent Particles, 3.08 μm. The cells were separated by adjusting the voltages, according to size and complexity: forward scatter (FCS) versus side scatter (SSC), respectively. Cell counts were adjusted to count for 10 s or 1000,000 events. To measure the growth rates (μ) and duplication times (T_g), we followed the equations used in Fernández-Juárez et al. (2020) [31]. To evaluate the effect of the low nutrient concentration (i.e., serial, simultaneous, or independent) of the growth response to P and Fe (with N replete), the log ratio effect-size criteria based on the mean treatment and control response was assessed as in Fernández-Juárez et al. (2020) [31].

Microscopical Analysis

Microscopical images were taken with the Leica TCS SPE confocal microscope, Leica Microsystems. The samples were placed on a clean slide with DAPI at a final concentration of 0.1 mg mL^{-1}. The samples were kept in the dark until reading, taking the images with the ×100 objective combining the brief-field I (BF) channel. Images were processed with ImageJ software, and cell volume was calculated following Hillebrand et al. (1999) [57].

Alkaline Phosphatase Activity

Alkaline phosphatase activity (APA) was evaluated using a fluorometric assay and following the MUF-P hydrolysis [30]. At the end of the experiment, APA was tested at low levels of PO_4^{3-} (i.e., 0.005 μM) with low or high levels of Fe (1 nm or 1 μM) combined with different pH levels (pH 6–8). Moreover, a battery of concentrations of PO_4^{3-} (0.005, 0.05, 0.5, 5, 50, and 100 μM) combined with different levels of Fe (1 nm and 1 μM) at pH 8 was performed (Supplementary Table S1). An endpoint assay was conducted, using 5 μM MUF-P. After 1 h of incubation in darkness at room temperature, APA was measured in a microtiter plate that contained buffer borate pH 10 (3:1 of sample: buffer). With a Cary Eclipse spectrofluorometer (FL0902M009, Agilent Technologies), MUF production (fmol MUF $cell^{-1}$ h^{-1}) was measured at 359 nm (excitation) and 449 nm (emission), using a calibration standard curve with commercial MUF (Sigma-Aldrich). Results were normalized by cell number.

Structural Analysis of the Alkaline Phosphatase

Sequences of PhoD of the UIB 001 and 4B UA (locus_tag: HA399_02660 and H2O77_02640) in FASTA format were sent to the I-Tasser server for protein 3D-structure prediction [58], with their domains previously checked in Pfam 32.0

[59]. The predicted structures were sent to POSA for a structural alignment between them [60]. The description of the Ca^{2+} and Fe^{3+} coordination positions of these proteins was based on the descriptions of the catalytic center of the PhoD from *C. amphilecti* KMM 296 (WP_043333989) [61] and the PhoD crystal structure of *Bacillus subtilis* (PDB: 2YEQ). Residues from PhoD from UIB 001 and 4B UA strains against the PhoD of *C. amphilecti* KMM 296 were mapped through alignments with Uniprot Clustal Omega [62]. The predicted structures and the corresponding structural alignments were visualized with Pymol [63].

Reactive Oxygen Species Production

ROS detection was measured with the molecular probe 2′,7′-dichlorofluorescein diacetate (DCFH-DA, Sigma) [31]. Briefly, bacterial samples were placed in a 96-well microplate (Thermo Scientific) spiked with DCFH-DA at a final concentration of 15 μg mL^{-1}. The green fluorescence product, 2′,7′-dichlorofluorescein (DCF), generated after its oxidation by ROS was measured at 25 °C in the Eclipse spectrofluorometer (FL0902M009, Agilent Technologies) for 1 h with an excitation of 480 nm and emission of 530 nm. The results were expressed as the slope of the linear regression obtained and normalized by cell (arbitrary units [AU] $cell^{-1}$). DCFH-DA was added in ASW without cells as blanks under the same conditions.

Statistical Analysis

A parametric univariate analysis of variance (ANOVA) factor and post hoc (Bonferroni) was used to study the effect of N, P, and Fe concentrations in the UIB 001 and 4B UA strains. The statistical analyses were performed using the SPSS software v21 (IBM Corp year 2012).

Results

Characterizing *Cobetia* Sp. UIB 001 and 4B UA

Genomic Analyses

Based on 16S rRNA, ANIb, and GGDC analyses, we revealed that both strains from the endemic Mediterranean seagrass *P. oceanica* and the endemic HCS seagrass *H. chilensis*, respectively, corresponded to the same species and belonging to the *Cobetia* genus (Table 1, Fig. 1, Supplementary Tables S2, S3 and S4). The 16s rRNA analysis of the UIB 001 and 4B UA strains showed a similarity between 99.5 and 99.9% with the type strains *C. amphilecti* KMM 1516^T, *C. litoralis* KMM 3880^T, *Cobetia marina* JCM 21022^T, and *C. pacifica* KMM 3879^T (Supplementary Table S2). Besides, the 16S rRNA phylogenetic tree showed a clade formed by these species, supported with high bootstrap values (Fig. 1). Based on these results, the UIB 001 and 4B UA strains seem to be more closely related to *C. amphilecti* and *C. litoralis* (Supplementary Table S2). In agreement with the 16s rRNA analysis, ANIb and DDH analyses also confirmed that strains UIB 001 and 4B UA belong to the same species, showing a similarity over 96% (ANIb) and 70% (dDDH) between them (Table 1 and Supplementary Tables S3 and S4). Comparisons with genomes of the *Cobetia* genus present in GenBank were carried out to provide deeper insights into their taxonomic affiliation (Supplementary Table S3 and S4). There is an important lack of genome sequences of type strains inside the *Cobetia* genus, being *C. marina* the unique species for which the type strain has been genome sequenced (JCM 21022^T, accession number CP017114). The genome of *C. amphilecti* KMM 296, which is not the type strain, showed the highest score by ANIb and dDDH (over 96 and 70%, respectively), indicating that, presumably, our strains might be representatives of *C. amphilecti* (Supplementary Tables S3 and S4). However, due to the lack of type strain genomic information, it was not possible to perform an accurate final taxonomic classification at the species level. Overall, with our results, we can affirm that the strains isolated belong to the *Cobetia* genus, and they are not *C. marina*. Thus, the strains were named *Cobetia* sp. UIB 001 and 4B UA.

Genomic Features

Sequencing and assembly procedures generated two complete and closed genomes. The genome sequence of the strain UIB 001 was composed of one chromosome (4,177,647 bp) and one putative plasmid (10,679 bp), while the genome of strain 4B UA was composed of one chromosome (4,319,205 bp) and two putative plasmids (4702 and 2015 bp). The main genomic features of each genome are included in Table 1 and Fig. 2A and B. The complete genome sequences were deposited at DDBJ/EMBL/GenBank under the accession numbers CP058244 to CP058245 (*Cobetia* sp. UIB 001) and CP059843 to CP059845 (*Cobetia* sp. 4B UA).

Genomic Differences

The pan-genome analysis determined that both strains shared 3087 homologous proteins (Fig. 3A). Functional analysis of the entire set of proteins of each strain displayed that both strains shared almost the same distribution of gene functions (Supplementary Fig. S1). Additionally, 197 proteins were exclusively present in the strain UIB 001, whereas the strain 4B UA had 278 specific proteins (Fig. 3A). It is worth mentioning that the functional category with the most representatives was "Function unknown" (Fig. 3B). Results from the SNPs

Table 1 Genomic features of *Cobetia* sp. UIB 001 and 4B UA

	UIB 001	4B UA
Genome length (bp)	4,177,647	4,319,205
G+C (%)	62.78%	62.56%
Genes	3488	3562
Protein-coding genes	3391	3474
rRNA operons	7	7
tRNA genes	74	72
Putative plasmids	1 (10,679 bp)	2 (4702 and 2015 bp)
16s rRNA identity (%, between each other)	100%	100%
ANib (%,between each other)	96.99%	96.93%
dDDH (%,between each other)	75.80	75.80%

analysis showed up to 66,929 SNPs between both strains. Among the "classical" proteins implicated in the adaptation and survival to low N, P, and Fe availability, we detected up to 1045 SNPs, 470 SNPs for proteins related to N-metabolism, 277 SNPs for proteins related to P-metabolism, and 298 SNPs for proteins related to Fe-metabolism (Fig. 3C).

Phenotypic Features

From the phenotypic point of view, these rod-shaped bacteria (1–1.5 μm length and 0.7–0.8 μm width) were able to grow in nutrient-depleted media, i.e., in N-, P-, and Fe-depleted solid media (with 1.5% (p/v) agarose), as long as carbon (C)

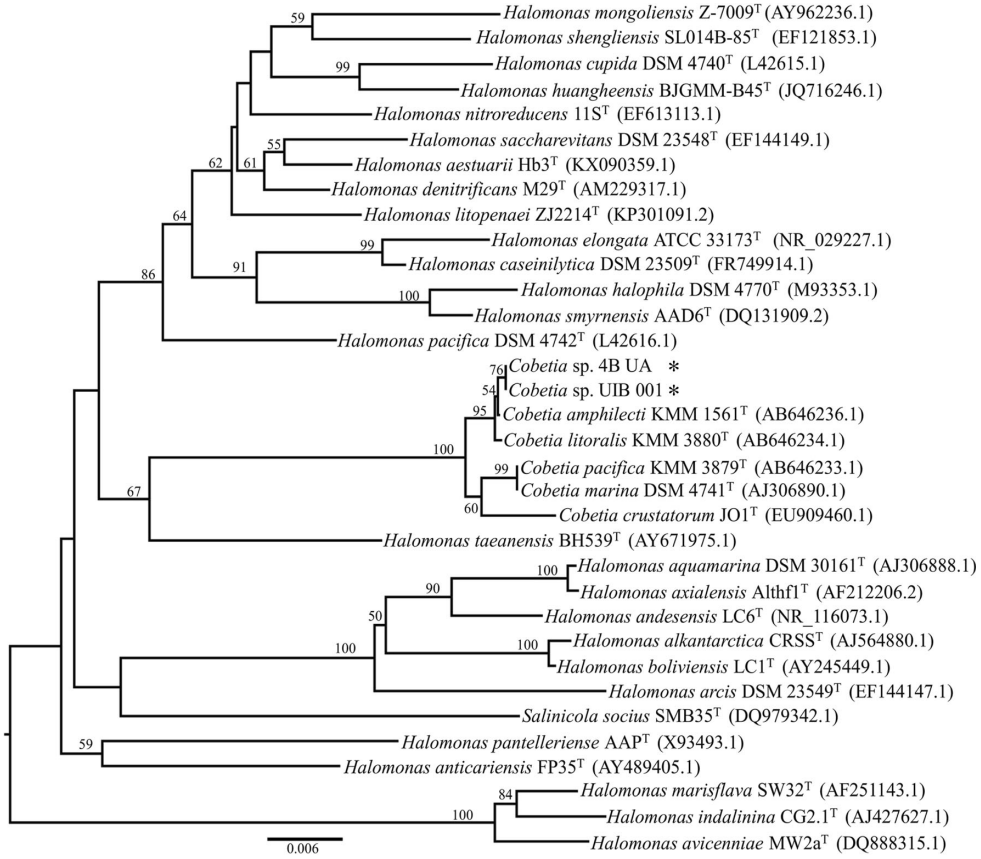

Fig. 1 Complete 16s rDNA phylogenetic tree of *Cobetia* spp. and other closely related groups, including the strains *Cobetia* sp. UIB 001 and 4B UA (*)

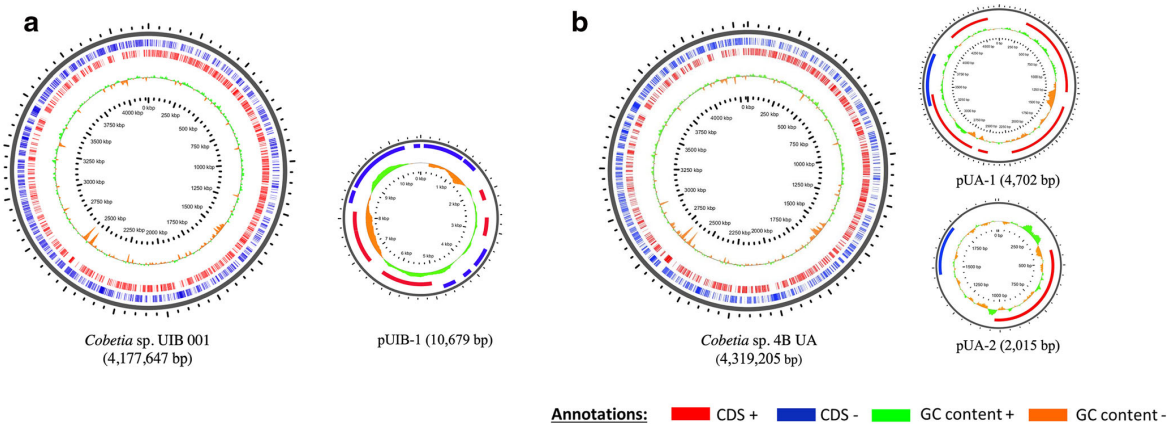

Fig. 2 Genome BLAST atlas of the chromosomes for the strains **A** UIB 001 and **B** 4B UA, showing the overall similarity of the chromosome organization between them. Position of CDS+ and CDS−, as well as GC content, is indicated

source was present (Table 2). In agreement with the species more related to them (*C. amphilecti* KMM 1516^T and *C. litoralis* KMM 3880^T), both isolated had a tolerance over 15% NaCl (yet growth was not detected at 20% NaCl) and up to 42 °C (Table 2). Overall, biochemical tests showed that both *Cobetia* sp., UIB 001 and 4B UA, had the same metabolic profiles and similar to the most related type strains (Table 2).

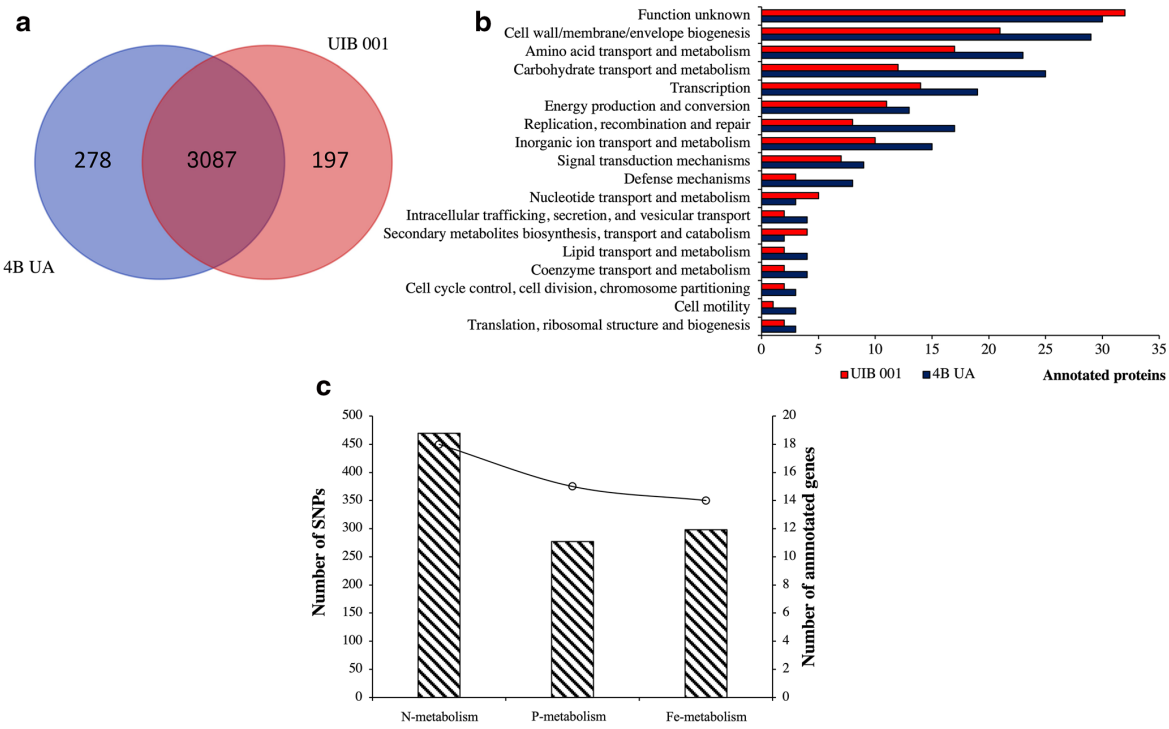

Fig. 3 Genomic differences between *Cobetia* sp. UIB 001 and 4B UA. **A** Pan-genomic analysis between *Cobetia* sp. UIB 001 and 4B UA, showing the number of shared proteins between the strains, as well as the number of exclusive proteins of each strain. **B** Functional categorization by COG analyses of the exclusive proteins of UIB 001 and 4B UA strains. **C** Number of SNPs detected in genes implicated in N, P, and Fe metabolism. The bar chart represents the number of SNPs, whereas, lines represent the number of annotated genes implicated in N, P, and Fe metabolism

Table 2 Differential phenotypic characteristics of the *Cobetia* sp. UIB 001 and 4B UA and the most related *Cobetia* sp. species, *Cobetia amphilecti* KMM 1516^T and *Cobetia litoralis* KMM 3880^T, whose results were obtained from Romanenko et al. (2016)

		UIB 001	4B UA	KMM 1516^T	KMM 3880^T
	Habitat	Mediterranean Sea (Balearic Islands, Spain)	Humboldt Current System (Puerto Aldea, Chile)	Internal tissue of the sponge *Amphilectus digitatus* (Alaska)	Sandy sediment sample collected at a depth of 1 m from the shore of the Sea of Japan, Russia
	Motility	–	–	+	+
	Morphology	Rod-shaped (0.76 μm width and 1.2 μm length)	Rod-shaped (0.76 μm width and 1.1 μm length)	Rod-shaped (0.8–0.9 μm width and 1.1–1.6 μm length)	Rod-shaped (0.7–0.9 μm width and 1.8–2.2 μm length)
Growth Nacl (%)	0%	–	–	s	s
	1%	+	+	+	+
	10%	+	+	+	+
	20%	–	–	+	+
Growth (°C)	4 °C	+	+	+	+
	42 °C	+	+	+	+
Optimum pH		≅ 8	≅ 8	6.5–8.5	7.5–8.5
Growth under very low nutrient concentration	(+P+Fe+N+C)	++	++	Non-tested	Non-tested
	(−P−Fe+N+C)	++	+		
	(+P+Fe−N+C)	+	+		
	(−P−Fe−N+C)	+	+		
	(+P+Fe+N−C)	–	–		
	(−P−Fe−N−C)	–	–		
API 20NE test	PNPG test; assimilation D-glucose, D-mannitol, maltose and D-gluconate	+	+	+	+
	Nitrate reduction, indole production, glucose fermentation, arginine dihydrolase and urease activity, aesculin hydrolysis, gelatinase; assimilation of L-arabinose, N-acetylglucosamine, D-mannose	–	–	–	–
	Caprate	–	w	–	+
	Adipate	–	w	–	–
	L-Malate	w	w	+	+
	Citrate and phenylacetate	w	w	–	–
Enzyme activities (API ZYM)	Alkaline phosphate, esterase (C4), esterase lipase (C8), acid phosphatase, *a*-glucosidase naphthol-AS-BI-phosphohydrolase	+	+	+	+
	Lipase (C14), cystine arylamidase, trypsin, *a*-chymotrypsin, *a*-galactosidase, β-glucuronidase, β-glucosidase, N-acetyl-β-glucosaminidase, *a*-mannosidase, *a*-fucosidase	–	–	–	–
	Valine arylamidase, β-galactosidase	–	–	w	–

Symbols +, −, w, and s, indicate positive, negative, weak, and slow reaction, respectively

Long- and Short-Term Effects of Varying Nutrient Concentration (N, P, and Fe)

Effect on Morphology

Nitrogen, P, and Fe triggered differential responses on the morphology of the UIB 001 and 4B UA strains (Fig. 4A–I). With N_2 as the sole N source, rod-shaped cells became more circular (≃1.2 μm length and 0.97 μm width) than under optimal nutrient conditions (≃1.16 μm length and 0.76 μm width) (Fig. 4C, D, and I). Under P/Fe or total nutrient (N, P, and Fe) depletion, cells became larger and wider (≃1.68 μm length and 0.95 μm width) than under optimal concentrations (≃1.16 μm length and 0.76 μm width) (Fig. 4E–I). Overall,

under low nutrient concentrations, both strains' volume (μm^3) significantly increased (Fig. 4I).

Changes of N Concentrations

Long-Term Effect of N Long-term studies testing N_2 as the sole N source showed differential effects between UIB 001 and 4B UA (ANOVA, $p < 0.05$, Fig. 5A and B). N-depletion for UIB 001 reduced cell growth by 3-fold (μ, 0.18 d^{-1} and *Tg*, 3.87 d) compared to optimal nutrient conditions (μ, 0.51 d^{-1} and *Tg*, 1.37 d) (Bonferroni test, $p < 0.05$, Fig. 5B). Nevertheless, UIB 001 strain was capable to grow under this condition, showing its diazotrophic features. Although we did not find any annotated *nif* genes, UIB 001 possesses a cbb3-type cytochrome oxidase (locus_Tag: HA399_01480) found in N_2-fixing organisms and had active N_2-fixation rates (Supplementary Fig. S2A). Besides, both strains were capable of growth in Burk's N-free medium, recommended for detecting N_2-fixing organisms [64] (Supplementary Fig. S2B).

Short-Term Effects of N along with pH Different N sources (i.e., inorganic, NH_3, and/or organic, Tris) triggered different effects on UIB 001 and 4B UA at pH 8 after 96 h (ANOVA, $p < 0.05$, Fig. 5C). For both, increasing N sources had a positive impact, reaching the highest growths at 0.8 mM of NH_3 and 1 mM of Tris for UIB 001 and 4B UA, respectively (Fig. 5C). However, combining inorganic and organic N sources (i.e., 1 mM Tris + 0.8 mM NH_3) impaired the growth of both strains (Bonferroni test, $p < 0.05$, Fig. 5C). At low N levels (i.e., 0.08 mM NH_3), UIB 001 responded better than 4B UA. However, organic N (i.e., 1 mM Tris) was more toxic to UIB 001 than 4B UA (Bonferroni test, $p < 0.05$, Fig. 5C).

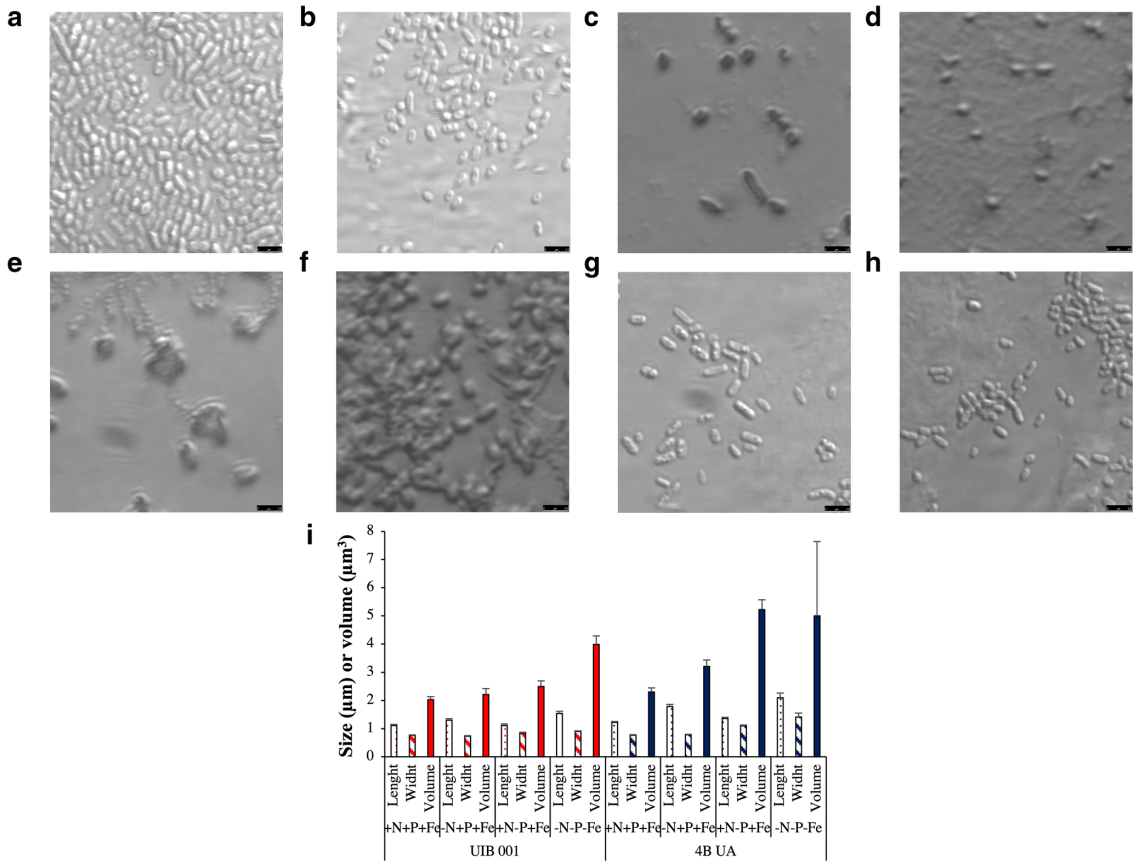

Fig. 4 Microscopic analysis of *Cobetia* sp. UIB 001 and 4B UA under different N, P, and Fe nutrient regimes. **A** Optimal condition, +N + P + Fe + C, for the UIB 001 strain. **B** Optimal condition, +N + P + Fe + C, for the 4B UA strain. **C** N_2 as the sole N source, −N + P + Fe + C, for the UIB 001 strain. **D** N_2 as the sole N source, −N + P + Fe + C, for the 4B UA strain. **E** P- and Fe-depleted condition, +N−P−Fe + C, for the UIB 001 strain. **F** P- and Fe-depleted condition, +N−P−Fe + C, for the 4B UA strain. **G** Nutrient-depleted condition, −N−P−Fe + C, for the UIB 001 strain. **H** Nutrient depleted condition, −N−P−Fe + C, for the 4B UA strain. **I** Length, width, and volume changes derived from changes in nutrient regimes for *Cobetia* sp. UIB 001 and 4B UA. For **A–H**, microscopical images were taken at ×100 with 4.73 of zoom

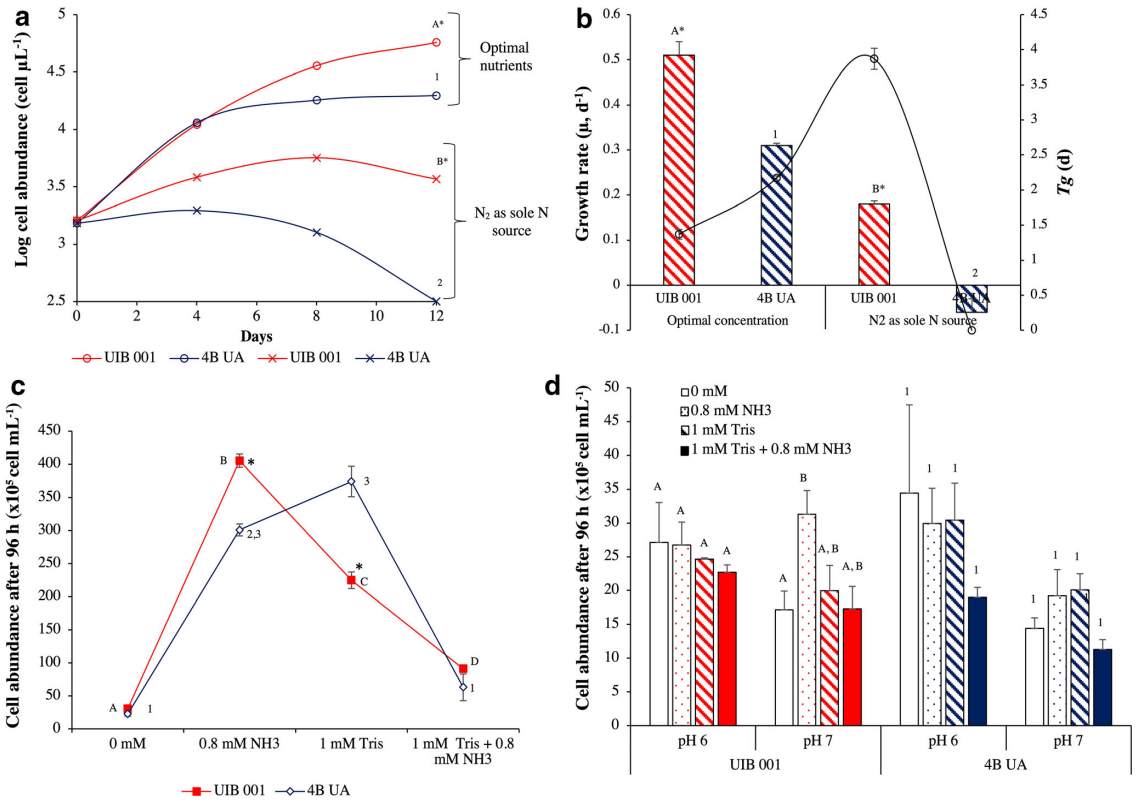

Fig. 5 Nitrogen (N) concentration effect for *Cobetia* sp. UIB 001 and 4B UA. **A–B** Long-term effect. **A** Growth curve under the optimal condition and N_2 as the sole N source and **B** growth rate (µ, d^{-1}, as a bar chart) and duplication time (*Tg*, d, as a line) under the optimal condition and N_2 as the sole N source. **C–D** Short-term (cell abundance, cell mL^{-1}) after 96 h under different N sources (inorganic, NH_3, or organic, Tris) at **C** pH 8 and **D** at pH 6 and 7. Values are the mean ± SE between the replicates. Letters (for UIB 001) and numbers (for 4B UA) indicate significant differences according to the treatment inside each strain, and asterisks (*) indicate significant differences between each strain inside each treatment, using a post hoc test (Bonferroni test, $p < 0.05$) after ANOVA over the whole dataset

Lowering pH to 6 or 7 affected growth to a higher degree than the N source itself (ANOVA, $p < 0.05$, Fig. 5D). Indeed, the significant differences found previously were banished when pH was dropped, without any differences between strains (ANOVA, $p > 0.05$, Fig. 5D), except for UIB 001 at pH 7, in which 0.8 mM of NH_3 had a positive impact on cell abundance (Bonferroni test, $p < 0.05$, Fig. 5D).

Changes of P and Fe Concentrations

Long-Term Effect of P and Fe Not surprisingly, higher growth rates (µ) were reached under optimal PO_4^{3-} and Fe concentrations than at low PO_4^{3-}, decreasing growth ≃ 2-fold for both strains, and more pronouncedly at low Fe levels (ANOVA, $p < 0.05$, Fig. 6A and B). Noteworthy, higher µ and lower *Tg* were reached by UIB 001, compared to 4B UA, independently of the nutrient levels (Bonferroni test, $p < 0.05$, Fig. 6B).

Short-Term Effects of P and Fe Along with pH Short-term studies (during 96 h) showed that for both strains, PO_4^{3-}/Fe concentrations and pH levels (6, 7, and 8) variations significantly affected cell abundances (ANOVA, $p < 0.05$, Fig. 6C). Overall, low concentrations of PO_4^{3-} and Fe combined with different pH levels (6–8) did not significantly differ between strains (ANOVA, $p > 0.05$, Fig. 6C), albeit a higher tolerance to lower pH was observed for the UIB 001 strain. However, at pH 8 and low PO_4^{3-} and Fe levels, UIB 001 grew as it did at high PO_4^{3-} and Fe levels (Bonferroni test, $p > 0.05$, Fig. 6C), as opposed to 4B UA (Bonferroni test, $p < 0.05$, Fig. 6C). Decreasing pH levels had a dramatic effect on cell abundances (i.e., pH 6 and 7) (Bonferroni test, $p < 0.05$, Fig. 6C), showing that pH 8 was the optimum for UIB 001 and 4B UA strains independently of PO_4^{3-} and Fe levels (Fig. 6C).

Effect of Low Concentrations of P and Fe The responses to low PO_4^{3-} and Fe availability (under long term or short term) for both strains revealed an independent effect of P and Fe (P

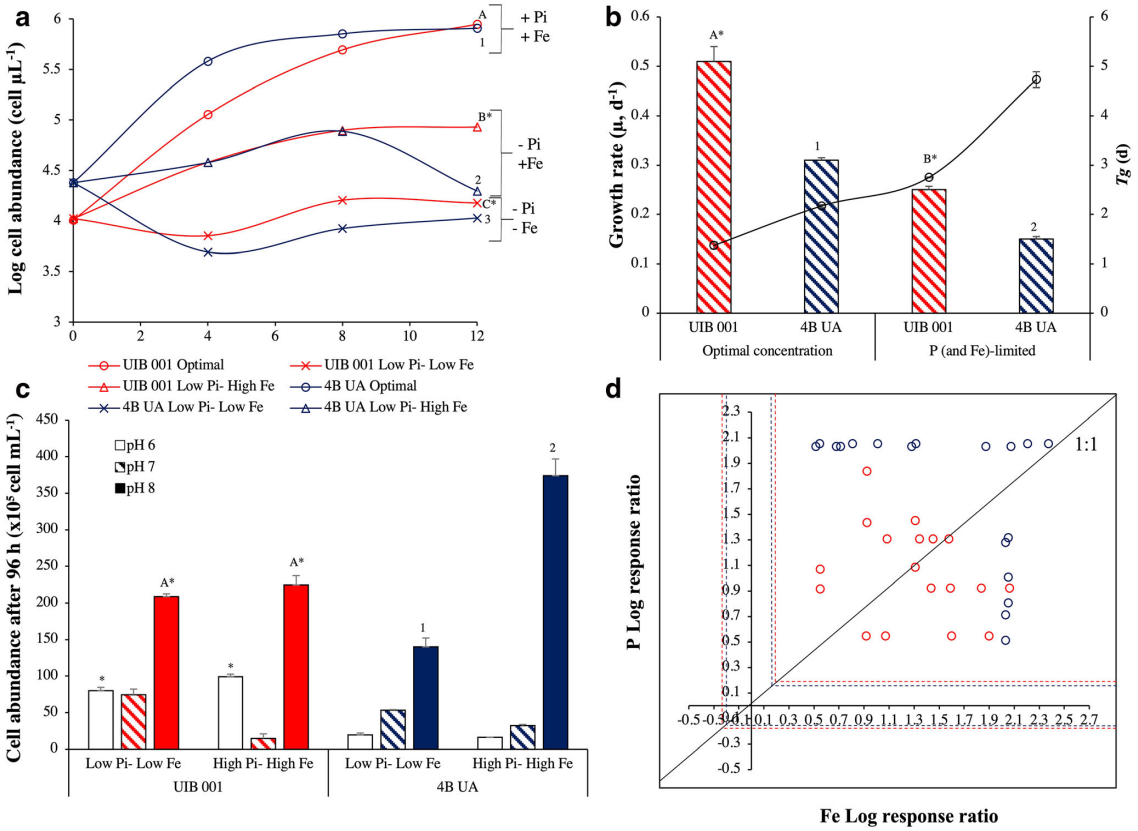

Fig. 6 Phosphorus (P) and Fe concentration effect for *Cobetia* sp. UIB 001 and 4B UA. **A–B** Long-term effect studies. **A** Growth curve under optimal nutrient condition and low PO_4^{3-} and/or Fe concentrations (0.005 µM and/or 1 nM, respectively) and **B** growth rate (µ, d^{-1}, as a bar chart) and duplication time (*Tg*, d, as a line) curve under optimal nutrient condition and low PO_4^{3-} and/or Fe concentrations. **C** Short-term studies (cell abundance, cell mL^{-1}) after 96 h under different PO_4^{3-} and Fe concentrations at pH 6, 7, and 8. In **A-C** values are the mean ± SE between the replicates. Letters (for UIB 001) and numbers (for 4B UA) indicate significant differences according to the treatment inside each strain, and asterisks (*) indicate significant differences between each strain inside each treatment, using a post hoc test (Bonferroni test, $p < 0.05$) after ANOVA over the whole dataset. PO_4^{3-} is represented as Pi**. D** Log P and Fe responses. Each data point represents each replicate (red: UIB 001; blue: 4B UA) in which *X*-axis is the P log response and *Y*-axis is the Fe log response. Dashed red (for *Cobetia* sp. UIB 001) and blue lines (*Cobetia* sp. 4B UA) represent the critical threshold values (data points outside the critical values are significantly different (at $p = 0.05$) from P_0Fe_0)

response >0, Fe response >0 and P + Fe response >0, $p < 0.05$, Fig. 6D). The threshold for P and Fe was slightly lower for UIB 001 than 4B UA, displaying a better response to low concentrations of P and Fe.

Effects of P on APA and Structure of PhoD The alkaline phosphatase activity (APA) was extremely influenced by pH at low PO_4^{3-} levels, i.e., 0.005 µM (ANOVA, $p < 0.05$, Fig. 7A). Alkaline pH (i.e., pH 8) enhanced APA an average of 40-fold in both strains compared with the acidify conditions (Bonferroni test, $p < 0.05$, Fig. 7A). Different Fe levels (1 nM–1 µM) did not cause any significant differences in APA at [Low PO_4^{3-}], i.e., 0.005 µM (ANOVA, $p < 0.05$, Fig. 7A). Increasing levels of PO_4^{3-} (up to 100 µM) induced different inhibition responses on each strain (ANOVA, $p < 0.05$, Fig. 7B), detecting positive feedback with Fe, especially for the *Cobetia* sp. UIB 001 (Fig. 7B). For the UIB 001, at pH 8 and high levels of Fe (1 µM), APA did not respond to higher P levels (up to 50 µM) and required the highest PO_4^{3-} level (100 µM) to inhibit its activity (Bonferroni test, $p < 0.05$, Fig. 7B), unlike for 4B UA in which APA at 50 µM was significantly inhibited (Bonferroni test, $p < 0.05$, Fig. 7B).

Structural analysis revealed the potential protein structure and the catalytic center for both PhoD of UIB 001 and 4B UA (Fig. 7 C and D). PhoD sequences shared an identity of 88%, while at the structural level, they shared an identity of 76%. Both PhoD had the same catalytic center as predicted for the PhoD of *C. amphilecti* KMM 296 (WP_043333989): ASP (241/238), TYR (244/241), ASP (306/303), HIS (308/305),

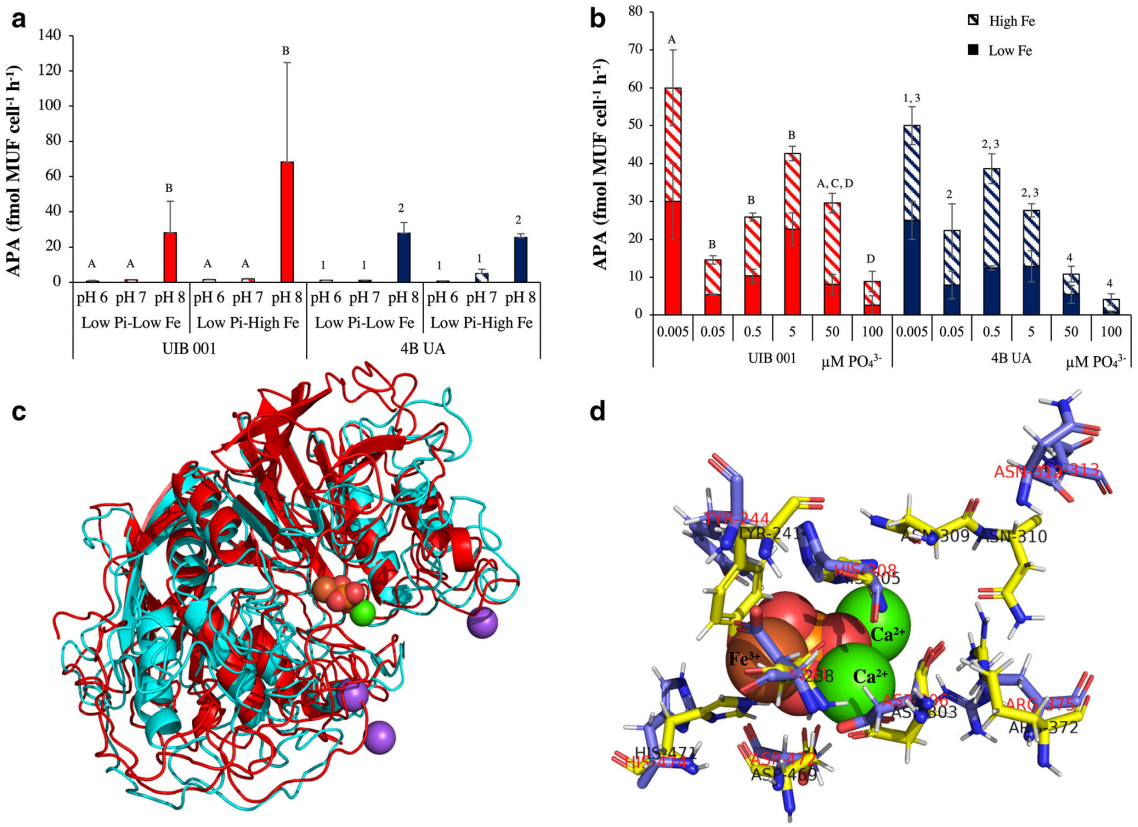

Fig. 7 P-acquisition mechanisms for *Cobetia* sp. UIB 001 and 4B UA. **A** Alkaline phosphatase activity (APA) under low levels of PO_4^{3-} (0.005 μM) and differential concentration of Fe (1 nm and 1 μM). **B** APA under different levels of PO_4^{3-} (0.005–100 μM). Solid bars are low Fe level conditions, whereas the stripped bars are under high levels conditions. Values are the mean ± SE between the replicates. Letters (for UIB 001) and numbers (for 4B UA) indicate significant differences according to the treatment inside each strain using a post hoc test (Bonferroni test, $p < 0.05$) after ANOVA over the whole dataset. PO_4^{3-} is represented as Pi. **C–D** Protein structural analysis base on the description of the PhoD of *C. amphilecti* KMM 296. **C** Structural analysis of PhoD from UIB 001 (red) and 4B UA (blue) strains. **D** Catalytic center for PhoD: UIB 001 strain, in red (aa letters) and blue (aa structure), and 4B UA, in black (aa letters) and yellow (aa structure)

ASN (312/309), ASN (313/310), ARG (375/372), ASP (472/469), and HIS (474/471) (Fig. 7D).

Effects of N, P, and Fe on ROS Production Along with pH

Different pH levels had a significant effect on ROS production for both strains (ANOVA, $p < 0.05$, Fig. 8A). Alkaline pH (i.e., pH 8) reduced an average of 15-fold ROS compared with the acidify conditions (Bonferroni test, $p < 0.05$, Fig. 8A). At pH 8, ROS production was affected by the different sources of inorganic and organic N (ANOVA, $p < 0.05$, Fig. 8B). However, no significant differences were achieved between strains (ANOVA, $p > 0.05$, Fig. 8B), decreasing ROS production with an increase of N (ANOVA, $p < 0.05$, Fig. 8B). Indeed, different PO_4^{3-} and Fe levels did not have any effect on ROS production for both strains (ANOVA, $p > 0.05$, Fig. 8C), except for 4B UA at high concentrations of PO_4^{3-} and Fe, with ROS production decreasing significantly compared to [Low PO_4^{3-}-High PO_4^{3-}] condition (Bonferroni test, $p < 0.05$, Fig. 8C).

Discussion

For decades, the study of microbial biodiversity has sought to determine why microbes live where they live, embracing the tenet that "Everything is everywhere, but the environment selects" [33]. Here, we isolate and identify two strains of the same species (i.e., as endophytic and epiphytic bacteria, *Cobetia* sp. UIB 001 and 4B UA) which thrive on two different seagrasses in contrasting environments: *Posidonia oceanica* found in the Mediterranean Sea (MS) and the *Heterozostera chilensis* (formerly *H. nigricaulis*) found in the Humboldt current system (HCS). As noticed before, the MS is an oligotrophic semi-enclosed sea, where *P. oceanica* is

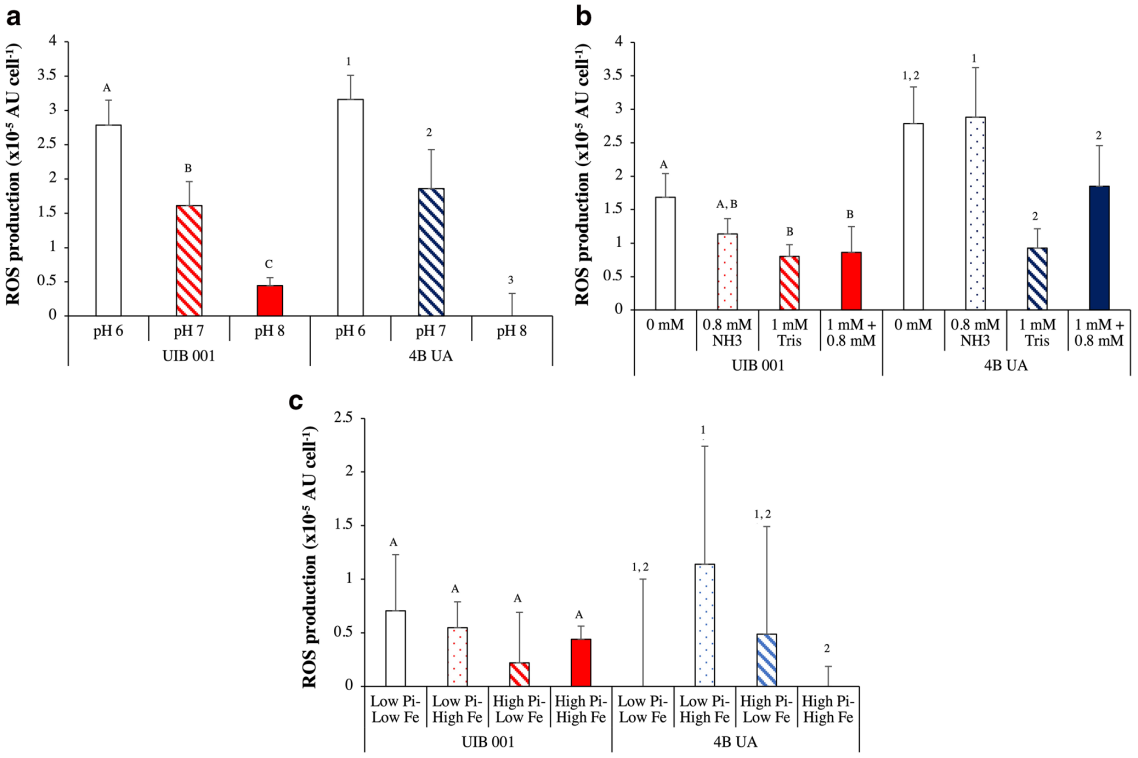

Fig. 8 Reactive oxygen production (ROS) production for *Cobetia* sp. UIB 001 and 4B UA. **A** At different pH levels (6–8). **B** At different concentrations of N source. **C** At different combinations of PO_4^{3-} and Fe. Values are the mean ± SE between the replicates. Letters (for UIB 001) and numbers (for 4B UA) indicate significant differences according to the treatment inside each strain using a post hoc test (Bonferroni test, $p < 0.05$) after ANOVA over the whole dataset. PO_4^{3-} is represented as Pi

widely extended, while the HCS is a nutrient-rich cold current where *H. chilensis* thrives in just a few locations, settled relatively recently [21]. Our results suggest that regardless of the contrasting environments considered, the same endophytic and epiphytic bacteria can perform analogous functions and adapt similarly to stressful scenarios.

After culturing the whole epiphytic community of both seagrasses, the gamma-proteobacteria *Cobetia* sp. (UIB 001 and 4B UA) arose above all in both seagrasses. Although we made an effort to taxonomic classify these isolates, it was only possible to determine that both strains are the same *Cobetia* species, presumably *C. amphilecti*, and they do not belong to the *Cobetia marina* species. Due to the lack of type strain genome sequences of the genus *Cobetia*, precise taxonomic classifications cannot be performed from the genomic point of view. From a genomic view, high G + C % contents were detected in both strains (i.e., 62–63%), which has previously been correlated to N availability [65]. This means that the ecological niche of *Cobetia* sp. UIB 001 and 4B UA are rich in N, probably by the high rates of N_2-fixation detected in *P. oceanica* (i.e., higher than the rest of tropical seagrasses) [9] and the high N availability in the HCS [19]. Even though Balabanova et al. (2016ab) did not show physiological data, it revealed the potential genomic adaptation to the changing nutrient regimes of *C. amphilecti*, reporting different metabolic and biochemical profiles between differential strains placed in different marine niches [66, 67]. Yet, this work reveals that the *Cobetia* sp. isolates respond differently to seawater conditions. Thus, we hypothesize that these different traits might be the consequence of a different genomic evolution subjected to environmental pressures that led to the development of specific proteins and the significant number of SNPs that were found.

According to classical classifications [68, 69], both *Cobetia* sp. strains (UIB 001 and 4B UA), might belong to the group of oligotrophic bacteria, as they were capable of growing with minimal content of organic matter and nutrients (i.e., 1–15 mg of C mL^{-1} and N_2 as the sole N source). Indeed, these strains may be considered as extreme oligotrophic bacteria, as they were able to grow with N_2 as the sole N source, and P- and Fe-depleted conditions, being just dependent on the carbon (C) source (e.g., citrate or glucose), as metabolic tests revealed. Oligotrophic bacteria usually have small sizes (≤ 1 μm) to optimize the low availability of resources

available by increasing their S/V ratio. However, microbes can expand their size to increase the cell surface area to accommodate enough uptake sites to meet uptake demands [70], as observed in both *Cobetia* sp. Through this plasticity to respond to the changing environment, bacteria play a key role in marine food webs and nutrient recycling (e.g., accumulation, export, remineralization, and transformation of nutrients), being a reservoir for nutrients as C, N, and P [71, 72], as *Cobetia* sp. does for the sustenance and maintenance of both seagrasses.

The ability to grow with N_2 as the sole N source and the N_2-fixation activity found in the UIB 001, remarks its potential role as N_2-fixer, as previously seen in other *Cobetia* spp., isolated as hydrocarbon-utilizing microbiota [73, 74]. Although non-putative N_2-fixation genes annotated were found in their genomes (i.e., UIB 001 and 4B UA), genes typically involved in N_2-fixing bacteria as ADP-ribosyl (dinitrogen reductase) glycohydrolase (*draG*), which products can regulate the nitrogenase complex (i.e., formed by NifH, NifK, and NifD) [75], and cbb3-type cytochrome c oxidase, required for symbiotic N_2-fixation [76], were found in both bacteria. This observation may suggest that the UIB 001 might contain alternative genes for N_2-fixation. Noteworthy, the utilization of trace amounts of atmospheric ammonia through high-affinity ammonium transporters (AmtB) might be also a potential source of N for extreme oligotrophic bacteria [77], which explains why isolated 4B UA was capable of growth in (semi)solid media with N_2 as sole N source.

In vast oligotrophic areas of the ocean, N_2-fixation is limited by P [78], while, in eutrophic coastal areas, P can trigger harmful algal blooms [79]. In our experiments, only the 4B UA strain isolated from the eutrophic HCS was P limited, as opposed to the oligotrophic MS isolate (UIB 001) that was relatively unaffected. Contrariwise, APA of the UIB 001 strain was prolonged with a higher concentration of PO_4^{3-} (without enhancing ROS production, unlike the 4B UA), suggesting a higher P-demand to achieve homeostasis. Previously, it was observed that under low concentrations of P, bacteria associated with *P. oceanica* (e.g., *Halothece* sp. species) were able to release dissolved inorganic phosphorus (DIP) from dissolved organic phosphorus (DOP) through the alkaline phosphatases (APases), which are expressed and activated through the PhoB-PhoR system [30]. Alkaline phosphatase D (PhoD) varied between the two strains at the sequence and structural levels, 88% and 76%, respectively, pointing to the structural differences as the most relevant in the differential APA, due to the lack of differences at the catalytic center.

Both APases are Fe-dependent (such as antioxidant enzymes or the nitrogenase complex [27, 80]) and are therefore impacted by the extended iron limitation throughout the ocean, including the MS and the HCS [17]. For both strains, APA was enhanced by increasing Fe levels since we predict in our PhoD model the coordination with one Fe^{3+} atom. However, high Fe levels did not induce ROS production at the optimal pH 8. Ferric iron, Fe^{3+}, is insoluble at neutral pH, but at a lower pH, its solubility increases. At acidified pH, organic ligands have less affinity for Fe, reducing Fe absorption and thus affecting cell growth [81]. Moreover, ROS production was enhanced under acidic pH (i.e., pH 6), possibly by lower intracellular Fe content for antioxidant enzymes (e.g., superoxide dismutase, catalase, glutathione reductase, or glutathione peroxidase).

The increasing carbon dioxide (CO_2) concentrations emitted to the atmosphere are irremissibly increasing ocean acidification (OA), posing serious risks to marine life [82]. However, lower pH levels may ameliorate some of the concomitant impacts of OA, i.e., reducing the impacts of un-ionized NH_3 on the activity of some cytosolic enzymes [83]. Both *Cobetia* sp. were significantly affected by high N sources at pH 8, but not at pH 6 or 7, not accompanied by ROS increments, suggesting that antioxidant enzymes were not affected by un-ionized NH_3. Moreover, it has been observed that OA may play a significant role in P eutrophication [84]. Previous works pointed to the sensitivity of the APA of *Cobetia* spp. exposed to acidification [61, 85, 86].

Our multifactorial design showed that the same species growing in different ocean basins (i.e., MS or HCS) displays different physiological and biochemical responses to different nutrient regimes (N, P, and/or Fe). Not surprisingly, the Mediterranean strain (exposed to oligotrophic water of the MS) coped with low N and P concentrations more efficiently. Nonetheless, the appearance of oligotrophic bacteria in nutrient replete waters (i.e., 4B UA) may point to the origin of this species, as its host, *H. chilensis*, reached the Chilean coast after long-distance dispersal from its native East Australian Current [21], characterized by warm waters and oligotrophy. Moreover, this species settled ~30°S, where a drop in primary production has been associated with the poleward migration of the South Pacific Anticyclone [87], pointing to substrate availability as the more important factor controlling bacterial activity and abundance in the HCS [88].

Conclusions

In summary, the present study brings new clues to better understand how biotic (host) and abiotic (i.e., nutrient levels and pH) interactions affect the plasticity and phenotypic acclimation of epiphytic bacteria thriving in contrasting environments, pointing to the intriguing relationships between epiphytes and seagrasses on the nutrients cycling around the global ocean.

Supplementary Information The online version contains supplementary material available at https://doi.org/10.1007/s00248-021-01766-z.

Acknowledgements VFJ acknowledges the travel funds provided by the Santander Iberoamérica 2019–2020 fellowship. We are grateful to Prof. Mario Edding and Felipe Sáez of the Laboratorio de Botánica Marina at the Universidad Católica del Norte for providing us with leaves of *H. chilensis*.

Author Contribution VFJ and PE designed the experiments. VFJ conducted all the laboratory experiments and isolated the UIB 001 strain. JBE isolated the Pacific 4B UA strain. DJL conducted the bioinformatic analyses. All the authors, VFJ, DJL, JBE, ABF, NSRA, and PE, led the writing of the paper.

Funding NSRA was funded through the Ministerio de Economía, Industria y Competitividad-Agencia Estatal de Investigación and the European Regional Development Funds project (CTM2016-75457-P). PE acknowledges the financial support of the research grants Fondecyt Iniciación 11170837, FONDEQUIP EQM120137, and REDI170403.

Data and Availability and Code Availability This manuscript contains previously unpublished data. The name of the repository and accession number(s) are CP058244 to CP058245 (*Cobetia* sp. UIB 001) and CP059843 to CP059845 (*Cobetia* sp. 4B UA).

Declarations

Studies Involving Animal Subjects No animal studies are presented in this manuscript.

Studies Involving Human Subjects No human studies are presented in this manuscript.

Inclusion of Identifiable Human Data No potentially identifiable human images or data is presented in this study.

Consent to Participate Not applicable.

Consent for Publication Not applicable.

Conflict of Interest The authors declare no competing interests.

References

1. Hemminga MA, Duarte CM (2002) Seagrass ecology. Cambridge University Press. James W. Fourqurean. https://doi.org/10.4319/lo.2002.47.2.0611
2. Gutiérrez JL, Jones CG, Byers JE, Arkema KK, Berkenbusch K, Commito A et al (2012) Physical ecosystem engineers and the functioning of estuaries and coasts. Treatise Estuar Coast Sci 7:58–81. https://doi.org/10.1016/B978-0-12-374711-2.00705-1
3. Renn CE (1937) Bacteria and the phosphorus cycle in the sea. Biol Bull 72:190–195
4. Tortell PD, Maldonado MT, Price NM (1996) The role of heterotrophic bacteria in iron-limited ocean ecosystems. Nature. 383:330–332. https://doi.org/10.1038/383330a0
5. Anderson OR (2018) Evidence for coupling of the carbon and phosphorus biogeochemical cycles in freshwater microbial communities. Front Mar Sci 5:1–6. https://doi.org/10.3389/fmars.2018.00020
6. Flombaum P, Gallegos JL, Gordillo RA, Rincon J, Zabala LL, Jiao N, Karl DM, Li WKW, Lomas MW, Veneziano D, Vera CS, Vrugt JA, Martiny AC (2013) Present and future global distributions of the marine Cyanobacteria *Prochlorococcus* and *Synechococcus*. Proc Natl Acad Sci 110:9824–9829. https://doi.org/10.1073/pnas.1307701110
7. Ugarelli K, Chakrabarti S, Laas P, Stingl U (2017) The seagrass holobiont and its microbiome. Microorganisms 5:81. https://doi.org/10.3390/microorganisms5040081
8. Sohm JA, Webb EA, Capone DG (2011) Emerging patterns of marine nitrogen fixation. Nat Rev Microbiol 9:499–508. https://doi.org/10.1038/nrmicro2594
9. Agawin NSR, Ferriol P, Cryer C, Alcon E, Busquets A, Sintes E, Vidal C, Moyà G (2016) Significant nitrogen fixation activity associated with the phyllosphere of Mediterranean seagrass *Posidonia oceanica*: first report. Mar Ecol Prog Ser 551:53–62. https://doi.org/10.3354/meps11755
10. Agawin NSR, Ferriol P, Sintes E, Moyà G (2017) Temporal and spatial variability of in situ nitrogen fixation activities associated with the Mediterranean seagrass *Posidonia oceanica* meadows. Limnol Oceanogr 62:2575–2592. https://doi.org/10.1002/lno.10591
11. Agawin NSR, Ferriol P, Sintes E (2019) Simultaneous measurements of nitrogen fixation activities associated with different plant tissues of the seagrass *Posidonia oceanica*. Mar Ecol Prog Ser 611:111–127. https://doi.org/10.3354/meps12854
12. Perry CJ, Dennison WC (1999) Microbial nutrient cycling in seagrass sediment. J Aust Geol Geophys 17:227–231
13. Tanhua T, Hainbucher D, Schroeder K, Cardin V, Álvarez M, Civitarese G (2013) The Mediterranean Sea system: a review and an introduction to the special issue. Ocean Sci 9:789–803. https://doi.org/10.5194/os-9-789-2013
14. Thingstad TF, Krom MD, Mantoura RFC, Flaten GA, Groom S, Herut B, Kress N, Law CS, Pasternak A, Pitta P, Psarra S, Rassoulzadegan F, Tanaka T, Tselepides A, Wassmann P, Woodward EM, Riser CW, Zodiatis G, Zohary T (2005) Nature of phosphorus limitation in the ultraoligotrophic eastern Mediterranean. Science (80-) 309:1068–1071. https://doi.org/10.1126/science.1112632
15. Ridame C, Le Moal M, Guieu C et al (2011) Nutrient control of N_2 fixation in the oligotrophic Mediterranean Sea and the impact of Saharan dust events. Biogeosciences 8:2773–2783. https://doi.org/10.5194/bg-8-2773-2011
16. Statham PJ, Hart V (2005) Dissolved iron in the Cretan Sea (eastern Mediterranean). Limnol Oceanogr 50:1142–1148. https://doi.org/10.4319/lo.2005.50.4.1142
17. Moore JK, Doney SC, Glover DM, Fung IY (2001) Iron cycling and nutrient-limitation patterns in surface waters of the world ocean. Deep Res Part II Top Stud Oceanogr 49:463–507. https://doi.org/10.1016/S0967-0645(01)00109-6
18. Thiel M, Macaya EC, Acuña E, Arntz WE, Bastias H, Brokordt K, Camus PA, Castilla JC, Castro LR, Cortés M, Dumont CP, Escribano R, Fernández M, Gajardo JA, Gaymer CF, Gomez I, González AE, González HE, Haye PA et al (2007) The Humboldt Current System of Northern and Central Chile oceanographic processes, ecological interactions and socioeconomic feedback. Oceanogr Mar Biol 195–344
19. Montecino V, Lange CB (2009) The Humboldt Current System: ecosystem components and processes, fisheries, and sediment studies. Prog Oceanogr 83:65–79. https://doi.org/10.1016/j.pocean.2009.07.041
20. Kuo J (2005) A revision of the genus *Heterozostera* (*Zosteraceae*). Aquat Bot 81:97–140. https://doi.org/10.1016/j.aquabot.2004.10.005

21. Smith TM, York PH, Broitman BR, Thiel M, Hays GC, van Sebille E, Putman NF, Macreadie PI, Sherman CDH (2018) Rare long-distance dispersal of a marine angiosperm across the Pacific Ocean. Glob Ecol Biogeogr 27:487–496. https://doi.org/10.1111/geb.12713
22. Santelices B (1980) Phytogeographic characterization of the temperate coast of Pacific South America. Phycologia. 19:1–12. https://doi.org/10.2216/i0031-8884-19-1-1.1
23. Mahowald NM, Hamilton DS, Mackey KRM, Moore JK, Baker AR, Scanza RA, Zhang Y (2018) Aerosol trace metal leaching and impacts on marine microorganisms. Nat Commun 9:2614. https://doi.org/10.1038/s41467-018-04970-7
24. Moore CM, Mills MM, Arrigo KR, Berman-Frank I, Bopp L, Boyd PW, Galbraith ED, Geider RJ, Guieu C, Jaccard SL, Jickells TD, la Roche J, Lenton TM, Mahowald NM, Marañón E, Marinov I, Moore JK, Nakatsuka T, Oschlies A, Saito MA, Thingstad TF, Tsuda A, Ulloa O (2013) Processes and patterns of oceanic nutrient limitation. Nat Geosci 6:701–710. https://doi.org/10.1038/ngeo1765
25. Bristow LA, Mohr W, Ahmerkamp S, Kuypers MMM (2017) Nutrients that limit growth in the ocean. Curr Biol 27:R474–R478. https://doi.org/10.1016/j.cub.2017.03.030
26. Sebastian M, Ammerman JW (2011) Role of the phosphatase PhoX in the phosphorus metabolism of the marine bacterium *Ruegeria pomeroyi* DSS-3. Environ Microbiol Rep 3:535–542. https://doi.org/10.1111/j.1758-2229.2011.00253.x
27. Lesser MP (2006) Oxidative stress in marine environments: biochemistry and physiological ecology. Annu Rev Physiol 68:253–278
28. Yang M, Zhao W, Xie X (2014) Effects of nitrogen, phosphorus, iron and silicon on growth of five species of marine benthic diatoms. Acta Ecol Sin 34:311–319. https://doi.org/10.1016/j.chnaes.2014.10.003
29. Garcia NS, Fu F, Sedwick PN, Hutchins DA (2015) Iron deficiency increases growth and nitrogen-fixation rates of phosphorus-deficient marine cyanobacteria. ISME J 9:238–245. https://doi.org/10.1038/ismej.2014.104
30. Fernández-Juárez V, Bennasar-Figueras A, Tovar-Sanchez A, Agawin NSR (2019) The role of iron in the P-acquisition mechanisms of the unicellular N_2-fixing cyanobacteria *Halothece* sp., found in association with the Mediterranean seagrass *Posidonia oceanica*. Front Microbiol 10. https://doi.org/10.3389/fmicb.2019.01903
31. Fernández-Juárez V, Bennasar-Figueras A, Sureda-Gomila A, Ramis-Munar G, Agawin NSR (2020) Differential effects of varying concentrations of phosphorus, iron, and nitrogen in N_2-fixing cyanobacteria. Front Microbiol 11. https://doi.org/10.3389/fmicb.2020.541558
32. Browning TJ, Achterberg EP, Yong JC, Rapp I, Utermann C, Engel A, Moore CM (2017) Iron limitation of microbial phosphorus acquisition in the tropical North Atlantic. Nat Commun 8:1–7. https://doi.org/10.1038/ncomms15465
33. Baas-Becking LGM (1934) Geobiologie of inleiding tot de milieukunde. W.P. Van Stockum & Zoon, The Hague, the Netherlands
34. Sanz-Sáez I, Salazar G, Sánchez P, Lara E, Royo-Llonch M, Sà EL, Lucena T, Pujalte MJ, Vaqué D, Duarte CM, Gasol JM, Pedrós-Alió C, Sánchez O, Acinas SG (2020) Diversity and distribution of marine heterotrophic bacteria from a large culture collection. BMC Microbiol 20:1–16. https://doi.org/10.1186/s12866-020-01884-7
35. Arahal DR, Ventosa A (2006) The family *Halomonadaceae*. In: E S (ed) The Prokaryotes. Springer, New York, pp 811–835
36. De La Haba RR, Arahal DR, Márquez MC, Ventosa A (2010) Phylogenetic relationships within the family *Halomonadaceae* based on comparative 23S and 16S rRNA gene sequence analysis. Int J Syst Evol Microbiol 60:737–748. https://doi.org/10.1099/ijs.0.013979-0
37. Romanenko LA, Tanaka N, Svetashev VI, Falsen E (2013) Description of *Cobetia amphilecti* sp. nov., *Cobetia litoralis* sp. nov. and *Cobetia pacifica* sp. nov., classification of Halomonas halodurans as a later heterotypic synonym of *Cobetia marina* and emended descriptions of the genus *Cobetia* and *Cobetia* marina. Int J Syst Evol Microbiol 63:288–297. https://doi.org/10.1099/ijs.0.036863-0
38. Kim MS, Roh SW, Bae JW (2010) *Cobetia crustatorum* sp. nov., a novel slightly halophilic bacterium isolated from traditional fermented seafood in Korea. Int J Syst Evol Microbiol 60:620–626. https://doi.org/10.1099/ijs.0.008847-0
39. Arahal DR, Castillo AM, Ludwig W, Schleifer KH, Ventosa A (2002) Proposal of *Cobetia marina* gen. nov., comb. nov., within the family *Halomonadaceae*, to include the species Halomonas marina. Syst Appl Microbiol 25:207–211. https://doi.org/10.1078/0723-2020-00113
40. Yumoto I, Hirota K, Iwata H, Akutsu M, Kusumoto K, Morita N, Ezura Y, Okuyama H, Matsuyama H (2004) Temperature and nutrient availability control growth rate and fatty acid composition of facultatively psychrophilic *Cobetia marina* strain L-2. Arch Microbiol 181:345–351. https://doi.org/10.1007/s00203-004-0662-8
41. Ivanova EP, Christen R, Sawabe T, Alexeeva YV, Lysenko AM, Chelomin VP, Mikhailov VV (2005) Presence of ecophysiologically diverse populations within *Cobetia marina* strains isolated from marine invertebrate, algae and the environments. Microbes Environ 20:200–207. https://doi.org/10.1264/jsme2.20.200
42. Ibacache-Quiroga C, Ojeda J, Espinoza-Vergara G, Olivero P, Cuellar M, Dinamarca MA (2013) The hydrocarbon-degrading marine bacterium *Cobetia* sp. strain MM1IDA2H-1 produces a biosurfactant that interferes with quorum sensing of fish pathogens by signal hijacking. Microb Biotechnol 6:394–405. https://doi.org/10.1111/1751-7915.12016
43. Lv N, Pan L, Zhang J, Li Y, Zhang M (2019) A novel microorganism for removing excess ammonia-N in seawater ponds and the effect of *Cobetia amphilecti* on the growth and immune parameters of *Litopenaeus vannamei*. J World Aquacult Soc 50:448–459. https://doi.org/10.1111/jwas.12561
44. Fernández-juárez V, López-alforja X, Frank-comas A, Echeveste P (2021) "The good, the bad and the double-sword" effects of microplastics and their organic additives in marine bacteria. Front Microbiol 11:1–12. https://doi.org/10.3389/fmicb.2020.581118
45. Salvà Serra F, Salvà-Serra F, Svensson-Stadler L, Busquets A, Jaén-Luchoro D, Karlsson R, R. B. Moore E, Gomila M (2018) A protocol for extraction and purification of high-quality and quantity bacterial DNA applicable for genome sequencing: a modified version of the Marmur procedure. Protoc Exch. https://doi.org/10.1038/protex.2018.084
46. Wick RR, Judd LM, Gorrie CL, Holt KE (2017) Unicycler: resolving bacterial genome assemblies from short and long sequencing reads. PLoS Comput Biol 13:e1005595. https://doi.org/10.1371/journal.pcbi.1005595
47. Gurevich A, Saveliev V, Vyahhi N, Tesler G (2013) QUAST: quality assessment tool for genome assemblies. Bioinformatics. 29:1072–1075. https://doi.org/10.1093/bioinformatics/btt086
48. Tatusova T, Dicuccio M, Badretdin A et al (2016) NCBI prokaryotic genome annotation pipeline. Nucleic Acids Res 44:6614–6624. https://doi.org/10.1093/nar/gkw569
49. Haft DH, DiCuccio M, Badretdin A, Brover V, Chetvernin V, O'Neill K, Li W, Chitsaz F, Derbyshire MK, Gonzales NR, Gwadz M, Lu F, Marchler GH, Song JS, Thanki N, Yamashita RA, Zheng C, Thibaud-Nissen F, Geer LY, Marchler-Bauer A, Pruitt KD (2018) RefSeq: an update on prokaryotic genome

annotation and curation. Nucleic Acids Res 46:D851–D860. https://doi.org/10.1093/nar/gkx1068

50. Yoon SH, Ha SM, Kwon S, Lim J, Kim Y, Seo H, Chun J (2017) Introducing EzBioCloud: a taxonomically united database of 16S rRNA gene sequences and whole-genome assemblies. Int J Syst Evol Microbiol 67:1613–1617. https://doi.org/10.1099/ijsem.0.001755
51. Kumar S, Stecher G, Tamura K (2016) MEGA7: molecular evolutionary genetics analysis version 7.0 for bigger datasets. Mol Biol Evol 33:1870–1874. https://doi.org/10.1093/molbev/msw054
52. Richter M, Rosselló-Móra R, Oliver Glöckner F, Peplies J (2016) JSpeciesWS: a web server for prokaryotic species circumscription based on pairwise genome comparison. Bioinformatics. 32:929–931. https://doi.org/10.1093/bioinformatics/btv681
53. Meier-Kolthoff JP, Auch AF, Klenk HP, Göker M (2013) Genome sequence-based species delimitation with confidence intervals and improved distance functions. BMC Bioinformatics 14:60. https://doi.org/10.1186/1471-2105-14-60
54. Jaén-Luchoro D, Gonzales-Siles L, Karlsson R, Svensson-Stadler L, Molin K, Cardew S, Jensie-Markopolous S, Ohlén M, Inganäs E, Skovbjerg S, Tindall BJ, Moore ERB (2020) Corynebacterium sanguinis sp. nov., a clinical and environmental associated corynebacterium. Syst Appl Microbiol 43:126039. https://doi.org/10.1016/j.syapm.2019.126039
55. Contreras-Moreira B, Vinuesa P (2013) GET_HOMOLOGUES, a versatile software package for scalable and robust microbial pangenome analysis. Appl Environ Microbiol 79:7696–7701. https://doi.org/10.1128/aem.02411-13
56. Huerta-Cepas J, Szklarczyk D, Heller D, Hernández-Plaza A, Forslund SK, Cook H, Mende DR, Letunic I, Rattei T, Jensen LJ, von Mering C, Bork P (2018) eggNOG 5.0: a hierarchical, functionally and phylogenetically annotated orthology resource based on 5090 organisms and 2502 viruses. Nucleic Acids Res 47:309–314. https://doi.org/10.1093/nar/gky1085
57. Hillebrand H, Dürselen CD, Kirschtel D, Pollingher U, Zohary T (1999) Biovolume calculation for pelagic and benthic microalgae. J Phycol 35:403–424. https://doi.org/10.1046/j.1529-8817.1999.3520403.x
58. Zhang Y (2008) I-TASSER server for protein 3D structure prediction. BMC Bioinformatics 9:40. https://doi.org/10.1186/1471-2105-9-40
59. Finn RD, Coggill P, Eberhardt RY, Eddy SR, Mistry J, Mitchell AL, Potter SC, Punta M, Qureshi M, Sangrador-Vegas A, Salazar GA, Tate J, Bateman A (2016) The Pfam protein families database: towards a more sustainable future. Nucleic Acids Res 44:D279–D285. https://doi.org/10.1093/nar/gkv1344
60. Li Z, Natarajan P, Ye Y, Hrabe T, Godzik A (2014) POSA: a user-driven, interactive multiple protein structure alignment server. Nucleic Acids Res 42:W240–W245. https://doi.org/10.1093/nar/gku394
61. Noskova Y, Likhatskaya G, Terentieva N, Son O, Tekutyeva L, Balabanova L (2019) A novel alkaline phosphatase/phosphodiesterase, CamPhoD, from marine bacterium *Cobetia amphilecti* KMM 296. Mar Drugs 17:1–20. https://doi.org/10.3390/md17120657
62. The UniProt Consortium (2014) UniProt: a hub for protein information. Nucleic Acids Res 43:D204–D212. https://doi.org/10.1093/nar/gku989
63. DeLano WL (2002) The PyMOL molecular graphics system. Schrödinger, LLC. Available online at: http://www.pymol.org
64. Park M, Kim C, Yang J, Lee H, Shin W, Kim S, Sa T (2005) Isolation and characterization of diazotrophic growth promoting bacteria from rhizosphere of agricultural crops of Korea. Microbiol Res 160:127–133. https://doi.org/10.1016/j.micres.2004.10.003
65. Hellweger FL, Huang Y, Luo H (2018) Carbon limitation drives GC content evolution of a marine bacterium in an individual-based genome-scale model. ISME J 12:1180–1187. https://doi.org/10.1038/s41396-017-0023-7
66. Balabanova LA, Golotin VA, Kovalchuk SN, Babii AV, Shevchenko LS, Son OM, Kosovsky GY, Rasskazov VA (2016) The genome of the marine bacterium *Cobetia marina* KMM 296 isolated from the mussel *Crenomytilus grayanus* (dunker, 1853). Russ J Mar Biol 42:106–109. https://doi.org/10.1134/S106307401601003X
67. Balabanova L, Nedashkovskaya O, Podvolotskaya A, Slepchenko L, Golotin V, Belik A, Shevchenko L, Son O, Rasskazov V (2016) Data supporting functional diversity of the marine bacterium *Cobetia amphilecti* KMM 296. Data Br 8:726–732. https://doi.org/10.1016/j.dib.2016.06.034
68. Kuznetsov SI, Dubinina GA, Lapteva NA (1979) Biology of oligotrophic bacteria. Annu Rev Microbiol 33:377–387. https://doi.org/10.1146/annurev.mi.33.100179.002113
69. Schut F, Prins RA, Gottschal JC (1997) Oligotrophy and pelagic marine bacteria: facts and fiction. Aquat Microb Ecol 12:177–202
70. Dao MH (2013) Reassessment of the cell surface area limitation to nutrient uptake in phytoplankton. Mar Ecol Prog Ser 489:87–92. https://doi.org/10.3354/meps10434
71. Cole J, Findlay S, Pace M (1988) Bacterial production in fresh and saltwater ecosystems: a cross-system overview. Mar Ecol Prog Ser 43:1–10. https://doi.org/10.3354/meps043001
72. Biddanda B, Ogdahl M, Cotner J (2001) Dominance of bacterial metabolism in oligotrophic relative to eutrophic waters. Limnol Oceanogr 46:730–739. https://doi.org/10.4319/lo.2001.46.3.0730
73. Radwan S, Mahmoud H, Khanafer M, al-Habib A, al-Hasan R (2010) Identities of epilithic hydrocarbon-utilizing diazotrophic bacteria from the Arabian gulf coasts, and their potential for oil bioremediation without nitrogen supplementation. Microb Ecol 60:354–363. https://doi.org/10.1007/s00248-010-9702-x
74. Al-Awadhi H, Al-Mailem D, Dashti N et al (2012) Indigenous hydrocarbon-utilizing bacterioflora in oil-polluted habitats in Kuwait, two decades after the greatest man-made oil spill. Arch Microbiol 194:689–705. https://doi.org/10.1007/s00203-012-0800-7
75. Zhang Y, Burris RH, Ludden PW, Roberts GP (1997) Regulation of nitrogen fixation in *Azospirillum brasilense*. FEMS Microbiol Lett 152:195–204. https://doi.org/10.1016/S0378-1097(97)00187-0
76. Argandoña M, Fernández-Carazo R, Llamas I et al (2005) The moderately halophilic bacterium *Halomonas maura* is a free-living diazotroph. FEMS Microbiol Lett 244:69–74. https://doi.org/10.1016/j.femsle.2005.01.019
77. Yoshida N, Inaba S, Takagi H (2014) Utilization of atmospheric ammonia by an extremely oligotrophic bacterium, *Rhodococcus erythropolis* N9T-4. J Biosci Bioeng 117:28–32. https://doi.org/10.1016/j.jbiosc.2013.06.005
78. Sañudo-Wilhelmy SA, Kustka AB, Gobler CJ, Hutchins DA, Yang M, Lwiza K, Burns J, Capone DG, Raven JA, Carpenter EJ (2001) Phosphorus limitation of nitrogen fixation by *Trichodesmium* in the central Atlantic Ocean. Nature 411:66–69
79. Mackey KRM, Mioni CE, Ryan JP, Paytan A (2012) Phosphorus cycling in the red tide incubator region of Monterey Bay in response to upwelling. Front Microbiol 3:1–14. https://doi.org/10.3389/fmicb.2012.00033
80. Hoffman BM, Lukoyanov D, Yang Z-Y, Dean DR, Seefeldt LC (2014) Mechanism of nitrogen fixation by nitrogenase: the next stage. Chem Rev 114:4041–4062. https://doi.org/10.1021/cr400641x
81. Shi D, Xu Y, Hopkinson BM, Morel FMM (2010) Effect of ocean acidification on iron availability to marine phytoplankton. Science (80-) 327:676–679. https://doi.org/10.1126/science.1183517

82. Doney SC, Fabry VJ, Feely RA, Kleypas JA (2009) Ocean acidification: the other CO2 problem. Annu Rev Mar Sci 1:169–192. https://doi.org/10.1146/annurev.marine.010908.163834
83. Kadam PC, Boone DR (1996) Influence of pH on ammonia accumulation and toxicity in halophilic, methylotrophic methanogens. Appl Environ Microbiol 62:4486–4492. https://doi.org/10.1128/aem.62.12.4486-4492.1996
84. Ge C, Chai Y, Wang H, Kan M (2017) Ocean acidification: one potential driver of phosphorus eutrophication. Mar Pollut Bull 115:149–153. https://doi.org/10.1016/j.marpolbul.2016.12.016
85. Yu Plisova E, Balabanova LA, Ivanova EP, Kozhemyako VB, Mikhailov VV, Agafonova EV, Rasskazov VA (2005) A highly active alkaline phosphatase from the marine bacterium *Cobetia*. Mar Biotechnol 7:173–178. https://doi.org/10.1007/s10126-004-3022-4
86. Balabanova L, Golotin V, Kovalchuk S, Bulgakov A, Likhatskaya G, Son O, Rasskazov V (2014) A novel bifunctional hybrid with marine bacterium alkaline phosphatase and far eastern holothurian mannan-binding lectin activities. PLoS One 9:e112729. https://doi.org/10.1371/journal.pone.0112729
87. Weidberg N, Ospina-Alvarez A, Bonicelli J, Barahona M, Aiken CM, Broitman BR, Navarrete SA (2020) Spatial shifts in productivity of the coastal ocean over the past two decades induced by migration of the Pacific anticyclone and Bakun's effect in the Humboldt upwelling ecosystem. Glob Planet Chang 193:103259. https://doi.org/10.1016/j.gloplacha.2020.103259
88. Troncoso VA, Daneri G, Cuevas LA, Jacob B, Montero P (2003) Bacterial carbon flow in the Humboldt Current System off Chile. Mar Ecol Prog Ser 250:1–12. https://doi.org/10.3354/meps250001

SECTION II: EFFECT OF ANTHROPOGENIC FACTORS IN DIAZOTROPHS: GLOBAL CLIMATE CHANGE FACTORS AND EMERGING POLLUTANTS

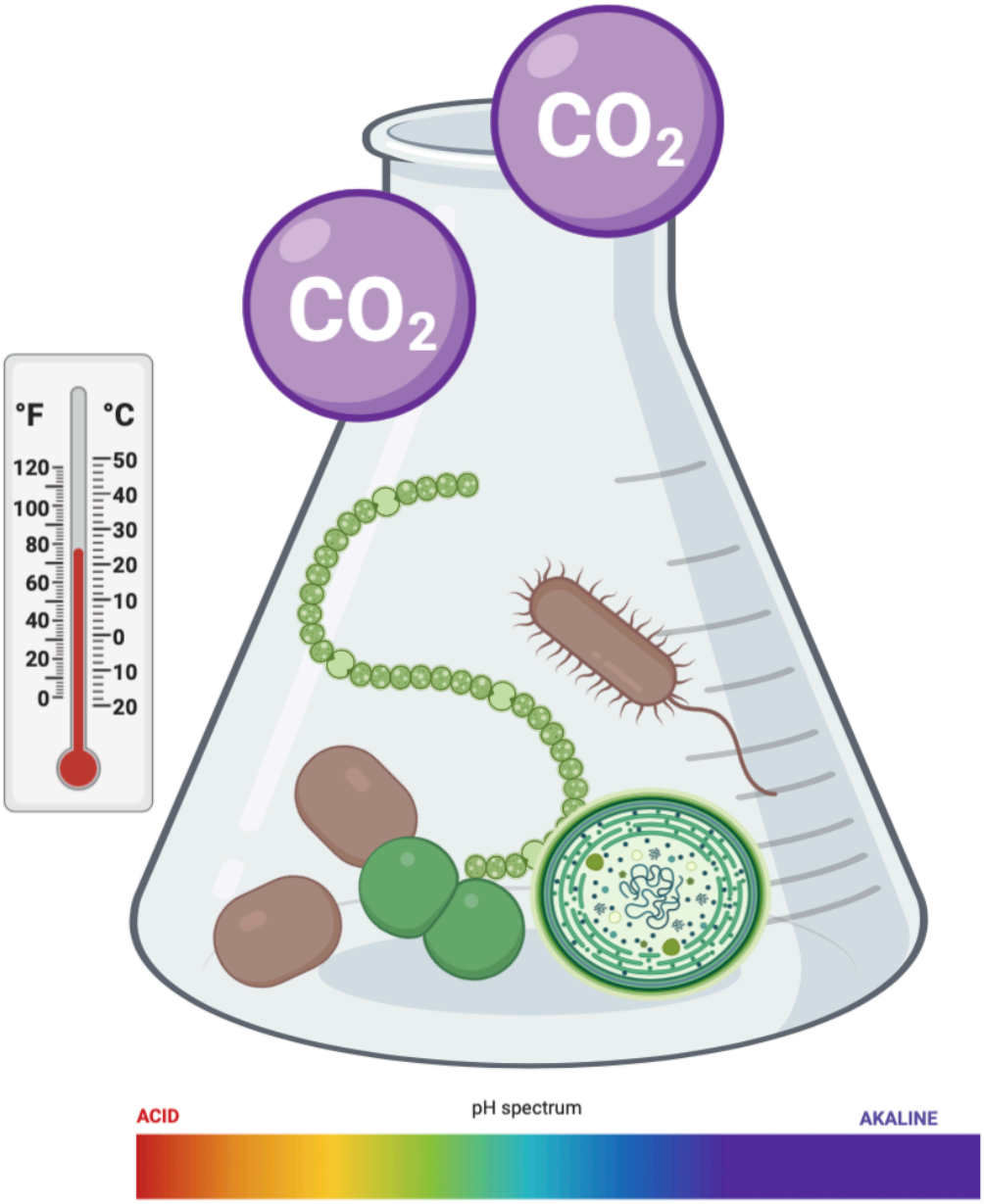
CO_2
CO_2
°F
°C
120
100
80
60
40
20
0
50
40
30
20
10
0
10
20
ACID
pH spectrum
AKALINE

3.4 Chapter 4

Limnology and Oceanography

Dependence of the effects of pH changes, temperature and elevated levels of CO2 on the nutrient status of N2-fixing bacteria

Journal:	*Limnology and Oceanography*
Manuscript ID	LO-21-0168
Wiley - Manuscript type:	Original Article
Date Submitted by the Author:	30-Mar-2021
Complete List of Authors:	Fernández-Juárez, Victor; University of the Balearic Islands H. Zech, Elisa ; Universität Wien, Archaea Physiology & Biotechnology Group, Department of Functional and Evolutionary Ecology Pol-Pol, Elisabet ; University of the Balearic Islands Faculty of Sciences Agawin, Nona Sheila; Universitat de les Illes Balears Facultat de Ciencies, Biology
Keywords:	Ocean acidification and warming, CO2, Phosphorus and iron, Diazotrophs, Reactive oxygen species, Alkaline phosphatase activity
Abstract:	Ocean acidification and warming are current global challenges that marine bacteria have to cope with, including those that are involved in N-cycles (i.e., N2-fixers or diazotrophs). However, there is scarce information about the effects of global climate change factors (i.e., changes in pH and temperature with increased CO2 levels) in combination with other environmental factors (e.g., nutrient availability) in diazotrophs. We tested different pH (from pH 4 to 8) and temperature levels (12-30 ºC), both under different nutrient availability of phosphorus (P) and iron (Fe). We also tested different CO2 concentrations (410 and 1000 µmol CO2 mol-1) under different levels of Fe (1 µM and 2 nM) and temperatures (18 ºC and 30 ºC), both under different P-concentrations. Our results reveal that the heterotrophic species are more susceptible to changes in pH and temperature than the phototrophic species. Generally, high CO2 levels (i.e., 1000 µmol CO2 mol-1) negatively affected the growth for heterotrophic N2-fixing bacteria, but only when cultures were Fe and/or P-limited. Generally, continuous CO2 influx, 410 and 1000 µmol CO2 mol-1 (according to the Fe and/or temperature levels), in the heterotrophic bacterial cultures resulted in higher reactive oxygen species (ROS) production, and higher N2-fixation rates than in cultures without added CO2. Overall, the alkaline phosphatase activity in cyanobacteria and heterotrophic bacteria decreased with increasing CO2 levels, according to the Fe and/or temperature levels. Our findings suggest that diazotrophic responses to climate change factors can be dependent on their nutrient status and their mode of life (phototrophic or heterotrophic).

Dependence of the effects of pH changes, temperature and elevated levels of CO_2 on the nutrient status of N_2-fixing bacteria

Víctor Fernández-Juárez[1*], Elisa H. Zech[2], Elisabet Pol-Pol[1] and Nona S.R. Agawin[1*]

[1]Marine Ecology and Systematics (MarES) Department of Biology, University of the Balearic Islands, Palma, Mallorca, Spain

[2]Archaea Physiology & Biotechnology Group, Department of Functional and Evolutionary Ecology Universität Wien, Wien, Austria

*Corresponding author: victor.fernandez@uib.es and nona.agawin@uib.es

Running title: Effects of climate change factors in diazotrophs.

Keywords: ocean acidification and warming, CO_2, phosphorus and iron, diazotrophs, reactive oxygen species (ROS), alkaline phosphatase activity.

Abstract

Ocean acidification and warming are current global challenges that marine bacteria have to cope with, including those that are involved in N-cycles (i.e., N_2-fixers or diazotrophs). However, there is scarce information about the effects of global climate change factors (i.e., changes in pH and temperature with increased CO_2 levels) in combination with other environmental factors (e.g., nutrient availability) in diazotrophs. We tested different pH (from pH 4 to 8) and temperature levels (12-30 ºC), both under different nutrient availability of phosphorus (P) and iron (Fe). We also tested different CO_2 concentrations (410 and 1000 µmol CO_2 mol^{-1}) under different levels of Fe (1 µM and 2 nM) and temperatures (18 ºC and 30 ºC), both under different P-concentrations. Our results reveal that the heterotrophic species are more susceptible to changes in pH and temperature than the phototrophic species. Generally, high CO_2 levels (i.e., 1000 µmol CO_2 mol^{-1}) negatively affected the growth for heterotrophic N_2-fixing bacteria, but only when cultures were Fe and/or P-limited. Generally, continuous CO_2 influx, 410 and 1000 µmol CO_2 mol^{-1} (according to the Fe and/or temperature levels), in the heterotrophic bacterial cultures resulted in higher reactive oxygen species (ROS) production, and higher N_2-fixation rates than in cultures without added CO_2. Overall, the alkaline phosphatase activity in cyanobacteria and heterotrophic bacteria decreased with increasing CO_2 levels, according to the Fe and/or temperature levels. Our findings suggest that diazotrophic responses to climate change factors can be dependent on their nutrient status and their mode of life (phototrophic or heterotrophic).

1. Introduction

Carbon dioxide (CO_2) emissions have been increasing since the start of the industrial revolution in 1750 (Etheridge et al., 1996). Anthropogenic activities will continuously emit CO_2 into the atmosphere and projected to reach 750 µmol CO_2 mol^{-1} or more than 1000 µmol CO_2 mol^{-1} by the end of this century (Raupach et al., 2007), from the current atmospheric levels of 417 µmol CO_2 mol^{-1} (National Oceanic and Atmospheric Administration [NOAA], https://www.esrl.noaa.gov/gmd/ccgg/trends/weekly.html, retrieved March 23, 2021). Increasing CO_2 levels have clear consequences on the chemistry of marine environments since one-third of anthropogenic emissions are accumulated in the oceans (Global Carbon Project, 2020). Carbon dioxide molecules can chemically react with seawater forming carbonic acid (H_2CO_3) and then bicarbonate (HCO_3^-) which dissociates to carbonate (CO_3^{-2}), releasing protons (H^+) which causes acidification of the oceans. Future acidification scenarios are predicted to be at pH 7.7 by the end of the century (2100) from current pH values of between pH 8 to 8.25 (Jiang et al., 2019), and warming scenarios predict an increase of 2 to 6 ºC in the ocean temperature (Sarmento et al., 2010). The effect of increased CO_2 levels and concomitant changes in pH and temperature have been studied in phytoplankton or microorganisms in general but often with contradictory results. Oliver et al. (2014) reported that increasing CO_2 levels do not have deleterious effects on phytoplanktonic communities, and even can stimulate cell abundance (Kim et al., 2006). Some reports speculate that marine phytoplankton can be resistant to ocean acidification (Berge et al., 2010; Nielsen et al., 2012). However, others affirm that small changes in the pH might change the microbial structure (Krause et al., 2012), while warmer temperatures can enhance phytoplanktonic abundance and activity, triggering algal blooms (Sarmento et al., 2010).

For N_2-fixing microorganisms or diazotrophs which play important roles in N-cyles (Hoffman et al., 2014), several studies have been focus on the effect of increasing levels of CO_2 and temperature. However, these reports are focused on the filamentous cyanobacteria *Trichodesmium* (and *Nodularia spumigena*) or in the unicellular cyanobacteria *Cyanothece* and *Crocosphaera* (Barcelos e Ramos et al., 2007; Breitbarth et al., 2007; Hutchins et al., 2007; Levitan et al., 2007; Fu et al., 2008; Czerny et al., 2009; Garcia et al., 2011, 2013ab; Shi et al., 2012; Eichner et al., 2014ab; Boatman et al., 2017), and to our knowledge, none has investigated the effects of climate change factors to heterotrophic N_2-fixing bacteria, which are suggested to contribute significantly to global N_2-fixation (Shiozaki et al., 2014; Zehr and Capone, 2020). It has been predicted

that N_2-fixation rates will increase to 22 to 27% due to an increase in water temperature by the end of this century (Boyd and Doney, 2002; Fu et al., 2014; Jiang et al., 2018), but these general predictions should be viewed with caution since the N_2-fixing community is composed of different groups, which can differ with their optimal pH, temperature, and nutrient requirements for their growth and activities (Lagus et al., 2004; Thackeray et al., 2008; Striebel et al., 2016), which can regulate their response in future ocean acidification and warming scenarios (Wrightson and Tagliabue, 2020). Diazotrophs have a particularly higher demand for phosphorus (P) and iron (Fe) than other microorganisms (Falkowski, 1997; Ward et al., 2013), because of their N_2-fixation and P-acquisition mechanisms and the dependence of their activities on available N concentrations (Fernández-Juárez et al., 2019, 2020). The availability of these nutrients may also affect their responses to changes in climate change factors (CO_2, pH and temperature).

Here, we studied the effect of climate change factors (i.e., changes in pH, increased temperature and CO_2 levels) in N_2-fixing bacteria, using selected cultures of diazotrophic species found in association with the endemic Mediterranean *Posidonia oceanica* seagrass (Agawin et al., 2017). From our previous studies, these test species were sensitive to different nutrient concentrations of P, Fe and N (Fernández-Juárez et al., 2019, 2020), and we hypothesize that their response to changes in pH, increased temperature and CO_2 levels are dependent on their nutrient status. Specifically, we investigated the response of four diazotrophic bacteria (phototrophic and heterotrophic) in batch cultures, testing the effects of (**I**) changes in pH (from pH 4 to 8) and (**II**) different temperature levels (12-30 ºC), both under different nutrient concentrations of inorganic phosphorus (i.e., PO_4^{3-}) and Fe. We also tested the effects of (**III**) different levels of CO_2 (atmospheric CO_2, aCO_2: 410 µmol CO_2 mol^{-1} and elevated CO_2 as predicted at the end of the century, eCO_2: 1000 µmol CO_2 mol^{-1}) under (**i**) different levels of Fe (1 µM and 2 nM) at 24 ºC and (**ii**) different temperatures (18 ºC and 30 ºC), both under different P-concentrations.

2. Materials and methods

2.1 Culture strains tested

We selected three N_2-fixers found in association with *P. oceanica* (Agawin et al., 2017), represented by their culturable strains: two cyanobacteria (i.e., unicellular *Halothece* sp. PCC 7418 and filamentous heterocyst-forming *Fischerella muscicola* PCC

73103), and one heterotrophic bacterium (i.e., *Pseudomonas azotifigens* DSM 17556^T) (**Supplementary Table S1**). Additionally, we tested another heterotrophic bacterium, *Cobetia* sp. UIB 001, isolated from the roots of *P. oceanica*, identified as a potential N_2-fixer (unpublished data). Before the experiments, the stock cultures were maintained in their optimal culture media: ASNIII + Turks Island Salts 4X for *Halothece* sp., $BG11_0$ for *F. muscicola* and Marine Broth for the heterotrophic bacteria, and they were incubated at 24 ºC and 120 rpm in a rotatory shaker with a photoperiod of 12 h dark:12 h light under low-intensity fluorescent light (30 μE m^{-2} s^{-1}).

2.2 Experimental culture conditions

All the experiments were performed at least in triplicates (n = 3) and carried out in 2 mL microtiter plates (2 mL) or 50 mL falcon tubes (30 mL) in batch cultures, using modified artificial seawater medium, following in Fernández-Juárez et al. (2021). Inorganic phosphorus (P, in the form of K_2HPO_4), iron [Fe, in the form of ferric citrate, ($C_6H_5FeO_7$)] and inorganic nitrogen (N, in the form of NH_3Cl) were added depending on the nutrient regimen and the response variable selected (**Supplementary Table S1**). Cells were precipitated and washed with artificial seawater without P, Fe and N, inoculating in each treatment ~20-60 x10^4 cells mL^{-1}. Cells were then maintained again at the initial conditions of 120 rpm, 12 h dark:12 h light and under low-intensity fluorescent light (30 μE m^{-2} s^{-1}) for 72 h. To avoid Fe contamination, all the samples were manipulated in a class-100 clean hood. Cell abundance, N_2-fixation rates, reactive oxygen species (ROS) and alkaline phosphatase activity were measured as response variables (**Supplementary Table S1**).

Effects of variation in pH and temperature levels

We tested varying levels of pH and temperature for the four bacteria mentioned above (**Supplementary Table S1**). For the first part of the experiment, the pH levels of the cultures were adjusted to different levels (pH 4, 5, 6, 7 and 8), using Tris-HCl or Trizma base (Sigma-Aldrich) at 0.1 mM (final concentration) in a calibrated pH-Meter BASIC 20 (CRISON). Moreover, for *Halothece* sp. and *Cobetia* sp., we tested the effects of pH between pH 6.5 to 8 (**Supplementary Table S1**). Cells were incubated at a constant temperature (24 ºC), which is the temperature at which all the bacterial species tested have high growth rates. For the second part, the cultures were incubated at different

temperatures (12, 18, 24 and 30 ºC) with coolers and thermostats and the pH was adjusted to 8 (**Supplementary Table S1**). The cultures were incubated at different nutrient concentrations in both pH and temperature experiments: at optimal nutrient concentrations (1.5 mM PO_4^{3-}, 1 µM Fe) and under nutrient limitation (0.1 µM PO_4^{3-}, 2 nM Fe), both under low levels of NH_3 (0.15 mM) to avoid inhibition of N_2-fixation (Knapp, 2012).

Effects of increased CO_2 levels

To investigate the effects of increased CO_2 levels (without bubbling), we used the unicellular cyanobacterium, *Halothece* sp., and the heterotrophic bacterium, *Cobetia* sp., as our test species following Fernández-Juárez et al. (2021). We tested two different levels of CO_2: atmospheric, aCO_2: 410 µmol CO_2 mol^{-1} and elevated, eCO_2: 1000 µmol CO_2 mol^{-1} (as predicted at the end of the century, IPCC, 2014), and included a control with no CO_2 influx. All the experiments were performed under low levels of NH_3 (0.15 mM). Combinations with two variables (Fe and temperature) with the different levels of CO_2 were conducted: (**i**) CO_2 and Fe (1 µM and 2 nM) at constant temperature (24 ºC) and (**ii**) CO_2 and temperature (18 ºC and 30 ºC) with 1 µM of Fe. Both types of experiments were subject to different concentrations of PO_4^{3-} (optimal, 1.5 mM; limited, 0.1 µM). The initial pH was adjusted to pH 8 in each treatment.

The microplates and Falcon tubes with the cultures were placed inside hermetic tanks (**Supplementary Figure S1**). Mass flow controllers (MFCs, Aalborg) were set-up to control the air mixture. The gas mixture was introduced inside the hermetic tanks, with an outlet hole to allow the flow-through of the gas mixture. To achieve these mixes, air from an air-pump was connected to a filter with soda lime to remove CO_2 and mixed with pure CO_2 from a bottle to reach the desired concentration. Mixing was achieved in a tube with marbles to assure the homogenization of gases. After splitting the resulting treatment air gas mixture, the volume that entered each tank was regulated by a flow meter with a volume of 2.5 L min^{-1} (LPM). The pH was continuously measured and monitored (ENV-40-pH) every 30 min, and the resulting data was stored in two control boxes (IKS-AQUASTAR) (**Supplementary Figure S1**).

2.3 Flow cytometry and growth measurement

Fresh unfixed cells at the initial (T_o) and the final time point (T_f) of the experiments were counted with a Becton Dickinson FACS-Verse cytometer (Beckton and Dickinson, Franklin Lakes, New Jersey, USA). Fluorescent beads, BD FACSuite™ CS&T research beads (Beckton and Dickinson and Company BD Biosciences, San Jose, USA), were used as an internal standard to calibrate the instrument. Cells were separated by combinations of the flow cytometer parameters: forward scatter (FSC, reflecting cell size), side scatter (SSC, reflecting internal complexity of the cells) and/or fluorescein isothiocyanate (FITC, 488 nm excitation, 530/30 nm emission) parameters, recording for each sample a total of 1 x10^4 cells.

2.4 Nitrogen fixation activity

Nitrogen fixation rates were measured through the acetylene reduction assay at the end of the experiments (i.e., after 72 h), following the general method described in Agawin et al., (2014). Nitrogen fixation activities were measured under the dark period and at high P concentrations, as these conditions are previously found to be optimal for N_2-fixation of the species tested (Fernández-Juárez et al., 2019; 2020). Briefly, a known volume of the culture media (8 mL) was transferred into a 10 mL vial. Liquid saturated acetylene was injected in these vials achieving a final concentration of 20% (v/v) and incubated for 3 h. Ethylene and acetylene were determined using a gas chromatograph (model HP-5890, Agilent Technologies) equipped with a flame ionization detector (FID). The column was a Varian wide-bore column (ref. CP7584) packed with CP-PoraPLOT U (27.5 m length, 0.53 mm inside diameter, 0.70 mm outside diameter, 20 μm film thickness), using the set up described in Fernández-Juárez et al. (2019 and 2020). Ethylene produced was calculated using the equations in Stal (1988). The acetylene reduction rates were converted to N_2-fixation rates (nmol mL^{-1} h^{-1}) using a factor of 4:1 (Jensen and Cox, 1983).

2.5 Determination of reactive oxygen species (ROS)

The molecular probe 2'-7'-dichlorofluorescein diacetate (Sigma) was used to measured ROS production after 72 h, following Fernández-Juárez et al. (2020). The 2'-7'-dichlorofluorescein diacetate diluted in artificial seawater (previously stabilized in acetone at 1 mg mL^{-1}) was added in a 96-well microplate (Thermo Scientific) containing

the bacterial samples, achieving a final concentration of 15 μg mL^{-1}. The emission of the green fluorescence of the resulting 2'-7'-dichlorofluorescein was measured by a Cary Eclipse spectrofluorometer (FL0902M009, Agilent Technologies). Fluorescence was monitored for 1 h with an excitation of 480 nm and an emission of 530 nm. The slope of the linear regression between the fluorescence and time elapsed is reported as the ROS production expressed in arbitrary units (A.U.) and normalized by the cell number. The 2'-7'-dichlorofluorescein diacetate was added in artificial seawater without cells under the same conditions as above and served as blanks. To avoid the effect of nutrient limitation, described in Fernández-Juárez et al. (2020), all the variables were measured under P (or Fe) optimal conditions.

2.6 Determination of the alkaline phosphatase activity

Alkaline phosphatase activity was evaluated after 72 h through a fluorometric assay following the hydrolysis of the substrate 4-methylumbelliferyl phosphate (MUF-P, Sigma-Aldrich) to 4-methylumbelliferyl (MUF) following Fernández-Juárez et al. (2019). The culture media was PO_4^{3-} limited (0.1 μM, PO_4^{3-}) to induce the activity of the alkaline phosphatases. An endpoint enzymatic assay was conducted at the end of the experiment with 8 μM of MUF-P (**Supplementary Table S1**). For the pH experiments, we tested *Halothece* sp. and *Cobetia* sp. at the pH range of 6.5 to 8. After 1 h incubation in darkness, alkaline phosphatase activity was measured in a microtiter plate that contained borate pH buffer 10 (3:1 of sample: buffer). The MUF production was measured at 359 nm (excitation) and 449 nm (emission), using a calibration standard curve with commercial MUF (Sigma-Aldrich), with the Cary Eclipse spectrofluorometer (FL0902M009, Agilent Technologies).

2.7 Statistical analysis

Normality and homogeneity of variances were checked, and the statistical significance level was set at $p < 0.05$. Parametric analysis was used to examine normally distributed data using ANOVAs with Bonferroni post-hoc test. Spearman correlation analysis was used to determine the relationships between ROS vs. cell abundance, and alkaline phosphatase activity vs. cell abundance. All analyses were done in R-Studio, R version 3.6.3 (2020-02-29).

3. Results and discussion

3.1 Effect of varying levels of pH and temperature in N_2-fixing bacteria

Growth responses

The growth responses of the diazotrophs tested to varying pH and temperature levels were dependent on the nutrient status of the cells (ANOVA, $p < 0.05$, n = 3, **Figures 1** and **2**), with generally higher growth in nutrient (P and Fe) replete cells than in nutrient-limited cells across the pH and temperature treatments. Diazotrophs require large amounts of P to fuel the N_2-fixation process (i.e., requiring up to 16 ATP) (Sañudo-Wilhelmy, 2001; Fernández-Juárez et al., 2019 and 2020), while Fe is a co-factor of the nitrogenase complex (i.e., contains 38 Fe atoms per holoenzyme) (Hoffman et al., 2014), which can explain the higher growth in nutrient replete cells. Moreover, Fe has a key role in P-acquisition mechanisms, being a co-factor of the alkaline phosphatases, through which inorganic P (PO_4^{3-}) is released from the dissolved organic phosphorus, further fueling the N_2-fixation processes (Fernández-Juárez et al., 2019 and 2020). The lower growth in nutrient-limited cells here can be due to higher oxidative stress, cell breaks, and apoptotic processes, as reported in a previous study (Fernández-Juárez et al., 2020).

The growth of *Halothece* sp. and *Cobetia* sp. at pH between 6.5 to 8 generally were not affected (ANOVA, $p > 0.05$, n = 3, **Figure 1A**), in agreement with previous reports in marine microorganisms (Nielsen et al., 2012). However, under low pH (pH < 6.5), the magnitude of the difference between the growth of nutrient replete and nutrient-limited cells varies among the species tested and the pH (**Figures 1A** and **1B**). Under nutrient replete conditions, very low pH (between pH 4-5) negatively affected the growth of all species tested with an average of 14-fold lower compared with the growth in higher pH (Bonferroni test, $p < 0.05$, n = 3, **Figure 1B**). The cyanobacterium, *F. muscicola*, and the heterotrophic bacterium, *Cobetia* sp. were the most affected species to low pH levels (Bonferroni test, $p < 0.05$, n = 3, **Figure 1B**). The sensitivity to low pH under nutrient replete situation is consistent with reports in other phytoplanktonic groups conducted under nutrient replete conditions (Berge et al., 2010). Under nutrient-limiting conditions, the optimal pH for growth in the cyanobacteria species tested shifted towards an acidic pH (i.e., pH 5), with 9-fold higher growth compared with the rest of the pH treatments (Bonferroni test, $p < 0.05$, n = 3, **Figure 1B**). A slight change from optimal pH of growth towards the acidic-neutral pH (at pH 6-7) rather than pH 8 was also observed for the heterotrophic species tested under nutrient limitation (**Figure 1B**). These results suggest

species-specific responses on changes in pH and dependence of the responses on the nutrient status of cells. The negative effect observed under low pH levels (e.g., pH < 6.5) could be due to a decrease in nutrient uptake. Under lower pH levels, Fe (III) is less available for organic chelators (e.g., siderophores), and Fe (II) can be oxidized in non-bioassimilable forms (Samperio-Ramos et al., 2016) and thus Fe-uptake may be reduced. The reduction of Fe-uptake along with changes in cell membranes and gene expression can limit microbial activity and growth (Millero et al., 2009; Shi et al., 2010, 2012; Yu and Chen, 2019) with low pH levels as observed here (**Figure 1B**). The cyanobacterial species (*Halothece* sp. and *F. muscicola*) are suggested to be more resistant to lower pH than the heterotrophic bacteria (*Cobetia* sp.) under nutrient P and Fe limitation (**Figure 1B**). The mechanisms behind the higher tolerance to lower pH of cyanobacteria over heterotrophs need to be investigated further.

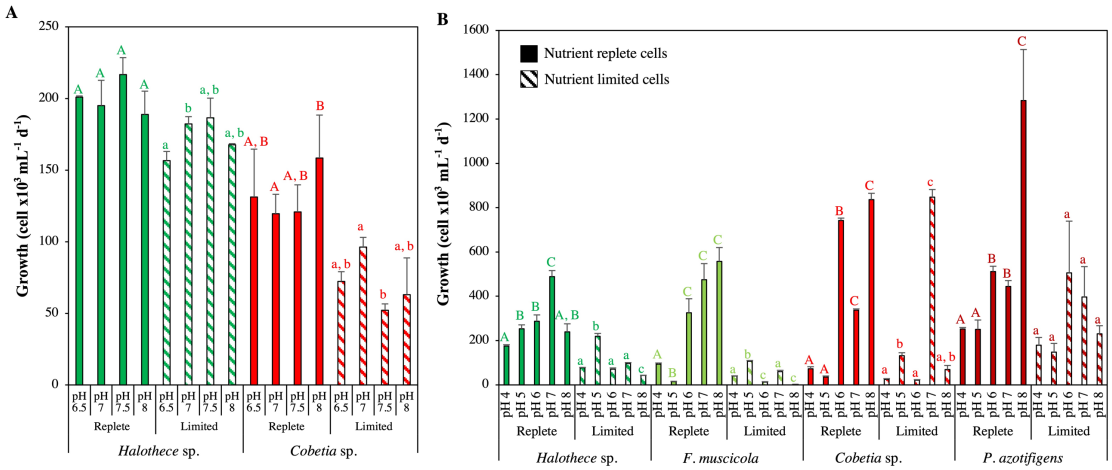

Figure 1. Effect of different levels of pH on growth after 72 h under different nutrient concentrations at 24 ºC, **A)** at the pH range of 6.5 to 8, and **B)** at the pH range of 4 to 8. Values are the mean ± SE (n = 3). Letters (i.e., capital letters or lower case) indicate significant differences ($p < 0.05$) with the rest of the treatments for each strain and nutrient level, using a posthoc test (Bonferroni test) after ANOVA over the whole dataset.

The response of the N_2-fixers tested at different temperatures was also dependent on the nutrient status of the cells and the species (ANOVA, $p < 0.05$, n = 3, **Figure 2**). Generally, nutrient replete cells of heterotrophic bacteria, *Cobetia* sp. and *P. azotifigens*, grew better in warmer temperatures (24-30 ºC) than the cyanobacterial strains, *Halothece* sp. and *F. muscicola* (12-18 ºC) (**Figure 2**). However, under nutrient limiting conditions, the optimal growth temperature of *Cobetia* sp. was 12 ºC (Bonferroni test, $p < 0.05$, n = 3, **Figure 2**). For the cyanobacterial strains, their optimal temperature range increased up

to 24 ºC (Bonferroni test, $p < 0.05$, n = 3, **Figure 2**). For *P. azotifigens* we did not detect significant changes under nutrient limitation (Bonferroni test, $p > 0.05$, n = 3, **Figure 2**). The mechanisms behind these results need to be further studied, but there are reports in which under nutrient replete conditions, warmer temperatures can stimulate heterotrophic bacteria respiration and enhances growth (Pomeroy and Wiebe, 2001), while lower temperatures reduce the ability to obtain inorganic nitrogen from the medium and decrease growth (Reay et al., 1999). Our results suggest that temperature-nutrient interactions can change the optimal growth temperature, in agreement with Thomas et al. (2017) and Marañón et al. (2018), which report changes of 3-6 ºC in the optimal temperature according to the nutritional status in *Synechococcus* sp., *Skeletonema costatum*, *Emiliania huxleyi* or *Thalassiosira pseudonana*, probably by alterations in enzymatic kinetics.

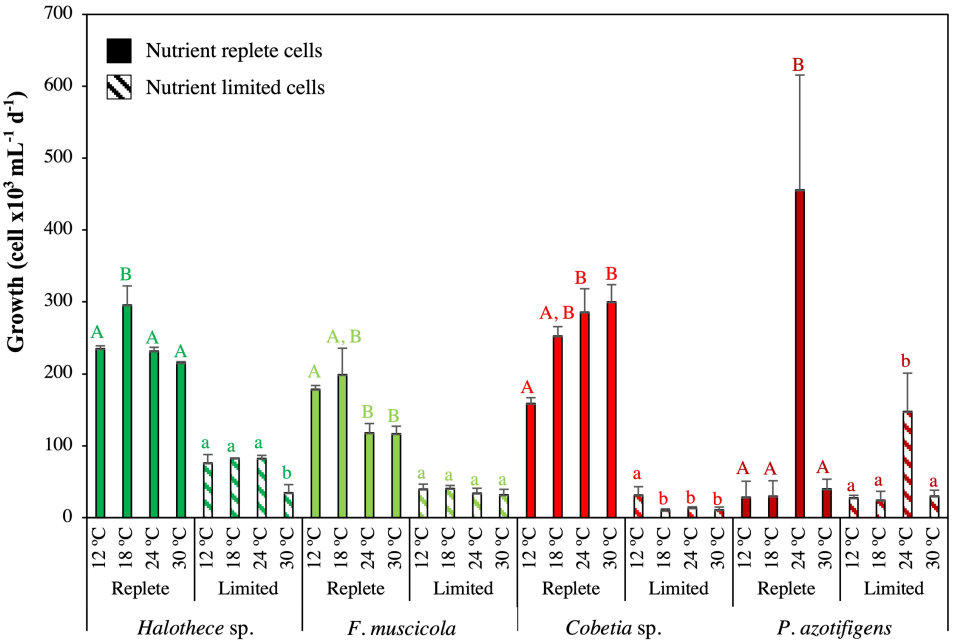

Figure 2. Effect of different levels of temperature on growth after 72 h under different nutrient concentrations. Values are the mean ± SE (n = 3). Letters (i.e., capital letters or lower case) indicate significant differences ($p < 0.05$) with the rest of the treatments for each strain and nutrient level, using a posthoc test (Bonferroni test) after ANOVA over the whole dataset.

Changes in N_2-fixation rates

We did not detect any significant changes in N_2-fixation rates in response to changes in pH and temperature (ANOVA, $p > 0.05$, n = 3, **Figures 3A** and **3B**). However, we detected clear differential trends in the N_2-fixation rates between cyanobacteria and

heterotrophs (**Figures 3A** and **3B**). Heterotrophic bacteria maintained active N_2-fixation rates at pH 5-8 (**Figure 3A**), in agreement with the chemolithotroph *Azotobacter vinelandii* (Pham and Burgess, 1993), and cyanobacteria have active N_2-fixation rates under acidic conditions (< pH 7) (**Figure 3A**). Low cytosolic pH can decrease N_2-fixation rates (Hong et al., 2017), and as our results show, heterotrophic bacteria could be more sensitive to low pH than cyanobacteria (**Figure 1B**). The exact mechanisms by which N_2-fixation rates are enhanced under acidic conditions in cyanobacteria remain to be investigated (**Figure 3A**), because to date, this is the first study that considers the independent effect of water acidification (aside from the effects of increased CO_2) on N_2-fixation activity for marine diazotrophs.

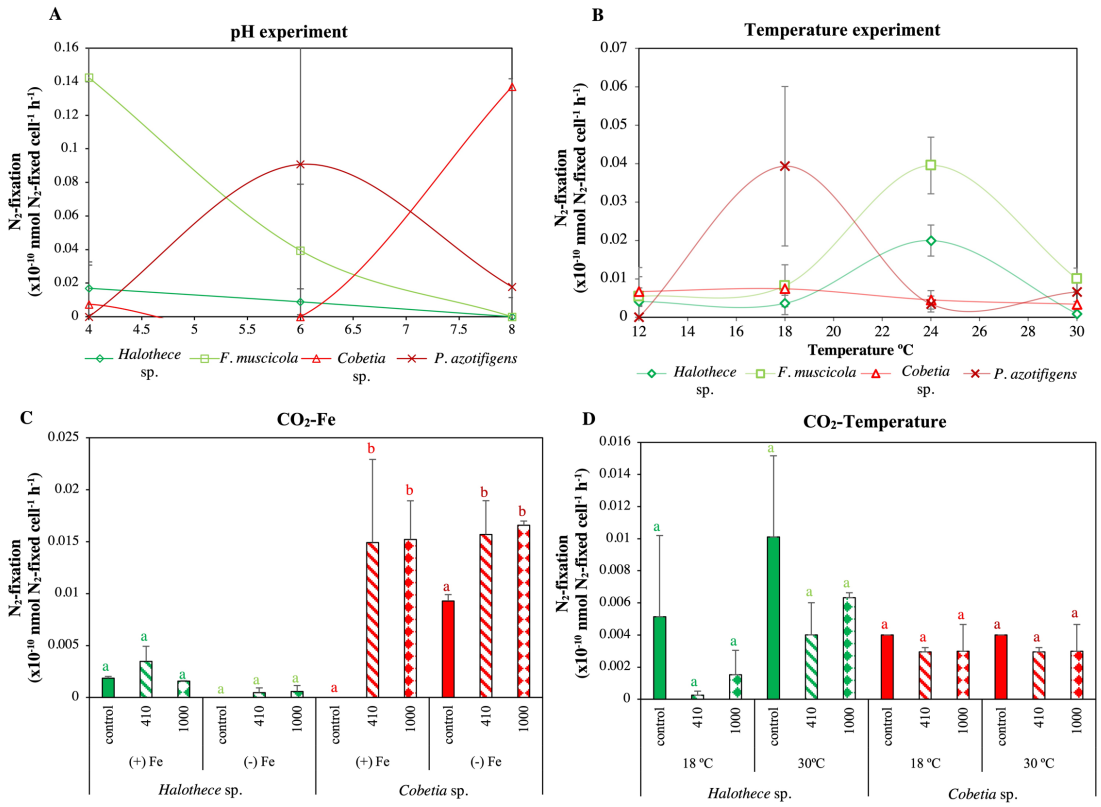

Figure 3. Effect in N_2-fixation rates after 72 h, under different **A)** pH and **B)** temperature levels, and **C-D)** different concentrations of CO_2 [control, atmospheric CO_2 (aCO_2): 410 µmol CO_2 mol^{-1}, and elevated CO_2 (eCO_2): 1000 µmol CO_2 mol^{-1}] in combination with different **C)** Fe (+Fe, 1 µM and -Fe, 2 nM) and **D)** temperature levels (18 ºC and 30 ºC). All the measurements were taken under optimal P-concentration to promote the N_2-fixation. Values are the mean ± SE (n = 3). Letters indicate significant differences ($p < 0.05$) with the rest of the treatments for each strain and experimental set-up, using a posthoc test (Bonferroni test) after ANOVA over the whole dataset.

Cyanobacteria (i.e., *Halothece* sp. and *F. muscicola*) reached the maximum N_2-fixation rates at 24 ºC, while in the heterotrophic bacteria, it was at 18 ºC (**Figure 3B**). These differential responses between the photosynthetic and heterotrophic species remain to be investigated, but in both, temperatures over 30 ºC have an inhibitory effect (**Figure 3B**). Studies conducted in marine bacteria show that N_2-fixation rates are active within the temperature range of 24 to 30 ºC, but at temperatures > 30 ºC the activity decrease, suggesting that temperature levels can control nitrogenase activity and expression (Breitbarth et al., 2007; Fu et al., 2014). Considering the pH and temperature effects on the growth of N_2-fixing cells tested (**Figures 1** and **2**), changes in their abundance can affect the bulk N_2-fixation rates.

Responses at the biochemical level and P-mechanisms

Significantly high ROS production was measured for *Halothece* sp., *F. muscicola* and *P. azotifigens* at the pH of normal ocean water (i.e., pH 8) compared to other pH treatments while for *Cobetia* sp. at this pH ROS was the lowest (ANOVA, $p < 0.05$, n = 3, **Figure 4A**). In other studies in phytoplankton cells, e.g., *Chattonella marina* and *Heterosigma akashiwo*, alkaline pH increases ROS production (Twiner, 2000; Liu et al., 2007), but our results indicate species-specific ROS production responses to alkaline pH (**Figure 4A**). Under acidified conditions, in most of the species tested, generally low ROS levels were measured and may suggest that the diazotrophic population must have mechanisms or efficient antioxidant defenses for low pH conditions (**Figure 4A**). Temperature also affected ROS production, but their response was also dependent on the species tested (**Figure 4B**). For *Halothece* sp. and *P. azotifigens*, ROS production was lower at intermediate temperatures than at the lowest (i.e., 12 ºC) and highest (i.e., 30 ºC) temperature treatments (Bonferroni test, $p < 0.05$, n = 3, **Figure 4B**), while for the other species, i.e., *F. muscicola* and *Cobetia* sp., no significant differences were detected (Bonferroni test, $p > 0.05$, n = 3, **Figure 4B**). Cooler and warmer temperatures may promote adaptative responses to survive and adapt to non-optimal conditions which can trigger higher ROS production (Twiner, 2000; Chattopadhyay, 2006).

For *Halothece* sp. and *Cobetia* sp., the maximum alkaline phosphatase activity was achieved at alkaline pH (i.e., above pH 7) (**Figure 5A**), and the rates dropped significantly from pH 8 to 6.5 for both bacteria (ANOVA, $p < 0.05$, n =3, **Figure 5A**). These results are consistent with studies in cyanobacteria (e.g., *Nostoc flagelliforme*) and heterotrophic bacteria (e.g., *Cobetia amphilecti* KMM 296), wherein alkaline phosphatase activities

were dramatically inhibited with acidification, possibly due to loss of the stability of the enzyme (Li et al. 2013; Noskova et al. 2019; Yu Plisova et al. 2005). Different temperature levels also affected the alkaline phosphatase activity in the diazotrophs tested (ANOVA, $p < 0.05$, n = 3, **Figure 5B**). The optimal temperature for the alkaline phosphatase activity varied by species (i.e., for cyanobacteria at 24 °C and heterotrophic bacteria at 12-18 °C), but for all the species we tested, the phosphatase enzymatic activities tended to have lower rates at 30 °C (**Figure 5B**) consistent with nitrogenase activities (**Figure 3B**). This suggests that alkaline phosphatase activity fuels the N_2-fixation processes (Fernández-Juárez et al., 2019; Agawin et al., 2021). The stability of the enzyme, the velocity of organic phosphate breakdown, and enzyme-substrate affinity are controlled by temperature (Hernández et al., 2002). Contrary to our results, *in vitro* studies with the purified alkaline phosphatase (e.g., PhoD) show that for cyanobacteria (e.g., *N. flagelliforme*) and heterotrophic bacteria (e.g., *C. amphilecti* KMM 296) the optimal alkaline phosphatases activity is within a range of 40 to 45 ºC (Noskova et al., 2019; Li et al., 2013). To date, this is the first study reporting the *in vivo* temperature effect of the alkaline phosphatase activity in marine N_2-fixing bacteria. Moreover, in some of the bacteria tested (i.e., *Halothece* sp. or *P. azotifigens*, **Figure 5B**), the alkaline phosphatases might be adapted to cold temperatures, as in the case for the marine *Vibrio* sp. (Hauksson et al., 2000). More studies about P-acquisition mechanisms should be carried out under *in vivo* conditions to understand the mechanisms behind the temperature responses in the marine diazotrophs.

3.2 Varying levels of CO_2 (aCO_2: 410 µmol CO_2 mol^{-1} and eCO_2: 1000 µmol CO_2 mol^{-1})

Growth responses

Elevated CO_2 (eCO_2, 1000 µmol CO_2 mol^{-1}) resulted in lower pH than at ambient levels (aCO_2, 410 µmol CO_2 mol^{-1}) (**Supplementary Figure S2**). The differences of pH between the two CO_2 treatments were lower for the cyanobacterium, *Halothece* sp. (an average of 0.21 units of pH), than for the heterotrophic bacterium, *Cobetia* sp. (an average of 0.55 units of pH). These results follow the premise that cyanobacterial, as phototrophs, perform photosynthesis, removing CO_2 from the media through efficient carbon concentration mechanisms (CCMs) which transport and concentrate CO_2 into the carboxysomes (i.e., structures in which CO_2-fixing enzyme, RuBisCO, is encapsulated).

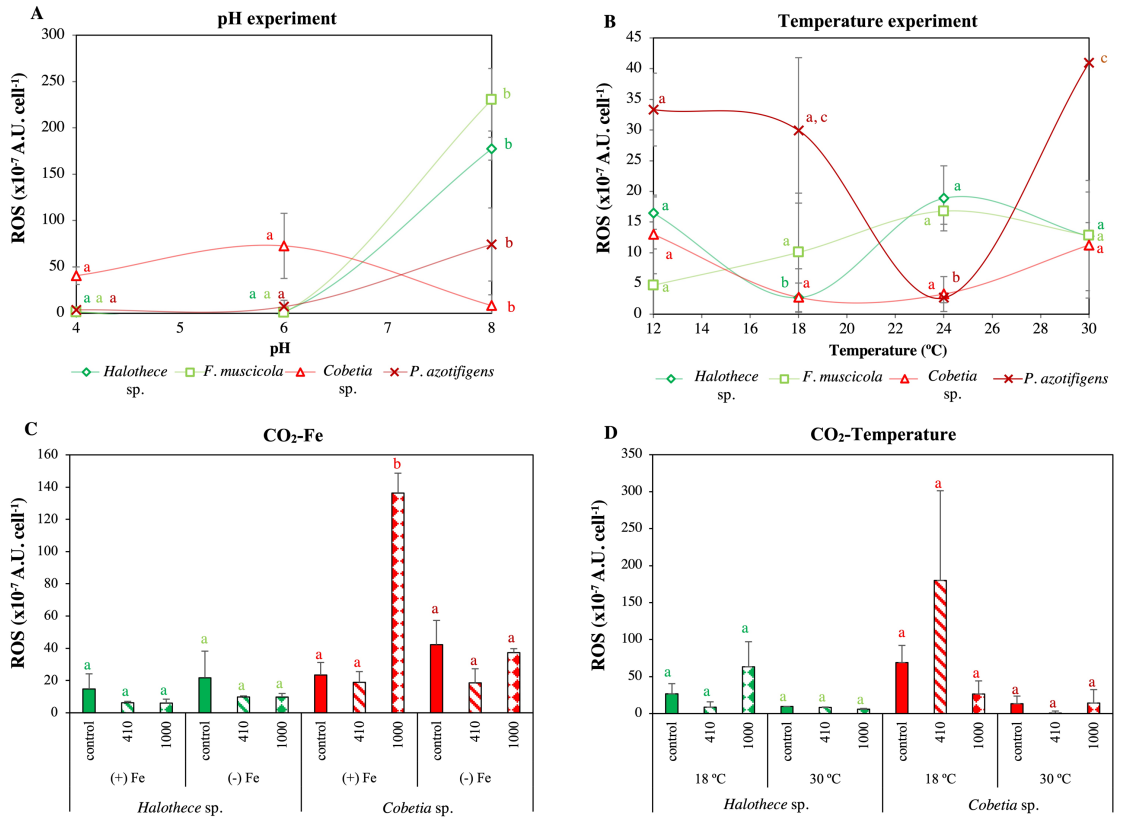

Figure 4. Effect at the biochemical level (i.e., reactive oxygen species, ROS), after 72 h, under different **A)** pH and **B)** temperature levels, and **C-D)** different concentration of CO_2 [control, atmospheric CO_2 (aCO_2): 410 µmol CO_2 mol^{-1}, and elevated CO_2 (eCO_2): 1000 µmol CO_2 mol^{-1}] in combination with different **C)** Fe (+Fe, 1 µM and -Fe, 2 nM) and **D)** temperature levels (18 ºC and 30 ºC). Values are the mean ± SE (n = 3). Letters indicate significant differences ($p < 0.05$) with the rest of the treatments for each strain and experimental set-up, using a posthoc test (Bonferroni test) after ANOVA over the whole dataset.

Thus, cyanobacteria can buffer the effect of acidification (Zhang et al., 2017). The growth of unicellular cyanobacterium tested (*Halothece* sp.) did not vary significantly at the different CO_2 levels applied in our study under different nutrient regimes (PO_4^{3-} and/or Fe) nor temperature levels (i.e., 18 ºC and 30 ºC) (ANOVA, $p > 0.05$, n = 3, **Figures 6A-D**). Our results are consistent with other studies on known cultures of N_2-fixing cyanobacteria (i.e., *Cyanothece* sp. ATCC51142, *Crocosphaera watsonii* WH850 /WH0401/WH0402 and *Trichodesmium erythraeum* IMS101) (Barcelos e Ramos et al., 2007; Fu et al., 2008; Kranz et al., 2009; Garcia et al., 2011, 2013a; Eichner et al., 2014b). However, in other reports of N_2-fixing cyanobacteria (i.e., *Crocosphaera*, *Cyanothece*, *Trichodesmium* and *Nodularia*), the authors report a growth increase or decrease due to elevated CO_2 levels depending on the nutritional status (Levitan et al., 2007; Garcia et al.,

2011, 2013b; Wannicke et al., 2012). According to Eichner et al. (2014b) cyanobacteria may have different CCMs, which causes different CO_2 sensitivities and depending on the habitat in which the different species live, they have to cope with different carbonate chemistry, and differentially adapted, suggesting that the effect increased CO_2 levels in cyanobacteria is species-specific.

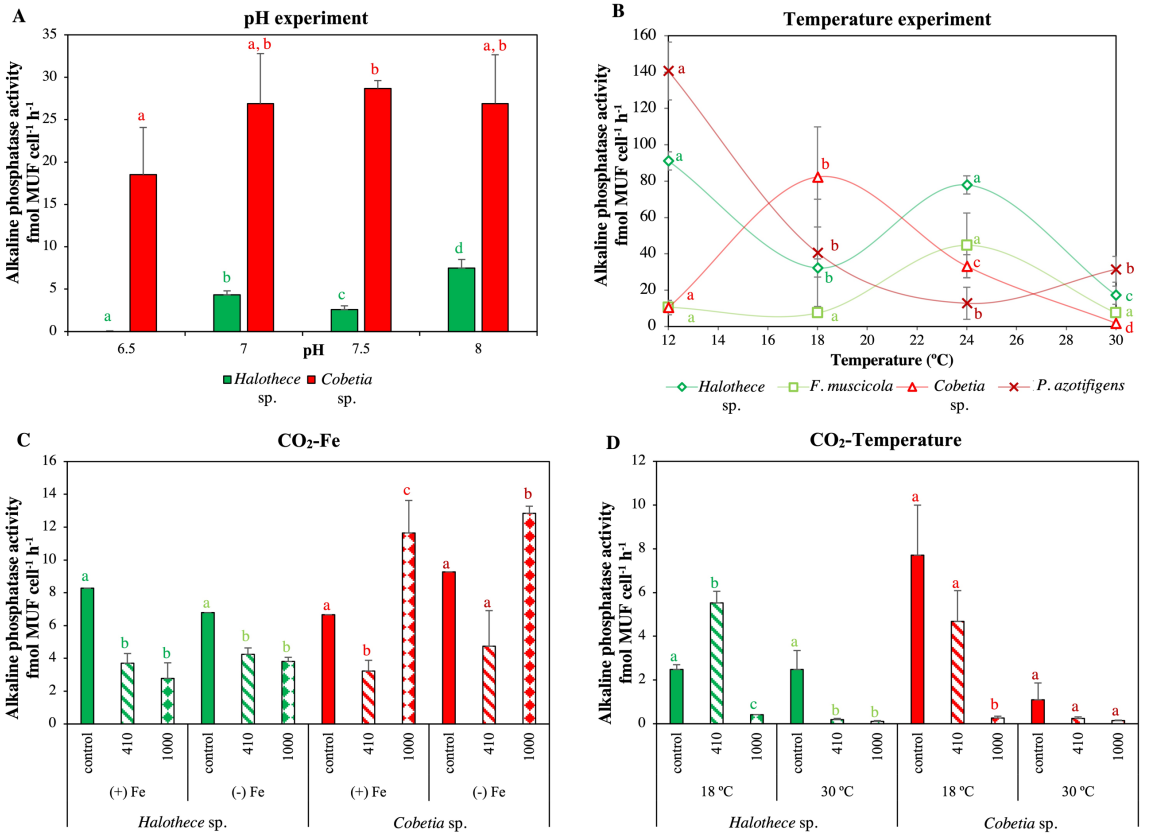

Figure 5. Effect in P-mechanisms (alkaline phosphatase activity), after 72 h, under different **A)** pH (6.5-8) and **B)** temperature levels (12-30 ºC), and **C-D)** different concentration of CO_2 [control, atmospheric CO_2 (aCO_2): 410 µmol CO_2 mol^{-1}, and elevated CO_2 (eCO_2): 1000 µmol CO_2 mol^{-1}] in combination with different **C)** Fe (+Fe, 1 µM and -Fe, 2 nM) and **D)** temperature levels (18 ºC and 30 ºC). The measurements were taken under P limitation (0.1 µM) to induce the activity of alkaline phosphatases. Values are the mean ± SE (n = 3). Letters indicate significant differences ($p < 0.05$) with the rest of the treatments for each strain and experimental set-up, using a posthoc test (Bonferroni test) after ANOVA over the whole dataset.

For the heterotrophic species, *Cobetia* sp., different CO_2 concentrations combined with varying Fe and temperature levels had a significant effect on their growth (ANOVA $p < 0.05$, n = 3, **Figures 6A-D**). In the CO_2-Fe experiments, growth was significantly lower at eCO_2 compared to the control (i.e., no CO_2 influx) without Fe at optimal P

concentration (Bonferroni test, $p < 0.05$, n = 3, **Figure 6A**). Under P-limitation, growth was drastically reduced at eCO_2 compared to the control, independently of the Fe level (Bonferroni test, $p < 0.05$, n = 3, **Figure 6A**). In the CO_2-temperature experiments, under P-optimal concentrations, growth was higher at aCO_2 and eCO_2 compared to the control, irrespective of the temperature level (Bonferroni test, $p < 0.05$, n = 3, **Figures 6C**), while under P-limited conditions, growth at eCO_2 was lower compared to the control, irrespective of the temperature level (Bonferroni test, $p < 0.05$, n = 3, **Figures 6C** and **6D**). In both CO_2-Fe and CO_2-temperature experiments, growth at eCO_2 was lower compared with aCO_2, only when cultures were P-limited (Bonferroni test, $p < 0.05$, n = 3, **Figures 6B** and **6D**). These results suggest the nutrient control (i.e., P and Fe) in *Cobetia* sp. responses with increased CO_2 levels. There have been few studies investigating the effect of CO_2 effect in heterotrophic bacteria in general, and one reports that continuous bubbling with elevated CO_2 levels in heterotrophic bacteria cultured in enriched nutrient media (i.e., P and Fe) does not affect microbial growth (Teira et al., 2012). However, nothing is known about N_2-fixing heterotrophic bacteria, and this study reports for the first time the interactive effect between CO_2 and nutrient limitation for the diazotrophic heterotrophic bacteria (**Figures 6A-6D**), which can be due to (**I**) limitation of protein synthesis and enzymatic activities under Fe and P-limitation (Bristow et al., 2017, Fernández-Juárez et al., 2019) and (**II**) the lowered pH due to increased CO_2 can limit nutrient uptake and microbial activity (**Figures 1A** and **1B**).

Changes in N_2-fixation rates

No significant changes in the N_2-fixation rates, irrespective of the CO_2, Fe and/or temperature levels (ANOVA, $p > 0.05$, n = 3, **Figures 3C** and **3D**) were found for *Halothece* sp. This is contrary to the previous reports conducted in other cyanobacterial species, in which CO_2 can enhance N_2-fixation rates (Fu et al., 2008; Hutchins et al., 2007; Levitan et al,. 2007) or reduce N_2-fixation rates depending on Fe concentrations (Shi et al., 2012). In some cyanobacteria, high CO_2 levels can downregulate carboxysome genes (Morris et al., 2008), decreasing the energy used for concentrating CO_2 in these organelles. It is hereby suggested that cyanobacteria can save energy by concentrating CO_2 and use this energy instead for N_2-fixation (Kranz et al., 2011; Eichner et al., 2014a). However, the absence of effect of increased CO_2 in the cyanobacteria tested here (*Halothece* sp.) suggests that regulatory processes of carbon concentrating mechanisms

or carbon uptake mechanisms can be species-specific, and thus N_2-fixing responses in diazotrophic cyanobacteria to global climate change factors cannot be generalized.

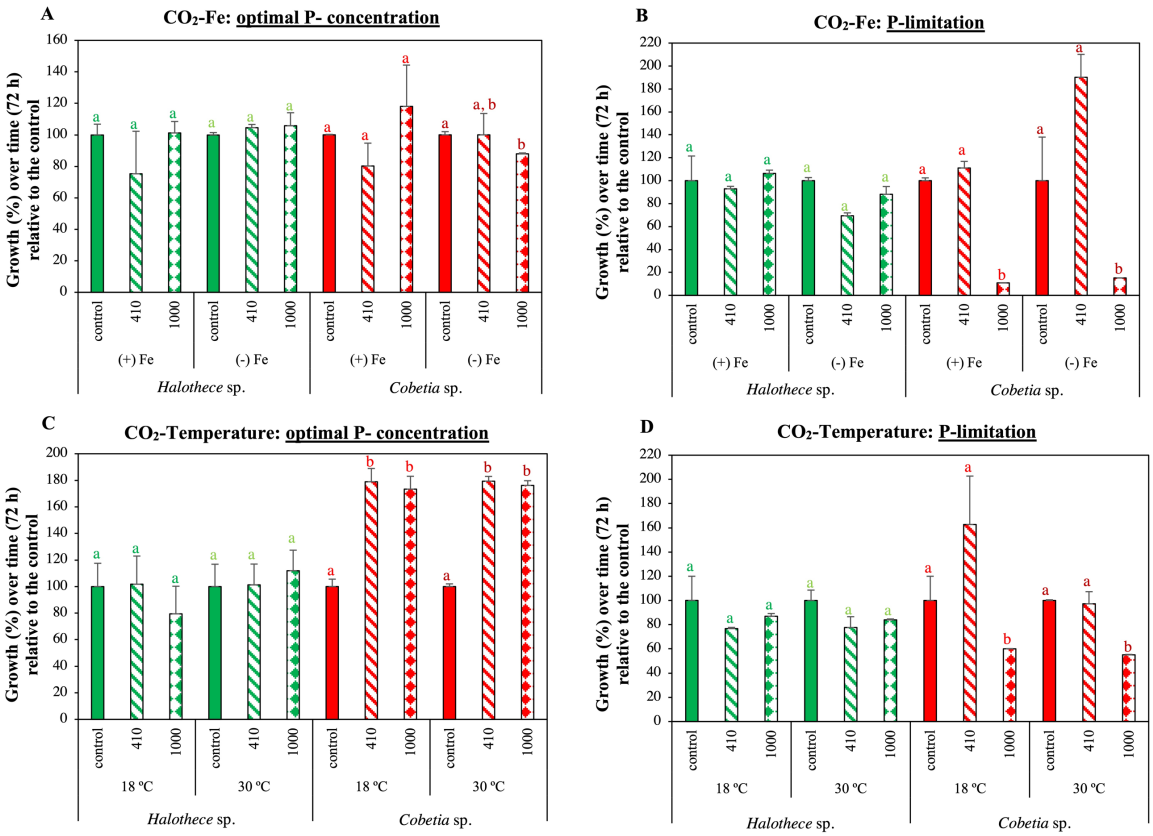

Figure 6. Growth (calculated as % difference relative to the control over the incubation time of 72 h) after the exposure to atmospheric CO_2 (aCO_2, 410 µmol CO_2 mol^{-1}) and elevated CO_2 (eCO_2, 1000 µmol $CO_2 mol^{-1}$). **A-B)** Exposure with CO_2 at different concentrations of Fe (+Fe, 1 µM and -Fe, 2 nM) under **A)** P-optimal conditions (1.5 mM) and **B)** P-limitation (0.1 µM). **C-D)** Exposure with CO_2 at different temperature levels (18 ºC and 30 ºC), under **C)** P-optimal conditions and **D)** P- limitation. Values are the mean ± SE (n = 3). Letters indicate significant differences ($p < 0.05$) with the rest of the treatments for each strain and experimental set-up, using a posthoc test (Bonferroni test) after ANOVA over the whole dataset.

For the heterotrophic species tested, *Cobetia* sp., continuous influx of CO_2 (i.e., both aCO_2 and eCO_2) significantly enhance the N_2-fixation rates compared to the control in the CO_2-Fe experiments at 24 ºC, irrespective of the Fe level, (Bonferroni test, $p < 0.05$, n = 3, **Figure 3C**). This suggests that CO_2 may regulate N_2-fixation processes in heterotrophic bacteria. Some heterotrophic bacteria can fix CO_2 through different carboxylation reactions catalyzed by the phosphoenolpyruvate (PEP) carboxylase and pyruvate carboxylase. These enzymes are capable of converting HCO_3^- in oxalacetate which can be included in the Krebs cycles (Santruckova et al., 2005), contributing to 2-

8% of the cell's biomass carbon abundance (Spona-Friedl et al., 2020). Thus, heterotrophic bacteria can take advantage of increasing CO_2 levels, increasing the ATP synthesis, which can fuel N_2-fixation processes. In the genome of *Cobetia* sp. (UIB 001) (accession number: CP058244-CP058245), we found that this bacterium contains a PEP carboxylase (locus tag: HA399_04700) and two SulP family inorganic anion transporters (locus_tag: HA399_00940 and HA399_13445), responsible for bicarbonate transport into the cells. These findings suggest its potential as CO_2-fixing bacteria. Hence, this explains their enhanced growth under aCO_2 and eCO_2 in the CO_2-temperature experiment **(Figure 6C**).

Responses at the biochemical level and P-mechanisms

Production of ROS was not significantly affected (ANOVA, $p < 0.05$, n = 3, **Figure 4C**) in response to the addition of CO_2 combined with different Fe and temperature levels for *Halothece* sp. For *Cobetia* sp. no significant ROS production was also observed with the addition of CO_2 at different temperature levels (ANOVA, $p > 0.05$, n = 3, **Figure 4**D). However, for *Cobetia* sp., eCO_2 levels with added Fe, ROS production increased 5-fold compared with the control and aCO_2 (Bonferroni test, $p < 0.05$, n = 3, **Figure 4C**). The exact molecular mechanisms behind the response remain unknown, but high Fe-levels can enhance Fenton and Haber-Weiss reactions, which generate free radicals such as hydroxyl radicals (·OH) which are extremely toxic for cells (Diaz and Plummer 2018). On the other hand, CO_2 can downregulate the catalase expression, which is responsible for the detoxification of the H_2O_2, and thus, causing a 6-fold decrease in ROS removal (Hennon et al., 2017). This suggests a negative interactive effect between CO_2 and Fe, which cannot be compensated by the antioxidant defenses of the N_2-fixing heterotrophic bacteria.

Generally, under both, aCO_2 (except in the temperature experiments) and eCO_2 levels, alkaline phosphatase activity decreased significantly compared to the control treatment (Bonferroni test, $p < 0.05$, n = 3, **Figures 5C** and **5D**) for *Halothece* sp. However, we did not find any significant differences between aCO_2 and eCO_2 (Bonferroni test, $p < 0.05$, n = 3, **Figures 5C** and **5D**). Moreover, alkaline phosphatase activity was negatively affected with increasing temperatures (i.e., 30 ºC) (ANOVA, $p < 0.05$, n = 3, **Figure 5C**), as we previously reported in the temperature experiments (**Figure 5B**). Although CO_2 per se did not affect significantly the growth of *Halothece* sp. (**Figures 6A-D**), our results show the alkaline phosphatase activity is sensitive to lower pH levels (i.e., pH < 7.5)

(**Figure 5A**), and may affect the viability of the cyanobacterial cells with the concomitant acidification of water from increased CO_2 levels. For the heterotrophic species, *Cobetia* sp., elevated CO_2 levels enhanced the alkaline phosphatase activity irrespective of the Fe levels at 24 ºC compared with the control and compared with aCO_2 levels in the Fe-CO_2 experiments (Bonferroni test, $p < 0.05$, n = 3, **Figure 5C**). Elevated CO_2 levels significantly reduced alkaline phosphatase activity at 18 ºC, compared to the control and aCO_2 levels in the CO_2-temperature experiments (Bonferroni test, $p < 0.05$, n = 3, **Figure 5D**). At 30 ºC, we did not find any significant differences among treatments (ANOVA, $p > 0.05$, n = 3, **Figure 5D**), but the enzymatic activity was again lower than compared to 18 ºC (Bonferroni test, $p > 0.05$, n = 3, **Figure 5D**). Phosphorus (P) availability can be controlled by pH, and lower pH (e.g., < pH 5.5) can cause fewer free phosphate ions to be transported into the cells (Cerozi and Fitzsimmons, 2016), and consequently increasing alkaline phosphatase activity, as evidenced by the enhancement of the alkaline phosphatase activity of *Cobetia sp*. at eCO_2 levels in the CO_2-Fe experiments at 24 ºC (**Figure 5C**). However, at 18 ºC, the sensitivity of the alkaline phosphatases from *Cobetia* sp. to pH decrease may be different, suggesting that the regulation of the activity of alkaline phosphatases depends on the interaction between pH and temperature and this interaction should be investigated further.

3.3 Reactive oxygen species (ROS) and alkaline phosphatase activity as molecular biomarkers

Cell abundance of all the species tested were negatively correlated with specific production of ROS and specific alkaline phosphatase activity (Spearman's correlation, $p < 0.05$, n = 144, $r^2 = -0.41$ and $r^2 = -0.34$, respectively, **Figures 7A** and **7B**). These results suggest that under optimal nutrient availability, pH, temperature and/or CO_2 conditions in which cell abundance may be higher and presumably the cells are healthy and growing, ROS production (i.e., triggered as a consequence of the biochemical metabolism) and alkaline phosphatase activity (i.e., triggered as a mechanism for obtaining P) are lower, indicating cells are not under stress. These correlations imply that ROS production and alkaline phosphatase activity can be used as molecular biomarkers to assess the health of diazotrophic microorganisms exposed to global climate change factors and other environmental stressors.

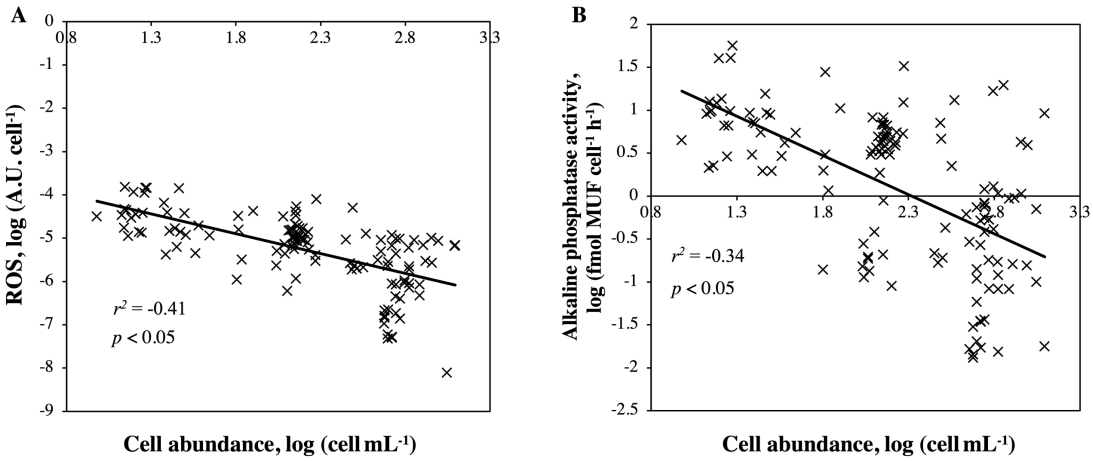

Figure 7. Linear regression analyses between **A)** cell abundance and the reactive oxygen species (ROS) per cell, and **B)** cell abundance and alkaline phosphatase activity per cell. All replicates of all treatments and species from the pH, temperature and CO_2 experiments were combined.

4. Conclusions

Ocean acidification and warming due to increased CO_2 levels may have a significant impact on N_2-fixing microorganisms. However, the impact may depend on whether they are phototrophic or heterotrophic bacteria, suggesting that the community structure of the N_2-fixing community may also change. The response of N_2-fixing microorganisms with climate change factors depends on their nutritional status. Moreover, climate change factors affect nutrient acquisition mechanisms, impairing the diazotrophic activities. The measurement of nutrient acquisition mechanisms such as phosphatase alkaline activities and production of ROS can be used as molecular biomarkers to assess the response of diazotrophic cells to climate change factors.

5. Declarations

5.1 Funding

This work was supported by funding to NSRA through the Ministerio de Economía, Industria y Competitividad- Agencia Estatal de Investigación and the European Regional Development Funds project (CTM2016-75457-P).

5.2 Conflict of interest

The authors declare that the research was conducted in the absence of any commercial or financial relationships that could be construed as a potential conflict of interest.

5.3 Authors contributions

VFJ conducted all experiments with the help of EHZ, EPP and NSRA in the various parameters measured in the study. VFJ and NSRA led the writing of the MS, and NRSA is the supervisor of the laboratory.

5.4 Acknowledgments

We acknowledge the support and help of the Scientific Technical Service (Dr. Guillem Ramis Munar and Maria Trinidad Garcia Barceló) of the University of the Balearic Islands (UIB) for cytometry and gas-chromatography analyses, respectively. We acknowledge Aida Frank Comas and Xabier López-Alforja for the help in the CO_2 set-up. We also thank Dr. Pere Ferriol Buñola, Alba Coma Ninot, and Group de Microbiologia de la UIB for the help in the acquisition of the diazotrophic cultures.

6. References

Agawin, N. S. R., Benavides, M., Busquets, A., Ferriol, P., Stal, L. J., and Arístegui, J. (2014). Dominance of unicellular cyanobacteria in the diazotrophic community in the Atlantic Ocean. *Limnol. Oceanogr.* 59, 623–637. doi:10.4319/lo.2014.59.2.0623.

Agawin, N. S. R., Ferriol, P., Sintes, E., and Moyà, G. (2017). Temporal and spatial variability of in situ nitrogen fixation activities associated with the Mediterranean seagrass *Posidonia oceanica* meadows. *Limnol. Oceanogr.* 62, 2575–2592. doi:10.1002/lno.10591.

Agawin, N. S. R, Gil Atorrasagasti, M. G, Frank Comas, A., Fernández-Juárez, V., López-Alforja, X, and Hendriks, I.E (2021). Response of the seagrass *Posidonia oceanica* and its associated N_2 fixers to high business-as-usual climate change scenario in winter. *Limnol. Oceanogr.*

Barcelos e Ramos, J., Biswas, H., Schulz, K. G., LaRoche, J., and Riebesell, U. (2007). Effect of rising atmospheric carbon dioxide on the marine nitrogen fixer *Trichodesmium*. *Global Biogeochem. Cycles* 21, 1–6. doi:10.1029/2006GB002898.

Berge, T., Daugbjerg, N., Andersen, B. B., and Hansen, P. J. (2010). Effect of lowered pH on marine phytoplankton growth rates. *Mar. Ecol. Prog. Ser.* 416, 79–91. doi:10.3354/meps08780.

Boatman, T. G., Lawson, T., and Geider, R. J. (2017). A key marine diazotroph in a changing ocean: the interacting effects of temperature, CO_2 and light on the growth of *Trichodesmium erythraeum* IMS101. *PLoS One* 12, 1–20. doi:10.1371/journal.pone.0168796.

Boyd, P. W., and Doney, S. C. (2002). Modelling regional responses by marine pelagic ecosystems to global climate change. *Geophys. Res. Lett.* 29, 53-1-53–4. doi:10.1029/2001gl014130.

Breitbarth, E., Oschlies, A., and LaRoche, J. (2007). Physiological constraints on the global distribution of *Trichodesmium*-Effect of temperature on diazotrophy. *Biogeosciences* 4, 53–61. doi:10.5194/bg-4-53-2007.

Bristow, L. A., Mohr, W., Ahmerkamp, S., and Kuypers, M. M. M. (2017). Nutrients that limit growth in the ocean. *Curr. Biol.* 27, R474–R478. doi:10.1016/j.cub.2017.03.030.

Cerozi, B. da S., and Fitzsimmons, K. (2016). The effect of pH on phosphorus availability

and speciation in an aquaponics nutrient solution. *Bioresour. Technol.* 219, 778–781. doi:10.1016/j.biortech.2016.08.079.

Chattopadhyay, M.K (2006). Mechanism of bacterial adaptation to low temperature. *J. Biosci.* 31, 157–65. doi: 10.1007/BF02705244.

Dutkiewicz, S., Morris, J. J., Follows, M. J., Scott, J., Levitan, O., Dyhrman, S. T., et al. (2015). Impact of ocean acidification on the structure of future phytoplankton communities. *Nat. Clim. Chang.* 5, 1002–1006. doi:10.1038/nclimate2722.

Eichner, M., Kranz, S. A., and Rost, B. (2014a). Combined effects of different CO_2 levels and N sources on the diazotrophic cyanobacterium *Trichodesmium*. *Physiol. Plant.* 152, 316–330. doi:10.1111/ppl.12172.

Eichner, M., Rost, B., and Kranz, S. A. (2014b). Diversity of ocean acidification effects on marine N_2 fixers. *J. Exp. Mar. Bio. Ecol.* 457, 199–207. doi:10.1016/j.jembe.2014.04.015.

Etheridge, D. M., Steele, L. P., Langenfelds, R. L., Francey, R. J., Barnola, J. M., and Morgan, V. I. (1996). Natural and anthropogenic changes in atmospheric CO_2 over the last 1000 years from air in Antarctic ice and firn. *J. Geophys. Res. Atmos.* doi:10.1029/95JD03410.

Falkowski, P. G. (1997). Evolution of the nitrogen cycle and its influence on the biological sequestration of CO_2 in the ocean. *Nature* 387, 272–275. doi:10.1038/387272a0.

Fernández-Juárez, V., Bennasar-Figueras, A., Tovar-Sanchez, A., and Agawin, N. S. R. (2019). The role of iron in the P-acquisition mechanisms of the unicellular N_2-fixing cyanobacteria *Halothece* sp ., found in association with the Mediterranean seagrass *Posidonia oceanica*. *Front. Microbiol.* 10, 1–22. doi:10.3389/fmicb.2019.01903.

Fernández-Juárez, V., Bennasar-Figueras, A., Sureda-Gomila, A., Ramis-Munar, G., and Agawin, N. S. R. (2020). Differential effects of varying concentrations of phosphorus, iron, and nitrogen in N_2-fixing cyanobacteria. *Front. Microbiol.* 11, 1–19. doi:10.3389/fmicb.2020.541558.

Fernández-Juárez, V., López-Alforja, X., Frank-Comas, A., Echeveste, P., Bennasar-Figueras, A., Ramis-Munar, G., Gomila, R. M., and Agawin, N. S. R. (2021). " The good , the bad and the double-sword" Effects of microplastics and their organic additives in marine bacteria. *Front. Microbiol.* 11, 1–12. doi:10.3389/fmicb.2020.581118.

Fu, F. X., Mulholland, M. R., Garcia, N. S., Beck, A., Bernhardt, P. W., Warner, M. E., Sañudo-Wilhelmy, S. A, and Hutchins, D. A. (2008). Interactions between changing pCO_2, N_2 fixation, and Fe limitation in the marine unicellular cyanobacterium *Crocosphaera*. *Limnol. Oceanogr.* 53, 2472–2484. doi:10.4319/lo.2008.53.6.2472.

Fu, F. X., Yu, E., Garcia, N. S., Gale, J., Luo, Y., Webb, E. A., and Hutchins, D. A. (2014). Differing responses of marine N_2 fixers to warming and consequences for future diazotroph community structure. *Aquat. Microb. Ecol.* 72, 33–46. doi:10.3354/ame01683.

Garcia, N. S., Fu, F. X., Breene, C. L., Bernhardt, P. W., Mulholland, M. R., Sohm, J. A., and Hutchins, D. A. (2011). Interactive effects of irradiance and CO_2 on CO_2 fixation and N_2 fixation in the diazotroph *Trichodesmium erythraeum* (cyanobacteria). *J. Phycol.* 47, 1292–1303. doi:10.1111/j.1529-8817.2011.01078.x.

Garcia, N. S., Fu, F. X., Breene, C. L., Yu, E. K., Bernhardt, P. W., Mulholland, M. R., and Hutchins, D. A. (2013a). Combined effects of CO_2 and light on large and small isolates of the unicellular N_2-fixing cyanobacterium *Crocosphaera watsonii* from the western tropical Atlantic Ocean. *Eur. J. Phycol.* 48, 128–139. doi:10.1080/09670262.2013.773383.

Garcia, N. S., Fu, F. X., and Hutchins, D. A. (2013b). Colimitation of the unicellular photosynthetic diazotroph *Crocosphaera watsonii* by phosphorus, light, and carbon dioxide. *Limnol. Oceanogr.* 58, 1501–1512. doi:10.4319/lo.2013.58.4.1501.

Hauksson, J. B., Andrésson, Ó. S., and Ásgeirsson, B. (2000). Heat-labile bacterial alkaline phosphatase from a marine *Vibrio* sp. *Enzyme Microb. Technol.* 27, 66–73. doi:10.1016/S0141-0229(00)00152-6.

Hennon, G. M., Morris, J. J., Haley, S. T., Zinser, E. R., Durrant, A. R., Entwistle, E., et al. (2017). The impact of elevated CO_2 on *Prochlorococcus* and microbial interactions with a 'helper' bacterium *Alteromonas*. *ISME J.* 12, 520–531. doi:10.1038/ismej.2017.189.

Hernández, I., Niell, F. X., and Whitton, B. A. (2002). Phosphatase activity of benthic marine algae. An overview. *J. Appl. Phycol.* 14, 475–487. doi:10.1023/A:1022370526665.

Hoffman, B. M., Lukoyanov, D., Yang, Z.-Y., Dean, D. R., and Seefeldt, L. C. (2014). Mechanism of nitrogen fixation by nitrogenase: The Next Stage. *Chem. Rev.* 114, 4041–4062. doi:10.1021/cr400641x.

Hong, H., Shen R., and Zhang, F. (2017). The complex effects of ocean acidification on

the prominent N_2-fixing cyanobacterium *Trichodesmium*. *Science (80-.).* 357, 527–531. doi:10.1126/science.aao0067.

Hutchins, D. A., Fu, F. X., Zhang, Y., Warner, M. E., Feng, Y., Portune, K., Bernhardt, P. W, and Mulholland, M. R. (2007). CO_2 control of *Trichodesmium* N_2 fixation, photosynthesis, growth rates, and elemental ratios: implications for past, present, and future ocean biogeochemistry. *Limnol. Oceanogr.* 52, 1293–1304. doi:10.4319/lo.2007.52.4.1293.

Jensen, B. B., and Cox, R. P. (1983). Direct measurements of steady-state kinetics of cyanobacterial N_2 uptake by membrane-leak mass spectrometry and comparisons between nitrogen fixation and acetylene reduction. *Appl. Environ. Microbiol.* 45, 1331–1337.

Jiang, H. B., Fu, F. X., Rivero-Calle, S., Levine, N. M., Sañudo-Wilhelmy, S. A., Qu, P. P., Wang, X. W., Pinedo-Gonzalez, P., Zhu, Z., and Hutchins D. A. (2018). Ocean warming alleviates iron limitation of marine nitrogen fixation. *Nat. Clim. Chang.* 8, 709–712. doi:10.1038/s41558-018-0216-8.

Jiang, L. Q., Carter, B. R., Feely, R. A., Lauvset, S. K., and Olsen, A. (2019). Surface ocean pH and buffer capacity: past, present and future. *Sci. Rep.* 9, 1–11. doi:10.1038/s41598-019-55039-4.

Kim, J. M., Lee, K., Shin, K., Kang, J. H., Lee, H. W., Kim, M., et al. (2006). The effect of seawater CO_2 concentration on growth of a natural phytoplankton assemblage in a controlled mesocosm experiment. *Limnol. Oceanogr.* 51, 1629–1636. doi:10.4319/lo.2006.51.4.1629.

Knapp, A. N. (2012). The sensitivity of marine N_2 fixation to dissolved inorganic nitrogen. *Front. Microbiol.* 3, 1–14. doi:10.3389/fmicb.2012.00374.

Kranz, S. A., Sültemeyer, D., Richter, K. U., and Rost, B. (2009). Carbon acquisition by *Trichodesmium*: the effect of pCO_2 and diurnal changes. *Limnol. Oceanogr.* 54, 548–559. doi:10.4319/lo.2009.54.2.0548.

Kranz, S. A., Eichner, M., and Rost, B. (2011). Interactions between CCM and N_2 fixation in *Trichodesmium*. *Photosynth. Res.* 109, 73–84. doi:10.1007/s11120-010-9611-3.

Krause, E., Wichels, A., Giménez, L., Lunau, M., Schilhabel, M. B., and Gerdts, G. (2012). Small changes in ph have direct effects on marine bacterial community composition: a microcosm approach. *PLoS One* 7. doi:10.1371/journal.pone.0047035.

Lagus, A., Suomela, J., Weithoff, G., Heikkilä, K., Helminen, H., and Sipura, J. (2004).

Species-specific differences in phytoplankton responses to N and P enrichments and the N:P ratio in the Archipelago Sea, northern Baltic Sea. *J. Plankton Res.* 26, 779–798. doi:10.1093/plankt/fbh070.

Levitan, O., Rosenberg, G., Setlik, I., Setlikova, E., Grigel, J., Klepetar, J., Prasil, O. and Berman-FranK, I. (2007). Elevated CO_2 enhances nitrogen fixation and growth in the marine cyanobacterium *Trichodesmium*. *Glob. Chang. Biol.* 13, 531–538. doi:10.1111/j.1365-2486.2006.01314.x.

Li, P., Liu, W., and Gao, K. (2013). Effects of temperature, pH, and UV radiation on alkaline phosphatase activity in the terrestrial cyanobacterium *Nostoc flagelliforme*. *J. Appl. Phycol.* 25, 1031–1038. doi:10.1007/s10811-012-9936-8.

Liu, W., Au, D. W. T., Anderson, D. M., Lam, P. K. S., and Wu, R. S. S. (2007). Effects of nutrients, salinity, pH and light:dark cycle on the production of reactive oxygen species in the alga Chattonella marina. *J. Exp. Mar. Bio. Ecol.* 346, 76–86. doi:10.1016/j.jembe.2007.03.007.

Marañón, E., Lorenzo, M. P., Cermeño, P., and Mouriño-Carballido, B. (2018). Nutrient limitation suppresses the temperature dependence of phytoplankton metabolic rates. *ISME J.* 12, 1836–1845. doi:10.1038/s41396-018-0105-1.

Morris, J. J., Kirkegaard, R., Szul, M. J., Johnson, Z. I., and Zinser, E. R. (2008). Facilitation of robust growth of Prochlorococcus colonies and dilute liquid cultures by 'helper' heterotrophic bacteria. *Appl. Environ. Microbiol.* doi:10.1128/AEM.02479-07.

Millero, F. J., Woosey, R., Ditrolio, B., and Water J. (2009). Effect of ocean acidification on the speciation of metals in seawater. *Oceanography* 22, 72–85. doi:10.5670/oceanog.2009.98

Nielsen, L. T., Hallegraeff, G. M., Wright, S. W., and Hansen, P. J. (2012). Effects of experimental seawater acidification on an estuarine plankton community. *Aquat. Microb. Ecol.* 65, 271–285. doi:10.3354/ame01554.

Noskova, Y., Likhatskaya, G., Terentieva, N., Son, O., Tekutyeva, L., and Balabanova, L. (2019). A novel alkaline phosphatase/phosphodiesterase, CamPhoD, from marine bacterium *Cobetia amphilecti* KMM 296. *Mar. Drugs* 17, 1–20. doi:10.3390/md17120657.

Oliver, A. E., Newbold, L. K., Whiteley, A. S., and van der Gast, C. J. (2014). Marine bacterial communities are resistant to elevated carbon dioxide levels. *Environ. Microbiol. Rep.* 6, 574–582. doi:10.1111/1758-2229.12159.

Pham, D. N., and Burgess, B. K. (1993). Nitrogenase reactivity: effects of pH on substrate reduction and CO inhibition. *Biochemistry* 32, 13725–13731. doi:10.1021/bi00212a043.

Pomeroy, L. R., and Wiebe, W. J. (2001). Temperature and substrates as interactive limiting factors for marine heterotrophic bacteria. *Aquat. Microb. Ecol.* 23, 187–204 doi:10.3354/ame023187

Stal, L. J. (1988). Acetylene reduction technique for assay of nitrogenase. *Methods Enzymol*. 167, 474–484.

Striebel, M., Schabhüttl, S., Hodapp, D., Hingsamer, P., and Hillebrand, H. (2016). Phytoplankton responses to temperature increases are constrained by abiotic conditions and community composition. *Oecologia* 182, 815–827. doi:10.1007/s00442-016-3693-3.

Teira, E., Fernández, A., Álvarez-Salgado, X. A., García-Martín, E. E., Serret, P., and Sobrino, C. (2012). Response of two marine bacterial isolates to high CO_2 concentration. *Mar. Ecol. Prog. Ser.* 453, 27–36. doi:10.3354/meps09644.

Thackeray, S. J., Jones, I. D., and Maberly, S. C. (2008). Long-term change in the phenology of spring phytoplankton: species-specific responses to nutrient enrichment and climatic change. *J. Ecol.* 96, 523–535. doi:10.1111/j.1365-2745.2008.01355.x.

Thomas, M. K., Aranguren-Gassis, M., Kremer, C. T., Gould, M. R., Anderson, K., Klausmeier, C. A., et al. (2017). Temperature–nutrient interactions exacerbate sensitivity to warming in phytoplankton. *Glob. Chang. Biol.* 23, 3269–3280. doi:10.1111/gcb.13641.

Twiner, M. J. (2000). Possible physiological mechanisms for production of hydrogen peroxide by the ichthyotoxic flagellate *Heterosigma akashiwo*. *J. Plankton Res.* 22, 1961–1975. doi:10.1093/plankt/22.10.1961.

Wannicke, N., Endres, S., Engel, A., Grossart, H.-P., Nausch, M., Unger, J., and Voss, M (2012). Response of *Nodularia spumigena* to pCO_2 - Part 1: growth, production and nitrogen cycling. *Biogeosciences* 9, 2973–2988. doi:10.5194/bg-9-2973-2012.

Ward, B. A., Dutkiewicz, S., Moore, C. M., and Follows, M. J. (2013). Iron, phosphorus, and nitrogen supply ratios define the biogeography of nitrogen fixation. *Limnol. Oceanogr.* 58, 2059–2075. doi:10.4319/lo.2013.58.6.2059.

Wrightson, L., and Tagliabue, A. (2020). Quantifying the impact of climate change on marine diazotrophy: insights from earth system models. *Front. Mar. Sci.* 7, 1–9.

doi:10.3389/fmars.2020.00635.

Yu Plisova, E., Balabanova, L. A., Ivanova, E. P., Kozhemyako, V. B., Mikhailov, V. V., Agafonova, E. V., et al. (2005). A highly active alkaline phosphatase from the marine bacterium *Cobetia*. *Mar. Biotechnol.* 7, 173–178. doi:10.1007/s10126-004-3022-4.

Yu, T., and Chen, Y. (2019). Effects of elevated carbon dioxide on environmental microbes and its mechanisms: A review. *Sci. Total Environ.* 655, 865–879. doi:10.1016/j.scitotenv.2018.11.301.

Zehr, J. P., and Capone, D. G. (2020). Changing perspectives in marine nitrogen fixation. *Science (80-.).* 368. doi:10.1126/science.aay9514.

Zhang, A., Carroll, A. L., and Atsumi, S. (2017). Carbon recycling by cyanobacteria: Improving CO_2 fixation through chemical production. *FEMS Microbiol. Lett.* 364, 1–7. doi:10.1093/femsle/fnx165.

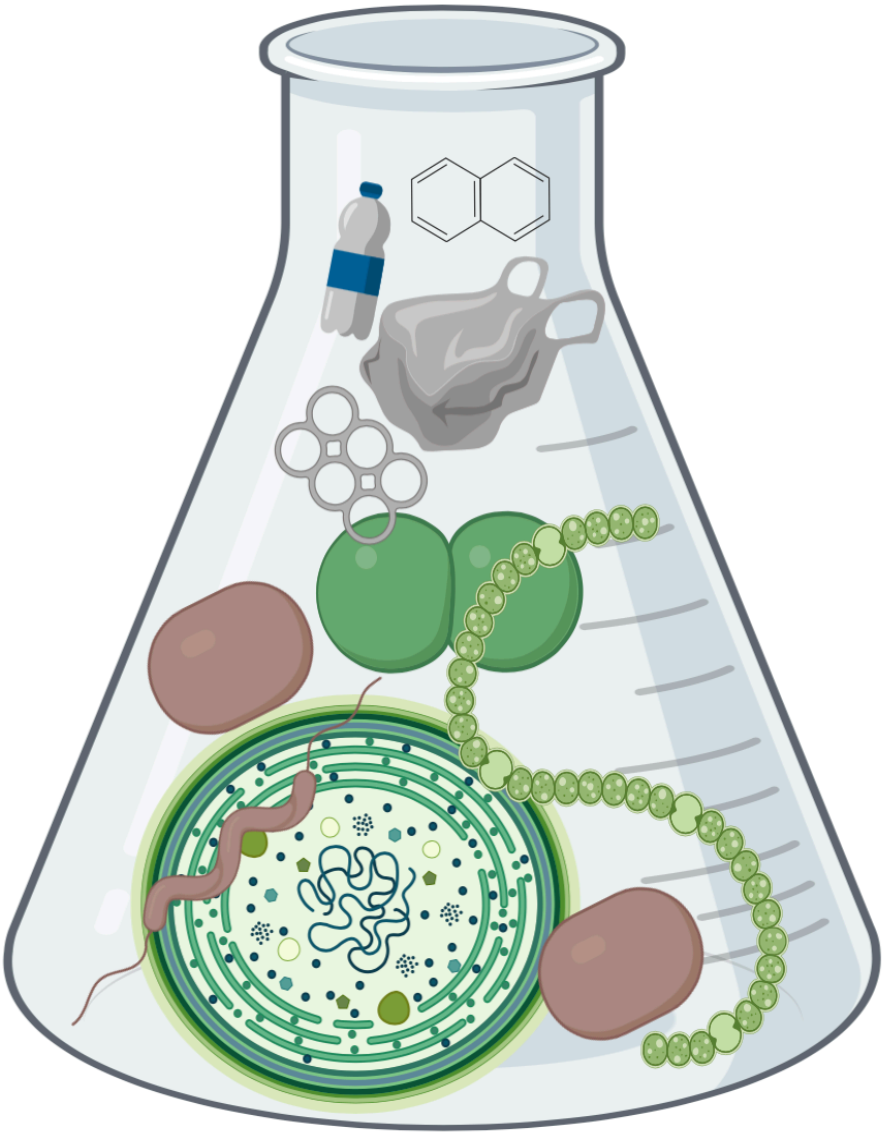

3.5 Chapter 5

frontiers in Microbiology

ORIGINAL RESEARCH
published: 20 January 2021
doi: 10.3389/fmicb.2020.581118

"The Good, the Bad and the Double-Sword" Effects of Microplastics and Their Organic Additives in Marine Bacteria

Víctor Fernández-Juárez[1], Xabier López-Alforja[1], Aida Frank-Comas[1], Pedro Echeveste[2], Antoni Bennasar-Figueras[3], Guillem Ramis-Munar[4], Rosa María Gomila[5] and Nona S. R. Agawin[1]**

[1] Marine Ecology and Systematics (MarES), Department of Biology, University of the Balearic Islands, Palma de Mallorca, Spain, [2] Instituto de Ciencias Naturales Alexander von Humboldt, Universidad de Antofagasta, Antofagasta, Chile, [3] Grup de Recerca en Microbiologia, Departament de Biologia, Universitat de les Illes Balears, Palma de Mallorca, Spain, [4] Celomic Unit of the University Institute of Research in Health Sciences of the Balearic Islands, Palma de Mallorca, Spain, [5] Servicio Científico-Técnicos, University of the Balearic Islands, Palma de Mallorca, Spain

OPEN ACCESS

Edited by:
Ondrej Prasil,
Academy of Sciences of the Czech Republic (ASCR), Czechia

Reviewed by:
Edo Bar Zeev,
Ben-Gurion University of the Negev, Israel
Olivier Pringault,
Institut de Recherche Pour le Développement (IRD), France

***Correspondence:**
Víctor Fernández-Juárez
victorfj@hotmail.es
Nona S. R. Agawin
nona.agawin@uib.es

Specialty section:
This article was submitted to Aquatic Microbiology, a section of the journal Frontiers in Microbiology

Received: 07 July 2020
Accepted: 21 December 2020
Published: 20 January 2021

Citation:
Fernández-Juárez V, López-Alforja X, Frank-Comas A, Echeveste P, Bennasar-Figueras A, Ramis-Munar G, Gomila RM and Agawin NSR (2021) "The Good, the Bad and the Double-Sword" Effects of Microplastics and Their Organic Additives in Marine Bacteria. Front. Microbiol. 11:581118. doi: 10.3389/fmicb.2020.581118

Little is known about the direct effects of microplastics (MPs) and their organic additives on marine bacteria, considering their role in the nutrient cycles, e.g., N-cycles through the N_2-fixation, or in the microbial food web. To fill this gap of knowledge, we exposed marine bacteria, specifically diazotrophs, to pure MPs which differ in physical properties (e.g., density, hydrophobicity, and/or size), namely, polyethylene, polypropylene, polyvinyl chloride and polystyrene, and to their most abundant associated organic additives (e.g., fluoranthene, 1,2,5,6,9,10-hexabromocyclododecane and dioctyl-phthalate). Growth, protein overproduction, direct physical interactions between MPs and bacteria, phosphorus acquisition mechanisms and/or N_2-fixation rates were evaluated. Cyanobacteria were positively affected by environmental and high concentrations of MPs, as opposed to heterotrophic strains, that were only positively affected with high concentrations of ∼120 μm-size MPs (detecting the overproduction of proteins related to plastic degradation and C-transport), and negatively affected by 1 μm-size PS beads. Generally, the organic additives had a deleterious effect in both autotrophic and heterotrophic bacteria and the magnitude of the effect is suggested to be dependent on bacterial size. Our results show species-specific responses of the autotrophic and heterotrophic bacteria tested and the responses (beneficial: the "good," deleterious: the "bad" and/or both: the "double-sword") were dependent on the type and concentration of MPs and additives. This suggests the need to determine the threshold levels of MPs and additives concentrations starting from which significant effects can be observed for key microbial populations in marine systems, and these data are necessary for effective environmental quality control management.

Keywords: microplastics, organic additives, marine pollution, cyanobacteria and heterotrophic bacteria, N2-fixing bacteria

INTRODUCTION

Marine coastal ecosystems are the most impacted zones by the pollution of plastics. Up to 10 million tons of plastic enter annually in the oceans (Almroth and Eggert, 2019). This oceanic "soup" of plastic is composed of different particle sizes: macroplastics (>250 mm), mesoplastics (1–25 mm), microplastics (MPs) (1–1,000 μm), and nanoplastics (NPs) (<1 μm) (Hartmann et al., 2019). The most abundant polymers (at the macro- and micro-size scale) on the surface of the oceans and seas are polyethylene (PE), followed by polypropylene (PP) and then by others such as polyvinyl chloride (PVC) or polystyrene (PS) (Suaria et al., 2016). MPs have associated chemical additives (usually organic) that have been added to them to improve their chemical properties, and these low molecular weight additives can leach from the plastic polymers, being also sorbed onto them (Bakir et al., 2014). Therefore, MPs can also be sources and vectors for these organic pollutants, which are deleterious for marine organisms (Hahladakis et al., 2018).

The abundance of plastic particles declines exponentially with depth according to their densities, resulting in low-density polymers (e.g., PE and PP) predominating in the surface waters and higher density polymers (e.g., PS) in the deeper areas (Erni-Cassola et al., 2019). However, some evidence suggests that much of the small plastic particles at the surface, independently of their density, end up in sediments by transport mechanisms (Reisser et al., 2015; Urbanek et al., 2018). The accumulation of MPs at depth indicates the susceptibility of planktonic and benthic macro- and micro-organisms to the effects of these pollutants.

In eukaryotic microorganisms, the deleterious effects of plastics have already been described (Wang and Zheng, 2008; Cole and Galloway, 2015; Nelms et al., 2018). However, studies investigating the direct effects of plastics, especially MPs, on marine prokaryotic organisms (e.g., in their growth, biochemistry or nutrient acquisition mechanisms) are still scarce (Harrison et al., 2011; Bryant et al., 2016; Romera-Castillo et al., 2018; Tetu et al., 2019; Machado et al., 2020; Piccardo et al., 2020; Sarker et al., 2020; Seeley et al., 2020). None have investigated the direct effect of MPs, for example, on marine diazotrophs, which are capable of converting the nitrogen gas (N_2) into ammonia (NH_3) through the nitrogenase enzyme complex and playing an important role in the marine N cycle. The few studies that have been done on other microorganisms usually are focused on plastic degradation and biofilm formation (Urbanek et al., 2018). Nonetheless, Machado et al. (2020) and Seeley et al. (2020) suggest that MPs can be anthropogenic stressors affecting microbial diversity and N-cycles. Other studies have reported changes in the microbial communities associated with the floating plastics through metagenomic analysis (Yang et al., 2019), suggesting that the response to plastic pollution can be species-specific. Tetu et al. (2019), Sarker et al. (2020), and Piccardo et al. (2020) also revealed the importance of concentration levels of leached plastic in cyanobacteria and heterotrophic bacteria. Considering these previous results, experimental studies investigating the effect of MPs and their additives should take into account the response of different bacterial test species and different concentration levels of the pollutants. Moreover, the previous studies investigating the effect of plastic pollution use plastics with unknown chemical additives, and to separate the effects of plastics and additives, pure MPs and their known additives must be tested. Furthermore, varying physical properties of MPs have to be considered (e.g., density, hydrophobic, or size) since could affect the response of microorganisms.

Here, we report the responses of different bacterial species, specifically N_2-fixing phototrophic and heterotrophic bacteria to different concentrations of pure MPs (i.e., PE, PP, PVC, and PS) and their most predominant organic chemical additives [fluoranthene, 1,2,5,6,9,10-hexabromocyclododecane (HBCD) and dioctyl-phthalate (DEHP)]. Our results show beneficial, detrimental or both effects, depending on the species tested and the type and concentrations of MPs and additives added.

MATERIALS AND METHODS

Culture Strains Tested

Five marine N_2-fixing species (two cyanobacteria and three heterotrophic bacteria), found in association with *P. oceanica* (Agawin et al., 2017; Fernández-Juárez et al., in prep), were selected according to the experimental design described in **Supplementary Table 1**. Before the experiments, the cells were acclimatized and cultured in their respective optimal culture media to achieve their exponential phase. Culture media were composed of synthetic seawater medium (ASN-III) + Turks island salts 4X for *Halothece* sp., $BG11_0$ for *F. muscicola* and marine broth (MB) for the rest of the heterotrophic bacteria (Rippka et al., 1979). The cells were acclimated at 25°C at 120 r.p.m in a rotatory shaker with a photoperiod of 12 h (hours) dark:12 h light under low-intensity fluorescent light (30 μE m^{-2} s^{-1}).

Experimental Culture Conditions

All the experiments and response variables were performed in triplicate ($n = 3$) in artificial seawater (ASW) medium following Kim et al. (2007) at pH 7, adding 1 mL^{-1} per L of trace metal [L^{-1}: 2.86 g H_3BO_3, 1.81 g $MnCl_2{\cdot}4H_2O$, 0.22 g $ZnSO_4{\cdot}7H_2O$, 0.39 g $NaMoO_4{\cdot}2H_2O$, 0.079 g $CuSO_4{\cdot}5H_2O$ and 0.049 g $Co(NO_3)_2{\cdot}6H2O$], glucose (final concentration 0.1% [v/v]), and with the respective MPs and/or organic additives. Inorganic phosphorus (PO_4^{3-}, 0.04 g L^{-1} K_2HPO_4), iron (Fe, 0.006 g L^{-1} ferric citrate) and inorganic nitrogen (NH_3, 0.5 g L^{-1} NH_3Cl) were added according to the response variable measured as we described below. Bacteria at their exponential phase were inoculated in the treatments (**Supplementary Table 1**) and incubated for 72 h under the same conditions as when they were previously acclimatized (i.e., at 25°C, 120 r.p.m in a rotatory shaker with a photoperiod of 12 h dark:12 h light, under low-intensity fluorescent light, 30 μE m^{-2} s^{-1}).

The pure MPs (low-density polyethylene [PE] with size 109 ± 6.29 μm, polypropylene [PP] with size 90 ± 7.56 μm and low-density polyvinyl chloride [PVC] with size 164 ± 8.03 μm) and organic additives (fluoranthene, 1,2,5,6,9,10-hexabromocyclododecane [HBCD] and dioctyl-phthalate

[DEHP]) used were obtained from Sigma-Aldrich. Besides, we used fluorescent polystyrene (PS)-based latex beads (Fluoresbrite® YG Microspheres 1.00 μm, Polysciences, Inc.) as the lowest sized MPs, based on the definition of MPs (Hartmann et al., 2019). The stock solution of MPs was made at 100 mg mL^{-1}, resuspending the MPs (previously UV-sterilized for 15 min) in acetone (98% [v/v]) to avoid aggregation of MPs and for easier manipulation of the workings solutions. To prevent chemical damages of MPs by acetone, the stock solution was rapidly diluted to working solutions of 1 mg mL^{-1} in ASW. The organic additives, i.e., fluoranthene and HBCD, were initially prepared in 1 mg mL^{-1} in absolute ethanol and acetone (98% [v/v]), respectively. For the DEHP additive that was in liquid form, a stock solution of 1 mg mL^{-1} was also prepared. We diluted these stock solutions to working solutions of 3 mg L^{-1} in ASW. Fluorescent PS beads were sterilized following the manufacturer's instructions, and the different concentrations in ASW were made from a stock solution of 4.55×10^{10} particles mL^{-1}. The controls were made with the respective amounts of acetone and/or ethanol (without any MPs nor organic additives). All the treatments have ≤ 1% acetone or ethanol to avoid any biological effect in the cells, and co-solvents effect in water (Schwarzenbach et al., 2002).

Experiments were performed in two parts (**Supplementary Table 1**), i.e., (I) under environmentally relevant concentrations (in which we performed an initial screening of the five strains selected) and (II) the "worst-case" scenario (in which we selected two strains, one cyanobacterium and one heterotrophic bacterium as our model strains). Ecotoxicology thresholds for MPs were determined following (Reddy et al., 2006; Suaria et al., 2016; Everaert et al., 2018; Kane et al., 2020), which established that MPs can accumulate up to 29–133 μg mL^{-1} in the water column and seafloor. For organic additives, we followed the concentrations reported in Hermabessiere et al. (2017), in which it is reported that additives can accumulate between from pg L^{-1} to μg L^{-1}, finding up to 44.39 μg L^{-1} in the water column.

Under Environmental Concentrations

In the first part, we made an overall screening of the five culture strains in sterile 2 mL well microplates (with 2 mL of culture media) to study their growth response under marine environmentally relevant concentrations of MPs and additives, with optimal nutrient conditions of PO_4^{3-}, Fe and NH_3 ($n = 3$). We used five concentration for MPs (0, 0.01, 0.1, 1, and 100 μg mL^{-1}) and organic additives (0, 0.3, 3, 30, and 300 μg L^{-1}) (**Supplementary Table 1**). Additional treatments combining MPs and plastic additives (e.g., PE-fluoranthene, PP-HBCD, and PVC-DEHP) were done by combining the lowest and the highest number of MPs and additives to test for possible interacting effects of MPs and their organic additives (**Supplementary Table 1**). Growth analysis was assessed through flux cytometry ($n = 3$).

Under the "Worst-Case" Scenario

In the second part, we selected two strains, one autotrophic (*Halothece* sp., being our model phototrophic bacteria) and one heterotrophic (*Cobetia* sp., which was our model heterotrophic bacteria). We established two levels MPs and additives concentration: 100 and 1,000 μg mL^{-1} for MPs, and 300 and 3,000 μg L^{-1} for the organic additives. We also selected a concentration of 4.55×10^6 and 4.55×10^7 particles mL^{-1} for PS beads. We cultured the test bacteria in 50 mL falcon (with 30 mL of culture media) tubes under N_2-fixing conditions (limiting NH_3 [∼ 0.15 mM] and with optimal PO_4^{3-} and Fe) for growth, protein overproduction, microscopical analysis, PO_4^{3-}-uptake and N_2-fixation assays, or under PO_4^{3-}-limiting conditions (with optimal NH_3 and Fe) for alkaline phosphatase activity (APA) ($n = 3$, **Supplementary Table 1**).

Flow Cytometry

Aliquots of cultures from all the experiments were taken initially and after 72 h of incubation and counted in fresh (without freezing nor fixing) with a Becton Dickinson FACS-Verse cytometer (Beckton & Dickinson, Franklin Lakes, New Jersey, USA). Fluorescent beads, BD FACSuite™ CS&T research beads (Beckton & Dickinson and Company BD Biosciences, San Jose, USA), were used as internal standards to calibrate the instrument. Cells were separated by combinations of the scatter plots of the flow cytometer parameters: forward scatter (FSC, reflecting cell size), side scatter (SSC, reflecting internal complexity of the cells), and/or fluorescein isothiocyanate filter (FITC, reflecting fluorescence, 488 nm excitation, 530/30 nm emission). For treatments with fluorescent PS beads, adsorption to them was measured (without detaching cells from the beads) using the FSC and FITC cytometer signals (**Supplementary Figure 1**). Adsorbed bacteria were those with intermediate intensity fluorescence signals between the free bacteria and the beads (**Supplementary Figure 1**). In all the experiments, a total of 10,000 cells (or cells recorded in 30 s) were counted in each sample. Changes in growth were calculated as the changes in cell concentrations after 72 h.

Protein Identification: MALDI-TOF Assay and Protein Structure Prediction

Crude cell extracts were done following the methods described in Ivleva and Golden (2007), using the cultures of *Halothece* sp. and *Cobetia* sp. after 72 h of incubation in the "worst-case" scenario (at the highest concentration treatment of MPs/additives and the control). Protein concentrations were determined with Bradford protein assay (Thermofisher), following the manufacturer's instructions. The protein extracts were run into polyacrylamide gels, 4–20% (p/v) Amersham ECL Gel (GE Healthcare, Chicago, Illinois, EEUU), using the ECL Gel Box system (GE Healthcare, Chicago, Illinois, EEUU) following the manufacturer's instructions.

The different bands detected only in *Cobetia* sp. exposed to high concentrations of MPs (1,000 ug mL^{-1} of PE, PP, and PVC), which did not appear at the control, were excised from the gel with a clean scalpel and sent to MALDI-TOF analysis. Each gel slice was cut into small pieces and then transferred to a clean and sterile Eppendorf tube. Protein identification was performed following Jaén-Luchoro et al. (2017). The samples were then analyzed with an Autoflex III MALDI-TOF-TOF

(BrukerDaltonics) spectrometer using the software Compassflex series v1.4 (flexControl v3.4, flexAnalysis v3.4 and BioTools 3.2). The spectra were calibrated using the peptide calibration standard (BrukerDaltonics). The obtained mass spectra were used for the protein identification and the in-house database was created with the predicted protein sequence of the annotated genome of *Cobetia* sp. The search process was performed with the algorithm MASCOT (MatrixSciences).

Fasta sequence of the alcohol dehydrogenase (ADH) (detected through MALDI-TOF) was sent to the I-Tasser server for protein 3D-structure prediction (Zhang, 2008), with their domains previously checked in Pfam 32.0 (Finn et al., 2016). The predicted structure was sent to the FunFOLD2 server for the prediction of protein–ligand interactions (Roche et al., 2013). Besides, we detected the potential sites of ligand or "pockets" through MetaPocket 2.0 (Huang, 2009). Finally, we predicted the orientation and position of the protein-ligand complex between polyethylene glycol (PEG) and ADH, docking these with Swissdock (Zoete and Michielin, 2011). All the structures were visualized by Pymol (DeLano, 2002).

Microscopic Observations

At the final time (after 72 h), the five strains tested were placed onto a microplate for inverted microscopy visualization of the physical interactions between bacterial cells and the MPs (i.e., PE, PP, and PVC) at 100x objective (Leica DM IRB). For *Halothece* sp. and *Cobetia* sp., their interaction with PS fluorescent beads (with an excitation of 441 nm and emission of 485 nm) were visualized by confocal microscopy (Leica TCS SPE, Leica Microsystems). Images were processed using the software Leica application suite (Leica Microsystems). The specific autofluorescence for *Halothece* sp. was observed with an excitation of 532 nm and an emission of 555–619 nm. For *Cobetia* sp., the cells were stained with Sybr green (Sigma-Aldrich), or propidium iodide (Sigma) to properly visualize the cells distinguishing them from the PS beads.

P-Metabolism Analysis

Alkaline phosphatase activity (APA) was evaluated through fluorometric assay following the hydrolysis of the substrate (S) 4-methylumbelliferyl phosphate (MUF-P, Sigma-Aldrich) to 4-methylumbelliferyl (MUF), following Fernández-Juárez et al. (2019). The culture media, i.e., in the "worst-case" scenario, was PO_4^{3-} limited (but with optimal NH_3 and Fe) to promote APA. Saturation curves of velocity (V, fmol MUF cell^{-1} h^{-1}) vs. substrate (S, μM) were made for each experimental condition for each of the two selected strains (*Halothece* sp. and *Cobetia* sp.). We used different concentrations of MUF-P: 0, 0.05, and 5 μM of MUF-P. After 1 h incubation in darkness at room temperature, APA was measured in a microtiter plate that contained buffer borated pH 10 (3:1 of sample: buffer). The MUF production (fmol MUF cell^{-1} h^{-1}) was measured with a Cary Eclipse spectrofluorometer (FL0902M009, Agilent Technologies) at 359 nm (excitation) and 449 nm (emission), using a calibration standard curve with commercial MUF (Sigma-Aldrich). The maximum velocity (V_{max}) at saturating substrate concentrations was obtained from each plot of V vs. S, using the Lineweaver-Burk plot.

For the determination of inorganic PO_4^{3-} concentrations for *Halothece* sp. and *Cobetia* sp. experiments, 1 mL of the culture was centrifuged for 15 min at 16,000 × g under 4°C. The bacteria-free clear supernatant was collected and used for PO_4^{3-} determinations following standard spectrophotometric methods (Hansen and Koroleff, 2007). The PO_4^{3-} concentrations in the culture media were determined at the initial and final time (after 72 h). Specific PO_4^{3-}-uptake rates (pmol PO_4^{3-} cell^{-1} d^{-1}) were calculated as described in Fernández-Juárez et al. (2019) and Ghaffar et al. (2017).

Determination of N_2-Fixation Rates Through Acetylene Reduction Assay (ARA)

Rates of N_2-fixation were measured for *Halothece* sp. as our model strain, described in Fernández-Juárez et al. (2019, 2020), under the "worst-case" scenario. A known volume of culture (8 mL) was sampled during the dark photoperiod and transferred to a closed hermetic vial and oxygen was flushed from the sample through bubbling with N_2 gas. A medium with saturated acetylene was injected at 20% (v/v) final concentration in each vial with a sterile syringe. Samples were incubated for 3 h at room temperature (24°C) in the dark. After the 3 h incubation time, 10 mL of liquid was removed and transferred to Hungate tubes containing 1.25 mL of 20% trichloroacetic acid (Agawin et al., 2014). Prior to analysis with the gas chromatograph (GC), the Hungate tubes were incubated at 37°C overnight in a water bath. Ethylene and acetylene gas from the gas phase of the Hungate tubes were determined using a GC (model GC-7890, Agilent Technologies) equipped with a flame ionization detector (FID), following the set up described in Fernández-Juárez et al. (2019, 2020). Ethylene produced was calculated using the equation in Stal (1988). The acetylene reduction rates were converted to N_2-fixation rates (nmol mL^{-1} h^{-1}) using a factor of 4:1 (Jensen and Cox, 1983).

Statistical Analysis

Non-normally distributed data, the Kruskal-Wallis rank-sum non-parametric test was used since the size sample was $n < 20$. An unpaired two-sample Wilcoxon test was used to determine the significant effects among different concentrations of MPs and additives. All analyses were done in R-Studio, R version 3.5.3 (2019-03-11).

RESULTS AND DISCUSSION

Effects of Varying Concentrations of MPs and Additives, Under Relevant Concentrations in the Marine Environment

The addition of PE within the range of 0–100 μg mL^{-1} did not significantly affect all the diazotrophs tested ($p > 0.05$, $n = 3$, **Figure 1A**), in agreement with Machado et al. (2020). Moreover, PP and PVC within the range of 0–100 μg mL^{-1} did not significantly affect the growth of heterotrophic bacteria (*Cobetia* sp., *Marinobacterium litorale* and *Pseudomonas azotifigens*)

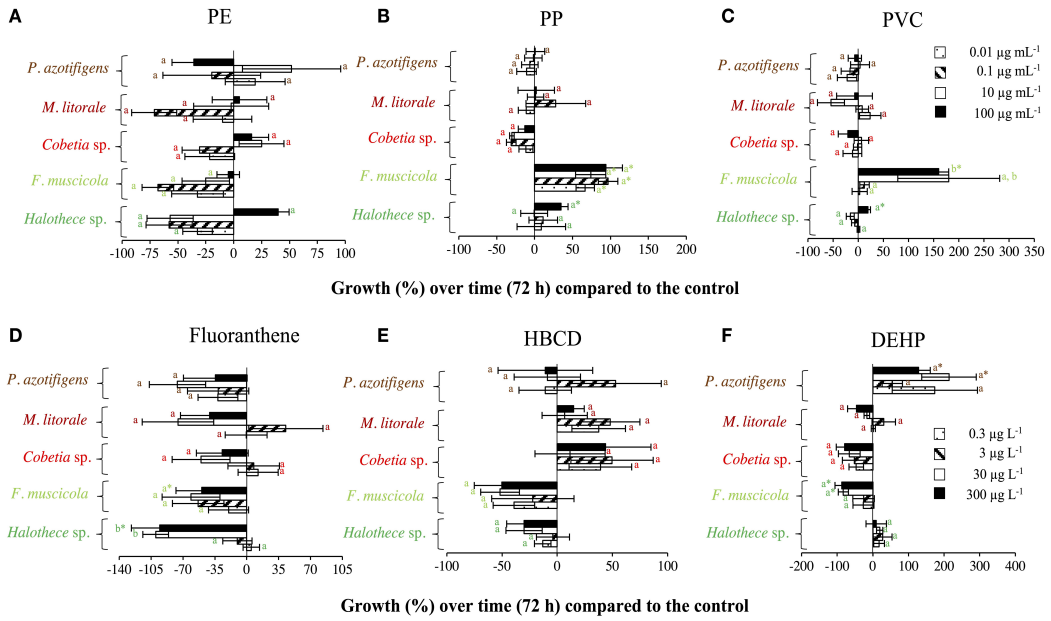

FIGURE 1 | Growth responses of diazotrophs subject to MPs and organic additives under relevant concentrations in the marine environment after 72 h, compared with the control value. **(A)** PE, **(B)** PP, and **(C)** PVC, with 0, 0.01, 0.1, 10, and 100 µg mL^{-1}. **(D)** Fluoranthene, **(E)** HBCD, and **(F)** DEHP, with 0, 0.3, 3, 30, and 300 µg L^{-1}. Values are the mean, and the error bar is the standard error between the replicates ($n = 3$). Letters indicate pairwise analysis among the variables (i.e., concentration) inside each strain (see the different colors), and asterisks (*) indicate pairwise significant differences between variables and the control ($p < 0.05$), using a *post-hoc* test (Wilcoxon) after Kruskal-Wallis over the whole dataset.

($p > 0.05$, $n = 3$, **Figures 1B,C**). This is consistent with the results obtained by Piccardo et al. (2020), in which PET microparticles at 100 µg mL^{-1} do not have affect in the heterotrophic bacteria (e.g., *Vibrio fischeri*). However, species-specific growth responses of the bacteria tested with the addition of MPs were exemplified here when PVC and PP addition (at 100 µg mL^{-1}) significantly enhanced the growth of the autotrophic cyanobacterial diazotrophs (*Halothece* sp. and *Fischerella muscicola*) by 1.5- to 4- fold ($p < 0.05$, $n = 3$, **Figures 1B,C**). This supports the idea that MPs may be selecting bacterial communities in the ocean (Seeley et al., 2020).

The effect of organic additives on bacterial growth is suggested here to be dependent on the type of additive (i.e., fluoranthene, HBCD and DEHP) (**Figures 1D–F**). Fluoranthene reduced the growth of *Halothece* sp. and *F. muscicola*, by 22- and 7- fold, respectively, at the highest concentrations compared to the control ($p < 0.05$, $n = 3$, **Figure 1D**). Besides, DEHP significantly reduced the growth of *F. muscicola* at the highest concentrations compared to the control ($p < 0.05$, $n = 3$, **Figure 1F**). On the contrary, the additive HBCD did not affect the growth of any species ($p > 0.05$, $n = 3$, **Figure 1E**), while the additive DEHP significantly enhanced the growth of the heterotrophic *P. azotifigens* by 4-fold, being significative at 30 and 300 µg L^{-1} compared to the control ($p < 0.05$, $n = 3$, **Figure 1F**). Additives can be sorbed and/or liberated by MPs in marine environments, with contrasting consequences (Gallo et al., 2018; Hahladakis et al., 2018). If sorbed, these chemicals may be less available for cells, being less harmful to sensitive species (Hahladakis et al., 2018), but detrimental to species making use of them as a C-source (Cao et al., 2015; Wang et al., 2015). If liberated, the increased availability of additives may be more harmful to

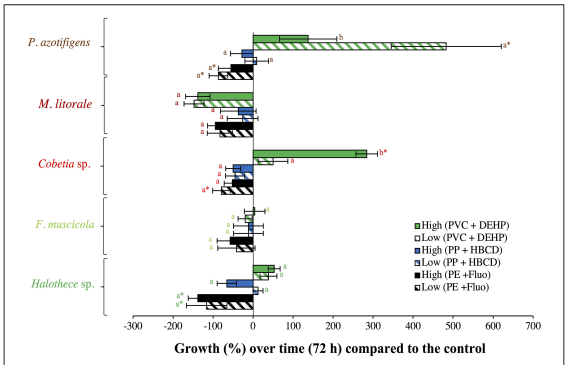

FIGURE 2 | Growth responses of diazotrophs subject to MP-additive interactions (PE + fluoranthene, PP + HBCD, and PVC + DEHP) after 72 h (under relevant concentrations), compared with the control value. "Low" and "High" represent low and high concentrations of MPs (0.01 and 100 µg mL^{-1}, respectively) and plastic additive (0.3 and 300 µg L^{-1}, respectively). Values are the mean, and the error bar is the standard error between the replicates ($n = 3$). Letters indicate pairwise analysis among the variables (i.e., concentration) inside each strain (see the different colors), and asterisks (*) indicate pairwise significant differences between variables and the control ($p < 0.05$), using a *post-hoc* test (Wilcoxon) after Kruskal-Wallis over the whole dataset.

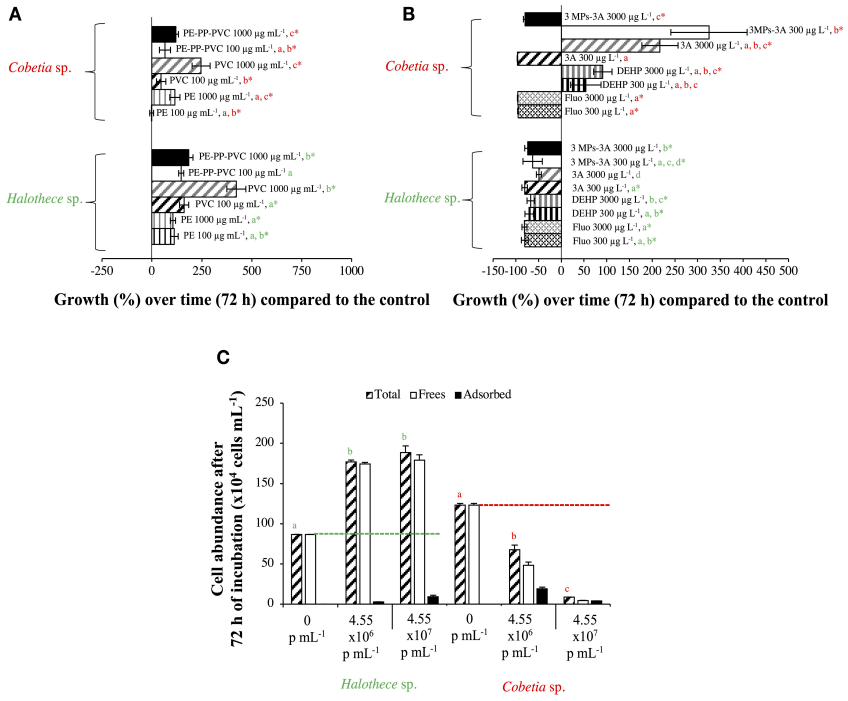

FIGURE 3 | Growth responses of diazotrophs subject to high concentrations (the "worst-case" scenario) of MPs and additives after 72 h, compared with the control value. **(A)** Effect of MPs (PE, PP, and/or PVC, 100/1,000 µg mL^{-1}). The effect of PP alone with non-significant results is not included in the graph. **(B)** Effect of organic additives (fluoranthene, HBCD, and/or DEHP, 300/3,000 µg L^{-1}). The effect of HBCD alone with non-significant results is not included in the graph. **(C)** Effect of PS beads. Total, free and adsorbed bacteria (to the beads) are differentiated. Values are the mean, and the error bar is the standard error between the replicates ($n = 3$). Letters indicate pairwise analysis among the variables (i.e., concentration) inside each strain (see the different colors), and asterisks (*) indicate pairwise significant differences between variables and the control ($p < 0.05$), using a *post-hoc* test (Wilcoxon) after Kruskal-Wallis over the whole dataset.

sensitive species (Tetu et al., 2019; Sarker et al., 2020), but benefit species using them (Cao et al., 2015; Wang et al., 2015). In our experiments, PVC + DEHP significantly enhanced the growth of *P. azotifigens* and *Cobetia* sp. (synergism), but significantly altered it when PE + fluoranthene were added (antagonism) ($p < 0.05$, $n = 3$, **Figure 2**), while the addition of PP + HBCD did not have any further effect ($p > 0.05$, $n = 3$, **Figure 2**).

Effect of Varying Concentrations of MPs and Additives, Under the "Worst-Case" Scenario

Effect of High Concentration of MPs

High MPs concentrations stimulated cell growth, especially with the addition of PVC in both strains compared with the control by 6- to 8- fold ($p < 0.05$, $n = 3$, **Figure 3A**). The enhancement of the bacterial growth, especially in the heterotrophic strain, *Cobetia* sp., after 72 h of incubation can be due to increased dissolved organic carbon (DOC) pool in the medium that could have leached from the MPs added (Romera-Castillo et al., 2018). Unfortunately, DOC was not measured.

Species-specific responses based on protein production profile are also shown here when two proteins related to plastic degradation (alcohol dehydrogenase [ADH] of 342 amino acids, HA399_02440) and carbon transport (C4-dicarboxylate ABC transporter substrate-binding protein [C4-ABCS] of 329 amino acids, HA399_06715) were overproduced in the heterotroph *Cobetia* sp., but were not detectable with the MALDI-TOF analyses in the cyanobacteria *Halothece* sp. after the addition of MPs at high concentrations. ADHs from *Rhodopseudomonas acidophila* M402 and *Pseudomonas oleovorans* have been shown to oxidize plastic polymers (e.g., PEG), being NAD-dependent (Ohta et al., 2006; Kawai, 2010), consistent with our *in silico* structural analysis for *Cobetia* sp. (**Figures 4A–C**). Further experimental studies have to be performed to evaluate if *Cobetia* sp. can degrade PEG polymers or similar ones, and indeed if the carbon released by ADH is transported by C4-ABCS inside the cells since C4-ABCS is a carbon transporter (Rosa et al., 2019).

Effect of the Size of MPs

Larger-sized MPs (i.e., 120 µm) enhanced the growth of autotropic and heterotrophic bacteria at high concentrations of MPs (**Figure 3A**). Larger-sized MPs may provide more surface area for the cells to adhere and attach as observed in the

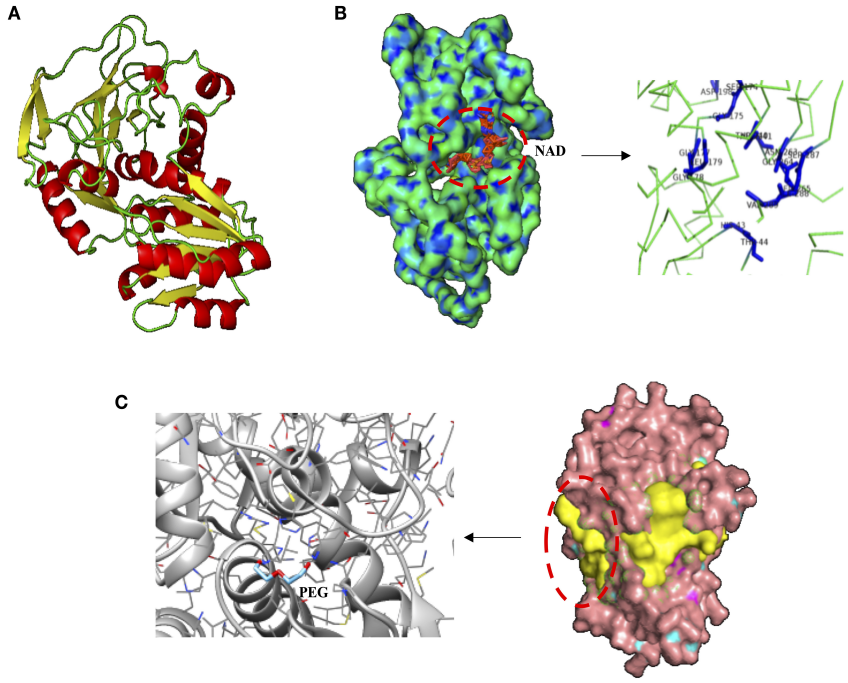

FIGURE 4 | Structural analysis of alcohol dehydrogenase (ADH) from *Cobetia* sp. (HA399_02440). **(A)** Protein prediction of ADH showing, **(B)** the nicotinamide-adenine-dinucleotide (NAD) dependence, displaying the ligand binding residues HIS 43, THR 44, SER 174, GLY 175, GLY 177, GLY 178, LEU 179, ASP 198, THR 240, ASP 241, ASN 263, GLY 264, LYS 265, SER 287, ILE 288, and VAL 289. **(C)** The three of the most probable pockets of the ADH (potential sites of ligand binding, in yellow), and the docking site (prediction of the orientation and position of protein-ligand complex) between the polyethylene glycol (PEG) and ADH.

heterotrophs tested here (**Figures 5B–E**). Surface attachment of the cells to the MPs through hydrodynamic and electrostatic interactions may enhance growth and facilitate nutrient uptake (especially under oligotrophic conditions), in most of the cases by the biofilm formation, increasing the surface of the substrates. This can aid the uptake of the necessary metabolites and co-factors, as suggested in Tuson and Weibel (2013). Smaller-sized MPs (i.e., PS beads of 1 μm-size), however, affected negatively the smallest size heterotrophic bacteria (i.e., *Cobetia* sp. of ∼ 1 μm-size, $p < 0.05$, $n = 3$, **Figure 3C**), and not the unicellular cyanobacteria (i.e., *Halothece* sp. of ∼ 4 to 7 μm-size) ($p > 0.05$, $n = 3$, **Figure 3C**). This can be due to the differences in the degree of physical adsorption between the PS beads and the different bacterial species. Approximately 40–87% of *Cobetia* sp. cells were adsorbed to PS (**Figures 3C**, **5H,I**), while only ∼2–5% of *Halothece* sp. cells were adsorbed (**Figure 3C**). The mechanisms behind the negative effect of small-sized MP in small-sized bacteria needs to be further studied and can possibly be due to disruption of bacterial cell division by the aggregation of the cells and beads. Although fewer PS beads were adsorbed on *Halothece* sp. cells, an invagination of the cell membranes by PS beads has been observed, possibly being engulfed or included as a carbon source (**Figures 5F,G**).

Physicochemical Properties of MPs

The physicochemical properties (e.g., hydrophobicity, electrostatic attraction, or roughness) of different MPs may affect the responses of bacterial communities (Ogonowski et al., 2018). Hydrophobicity, for example, can directly affect the bacterial colonization of MPs. PS polymers, which have aromatic phenyl groups, are one of the most hydrophobic polymers (Ogonowski et al., 2018), and this may explain the adherence of both autotrophic and heterotrophic bacteria to PS beads (**Figures 5F–I**). Contrary to the cyanobacterial diazotrophs (*Halothece* sp. and *F. muscicola*), which were not capable of adhering to the MPs, heterotrophic N_2-fixers (*Cobetia* sp., *M. litorale*, and *P. azotifigens*) tested were able to adhere to other types of MPs (i.e., PE, PP, and PVC, **Figures 5A–E**) which are less hydrophobic than PS. Moreover, PVC polymers are slightly more hydrophilic than PE (Kennedy, 2014), suggesting that they can be less available for adhesion and more available for bacterial growth. This may explain why PVC polymers were the MPs that most enhanced bacteria growth (**Figure 3A**).

Effect of High Concentrations of Organic Additives

Contrary to the effects of MPs, the addition of different types of organic additives (fluoranthene, HBCD and/or DEHP up to 3,000

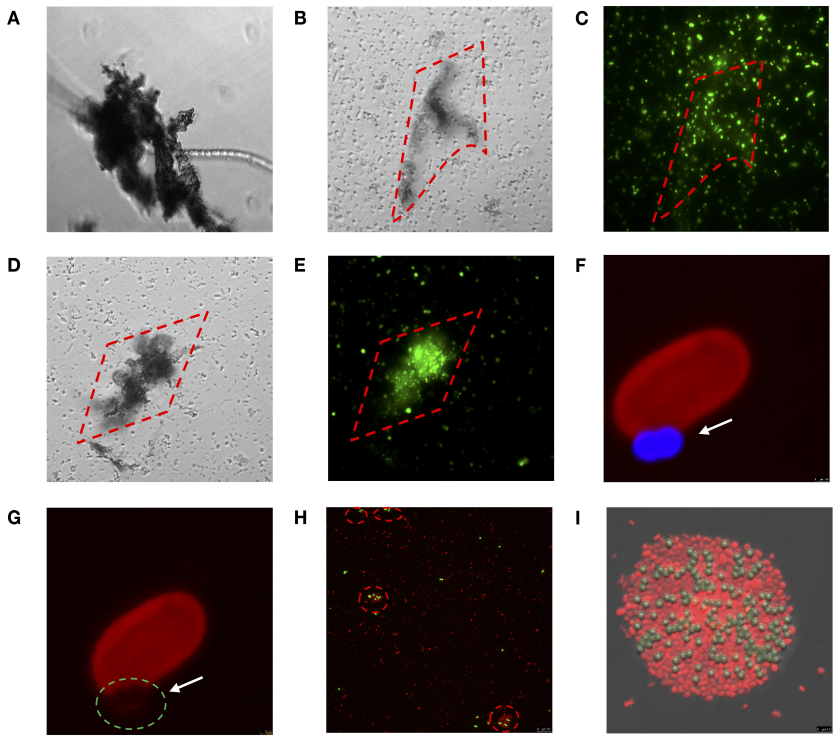

FIGURE 5 | Direct physical interaction between MPs and bacterial species tested in which **(A–E)** show the interaction between diazotrophs and mix of MPs (PE, PP, and PVC) at 100 μg mL^{-1} through inverted microscopy: **(A)** *Fischerella muscicola* under bright-field (BF), **(B,C)** *Cobetia* sp. under BF and Sybr-green channel, respectively, **(D,E)** *Marinobacterium litorale* under BF and Sybr-green channel, respectively; **(F–I)** show the physical interaction between diazotrophs and PS 1 μm beads (excitation of 441 nm and emission of 485 nm) through confocal microscopy: **(F,G)** *Halothece* sp. under excitation of 532 nm wavelength and emission of 555–619 nm. The arrows and green dashed circle show where the cell membrane is interacting with the PS bead (blue). **(H,I)** *Cobetia* sp. under excitation of 493 and 636 nm of emission. The dashed red circles show cell agglomeration on the PS beads (yellow). Images were taken at 1000x **(A–E** and **H)** and further magnified **(F,G,I)**.

μg L^{-1}) affected negatively the growth of *Halothece* sp. by 8-fold ($p < 0.05$, $n = 3$, **Figure 3B**). For the heterotrophic bacteria, different responses were observed, being the fluoranthene the most toxic pollutant ($p < 0.05$, $n = 3$, **Figure 3B**). The differing sensitivities of different species of bacteria to a particular type of additive can be due to cell-size dependent toxicity. For example, here we found an increasing toxicity to a PAH additive, fluoranthene, from bigger- to smaller-sized: *Cobetia* sp. (~1 μm) > unicellular cyanobacteria *Halothece* sp. (4–7 μm), > filamentous cyanobacteria *F. muscicola* (~7 μm) ($p < 0.05$, Spearman's correlation, $n = 21$, $r^2 = 0.7$) (**Figures 1D**, **3B**). The negative correlation between cell size and PAH toxicity is consistent with the study of Echeveste et al. (2010), and may be due to the higher surface to volume ratio of smaller-sized cells which increases the potential of the additives to be adsorbed or consumed by the cells. The DEHP additive (at high concentrations) and the interaction of the three MPs with the three plastic additives at low concentrations enhanced the growth of *Cobetia* sp. ($p < 0.05$, $n = 3$, **Figure 3B**), indicating that this species might use DEHP as a C-source and can be a possible bioremediator of DEHP-contaminated environments like *Rhodococcus* (Wang et al., 2015). Nevertheless, here we did not intend to reproduce an environmental situation since it may be improbable to find such high concentrations in the water column due to their solubility. However in marine sediments, concentrations of up to 2,988 μg Kg^{-1} of organic pollutants can be found in extremely impacted areas (Hermabessiere et al., 2017), and thus our results provide useful data to understand the response of the microorganisms associated with the benthic organisms.

Effect of MPs Pollution in the P and N-Metabolism

P-Acquisitions Mechanisms

The MPs and their plastic additives generally enhanced the alkaline phosphatase activity (APA) of *Halothece* sp. The addition of PS beads (at 4.55×10^7 particles mL^{-1}) increased the maximum rate of reaction (V_{max}) up to 0.21 fmol MUF $cell^{-1}$ h^{-1}, significantly higher than controls with a V_{max} of 0.033 fmol MUF $cell^{-1}$ h^{-1} ($p < 0.05$, $n = 3$, **Figure 6A**). In previous experiments, we described that the cyanobacterial N_2-fixer *Halothece* sp. synthesizes an alkaline phosphatase D (PhoD)

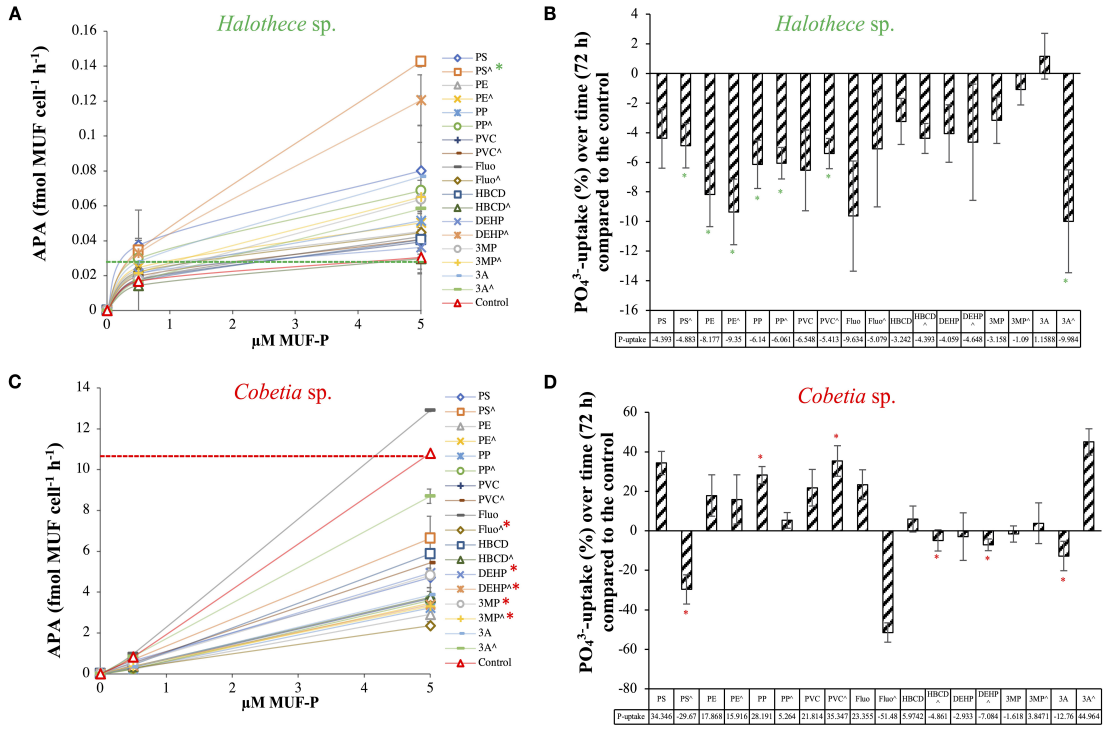

FIGURE 6 | Phosphorus acquisition mechanisms for two species of N_2-fixers exposed to different MPs and their plastic additives: **(A)** Alkaline phosphatase activity (APA, fmol MUF cell^{-1} h^{-1}) and (**B**) PO_4^{3-}-uptake (pmol PO_4^{3-} cell^{-1} d^{-1}) for *Halothece* sp., using relative values (with the control as reference). **(C)** APA and **(D)** PO_4^{3-}-uptake for *Cobetia* sp., using relative values (with the control as reference). (∧) indicates treatments up to 1,000 µg mL^{-1} (MPs) and 3,000 µg L^{-1} (organic additives), without (∧) indicates treatments with 100 µg mL^{-1} (MPs) and 300 µg L^{-1} (organic additives). Values are the mean, and the error bar is the standard error between the replicates ($n = 3$). Asterisks (*) indicate significant differences ($p < 0.05$) compared with the controls, using a *post-hoc* test (Wilcoxon) after Kruskal-Wallis over the whole dataset.

that is Fe dependent (Fe as metal co-factor) (Fernández-Juárez et al., 2019). Since metals (i.e., Fe) can be accumulated onto the plastics (Rochman et al., 2014), it is hypothesized that MPs may promote an environment rich in Fe co-factors. Considering the P-dependence of important processes (e.g., N_2-fixation, Fernández-Juárez et al., 2019), stimulation of APA can promote the growth of *Halothece* sp. For this unicellular cyanobacterium, PO_4^{3-}-uptake rates were significantly downregulated by the addition of MPs and their plastic additives ($p < 0.05$, $n = 3$, **Figure 6B**). Comparisons between treatments were made (**Supplementary Table 2**), showing that the combination of the three MPs (i.e., high levels) and the three additives (i.e., low levels) were the treatments with lower reduction of the PO_4^{3-}-uptake. The decreased PO_4^{3-}-uptake rates observed in *Halothece* sp. may be due to the adsorption of phosphate ions by PE and PVC (Hassenteufel et al., 1963).

Unlike *Halothece* sp., APA for *Cobetia* sp. was generally reduced by MPs and their organic additives ($p < 0.05$, $n = 3$, **Figure 6C**). Among the MPs, PE addition at high concentrations caused the most significant decrease in APA ($V_{max} = 8.52$ fmol MUF cell^{-1} h^{-1}) compared to controls ($V_{max} = 32.78$ fmol MUF cell^{-1} h^{-1}) ($p < 0.05$, **Figure 6C**). Among the plastic additives, fluoranthene caused the highest decrease in APA ($V_{max} = 11.52$ fmol MUF cell^{-1} h^{-1}) compared to controls ($p < 0.05$, **Figure 6C**). Significant differences in PO_4^{3-}-uptake rates were observed among the treatments tested ($p < 0.05$, $n = 3$, **Figure 6D** and **Supplementary Table 2**). Contrary to *Halothece* sp., PO_4^{3-}-uptake was increased with the addition of PP and PVC ($p < 0.05$, $n = 3$, **Figure 6D**), maybe as a consequence of higher nutrient and energy requirements for growth. Hence, we show species-specific differences of the P-mechanisms and P-requirements and the responses of these processes to MPs and their additives, showing that P-homeostasis can be disturbed with the addition of MPs and their organic additives associated.

Effect on N_2-Fixation in Cyanobacteria

In a seminal paper, Bryant et al. (2016) claimed that MPs may be hot spots of N_2-fixing autotrophic bacteria, based on the high abundances of N_2-fixation genes (*nifH*, *nifD*, and *nifK*) in the metagenomes associated with the plastic. Unfortunately, the authors did not measure the N_2-fixation activities, considering

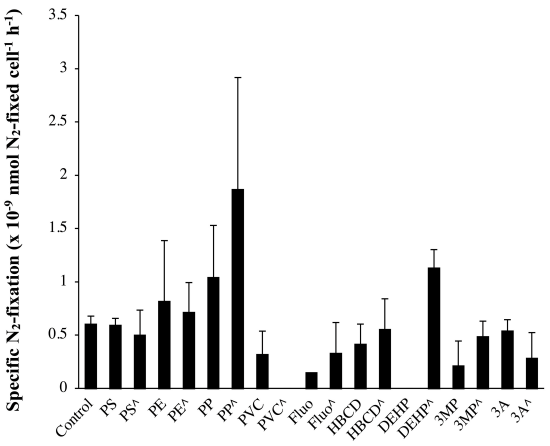

FIGURE 7 | Specific N_2-fixation rates (nmol N_2-fixed cell^{-1} h^{-1}) in the unicellular cyanobacteria *Halothece* sp. exposed to MPs and their plastic additives. (∧) indicates treatments up to 1,000 μg mL^{-1} (MPs) and 3,000 μg L^{-1} (organic additives), and without (∧) indicates treatments with 100 μg mL^{-1} (MPs) and 300 μg L^{-1} (organic additives). Values are the mean, and the error bar is the standard error between the replicates ($n = 3$).

that N_2-fixation rates in the open ocean are largely maintained by cyanobacteria (Zehr and Capone, 2020). Hence, cyanobacteria N_2-fixers can be one of the most impacted groups. Here, the effects of MPs and their additives on N_2-fixation rates are reported for the first time in cyanobacteria (i.e., *Halothece* sp., **Figure 7**). However, MPs and their additives did not have a significant effect on specific N_2-fixation rates of *Halothece* sp. ($p > 0.05$, $n = 3$, **Figure 7**), but as we showed that growth was positively enhanced with the addition of MPs (**Figure 3A**), or negatively affected by the addition of organic additives (**Figure 3B**), these pollutants could eventually enhance/inhibit global N_2-fixation rates in the environment.

In summary, this study shows that the most predominant MPs (e.g., PE, PP, PVC, and PS) in the oceans and their commonly associated organic additives (i.e., fluoranthene, HBCD, and DEHP) can be beneficial (the "good"), deleterious (the "bad"), or both (the "double-sword") to marine bacteria. Our study provides useful data to understand the response of marine bacteria, especially the diazotrophs to MPs pollution. Nevertheless, the transposition of the results obtained under *in vitro* controlled conditions must be taken with precautions since our study used concentrations that may not be representative of all marine environments. Open questions such as how the hydrophobicity of MPs can affect the growth responses, or if N_2-fixers may have another important environmental role of biodegrading synthetic plastic polymers aside from their important ecological role of providing new N into marine ecosystems, have to be addressed. The use of next-generation analysis (i.e., transcriptomic or proteomic assays) to identify changes in gene expression or protein profiles derived from MPs and plastic additives may allow a better comprehension of the molecular responses behind the plastic threat in oceans.

DATA AVAILABILITY STATEMENT

The datasets presented in this study can be found in online repositories. The names of the repository/repositories and accession number(s) can be found in the article/ **Supplementary Material**.

AUTHOR CONTRIBUTIONS

VF-J and XL-A conducted all experiments with the help of AF-C, PE, AB-F, GR-M, and RG in the various parameters measured in the study. VF-J and NA led the writing of the MS. NA is the supervisor of the laboratory. All authors contributed to the article and approved the submitted version.

FUNDING

This work was supported by funding to NA through the Ministerio de Economía, Industria y Competitividad-Agencia Estatal de Investigación, and the European Regional Development Funds project (CTM2016-75457-P).

ACKNOWLEDGMENTS

We acknowledge the support and help of scientific technical service (Maria Trinidad Garcia Barceló) of the University of the Balearic Islands for gas-chromatography analyses. We also thank Pere Ferriol Buñola and Alba Coma Ninot for the help in the acquisition of the cultures, and project AAEE117/2017 of the Dirección General Innovación y Recerca CAIB.

SUPPLEMENTARY MATERIAL

The Supplementary Material for this article can be found online at: https://www.frontiersin.org/articles/10.3389/fmicb.2020.581118/full#supplementary-material

REFERENCES

Agawin, N. S. R., Benavides, M., Busquets, A., Ferriol, P., Stal, L. J., and Arístegui, J. (2014). Dominance of unicellular cyanobacteria in the diazotrophic community in the Atlantic Ocean. *Limnol. Oceanogr.* 59, 623–637. doi: 10.4319/lo.2014.59.2.0623

Agawin, N. S. R., Ferriol, P., Sintes, E., and Moyà, G. (2017). Temporal and spatial variability of in situ nitrogen fixation activities associated with the Mediterranean seagrass *Posidonia oceanica* meadows. *Limnol. Oceanogr.* 62, 2575–2592. doi: 10.1002/lno.10591

Almroth, B.C., and Eggert, H. (2019). Marine plastic pollution: sources, impacts, and policy issues. *Rev. Environ. Econ. Policy*, 13, 2, 317–326, doi: 10.1093/reep/rez012

Bakir, A., Rowland, S.J., and Thompson, R.C. (2014). Enhanced desorption of persistent organic pollutants from microplastics under simulated physiological conditions. *Environ. Pollut.* 185, 16–23. doi: 10.1016/j.envpol.2013.10.007

Bryant, J.A., Clemente, T.M., Viviani, D.A., Fong, A.A., Thomas, K.A., Kemp, P., et al. (2016). Diversity and activity of communities inhabiting plastic debris in the North Pacific Gyre. *mSystems* 1, 1–19. doi: 10.1128/mSystems.00024-16

Cao, J., Lai, Q., Yuan, J., and Shao, Z. (2015). Genomic and metabolic analysis of fluoranthene degradation pathway in *Celeribacter indicus* P73 T. *Sci. Rep.* 5, 1–12. doi: 10.1038/srep07741

Cole, M., and Galloway, T.S. (2015). Ingestion of nanoplastics and microplastics by pacific oyster larvae. *Environ. Sci. Technol.* 49, 14625–14632. doi: 10.1021/acs.est.5b04099

DeLano, W. (2002). *The PyMOL Molecular Graphics System*. Schrödinger, LLC. Available online at: http://www.pymol.org

Echeveste, P., Agustí, S., and Dachs, J. (2010). Cell size dependent toxicity thresholds of polycyclic aromatic hydrocarbons to natural and cultured phytoplankton populations. *Environ. Pollut.* 158, 299–307. doi: 10.1016/j.envpol.2009.07.006

Erni-Cassola, G., Zadjelovic, V., Gibson, M. I., and Christie-oleza, J. A. (2019). Distribution of plastic polymer types in the marine environment : a meta-analysis. *J. Hazard. Mater.* 369, 691–698. doi: 10.1016/j.jhazmat.2019.02.067

Everaert, G., Van Cauwenberghe, L., De Rijcke, M., Koelmans, A. A., Mees, J., Vandegehuchte, M., et al. (2018). Risk assessment of microplastics in the ocean: Modelling approach and first conclusions. *Environ. Pollut.* 242, 1930–1938. doi: 10.1016/j.envpol.2018.07.069

Fernández-Juárez, V., Bennasar-Figueras, A., Sureda-Gomila, A., Ramis-Munar, G., and Agawin, N. S. R. (2020). Differential effects of varying concentrations of phosphorus, Iion, and nitrogen in N_2-Fixing Cyanobacteria. *Front. Microbiol.* 11, 1–19. doi: 10.3389/fmicb.2020.541558

Fernández-Juárez, V., Bennasar-Figueras, A., Tovar-Sanchez, A., and R. Agawin, N. S. (2019). The role of iron in the P-acquisition mechanisms of the unicellular N_2-fixing cyanobacteria *Halothece* sp. found in association with the Mediterranean seagrass Posidonia oceanica. *Front. Microbiol.* 10, 1–22. doi: 10.3389/fmicb.2019.01903

Finn, R.D., Coggill, P., Eberhardt, R.Y., Eddy, S.R., Mistry, J., Mitchell, A.L., et al. (2016). The Pfam protein families database: towards a more sustainable future. *Nucleic Acids Res.* 44, D279–D285. doi: 10.1093/nar/gkv1344

Gallo, F., Fossi, C., Weber, R., Santillo, D., Sousa, J., Ingram, I., et al. (2018). Marine litter plastics and microplastics and their toxic chemicals components: the need for urgent preventive measures. *Environ. Sci. Eur.* 30:139. doi: 10.1186/s12302-018-0139-z

Ghaffar, S., Stevenson, R.J., and Khan, Z. (2017). Effect of phosphorus stress on *Microcystis aeruginosa* growth and phosphorus uptake. *PLoS ONE* 12:174349. doi: 10.1371/journal.pone.0174349

Hahladakis, J.N., Velis, C.A., Weber, R., Iacovidou, E., and Purnell, P. (2018). An overview of chemical additives present in plastics: migration, release, fate and environmental impact during their use, disposal and recycling. *J. Hazard. Mater.* 344, 179–199. doi: 10.1016/j.jhazmat.2017.10.014

Hansen, H. P., and Koroleff, F. (2007). "Determination of nutrients," in *Methods of Seawater Analysis, 3rd Edn*, eds K. Grasshoff, K. Kremling, and M. Ehrhard (Weinheim: Wiley – VCH Verlag), 159–228. doi: 10.1002/9783527613984.ch10

Harrison, P., Sapp, M., Schratzberger, M., and Osborn, A.M. (2011). Interactions between microorganisms and marine microplastics: a call for re- search. *Mar. Technol. Soc. J.* 45, 12–20. doi: 10.4031/MTSJ.45.2.2

Hartmann, N.B., Hüffer, T., Thompson, R.C., Hassellöv, M., Verschoor, A., Daugaard, A.E., et al. (2019). Are we speaking the same language? Recommendations for a definition and categorization framework for plastic debris. *Environ. Sci. Technol.* 53, 1039–1047. doi: 10.1021/acs.est.8b05297

Hassenteufel, W., Jagitsch, R., and Koczy, F. F. (1963). Impregnation of glass surfacae against sortion of phospahate traces. *Limnol. Oceanogr.* 8, 152–156. doi: 10.4319/lo.1963.8.2.0152

Hermabessiere, L., Dehaut, A., Paul-Pont, I., Lacroix, C., Jezequel, R., Soudant, P., et al. (2017). Occurrence and effects of plastic additives on marine environments and organisms: a review. *Chemosphere* 182, 781–793. doi: 10.1016/j.chemosphere.2017.05.096

Huang, B. (2009). MetaPocket: a meta approach to improve protein ligand binding site prediction. *OMICS* 13, 325–330. doi: 10.1089/omi.2009.0045

Ivleva, N. B., and Golden, S.S. (2007). Protein extraction, fractionation, and purification from cyanobacteria. *Methods Mol. Biol.* 362, 365-73. doi: 10.1007/978-1-59745-257-1_26

Jaén-Luchoro, D., Aliaga-Lozano, F., Gomila, R. M., Gomila, M., Salvà-Serra, F., Lalucat, J., et al. (2017). First insights into a type II toxin-antitoxin system from the clinical isolate *Mycobacterium* sp. MHSD3, similar to epsilon/zeta systems. *PLoS ONE* 12, 1–20. doi: 10.1371/journal.pone.0189459

Jensen, B. B., and Cox, R. P. (1983). Direct measurements of steady-state kinetics of cyanobacterial N_2 uptake by membrane-leak mass spectrometry and comparisons between nitrogen fixation and acetylene reduction. *Appl. Environ. Microbiol.* 45, 1331–1337. doi: 10.1128/AEM.45.4.1331-1337.1983

Kane, I.A., Clare, M.A., Miramontes, E., Wogelius, R., Rothwell, J.J., Garreau, P., et al. (2020). Seafloor microplastic hotspots controlled by deep-sea circulation. *Science* 5899:aba5899. doi: 10.1126/science.aba5899

Kawai, F. (2010). The biochemistry and molecular biology of xenobiotic polymer degradation by microorganisms. *Biosci. Biotechnol. Biochem.* 74, 1743–1759. doi: 10.1271/bbb.100394

Kennedy, E. J. (2014). Biological drug products: development and strategies. *ChemMedChem* 9, 2814–2815. doi: 10.1002/cmdc.201402432

Kim, H., Choo, Y. J., Song, J., Lee, J. S., Lee, K. C., and Cho, J. C. (2007). *Marinobacterium litorale* sp. nov. in the order Oceanospirillales. *Int. J. Syst. Evol. Microbiol.* 57, 1659–1662. doi: 10.1099/ijs.0.64892-0

Machado, M. C., Vimbela, G. V., Silva-Oliveira, T. T., Bose, A., and Tripathi, A. (2020). The response of *Synechococcus* sp. PCC 7002 to micro-/nano polyethylene particles - investigation of a key anthropogenic stressor. *PLoS ONE* 15, 1–14. doi: 10.1371/journal.pone.0232745

Nelms, S. E., Galloway, T. S., Godley, B. J., Jarvis, D. S., and Lindeque, P. K. (2018). Investigating microplastic trophic transfer in marine top predators. *Environ. Pollut.* 238, 999–1007. doi: 10.1016/j.envpol.2018.02.016

Ogonowski, M., Motiei, A., Ininbergs, K., Hell, E., Gerdes, Z., Udekwu, K. I., et al. (2018). Evidence for selective bacterial community structuring on microplastics. *Environ. Microbiol.* 20, 2796–2808. doi: 10.1111/1462-2920.14120

Ohta, T., Kawabata, T., Nishikawa, K., Tani, A., Kimbara, K., and Kawai, F. (2006). Analysis of amino acid residues involved in catalysis of polyethylene glycol dehydrogenase from *Sphingopyxis terrae*, using three-dimensional molecular modeling-based kinetic characterization of mutants. *Appl. Environ. Microbiol.* 72, 4388–4396. doi: 10.1128/AEM.02174-05

Piccardo, M., Provenza, F., Grazioli, E., Cavallo, A., Terlizzi, A., and Renzi, M. (2020). PET microplastics toxicity on marine key species is influenced by pH, particle size and food variations. *Sci. Total Environ.* 715, 136947. doi: 10.1016/j.scitotenv.2020.136947

Reddy, M.S., Shaik Basha, Adimurthy, S., and Ramachandraiah, G. (2006). Description of the small plastics fragments in marine sediments along the Alang-Sosiya ship-breaking yard, India. *Estuar. Coast. Shelf Sci.* 68, 656–660. doi: 10.1016/j.ecss.2006.03.018

Reisser, J., Slat, B., Noble, K., Plessis, K., Epp, M., Proietti, M., et al. (2015). The vertical distribution of buoyant plastics at sea: an observational study in the North Atlantic Gyre. *Biogeosciences* 12, 1249–1256. doi: 10.5194/bg-12-1249-2015

Rippka, R., Deruelles, J., Waterbury, J. B., Herdman, M., and Stanier, R. Y. (1979). Generic assignments, strain histories and properties of pure cultures of cyanobacteria. *Microbiology* 111, 1–61. doi: 10.1099/00221287-111-1-1

Roche, D. B., Buenavista, M. T., and McGuffin, L. J. (2013). The FunFOLD2 server for the prediction of protein-ligand interactions. *Nucleic Acids Res.* 41, 303–307. doi: 10.1093/nar/gkt498

Rochman, C.M., Hentschel, B.T., and Teh, S.J. (2014). Long-term sorption of metals is similar among plastic types: implications for plastic debris in aquatic environments. *PLoS ONE* 9:e85433. doi: 10.1371/journal.pone.0085433

Romera-Castillo, C., Pinto, M., Langer, T.M., Álvarez-Salgado, X.A., and Herndl, G.J. (2018). Dissolved organic carbon leaching from plastics stimulates microbial activity in the ocean. *Nat. Commun.* 9:1430. doi: 10.1038/s41467-018-03798-5

Rosa, L. T., Dix, S. R., Rafferty, J. B., and Kelly, D. J. (2019). A New Mechanism for high-affinity uptake of C4-dicarboxylates in Bacteria revealed by the structure of *Rhodopseudomonas palustris* MatC (RPA3494), a periplasmic binding protein of the Tripartite Tricarboxylate Transporter (TTT) Family. *J. Mol. Biol.* 431, 351–367. doi: 10.1016/j.jmb.2018.11.016

Sarker, I., Moore, L. R., Paulsen, I. T., and Tetu, S. G. (2020). Assessing the toxicity of leachates from weathered plastics on photosynthetic marine

bacteria prochlorococcus. *Front. Mar. Sci.* 7, 1–14. doi: 10.3389/fmars.2020.571929

Schwarzenbach, R. P., Gschwend, P. M., and Imboden, D. M. (2002). *Environmental Organic Chemistry*. Hoboken, NJ: John Wiley & Sons, Wiley-Interscience, 2003. doi: 10.1002/0471649643

Seeley, M. E., Song, B., Passie, R., and Hale, R. C. (2020). Microplastics affect sedimentary microbial communities and nitrogen cycling. *Nat. Commun.* 11, 1–10. doi: 10.1038/s41467-020-16235-3

Stal, L. J. (1988). Acetylene reduction technique for assay of nitrogenase. *Methods Enzymol.* 167, 474–484. doi: 10.1016/0076-6879(88)67052-2

Suaria, G., Avio, C. G., Mineo, A., Lattin, G. L., Magaldi, M. G., Belmonte, G., et al. (2016). The Mediterranean Plastic Soup: synthetic polymers in Mediterranean surface waters. *Sci. Rep.* 6:37551. doi: 10.1038/srep37551

Tetu, S.G., Sarker, I., Schrameyer, V., Pickford, R., Elbourne, L.D.H., Moore, L.R., et al. (2019). Plastic leachates impair growth and oxygen production in *Prochlorococcus*, the ocean's most abundant photosynthetic bacteria. *Commun. Biol.* 2:184. doi: 10.1038/s42003-019-0410-x

Tuson, H. H., and Weibel, D. B. (2013). Bacteria-surface interactions. *Soft Matter* 9, 4368–4380. doi: 10.1039/c3sm27705d

Urbanek, A. K., Rymowicz, W., and Mirończuk, A. M. (2018). Degradation of plastics and plastic-degrading bacteria in cold marine habitats. *Appl. Microbiol. Biotechnol.* 102, 7669–7678. doi: 10.1007/s00253-018-9195-y

Wang, J., Zhang, M. Y., Chen, T., Zhu, Y., Teng, Y., Luo, Y. M., et al. (2015). Isolation and identification of a di-(2-ethylhexyl) phthalate-degrading bacterium and its role in the bioremediation of a contaminated soil. *Pedosphere* 25, 202–211. doi: 10.1016/S1002-0160(15)60005-4

Wang, L., and Zheng, B. (2008). Toxic effects of fluoranthene and copper on marine diatom *Phaeodactylum tricornutum*. *J. Environ. Sci.* 20, 1363–1372. doi: 10.1016/S1001-0742(08)62234-2

Yang, Y., Liu, G., Song, W., Ye, C., Lin, H., Li, Z., et al. (2019). Plastics in the marine environment are reservoirs for antibiotic and metal resistance genes. *Environ. Int.* 123, 79–86. doi: 10.1016/j.envint.2018.11.061

Zehr, J. P., and Capone, D. G. (2020). Changing perspectives in marine nitrogen fixation. *Science* 368:aay9514. doi: 10.1126/science.aay9514

Zhang, Y. (2008). I-TASSER server for protein 3D structure prediction. *BMC Bioinformatics* 9:40. doi: 10.1186/1471-2105-9-40

Zoete, V., and Michielin, O. (2011). SwissDock, a protein-small molecule docking web service based on EADock DSS. *Nucleic Acids Res.* 39, 270–277. doi: 10.1093/nar/gkr366

Conflict of Interest: The authors declare that the research was conducted in the absence of any commercial or financial relationships that could be construed as a potential conflict of interest.

4. GENERAL DISCUSSION

GENERAL DISCUSSION

Environmental factors and emerging pollutants can affect diazotrophs at physiological and molecular levels, affecting their N_2-fixation activities. Here was investigated the effect of different nutrient concentrations (i.e., P, Fe and N) (**Chapters 1-3**) and anthropogenic factors [i.e., increasing CO_2 levels (and its concomitant effect in ocean acidification and warming), and emerging pollutants (MPs and their associated organic additives) (**Chapters 4-5**)] in the survival and adaptation of the diazotrophic population found in association with *P. oceanica* meadows (*objective 1*). The results suggest that N_2-fixing microbial structure could eventually change since species-specific responses were found. The molecular mechanisms that are triggered by environmental and anthropogenic stressors in marine diazotrophs associated with benthic systems were also unveiled, (*objective 2*). The most relevant results are summarized in the **Table 4.1**.

Table 4.1. Summary of the relevance and the main results presented in this thesis, structured in five chapters and two sections. **Abbreviations:** OA, ocean acidification; OW, ocean warming; MPs, microplastics; HCS, Humboldt Current System. Green panels display the results for the cyanobacteria, while the orange panel shows the results for the heterotrophic bacteria.

Chapter 1	Chapter 2	Chapter 3	Chapter 4	Chapter 5
Environmental factors and emerging pollutants				
Section I: Effect of nutrient availability			Section II: Effect of anthropogenic factors	
Effect of different concentrations of P, Fe and N in phototrophic and heterotrophic bacteria			Effect of increasing CO_2 levels (OA and OW)	Plastic (MPs) pollution and their associated organic additives
P-acquisition mechanisms can be Fe dependent in cyanobacteria containing PhoD	Nutrient limitation (P, Fe and/or N) can reduce growth and N_2-fixation rates in cyanobacteria	"Everything is everywhere, but the environment selects"	CO_2, pH and temperature effects are controlled by nutrient availability, suggesting an interactive effect between global climate change factors and nutrients. CO_2 might have a deleterious effect, only when cultures are P-limited (in the heterotrophic bacteria)	This is the first study where the exposure to MPs and organic additives were evaluated in diazotrophs
Alkaline phosphatase activity (APA) and P-uptake in unicellular cyanobacteria may be controlled by DIN concentration (i.e., higher APA under low N levels)	Reactive oxygen species (ROS), morphological changes, and apoptosis processes are enhanced in cyanobacteria under nutrient limitation	Ecological niches (i.e., Mediterranean Sea and HCS) might determine, select and modify the genomic and phenotypic features of cosmopolitan bacteria	P-acquisition mechanisms are negatively affected by decreasing pH and increasing temperatures levels	MPs and organic additives trigger species-specific responses, generally enhancing or decreasing the growth at high levels, respectively
APA can fuel the N_2-fixation processes	Low DIN levels may inhibit cell growth of unicellular cyanobacteria, questioning the "classical" diazotrophic response	Bacteria found in the Mediterranean oligotrophic waters can be better adapted than those found in eutrophic waters (e.g., HCS)	N_2-fixing cyanobacteria can be more resistant than heterotrophic N_2-fixing bacteria, suggesting a shift in the N_2-fixing structure of benthic systems	Cell responses to plastic pollution are suggested to be dependent on the physical properties of MPs and characteristics of the bacteria tested

4.1. *Objective 1*: What is the role of the environmental factors and emerging pollutants in regulating the functioning of N_2-fixers associated with *Posidonia oceanica*?

The prediction of how the N_2-fixing community will respond to environmental factors and emerging pollutants are currently major challenges for marine microbiologists in the field of research on the disturbances of N-cycles (Zehr and Capone, 2020). The outcome of this work reveals that the microbial responses can be species-specific (**Chapters 1-5**), suggesting the change of the N_2-fixing microbial communities found in association with *P. oceanica* cause by the abiotic factors (i.e., changes in nutrient availabilities, anthropogenic CO_2 and emerging pollutants). This thesis was centered on answering the following questions in the context of diazotrophs associated with benthic systems: "Will the biomass/N_2-fixation rates of diazotrophs decline or increase in the future? What taxonomic groups and individual species could benefit or be hit especially hard by changing environmental conditions?" (Litchman et al., 2012). The environmental factors and emerging pollutants tested may select the responses of N_2-fixers, with "winners" and "losers" according to the taxonomic group (i.e., phototrophs vs. heterotrophic bacteria) since negative, neutral and positive effects were detected at the growth, N_2-fixation rates and biochemical levels (**Chapters 1-5**). Generally, cyanobacteria were more sensitive to changes for nutrient regimes, while heterotrophic bacteria were more sensitive to anthropogenic threats (i.e., ocean acidification and warming) and emerging pollutants (i.e., MPs and their organic additives associated) (**Figure 4.1**).

According to several studies, marine microorganisms are strongly influenced by environmental stressors (e.g., by changes in the nutrients regimes or anthropogenic factors), affecting their growth and composition (Doney et al., 2009; Li et al., 2009; Hoegh-Guldberg and Bruno, 2010; Litchman et al., 2012). The environmental stressors can affect at different levels the microbial populations: (**I**) at phenotypic plasticity (i.e., the ability to persist when they are subject to an environmental stressor), (**II**) at species sorting (i.e., those species with higher plasticity or bacteria will be more abundant in the community), (**III**) at genetic adaptation (i.e., mutations, recombination or horizontal gene transfer may select species), or a combination of all these processes (Litchman et al., 2012). This work focused on the plasticity of the phototrophic and heterotrophic bacteria through the measurement of physiological and biochemical parameters, e.g., growth, P-acquisition mechanisms [i.e., alkaline phosphatase activity (APA) and P-uptake], oxidative stress [i.e., reactive oxygen species (ROS)], and changes in the cell morphology

and apoptotic processes (**Chapters 1-5**). Based on the differential responses obtained in the cyanobacteria and heterotrophic bacteria tested (**Chapters 1-5**), those better-adapted species to the environmental pressure, e.g., with higher plasticity, will compensate for the loss of the less poorly adapted species. Hence, this suggests that the "system" (i.e., the epiphytic and endophytic community of *P. oceanica*) might compensate for the decrease in the growth and N_2-fixation rates, at the cost of the loss of microbial diversity (**Figure 4.1**). However, the consequences on the plant remain to be investigated. Therefore, further studies in *P. oceanica* meadows investigating if indeed the N_2-fixing bacterial communities will change are needed for evaluating the environmental consequences in this marine phanerogam.

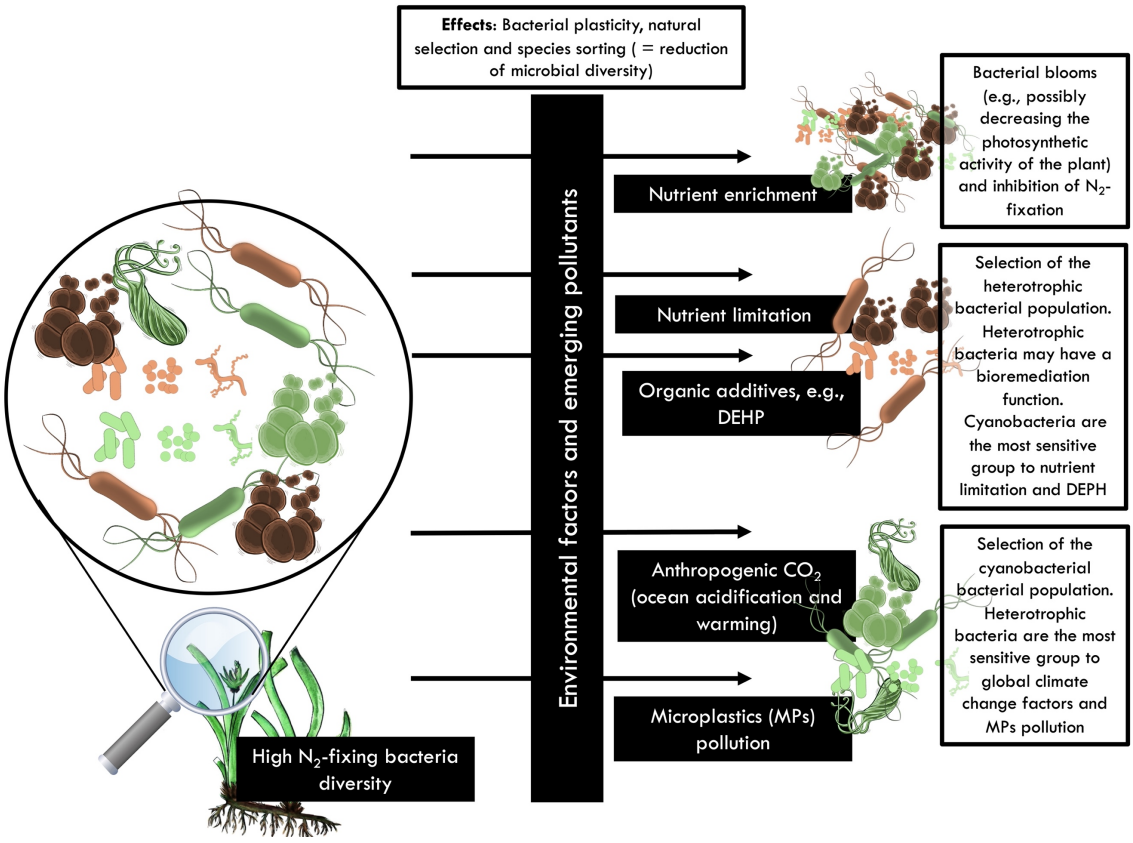

Figure 4.1. Effect of environmental factors and emerging pollutants on the N_2-fixers found in association with *Posidonia oceanica*. According to the results, changes in the microbiota composition (e.g., N_2-fixing bacteria) may be occurring in *P. oceanica* meadows. Considering the detrimental/beneficial effect of environmental factors and emerging pollutants on the diazotrophic population, the selection for the dominance of the diazotrophic cyanobacteria or heterotrophic bacteria may take place in *P. oceanica*. **Source:** own production.

Role of different concentrations of phosphorus, iron and nitrogen in regulating the functioning of N_2-fixers

This thesis revealed the interactive effect of nutrient availability (i.e., P, Fe and N) in N_2-fixers, providing useful data in a poorly explored research field on marine diazotrophs associated with marine benthic systems (**Chapters 1-3**). The P, Fe and N availabilities may be the main factors regulating the functioning of marine N_2-fixers (**Chapters 1-3**), consistent with Sohm et al. (2011) and Knapp (2012). Studies with cultures of N_2-fixers, e.g., *Trichodesmium* spp. and *Crocosphaera watsonii*, show that the limitation of either P or Fe can limit growth and N_2-fixation of diazotrophs (Berman-Frank et al., 2001; Dyhrman and Haley, 2006; Krauk et al., 2006; Küpper et al., 2008). Here, P, Fe, and N co-limitation dramatically affect the diazotrophic activity, increasing the ROS levels and even provoking cell disruption and death (**Chapter 2**). For all the diazotrophic bacteria tested, the dissolved inorganic phosphorus (DIP) was the main nutrient controlling the growth and N_2-fixation rates, when N_2-fixation was stimulated at low dissolved inorganic nitrogen (DIN) levels (Knapp, 2012) (**Chapters 1-3**). Under this situation, the N_2-fixation rates increased linearly with increasing P-levels (see discussion in **Chapters 1** and **2**). Moreover, low DIN concentrations enhanced the APA rates, suggesting a release of DIP from dissolved organic phosphorus (DOP) to fuel the N_2-fixation rates (**Chapter 1**). These results confirm the P-dependence of growth and N_2-fixation rates of diazotrophs. Iron (Fe) had a positive effect on the growth and N_2-fixation rates, e.g., in the filamentous heterocyst-forming *Fischerella muscicola* PCC 73103 or the heterotrophic bacteria *Cobetia* sp. UIB 001. However, its effect cannot be generalized since in the unicellular cyanobacterium *Halothece* sp. PCC 7418, their growth and N_2-fixation rates decreased at high Fe levels (**Chapter 2**), suggesting different Fe requirements for cyanobacteria and heterotrophic bacteria. Although N_2-fixers are generally not limited by N, the results obtained in *Halothece* sp. PCC 7418 suggest that limiting levels of N can be important in controlling the diazotrophic activity (**Chapter 2**). To date, this is the first report in which N_2-fixers are limited by DIN, requiring a minimum amount of DIN for survival. It remains to be investigated whether these cells in the natural environment require a combined source of inorganic nitrogen and if this requirement can be supplied by other diazotrophs in N-limited waters. Therefore, this work opens new questions about the responses of N_2-fixers in marine environments, questioning the classical functioning of diazotrophs.

The cyanobacterial population (e.g., *Halothece* sp. PCC 7418 and *F. muscicola* PCC 7418) was more sensitive to nutrient limitation (P, Fe and/or N) than the heterotrophic

bacteria (e.g., *Cobetia* sp. UIB 001) (**Chapters 1-3**). The sensitivity of cyanobacteria to limiting concentrations of nutrients may be due to their higher nutrient requirements than other phytoplanktonic taxa, as suggested by their Redfield N:P ratio of 25, which is significantly higher than other marine microbial groups with a ratio of 16 (Redfield, 1934; Geider and La Roche, 2002; Quigg et al., 2011). This is because cyanobacteria contain membrane-anchored multimeric light-scavenging proteins called phycobiliproteins (that contain phycocyanin and phycoerythrin pigments) which capture light for photosynthetic activities, and these proteins are rich in N (Pagels et al., 2019). Under nutrient limitation, phycobiliproteins are degraded as a N source through the expression of the NblA protein, which causes chlorosis (**Chapter 2**). Unlike cyanobacteria, the heterotrophic bacteria generally have smaller sizes, and a higher surface: volume ratio which makes them more efficient in acquiring nutrients (**Chapter 3**). However, the nutrient responses in heterotrophic bacteria, even between strains of the same species, can be controlled by the marine environment in which they are found, as shown for *Cobetia* spp. isolated from *P. oceanica* (Spain) and *Heterozostera chilensis* (Chile) (**Chapter 3**).

In situ and mesocosm experiments were conducted to test the effect of increasing concentrations of P and Fe in the water column and sediment in the *nifH* expression for the diazotrophs associated with *P. oceanica*. The results revealed that N_2-fixation activity associated with the plant is mainly due to activities of the unicellular cyanobacterial population, especially UCYN-B and UCYN-C (**Figures 4.2A-D**) (Fernández-Juárez and Agawin, unpublished data). Water column nutrient enrichment (i.e., P and Fe) might increase *nifH* gene expression, increasing N_2-fixation rates (**Figures 4.2A** and **4.2B**), consistent with the studies conducted by Turk-Kubo et al. (2012). The additional nutrient supply could be beneficial to the plant in the short-term. However, long-term nutrient load on the water column might trigger the epiphytic bloom on *P. oceanica*'s leaves, which can cause a decrease in the photosynthetic activities of the plant due to the reduction of light. On the contrary, nutrient enrichment in marine sediments can have the opposite effect, downregulating the expression of the *nifH* gene (**Figures 4.2C** and **4.2D**). Sediment nutrient enrichment may increase the oxidative stress in *P. oceanica* leaves and can affect the symbiotic relationship between the plant and the epiphytic population (Fernández-Juárez, unpublished results). Thus, the nutrient enrichment can regulate the epiphyte and endophyte community composition and N_2-fixing activities associated with *P. oceanica* meadows.

Role of anthropogenic threats in N_2-fixers associated with Posidonia oceanica

CO_2 effect and its concomitant effect in ocean acidification and warming

This work sheds light on the effect of CO_2 and its concomitant effect (i.e., ocean acidification and warming) in phototrophic and heterotrophic N_2-fixers found in association with *P. oceanica* meadows. The experimental design [i.e., testing varying pH (pH 4-8) and temperature levels (12-30 ºC), and different concentrations of CO_2 (i.e., atmospheric, aCO_2, 410 and expected, eCO_2, 1000 ppm) in combination with different nutrient regimes and temperatures] conducted in monocultures of N_2-fixers revealed that (**I**) the effect of global climate change factors (i.e., CO_2, pH and temperature) may be dependent on nutrient concentrations and negatively affecting heterotrophic bacteria, and (**II**) lowering pH and increasing temperature affect microbial activity according to the nature of the bacteria (i.e., phototrophic or heterotrophic), decreasing the rates of the nutrient acquisition mechanisms (i.e., APA). The pH drop can enhance protein instability, while warmer temperatures may downregulate the expression APases, and altogether decreasing the APA rates (see results and discussion of **Chapter 4**).

According to the results obtained, nutrient availability is an important factor to consider when looking at the effect of global climate change factors (i.e., CO_2, pH and temperature) in N_2-fixing bacteria (**Chapter 4**). This is consistent with models that consider the role of P, Fe, and N limitation in predicting how N_2-fixation will be affected by climate change at the end of this century (Wrightson and Tagliabue, 2020). A decrease in pH can limit nutrient uptake, while temperature increased can rise ocean stratification, affecting P and N vertical distribution and limiting nutrient availability (Cavicchioli et al., 2019). Some studies predict that global N_2-fixation in the ocean will decrease by 2100, affecting the net primary production of the oceans (Wrightson and Tagliabue, 2020), while other studies predict an increase of the global N_2-fixation rates by the end of the century to 22-27% (Boyd and Doney, 2002). However, the latter studies do not consider competition between diazotrophs and non-diazotroph for nutrients.

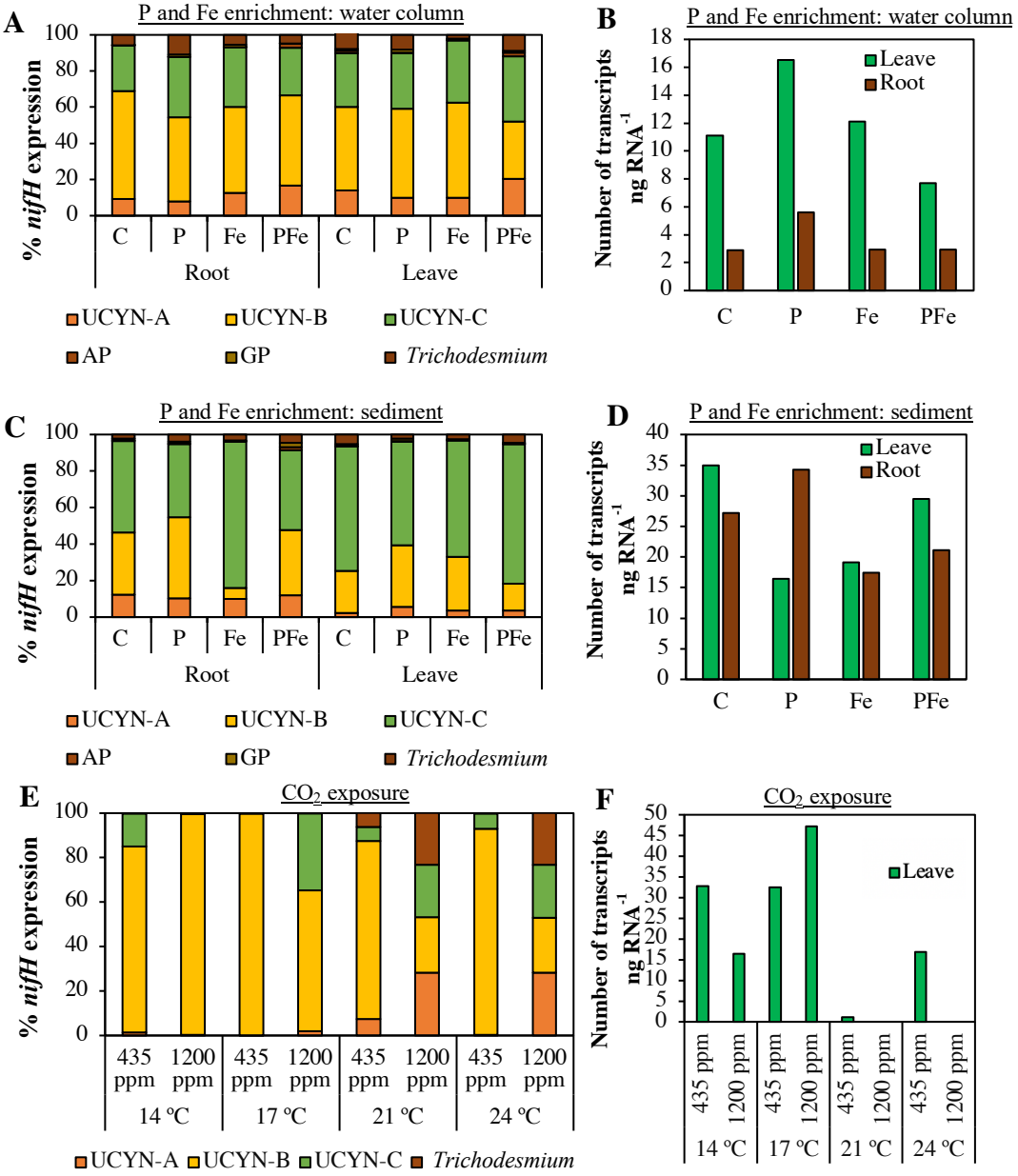

Figure 4.2. RT-qPCR analyses of the *nifH* gene expression of groups UCYN-(A, B and C), *Trichodesmium*, α-proteobacteria (AP) and γ-proteobacteria (GP) measured by RT- qPCR from leaves and roots of *Posidonia oceanica*. **A-B)** P and Fe enrichment concentrations in the water column, **C-D)** P and Fe enrichment concentrations in the sediment, and **E-F)** changing CO_2 concentration together with different temperature levels. It is shown the relative % of *nifH* by N_2-fixer groups and the number of transcripts ng RNA^{-1}. **Source:** Fernández-Juárez and Agawin (unpublished results).

These predictions were done using a few N_2-fixers as models, but N_2-fixing heterotrophic bacteria might be more sensitive to global climate change factors than N_2-fixing cyanobacteria (**Chapter 4**). Cyanobacteria have efficient carbon concentration mechanisms (CCMs) via carboxysomes (i.e., structures in which CO_2-fixing enzyme,

RuBisCO, is encapsulated) which remove inorganic carbon from the media (Rae et al., 2013), and thus, they can be less affected by increased CO_2 or concomitant changes in pH compared to heterotrophic bacteria. Here it is suggested that diazotrophic bacteria might have different types and functioning of CCMs, which could explain the different sensibility to CO_2 for different cyanobacterial species (Eichner et al., 2014b) (**Chapter 4**). The increase in CO_2 levels combined with other environmental factors may select for less sensitive species in the microbial community, reducing the diversity of the diazotrophic population (Joint et al., 2011; He et al., 2014). The results obtained not only suggest that a change in the structure of the diazotrophic community may occur with increased CO_2, but also a decrease in the expression of the *nifH* gene (**Figures 4.2E** and **4.2F**). Therefore, considering the sensibility to the pH and temperature for the N_2-fixers associated with *P. oceanica* (**Chapter 4**), ocean acidification and warming may potentially impact the N_2-fixing structure of *P. oceanica* meadows. The consequences on the plant itself should be further investigated with the possible change in the activity of the diazotrophic community.

Effect of microplastics (MPs) and their associated organic additives

The interest in finding out the effect of MPs in the environments and human health has increased exponentially with more than 3000 reports about MPs (in US National Library of Medicine National Institutes of Health, PubMed, retrieved January 2021) in the last ten years. Yet, there are only a few papers that discuss the direct effect of MPs in bacteria. In the strains tested in this work, MPs and their associated organic additives did not have a significant effect on N_2-fixation rates, but changes in growth (and abundance) of the cells may affect the global N_2-fixation rates in the marine environment (**Chapter 5**). Further studies are needed to evaluate the potential impacts of increasing levels of MPs and their organic associated additives in N_2-fixation activities. It can be hypothesized that N_2-fixation activities can be affected in three different ways: (**I**) since N_2-fixation is P-dependent, P-scavenging of MPs would inhibit N_2-fixation (Hassenteufel et al., 1963); (**II**) as N_2-fixation is an energy-costly process, species that also degrade MPs would require additional energy, with N_2-fixation activities being lowered by changes in energy allocation of the cells; (**III**) since MPs and their additives affect the production of reactive oxygen species (ROS) (Fernández-Juárez and López-Alforja, unpublished data), N_2-fixation activities could decrease by redox processes in the nitrogenase complex, considering its sensitivity to the radical species (Alquéres et al., 2010). Although the

experiments conducted cannot be ecologically relevant since we did not use natural MPs (with the organic additives) (Paul-Pont et al., 2018) and instead it was used non-processed MPs without additives, this work suggest that MPs pollution (MPs: PS, PE, PP and PVC, and organic additives: fluoranthene, HBCD and DEHP) may affect the N and P cycles in the ocean (**Figure 4.3** and **Chapter 5**).

Several reports support the idea that MPs can select bacterial communities in the ocean. Bryant et al. (2016) reported a core group of microbes associated (e.g., *Bryozoa*, *Cyanobacteria*, *Alphaproteobacteria*, and *Bacteroidetes*) with small plastic fragments in oligotrophic surface waters. This microbial community composition associated with plastics can differ from that of their water column-counterparts (Zettler et al., 2013; Oberbeckmann et al., 2014; Bryant et al., 2016). Plastic accumulation in benthic systems may also trigger a potential change of microbial structure. Considering the beneficial effect of MPs on growth of diazotrophic cyanobacteria but not on heterotrophs (**Chapter 5**), the selection for the dominance of the diazotrophic cyanobacteria may take place in *P. oceanica*. Contrary to the effect of MPs, organic additives, except those that can be degraded, may have detrimental effects on diazotrophs and consequently affect the maintenance of the productivity of *P. oceanica* since the activity of these N_2-fixers may provide up to 100% of the N demand of plants (Agawin et al., 2016). Moreover, different physical processes such as currents or eddies could transport both MPs and the diazotrophs in adjacent seawater environments [since these cells can adhere with the MPs (**Chapter 5**)], allowing them to settle and colonize other ecological niches. The role of MPs as vectors for the transport of microorganisms has already been reported for pathogenic bacteria and harmful algal bloom-forming species (HABs) (Curren and Leong, 2019; Naik et al., 2019), but more studies are needed to investigate the role of natural MPs in N_2-fixing communities in the marine environment.

4.2. *Objective 2*: Investigation of the molecular responses with exposure to environmental factors and emerging pollutants

The second main objective of this thesis was to study the molecular mechanisms behind the diazotrophic responses against exposure to environmental factors and emerging pollutants. The goal was to find out molecular responses which can be used as molecular biomarkers to indicate the health status of N_2-fixing communities associated with benthic systems. According to the US National Academy of Sciences (NAS)-National Research Council (NRC), “biomarker” is defined as an indicator to report about

the health of biological systems (e.g., bacteria) exposed to an exogenous factor (e.g., different nutrient regimes or anthropogenic factors) (Committee on Biological Markers of the National Research Council, 1987). With this aim, the molecular mechanisms studied here were the P-mechanisms, through the measurement of the alkaline phosphatase activity (APA) and P-uptake analyses (**Chapters 1**, **3-5**); the oxidative stress responses, through the measurement of the reactive oxygen species (ROS) (**Chapters 2, 3,** and **4**); the morphological changes, monitoring changes in cell size; the apoptotic processes, via the phosphatidylserine detection (**Chapter 2**); and the protein overproduction, using MALDI-TOF analyses (**Chapter 5**). The APA and the ROS production were the better biomarkers tested in these studies, as discussed below. The increase of these biological markers was correlated with the decrease in the cell population (**Chapter 4**), one of the main characteristics to be a good biomarker (Committee on Biological Markers of the National Research Council, 1987).

This thesis reveals the use of APA as a physiological biomarker to assess the phosphorous nutritional status and energy requirements of diazotrophic cells. The APA is activated as a mechanism of adaptation and survival to P-limitation, or when the P-cellular demand increases, e.g., for synthetizing ATP for fueling ATP-dependent reactions (e.g., N_2-fixation) (Santos-Beneit, 2015). Thus, through the measurement of APA, it can be assessed whether the cells are P-limited or whether they have fulfilled their P-requirements (**Chapter 2**). The abiotic factors that N_2-fixers have to cope with could change the P-requirement and energy demand, and hence, the evaluation of APA can shed light to investigate how environmental stressors are affecting their responses. Generally, it can be interpreted that if an environmental stressor is enhancing APA, this is probably a factor that potentially might trigger a deleterious effect in the short or long-term since cells require higher P-requirements (e.g., for protein synthesis or ATP-dependent enzymes) as a response of this factor. However, some abiotic factors can inhibit APA (e.g., increasing temperatures, **Chapter 4**), decreasing the ability of cells to obtain DIP from DOP, and thus decreasing the survival of N_2-fixers. These findings are coherent with results from several mesocosms experiments in *P. oceanica* (Fernández-Juárez and Agawin, unpublished data; Frank et al., unpublished data). The results show that APA can be utilized as a biomarker for evaluating coastal P and Fe enrichment, increasing CO_2 levels, and MPs exposure in *P. oceanica* (**Figures 4.4A-F)**. Alkaline phosphatase activity (APA) has also been used as a biomarker for coastal nutrient enrichment in other studies of *P. oceanica* (Martínez-Crego et al., 2006). Briefly, the

results show that P enrichment in the water column decreased APA, whereas Fe has no significant effect on APA rates (**Figures 4.4A** and **4.4B**); increasing CO_2 and temperature levels decreased APA (in agreement with the results of **Chapter 4**) (**Figures 4.4C** and **4.4D**); and plastic exposure can promote APA, probably due to the higher energy demand required for plastic-degrading bacteria (**Figures 4.4E** and **4.4F**). Considering the narrow connection between the N_2-fixation rates and APA in *P. oceanica* (Agawin et al., 2021), the P-metabolism of its associated microbiota should be further studied in-depth.

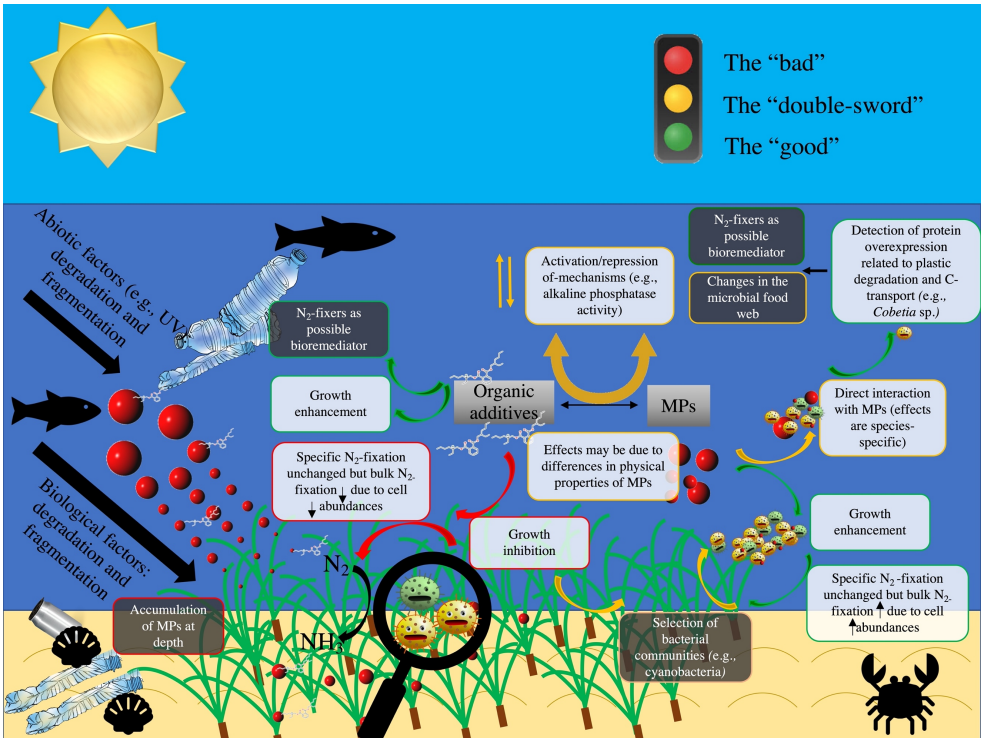

Figure 4.3. Effects of MPs and their organic additives in the bacteria associated with benthic systems (e.g., the endemic Mediterranean *Posidonia oceanica*). These can be beneficial or "the good" (green arrows), detrimental or "the bad" (red arrows), and "double-sword" (yellow arrows) (**Chapter 5**). White boxes represent the results obtained in the present study, while the black boxes represent the implications of our results. MPs and their organic additives can trigger species-specific responses, and these responses are suggested to be dependent on the physical properties of the different MPs tested. The species that could grow with particular types of MP/additives can have a bioremediation function, and the results also imply the selection for specific bacterial communities and changes in the microbial food web. **Source:** own production.

Reactive oxygen species (ROS) are biochemical biomarkers used in marine plants and animals (Ferrat et al., 2003; Benedetti et al., 2015), and in bacteria, it can be used to evaluate the plasticity of the bacterial community against different abiotic factors (Lesser, 2006; Litchman et al., 2012). Here, the increased ROS levels depend on the type of bacteria, showing that cyanobacteria accumulate more ROS than heterotrophic bacteria under nutrient-limited conditions (**Chapters 2** and **3**). The detection of high levels of

ROS [e.g., caused by nutrient limitation (**Chapters 2** and **3**), climate change factors (**Chapter 4**), and exposure to MPs (Fernández-Juárez and López-Alforja, unpublished data)] does not necessarily mean that the cells have oxidative stress that can end up in cell death. Cells can compensate ROS by enzymatic and non-enzymatic defenses without any effect on cell growth. However, if the stimulus persists and ROS are not removed, the increase of ROS can end up in oxidative stress, and consequently lead to programmed cell death (Diaz and Plummer, 2018). Thus, ROS can provide information on the biochemical status of bacteria against an environmental stressor, although there is no visible physiological damage. Abiotic factors (e.g., nutrient limitation or anthropogenic factors) on diazotrophs not only produce ROS but also may induce apoptosis, which was never reported in previous studies (**Chapter 2**). Programmed cell death can be monitored by investigating cell apoptosis, using a typical kit designed for eukaryotic cells (Alexa Fluor 488 Annexin V / Dead Cell Apoptosis Kit, Thermo Fisher) (**Chapter 2)**. Moreover, morphological changes may be useful for studying the effect of environmental stressors on N_2-fixing communities. Different nutrient concentrations (i.e., P, Fe, and N) provoked morphological changes in N_2-fixing bacteria, in which cells become bigger and larger under nutrient limitation both in cyanobacteria (e.g., triggering cell breaks) and heterotrophic bacteria (**Chapters 2** and **3**). This can be due to the cessation of cell division with limitations of P, Fe, and N (Klotz et al., 2016). Thus, cell size may be used as an indicator for bacterial nutritional status. Protein profiles (through proteomic analyses) can also be utilized as a molecular parameter for evaluating diazotrophic responses to environmental stressors (**Chapter 5**).

The use of bioinformatics can help open new hypotheses about the genetic mechanisms that diazotrophs use to thrive under nutrient limitation. The complete genome of the diazotrophic *Halothece* sp. PCC 7418 was used as a model to try to investigate which genetic pathways or functions would be triggered by the transcriptional factors Pho, Fur and NtcA, under P, Fe and N limiting conditions (**Chapter 2** and **Annex Chapters 1** and **2**). Among all the genes detected, it can be highlighted the N_2-fixation regulator gene, *nifB*, which was predicted under the control of NtcA, and whose product is crucial in iron–molybdenum biosynthesis. Downstream of this gene, an entire cluster of twenty genes related to N_2-fixation is localized: Fd III 4Fe-4S, *nifS*, *nifU*, *nifH*, *nifD*, *nifK*, *nifZ*, *nifE*, *nifN*, *nifX*, DUF683, and *nifW* (**Figure 4.5**). Chip analyses revealed that the *nifB* from *Anabaena* sp. PCC 7120 contains upstream a NtcA box, suggesting the role

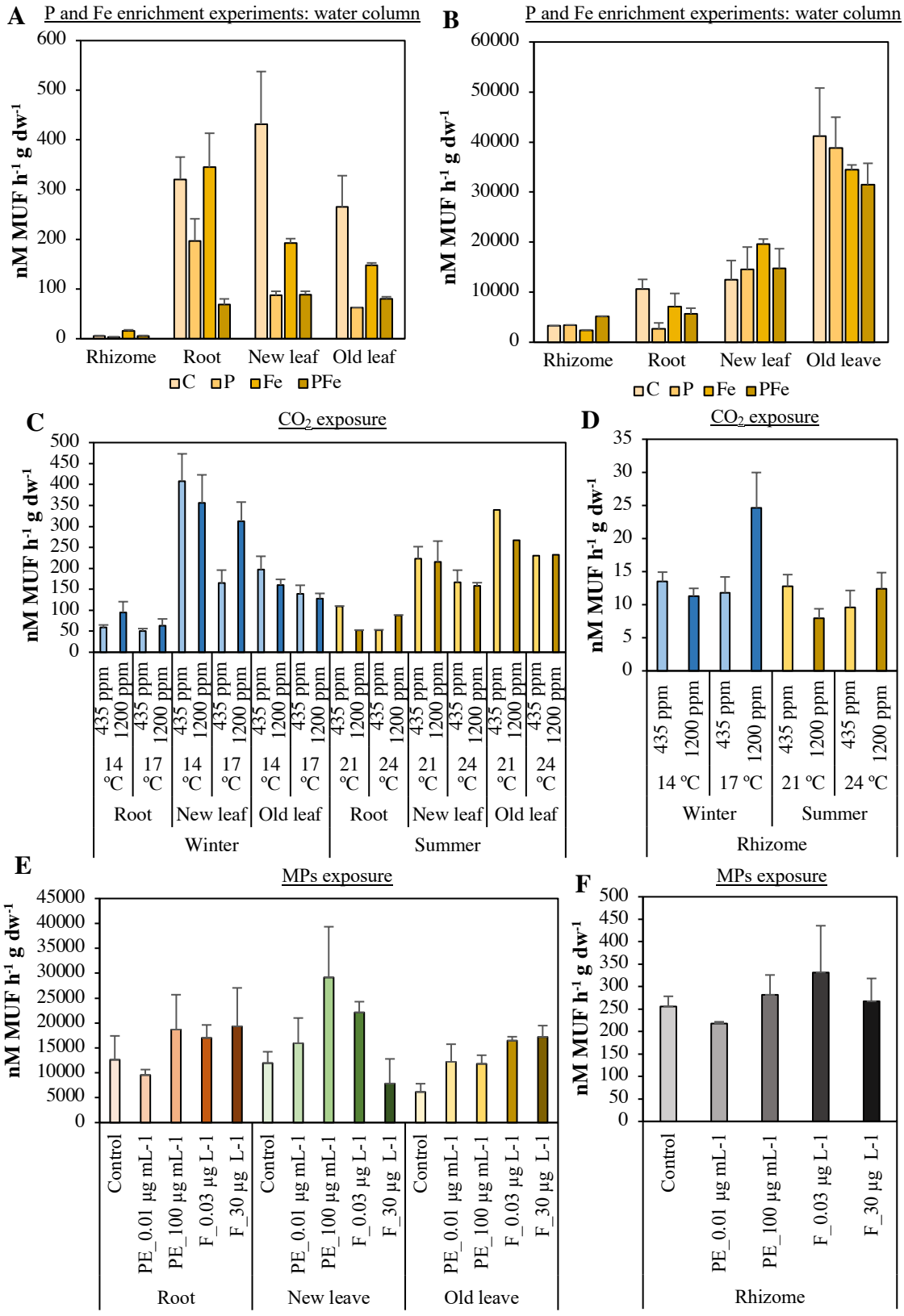

Figure 4.4. Alkaline phosphatase activity (APA) in *Posidonia oceanica* under different experimental set-ups. **A-B)** P and Fe enrichment experiments, **A)** in the water column and **B)** in sediment. **C-D)** CO_2 exposure, testing different temperature levels. **E-F)** Microplastics (MPs) exposure, i.e., polyethylene (PE), and its organic additive effect, i.e., fluoranthene (F). **Source: A-D**) Fernández-Juárez and Agawin (unpublished results), and **E-F**) Frank et al. (unpublished results).

of NtcA in N_2-fixation regulation (Picossi et al., 2014). Contrary to other N_2-fixing bacteria in which *nif* genes are found in different and distant clusters, the genome of *Halothece* sp. PCC 7418 stands out for co-locating the complete N_2-fixation cluster in just 17.8 kb with all the genes necessary for the N_2-fixation process (**Figure 4.5**). These characteristics make *Halothece* sp. PCC 7418 a potential model organism in which different biotechnological approaches can be carried out to reveal the role of *nif* genes. These findings may open new hypotheses about the genetic mechanisms that cyanobacteria use to thrive under nutrient limitation (**Chapter 2**).

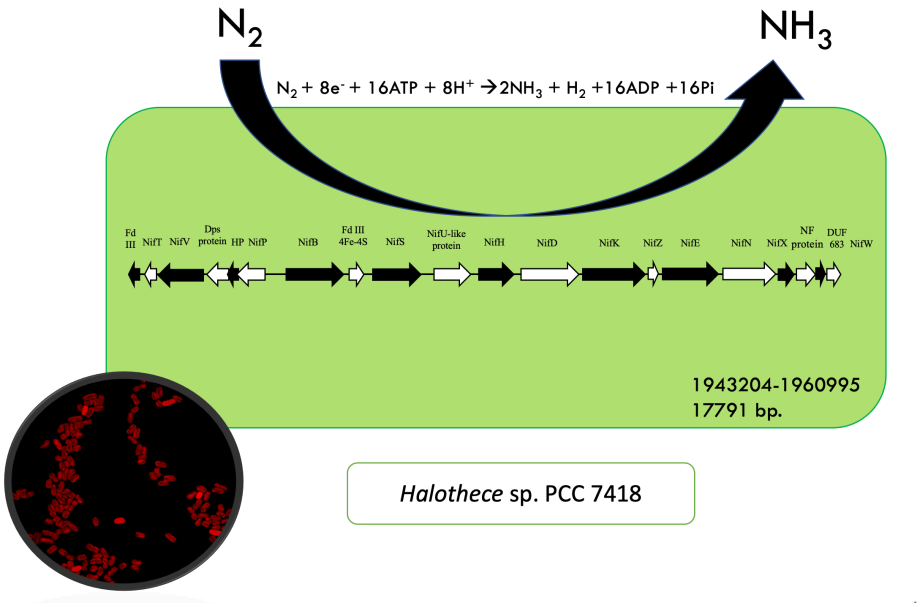

Figure 4.5. Complete N_2-fixation cluster in *Halothece* sp. PCC 7418. The *nif* cluster of the PCC 7418 strain occupies 17.8 kb in the genome. **Source:** Own production.

4.3 Future directions

The present work dealt with abiotic environmental factors and stressors regulating the functioning of the N_2-fixers associated with the seagrass *P. oceanica*. Future works should consider biotic factors, e.g., ecological interactions between other microorganisms and N_2-fixers, or the influence of viruses in N_2-fixation. For these general purposes, it is necessary to build synthetic microbial communities with two or more bacteria in chemostat experiments (i.e., continuous culture) (Großkopf and Soyer, 2014; Widder et al., 2016). The implementation of novel approaches like microfluidics is required for these studies (Großkopf and Soyer, 2014), through which to evaluate the interactions that diazotrophs can be establishing, e.g., commensalism, competition, predation, no interaction, cooperation or amensalism, between them and other marine microbial groups

found as the epiphytic or endophytic population on the plant. On the other hand, viruses can control bacterial communities participating in the genetic diversity and success of microbial species, considering that in the seawater, viruses can reach 10^7 viruses mL^{-1} (Whitton, 2012). Among them, cyanophages synthesize bacterial gene homologs, which can control the photosynthetic activities in *Prochlorococcus* and *Synechococcus*, obtaining the energy necessary for viral replication (Puxty et al., 2015). It is hypothesized that according to different abiotic conditions (e.g., temperature, light or nutrient regimes), the viral infection dynamics may be affected (Puxty et al., 2018). Novel research in diazotrophs suggests that in the filamentous heterocyst forming cyanobacterium *Aphanizomenon flos-aquae*, viral infection can impair the flow of the fixed N_2 within the filaments. However, the *nifH* gene expression and N_2-fixation rates were not affected (Kuznecova et al., 2020). Further research should assess the viral effects on the N_2-fixation rates in diazotrophs and the consequences for marine systems (e.g., *P. oceanica*), and how environmental factors (e.g., nutrient availability) can control these responses.

In a more ecological context, future research plans should consider experiments (field or mesocosm) carried out in natural N_2-fixing communities associated with *P. oceanica*, investigating whether there is indeed a change in the N_2-fixing community structure and how the plants cope with the environmental stressors and emerging pollutants tested in this thesis (i.e., nutrient availabilities, global climate change factors and emerging pollutants). High throughput analyses, e.g., metagenomics, metatranscriptomics and metaproteomics approaches, might be useful to know which genes and proteins are responsible for the adaptation and survival of diazotrophic microorganisms to the different abiotic factors tested. Seasonal field experiments on *P. oceanica* beds are also needed to know how the N_2-fixing bacterial community structure change over the seasons and how these relate to changes of the different environmental factors studied during this thesis.

5. CONCLUSIONS

CONCLUSIONS

In summary, this thesis shows for the first time the role of environmental factors and emerging pollutants in N_2-fixing bacteria associated with the endemic Mediterranean seagrass *Posidonia oceanica*. These studies will contribute to predict and anticipate changes in the *P. oceanica* meadows in response to anthropogenic impacts (e.g., nutrient enrichment, anthropogenic increase in CO_2 or plastic pollution) in the Mediterranean Sea. Throughout this work, the plasticity of N_2-fixers to abiotic global stressors was described and discussed. The conclusions of this work are as follows:

1- The responses of the N_2-fixing bacteria to environmental factors and emerging pollutants tested are species-specific. As a consequence, some species may be favored or selected when they are subject to environmental stressors, and thus, changes in the microbial N_2-fixing structure (i.e., selecting the cyanobacterial or heterotrophic population) of *Posidonia oceanica* might be occurring as a consequence of the abiotic factors tested, according to the nature of the N_2-fixing bacteria (**Chapters 1-5**).

2- Nutrient limitation (i.e., P, N and Fe) affects nutrient acquisition mechanisms for diazotrophs, e.g., the alkaline phosphatase and N_2-fixation activities. Whatever processes, natural or anthropogenic that can change nutrient concentrations, could consequently affect nutrient acquisition mechanisms, and therefore regulate the diazotrophic responses in benthic systems (**Chapter 1**).

3- This work opens new questions and hypotheses about the responses of N_2-fixers in marine environments, questioning the "classical" diazotrophic responses since some N_2-fixer cyanobacteria can have a threshold dependence of dissolved inorganic nitrogen (DIN) and in theory, N_2-fixing bacteria are independent of the availability of DIN since they can use atmospheric N_2 (**Chapter 2**).

4- The marine environment is suggested to select and determine the genomic and phenotypic responses of the same bacterial species found in different regions as evidenced in this thesis. *Cobetia* spp., found associated with the Mediterranean seagrass *Posidonia oceanica* may be better adapted to oligotrophic conditions than

those found in nutrient-rich waters in the Humboldt Current System and associated with the Chilean seagrass *Heterozostera chilensis* (**Chapter 3**).

5- Ocean acidification and warming due to increased CO_2 levels may have a significant impact on N_2-fixing microorganisms. However, the impact may depend on whether they are phototrophic or heterotrophic bacteria, suggesting that the community structure of the N_2-fixing community may also change. The response of N_2-fixing microorganisms with climate change factors depends on their nutritional status. Moreover, climate change factors affect nutrient acquisition mechanisms, impairing the diazotrophic activities (**Chapter 4**).

6- For the first time, the role of exposure to microplastics (MPs) and their organic additives in marine diazotrophs was investigated, revealing that generally, non-processed MPs increase growth, unlike organic additives. The diazotrophic cell responses can be dependent on the concentration and physical properties of MPs. Although N_2-fixation rates were not affected, changes in growth or abundance of the diazotrophic cells may affect global N_2-fixation rates. Microplastics (MPs) and their associated organic additives trigger species-specific responses, and thus, the structure of the diazotrophic microbial population associated with the seagrass *Posidonia oceanica* can eventually change with exposure to these contaminants (**Chapter 5**).

6. ANNEXES

ANNEXES

Chapter 1

Supplementary Table 1. All genes and Locus Tags of the predicted Pho regulon of all the tested strains.

***Nostoc punctiforme* PCC 73102 (CP001037)**			***Chroococcidiopsis thermalis* PCC 7203 (CP003598)**		
Genes	**Annotation (Patric)**	**Locus Tag**	**Genes**	**Annotation (Patric)**	**Locus Tag**
phoU	-	-	*phoU*	-	-
pstS	-	-	*pstS*	-	-
pstC	-	-	*pstC*	-	-
pstA	-	-	*pstA*	-	-
pstB	-	-	*pstB*	-	-
phoR	-	-	*phoR*	Phosphate regulon sensor protein PhoR (SphS)	Chro_5919
phoB	-	-	*phoB*	-	-
APase	-	-	APase	Alkaline phosphatase	Chro_5919
ppK	-	-	*ppK*	-	-
ppX	-	-	*ppX*	-	-
ppA	-	-	*ppA*	-	-
***Spirulina subsalsa* PCC 9445 (NZ_ALVR01000000)**			***Crocosphaera watsonii* WH 8501 (NZ_AADV02000000)**		
Genes	**Annotation (Patric)**	**Locus Tag**	**Genes**	**Annotation (Patric)**	**Locus Tag**
phoU	Phosphate transport system regulatory protein PhoU	SPI9445_RS0119485	*phoU*	Phosphate transport system regulatory protein PhoU	CwatDRAFT_5911
pstS	Phosphate ABC transporter, substrate-binding protein PstS	SPI9445_RS0105090	*pstS*	Phosphate ABC transporter, substrate-binding protein PstS	CwatDRAFT_6534

	Phosphate ABC transporter, substrate-binding protein PstS	SPI9445_RS0120490		Phosphate ABC transporter, substrate-binding protein PstS	CwatDRAFT_5160
	Phosphate ABC transporter, substrate-binding protein PstS	SPI9445_RS0121920		Phosphate ABC transporter, substrate-binding protein PstS	CwatDRAFT_4928
pstC	Phosphate ABC transporter, permease protein PstC	SPI9445_RS0120485	*pstC*	Phosphate ABC transporter, permease protein PstC	CwatDRAFT_4929
pstA	Phosphate ABC transporter, permease protein PstA	SPI9445_RS0120480	*pstA*	Phosphate ABC transporter, permease protein PstA	CwatDRAFT_4930
pstB	Phosphate ABC transporter, permease protein PstB	SPI9445_RS0107060		Phosphate ABC transporter, permease protein PstA	CwatDRAFT_4931
phoR	Phosphate regulon sensor protein PhoR (SphS)	SPI9445_RS0119490	*pstB*	Phosphate ABC transporter, permease protein PstB	CwatDRAFT_4932
phoB	Phosphate regulon transcriptional regulatory protein PhoB (SphR)	SPI9445_RS0119495		Phosphate ABC transporter, permease protein PstB	CwatDRAFT_4933
APase	-	-		Phosphate ABC transporter, permease protein PstB	CwatDRAFT_1348
ppK	Polyphosphate kinase	SPI9445_RS0118550	*phoR*	Phosphate regulon sensor protein PhoR (SphS)	CwatDRAFT_5910
ppX	Exopolyphosphatase	SPI9445_RS0101940	*phoB*	Phosphate regulon transcriptional regulatory protein PhoB (SphR)	CwatDRAFT_2775
ppA	Inorganic pyrophosphatase	SPI9445_RS0119415	APase	Alkaline phosphatase	CwatDRAFT_1549
				Alkaline phosphatase	CwatDRAFT_1629
			ppK	Polyphosphate kinase	CwatDRAFT_6491
			ppX	Exopolyphosphatase	CwatDRAFT_1948
			ppA	Inorganic pyrophosphatase	CwatDRAFT_2235
***Synechocystis* sp. PCC 7509 (NZ_ALVU02000000)**			***Pleurocapsa* sp. PCC 7327 (CP003590)**		
Genes	**Annotation (Patric)**	**Locus Tag**	**Genes**	**Annotation (Patric)**	**Locus Tag**
phoU	Phosphate transport system regulatory protein PhoU	SYN7509_RS0215960	*phoU*	Phosphate transport system regulatory protein PhoU	Ple7327_4124
pstS	Phosphate ABC transporter, substrate-binding protein PstS	SYN7509_RS0206650	*pstS*	Phosphate ABC transporter, substrate-binding protein PstS	Ple7327_1250
	Phosphate ABC transporter, substrate-binding protein PstS	SYN7509_RS0207360		Phosphate ABC transporter, substrate-binding protein PstS	Ple7327_3388
	Phosphate ABC transporter, substrate-binding protein PstS	SYN7509_RS0215920		Phosphate ABC transporter, substrate-binding protein PstS	Ple7327_3389

	Phosphate ABC transporter, substrate-binding protein PstS	SYN7509_RS0215925		Phosphate ABC transporter, substrate-binding protein PstS	Ple7327_3618
pstC	Phosphate ABC transporter, permease protein PstC	SYN7509_RS0206655	*pstC*	Phosphate ABC transporter, permease protein PstC	Ple7327_1249
	Phosphate ABC transporter, permease protein PstC	SYN7509_RS0207365		Phosphate ABC transporter, permease protein PstC	Ple7327_3387
pstA	Phosphate ABC transporter, permease protein PstA	SYN7509_RS0206660	*pstA*	Phosphate ABC transporter, permease protein PstA	Ple7327_1248
	Phosphate ABC transporter, permease protein PstA	SYN7509_RS0207370		Phosphate ABC transporter, permease protein PstA	Ple7327_3386
pstB	Phosphate ABC transporter, permease protein PstB	SYN7509_RS0206665	*pstB*	Phosphate ABC transporter, permease protein PstB	Ple7327_1247
	Phosphate ABC transporter, permease protein PstB	SYN7509_RS0207375		Phosphate ABC transporter, permease protein PstB	Ple7327_3385
phoR	Phosphate regulon sensor protein PhoR (SphS)	SYN7509_RS0215965	*phoR*	Phosphate regulon sensor protein PhoR (SphS)	Ple7327_4123
phoB	Phosphate regulon transcriptional regulatory protein PhoB (SphR)	SYN7509_RS0215970	*phoB*	Phosphate regulon transcriptional regulatory protein PhoB (SphR)	Ple7327_4122
APase	Alkaline phosphatase	SYN7509_RS0210500	APase	Phosphodiesterase/alkaline phosphatase D	Ple7327_0042
ppK	Polyphosphate kinase	SYN7509_RS0202140		Alkaline phosphatase	Ple7327_1998
	Polyphosphate kinase 2	SYN7509_RS0205545		Alkaline phosphatase like protein	Ple7327_4613
ppX	Exopolyphosphatase	SYN7509_RS0215695	*ppK*	Polyphosphate kinase	Ple7327_2011
ppA	Inorganic pyrophosphatase	SYN7509_RS0218560	*ppX*	Exopolyphosphatase	Ple7327_1164
			ppA	Inorganic pyrophosphatase	Ple7327_3589

***Anabaena* sp. PCC 7108 (NZ_AJWF01000000)**			***Dactylococcopsis salina* PCC 8305 (CP003944)**		
Genes	**Annotation (Patric)**	**Locus Tag**	**Genes**	**Annotation (Patric)**	**Locus Tag**
phoU	Phosphate transport system regulatory protein PhoU	ANA7108_RS010733	*phoU*	Phosphate transport system regulatory protein PhoU	Dacsa_1982
pstS	Phosphate ABC transporter, substrate-binding protein PstS	ANA7108_RS0104250	*pstS*	Phosphate ABC transporter, substrate-binding protein PstS	Dacsa_0981
	Phosphate ABC transporter, substrate-binding protein PstS	ANA7108_RS0114535		Phosphate ABC transporter, substrate-binding protein PstS	Dacsa_1219
	Phosphate ABC transporter, substrate-binding protein PstS	ANA7108_RS0124135		Phosphate ABC transporter, substrate-binding protein PstS	Dacsa_1417

	Phosphate ABC transporter, substrate-binding protein PstS	ANA7108_RS0125995		Phosphate ABC transporter, substrate-binding protein PstS	Dacsa_1575
pstC	Phosphate ABC transporter, permease protein PstC	ANA7108_RS0114530		Phosphate ABC transporter, substrate-binding protein PstS	Dacsa_3076
	Phosphate ABC transporter, permease protein PstC	ANA7108_RS0124130	*pstC*	Phosphate ABC transporter, permease protein PstC	Dacsa_1220
pstA	Phosphate ABC transporter, permease protein PstA	ANA7108_RS0114525		Phosphate ABC transporter, permease protein PstC	Dacsa_1416
	Phosphate ABC transporter, permease protein PstA	ANA7108_RS0124125		Phosphate ABC transporter, permease protein PstC	Dacsa_3114
pstB	Phosphate ABC transporter, permease protein PstB	ANA7108_RS0114520	*pstA*	Phosphate ABC transporter, permease protein PstA	Dacsa_1224
	Phosphate ABC transporter, permease protein PstB	ANA7108_RS0111425		Phosphate ABC transporter, permease protein PstA	Dacsa_1415
	Phosphate ABC transporter, permease protein PstB	ANA7108_RS0124120	*pstB*	Phosphate ABC transporter, permease protein PstB	Dacsa_1414
phoR	Phosphate regulon sensor protein PhoR (SphS)	ANA7108_RS0107330		Phosphate ABC transporter, permease protein PstB	Dacsa_3115
phoB	Phosphate regulon transcriptional regulatory protein PhoB (SphR)	ANA7108_RS0107325	*phoR*	Phosphate regulon sensor protein PhoR (SphS)	Dacsa_1981
Apase	Alkaline phosphatase	ANA7108_RS0104615	*phoB*	Phosphate regulon transcriptional regulatory protein PhoB (SphR)	Dacsa_1980
	Alkaline phosphatase	ANA7108_RS0104600	APase	Alkaline phosphatase	Dacsa_0439
	Alkaline phosphatase	ANA7108_RS0100780		Alkaline phosphatase	Dacsa_1692
	Alkaline phosphatase	ANA7108_RS0111735		Alkaline phosphatase	Dacsa_1693
ppK	Polyphosphate kinase 2	ANA7108_RS0119175		Alkaline phosphatase	Dacsa_1695
	Polyphosphate kinase	ANA7108_RS0109985		Alkaline phosphatase	Dacsa_1696
ppX	Exopolyphosphatase	ANA7108_RS0118330		Alkaline phosphatase	Dacsa_2870
ppA	Inorganic pyrophosphatase	ANA7108_RS0101510	*ppK*	Polyphosphate kinase	Dacsa_1689
			ppX	Exopolyphosphatase	Dacsa_0957
			ppA	Inorganic pyrophosphatase	Dacsa_3296
***Microcystis aeruginosa* PCC 7806SL (CP020771)**			***Fischerella* sp. PCC 9339 (NZ_ALVS01000000)**		

Genes	Annotation (Patric)	Locus Tag	Genes	Annotation (Patric)	Locus Tag
phoU	Phosphate transport system regulatory protein PhoU	BH695_5315	*phoU*	Phosphate transport system regulatory protein PhoU	PCC9339_RS0124490
pstS	Phosphate ABC transporter, substrate-binding protein PstS	BH695_0746	*pstS*	Phosphate ABC transporter, substrate-binding protein PstS	PCC9339_RS0107315
	Phosphate ABC transporter, substrate-binding protein PstS	BH695_0747		Phosphate ABC transporter, substrate-binding protein PstS	PCC9339_RS0115315
	Phosphate ABC transporter, substrate-binding protein PstS	BH695_1907		Phosphate ABC transporter, substrate-binding protein PstS	PCC9339_RS0118145
	Phosphate ABC transporter, substrate-binding protein PstS	BH695_1911		Phosphate ABC transporter, substrate-binding protein PstS	PCC9339_RS0124050
	Phosphate ABC transporter, substrate-binding protein PstS	BH695_4434		Phosphate ABC transporter, substrate-binding protein PstS	PCC9339_RS013259
pstC	Phosphate ABC transporter, permease protein PstC	BH695_0748	*pstC*	Phosphate ABC transporter, permease protein PstC	PCC9339_RS0107310
	Phosphate ABC transporter, permease protein PstC	BH695_1910		Phosphate ABC transporter, permease protein PstC	PCC9339_RS0124055
pstA	Phosphate ABC transporter, permease protein PstA	BH695_0749		Phosphate ABC transporter, permease protein PstC	PCC9339_RS0132595
	Phosphate ABC transporter, permease protein PstA	BH695_1909	*pstA*	Phosphate ABC transporter, permease protein PstA	PCC9339_RS0107305
pstB	Phosphate ABC transporter, permease protein PstB	BH695_0750		Phosphate ABC transporter, permease protein PstA	PCC9339_RS0124060
	Phosphate ABC transporter, permease protein PstB	BH695_0752		Phosphate ABC transporter, permease protein PstA	PCC9339_RS0132600
	Phosphate ABC transporter, permease protein PstB	BH695_1908	*pstB*	Phosphate ABC transporter, permease protein PstB	PCC9339_RS0107300
phoR	Phosphate regulon sensor protein PhoR (SphS)	BH695_3368		Phosphate ABC transporter, permease protein PstB	PCC9339_RS0124065
	Phosphate regulon sensor protein PhoR (SphS)	BH695_5316		Phosphate ABC transporter, permease protein PstB	PCC9339_RS0132605
phoB	Phosphate regulon transcriptional regulatory protein PhoB (SphR)	BH695_5317	*phoR*	Phosphate ABC transporter, permease protein PstB	PCC9339_RS0124065
Apase	Alkaline phosphatase	BH695_2564	*phoB*	Phosphate ABC transporter, permease protein PstB	PCC9339_RS0132605
	Alkaline phosphatase	BH695_2565	Apase	Alkaline phosphatase	PCC9339_RS0114510
	Alkaline phosphatase	BH695_2649		Alkaline phosphatase	PCC9339_RS0133125

	Alkaline phosphatase	BH695_3440		Alkaline phosphatase	PCC9339_RS0120820
	Alkaline phosphatase-like protein	BH695_4984	*ppK*	Polyphosphate kinase	PCC9339_RS0116345
ppK	Polyphosphate kinase	BH695_2980		Polyphosphate kinase 2	PCC9339_RS0129015
ppX	Exopolyphosphatase	BH695_0037		Polyphosphate kinase	PCC9339_RS0129835
	Exopolyphosphatase	BH695_5350	*ppX*	Exopolyphosphatase	PCC9339_RS0123895
ppA	Inorganic pyrophosphatase	BH695_0664	*ppA*	Inorganic pyrophosphatase	PCC9339_RS0115895
***Halothece* sp. PCC 7418 (CP003945)**			***Cyanothece* sp. ATCC 51472 (NZ_AGJC02000000)**		
Genes	**Annotation (Patric)**	**Locus Tag**	**Genes**	**Annotation (Patric)**	**Locus Tag**
phoU	Phosphate transport system regulatory protein PhoU	PCC7418_3123	*phoU*	Phosphate transport system regulatory protein PhoU	CY51472DRAFT_RS0222590
pstS	Phosphate ABC transporter, substrate-binding protein PstS	PCC7418_0041	*pstS*	Phosphate ABC transporter, substrate-binding protein PstS	CY51472DRAFT_RS0201580
	Phosphate ABC transporter, substrate-binding protein PstS	PCC7418_0390		Phosphate ABC transporter, substrate-binding protein PstS	CY51472DRAFT_RS0209720
	Phosphate ABC transporter, substrate-binding protein PstS	PCC7418_1750		Phosphate ABC transporter, substrate-binding protein PstS	CY51472DRAFT_RS0209725
	Phosphate ABC transporter, substrate-binding protein PstS	PCC7418_3269		Phosphate ABC transporter, substrate-binding protein PstS	CY51472DRAFT_RS0210980
pstC	Phosphate ABC transporter, permease protein PstC	PCC7418_1749		Phosphate ABC transporter, substrate-binding protein PstS	CY51472DRAFT_RS0211095
	Phosphate ABC transporter, permease protein PstC	PCC7418_1912		Phosphate ABC transporter, substrate-binding protein PstS	CY51472DRAFT_RS0214500
	Phosphate ABC transporter, permease protein PstC	PCC7418_3270		Phosphate ABC transporter, substrate-binding protein PstS	CY51472DRAFT_RS0224580
pstA	Phosphate ABC transporter, permease protein PstA	PCC7418_1748	*pstC*	Phosphate ABC transporter, permease protein PstC	CY51472DRAFT_RS0209715
	Phosphate ABC transporter, permease protein PstA	PCC7418_3271		Phosphate ABC transporter, permease protein PstC	CY51472DRAFT_RS0211100
pstB	Phosphate ABC transporter, permease protein PstB	PCC7418_1747	*pstA*	Phosphate ABC transporter, permease protein PstA	CY51472DRAFT_RS0209710
	Phosphate ABC transporter, permease protein PstB	PCC7418_1911		Phosphate ABC transporter, permease protein PstA	CY51472DRAFT_RS0211105
	Phosphate ABC transporter, permease protein PstB	PCC7418_3272	*pstB*	Phosphate ABC transporter, permease protein PstB	CY51472DRAFT_RS0201590

phoR	Phosphate regulon sensor protein PhoR (SphS)	PCC7418_3124		Phosphate ABC transporter, permease protein PstB	CY51472DRAFT_RS0224545
phoB	Phosphate regulon transcriptional regulatory protein PhoB (SphR)	PCC7418_3124		Phosphate ABC transporter, permease protein PstB	CY51472DRAFT_RS0209700
Apase	Alkaline phosphatase	PCC7418_0071		Phosphate ABC transporter, permease protein PstB	CY51472DRAFT_RS0211110
	Alkaline phosphatase	PCC7418_0077		Phosphate ABC transporter, permease protein PstB	CY51472DRAFT_RS0209705
	Alkaline phosphatase	PCC7418_0571		Phosphate ABC transporter, permease protein PstB	CY51472DRAFT_RS0224540
	Alkaline phosphatase	PCC7418_1065	*phoR*	Phosphate regulon sensor protein PhoR (SphS)	CY51472DRAFT_RS0221650
	Phosphodiesterase/alkaline phosphatase D	PCC7418_1982	*phoB*	Phosphate regulon transcriptional regulatory protein PhoB (SphR)	CY51472DRAFT_RS0201450
	Alkaline phosphatase	PCC7418_2858	Apase	Alkaline phosphatase	CY51472DRAFT_RS0203850
	Alkaline phosphatase	PCC7418_3483		Alkaline phosphatase	CY51472DRAFT_RS0203450
	Alkaline phosphatase	PCC7418_3485		Alkaline phosphatase	CY51472DRAFT_RS0222455
ppK	Polyphosphate kinase	PCC7418_1073		Alkaline phosphatase	CY51472DRAFT_RS0204765
ppX	Exopolyphosphatase	PCC7418_2036	*ppK*	Polyphosphate kinase	CY51472DRAFT_RS0216060
ppA	Inorganic pyrophosphatase	PCC7418_0708		Polyphosphate kinase	CY51472DRAFT_RS0224465
			ppX	Exopolyphosphatase	CY51472DRAFT_RS0208320
			ppA	Inorganic pyrophosphatase	CY51472DRAFT_RS0203230

***Calothrix* sp. PCC 7507 (CP003943)**			***Gloeocapsa* sp. PCC 7428 (CP003646)**		
Genes	**Annotation (Patric)**	**Locus Tag**	**Genes**	**Annotation (Patric)**	**Locus Tag**
phoU	Phosphate transport system regulatory protein PhoU	Cal7507_1625	*phoU*	Phosphate transport system regulatory protein PhoU	Glo7428_3037
pstS	Phosphate ABC transporter, substrate-binding protein PstS	Cal7507_0340	*pstS*	Phosphate ABC transporter, substrate-binding protein PstS	Glo7428_0758
	Phosphate ABC transporter, substrate-binding protein PstS	Cal7507_1013		Phosphate ABC transporter, substrate-binding protein PstS	Glo7428_0759
	Phosphate ABC transporter, substrate-binding protein PstS	Cal7507_1206		Phosphate ABC transporter, substrate-binding protein PstS	Glo7428_1132
	Phosphate ABC transporter, substrate-binding protein PstS	Cal7507_1927		Phosphate ABC transporter, substrate-binding protein PstS	Glo7428_1752

	Phosphate ABC transporter, substrate-binding protein PstS	Cal7507_1928		Phosphate ABC transporter, substrate-binding protein PstS	Glo7428_1886
	Phosphate ABC transporter, substrate-binding protein PstS	Cal7507_4798		Phosphate ABC transporter, substrate-binding protein PstS	Glo7428_2342
	Phosphate ABC transporter, substrate-binding protein PstS	Cal7507_5691		Phosphate ABC transporter, substrate-binding protein PstS	Glo7428_4983
	Phosphate ABC transporter, substrate-binding protein PstS	Cal7507_5816	*pstC*	Phosphate ABC transporter, permease protein PstC	Glo7428_1133
pstC	Phosphate ABC transporter, permease protein PstC	Cal7507_0341		Phosphate ABC transporter, permease protein PstC	Glo7428_2341
	Phosphate ABC transporter, permease protein PstC	Cal7507_1207		Phosphate ABC transporter, permease protein PstC	Glo7428_4984
	Phosphate ABC transporter, permease protein PstC	Cal7507_4797	*pstA*	Phosphate ABC transporter, permease protein PstA	Glo7428_1134
pstA	Phosphate ABC transporter, permease protein PstA	Cal7507_0342		Phosphate ABC transporter, permease protein PstA	Glo7428_2340
	Phosphate ABC transporter, permease protein PstA	Cal7507_1208		Uncharacterized protein Psta_3961	Glo7428_3942
	Phosphate ABC transporter, permease protein PstA	Cal7507_4796		Phosphate ABC transporter, permease protein PstA	Glo7428_4985
pstB	Phosphate ABC transporter, permease protein PstB	Cal7507_0343	*pstB*	Phosphate ABC transporter, permease protein PstB	Glo7428_1135
	Phosphate ABC transporter, permease protein PstB	Cal7507_1209		Phosphate ABC transporter, permease protein PstB	Glo7428_2339
	Phosphate ABC transporter, permease protein PstB	Cal7507_1210	*phoR*	Phosphate regulon sensor protein PhoR (SphS)	Glo7428_0220
	Phosphate ABC transporter, permease protein PstB	Cal7507_4795		Phosphate regulon sensor protein PhoR (SphS)	Glo7428_3038
phoR	Phosphate regulon sensor protein PhoR (SphS)	Cal7507_1624		Phosphate regulon sensor protein PhoR (SphS)	Glo7428_5081
phoB	Phosphate regulon transcriptional regulatory protein PhoB (SphR)	Cal7507_1623	*phoB*	Phosphate regulon transcriptional regulatory protein PhoB (SphR)	Glo7428_0934
Apase	Alkaline phosphatase	Cal7507_1562		Phosphate regulon transcriptional regulatory protein PhoB (SphR)	Glo7428_3039
	Alkaline phosphatase	Cal7507_2517	Apase	Alkaline phosphatase	Glo7428_0109
	Alkaline phosphatase	Cal7507_2523		Alkaline phosphatase	Glo7428_0424
ppK	Polyphosphate kinase	Cal7507_0098		Alkaline phosphatase	Glo7428_0645

	Polyphosphate kinase	Cal7507_2880
	Polyphosphate kinase	Cal7507_4641
ppX	Exopolyphosphatase	Cal7507_4902
ppA	Inorganic pyrophosphatase	Cal7507_2098

	Alkaline phosphatase	Glo7428_0796
	Alkaline phosphatase	Glo7428_0846
	Alkaline phosphatase	Glo7428_1248
	Alkaline phosphatase	Glo7428_1514
	Alkaline phosphatase	Glo7428_1646
	Alkaline phosphatase	Glo7428_1647
	Phosphodiesterase/alkaline phosphatase D	Glo7428_3016
	Alkaline phosphatase	Glo7428_3293
	Alkaline phosphatase	Glo7428_3370
	Alkaline phosphatase	Glo7428_3554
	Alkaline phosphatase	Glo7428_3943
	Alkaline phosphatase	Glo7428_4190
	Alkaline phosphatase	Glo7428_4312
	Alkaline phosphatase	Glo7428_4364
	Alkaline phosphatase	Glo7428_4414
	Phosphodiesterase/alkaline phosphatase D	Glo7428_4942
ppK	Polyphosphate kinase	Glo7428_1568
	Polyphosphate kinase 2	Glo7428_1966
ppX	Exopolyphosphatase	Glo7428_1713
ppA	Inorganic pyrophosphatase	Glo7428_1953

Chapter 2

Supplementary Table 1. List of all experimental treatments conducted in this study.

Experiments on *Halothece* sp. PCC 7418 and *Fischerella muscicola* PCC 73103			
Treatments			**Description**
[Low PO_4^{3-}- Low Fe]	[Medium PO_4^{3-} - Low Fe]	[High PO_4^{3-}- Low Fe]	1st experiment Optimal NO_3^- (4.4 mM) for *Halothece* sp.
[Low PO_4^{3-}- Medium Fe]	[Medium PO_4^{3-} - Medium Fe]	[High PO_4^{3-}- Medium Fe]	2nd experiment Low NO_3^- (0.15 mM) for *Halothece* sp. and N_2 as sole N source for *F. muscicola*
[Low PO_4^{3-}- High Fe]	[Medium PO_4^{3-} - High Fe]	[High PO_4^{3-}- High Fe]	3rd experiment Extremely limiting NO_3^- conditions (6.66 nM), comparing with optimal NO_3^- in selected treatments ([Low PO_4^{3-}- Low Fe], [High PO_4^{3-}- Low Fe], [Low PO_4^{3-}- High Fe] and [High PO_4^{3-}- High Fe]) for *Halothece* sp.
Recovery experiments on *Halothece* sp. PCC 7418			
Initial Treatment	**Condition of NO_3^-**	**Nutrient added (at day 12)**	**Resulting treatment (maintained for 4 days)**
[Low PO_4^{3-}- Low Fe]	Optimal NO_3^- (4.4 mM)	PO_4^{3-} and Fe	[High PO_4^{3-}- High Fe] in optimal NO_3^- treatment
[Low PO_4^{3-}- Low Fe]	Extremely limiting NO_3^- conditions (6.66 nM)	PO_4^{3-}, Fe and NO_3^-	[High PO_4^{3-}- High Fe] in optimal NO_3^- treatment
[High PO_4^{3-}- High Fe]	Extremely limiting NO_3^- conditions (6.66 nM)	NO_3^-	[High PO_4^{3-}- High Fe] in optimal NO_3^- treatment

In the recovery experiments, PO_4^{3-}, Fe, and/or NO_3^- were added to the different initial treatments to achieve optimal conditions (45 μM, 7.5 μM and 4.4 mM, respectively). Initial treatment for PO_4^{3-}: [Low PO_4^{3-}] (0.1 μM), [Medium PO_4^{3-}] (1 μM) and [High PO_4^{3-}] (45 μM). Initial treatments for Fe: [Low Fe] (2 nM), [Medium Fe] (20 nM) and [High Fe] (7.5 μM).

Supplementary multifasta 1, for PHO boxes in cyanobacteria:

>SYNPCC7002_A1357(SYNPCC7002_A1357) Score=7.8 Pos=-125 [Synechococcus sp. PCC 7002]
GCTAACCTNNNCTATATTTNNNTTTTATTT
>SYNPCC7002_A2352(phoA1) Score=7.5 Pos=-182 [Synechococcus sp. PCC 7002]
ATTTAATTNNNTTTAGTTGNNNCTTAGCTA
>SYNPCC7002_A2352(phoA1) Score=9.5 Pos=-91 [Synechococcus sp. PCC 7002]
ATTAAACTNNNCTTAGTTTNNNTTTAACTC
>SYNPCC7002_A1232(cysR) Score=8.7 Pos=-126 [Synechococcus sp. PCC 7002]
CTTAAACTNNNGATTACATNNNATTTAACT
>SYNPCC7002_A2120(ndbB) Score=7.6 Pos=-309 [Synechococcus sp. PCC 7002]
CTAAAATTNNNTTTTACTANNNTTTGATCA
>sll0679(sphX) Score=10.9 Pos=-135 [Synechocystis sp. PCC 6803]
TTTAACCANNNCTTTACTANNNCTTAACCT
>sll0654(phoA) Score=7.3 Pos=-210 [Synechocystis sp. PCC 6803]
TTTTACTTNNNCTTTCCCTNNNGTTAGCAA
>sll0654(phoA) Score=8.8 Pos=-175 [Synechocystis sp. PCC 6803]
CTTAACCTNNNCATAGTCTNNNCATAAGTT
>slr1247(pstS) Score=10.5 Pos=-342 [Synechocystis sp. PCC 6803]
CTTAATCTNNNCTTAATTCNNNCTTAATTT
>slr0115(rpaA) Score=7 Pos=-174 [Synechocystis sp. PCC 6803]
ATTACCCANNNTTTAGATGNNNTTTTTCTT
>cce_1163(pstS) Score=9.7 Pos=-109 [Cyanothece sp. ATCC 51142]
CTTAATCTNNNTTTTACTGNNNTTTAACCC
>cce_1859(sphX) Score=8.8 Pos=-141 [Cyanothece sp. ATCC 51142]
CTTAATAANNNGTTTAACTNNNCTTCATAT
>cce_0886(pstS) Score=7.5 Pos=-53 [Cyanothece sp. ATCC 51142]
GTTAGATTNNNCTTTAAGANNNGTTTAGTT
>cce_0886(pstS) Score=6.9 Pos=-358 [Cyanothece sp. ATCC 51142]
CTTGAAAANNNTATAAATANNNGTTATCAT
>cce_3317(SYNPCC7002_A1357) Score=8.4 Pos=-44 [Cyanothece sp. ATCC 51142]
CTTATCTANNNCTTTATTTNNNTTTATACT
>cce_1211(purF) Score=7.7 Pos=-143 [Cyanothece sp. ATCC 51142]
TATAATCTNNNGTTTTATTNNNGTCTATTT
>cce_4621(phoA) Score=8.7 Pos=-88 [Cyanothece sp. ATCC 51142]
TTTAAAGTNNNTTTAACATNNNCTTTAAAT
>cce_4758(fbp) Score=8.3 Pos=-125 [Cyanothece sp. ATCC 51142]
ATTAACCTNNNCTGAAATTNNNCTAAAGTT
>cce_5183(ackA) Score=9.6 Pos=-74 [Cyanothece sp. ATCC 51142]
GTTAATTTNNNTTTAATCANNNCTTAAAAT
>cce_4392(cce_4392) Score=8.8 Pos=20 [Cyanothece sp. ATCC 51142]
CTTTAACCNNNCTCAATCTNNNCTTAAACT
>cce_5174(ppk) Score=8.4 Pos=-70 [Cyanothece sp. ATCC 51142]
GATAAAAANNNCATAAAGTNNNCTTAAACT
>cce_0154(ndbB) Score=7.6 Pos=-83 [Cyanothece sp. ATCC 51142]
TTTTATCTNNNGATAATTANNNATTAATGA
>PCC8801_1024(pstS) Score=9.8 Pos=-108 [Cyanothece sp. PCC 8801]
TTTTATCANNNGTTTACCTNNNCTTAACCC
>PCC8801_4067(sphX) Score=8.1 Pos=-157 [Cyanothece sp. PCC 8801]
CTTAGCATNNNCTTTTTCTNNNGCTAAACT
>PCC8801_1433(spoT) Score=8.5 Pos=-224 [Cyanothece sp. PCC 8801]
TTTAACAGNNNCTAAACCTNNNTTTAAACT
>PCC8801_1847(SYNPCC7002_A1357) Score=7.5 Pos=-43 [Cyanothece sp. PCC 8801]
AATAAATTNNNTCTTATTTNNNATTATCTT

>PCC8801_4178(purF) Score=7.5 Pos=-104 [Cyanothece sp. PCC 8801]
GATAAGATNNNGTTAAAGANNNGTTAAAAT
>PCC8801_1683(nucH) Score=9.8 Pos=-246 [Cyanothece sp. PCC 8801]
ATTAAACTNNNCTTAAATTNNNGTTAAATA
>PCC8801_0430(fbp) Score=7.9 Pos=-278 [Cyanothece sp. PCC 8801]
TTAAAATTNNNTTTTATTTNNNCTTTTATT
>PCC8801_0346(cysR) Score=9.7 Pos=-91 [Cyanothece sp. PCC 8801]
TTTAATCTNNNGATTACCTNNNGTTTACCT
>PCC8801_3887(ackA) Score=9.1 Pos=-183 [Cyanothece sp. PCC 8801]
CTTTGACCNNNGTTTACCANNNCTTAACCT
>PCC8801_1625(ppk) Score=7.2 Pos=-95 [Cyanothece sp. PCC 8801]
TATTACCTNNNTATAGCCTNNNGATAGCCT
>PCC8801_3662(rsbU) Score=7.4 Pos=-162 [Cyanothece sp. PCC 8801]
ATTAACGCNNNGATTAACCNNNCCTAATTA
>PCC8801_2302(SYNPCC7002_A0979) Score=7.1 Pos=-232 [Cyanothece sp. PCC 8801]
CATAATGANNNTTTTAAGANNNGTTAAAAA
>Cyan7425_0207 Score=7.8 Pos=-81 [Cyanothece sp. PCC 7425]
TTTAACGANNNCTTTAGCANNNGATTACCT
>Cyan7425_4261(phoA1) Score=9 Pos=-146 [Cyanothece sp. PCC 7425]
ATTAATCANNNGTTTACCTNNNCATAAATC
>Cyan7425_4387(SYNPCC7002_A2263) Score=7.5 Pos=-102 [Cyanothece sp. PCC 7425]
ATTATCATNNNTATTACCTNNNCCTTACCC
>Cyan7425_1977(ppk) Score=8.4 Pos=-238 [Cyanothece sp. PCC 7425]
GTTATCCCNNNGTTAATTTNNNATTAAATC
>Cyan7425_0664(pstS) Score=10.1 Pos=-80 [Cyanothece sp. PCC 7425]
ATTAATCTNNNCTTAATCTNNNCTTTATCC
>MAE_18380(pstS) Score=9.5 Pos=-87 [Microcystis aeruginosa NIES-843]
TTTATTCANNNCTTAACCTNNNCTTTACCA
>MAE_23860(fbp) Score=7.6 Pos=-129 [Microcystis aeruginosa NIES-843]
ATTAGCCANNNCTAAAACTNNNCTAAAAAT
>MAE_18440(cysR) Score=9.6 Pos=-86 [Microcystis aeruginosa NIES-843]
GTTAATCTNNNGATTACCTNNNGTTTACCT
>MAE_02800(ackA) Score=8.8 Pos=-66 [Microcystis aeruginosa NIES-843]
TTTTATCTNNNCTTAACCTNNNTTTGATTA
>MAE_18310(pstS) Score=9.6 Pos=-139 [Microcystis aeruginosa NIES-843]
ATTAACCGNNNTTTTACCGNNNCTTAACCA
>all3651(purF) Score=7.7 Pos=-119 [Nostoc sp. PCC 7120]
TTTAATATNNNGTTAAAGANNNGTTAAGAC
>alr5291(phoA1) Score=10.4 Pos=-229 [Nostoc sp. PCC 7120]
GTTAACCTNNNTTTATATTNNNCTTAACTT
>all4021(fbp) Score=7 Pos=-136 [Nostoc sp. PCC 7120]
CGTAAACTNNNGATTTCTTNNNTTTATCTA
>alr5259(SYNPCC7002_A2263) Score=8.7 Pos=-329 [Nostoc sp. PCC 7120]
GTAAAACTNNNTTTATTTANNNCTTAATTT
>all1758(rsbU) Score=7.5 Pos=-49 [Nostoc sp. PCC 7120]
ATTTATTANNNGTCAATCTNNNATTAACCC
>all0129(rpaA) Score=7.3 Pos=-101 [Nostoc sp. PCC 7120]
TTTATGTTNNNTTTAAAATNNNTTTTATAA
>all3822(SYNPCC7002_A0979) Score=8.6 Pos=-149 [Nostoc sp. PCC 7120]
CTTAATTTNNNCTTAAGTANNNCTCAAATT
>alr4975(alr4975) Score=7.6 Pos=-10 [Nostoc sp. PCC 7120]
ATTAATTANNNTGTTACCTNNNATTTATAT
>alr2234(phoD) Score=9.6 Pos=-275 [Nostoc sp. PCC 7120]
ATTAACCTNNNCTTAGTCANNNATTAATTT
>all0207(phoD) Score=9.3 Pos=-98 [Nostoc sp. PCC 7120]

ATTAACCCNNNGATAACTCNNNCTTTACTT
>all0911(pstS) Score=10.8 Pos=-105 [Nostoc sp. PCC 7120]
CTTAACTTNNNGTTTACCTNNNCTTAACTT
>all4575(pstS) Score=8 Pos=-324 [Nostoc sp. PCC 7120]
TTTTATCTNNNCTTTTATTNNNCTTTTTTT
>Tery_3534(pstS) Score=9.7 Pos=-192 [Trichodesmium erythraeum IMS101]
TTTGATATNNNTTTAACCTNNNCTTAATCT
>Tery_2653(spoT) Score=7.8 Pos=-43 [Trichodesmium erythraeum IMS101]
AATAAACTNNNATTTGATANNNATTAACTC
>Tery_4322(SYNPCC7002_A1357) Score=7 Pos=-395 [Trichodesmium erythraeum IMS101]
CTTATTATNNNAATTATTTNNNATTTAGCT
>Tery_3699(purF) Score=8.3 Pos=-97 [Trichodesmium erythraeum IMS101]
GTTAAGGANNNCTTAAAGTNNNTTTAAGCT
>Tery_0682(fbp) Score=6.5 Pos=-336 [Trichodesmium erythraeum IMS101]
TTTTAGATNNNGTTTTTGTNNNCATTATCA
>Tery_2568(SYNPCC7002_A2263) Score=7.5 Pos=-208 [Trichodesmium erythraeum IMS101]
GATAAGATNNNATTAACCTNNNGTTTGCTA
>Tery_0739(rsbU) Score=8.3 Pos=-250 [Trichodesmium erythraeum IMS101]
TTAAAACTNNNCTTAATCTNNNACTAACTC
>Tery_4937(rpaA) Score=7 Pos=-158 [Trichodesmium erythraeum IMS101]
CTTGACAANNNAATAAATTNNNGTTAAAGA
>Tery_0954(SYNPCC7002_A0979) Score=8.3 Pos=-309 [Trichodesmium erythraeum IMS101]
ATTAACCANNNATTGAATTNNNATTGACTT
>Tery_2902(sphR) Score=10.4 Pos=-365 [Trichodesmium erythraeum IMS101]
GATAACCCNNNGTTAACCTNNNCTTAACCT
>Tery_3661(ndbB) Score=7.8 Pos=-342 [Trichodesmium erythraeum IMS101]
TTTTAATANNNAATTACCCNNNCTTAGCCT
>Synpcc7942_0004(purF) Score=7.8 Pos=-76 [Synechococcus elongatus PCC 7942]
GTTAAGTCNNNGTTAAATTNNNATTAGCCG
>Synpcc7942_1392(phoA) Score=9.4 Pos=-233 [Synechococcus elongatus PCC 7942]
TTTAACTANNNCATAATCTNNNCTCAATCT
>CYA_1552(pstS) Score=10.2 Pos=-203 [Synechococcus sp. JA-3-3Ab]
AATAACCTNNNTTTAACCTNNNGTTAACCA
>CYA_1732(pstS) Score=9.6 Pos=-75 [Synechococcus sp. JA-3-3Ab]
GTTAACCTNNNGATATCCTNNNGTTAACTT
>CYA_1541(cysR) Score=10.5 Pos=-172 [Synechococcus sp. JA-3-3Ab]
CTTAACCTNNNCATAACCTNNNCTTTACTT
>CYA_2506(phoD) Score=7.9 Pos=-129 [Synechococcus sp. JA-3-3Ab]
CTTAAACANNNGCTAACCCNNNTTTCACCG
>SYNW2391(phoA1) Score=9.2 Pos=-78 [Synechococcus sp. WH 8102]
TTTGATCANNNCTTAAACTNNNCCTAACTT
>tlr2164(pstS) Score=10.9 Pos=-51 [Thermosynechococcus elongatus BP-1]
TTTAAACANNNTTTTACCTNNNCTTAACTT
>tll1671(cysR) Score=8.1 Pos=-171 [Thermosynechococcus elongatus BP-1]
CTTAACCCNNNCTTGAACCNNNGATTATCT
>null(SYNPCC7002_A1357) Score=7.1 Pos=-268 [Thermosynechococcus elongatus BP-1]
ATTAAAAANNNATTAAAAANNNTTTCTCTT

Supplementary multifasta 2, for Fur boxes in cyanobacteria:

>SYNPCC7002_A2347(chlL) Score=3.6 Pos=-126 [Synechococcus sp. PCC 7002]
TTTTATAAAAACTCTAAGT
>SYNPCC7002_G0137(exbB) Score=4.2 Pos=-279 [Synechococcus sp. PCC 7002]
ATTAAGAGATTATCTCAAT
>SYNPCC7002_G0099(pchR) Score=3.7 Pos=-94 [Synechococcus sp. PCC 7002]
ATTTCTTATTAATATAAAT
>SYNPCC7002_G0006(iutA) Score=4.6 Pos=-38 [Synechococcus sp. PCC 7002]
TTTGAGAATTATTTTTAGT
>SYNPCC7002_A1631(apcF) Score=3.3 Pos=-257 [Synechococcus sp. PCC 7002]
TTTTATTATTTTTTTTAAA
>SYNPCC7002_A0913(SYNPCC7002_A0913) Score=2.2 Pos=-146 [Synechococcus sp. PCC 7002]
TTTTTACAACATTTTTAAA
>SYNPCC7002_A0913(SYNPCC7002_A0913) Score=3.8 Pos=-68 [Synechococcus sp. PCC 7002]
AATGAGAAAATTTTGATAT
>SYNPCC7002_A1018(chlH) Score=3.8 Pos=-57 [Synechococcus sp. PCC 7002]
ATAGTTATAAATTTTTAAT
>SYNPCC7002_A1443(nifJ) Score=2.2 Pos=-165 [Synechococcus sp. PCC 7002]
TTTTCTTATAACTTTTAGC
>SYNPCC7002_A0871(afuC) Score=5.1 Pos=-83 [Synechococcus sp. PCC 7002]
GTTGAGAATAGTTCTTAAT
>SYNPCC7002_A2351(SYNPCC7002_A2351) Score=2.9 Pos=-216 [Synechococcus sp. PCC 7002]
TTTATTATTGTTTTTTAGT
>SYNPCC7002_A1961(psaA) Score=3.4 Pos=-206 [Synechococcus sp. PCC 7002]
AGTTTTAAATATTGTTAAT
>SYNPCC7002_G0061(SYNPCC7002_G0061) Score=4.1 Pos=-62 [Synechococcus sp. PCC 7002]
ATTGATAAATAATTTAAGT
>SYNPCC7002_A1649(fur) Score=3.5 Pos=-88 [Synechococcus sp. PCC 7002]
GTTAGTATTTATTTGCAAT
>SYNPCC7002_G0138(iutA) Score=4.6 Pos=-67 [Synechococcus sp. PCC 7002]
ATTGAGATAATCTCTTAAT
>SYNPCC7002_G0090(SYNPCC7002_G0090) Score=5.2 Pos=-83 [Synechococcus sp. PCC 7002]
ATTGAAATAAATTCTTATT
>SYNPCC7002_G0104(pchR) Score=5.4 Pos=-68 [Synechococcus sp. PCC 7002]
ATTGAGAATAATTAGTAAT
>SYNPCC7002_G0103(fhuA) Score=3.2 Pos=-46 [Synechococcus sp. PCC 7002]
ATTAAGAACTTTTTGAAGT
>slr0749(chlL) Score=3.3 Pos=-173 [Synechocystis sp. PCC 6803]
ATTTTATTTTTGTCTCAAT
>ssr2333(feoA) Score=4.5 Pos=-31 [Synechocystis sp. PCC 6803]
GTTGAGAATTATTTGCAGT
>sll1406(fhuA) Score=3.4 Pos=-38 [Synechocystis sp. PCC 6803]
ATTAATAAAACTTTTTAAC
>sll1404(exbB) Score=6 Pos=-110 [Synechocystis sp. PCC 6803]
ATTGAAAATAGTTATCAAT
>slr1490(fhuA) Score=4.1 Pos=-86 [Synechocystis sp. PCC 6803]
TTTGAGAATTAGTTGCAGT
>slr1484(SYNPCC7002_G0090) Score=5.6 Pos=-255 [Synechocystis sp. PCC 6803]
ATTGATAACTATTTTCAAT

>slr1318(fecE) Score=4.1 Pos=-176 [Synechocystis sp. PCC 6803]
ATTCCTAATTATTCTTAAC
>slr1485(SYNPCC7002_G0089) Score=2.2 Pos=-9 [Synechocystis sp. PCC 6803]
GTTTTAATAATGTTTAAAT
>slr1316(fecC) Score=4.2 Pos=-78 [Synechocystis sp. PCC 6803]
ATTGATAATCTTTCCTAGT
>slr1485(SYNPCC7002_G0089) Score=2.7 Pos=-42 [Synechocystis sp. PCC 6803]
ACTGTGAAATTTATTTAAC
>sll1404(exbB) Score=4.6 Pos=-64 [Synechocystis sp. PCC 6803]
ATTGAGAATTACTCTTAAC
>sll1404(exbB) Score=4.6 Pos=-286 [Synechocystis sp. PCC 6803]
TATGTGAAATATTATTATT
>slr1295(sufA) Score=4.9 Pos=-44 [Synechocystis sp. PCC 6803]
ATTGAGAATTACTTTTATT
>sll1911(SYNPCC7002_A0913) Score=4.2 Pos=-59 [Synechocystis sp. PCC 6803]
GTTGTTAAAATTTAACAAT
>slr0513(sufA) Score=3.9 Pos=-240 [Synechocystis sp. PCC 6803]
AATAATAATCTCTTGCAAT
>slr0513(sufA) Score=4.1 Pos=-187 [Synechocystis sp. PCC 6803]
ATTGCACTTTATTTGCAAT
>sll0849(psbD) Score=3.3 Pos=-298 [Synechocystis sp. PCC 6803]
AATGTAAAATATTTGCTAA
>slr1181(psbA) Score=2.8 Pos=-242 [Synechocystis sp. PCC 6803]
ATTAAAATCTTTTTTTTAC
>slr1181(psbA) Score=4 Pos=-182 [Synechocystis sp. PCC 6803]
TTAAAGAAATATTATTAAT
>sll1867(psbA) Score=3.4 Pos=-124 [Synechocystis sp. PCC 6803]
ATTTACAAATTGTTACAAT
>slr1738(perR) Score=3 Pos=-194 [Synechocystis sp. PCC 6803]
ATTAATATTTTTTTTATAA
>sll0247(isiA) Score=2.8 Pos=-269 [Synechocystis sp. PCC 6803]
ATTTCTTAATAATTTTAGT
>ssr2333(feoA) Score=4.4 Pos=-69 [Synechocystis sp. PCC 6803]
TTTGATATTTATTCTGAAC
>slr1392(feoB) Score=4.5 Pos=-278 [Synechocystis sp. PCC 6803]
GTTGAGAATTATTTGCAGT
>cce_4533(cce_4533) Score=3.7 Pos=-118 [Cyanothece sp. ATCC 51142]
TTTGAGTTTTATTTAAAAT
>cce_0033(feoA) Score=4.5 Pos=-47 [Cyanothece sp. ATCC 51142]
GATAAGAATTATTCTTAAT
>cce_0033(feoA) Score=3.3 Pos=-298 [Cyanothece sp. ATCC 51142]
ATTAAAAAATACTGTTAAC
>cce_0660(psbD) Score=3.4 Pos=-298 [Cyanothece sp. ATCC 51142]
ATTGTAAATTTTTTGCTAA
>cce_0479(dpsA) Score=4.7 Pos=-144 [Cyanothece sp. ATCC 51142]
GATGCAATATATTCTCAAT
>cce_2632(sufA) Score=4.8 Pos=-20 [Cyanothece sp. ATCC 51142]
ATCAATAATAATTTTCAAT
>cce_4358(chlH) Score=2.7 Pos=-183 [Cyanothece sp. ATCC 51142]
AATAAATAATTTTTGTAAA
>cce_4358(chlH) Score=2.3 Pos=-138 [Cyanothece sp. ATCC 51142]
ATTTGTCAATATTTGTAAC
>cce_3801(afuC) Score=4.2 Pos=-163 [Cyanothece sp. ATCC 51142]
ATTGAAAATTAATGCTAAT
>cce_0989(psaA) Score=3.4 Pos=-205 [Cyanothece sp. ATCC 51142]

AATTTTAATTATTGTTAAG
>cce_3809(SYNPCC7002_A2351) Score=3.2 Pos=-132 [Cyanothece sp. ATCC 51142]
GTTTTTATTTTCTGTCAAT
>cce_1977(coxB) Score=3.7 Pos=-136 [Cyanothece sp. ATCC 51142]
AATTTCAATCAATTTCAAT
>cce_0019(SYNPCC7002_A0913) Score=3.1 Pos=-75 [Cyanothece sp. ATCC 51142]
TTTTTTAATATTTTTTGAT
>cce_1944(apcF) Score=4.4 Pos=-151 [Cyanothece sp. ATCC 51142]
ATTGCTAAAATCTATAATT
>cce_3895(SYNPCC7002_G0062) Score=2.8 Pos=16 [Cyanothece sp. ATCC 51142]
GTTTAAAAATTCTTTTAGT
>cce_0892(fdx) Score=3 Pos=-29 [Cyanothece sp. ATCC 51142]
TTTCTTATAATTTCTTAAC
>cce_1785(isiA) Score=4.4 Pos=-18 [Cyanothece sp. ATCC 51142]
ATTGCAAATCTTTTTAAAT
>cce_3031(isiB) Score=4.9 Pos=-66 [Cyanothece sp. ATCC 51142]
ATTGAGAATTATTCTAAAC
>cce_2330(fur) Score=5.1 Pos=-96 [Cyanothece sp. ATCC 51142]
GTTGCTAATTATTTTCAAT
>PCC8801_0791(chlL) Score=2.7 Pos=-242 [Cyanothece sp. PCC 8801]
ATTTAGTAAATTTTAAAGT
>PCC8801_2575(SYNPCC7002_A2351) Score=3.1 Pos=-247 [Cyanothece sp. PCC 8801]
ATTTCTCCTTATTTTTAAT
>PCC8801_0349(sll1407) Score=3.3 Pos=-107 [Cyanothece sp. PCC 8801]
AATAATTAATTTTTTTTAT
>PCC8801_0256(ctaA) Score=2.2 Pos=-185 [Cyanothece sp. PCC 8801]
TTTTATTAACTTATGTAAA
>PCC8801_2812(SYNPCC7002_A0913) Score=4.4 Pos=-67 [Cyanothece sp. PCC 8801]
TATGATAAAATTTATTAAA
>PCC8801_4320(chlH) Score=2.3 Pos=-186 [Cyanothece sp. PCC 8801]
ATTTGTCAATATTTGTAAC
>PCC8801_0567(coxB) Score=2.7 Pos=-152 [Cyanothece sp. PCC 8801]
TTTGTTTATTATTTGTTAC
>PCC8801_3918(nifJ) Score=3.4 Pos=-67 [Cyanothece sp. PCC 8801]
TTTGTCAATAATTTGTAAC
>PCC8801_1443(sufA) Score=4 Pos=-90 [Cyanothece sp. PCC 8801]
ATTAGGAATAATTAGCAAC
>PCC8801_1928(SYNPCC7002_G0061) Score=2 Pos=-184 [Cyanothece sp. PCC 8801]
AATATTTTATATTTATAGT
>PCC8801_2860(fdx) Score=3.8 Pos=-49 [Cyanothece sp. PCC 8801]
ATTGTAAAAAAATATTAAC
>PCC8801_0870(fur) Score=4.6 Pos=-97 [Cyanothece sp. PCC 8801]
GTTGCAAATTATTTGCAAT
>PCC8801_3039(SYNPCC7002_G0098) Score=5.5 Pos=-89 [Cyanothece sp. PCC 8801]
GTTGACAAAAATTCTCATT
>PCC8801_3017(exbB) Score=5.7 Pos=-38 [Cyanothece sp. PCC 8801]
ATTGATAACTTTTCTCAAT
>Cyan7425_2411(pchR) Score=4.9 Pos=-71 [Cyanothece sp. PCC 7425]
ATTGTTAATCTTTTTCATT
>Cyan7425_2410(fhuA) Score=5.8 Pos=-56 [Cyanothece sp. PCC 7425]
ATTGAGAATAATTCTTATT
>Cyan7425_2418(exbB) Score=4.6 Pos=-264 [Cyanothece sp. PCC 7425]
ATTGATGATTATTTTCAAC
>Cyan7425_2438(pchR) Score=4.5 Pos=-37 [Cyanothece sp. PCC 7425]
ATTAAGAATAAGTCTCAGT

>Cyan7425_2439(fhuA) Score=5.1 Pos=-66 [Cyanothece sp. PCC 7425]
ATTGAGAGTATTTCTTATT
>Cyan7425_1597(perR) Score=4.9 Pos=-88 [Cyanothece sp. PCC 7425]
TTTGAGAATTATACTAAAT
>Cyan7425_5031(psbD) Score=3.1 Pos=-91 [Cyanothece sp. PCC 7425]
GTTTATAAACTTTCGTAAA
>Cyan7425_4671(psaA) Score=3.4 Pos=-292 [Cyanothece sp. PCC 7425]
TCTATGAATTTTTATTAAT
>Cyan7425_3510(afuC) Score=4 Pos=-60 [Cyanothece sp. PCC 7425]
GTTGAATAATAGTCTTAAT
>Cyan7425_3510(afuC) Score=5.3 Pos=-105 [Cyanothece sp. PCC 7425]
ATTGAGAATAATTTTCAAA
>Cyan7425_1838(apcF) Score=3 Pos=-245 [Cyanothece sp. PCC 7425]
TTTTATATTATCTTTTAAC
>Cyan7425_1059(psbA) Score=3.4 Pos=-182 [Cyanothece sp. PCC 7425]
ATTATTAATAAGTTTCAAA
>Cyan7425_2984(cce_4396) Score=2.7 Pos=-78 [Cyanothece sp. PCC 7425]
TATATGAATATCTTGTAAT
>Cyan7425_2984(cce_4396) Score=3.9 Pos=-48 [Cyanothece sp. PCC 7425]
ATTGCAATTATATTACAAT
>Cyan7425_2434(isiA) Score=4.7 Pos=-61 [Cyanothece sp. PCC 7425]
ATTGAGTTTATTTCTCAAC
>Cyan7425_3508(sufA) Score=3.5 Pos=-165 [Cyanothece sp. PCC 7425]
ATTAGGAATGAATCGTAAT
>MAE_16250(chlN) Score=2.8 Pos=-107 [Microcystis aeruginosa NIES-843]
ATTAAGTAATTCTTTATAT
>MAE_16230(chlL) Score=2.8 Pos=-150 [Microcystis aeruginosa NIES-843]
ATTTATATAATTTTTAAGC
>MAE_12190(chlH) Score=2.8 Pos=-247 [Microcystis aeruginosa NIES-843]
ATTAAATATTAATTTTTGT
>MAE_41160(psbD) Score=2.9 Pos=-274 [Microcystis aeruginosa NIES-843]
ATTTGTAATTTTTTGCTAA
>MAE_47560(psaA) Score=3.2 Pos=-297 [Microcystis aeruginosa NIES-843]
ATTAATAAACTTTTGTAAA
>MAE_22930(coxB) Score=2.5 Pos=-216 [Microcystis aeruginosa NIES-843]
TTTTAGATATTCTTTAGAT
>MAE_38140(nifJ) Score=3.9 Pos=-292 [Microcystis aeruginosa NIES-843]
ATTCTGAATATTAATTAAT
>MAE_12460(afuC) Score=4.4 Pos=-117 [Microcystis aeruginosa NIES-843]
TTTGAGAAAGTTTCCTAAT
>MAE_56680(sufA) Score=4.9 Pos=-61 [Microcystis aeruginosa NIES-843]
GATAAGAATTATTCTCAAT
>MAE_22920(ctaA) Score=2.5 Pos=-282 [Microcystis aeruginosa NIES-843]
TCTTTTCAATATTTTTAAT
>all4365(chlH) Score=2.9 Pos=-272 [Nostoc sp. PCC 7120]
GTTTTTTATTTTTTTCATC
>all4365(chlH) Score=3 Pos=-232 [Nostoc sp. PCC 7120]
AATATTAATTTTTCTTTAC
>alr5154(psaA) Score=3.4 Pos=-177 [Nostoc sp. PCC 7120]
ATTTTGAATTATTGTTAAA
>alr0950(coxB) Score=3.7 Pos=-134 [Nostoc sp. PCC 7120]
TTTACTCAAGATTATTAAT
>alr2803(nifJ) Score=3.8 Pos=-92 [Nostoc sp. PCC 7120]
ATTTTTAATCAGTATTAAT
>alr3808(dpsA) Score=3.5 Pos=-204 [Nostoc sp. PCC 7120]

GTTTAGAAATTATTGCAAT
>alr2514(coxB) Score=3 Pos=-190 [Nostoc sp. PCC 7120]
AGTTAAAAAGTTAATAAGT
>all4001(isiA) Score=4.8 Pos=-161 [Nostoc sp. PCC 7120]
ATTAAGAATCTTTTTCAAT
>alr3727(psbA) Score=3.7 Pos=-105 [Nostoc sp. PCC 7120]
TTTAGTAATATTAATTAAT
>alr4592(psbA) Score=4.1 Pos=-28 [Nostoc sp. PCC 7120]
ATAAATAATTAATCGCAAT
>asl0884(fdx) Score=3.5 Pos=-90 [Nostoc sp. PCC 7120]
ATTCTTAATTTTTTGTAAT
>alr3155(SYNPCC7002_G0061) Score=4.1 Pos=-98 [Nostoc sp. PCC 7120]
ATTACGAATTAATATAAAT
>all3903(cce_4396) Score=4.6 Pos=-47 [Nostoc sp. PCC 7120]
TTTAATATAAATTGTCAAT
>all2367(all2367) Score=3.2 Pos=-181 [Nostoc sp. PCC 7120]
TATTGTAATATCTTTTAAT
>alr2405(isiB) Score=5 Pos=-235 [Nostoc sp. PCC 7120]
ATTGAAATAAATATTCAAT
>all1691(fur) Score=5.2 Pos=-94 [Nostoc sp. PCC 7120]
TTTAATAAATATTCTCAAT
>all1692(sigC) Score=3.5 Pos=-320 [Nostoc sp. PCC 7120]
AATAAACATAATTTTTACT
>all2158(fhuA) Score=4.6 Pos=-62 [Nostoc sp. PCC 7120]
ATTAAGAATTATTAGCAGT
>alr2175(fhuE) Score=4.4 Pos=-120 [Nostoc sp. PCC 7120]
GTTAATAATCTTTCGCAAT
>alr2626(fhuE) Score=4.7 Pos=-106 [Nostoc sp. PCC 7120]
TTTGATATTAATTACTAAT
>all2586(fecC) Score=4.6 Pos=-100 [Nostoc sp. PCC 7120]
TCTTATATTAATTCTCAAT
>all2586(fecC) Score=5 Pos=-32 [Nostoc sp. PCC 7120]
AATGACTATATTTTTCAAT
>all2237(pchR) Score=5.1 Pos=-40 [Nostoc sp. PCC 7120]
TTTGAGAAAGTTTATCTAT
>all2235(fecB) Score=3.5 Pos=12 [Nostoc sp. PCC 7120]
TTTTATTATCATATTCAAC
>all1101(fhuA) Score=3.8 Pos=-238 [Nostoc sp. PCC 7120]
ATTAATATTAAATCCTAAT
>all4924(fhuE) Score=5.5 Pos=-32 [Nostoc sp. PCC 7120]
ATTGAGAATTTTTATCTAT
>all5047(exbB) Score=4.7 Pos=-102 [Nostoc sp. PCC 7120]
TTTGATAATAATTTGCATC
>alr2184(pchR) Score=5.1 Pos=-39 [Nostoc sp. PCC 7120]
ATTGAGAAATAATATTATT
>alr2185(fhuE) Score=4.3 Pos=-69 [Nostoc sp. PCC 7120]
TTTGCAAAAAATTATTAAC
>alr2211(fhuA) Score=2.9 Pos=-272 [Nostoc sp. PCC 7120]
ATTTATTTAATTATTTAGT
>all2580(pchR) Score=5.5 Pos=-48 [Nostoc sp. PCC 7120]
ATTGAGAAATAATATCATT
>alr2174(pchR) Score=5.6 Pos=-96 [Nostoc sp. PCC 7120]
ATTGATAAATACTATCATT
>Tery_2879(feoA) Score=3.5 Pos=-270 [Trichodesmium erythraeum IMS101]
TTTTCCAAATTTTTTCAGT

>Tery_2644(SYNPCC7002_A2351) Score=4.2 Pos=-122 [Trichodesmium erythraeum IMS101]
AATTAGATTAATTTTGAAT
>Tery_4282(dpsA) Score=2.4 Pos=-285 [Trichodesmium erythraeum IMS101]
ATTTTTTAACAATTGAAAT
>Tery_0513(psbC) Score=3.5 Pos=-195 [Trichodesmium erythraeum IMS101]
TTTACAAAAAATTTGTAAT
>Tery_1780(ctaA) Score=3.3 Pos=-167 [Trichodesmium erythraeum IMS101]
ATTAAAAAAAAATTTAAAA
>Tery_4773(SYNPCC7002_A0913) Score=2.4 Pos=-64 [Trichodesmium erythraeum IMS101]
TTTATGAAATATTTATGAT
>Tery_3224(chlH) Score=3 Pos=-65 [Trichodesmium erythraeum IMS101]
GTTTAAAATTTTTTGATAT
>Tery_1781(ctaB) Score=4.1 Pos=-41 [Trichodesmium erythraeum IMS101]
AATTATAACCAGTTTCAAT
>Tery_4669(psaA) Score=4 Pos=-80 [Trichodesmium erythraeum IMS101]
ATTGATAATTCTTTACAAC
>Tery_3222(afuC) Score=5.1 Pos=-94 [Trichodesmium erythraeum IMS101]
AATGAAAAAAATATTCAAT
>Tery_2878(feoB) Score=3 Pos=-43 [Trichodesmium erythraeum IMS101]
TATTACATAATTTTTATAT
>Tery_3377(sufA) Score=4.4 Pos=-97 [Trichodesmium erythraeum IMS101]
ATTAAGAATAAATTGCAAT
>Tery_1667(isiA) Score=3.2 Pos=-156 [Trichodesmium erythraeum IMS101]
TTTTATAATTTCTTTTAAA
>Tery_4504(fdx) Score=2.6 Pos=-35 [Trichodesmium erythraeum IMS101]
GTTAATATTTTTTTATAAC
>Tery_1958(fur) Score=4.7 Pos=-44 [Trichodesmium erythraeum IMS101]
ATTGTGTATCATTGTCAAT
>Tery_1780(ctaA) Score=3.5 Pos=-278 [Trichodesmium erythraeum IMS101]
ATTGTTAAAATTATGAAAT
>Synpcc7942_2601(ctaA) Score=4.3 Pos=-158 [Synechococcus elongatus PCC 7942]
GATGACAATATTTTTCGAT
>Synpcc7942_1406(afuC) Score=4.2 Pos=-81 [Synechococcus elongatus PCC 7942]
ATTGAGAATAAATCGCAGA
>Synpcc7942_0938(cce_4396) Score=4 Pos=-30 [Synechococcus elongatus PCC 7942]
AATAAAAAAGTTTCGTAAT
>Synpcc7942_1542(isiA) Score=5.2 Pos=-45 [Synechococcus elongatus PCC 7942]
ATTGAGAATTATTGTAAAT
>Synpcc7942_2049(psaA) Score=3.3 Pos=-296 [Synechococcus elongatus PCC 7942]
TCTTTGAATTATTGTTAAT
>PMT1340(ctaA) Score=2.6 Pos=-30 [Prochlorococcus marinus str. MIT 9313]
ATTTAAATTATTTTATTGT
>CYA_2647(psbD) Score=3 Pos=-106 [Synechococcus sp. JA-3-3Ab]
TTTATTAATTTTTCGTAAG
>CYA_2794(afuC) Score=3.8 Pos=-26 [Synechococcus sp. JA-3-3Ab]
AGTGAAAATCTTTTGCAAC
>CYA_0643(fdx) Score=2.8 Pos=-92 [Synechococcus sp. JA-3-3Ab]
ATTAAAAATATGATTTAAA
>gvip470(psaA) Score=2.2 Pos=-195 [Gloeobacter violaceus PCC 7421]
TTTTTAAAAATTGTTAAGT
>glr3733(perR) Score=4.2 Pos=-58 [Gloeobacter violaceus PCC 7421]
AATTAGATCTATTCTAAAT
>gll1014(afuA) Score=3.7 Pos=-64 [Gloeobacter violaceus PCC 7421]
ATTGACAATTAATTGCAGC
>null(chlL) Score=2.8 Pos=-211 [Thermosynechococcus elongatus BP-1]

TTTTGTATTTTTGTTTAAT
>null(psbA) Score=3.8 Pos=-135 [Thermosynechococcus elongatus BP-1]
ATTTAGTTTTACTAACAAT
>null(apcF) Score=3.1 Pos=-157 [Thermosynechococcus elongatus BP-1]
AATTATGAACTTTTGTAAT
>null(cce_4396) Score=4 Pos=-45 [Thermosynechococcus elongatus BP-1]
AATTAAAATTATATTCATC
>null(isiA) Score=5.5 Pos=-121 [Thermosynechococcus elongatus BP-1]
AATGCTATTAATTCTCAAT
>null(fur) Score=4.4 Pos=-59 [Thermosynechococcus elongatus BP-1]
CATTGTAATTATTCTCAAT

Supplementary multifasta 3, for NtcA boxes in cyanobacteria:

>SYNPCC7002_A2208(amt1) Score=3.7 Pos=-52 [Synechococcus sp. PCC 7002]
GGTTACTTCTGCTACC
>SYNPCC7002_A0076(SYNPCC7002_A0076) Score=4.2 Pos=-97 [Synechococcus sp. PCC 7002]
AGTATTGAAATATACA
>SYNPCC7002_A2395(SYNPCC7002_A2395) Score=4.5 Pos=-200 [Synechococcus sp. PCC 7002]
TGTTACTTAAATTACA
>SYNPCC7002_A2395(SYNPCC7002_A2395) Score=4.5 Pos=-92 [Synechococcus sp. PCC 7002]
TGTAGTAGACGTTACA
>SYNPCC7002_A1954(SYNPCC7002_A1954) Score=4.7 Pos=-243 [Synechococcus sp. PCC 7002]
TGTAACAGGAGTTACA
>SYNPCC7002_A0643(cynS) Score=4.5 Pos=-237 [Synechococcus sp. PCC 7002]
CGTATCTTTAATTACA
>SYNPCC7002_A0860(cynA) Score=4.1 Pos=-221 [Synechococcus sp. PCC 7002]
TGTAATTGATTTAACA
>SYNPCC7002_A0582(gifA) Score=5 Pos=-96 [Synechococcus sp. PCC 7002]
TGTATCAAATTTTACA
>SYNPCC7002_A1630(glnA) Score=3.5 Pos=-125 [Synechococcus sp. PCC 7002]
TGTGACCCAGACTACA
>SYNPCC7002_A1827(nirA) Score=4 Pos=-111 [Synechococcus sp. PCC 7002]
CGTAGTTAACACTACA
>SYNPCC7002_A0496(nrrA) Score=4.1 Pos=-75 [Synechococcus sp. PCC 7002]
CGTAACCACGGTTACA
>SYNPCC7002_A1675(ntcA) Score=3.9 Pos=-177 [Synechococcus sp. PCC 7002]
TGAAGCAAAAAGTACA
>SYNPCC7002_A1632(ntcB) Score=3.9 Pos=-87 [Synechococcus sp. PCC 7002]
TGTAACATCCGGAACA
>SYNPCC7002_A2101(SYNPCC7002_A2101) Score=5 Pos=67 [Synechococcus sp. PCC 7002]
TGTATCATTAAATACA
>SYNPCC7002_A0264(SYNPCC7002_A0264) Score=5 Pos=-29 [Synechococcus sp. PCC 7002]
TGTATCAAATACTACA
>SYNPCC7002_A0398(urtA) Score=4.1 Pos=-127 [Synechococcus sp. PCC 7002]
TGTATCAAGTGTCACA
>SYNPCC7002_A1443(nifJ) Score=4.1 Pos=-272 [Synechococcus sp. PCC 7002]
TTTATCATTTTCTACA
>sll0108(amt1) Score=4 Pos=-189 [Synechocystis sp. PCC 6803]
AGTAGTAAATCATACA
>sll0108(amt1) Score=4.4 Pos=-18 [Synechocystis sp. PCC 6803]
TGTAGATTAAAGTACA
>ssr1562(SYNPCC7002_A0076) Score=4.5 Pos=-78 [Synechocystis sp. PCC 6803]
TGTAATCGATAATACA
>slr1147(SYNPCC7002_A1954) Score=4.7 Pos=-214 [Synechocystis sp. PCC 6803]
TGTAATGATAGTTACA
>ssl1911(gifA) Score=5 Pos=-89 [Synechocystis sp. PCC 6803]
TGTATAAAATGTTACA
>slr1756(glnA) Score=4.3 Pos=-98 [Synechocystis sp. PCC 6803]
GGTAGCGAAAAATACA
>ssl0707(glnB) Score=3.7 Pos=-184 [Synechocystis sp. PCC 6803]

GGTACTGATTTTTACA
>slr0851(ndh) Score=4.1 Pos=-72 [Synechocystis sp. PCC 6803]
TGTAACAACCATTACC
>sll1450(nrtA) Score=3.9 Pos=-96 [Synechocystis sp. PCC 6803]
AGTTACAAACTATACA
>slr0898(nirA) Score=4.7 Pos=-74 [Synechocystis sp. PCC 6803]
TGTAATTTACGTTACA
>sll1330(nrrA) Score=4.6 Pos=-75 [Synechocystis sp. PCC 6803]
GGTAACTGTTGTTACA
>slr0653(rpoD) Score=3.9 Pos=-246 [Synechocystis sp. PCC 6803]
TGTTATCGAGGCTACA
>sll1515(gifB) Score=4.2 Pos=-119 [Synechocystis sp. PCC 6803]
CGTAAAAATGGATACA
>slr0447(urtA) Score=4.5 Pos=-211 [Synechocystis sp. PCC 6803]
GGTATCCTATGCTACA
>slr0009(rbcL) Score=4.3 Pos=-228 [Synechocystis sp. PCC 6803]
TGTAATTTAAAAAACA
>sll0741(nifJ) Score=3.3 Pos=-181 [Synechocystis sp. PCC 6803]
AGAATCAACAAAAACA
>sll1733(ndhD) Score=4 Pos=-252 [Synechocystis sp. PCC 6803]
TGTAACAATTTTTAGT
>sll1732(ndhF) Score=4 Pos=-244 [Synechocystis sp. PCC 6803]
TGTAACAAATAACACT
>sll1712(hanA) Score=3.8 Pos=-264 [Synechocystis sp. PCC 6803]
GGTAGTTTTTGAAACT
>cce_3261(amt1) Score=3.5 Pos=-152 [Cyanothece sp. ATCC 51142]
TGTTAAGGTTGTAACA
>cce_0537(SYNPCC7002_A0076) Score=4 Pos=-137 [Cyanothece sp. ATCC 51142]
TGTAAACTATGATATA
>cce_0537(SYNPCC7002_A0076) Score=4.8 Pos=-93 [Cyanothece sp. ATCC 51142]
TGTAGTCTTTGTTACA
>cce_4355(SYNPCC7002_A0077) Score=4.7 Pos=-172 [Cyanothece sp. ATCC 51142]
TGTTACAATAGCTACA
>cce_2729(SYNPCC7002_A2395) Score=4 Pos=-148 [Cyanothece sp. ATCC 51142]
TGTAACATATGATAAC
>cce_2729(SYNPCC7002_A2395) Score=4.6 Pos=-87 [Cyanothece sp. ATCC 51142]
TGTAATATTGATTACA
>cce_3327(SYNPCC7002_A1954) Score=4.7 Pos=-210 [Cyanothece sp. ATCC 51142]
TGTAGTCATAGTTACA
>cce_3327(SYNPCC7002_A1954) Score=4 Pos=-46 [Cyanothece sp. ATCC 51142]
TTTATTTTCTGTTACA
>cce_3797(cce_3797) Score=4.9 Pos=-70 [Cyanothece sp. ATCC 51142]
TGTAGCTTAATATACA
>cce_0259(gifA) Score=5.2 Pos=-95 [Cyanothece sp. ATCC 51142]
TGTAGCAAATGTTACA
>cce_4432(glnA) Score=4.5 Pos=-89 [Cyanothece sp. ATCC 51142]
AGTATCCAATTATACA
>cce_4432(glnA) Score=4 Pos=-30 [Cyanothece sp. ATCC 51142]
TGTATATATTGAAACC
>cce_1063(hupS) Score=4.8 Pos=-204 [Cyanothece sp. ATCC 51142]
TGTAAAATTTAATACA
>cce_1063(hupS) Score=3.8 Pos=-159 [Cyanothece sp. ATCC 51142]
GGTAATAATTAATAGA
>cce_0624(ndh) Score=4.7 Pos=-47 [Cyanothece sp. ATCC 51142]
TGTAACTGTAGTTACT

>cce_1223(nirA) Score=4.7 Pos=-76 [Cyanothece sp. ATCC 51142]
TGTTACATTAGCTACA
>cce_1808(nrrA) Score=4.3 Pos=-76 [Cyanothece sp. ATCC 51142]
CGTAGCCGATGTTACA
>cce_0198(ntcB) Score=4.2 Pos=-73 [Cyanothece sp. ATCC 51142]
AGTATCAATTTCTACG
>cce_3797(SYNPCC7002_A2101) Score=4.9 Pos=-70 [Cyanothece sp. ATCC 51142]
TGTAGCTTAATATACA
>cce_0267(psbA3) Score=4.4 Pos=-58 [Cyanothece sp. ATCC 51142]
GGTAATCATTGATACA
>cce_0875(rpoD) Score=4.3 Pos=-232 [Cyanothece sp. ATCC 51142]
AGTAATCAAGGCTACA
>cce_2638(gifB) Score=5.2 Pos=-144 [Cyanothece sp. ATCC 51142]
TGTAACAATAGATACA
>cce_1944(apcF) Score=3.8 Pos=-177 [Cyanothece sp. ATCC 51142]
TGTGATAAGAAATACA
>cce_2390(trxQ) Score=3.7 Pos=-332 [Cyanothece sp. ATCC 51142]
AATAGCTATAATTACT
>cce_3633(psbZ) Score=4.2 Pos=-20 [Cyanothece sp. ATCC 51142]
TGTAACTGTATTAACA
>cce_0953(nifJ) Score=3.8 Pos=-52 [Cyanothece sp. ATCC 51142]
TGCAACAAAAATTACC
>PCC8801_1229(amt1) Score=5 Pos=-264 [Cyanothece sp. PCC 8801]
TGTATTTTTTGATACA
>PCC8801_1229(amt1) Score=4.1 Pos=-229 [Cyanothece sp. PCC 8801]
AGTAATAAAAAAAACA
>PCC8801_3101(SYNPCC7002_A0076) Score=4.6 Pos=-95 [Cyanothece sp. PCC 8801]
TGTATTGGTTGTTACA
>PCC8801_2066(SYNPCC7002_A2395) Score=4.8 Pos=-53 [Cyanothece sp. PCC 8801]
TGTAATATTAATTACA
>PCC8801_3053(SYNPCC7002_A1954) Score=4.8 Pos=-198 [Cyanothece sp. PCC 8801]
TGTAATCATAGTTACA
>PCC8801_3848(cce_3797) Score=5.1 Pos=-165 [Cyanothece sp. PCC 8801]
TGTAACTTTAGATACA
>PCC8801_2371(gifA) Score=4.9 Pos=-94 [Cyanothece sp. PCC 8801]
TGTATAAATTGCTACA
>PCC8801_0808(glnA) Score=4 Pos=-92 [Cyanothece sp. PCC 8801]
CGTATCATGGTATACA
>PCC8801_3212(hupS) Score=4.3 Pos=-127 [Cyanothece sp. PCC 8801]
TGTAACAACAATAACA
>PCC8801_3485(ndh) Score=4.6 Pos=-117 [Cyanothece sp. PCC 8801]
TGTAACCATAGCTACT
>PCC8801_3485(ndh) Score=3.8 Pos=-92 [Cyanothece sp. PCC 8801]
CGTAATTGGTTTTACA
>PCC8801_4396(nrtA) Score=4.6 Pos=-184 [Cyanothece sp. PCC 8801]
TGTAGCAAATAATACG
>PCC8801_4396(nrtA) Score=3.9 Pos=-106 [Cyanothece sp. PCC 8801]
AGTATTTATAGACACA
>PCC8801_2468(nirA) Score=4.6 Pos=-75 [Cyanothece sp. PCC 8801]
TGTTACAATTAATACA
>PCC8801_2463(narB) Score=4.4 Pos=-165 [Cyanothece sp. PCC 8801]
TGTATTACCAAATACA
>PCC8801_3375(nrrA) Score=4.5 Pos=-76 [Cyanothece sp. PCC 8801]
CGTAGCAGATGTTACA
>PCC8801_2329(ntcB) Score=4.7 Pos=-80 [Cyanothece sp. PCC 8801]

TGTATCAAATTCTACT
>PCC8801_3848(SYNPCC7002_A2101) Score=5.1 Pos=-165 [Cyanothece sp. PCC 8801]
TGTAACTTTAGATACA
>PCC8801_3216(psbA3) Score=4.4 Pos=-59 [Cyanothece sp. PCC 8801]
AGTAGTTATTGCTACT
>PCC8801_0154(rpoD) Score=4.4 Pos=-257 [Cyanothece sp. PCC 8801]
TGTAATCGAGGCTACA
>PCC8801_0807(apcF) Score=4 Pos=-251 [Cyanothece sp. PCC 8801]
TGTATACCATGATACG
>PCC8801_0870(fur) Score=3.4 Pos=-380 [Cyanothece sp. PCC 8801]
TGTTTATGCTAAAACA
>PCC8801_0567(coxB) Score=3.8 Pos=-148 [Cyanothece sp. PCC 8801]
TTTATTATTTGTTACC
>PCC8801_3918(nifJ) Score=3.5 Pos=-265 [Cyanothece sp. PCC 8801]
AGTAACCATAATTATT
>PCC8801_4247(ndhF) Score=3.6 Pos=-238 [Cyanothece sp. PCC 8801]
CGTATTATGAGTTAGA
>Cyan7425_0782(amt1) Score=4.4 Pos=-228 [Cyanothece sp. PCC 7425]
TGTATAACGTGATACA
>Cyan7425_0729(SYNPCC7002_A0076) Score=4.3 Pos=-128 [Cyanothece sp. PCC 7425]
TGTAACATTTGTTATT
>Cyan7425_0729(SYNPCC7002_A0076) Score=4.1 Pos=-71 [Cyanothece sp. PCC 7425]
AGTATTGGTGGATACA
>Cyan7425_0833(SYNPCC7002_A2395) Score=3.7 Pos=-38 [Cyanothece sp. PCC 7425]
AGTAGTTTAATAAACT
>Cyan7425_0732(cce_3797) Score=5.2 Pos=-33 [Cyanothece sp. PCC 7425]
TGTATCATAAGCTACA
>Cyan7425_1839(glnA) Score=4.9 Pos=-221 [Cyanothece sp. PCC 7425]
TGTAACTCATGATACA
>Cyan7425_4042(Cyan7425_4042) Score=4.4 Pos=-151 [Cyanothece sp. PCC 7425]
AGTAGCTCGTGATACA
>Cyan7425_4573(nirA) Score=4.5 Pos=-123 [Cyanothece sp. PCC 7425]
TGTAACTTAATATACC
>Cyan7425_0851(nrrA) Score=4.1 Pos=-82 [Cyanothece sp. PCC 7425]
AGTAGCTAGAGTTACG
>Cyan7425_0755(ntcA) Score=4.8 Pos=-173 [Cyanothece sp. PCC 7425]
TGTATCCGATGATACA
>Cyan7425_1599(ntcB) Score=4.6 Pos=-78 [Cyanothece sp. PCC 7425]
TGTATCACTATCTACA
>Cyan7425_0732(SYNPCC7002_A2101) Score=5.2 Pos=-33 [Cyanothece sp. PCC 7425]
TGTATCATAAGCTACA
>Cyan7425_1838(apcF) Score=4.9 Pos=-281 [Cyanothece sp. PCC 7425]
TGTATCATGAGTTACA
>Cyan7425_4369(nifJ) Score=3.1 Pos=-120 [Cyanothece sp. PCC 7425]
TCTAACGTATTCTCCA
>Cyan7425_2260(urtA) Score=3.7 Pos=-148 [Cyanothece sp. PCC 7425]
TGTATAATAGATCACA
>Cyan7425_1393(gifB) Score=4.7 Pos=-158 [Cyanothece sp. PCC 7425]
GGTATCATATAATACA
>MAE_62530(icd) Score=3.7 Pos=-30 [Microcystis aeruginosa NIES-843]
CGTATAGATAAATACT
>MAE_40010(amt1) Score=4.6 Pos=-213 [Microcystis aeruginosa NIES-843]
TGTATCAACGAATACA
>MAE_39690(SYNPCC7002_A0076) Score=4.3 Pos=-99 [Microcystis aeruginosa NIES-843]
TGTAATCGTCGATACA

>MAE_38700(SYNPCC7002_A2395) Score=4.2 Pos=-87 [Microcystis aeruginosa NIES-843]
TGTAATCATCTTTACA
>MAE_14410(SYNPCC7002_A1954) Score=3.7 Pos=-75 [Microcystis aeruginosa NIES-843]
TGTAAACTGGGAAACA
>MAE_14840(cce_3797) Score=4.9 Pos=-38 [Microcystis aeruginosa NIES-843]
TGTAAATTTAGATACA
>MAE_49490(gifA) Score=4.9 Pos=-42 [Microcystis aeruginosa NIES-843]
TGTAAAAATAGATACA
>MAE_19270(glnA) Score=4.7 Pos=-92 [Microcystis aeruginosa NIES-843]
TGTATCGAAAAATACA
>MAE_09050(glnN) Score=4.7 Pos=-244 [Microcystis aeruginosa NIES-843]
TGTAATGTTTGATACA
>MAE_18410(nirA) Score=4.1 Pos=-190 [Microcystis aeruginosa NIES-843]
TGTTACAGACAATACA
>MAE_14810(MAE_14810) Score=4.2 Pos=-177 [Microcystis aeruginosa NIES-843]
TGTAACAATCTATACG
>MAE_53960(narB) Score=4.8 Pos=-88 [Microcystis aeruginosa NIES-843]
TGTATTAATAACTACA
>MAE_09380(ntcB) Score=4.1 Pos=-80 [Microcystis aeruginosa NIES-843]
GGTAGCAATTTCTACC
>MAE_14840(SYNPCC7002_A2101) Score=4.9 Pos=-38 [Microcystis aeruginosa NIES-843]
TGTAAATTTAGATACA
>MAE_54470(rpoD) Score=4.9 Pos=-126 [Microcystis aeruginosa NIES-843]
TGTAATTAAAGCTACA
>MAE_18580(SYNPCC7002_A0264) Score=4.8 Pos=-68 [Microcystis aeruginosa NIES-843]
TGTATCTTTAGCTACT
>MAE_06220(urtA) Score=4.6 Pos=-140 [Microcystis aeruginosa NIES-843]
AGTAGCGAAAGTTACA
>MAE_06180(urtE) Score=3.8 Pos=-8 [Microcystis aeruginosa NIES-843]
GGTTGACAATGTTACA
>MAE_37080(fur) Score=3.7 Pos=-118 [Microcystis aeruginosa NIES-843]
AGTAATTTTTCATACT
>MAE_22930(coxB) Score=3.8 Pos=-141 [Microcystis aeruginosa NIES-843]
AGTTATTTTAAATACT
>MAE_06220(urtA) Score=4.7 Pos=-170 [Microcystis aeruginosa NIES-843]
AGTAGCAAAAATTACA
>all4968(gor) Score=4.1 Pos=-48 [Nostoc sp. PCC 7120]
AATAACAACTGTTACA
>alr1827(icd) Score=3.4 Pos=-6 [Nostoc sp. PCC 7120]
TGAAATATGTACAACA
>alr0992(amt1) Score=4.7 Pos=-50 [Nostoc sp. PCC 7120]
TGTAACTAAGTATACA
>alr0990(amt1) Score=4.7 Pos=-250 [Nostoc sp. PCC 7120]
TGTATTAACTAATACA
>asr0064(SYNPCC7002_A0076) Score=3.7 Pos=-107 [Nostoc sp. PCC 7120]
CGTATAGCAAAATACA
>alr4308(SYNPCC7002_A2395) Score=3.9 Pos=-64 [Nostoc sp. PCC 7120]
GGTAGTCGGAGTTACA
>alr3982(SYNPCC7002_A1954) Score=4.6 Pos=-250 [Nostoc sp. PCC 7120]
TGTAGTGATAGCTACA
>asl2329(gifA) Score=4.7 Pos=-78 [Nostoc sp. PCC 7120]
CGTAGCATAAGATACA
>alr2328(glnA) Score=4.8 Pos=-142 [Nostoc sp. PCC 7120]
TGTAACAAAGACTACA
>all2319(glnB) Score=3.8 Pos=-214 [Nostoc sp. PCC 7120]

AGTTACACAGACTACA
>all1127(ndh) Score=4.7 Pos=-146 [Nostoc sp. PCC 7120]
TGTAGCTTAAATTACT
>all4312(nrrA) Score=4.5 Pos=-75 [Nostoc sp. PCC 7120]
AGTAACAAAGACTACA
>alr4392(ntcA) Score=3.7 Pos=-151 [Nostoc sp. PCC 7120]
GGTATCATTATGAACA
>alr4392(ntcA) Score=3.7 Pos=-111 [Nostoc sp. PCC 7120]
AGTATAGGAAAGTACA
>all0602(ntcB) Score=4.5 Pos=-80 [Nostoc sp. PCC 7120]
TGTAACAAAATCTACC
>all0602(ntcB) Score=4.7 Pos=-21 [Nostoc sp. PCC 7120]
TGTAATTAAGGCTACA
>all1327(SYNPCC7002_A0264) Score=4.3 Pos=-52 [Nostoc sp. PCC 7120]
CGTAGTGTATGTTACA
>all2327(apcF) Score=4.8 Pos=-233 [Nostoc sp. PCC 7120]
TGTAGTCTTTGTTACA
>all1691(fur) Score=4.1 Pos=-218 [Nostoc sp. PCC 7120]
TGTAGCTTGAGATTCA
>alr1690(alr1690) Score=3.6 Pos=-91 [Nostoc sp. PCC 7120]
TGTGAATATAGAAACA
>alr2514(coxB) Score=3.5 Pos=-291 [Nostoc sp. PCC 7120]
AGAAGTAGAAGCTACT
>all4001(isiA) Score=3.7 Pos=-37 [Nostoc sp. PCC 7120]
AGTATTTCTGGCAACA
>alr1524(rbcL) Score=3.6 Pos=-32 [Nostoc sp. PCC 7120]
AGTAAAAAGAGTGACA
>alr4344(gltS) Score=3.5 Pos=-265 [Nostoc sp. PCC 7120]
TGGAAAAATTAAAACA
>all1258(psbZ) Score=3.4 Pos=-161 [Nostoc sp. PCC 7120]
TGTTACAAAAATTAGG
>alr1911(nifJ) Score=3.2 Pos=-281 [Nostoc sp. PCC 7120]
TGAATTTGATGTAACC
>alr4156(ndhF) Score=4 Pos=-260 [Nostoc sp. PCC 7120]
TGTCTTATAAAATACA
>alr0052(trxA) Score=3.7 Pos=17 [Nostoc sp. PCC 7120]
AGTTACAGATTCTACT
>asr3935(hanA) Score=3.6 Pos=-279 [Nostoc sp. PCC 7120]
GGTATTTTTTCCTACT
>all1951(urtA) Score=4.3 Pos=-116 [Nostoc sp. PCC 7120]
AGTATCAAAAATAACA
>Tery_4477(amt1) Score=4.9 Pos=-83 [Trichodesmium erythraeum IMS101]
AGTAGCATTTGATACA
>Tery_2891(SYNPCC7002_A0076) Score=4.1 Pos=-191 [Trichodesmium erythraeum IMS101]
TGTAATTTAGACAACA
>Tery_2891(SYNPCC7002_A0076) Score=4.6 Pos=-110 [Trichodesmium erythraeum IMS101]
TGTAACTATATATACT
>Tery_0672(SYNPCC7002_A2395) Score=4.3 Pos=-94 [Trichodesmium erythraeum IMS101]
AGTATTCAAAATTACA
>Tery_3912(SYNPCC7002_A1954) Score=4.3 Pos=-156 [Trichodesmium erythraeum IMS101]
TGTAGTTATGGCTACC
>Tery_3834(glnA) Score=4 Pos=-250 [Trichodesmium erythraeum IMS101]
CGTAACACCCGATACA
>Tery_3369(hupS) Score=4.3 Pos=-188 [Trichodesmium erythraeum IMS101]
AGTATCAAAAATAACA

>Tery_3368(hupL) Score=4.1 Pos=-64 [Trichodesmium erythraeum IMS101]
TGTAGCTACTGATAAA
>Tery_1068(nirA) Score=3.8 Pos=-276 [Trichodesmium erythraeum IMS101]
TGTATTTTTATATAGT
>Tery_1068(nirA) Score=4.1 Pos=-199 [Trichodesmium erythraeum IMS101]
TGTTATATAAGCTACG
>Tery_0675(nrrA) Score=4.7 Pos=-89 [Trichodesmium erythraeum IMS101]
AGTAGCTTCTGTTACA
>Tery_4333(ntcB) Score=4 Pos=-27 [Trichodesmium erythraeum IMS101]
TGTATAAAATAACACA
>Tery_5068(rpoD) Score=4 Pos=-199 [Trichodesmium erythraeum IMS101]
TGTAAAATTTTGTACC
>Tery_5068(rpoD) Score=3.7 Pos=-46 [Trichodesmium erythraeum IMS101]
TGTAAAATAATTTATT
>Tery_3029(gifB) Score=3.8 Pos=-349 [Trichodesmium erythraeum IMS101]
TGTATCTGATGTTAGG
>Tery_1958(fur) Score=3.5 Pos=-40 [Trichodesmium erythraeum IMS101]
TGTATCATTGTCAATA
>Tery_4410(rbcL) Score=3.4 Pos=-293 [Trichodesmium erythraeum IMS101]
GATAACTATTACTACG
>Tery_1667(isiA) Score=3.6 Pos=-134 [Trichodesmium erythraeum IMS101]
AGTAATTGATCATACT
>Tery_0466(gltS) Score=4.2 Pos=-228 [Trichodesmium erythraeum IMS101]
TGTATCCTAGGCAACA
>Tery_0130(urtA) Score=3.8 Pos=-390 [Trichodesmium erythraeum IMS101]
AGTTACAAAAAAAACA
>Tery_4747(gor) Score=3.9 Pos=-208 [Trichodesmium erythraeum IMS101]
TGTAGTCGTAGATATA
>Tery_4747(gor) Score=4.7 Pos=-120 [Trichodesmium erythraeum IMS101]
TGTAACTAATTATACT
>Synpcc7942_0442(amt1) Score=4.1 Pos=-151 [Synechococcus elongatus PCC 7942]
TGTTACATCGATTACA
>Synpcc7942_1845(cce_3797) Score=4.3 Pos=-27 [Synechococcus elongatus PCC 7942]
TGTATCCGTTGCTACC
>Synpcc7942_2107(cynA) Score=4.4 Pos=-67 [Synechococcus elongatus PCC 7942]
TGTAACGACGGCTACA
>Synpcc7942_2156(glnA) Score=4.8 Pos=-194 [Synechococcus elongatus PCC 7942]
TGTATCAGCTGTTACA
>Synpcc7942_0321(glnB) Score=4.8 Pos=-103 [Synechococcus elongatus PCC 7942]
TGTAGCAGTAACTACA
>Synpcc7942_1240(nirA) Score=4.9 Pos=-220 [Synechococcus elongatus PCC 7942]
TGTAGCAATTGCTACT
>Synpcc7942_1240(nirA) Score=4.3 Pos=-149 [Synechococcus elongatus PCC 7942]
AGTATCAATGATTACT
>Synpcc7942_1240(nirA) Score=4.4 Pos=-80 [Synechococcus elongatus PCC 7942]
TGTAGTTTCTGTTACC
>Synpcc7942_0127(ntcA) Score=4.7 Pos=-157 [Synechococcus elongatus PCC 7942]
AGTAGCAGTTGCTACA
>Synpcc7942_1241(nirB) Score=4.3 Pos=-153 [Synechococcus elongatus PCC 7942]
AGTAATCATTGATACT
>Synpcc7942_1241(nirB) Score=4.9 Pos=-82 [Synechococcus elongatus PCC 7942]
AGTAGCAATTGCTACA
>Synpcc7942_1845(SYNPCC7002_A2101) Score=4.3 Pos=-27 [Synechococcus elongatus PCC 7942]
TGTATCCGTTGCTACC

>Synpcc7942_2158(apcF) Score=4.8 Pos=-214 [Synechococcus elongatus PCC 7942]
TGTAACAGCTGATACA
>PMT1853(amt1) Score=3.8 Pos=-160 [Prochlorococcus marinus str. MIT 9313]
TGTAACAAAATGAACT
>PMT0601(glnA) Score=4.2 Pos=-79 [Prochlorococcus marinus str. MIT 9313]
GGTACCTGTTGCTACA
>PMT2229(urtA) Score=4 Pos=-146 [Prochlorococcus marinus str. MIT 9313]
TGTTGCAACAGCTACC
>PMT2229(urtA) Score=4.7 Pos=-95 [Prochlorococcus marinus str. MIT 9313]
TGTATCATTCACTACA
>CYA_0030(fur) Score=3.6 Pos=-66 [Synechococcus sp. JA-3-3Ab]
GCTATTATCAATTACA
>CYA_0570(SYNPCC7002_A2395) Score=3.9 Pos=-139 [Synechococcus sp. JA-3-3Ab]
GGTAAGATAAAATACA
>CYA_0570(SYNPCC7002_A2395) Score=4.2 Pos=-81 [Synechococcus sp. JA-3-3Ab]
CGTATCAAAGGCTACT
>CYA_1363(glnA) Score=4.3 Pos=-138 [Synechococcus sp. JA-3-3Ab]
CGTATCAGAAACTACA
>CYA_1508(glnB) Score=4.5 Pos=-74 [Synechococcus sp. JA-3-3Ab]
TGTATCCGTTTTTACA
>CYA_0612(nirA) Score=3.9 Pos=-72 [Synechococcus sp. JA-3-3Ab]
TGTAACTGCCAATACC
>CYA_1799(ntcA) Score=4.7 Pos=-181 [Synechococcus sp. JA-3-3Ab]
TGTAGCTCCTGCTACA
>CYA_0984(ntcB) Score=4.2 Pos=-89 [Synechococcus sp. JA-3-3Ab]
TGTAACGGTGTTTACA
>CYA_1920(urtE) Score=3.9 Pos=-248 [Synechococcus sp. JA-3-3Ab]
AGAAACAGAAGCTACA
>CYA_1924(urtA) Score=3.7 Pos=-272 [Synechococcus sp. JA-3-3Ab]
GGTATCCCGCGATACA
>SYNW0253(amt1) Score=4.2 Pos=-100 [Synechococcus sp. WH 8102]
TGTATCAATTAACACA
>SYNW0246(SYNPCC7002_A1954) Score=4.1 Pos=-143 [Synechococcus sp. WH 8102]
TGTAACTTTGGTTGCA
>SYNW2487(cynA) Score=4.1 Pos=-103 [Synechococcus sp. WH 8102]
TGTAGCAAGTGAGACA
>SYNW2487(cynA) Score=4.5 Pos=-66 [Synechococcus sp. WH 8102]
AGTATCACCTGATACA
>SYNW2442(urtA) Score=4 Pos=-118 [Synechococcus sp. WH 8102]
TGTTGCAACAGCTACC
>gvip146(glnA) Score=4 Pos=-116 [Gloeobacter violaceus PCC 7421]
CGTATCTCAGACTACA
>gvip212(nirA) Score=4 Pos=-146 [Gloeobacter violaceus PCC 7421]
TGTATCTGGGGTTACG
>gvip454(ntcA) Score=3.9 Pos=-77 [Gloeobacter violaceus PCC 7421]
AGTAGTCCCTAATACA
>gvip213(ntcB) Score=4 Pos=-46 [Gloeobacter violaceus PCC 7421]
CGTAACCCCAGATACA
>glr3304(fur) Score=3.9 Pos=-116 [Gloeobacter violaceus PCC 7421]
TGTAACAAATTGTAGA
>gll0880(trxA) Score=3.6 Pos=-379 [Gloeobacter violaceus PCC 7421]
TGTATCTAGAACTAGC
>null(gifB) Score=4.4 Pos=-175 [Thermosynechococcus elongatus BP-1]
TGTTAAATTAGATACA
>amt1(amt1) Score=4.4 Pos=-190 [Thermosynechococcus elongatus BP-1]

TGTATAACGTGATACA
>tsr2448(SYNPCC7002_A0076) Score=4.1 Pos=-63 [Thermosynechococcus elongatus BP-1]
AGTATTGGATATTACA
>tlr1468(SYNPCC7002_A2395) Score=4.3 Pos=-85 [Thermosynechococcus elongatus BP-1]
TGTAGTTGAGTTTACA
>tlr0194(tlr0194) Score=4.2 Pos=-111 [Thermosynechococcus elongatus BP-1]
TGTAACCTATCTTACA
>tll0591(glnB) Score=5.1 Pos=-80 [Thermosynechococcus elongatus BP-1]
TGTAGCTATTGCTACA
>tlr1349(nirA) Score=4.6 Pos=-82 [Thermosynechococcus elongatus BP-1]
AGTAGCAAAATTTACA
>tlr1330(nrrA) Score=4 Pos=-138 [Thermosynechococcus elongatus BP-1]
AGTATTATTCGTTACG
>null(ntcB) Score=3.9 Pos=-122 [Thermosynechococcus elongatus BP-1]
TGTATCAATCAACACA
>tlr1120(urtA) Score=4 Pos=-81 [Thermosynechococcus elongatus BP-1]
TGTAGCCTAGCATACA
>tlr2286(trxQ) Score=4 Pos=-130 [Thermosynechococcus elongatus BP-1]
AGTAGCAATGACAACA
>null(isiA) Score=3.8 Pos=-195 [Thermosynechococcus elongatus BP-1]
AGTTTCTGGAAATACA
>null(ndhF) Score=3.6 Pos=-220 [Thermosynechococcus elongatus BP-1]
GGTAACTTTTGCTATG
>null(gifB) Score=4.4 Pos=-146 [Thermosynechococcus elongatus BP-1]
TGTTAAATTAGATACA

Supplementary position frequency matrix (PFM 1) for PHO boxes in cyanobacteria:

A: 20	10	4	61	66	21	14	23	0	0	0	7
	18	3	43	61	24	4	16	0	0	0	12
	6	2	49	63	17	11	16				
C: 20	1	0	0	1	28	42	8	0	0	0	28
	2	2	0	1	30	38	6	0	0	0	34
	5	3	3	0	36	31	11				
G: 14	1	0	4	4	6	5	2	0	0	0	22
	1	1	2	7	2	7	4	0	0	0	18
	0	0	3	6	6	2	2				
N: 0	0	0	0	0	0	0	0	77	77	77	0
	0	0	0	0	0	0	0	77	77	77	0
	0	0	0	0	0	0	0				
T: 23	65	73	12	6	22	16	44	0	0	0	20
	56	71	32	8	21	28	51	0	0	0	13
	66	72	22	8	18	33	48				

Supplementary position frequency matrix (PFM 2) for Fur boxes in cyanobacteria:

A: 100	29	3	45	101	34	134	129	64	58	92	21
	13	26	11	26	147	127	18				
C: 1	5	1	4	18	9	8	1	6	18	2	18
	0	38	5	63	0	1	30				
G: 22	3	0	67	10	52	2	2	0	7	2	10
	2	10	41	2	4	25	2				
T: 44	130	163	51	38	72	23	35	97	84	71	118
	152	93	110	76	16	14	117				

Supplementary position frequency matrix (PFM 3) for NtcA boxes in cyanobacteria:

A: 47	3	6	201	99	29	108	94	90	88	71	88
	27	225	2	168							
C: 18	2	1	1	2	131	36	18	28	16	6	61
	7	1	211	19							
G: 20	220	1	3	52	1	19	43	21	33	113	8
	2	1	8	12							
T: 143	3	220	23	75	67	65	73	89	91	38	71
	192	1	7	29							

Supplementary Table 2. Pho regulon prediction. PHO boxes sequences, their position in the genome, orientation, the genes that are controlling (the Pho regulon), locus tag from these genes, the distance of the box from the gene and the gen function from single-letter of functional (COGs) are presented.

PHO boxes sequences	Position	Orientation	Pho regulon (genes)	Locus_tag	Distance	COG
GATATCCTTAACTATAATTTCTAATAACTT	37692	(+)	AbgT family transporter	PCC7418_RS00155	-342	H
TTTAATTTCATCCTAGTTTAGGCTTAAAGT	41629	(+)	serine hydrolase-HP-ABC transporter ATP-binding protein/permease	PCC7418_RS00180/RS00185/RS00190	-145	V, S, S
AATAAAACTTAATTAAAGCCATCTTAACCT	48034	(+)	PstS family phosphate ABC transporter substrate-binding protein (*pstS*)	PCC7418_RS00210	-51	P
AAGAAATAATGTGTTAAAGTTAATATAAAT	54813	(-)	PAS domain-containing protein response regulator	PCC7418_RS00225/RS00230	-315	T, T
GAGTAAACCAAAGGCTAAATTAACAATATT	59558	(-)	thioredoxin	PCC7418_RS00250	-262	O
TCTTAAAGTTACAGTTAATGAAAGATTATA	61353	(-)	mechanosensitive ion channel	PCC7418_RS00255	-316	M
GAGTTATCGGAAGAAAAAGATGAGTATAAT	63341	(-)	recombination protein RecR-tetratricopeptide repeat protein	PCC7418_RS00265/RS00270	-47	S, L
ATTTAATTACTTAGAAACTCTGCTTAACAA	73689	(+)	IS200/IS605 family element transposase accessoryprotein (*tnpB*)	PCC7418_RS00335	-175	L
TTTAAACTCAGCATTATCTTTAGATTTGAC	119529	(+)	RMD1 family protein-hypothetical protein (HP)-asparagine synthase	PCC7418_RS00490/RS00495/RS00500	-519	S, S, L, E
TTTAGCCTCTTTCTTACCCTTTTTTAACAA	163587	(+)	universal stress protein	PCC7418_RS00715	-112	T
TTTTGTGTTACTTTAACCTTCCTTTTAGCA	168098	(+)	ABC transporter substrate binding protein	PCC7418_RS00750	+34	G
AATTTAAAATGAAATTATGCAATCAAAAAT	187427	(-)	HP-glycoside hydrolase	PCC7418_RS00830/RS00835	-221	G, S
AATTAAACCTAAAATAGTTTCAAGGATAAT	192110	(-)	transposase	PCC7418_RS00850	-615	S
TCATTAAGTTTTTGTTAAAGGAAGGTTATC	193598	(-)	phosphoribosylformylglycinamidine cyclo-ligase	PCC7418_RS00865	-47	F
ATTAAGTTTTTGTTAAAGGAAGGTTATCAT	193600	(+)	septal ring lytic transglycosylase RlpA family protein	PCC7418_RS00870	-256	M
TTGTAAGGCAGAATCAAAATTCAGTTTATC	226059	(-)	HP	PCC7418_RS01010	-253	O
CTTAATGTGATTTAAAATACCATTTAAGTT	226508	(+)	HP	PCC7418_RS01025	-223	S
TTTAATATTAGTTTAATATTAGTTTAAGTA	227609	(+)	Nif11 like leader peptide family natural productprecursor	PCC7418_RS01030	-115	S
CTTAGCCCCAGCTTTAGTTAATATTAATAC	299142	(+)	archease RtcB family protein-phosphoribosyltransferase	PCC7418_0261/RS01330/RS01335	-274	S, L, S

GTTTACTTAATTTTTATTACAAAATAAGAT	323385	(+)	B12-binding domain-containing radical SAM protein	PCC7418_RS01445	-99	C
AATTTAAGACCTAGTAATCAACACGAAATT	345451	(-)	iron uptake porin	PCC7418_RS01525	-15	M
TTTAGTAATCGCTTAACCTTTTCTTAACTT	351477	(+)	thylakoid membrane photosystem I accumulation factor	PCC7418_RS01570	-439	CO
GTTTATCAACTTTTTACATAAGATTTAGCA	362063	(+)	NAD(P)H dependent glicerol 3 phosphate dehydrogenase	PCC7418_RS01620	-78	I
AGTCAAAAAAATATTAAATCAATCATTAAT	362100	(-)	NUDIX hydrolase	PCC7418_RS01615	-293	F
ATTAAACTTTTTAATATCAGAGTATAATCA	397041	(+)	HP-NblA/ycf18 family protein	PCC7418_RS01780/RS01785	-106	S, S
ATTATTTTAATGTTTTTCAGTCTTTTTATT	402390	(+)	3-isopropylmalate dehydrogenase (*leuB*)	PCC7418_RS01815	-308	CE
AGATTAAAGCCAATTTATGAAGAGGTTAAA	435783	(-)	bifunctional aminoglycoside phosphotransferase ATP binding protein	PCC7418_RS01975	-39	S
TTTTATTTATATTTACACTGCCTTTAACGA	440704	(+)	trypsin-like peptidase domain containing protein	PCC7418_RS02005	-238	O
AATTAAAGTTATGATAAAAGCGATCTTAAA	449261	(-)	SIMPL domain containing protein	PCC7418_RS02035	-714	S
AGGTTAAATATGGTTCAAAAACTATTCAAA	449976	(-)	uroporphyrinogen III C-methyltransferase	PCC7418_RS02045	0	H
GTTTAAGTTTCGATAAAATTTCGTTATCAT	456308	(+)	phosphomannose isomerase type II C-terminal cupin domain-lecithin retinol acyltransferase family protein	PCC7418_RS02090/RS02095	-115	G, KT
AAATGAAGAAGAAATTATGCTGATGCCAAA	456629	(-)	branched-chain amino acid ABC transporter permease	PCC7418_RS02085	-325	E
AAGTAAAGTCTTTTTAATAAAAATTTAATA	524155	(-)	response regulator-HP	PCC7418_RS02385/PCC7418_RS19225	-356	T, S
AATTCAACAAAATTATAAGGAGGGGTAAAA	543130	(-)	gas vesicle protein GvpG	PCC7418_RS02455	-185	S
GAATGAATTAAAGATTAATTTCTTTTAAAC	547534	(-)	gas vesicle structural protein GvpA (*gvpA*)-HP-gas vesicle protein GvpN/gas vesicle protein (*gvpN*)-HP-HP-gas vesicle protein K (*gvpK*)-GvpL /GvpF family gas vesicle protein (*gvpL/gvpF*)	PCC7418_RS02490/RS02485/RS02480/ RS02475/RS02470/ RS02465/RS02460	-103	S, S, S, S, S, J, S
AATGAATTAAAGATTAATTTCTTTTAAACT	547535	(+)	GvpL/GvpF family gas vesicle protein (*gvpL/gvpF*)	PCC7418_RS02495	-196	S
TTATGAAAAAATAATTAACAAAAGATAAAT	550498	(-)	histidine phosphatase family protein-glucokinase	PCC7418_RS02510/RS02505	-11	G, G
GAGTTAGAGGATGGTTATAAACATATAAAG	599343	(-)	(2Fe-2S) binding protein	PCC7418_RS02740	-365	C
ATTAAAATCCGATCAATCTAAAAATAAGTT	609687	(+)	ferredoxin nitrite reductase	PCC7418_RS02810	+11	C

TATGATTTTCAATTTAACTGTACCTATCTT	612817	(+)	UDP-N-acetylmuramoyl tripeptide D-alanyl-D-alanine ligase	PCC7418_RS02820	-1	M
TTTTCAATTCTTCTTAAAACCCTGATTAAC	641750	(-)	Ig like domain containing protein	PCC7418_RS02875	-148	S
TTTTACTGAATTTTAATTTAAACTTAGAAC	657612	(+)	ABC transporter ATP binding protein	PCC7418_RS02955	-191	V
TAATTTATATCTTTTTAAGGTTATTTTAAG	675681	(-)	CAP domain-containing protein	PCC7418_RS19240	-284	Q
TTTTACCTGAATTTGTTTTAACCTTAAGTC	677077	(+)	Uma2 family endonuclease-Uma2 family endonuclease	PCC7418_RS03075/RS03080	-73	S, S
TGGCTATCTTTATGTTATAATGATTTTAAC	683216	(-)	Response regulator	PCC7418_RS03100	-432	T
AATTATCTTCAGTTTAGTTTACGCTAATCT	728680	(+)	heme oxygenase (biliverdin-producing)	PCC7418_RS03280	-101	C
ATGAAAAACGTTAGATAAAAACAATTTAAA	739128	(-)	YvcK family protein	PCC7418_RS03330	-60	S
ATTTAATTAAATTTACAATTGATTTAAATT	766012	(+)	CRISPR associated endoribonuclease Cas6-CRISPR associated protein Cas4 type ID-CRISPR associated endonuclease Cas1-CRISPR associated endonuclease Cas2	PCC7418_RS03470/RS03475/RS03480/RS03485	-264	S, L, L, L
CGTAAACTAAGCATAGTTTGATCTTAATCC	787591	(+)	WYL domain containing protein	PCC7418_RS03530	-80	K
AGGCAAGGAGGAGATAAAAGCATGATCAAA	801527	(-)	LD carboxypeptidase	PCC7418_RS03590	-7	V
TTTAATGAGTGGTTTAAATTCAGTTGATTT	805778	(+)	UDP-N-acetylmuramate L-alanine ligase-UDP-N-acetylmuramate dehydrogenase	PCC7418_RS03620/RS03625	-3	M, M
TTTAATACTTGGTTAGTTCAAGATTATCTT	814733	(+)	glutathione S-transferase family protein	PCC7418_RS03660	-664	O
TTTAATAAACTTAAAAATTGTTATTTACAT	826909	(+)	tRNA (uridine(34)/cytosine(34)/5-carboxymethylaminomethyluridine(34)-2'-O) methyltransferase TrmL (*trmL*)	PCC7418_RS03720	-52	J
TATTAAATAATAGATCAAAATGAATTTTAT	832833	(-)	carotenoid biosynthesis protein	PCC7418_RS03740	-19	S
TGGTTAGTGAGTGATTAAACAATGGTTAGT	890284	(-)	precorrin 8X methylmutase	PCC7418_RS04085	-190	HK
GAATTAAGGAACATTTAACTTTTTGCAAAA	898154	(-)	FeoA domain-containing protein (*feoA*)-Fe(2+) transporter permease subunit FeoB (*feoB*)	PCC7418_RS04115/RS04120	-240	P, P
AAATAATGCTAAGATTATTATAACATAAAA	938858	(-)	IS200/IS605 family element transposase accessoryprotein TnpB (*tnpB*)	PCC7418_RS04310	-16	L
GTTAATCAAGTTTTTACGAATGATTTAGAT	939282	(+)	MFS transporter	PCC7418_RS04315	-19	G

TTTAATCCCCTGTTTATGGTAACTTTAGAA	953364	(+)	fused MFS/spermidine synthase	PCC7418_RS04390	-35	H
ATTAACTATCAATTAAAATAGCATTTGCTC	955972	(+)	methyltransferase domain-containing protein	PCC7418_RS04410	-27	Q
AGGTTAAGGCGAAAATAAACTCATTCCAAG	957937	(-)	ABC transporter ATP-binding protein	PCC7418_RS04415	-268	P
GAGTAAACGTTAAGCAAAAATCACATTAAT	961001	(-)	ABC transporter substrate binding protein-sugar ABC transporter permease arbohydrate ABC transporter permease	PCC7418_RS04430/RS04425/RS04420	-131	G, P, P
AGCAAAACCATAAGCAATGGGCAAGTTAAA	964557	(-)	ATP-grasp domain containing protein	PCC7418_RS04445	-352	F
GATTACCACTCGTTAAATTGGTAATAACAC	970920	(+)	membrane protein insertase YidC-nucleic acid binding protein	PCC7418_RS04500/RS04505	-105	S, U
TTTTTAATATAAAATTAATCAATAGTTAAC	1018379	(-)	DNA starvation/stationary phase protection protein	PCC7418_RS04685	-122	P
GAAAGTTAAAAGTTAACCATTTCTTAACTT	1047914	(+)	glycosyltransferase family 4 protein-amylo alpha 1,6-glucosidase	PCC7418_RS04835/RS04840	-439	M, G
ATCTTAAATTAAGGTTTAAATGAATTTTAA	1071732	(-)	solanesyl diphosphate synthase	PCC7418_RS04940	-313	H
CTTAAGATAAGATTAGTCAGTAATTAATCC	1072305	(+)	uracil-DNA glycosylase	PCC7418_RS04945	-506	L
CTTATACTAATTTTTTCAAAAGTTTATCCT	1132472	(+)	Uma2 family endonuclease	PCC7418_RS05220	-136	S
AGATTATGGGCTGGTTGACAACATATCAAG	1132816	(-)	phycobilisome rod core linker polypeptide	PCC7418_RS05215	-356	G
ATAAATATTATTATAAATTAACTTCAAAAT	1170761	(+)	circadian clock protein KaiC-polyphosphate kinase 1	PCC7418_RS05365/PCC7418_RS05370	-10	F, P
TTTACCATGGCTATGAATTAACCTTAACCA	1175011	(+)	MogA/MoaB family molybdenum cofactor biosynthesis protein	PCC7418_RS05380	-145	H
AAGTTAAGAGTGACTTGATCGGGGTTTAAA	1196246	(-)	HlyD family type I secretion periplasmic adaptorsubunit	PCC7418_RS05475	-191	M
TTTAAATATCTTTTTTATTTCTATTTTTAT	1234207	(+)	L-aspartate oxidase (*nadB*)	PCC7418_RS05635	-202	H
ATTAATCTCCTAATTATCAACACATCACTA	1249518	(+)	tRNA (adenosine(37)-N6)-threonylcarbamoyltransferase complex transferase subunit (*tsaD*)	PCC7418_RS05715	-681	J
TGATTGAGGAGAATTTAAATCAATGTCAAT	1261043	(-)	arsenate reductase, glutathione/glutaredoxin type (*arsC*)-arsenical resistance protein (*arsH*)	PCC7418_RS05760/RS05755	-346	T, S
ATTAAACTGCTCATAAGGAAACGTAAATTT	1360953	(+)	acyl-CoA desaturase	PCC7418_RS06160	-88	I
AAATAATGCTAAGATTATTATAACATAAA	1366037	(-)	IS200/IS605 family element transposase accessoryprotein TnpB (*tnpB*)	-	-15	S

AATTAAAAATAGGAATAAAACTAAGCTAAT	1371373	(-)	tetratricopeptide repeat protein	PCC7418_RS06205	-12	S
TTAGAAAAAGAGTTAAATTCTCGTTAAAAT	1375855	(+)	TIGR04282 family arsenosugar biosynthesis glycosyltransferase	PCC7418_RS06240	-215	S
GTTATTTTGTTCTTTGTTGGCTGTTAATCA	1425334	(+)	transposase	PCC7418_RS06495	-115	S
GTTAATCAACTTTTTACATAAGATTTAGAA	1439381	(+)	CRISPR associated endonuclease Cas1-CRISPR associated endonuclease Cas2	PCC7418_RS06595/RS06600	-501	L, L
TGATAAACAATAGGTAAAGTAAGGACTTAC	1558203	(-)	type I restriction endonuclease subunit R	PCC7418_RS07055	-251	S
GTTATTTTGTTCTTTGTTGGCTGTTAATCA	1594235	(+)	transposase	PCC7418_RS07215	-108	S
AGCTGATGACTAGGTTAAGGCTTTCTTAAT	1613769	(-)	ABC transporter substrate binding protein	PCC7418_RS07290	-265	E
CTTTTTCCCACCTTTGACCTGTGTTAAATT	1623103	(+)	glutathione S-transferase family protein	PCC7418_RS07335	-249	S
AGATTAAGGAAAATTAAACCTCAACTTAAA	1664840	(-)	sodium:proton antiporter	PCC7418_RS07540	-114	P
ATTAAAACAATATTAAAACAAATTTTACTA	1665092	(+)	ATP-dependent zinc protease	PCC7418_RS07545	-115	O
TATAATCTTCGCTATAGCTCATTTTTAGTT	1679832	(+)	response regulator	PCC7418_RS07610	-364	T
TGTTAAAGACGCAGAAAATCTTATTTTAAA	1708354	(-)	site-specific DNA-methyltransferase	PCC7418_RS07755	-130	L
AACTTAATTTCTGAAAAATTCAGGGTTAAT	1744927	(-)	sedoheptulose 7-phosphate cyclase	PCC7418_RS07910	-329	E
AAATAAATCCCTGTTAAAGCTCATAAAAAT	1754941	(-)	response regulator-EAL domain containing response regulator-response regulator	PCC7418_RS07930/RS07935/RS07940	-60	T, T, T
AAATTAATGTTTCATAATGAGGTGGATTAA	1766429	(-)	N(2) fixation sustaining protein CowN	PCC7418_RS07995	-601	S
AGATCATGAGTAATAAATAAATAGGTTAAA	1767932	(-)	D-alanyl-D-alanine carboxypeptidase/D-alanyl-D-alanine endopeptidase	PCC7418_RS08000	-120	M
TTCATAATTAATCGTTAATAAATGATTAAG	1794333	(-)	ABC transporter substrate-binding protein	PCC7418_RS08120	-6	E
ATTTTTTTGTTTTTAATTATCCCTTGACTT	1810041	(+)	ATP phosphoribosyltransferase regulatory subunit	PCC7418_RS08205	-314	E
TTTTCCCTCACCTTAGATTTAAGTTTATTA	1811102	(+)	undecaprenyldiphospho-muramoylpentapeptide beta-N-acetylglucosaminyltransferase	PCC7418_RS08210	-449	M
TTCTAAATCATTCGTAAAAAGTTGATTAAC	1871218	(-)	copper-translocating P-type ATPase	PCC7418_RS08475	-151	P
TTTAAGCATGACCTTACCCCTAATTATCCT	1889348	(+)	NAD(P)H-quinone oxidoreductase subunit 4	PCC7418_RS08560	-648	C

TTTAATTGTAAATTTTCTTATTTTTTAGTT	1900730	(+)	glutathione synthase (*gshB*)	PCC7418_RS08590	-93	H
TGCTTGTGGTAAAGAAAAGGTTATGTTAAA	1919258	(-)	phosphate ABC transporter substrate binding protein PstS (*pstS*)-phosphate ABC transporter permease subunit PstC (*pstC*)-phosphate ABC transporter permease PstA (*pstA*)-phosphate ABC transporter ATP binding protein PstB (*pstB*)	PCC7418_RS08670/RS08665/ RS08660/RS08655	-256	P, P, P, P
GTTAATCACAGAGAAAATTAATCTTAAATT	1932831	(+)	endonuclease MutS2	PCC7418_RS08735	-136	L
GATTAAAGTTTTGATAAAGTCTTGATCTAG	1942813	(-)	cysteine synthase A (*cysK*)	PCC7418_RS08775	-162	E
ATTTATGTTATAATAATTTTACCATTATTT	1970080	(+)	IS200/IS605 family element transposase accessoryprotein TnpB (*tnpB*)	PCC7418_RS08950	-40	S
ATTGAACCTTTATTAAACTCGGTTTATCAA	1996480	(+)	response regulator-chemotaxis protein CheW (*cheW*)	PCC7418_RS09080/RS09085	-696	KT, NT
TTGTAATGGGCGGGTTTAGGAATGGTTAAA	2056920	(-)	glycosyltransferase family 2 protein	PCC7418_RS09320	-565	M
GAGCTAAGAAATGATAATGCTGTTCTAAAC	2134623	(-)	cobalt precorrin 8X methylmutase/bifunctional cobalt-precorrin-7 (C(5)) - methyltransferase cobalt precorrin-6B (C(15)) methyltransferase (*cbiE*)	PCC7418_RS09630/RS09625	-343	H, T
TTTAAAAAAGTAATTGTCTCCCGTTTTCCA	2186011	(+)	late competence development ComFB family protein	PCC7418_RS09865	-39	S
AGGTAATGACGATATTAATCCCATTATAAA	2244285	(-)	RNA methyltransferase	PCC7418_RS10105	-172	L
CGGTAAACGTAAAATTAGCCCCATGTAAAT	2251376	(-)	5-(carboxyamino)imidazole ribonucleotide synthase	PCC7418_RS10145	-205	F
AATAGTCTCATTTTTATTTTTAATTTTTAT	2285162	(+)	alanine:cation symporter family protein	PCC7418_RS10255	-415	U
ATTATTATAGATATTATCTCCGGCTAAAAT	2323958	(+)	serine O-acetyltransferase	PCC7418_RS10410	-391	E
TTAAATTTAATCATTACTTTAGGTTTAAGT	2388578	(+)	class 1 fructose-bisphosphatase	PCC7418_RS10725	-182	G
GATAAAAAGTTAAATCAACTAAAGATAAAT	2403390	(-)	citramalate synthase	PCC7418_RS10785	-453	E
TTTTGCCTAAATTTTATTTTCTATTAACCT	2442208	(+)	PAS domain S-box protein	PCC7418_RS19415	-102	T
AGTAAAAACAATCTTTAAATTGAATTAAAA	2467390	(-)	AAA family ATPase	PCC7418_RS11110	-140	O
AATAAAATATTACGTAAACCATAGGCTAAA	2476471	(-)	lipoprotein signal peptidase	PCC7418_RS11185	0	MU

TTTAACTGCAATTTTAATTTTAATTGGCTT	2487840	(+)	glucosylglycerol 3-phosphatase	PCC7418_RS11220	-321	S
GATTTAAAATAAAGATTTGCTAAGGTTAAA	2519448	(-)	saccharopine dehydrogenase NADP-binding domain containing protein	PCC7418_RS11355	-19	E
AAATTAAAAGAAGTTTTAAGATTTAATATA	2523201	(-)	cytochrome ubiquinol oxidase subunit I-cytochrome d ubiquinol oxidase subunit II (*cydB*)	PCC7418_RS11365/PCC7418_RS11370	-66	C, C
TTTTACGAAGAATTAAACTCATTTTTACCG	2523301	(+)	hemerythrin family protein	PCC7418_RS11375	-80	P
TTTAAATTTTTTATAACAATTGATTGATCA	2657664	(+)	EAL domain containing protein	PCC7418_RS19435	-99	T
GTATGAACGTTAATTAAAGGCATAATTAAT	2669847	(-)	macrophage migration inhibitory factor family protein	PCC7418_RS12020	-7	S
ATTAATCATTTGCTTACTCAGGATTAAACT	2686183	(+)	Crp/Fnr family transcriptional regulator	PCC7418_RS12095	-165	K
AATAATGAAACTTTTTCCTCTTCTTTTACT	2708076	(+)	NADAR family protein	PCC7418_RS12195	-219	O
TTTATTTTTATGTTATAATAATCTTAGCAT	2735781	(+)	IS200/IS605 family element transposase accessoryprotein TnpB (*tnpB*)	PCC7418_RS12340	-45	S
ATTAAGAAGAACTTAACGAATCTTTAATTT	2791405	(+)	Crp/Fnr family transcriptional regulator	PCC7418_RS12605	-41	K
TTTAACTTATATTTTTATTTCCCATGACTT	2871984	(+)	ureidoglycolate lyase	PCC7418_RS13060	-255	F
TTTAACTTTTTGTTTATTGCCACCTTTCCT	2922699	(+)	llutamate cysteine ligase (*gshA*)	PCC7418_RS13320	-19	S
CACTGAAAAACAAAAAAAGGCTAGTTTAAT	2930864	(-)	lysine tRNA ligase	PCC7418_RS13445	-191	J
TGTTCAAAACTACGCAATGTGAAAATTAAT	2954730	(-)	ribosome maturation factor RimM (*rimM*)	PCC7418_RS13700	-97	J
ATTTATATAATGATTAATTGACTTTGTTTT	3006109	(+)	polysaccharide pyruvyl transferase family protein	PCC7418_RS13700	-127	S
AGATTATTTCTGATTAAAACGAATACTAAA	3128024	(-)	translocation/assembly module TamB domain-containing protein	PCC7418_RS14210	-32	U
TACTTAAGTATAGTATAAGATTATAATAT	3138188	(-)	YqhA family protein- DUF202 domain containing protein	PCC7418_RS14255/RS14260	-89	S, S
AGTAAGAGGTGAATTAAAGGGGGGATCAAA	3146602	(-)	formylglycine generating enzyme family protein	PCC7418_RS14295	-69	S
TTTAAAAAATAATTAATTTTCTTCCAACAT	3179396	(+)	DMT family transporter	PCC7418_RS14440	-219	EG
ATTTATCTAAATATAAAACTGAATTAAATA	3191656	(+)	2Fe-2S iron sulfur cluster binding domain containing protein	PCC7418_RS14510	-279	C
ATATAAAACTGAATTAAATATAATTATAAC	3191666	(-)	M28 family peptidase	PCC7418_RS14505	-8	S
ATTGATGACTTATTAATTATCAATTAAGTT	3224851	(+)	o-succinylbenzoate synthase	PCC7418_RS14660	-11	M

GATAATATCATGATTATTTTTTTCTTATTA	3244402	(+)	glycosyltransferase	PCC7418_RS14775	-254	V
AAGCTAAACGTAGATAGAGTTGAGTAAAAA	3247808	(-)	glycosyltransferase-sulfotransferase	PCC7418_RS14780/RS14785	-94	M, S
CTTTATCTAATTTTGATCACTAGTTTTATA	3275429	(+)	DNA phosphorothioation system sulfurtransferase DndC (*dndC*)	PCC7418_RS14930	-56	EH
CTTAGAATTTAGTAAATCTTAACTTAATT	3309133	(+)	BCCT family transporter	PCC7418_RS15085	-305	M
ATTAGAATCAGTTTAAACTAAGCTCAATGT	3332712	(+)	nickel-type superoxide dismutase maturation protease	PCC7418_RS15220	0	U
GTTAATTGTTGCTTAAAATTACGTTTGCAT	3404962	(+)	peptide chain release factor 1 (*prfA)*	PCC7418_RS15625	-65	J
ATAATAAAGGGTGGTTATATGAAAGTAAAG	3410009	(-)	DNA (cytosine-5-) methyltransferase	PCC7418_RS15640	-359	H
CTCTAAAAAGTAATCTAAAAAAAATTTAAT	3427651	(-)	TdeIII family type II restriction endonuclease	PCC7418_RS15720	-49	L
AGGTTAGAAGCAACTAAAGTTTTCATAAAT	3454152	(-)	phycobilisome linker polypeptide	PCC7418_RS15845	-4	H
AAACAAAAAGAAAGTTAAATTTTTATAAAC	3455723	(-)	phycocyanin subunit beta	PCC7418_RS15855	-246	C
TTTAATTTCTCCTTAATAGGATATTAGTTA	3467427	(+)	translation initiation factor IF-2	PCC7418_RS15920	-123	S
ATTGACTTTTTGTTAGACTGAATTTAGTTT	3484159	(+)	IS200/IS605 family transposase	PCC7418_RS15965	-48	S
TTTTTTGTCAACTTAACCTTCCCTTTACTT	3516392	(+)	PstS family phosphate ABC transporter substrate binding protein (*pstS*)-phosphate ABC transporter permease subunit PstC (*pstC*)-phosphate ABC transporter permease PstA (*pstA*)-phosphate ABC transporter ATP binding protein PstB (*pstB*)	PCC7418_RS16135/RS16140/ RS16145/RS16150	-147	P, P, P, P
TCATTAAACATCGAATAAACTTTGATTAAA	3579899	(-)	LmeA family phospholipid binding protein	PCC7418_RS16405	0	S
ATTAAACATCGAATAAACTTTGATTAAAAT	3579901	(+)	rRNA pseudouridine synthase	PCC7418_RS16410	-53	-
ATTTTTTTGAGCATTATTTGAGCATTATTT	3596661	(+)	response regulator-chemotaxis protein CheW (*cheW*)	PCC7418_RS16505/RS16510	-120	KT, NT
ATTAATTTTTATTAAGATTATGTTTTTTTT	3799356	(+)	class I SAM-dependent methyltransferase	PCC7418_RS17370	-383	H
ATTTATTGATGTATTTTTTTGTCTTAACCC	3774649	(+)	alkaline phosphatase	PCC7418_RS17240	-76	P
ATTAATCATTCTCTATCCTCCAAATAACCA	3842069	(+)	pentapeptide repeat-containing protein	PCC7418_RS17560	-59	S
ATTATTATTTTTGTTATTCACGCTTAACCT	3866970	(+)	transposase	PCC7418_RS17665	-417	Q

ATTAACTTGCAATTATTTATCCCTTGATC	3887039	(+)	Hemolysin type calcium binding protein	PCC7418_RS17775	-48	S
TTTAGGCTGTAATTAAACTGATGTCAACAA	3896679	(+)	IS200/IS605 family element transposase accessoryprotein TnpB (*tnpB*)	PCC7418_RS17810	-155	S
ATTATAAAAATAATTTAAAATGAATATAAA	3944455	(-)	HindVP family restriction endonuclease	PCC7418_RS18040	0	L
TTTTTAAGCGAAATTTATCAAGGAGAAAA	3960433	(+)	glycogen debranching protein GlgX (*glgX*)	PCC7418_RS18135	-167	G
GTTAAATCAGAGTTAACCCATTATTAAATT	3992761	(+)	methyl-accepting chemotaxis sensory transducer	PCC7418_RS18275	-107	NT
TGGATAATAGCATATAAAGACTTAATAAAT	4015538	(-)	NAD(P)-dependent oxidoreductase	PCC7418_RS18405	-406	GM
ATAAAAAAGATTAATAATAGTAAGGTAAAA	4030328	(+)	glycosyltransferase	PCC7418_RS18495	-129	J
GATAAATTCTTCTTTTACTCTTCTTTTACA	4066330	(+)	D-alanyl-D-alanine carboxypeptidase family protein	PCC7418_RS18675	-233	M
TATAACCTATCATTTATTGTCAAATAACCA	4074906	(+)	ABC transporter ATP binding protein-ABC transporter permease	PCC7418_RS18715/RS18720	-61	V
TAGTTAATTTTAATTAATTTATTAATAATT	4087245	(+)	Na-Ca exchanger/integrin-beta4	PCC7418_RS18775	-319	S
AAATCATCAATTCGTTAAATTCAATTTAAT	4115030	(-)	SDR family oxidoreductase	PCC7418_RS18900	-148	IQ
AGTTTAAATTTATAATCAGTTCAGTTTAAT	4163771	(-)	SHOCT domain-containing protein	PCC7418_RS19070	-26	L
GCTAACCTTTTTATTATCTTAACTTAGATT	4174392	(+)	GNAT family N-acetyltransferase	PCC7418_RS19130	-255	K

Supplementary Table 3. Fur regulon prediction. Fur boxes sequences, their position in the genome, orientation, the genes that are controlling (the Fur regulon), locus tag from these genes, the distance of the box from the gene and the gen function from single-letter of functional (COGs) are presented.

Fur boxes sequences	Position	Orientation	Fur regulon (genes)	Locus_tag	Distance	COG
GTTAATAAATATTTTTTAC	1663	(+)	chromosomal replication initiator protein DnaA (*dnaA*)	PCC7418_RS00025	-472	L
GTTACAAAATATTTAGAAT	50660	(-)	alpha amylase	PCC7418_RS00215	-58	S
ATCTAAAGTTTTTATAAAA	54620	(-)	PAS domain containing protein	PCC7418_RS00230	-123	T
AATTCAAGAAATTTTAAAT	63574	(-)	recombination protein RecR	PCC7418_RS00270	-277	L
ATTAAAAACCATTTTTTAT	89952	(+)	esterase like activity of phytase family protein	PCC7418_RS20370	-355	F
TTTGTAAATTTTTATCATC	104461	(-)	SDR family oxidoreductase	PCC7418_RS00415	-85	G
ATCTAAAATTAATCATAAT	114408	(-)	ketol-acid reductoisomerase	PCC7418_RS00460	-250	E
AATTTGGATATTTTTTAAT	116549	(+)	glycosyltransferase family 2 protein	PCC7418_RS00475	-38	M
ATTTTGATTATATATAAAT	148165	(+)	prepilin-type N-terminal cleavage/methylation domain-containing protein	PCC7418_RS00635	-172	U
ATTTATAAATATTATCAAT	199345	(+)	energy transducer TonB (*tonB*)	PCC7418_RS00895	-13	M
ATTTATAAATATTATCAAT	199345	(-)	MotA/TolQ/ExbB proton channel family protein	PCC7418_RS00890	-192	U
ATTGCAAATATTTTTTGAT	200598	(+)	AraC family transcriptional regulator	PCC7418_RS00900	-38	K
ATTTTTCTTTTATTTTAAT	247069	(+)	DUF3298/DUF4163 domain containing protein	PCC7418_RS01105	-454	S
ATTAAGTAATATTACAAAA	379625	(-)	heavy metal translocating P-type ATPase	PCC7418_RS01685	-283	P
AATATTTATATTTCTTAAT	510372	(+)	4-alpha-glucanotransferase	PCC7418_RS02325	-227	G
ATAAAAATTTAATAATAAT	524171	(-)	response regulator	PCC7418_RS02385	-374	T
ATTGATAATATTTATTAAC	559257	(-)	coenzyme F420 hydrogenase	PCC7418_RS02560	-101	C
TTTTATGATTATTATCAAT	690115	(+)	ShlB/FhaC/HecB family hemolysin secretion/activation protein	PCC7418_RS03120	-17	M
ATTAATAAACTTTTTTAAC	746975	(+)	photosystem I reaction center protein subunit XI-photosystem I reaction center subunit VIII	PCC7418_RS03390	-246	S
ATTTAATTAAATTTACAAT	766012	(+)	CRISPR associated endoribonuclease Cas6	PCC7418_RS03470	-242	S
ATTGACAAAATTTCCTAAT	789753	(-)	photosystem II q(b) protein	PCC7418_RS03535	-74	C

ATTGAAAGTCATTCTTATT	898088	(-)	ferrous iron transport protein A-Fe (2+) (*feoA*)-transporter permease subunit FeoB (*feoB*)	PCC7418_RS04120/ RS04115	-93	P, P
ATTAGAAATTTTTCTAAAA	1004388	(-)	ISAs1 family transposase	PCC7418_RS20420	0	S
AATGTTAAATTTTTATAAA	1169323	(+)	KaiA family protein	PCC7418_RS05355	-185	S
ATTTATAACTTTTCTCTAT	1179409	(+)	MFS transporter	PCC7418_RS05400	-207	G
ATTTTTGATAATTATTAAT	1210254	(+)	HP	PCC7418_RS05535	-184	P
GTTGAAATAGATTCTTATT	1244480	(-)	adenylyl-sulfate kinase	PCC7418_RS05670	-147	P
ATTAGAAATTTTTCTAAAA	1277716	(-)	ISAs1 family transposase	PCC7418_RS05850	0	S
ATTTTAATTTTTTTGTTAT	1541282	(+)	HEAT repeat domain-containing protein	PCC7418_RS07010	-88	C
ACTAATATTTTTTCTAAAT	1613963	(-)	solute-ABC transporter substrate-binding protein	PCC7418_RS07285	-458	E
ATTAAAATAAAATCTAATC	1626439	(-)	CDP-diacylglycerol--glycerol-3-phosphate 3-phosphatidyltransferase	PCC7418_RS07355	-120	I
ATTAACAAATTATAAAATT	1638172	(-)	sensor domain-containing diguanylate cyclase	PCC7418_RS07405	-11	P
TTATAAAATTATTTACAAT	1773346	(-)	2-carboxy-1,4-naphthoquinone phytyltransferase (*menA*)	PCC7418_RS08020	-216	H
ATTACAAAAGATTCTCAAC	1846361	(-)	ferrous iron transport protein A-Fe (2+) (*feoA*)-transporter permease subunit FeoB (*feoB*)	PCC7418_RS08340/ RS08335	-31	P, P
AATTATTAAAATTATTAAT	1978529	(+)	photosystem II protein PsbX (*psbX*)	PCC7418_RS08985	-145	C
GTTCATAATATTTTATAAT	2010967	(+)	DUF2207 domain-containing protein	PCC7418_RS09130	-396	S
TTTTAGTATATTTCTCATT	2201702	(+)	30S ribosome-binding factor RbfA (*rbfA*)	PCC7418_RS09935	-165	H
ATTGACAACTATTTTTAGT	2226486	(+)	methyl-accepting chemotaxis protein	PCC7418_RS10065	-669	L
ATTGCAATTAAATTTAAAA	2226728	(-)	ferrous iron transport protein A-Fe (2+) (*feoA*)-transporter permease subunit FeoB (*feoB*)	PCC7418_RS10060/ RS10055	-316	P
TTTTGTAAATTTTTGTAAA	2234872	(+)	glutamate-1-semialdehyde-2,1-aminomutase (*gsaI*)	PCC7418_RS10080	-177	H
TTTGTAAATTTTTGTAAAT	2234873	(+)	magnesium chelatase subunit H (*chlH*)	PCC7418_RS10075	-214	H
TTTTAAAATAAAAAATAAT	2376830	(-)	hydrogenase maturation protease	PCC7418_RS10660	-207	C
ATTGCTATTTATTCATAAT	2425245	(-)	DUF1643 domain-containing protein	PCC7418_RS19410	-256	S

TTTTAGAAAAATTTCTAAT	2459685	(+)	ISAs1 family transposase	PCC7418_RS11060	0	S
TTTGTTATTTATTCTTAGT	2584479	(+)	HP	PCC7418_RS11685	-270	S
AATACAAAAATTTGTTAAA	2609963	(-)	ABC transporter ATP-binding protein	PCC7418_RS11810	-546	V
ATTTTTAATTTTTTGTTAA	2785156	(+)	cobalamin biosynthesis protein (*cobW)*	-	-64	S
ATTGCAAATTTTTTTTATT	2791453	(+)	Crp/Fnr family transcriptional regulator	PCC7418_RS12605	0	K
ATTAAGAAAAATTAATATT	2858373	(+)	argininosuccinate synthase	PCC7418_RS13005	0	E
ATTGTTATTTATTATTTGT	2864252	(+)	6-pyruvoyltetrahydropterin synthase	PCC7418_RS13025	-312	H
ACTGGAAAAAATTATCAAA	2874763	(-)	methyltransferase domain-containing protein	PCC7418_RS1306	-194	L
ATTGAGATATTTTATCGAT	2883764	(+)	transcription-repair coupling factor	PCC7418_RS13105	-64	L
ATTTTGAACAAATTTCAAT	2933424	(+)	SpoIID/LytB domain-containing protein	PCC7418_RS13340	-50	D
GTTTTAAAAAATAATTAAT	3179394	(-)	photosystem II reaction center protein Ycf12	PCC7418_RS14435	-25	S
ATTAAATATAATTATAACT	3191678	(-)	M28 family peptidase	PCC7418_RS14505	-21	S
GTTGAGATTAATTTTCATT	3379840	(-)	PAS domain-containing protein	PCC7418_RS15425	-46	T
ATTAATAAAGTTTTGCAAA	3441389	(+)	glutamate-5-semialdehyde dehydrogenase	PCC7418_RS15780	-102	E
GTTGCTAATTTTTAGCAAA	3460255	(-)	bifunctional phosphoribosylaminoimidazolecarboxamide formyltransferase/IMP cyclohydrolase (*purH*)	PCC7418_RS15885	-45	F
AATTGGAAATTTTTTCAGT	3692765	(+)	peptidase S13	PCC7418_RS16905	-39	S
ATTGCAATTTAATTTCAAT	3725995	(-)	alpha/beta hydrolase	PCC7418_RS17030	-21	S
ATTGTCAATTTTTTGTAAT	3727770	(+)	HU family DNA binding protein	PCC7418_RS17045	-245	L
ATTATAAAAAACTATTAAC	3774691	(+)	alkaline phosphatase	PCC7418_RS17240	-45	S
GTTAATTTTAATTTTTAAT	3840660	(+)	sensor protein	PCC7418_RS17555	-1	S
ATTGCAAAAGATATTCAAT	3885410	(-)	chlorophyll a/b binding light-harvesting protein-chlorophyll a/b binding light-harvesting protein	PCC7418_RS17760	-16	S
TTTGAAATTAACTTGCAAT	3887033	(+)	hemolysin type calcium binding protein	PCC7418_RS17775	-54	V

TATAAAAATAATTTAAAAT	3944457	(-)	HindVP family restriction endonuclease	PCC7418_RS18040	0	V
GATAAAAAAGATTAATAAT	4030327	(-)	glycosyltransferase family 2 protein	PCC7418_RS18475	-127	M
ATTGAAATAAATTGTCAAC	4047761	(+)	uracil phosphoribosyltransferase	PCC7418_RS18570	-188	F
ATTGAAATAAATTGTCAAC	4047761	(-)	carotene isomerase	PCC7418_RS18565	-141	F
ATTTAGCAAAATTATTAAA	4072511	(+)	magnesium-protoporphyrin IX monomethyl ester anaerobic oxidative cyclase	PCC7418_RS18705	-77	H
TTTGAGAATATTTCTTTTT	4095529	(+)	PadR family transcriptional regulator (*padR*)	PCC7418_RS18830	-139	K

Supplementary Table 4. NtcA regulon prediction. NtcA boxes sequences, their position in the genome, orientation, the genes that are controlling (the NtcA regulon), locus tag from these genes, the distance of the box from the gene and the gen function from single-letter of functional (COGs) are presented.

NtcA boxes sequences	Position	Orientation	NtcA regulon (genes)	Locus_tag	Distance	COG
TGTAATATTTGTTAAA	193565	(-)	phosphoribosylformylglycinamidine cyclo-ligase (*purM*)	PCC7418_RS00865	-14	F
TGTAACATTCGATACA	433503	(+)	DUF4278 domain-containing protein	PCC7418_RS01970	-53	P
TGTAAATTTTGATACC	435747	(+)	PstS phosphate ABC transporter substrate-binding protein (*pstS*)	PCC7418_RS01980	-166	P
TGTAAATTTTGATACC	435748	(-)	adenylyl-sulfate kinase (*cysC*)	PCC7418_RS01975	-3	S
CGTATATTATGATACA	609571	(+)	ferredoxin--nitrite reductase (*nirA*)	PCC7418_RS02810	-89	C
TGTAATAGTAAATAGA	676478	(+)	Uma2 family endonuclease	PCC7418_RS03075	-18	S
TGTATCTATTGTTACA	857460	(-)	DUF4278 domain-containing protein	PCC7418_RS03870	-116	S
TGTATCAAATATTACT	1222068	(-)	2-oxo acid dehydrogenase subunit E2	PCC7418_RS05590	-159	C
TGTATCAAATATTACT	1222069	(+)	response regulator	PCC7418_RS05595	-100	T
AGTAAAAACTGCTACA	1299552	(+)	hybrid sensor histidine kinase/response regulator	PCC7418_RS05925	-195	T
TGTATTGTTTTCTACA	1331526	(-)	helix turn helix domain-containing protein	PCC7418_RS06050	-183	C
AGTAGTTTTTGTTACA	1381373	(+)	glutamate synthase large subunit *(gltB*)	PCC7418_RS06265	-342	E
TGTATTTTTCGATACA	1487910	(+)	ammonium transporter (*amt*)	PCC7418_RS06755	-145	P
TGTATCTTTTTATACT	1496086	(+)	Crp/Fnr family transcriptional regulator	PCC7418_RS06790	-54	K
TATAACTTTTTTTACA	1502278	(-)	elongation factor G (*fusA*)-elongation factor Tu (*tuf*)	PCC7418_RS06815/ RS06810	-82	J, J
AGTAACAATTGATACA	1504147	(-)	cupin domain-containing protein-iron-sulfur cluster assembly accessory protein	PCC7418_RS06835	-14	G

TGTTTTTTCTGATACA	1613632	(-)	solute-ABC transporter substrate-binding protein	PCC7418_RS07290	-120	E
TGTATCATTTGTTACA	1907277	(-)	pyridoxal phosphate-dependent aminotransferase	PCC7418_RS08620	-77	E
TGTAGCGTTTGTTACT	1946907	(+)	nitrogenase cofactor biosynthesis protein (*nifB*)	PCC7418_RS08815	-629	C
AGTATTACTAAATACA	1963729	(+)	molybdate ABC transporter substrate-binding protein (*modA*)	PCC7418_RS08910	-352	P
TGTATAAATCGCTACA	1981610	(-)	ammonium transporter (*amt*)	PCC7418_RS08960	-56	P
AGTAACATTAAATACA	2022577	(-)	SulP family inorganic anion transporter	PCC7418_RS09170	-90	P
AGTAACATTAAATACA	2022578	(+)	TIGR03279 family radical SAM protein	PCC7418_RS09175	-78	C
TGTAGTTGCAATTACT	2077841	(-)	sugar transferase	PCC7418_RS09405	-75	M
TGTAGCTGATAATACC	2201041	(-)	orange carotenoid-binding protein	PCC7418_RS09925	-53	S
TCTAACAAAAGTTACA	2260357	(+)	photosystem II chlorophyll-binding protein CP47 (*psbB*)	PCC7418_RS10180	-161	S
TGTAACTTTAGATACG	2301793	(-)	alanine:cation symporter family protein	PCC7418_RS10335	-68	E
TGTAACTTGTATTACA	2496434	(+)	phosphodiesterase	PCC7418_RS11260	-145	E
TGTATTTAATGTTACA	2725914	(-)	type I glutamate--ammonia ligase *(glnN*)	PCC7418_RS12280	-72	E
TGTAGTTGAGGTTACA	2977247	(+)	NINE protein	PCC7418_RS13560	-195	E
AGTAGCAATTATTACA	3197191	(-)	sodium:glutamate symporter (*gltS*)	PCC7418_RS14540	-106	E
TGTATTTTTTGATACA	3288086	(-)	MinD/ParA family protein	PCC7418_RS14970	-204	D
AGTAAAATAAAATACA	3502170	(-)	rhodopsin	PCC7418_RS16035	-294	S
TGTACAAAATATTACA	3542559	(-)	tetratricopeptide repeat protein	PCC7418_RS16280	-70	S

TGTTATTTACGATACA	3690483	(-)	[acyl-carrier-protein] S-malonyltransferase (*fabD*)	PCC7418_RS16890	-7	I
TGTATTCACTAATACA	3817904	(+)	response regulator	PCC7418_RS17455	-61	T
AGTAATTATTGCTACA	3962735	(+)	transcriptional repressor (*fur*)	PCC7418_RS16465	-7	T
AGTATCTTTCGTTACA	4051198	(-)	L-histidine N(alpha)-methyltransferase (*egtD*)	PCC7418_RS18585	-41	S
CGTATCAAGAGATACA	4130890	(+)	ATP-grasp domain-containing protein	PCC7418_RS18945	-144	S

Chapter 3

Supplementary Table S1. List of all treatments and variables measured in this study.

<table>
<tr><td>Strains/Experiments</td><td colspan="5">(I) Long-term studies: growth curves (growth rate [μ] and duplication time [T_g])</td></tr>
<tr><td rowspan="11">UIB 001 (Balearic Islands, Spain)

4B UA (Puerto Aldea, Chile)</td><td>High PO_4^{3-} (50 μM)- High Fe (1 μM)</td><td>N_2 as sole N source</td><td>Low PO_4^{3-} (0.005 μM)- Low Fe (1 nM)</td><td>Low PO_4^{3-} (0.005)- High Fe (1 μM)</td><td>Growth curve for 12 days, with aliquots taken every 2-4 days, adjusted to pH 8.</td></tr>
<tr><td colspan="5">(II) Short-term studies: N concentration effect at different pH levels</td></tr>
<tr><td colspan="2">pH 6</td><td colspan="2">pH 7</td><td>pH 8</td><td rowspan="3">Experiment during 96 h (high PO_4^{3-}), in which it was measured cell abundance and ROS production.</td></tr>
<tr><td colspan="2">N_2 a sole N source</td><td colspan="3">0.8 mM of NH_3</td></tr>
<tr><td colspan="2">1 mM Tris NH_3</td><td colspan="3">1 mM + 0.8 mM NH_3</td></tr>
<tr><td colspan="5">(III) Short-term studies: P concentration effect at different pH levels</td></tr>
<tr><td colspan="2">pH 6</td><td colspan="2">pH 7</td><td>pH 8</td><td rowspan="3">Experiment during 96 h with N replete, in which it was measured cell abundance, ROS production and alkaline phosphatase activity (APA).</td></tr>
<tr><td colspan="2">Low PO_4^{3-} (0.005 μM)- Low Fe (1 nM)</td><td colspan="3">Low PO_4^{3-} (0.005 μM)- High Fe (1 μM)</td></tr>
<tr><td colspan="2">High PO_4^{3-}(50 μM)- Low Fe (1 nM)</td><td colspan="3">High PO_4^{3-} (50 μM)-High Fe (1 μM)</td></tr>
<tr><td colspan="5">(IV) Analysis of APA under increasing PO_4^{3-} concentrations</td></tr>
<tr><td colspan="3">(-Fe, 1 nM)</td><td colspan="2">(+Fe, 1 μM)</td><td rowspan="3">Experiment during 96 h with N replete at pH 8, in which it was measured APA with 5 μM of MUF-P at different levels of Fe.</td></tr>
<tr><td>0.005 μM</td><td colspan="2">0.05 μM</td><td>0.5 μM</td></tr>
<tr><td>5 μM</td><td colspan="2">50 μM</td><td>100 μM</td></tr>
</table>

Supplementary Table S2. 16S rRNA gene sequence identities of *Cobetia* sp. UIB 001, *Cobetia* sp. 4B UA and the type strains of the genus *Cobetia* (*C. amphilecti* KKM 1561^T, *C. litoralis* KMM 3880^T, *C. marina* JCM 21022^T, *C. pacifica* KMM 3879^T).

	***Cobetia* sp. UIB 001**	***Cobetia* sp. 4B UA**	***C. amphilecti* KMM 1561^T (AB646236)**	***C. litoralis* KMM 3880^T (AB646234)**	***C. marina* JCM 21022^T (CP017114)**	***C. pacifica* KMM 3879^T (AB646233)**
***Cobetia* sp. UIB 001**	*	100	99.9	99.8	99.4	99.4
***Cobetia* sp. 4B UA**	100	*	99.9	99.8	99.40	99.4
***C. amphilecti* KMM 1561^T (AB646236)**	99.9	99.9	*	99.9	99.5	99.5
***C. litoralis* KMM 3880^T (AB646234)**	99.8	99.8	99.9	*	99.4	99.4
***C. marina* JCM 21022^T (CP017114)**	99.4	99.4	99.5	99.4	*	100
***C. pacifica* KMM 3879^T (AB646233)**	99.4	99.4	99.5	99.4	100	*

Supplementary Table S3. Average nucleotide identity based on BLAST (ANIb) values between *Cobetia* sp. (UIB 001 and 4B UA), *C. pacifica* GPM2, *C. amphilecti* KMM 296 and *C. marina* JCM 21022^{T}.

Query genome	***C. marina* JCM 21022^{T} (NZ_CP017114)**	***C. pacifica* GPM2 (CP047970)**	***C. amphilecti* KMM 296 (GCF_000754225)**	***Cobetia* sp. UIB 001**	***Cobetia* sp. 4B UA**
***C. marina* JCM 21022^{T} (NZ_CP017114)**	*	97.97 [92.39]	86.34 [71.89]	86.58 [75.72]	86.53 [77.04]
***C. pacifica* GPM2 (CP047970)**	97.80 [92.34]	*	86.74 [74.05]	86.73 [76.22]	86.93 [79.32]
***C. amphilecti* KMM_296 (GCF_000754225)**	86.23 [75.71]	86.74 [77.84]	*	96.45 [90.42]	96.69 [94.27]
***Cobetia* sp. UIB 001**	86.43 [75.93]	86.67 [76.56]	96.30 [86.09]	*	96.99 [93.08]
***Cobetia* sp. 4B UA**	86.30 [75.09]	86.79 [77.50]	96.58 [87.69]	96.93 [90.71]	*

Supplementary Table S4. Digital DNA-DNA hybridization (dDDH) values between *Cobetia* sp. (UIB 001 and 4B UA) and the genomes of *C. pacifica* GPM2, *C. amphilecti* KMM 296 and *C. marina* JCM 21022^{T}.

Query genome	Reference genome	DDH	Model C.I.	Distance	Prob. DDH >= 70%
Cobetia sp. UIB 001	*C. pacifica* GPM2 (CP047970)	32.70	[30.3 - 35.2%]	0.1285	0.3
Cobetia sp. UIB 001	*Cobetia* sp. 4B UA	75.80	[72.8 - 78.6%]	0.0284	86.69
Cobetia sp. UIB 001	*C. amphilecti* KMM 296 (GCF_000754225)	72.00	[68.9 - 74.8%]	0.0334	81.6
Cobetia sp. UIB 001	*C. marina* JCM 21022^{T} (NZ_CP017114)	32.40	[30 - 34.9%]	0.1299	0.27

Query genome	Reference genome	DDH	Model C.I.	Distance	Prob. DDH >= 70%
Cobetia sp. 4B UA	*C. pacifica* GPM2 (CP047970)	33.10	[30.7 - 35.6%]	0.1265	0.35
Cobetia sp. 4B UA	*Cobetia* sp. UIB 001	75.80	[72.8 - 78.6%]	0.0284	86.69
Cobetia sp. 4B UA	*C. amphilecti* KMM 296 (GCF_000754225)	72.80	[69.8 - 75.6%]	0.0323	82.87
Cobetia sp. 4B UA	*C. marina* JCM 21022^{T} (NZ_CP017114)	32.20	[29.8 - 34.7%]	0.1307	0.25

Supplementary Figure S1. COG analysis of the annotated proteins of *Cobetia* sp. UIB 001 and 4B UA.

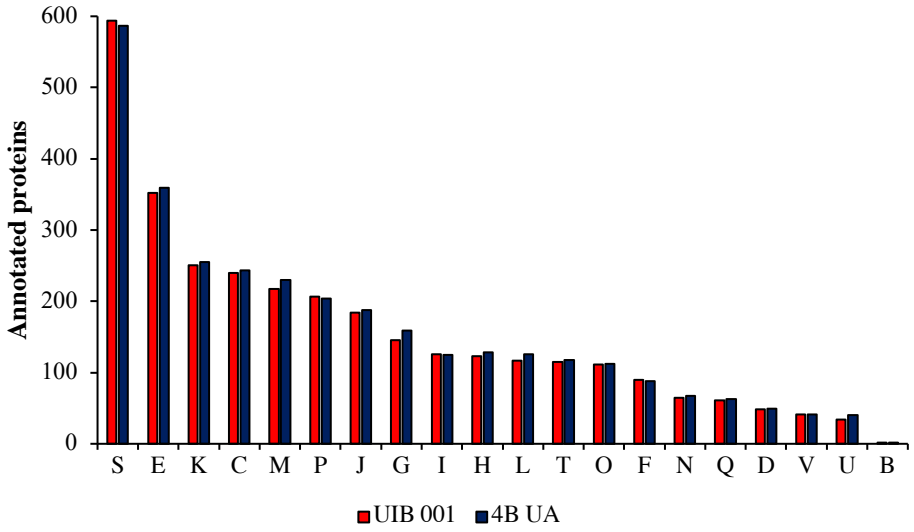

CELLULAR PROCESSES AND SIGNALING
[D] Cell cycle control, cell division, chromosome partitioning
[M] Cell wall/membrane/envelope biogenesis
[N] Cell motility
[O] Post-translational modification, protein turnover, and chaperones
[T] Signal transduction mechanisms
[U] Intracellular trafficking, secretion, and vesicular transport
[V] Defense mechanisms

INFORMATION STORAGE AND PROCESSING
[J] Translation, ribosomal structure and biogenesis
[K] Transcription
[L] Replication, recombination and repair

METABOLISM
[C] Energy production and conversion
[E] Amino acid transport and metabolism
[F] Nucleotide transport and metabolism
[G] Carbohydrate transport and metabolism
[H] Coenzyme transport and metabolism
[I] Lipid transport and metabolism
[P] Inorganic ion transport and metabolism
[Q] Secondary metabolites biosynthesis, transport, and catabolism

POORLY CHARACTERIZED
[S] Function unknown

Supplementary Figure S2. Diazotrophic features the *Cobetia* spp. isolated. **A)** N_2-fixation rates of *Cobetia* sp. UIB 001 compared with the diazotrophic *Pseudomonas azotifigens* DSM 17556^T, using the acetylene reduction assay (ARA), as is described in Fernández-Juárez et al. (2019, 2020). **B)** Growth of the UIB 001 and 4B UA in the Burk's N-free medium. Red circles indicate the growth of these strains in this medium.

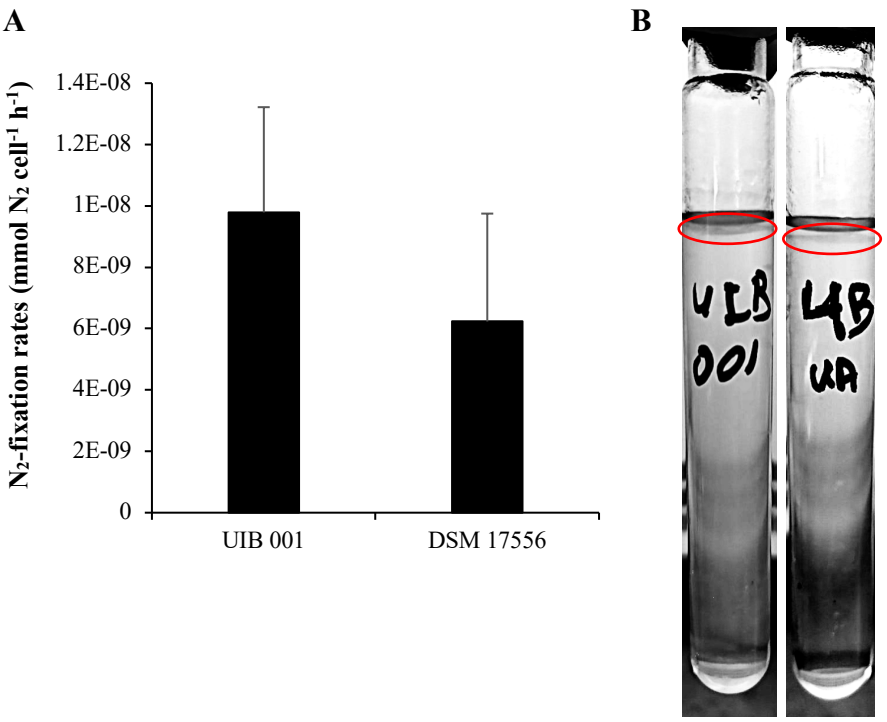

Chapter 4

Supplementary Table S1. List of all treatments, strains and variables studied in this report. * Only tested for *Halothece* sp. and *Cobetia* sp.

<table>
<tr><th colspan="7">(I, II) Without the infusion of CO_2</th></tr>
<tr><th>Strains</th><th colspan="3">(I) pH experiment (at 24º C)</th><th colspan="2">(II) Temperature experiment (adjusted to pH 8)</th><th>Description</th></tr>
<tr><td rowspan="5">Halothece sp. PCC 7418, Pasteur culture collection

Fischerella muscicola PCC 73103, Pasteur Culture Collection

Cobetia sp. UIB 001, obtained: isolated directly from P. oceanica roots (Fernández-Juárez et al., unpublished data). GenBank: CP058244-CP058245

Pseudomonas azotifigens DSM 17556^T, obtained: German Collection of Microorganisms and Cell Cultures GmbH (DSMZ)</td><td colspan="3">pH 4</td><td colspan="2">12 ºC</td><td rowspan="2">Under replete nutrients conditions: 1.5 mM PO_4^{3-}, 1 µM Fe and 0.15 mM NH_3</td></tr>
<tr><td colspan="3">pH 5</td><td colspan="2">18 ºC</td></tr>
<tr><td colspan="3">pH 6</td><td colspan="2">24 ºC</td><td rowspan="2">Under P and Fe limitation.: 0.1 µM PO_4^{3-}, 2 nM Fe and 0.15 mM NH_3</td></tr>
<tr><td>pH 6.5*</td><td>pH 7*</td><td colspan="3" rowspan="2">30 ºC</td></tr>
<tr><td>pH 7.5*</td><td>pH 8*</td><td>At 120 r.p.m 12:12 day: night photoperiod for 72 h</td></tr>
<tr><th colspan="7">(III) With the infusion of CO_2 (410 and 1000 µmol CO_2 mol^{-1})</th></tr>
<tr><th>Strains</th><th colspan="3">(i) CO_2-Fe (at 24ºC, adjusted to pH 8)</th><th colspan="2">(ii) CO_2-temperature (adjusted to pH 8)</th><th>Description</th></tr>
<tr><td rowspan="4">Halothece sp. PCC 7418

Cobetia sp. UIB 001</td><td rowspan="4">(+) Fe, 1 µM (+) PO_4^{3-}, 1.5 mM</td><td rowspan="4">(-) Fe, 2 nM (+) PO_4^{3-}, 1.5 mM</td><td rowspan="4">(+ or -) Fe, (-) PO_4^{3-}, 0.1 µM</td><td rowspan="4">18 ºC (+) Fe, 1000 nM (+) PO_4^{3-}, 1.5 mM</td><td rowspan="4">30 ºC (+) Fe, 1000 nM (+) PO_4^{3-}, 1.5 mM</td><td rowspan="4">18 ºC or 30ºC (-) PO_4^{3-},0.1 µM</td><td>Control, no CO_2 influx:</td></tr>
<tr><td>aCO2: 410 µmol CO_2 mol^{-1}</td></tr>
<tr><td>eCO2: 1000 µmol CO_2 mol^{-1}</td></tr>
<tr><td>At 120 r.p.m 12 h dark:12 h light photoperiod for 72 h, performed under 0.15 mM NH_3)</td></tr>
<tr><th colspan="7">Response variables</th></tr>
<tr><td colspan="2">(1) Growth</td><td colspan="2">(2) N_2-fixation rates</td><td colspan="2">(3) ROS production</td><td colspan="2">(4) P-mechanisms (APA)*</td></tr>
</table>

Supplementary Figure S1. Experimental set-up of the CO_2 experiments, considering two different levels of CO_2, aCO_2: 410 µmol CO_2 mol^{-1} and elevated, eCO_2: 1000 µmol CO_2 mol^{-1}, and included a control with no CO_2 influx. The pH level was monitored for aCO_2 and eCO_2.

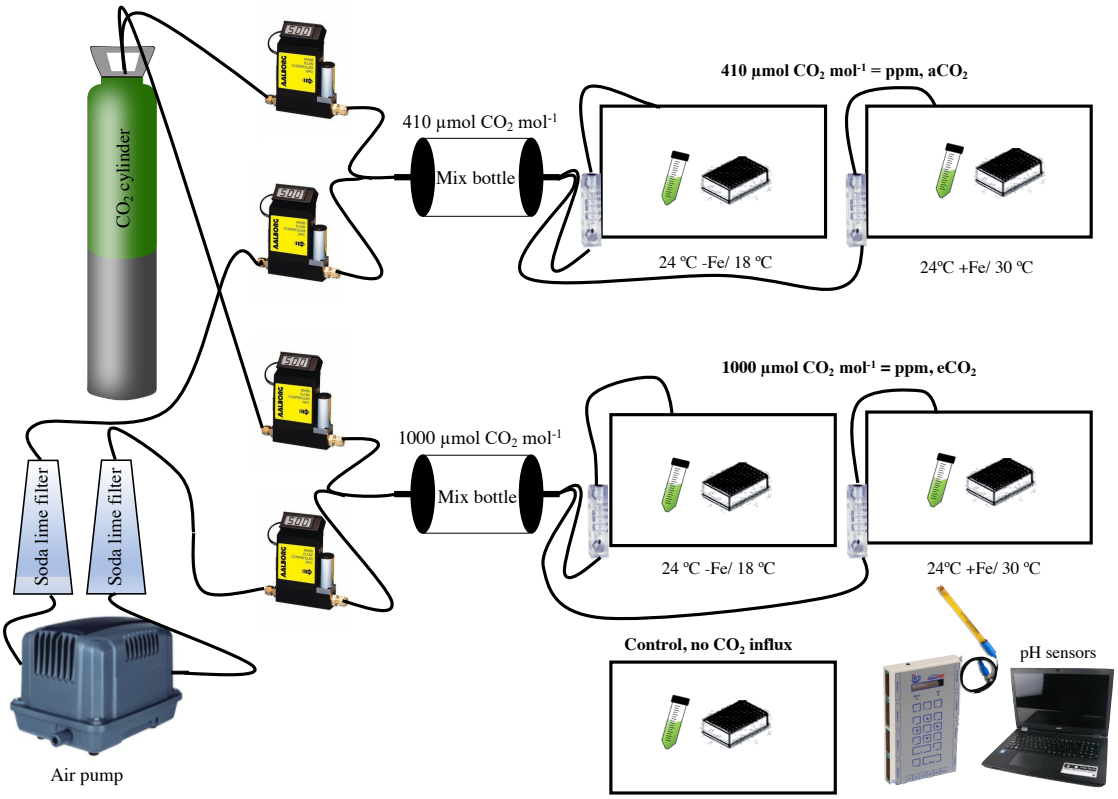

Supplementary Figure S2. pH monitoring under a continuous influx of atmospheric CO_2 410 µmol CO_2 mol^{-1} (atmospheric CO_2, aCO_2) and elevated CO_2 1000 µmol CO_2 mol^{-1} (elevated CO_2, eCO_2) for *Halothece* sp. and *Cobetia* sp.

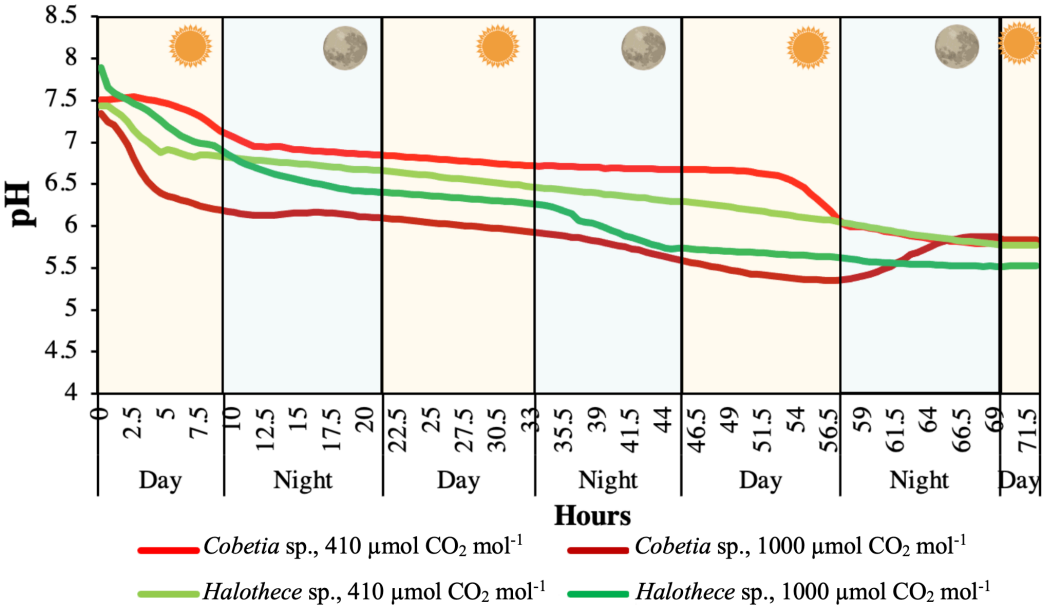

Chapter 5

Supplementary Table 1. List of all treatments performed in this study, divided into two parts: (**I**) Response to MPs at environmentally relevant concentrations and (**II**) Response to MPs at environmentally concentrations vs high concentrations (the "worst-case" scenario). Abbreviations: PE, polyethylene; PP, polypropylene; PVC, polyvinyl chloride; Fluo, fluoranthene; HBCD, 1,2,5,6,9,10-hexabromocyclododecane; DEHP, dioctyl-phthalate; PS, polystyrene. Response variables of each experiment are indicated in the table.

Experimental plan/treatments:		**MPs (PE, PP and/or PVC)**	**Additive (A) (Fluoranthene, HBCD and/or DEHP)**	**MPs and A: PE+Fluo/PP+HBCD/ PVC+DEHP or all interacting**	**PS (beads)**
I. Response to MPs at environmentally relevant concentrations					
Response variable: growth and microscopic analysis					
Species tested		0, 0.01, 0.1, 1, 100 µg mL^{-1}	0, 0.3, 3, 30, 300 µg L^{-1}	Low (L) MPs (0.01 µg ml^{-1}) and Low (L) A (0.3 µg L^{-1}) High (H) MPs (100 µg ml^{-1}) and High (H) A (300 µg L^{-1})	4.55×10^3 particles mL^{-1} In *Halothece* sp. PCC 7418 (data did not show)
Phototroph: unicellular autotroph	*Halothece* sp. PCC 7418 Source: Pasteur Culture Collection				
Phototroph: filamentous heterocyst-forming mixotroph	*Fischerella muscicola* PCC 73103 Source: Pasteur Culture Collection				
Heterotroph: isolated from roots of *P. oceanica*, benthic specie	*Cobetia* sp. UIB 001 Source: isolated directly from *P. oceanica* roots (Fernández-Juárez et al., in prep). GenBank: CP058244-CP058245				
Heterotroph: planktonic species	*Marinobacterium litorale* DSM 23545 Source: German Collection of Microorganisms and Cell Cultures GmbH (DSMZ)				
Heterotroph: planktonic species	*Pseudomonas azotifigens* DSM 17556^T: Source: German Collection of Microorganisms and Cell Cultures GmbH (DSMZ)				
II. Response to MPs at environmentally relevant concentrations vs high concentrations (the "worst-case" scenario)					
Response variable: growth, microscopic analysis, protein overexpression, alkaline phosphatase activity (APA), PO_4^{3-}-uptake and N_2-fixation					
Species tested		0, 100 and 1000 µg mL^{-1}	0, 300, 3000 µg L^{-1}	3MPs (100 µg mL^{-1}) and 3A (300 µg L^{-1}) (all combined) 3MPs (1000 µg mL^{-1}) and 3A (3000 µg L^{-1}) (all combined)	4.55×10^6 particles mL^{-1} 4.55×10^7 particles mL^{-1}
Phototroph: unicellular autotroph	*Halothece* sp. PCC 7418				
Heterotroph: isolated from roots of *P. oceanica*, benthic specie	*Cobetia* sp. UIB 001				

Supplementary Table 2. Comparison of PO_4^{3-}-uptake (pmol PO_4^{3-} $cell^{-1}$ d^{-1}) between treatments using a posthoc test (Wilcoxon) after Kruskal-Wallis over the whole dataset in *Halothece* sp. and *Cobetia* sp. (significant differences = $p < 0.05$).

Halothece sp. (p-value)	Control	PS	PS^	PE	PE^	PP	PP	PVC	PVC^	Fluo	Fluo^	Br	Br^	DEHP	DEHP^	3MP	3MP	3A	3A^
Control	-	-	-	-	-	-	-	-	-	-	-	-	-	-	-	-	-	-	-
PS	0.08	-	-	-	-	-	-	-	-	-	-	-	-	-	-	-	-	-	-
PS^	0.02	0.80	-	-	-	-	-	-	-	-	-	-	-	-	-	-	-	-	-
PE	0.03	0.16	0.17	-	-	-	-	-	-	-	-	-	-	-	-	-	-	-	-
PE^	0.02	0.09	0.10	0.64	-	-	-	-	-	-	-	-	-	-	-	-	-	-	-
PP	0.02	0.40	0.44	0.37	0.20	-	-	-	-	-	-	-	-	-	-	-	-	-	-
PP^	0.00	0.38	0.36	0.33	0.18	0.95	-	-	-	-	-	-	-	-	-	-	-	-	-
PVC	0.09	0.47	0.54	0.59	0.37	0.88	0.85	-	-	-	-	-	-	-	-	-	-	-	-
PVC^	0.00	0.57	0.66	0.23	0.14	0.46	0.42	0.66	-	-	-	-	-	-	-	-	-	-	-
Fluo	0.09	0.24	0.27	0.71	0.14	0.39	0.38	0.48	0.32	-	-	-	-	-	-	-	-	-	-
Fluo^	0.04	0.09	0.27	0.21	0.94	0.13	0.14	0.14	0.12	0.39	-	-	-	-	-	-	-	-	-
HBCD	0.14	0.56	0.31	0.07	0.30	0.13	0.09	0.27	0.16	0.17	0.07	-	-	-	-	-	-	-	-
HBCD^	0.04	0.25	0.08	0.05	0.04	0.04	0.01	0.17	0.01	0.14	0.07	0.37	-	-	-	-	-	-	-
DEHP	0.09	0.88	0.66	0.13	0.08	0.31	0.29	0.40	0.44	0.22	0.08	0.67	0.29	-	-	-	-	-	-
DEHP^	0.30	0.95	0.95	0.42	0.30	0.71	0.83	0.67	0.84	0.34	0.12	0.72	0.52	0.88	-	-	-	-	-
3MP	0.28	0.54	0.29	0.07	0.05	0.12	0.09	0.26	0.15	0.17	0.07	0.96	0.40	0.64	0.71	-	-	-	-
3MP^	0.21	0.20	0.04	0.04	0.03	0.03	0.00	0.12	0.00	0.11	0.06	0.16	0.25	0.16	0.40	0.18	-	-	-
3A	0.51	0.07	0.05	0.02	0.02	0.03	0.07	0.06	0.08	0.06	0.03	0.10	0.20	0.07	0.22	0.10	0.29	-	-
3A^	0.03	0.19	0.22	0.63	0.86	0.32	0.31	0.41	0.26	0.94	0.41	0.14	0.11	0.17	0.30	0.13	0.09	0.04	-

Cobetia sp. (p-value)	Control	PS	PS^	PE	PE	PP	PP^	PVC	PVC^	Fluo	Fluo^	Br	Br^	DEHP	DEHP^	3MP	3MP^	3A	3A^
Control	-	-	-	-	-	-	-	-	-	-	-	-	-	-	-	-	-	-	-
PS	0.08	-	-	-	-	-	-	-	-	-	-	-	-	-	-	-	-	-	-
PS^	0.01	0.00	-	-	-	-	-	-	-	-	-	-	-	-	-	-	-	-	-
PE	0.48	0.19	0.01	-	-	-	-	-	-	-	-	-	-	-	-	-	-	-	-
PE^	0.66	0.21	0.03	0.89	-	-	-	-	-	-	-	-	-	-	-	-	-	-	-
PP	0.00	0.39	0.00	0.34	0.36	-	-	-	-	-	-	-	-	-	-	-	-	-	-
PP^	0.13	0.07	0.01	0.27	0.41	0.00	-	-	-	-	-	-	-	-	-	-	-	-	-
PVC	0.26	0.24	0.01	0.74	0.67	0.47	0.14	-	-	-	-	-	-	-	-	-	-	-	-
PVC^	0.04	0.90	0.00	0.17	0.20	0.77	0.02	0.22	-	-	-	-	-	-	-	-	-	-	-
Fluo	0.13	0.23	0.00	0.62	0.20	0.48	0.07	0.87	0.20	-	-	-	-	-	-	-	-	-	-
Fluo^	0.01	0.01	0.00	0.01	0.57	0.00	0.01	0.00	0.00	0.00	-	-	-	-	-	-	-	-	-
HBCD	0.35	0.03	0.01	0.30	0.02	0.02	0.89	0.15	0.02	0.07	0.00	-	-	-	-	-	-	-	-
HBCD^	0.02	0.02	0.02	0.10	0.17	0.00	0.07	0.04	0.01	0.02	0.00	0.13	-	-	-	-	-	-	-
DEHP	0.30	0.04	0.10	0.19	0.26	0.08	0.50	0.12	0.04	0.10	0.03	0.48	0.87	-	-	-	-	-	-
DEHP^	0.01	0.06	0.05	0.09	0.14	0.00	0.03	0.05	0.01	0.03	0.04	0.08	0.40	0.64	-	-	-	-	-
3MP	0.01	0.04	0.03	0.10	0.17	0.00	0.02	0.05	0.01	0.02	0.01	0.11	0.91	0.83	0.28	-	-	-	-
3MP^	0.55	0.05	0.03	0.33	0.45	0.09	0.95	0.19	0.04	0.14	0.01	0.90	0.37	0.59	0.25	0.35	-	-	-
3A	0.04	0.01	0.09	0.05	0.09	0.01	0.06	0.02	0.00	0.01	0.01	0.06	0.29	0.45	0.50	0.30	0.16	-	-
3A^	0.07	0.29	0.00	0.08	0.10	0.17	0.07	0.09	0.33	0.08	0.01	0.03	0.03	0.03	0.06	0.05	0.06	0.01	-

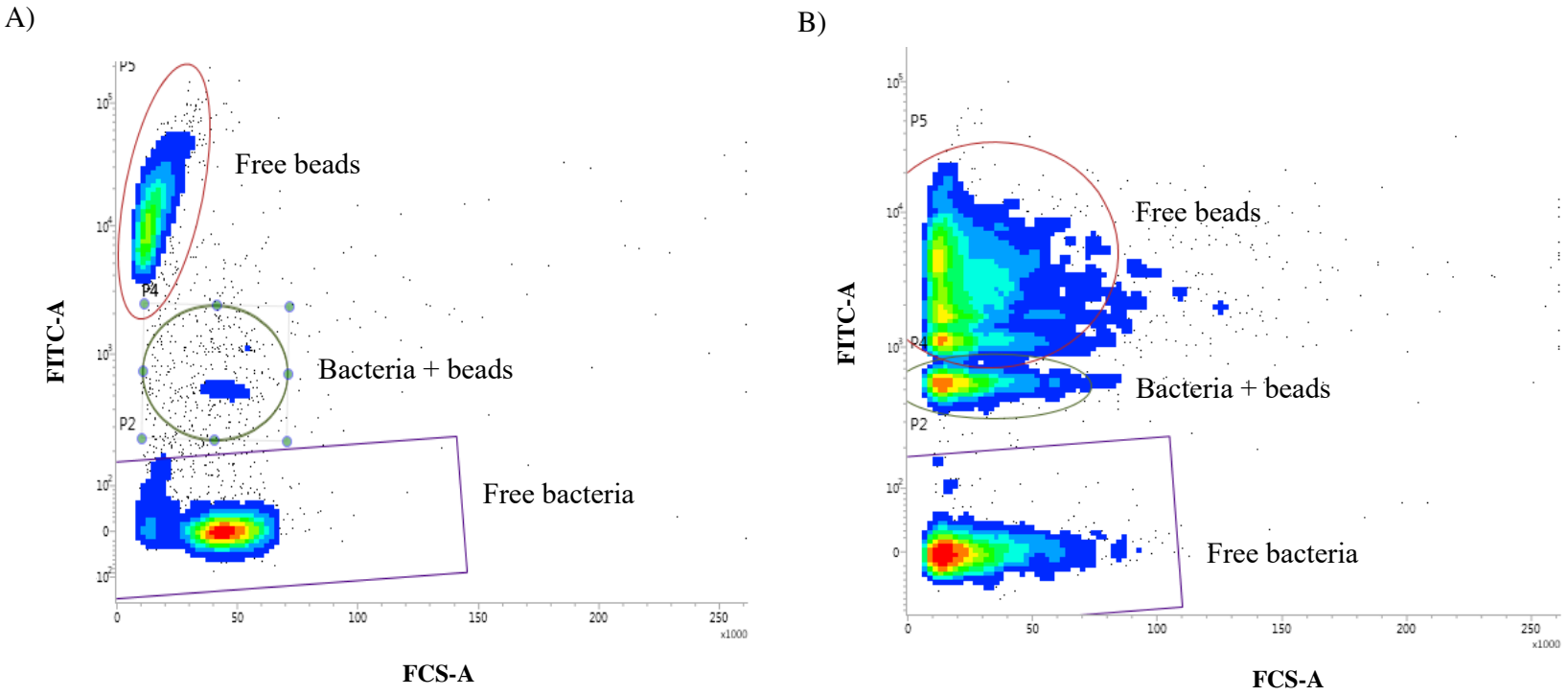

Supplementary Figure 1. Cytograms showing **A)** *Halothece* sp. and **B)** *Cobetia* sp. cells, being free or adsorbed with the PS-beads, using FITC-A and FCS-A as the flow cytometer parameters.

7. REFERENCES

REFERENCES

Agawin, N. S. R., Duarte, C. M., and Agusti, S. (2000). Nutrient and temperature control of the contribution of picoplankton to phytoplankton biomass and production. Am. Soc. *Limnol. Oceanogr*. 45, 591–600. doi: 10.4319/lo.2000.45.3.0591

Agawin, N. S. R., Rabouille, S., Veldhuis, M. J. W., Servatius, L., Hol, S., Van Overzee, M. J., et al. (2007). Competition and facilitation between unicellular nitrogen-fixing cyanobacteria and non – nitrogen-fixing phytoplankton species. *Limonol. Oceanogr*. 52, 2233–2248. doi: 10.4319/lo.2007.52.5.2233

Agawin, N. S. R., Benavides, M., Busquets, A., Ferriol, P., Stal, L. J., and Arístegui, J. (2014). Dominance of unicellular cyanobacteria in the diazotrophic community in the Atlantic Ocean. *Limnol. Oceanogr.* 59, 623–637. doi:10.4319/lo.2014.59.2.0623.

Agawin, N. S. R., Ferriol, P., Cryer, C., Alcon, E., Busquets, A., Sintes, E., et al. (2016). Significant nitrogen fixation activity associated with the phyllosphere of Mediterranean seagrass *Posidonia oceanica*: First report. *Mar. Ecol. Prog. Ser.* 551, 53–62. doi:10.3354/meps11755

Agawin, N. S. R., Ferriol, P., Sintes, E., and Moyà, G. (2017). Temporal and spatial variability of in situ nitrogen fixation activities associated with the Mediterranean seagrass *Posidonia oceanica* meadows. *Limnol. Oceanogr.* 62, 2575–2592. doi:10.1002/lno.10591.

Agawin, N. S. R., Ferriol, P., and Sintes, E. (2019). Simultaneous measurements of nitrogen fixation activities associated with different plant tissues of the seagrass *Posidonia oceanica. Mar. Ecol. Prog. Ser.* doi:10.3354/meps12854.

Agawin N. S. R, Gil Atorrasagasti M. G, Frank Comas A., Fernández-Juárez V., López-Alforja X and Hendriks I. E. (2021). Response of the seagrass *Posidonia oceanica* and its associated N_2 fixers to high business-as-usual climate change scenario in winter. *Limnol. Oceanogr.*

Al-Awadhi, H., Al-Mailem, D., Dashti, N., Khanafer, M., and Radwan, S. (2012). Indigenous hydrocarbon-utilizing bacterioflora in oil-polluted habitats in Kuwait, two decades after the greatest man-made oil spill. *Arch. Microbiol.* 194, 689–705. doi:10.1007/s00203-012-0800-7.

Alessi E., and Di Carlo G., (2018). “Out of the plastic trap: saving the Mediterranean from plastic pollution”. WWF Mediterranean Marine Initiative, Rome, Italy. 28 pp.

Almroth, B. C. (2019). marine plastic pollution: sources , impacts , and policy issues. 13, 317–326. doi:10.1093/reep/rez012.

Alquéres, S. M. C., Oliveira, J. H. M., Nogueira, E. M., Guedes, H. V., Oliveira, P. L., Câmara, F., et al. (2010). Antioxidant pathways are up-regulated during biological nitrogen fixation to prevent ROS-induced nitrogenase inhibition in *Gluconacetobacter diazotrophicus*. *Arch. Microbiol.* 192, 835–841. doi:10.1007/s00203-010-0609-1.

Anderson, O. R. (2018). Evidence for coupling of the carbon and phosphorus biogeochemical cycles in freshwater microbial communities. *Front. Mar. Sci.* 5, 1–6. doi:10.3389/fmars.2018.00020.

Argandoña, M., Fernández-Carazo, R., Llamas, I., Martínez-Checa, F., Caba, J. M., Quesada, E., et al. (2005). The moderately halophilic bacterium *Halomonas maura* is a free-living diazotroph. *FEMS Microbiol. Lett.* 244, 69–74. doi:10.1016/j.femsle.2005.01.019.

Arnaud-Haond, S., Duarte, C. M., Diaz-Almela, E., Marbà, N., Sintes, T., and Serrão, E. A. (2012). Implications of extreme life span in clonal organisms: millenary clones in meadows of the threatened seagrass *Posidonia oceanica*. *PLoS One* 7. doi:10.1371/journal.pone.0030454.

Arrigo, K. R. (2005). Marine microorganisms and global nutrient cycles. *Nature* 437, 343–348. doi:10.1038/nature04158.

Ascenzi, P., and Amiconi, G. (1987). Logarithmic plots in enzymology. Representation of the Michaelis-Menten equation. *Biochem. Educ.* doi:10.1016/0307-4412(87)90093-8.

Baas-Becking, L.G.M. (1934). Geobiologie of inleiding tot de milieukunde, The Hague, the Netherlands: W.P. Van Stockum & Zoon.

Baichoo, N., and Helmann, J. D. (2002). Recognition of DNA by Fur : a Reinterpretation of the Fur Box Consensus Sequence Recognition of DNA by Fur : a Reinterpretation of the Fur Box Consensus Sequence. *J. Bacteriol.* 184, 5826–5832. doi:10.1128/JB.184.21.5826.

Bakir, A., Rowland, S. J., and Thompson, R. C. (2014). Enhanced desorption of persistent organic pollutants from microplastics under simulated physiological conditions. *Environ. Pollut.* 185, 16–23. doi:10.1016/j.envpol.2013.10.007.

Balabanova, L., Golotin, V., Kovalchuk, S., Bulgakov, A., Likhatskaya, G., Son, O., et al. (2014). A novel bifunctional hybrid with marine bacterium alkaline phosphatase and far eastern holothurian mannan-binding lectin activities. *PLoS One* 9. doi:10.1371/journal.pone.0112729.

Balabanova, L. A., Golotin, V. A., Kovalchuk, S. N., Babii, A. V., Shevchenko, L. S., Son, O. M., et al. (2016a). The Genome of the marine bacterium *Cobetia marina* KMM 296 isolated from the mussel *Crenomytilus grayanus* (Dunker, 1853). *Russ. J. Mar. Biol.* 42, 106–109. doi:10.1134/S106307401601003X.

Balabanova, L., Nedashkovskaya, O., Podvolotskaya, A., Slepchenko, L., Golotin, V., Belik, A., et al. (2016b). Data supporting functional diversity of the marine bacterium *Cobetia amphilecti* KMM 296. *Data Br.* 8, 726–732. doi:10.1016/j.dib.2016.06.034.

Barcelos e Ramos, J., Biswas, H., Schulz, K. G., LaRoche, J., and Riebesell, U. (2007). Effect of rising atmospheric carbon dioxide on the marine nitrogen fixer *Trichodesmium*. *Global Biogeochem. Cycles* 21, 1–6. doi:10.1029/2006GB002898.

Benedetti, M., Giuliani, M. E., and Regoli, F. (2015). Oxidative metabolism of chemical pollutants in marine organisms: molecular and biochemical biomarkers in environmental toxicology. *Ann. N. Y. Acad. Sci.* 1340, 8–19. doi:10.1111/nyas.12698.

Berge, T., Daugbjerg, N., Andersen, B. B., and Hansen, P. J. (2010). Effect of lowered pH on marine phytoplankton growth rates. *Mar. Ecol. Prog. Ser.* 416, 79–91. doi:10.3354/meps08780.

Bergersen, F. J. (1970). The quantitative relationship between nitrogen fixation and the acetylene-reduction assay. *Aust. J. Biol. Sci.* doi:10.1071/BI9701015.

Berman-Frank, I., Cullen, J. T., Shaked, Y., Sherrell, R. M., and Falkowski, P. G. (2001). Iron availability, cellular iron quotas, and nitrogen fixation in *Trichodesmium*. *Limnol. Oceanogr.* 46, 1249–1260. doi:10.4319/lo.2001.46.6.1249.

Berner, C., Bertos-Fortis, M., Pinhassi, J., and Legrand, C. (2018). Response of microbial communities to changing climate conditions during summer cyanobacterial blooms in the Baltic Sea. *Front. Microbiol.* 9, 1–16. doi:10.3389/fmicb.2018.01562.

Biddanda, B., Ogdahl, M., and Cotner, J. (2001). Dominance of bacterial metabolism in oligotrophic relative to eutrophic waters. *Limnol. Oceanogr.* 46, 730–739. doi:10.4319/lo.2001.46.3.0730.

Blanco, A. G., Sola, M., Gomis-Rüth, F. X., and Coll, M. (2002). Tandem DNA Recognition by PhoB, a two-component signal transduction transcriptional activator. *Structure* 10, 701–713. doi:10.1016/S0969-2126(02)00761-X.

Boatman, T. G., Lawson, T., and Geider, R. J. (2017). A key marine diazotroph in a changing ocean: The interacting effects of temperature, CO_2 and light on the growth of *Trichodesmium erythraeum* IMS101. *PLoS One* 12, 1–20. doi:10.1371/journal.pone.0168796.

Boyd, P. W., and Doney, S. C. (2002). Modelling regional responses by marine pelagic ecosystems to global climate change. *Geophys. Res. Lett.* 29, 53-1-53–4. doi:10.1029/2001gl014130.

Breitbarth, E., Oschlies, A., and LaRoche, J. (2007). Physiological constraints on the global distribution of *Trichodesmium*-effect of temperature on diazotrophy. *Biogeosciences* 4, 53–61. doi:10.5194/bg-4-53-2007.

Brierley, A. S., and Kingsford, M. J. (2009). Impacts of climate change on marine organisms and ecosystems. *Curr. Biol.* 19, R602–R614. doi:10.1016/j.cub.2009.05.046.

Bristow, L. A., Mohr, W., Ahmerkamp, S., and Kuypers, M. M. M. (2017). Nutrients that limit growth in the ocean. *Curr. Biol.* 27, R474–R478. doi:10.1016/j.cub.2017.03.030.

Browning, T. J., Achterberg, E. P., Yong, J. C., Rapp, I., Utermann, C., Engel, A., et al. (2017). Iron limitation of microbial phosphorus acquisition in the tropical North Atlantic. *Nat. Commun.* 8, 1–7. doi:10.1038/ncomms15465.

Bryant, J. A., Clemente, T. M., Viviani, D. A., Fong, A. A., Thomas, K. A., Kemp, P., et al. (2016). Diversity and activity of communities inhabiting plastic debris in the North Pacific Gyre. *mSystems* 1, 1–19. doi:10.1128/msystems.00024-16.

By the Committee on biological markers of the national research council (1987). Biological markers in environmental health research. *Environ. Heal. Perspect.* 74, 3–9. doi:10.1210/endo-107-6-1820.

Cabiscol, E., Tamarit, J., and Ros, J. (2000). Oxidative stress in bacteria and protein damage by reactive oxygen species. *Int. Microbiol.* 3, 3–8. doi:10.2436/im.v3i1.9235.

Campagne, C. S., Salles, J. M., Boissery, P., and Deter, J. (2015). The seagrass *Posidonia oceanica*: ecosystem services identification and economic evaluation of goods and benefits. *Mar. Pollut. Bull.* 97, 391–400. doi:10.1016/j.marpolbul.2015.05.061.

Cao, J., Lai, Q., Yuan, J., and Shao, Z. (2015). Genomic and metabolic analysis of fluoranthene degradation pathway in *Celeribacter indicus* P73 T. *Sci. Rep.* 5, 1–12. doi:10.1038/srep07741.

Cavicchioli, R., Ostrowski, M., Fegatella, F., Goodchild, A., and Guixa-Boixereu, N. (2003). Life under nutrient limitation in oligotrophic marine environments: An eco/physiological perspective of *Sphingopyxis alaskensis* (formerly *Sphingomonas alaskensis*). *Microb. Ecol.* 45, 203–217. doi:10.1007/s00248-002-3008-6.

Cavicchioli, R., Ripple, W. J., Timmis, K. N., Azam, F., Bakken, L. R., Baylis, M., et al. (2019). Scientists' warning to humanity: microorganisms and climate change. *Nat. Rev. Microbiol.* 17, 569–586. doi:10.1038/s41579-019-0222-5.

Cerozi, B. da S., and Fitzsimmons, K. (2016). The effect of pH on phosphorus availability and speciation in an aquaponics nutrient solution. *Bioresour. Technol.* 219, 778–781. doi:10.1016/j.biortech.2016.08.079.

Chattopadhyay, M.K (2006). Mechanism of bacterial adaptation to low temperature. *J. Biosci.* 31, 157–65. doi: 10.1007/BF02705244.

Cole, M., and Galloway, T. S. (2015). Ingestion of nanoplastics and microplastics by pacific oyster larvae. *Environ. Sci. Technol.* 49, 14625–14632. doi:10.1021/acs.est.5b04099.

Coll, M., Piroddi, C., Steenbeek, J., Kaschner, K., Lasram, F. B. R., Aguzzi, J., et al. (2010). The biodiversity of the Mediterranean Sea: estimates, patterns, and threats. *PLoS One* 5. doi:10.1371/journal.pone.0011842.

Collier, J. L., and Grossman, A. R. (1994). A small polypeptide triggers complete degradation of light-harvesting phycobiliproteins. *EMBO J.* 13, 1039–1047.

Contreras-Moreira, B., and Vinuesa, P. (2013). GET_HOMOLOGUES, a versatile software package for scalable and robust microbial pangenome analysis. *Appl. Environ. Microbiol.* 79, 7696–7701. doi:10.1128/aem.02411-13.

Crooks, G. E., Hon, G., Chandonia, J. M., and Brenner, S. E. (2004). WebLogo: A sequence logo generator. *Genome Res.* doi:10.1101/gr.849004.

Curren, E., and Leong, S. C. Y. (2019). Profiles of bacterial assemblages from microplastics of tropical coastal environments. *Sci. Total Environ.* 655, 313–320. doi:10.1016/j.scitotenv.2018.11.250.

Dao, M. H. (2013). Reassessment of the cell surface area limitation to nutrient uptake in phytoplankton. *Mar. Ecol. Prog. Ser.* 489, 87–92. doi:10.3354/meps10434.

De Bruijn, *F. J. (2015). Biological Nitrogen Fixation.* Amsterdam: Elsevier Inc, doi: *10.1002/9781119053095*

de Haan, W. P., Sanchez-Vidal, A., and Canals, M. (2019). Floating microplastics and aggregate formation in the Western Mediterranean Sea. *Mar. Pollut. Bull.* 140, 523–535. doi:10.1016/j.marpolbul.2019.01.053.

de Jong, A., Pietersma, H., Cordes, M., Kuipers, O. P., and Kok, J. (2012). PePPER: a webserver for prediction of prokaryote promoter elements and regulons. *BMC Genomics* 13, 1. doi:10.1186/1471-2164-13-299.

DeLano, W. L. (2002). PyMOL: An open-source molecular graphics tool. *CCP4 Newsl. Protein Crystallogr.* doi:10.1038/s41598-017-03842-2.

Diaz, J., Ingall, E., Vogt, S., de Jonge, M. D., Paterson, D., Rau, C., et al. (2009). Characterization of phosphorus, calcium, iron, and other elements in organisms at sub-micron resolution using X-ray fluorescence spectromicroscopy. *Limnol. Oceanogr. Methods* 7, 42–51. doi:10.4319/lom.2009.7.42.

Diaz, J. M., and Plummer, S. (2018). Production of extracellular reactive oxygen species by phytoplankton: past and future directions. *J. Plankton Res.* 40, 655–666. doi:10.1093/plankt/fby039.

Doney, S. C., Fabry, V. J., Feely, R. A., and Kleypas, J. A. (2009). Ocean acidification: The other CO_2 problem. *Ann. Rev. Mar. Sci.* 1, 169–192. doi:10.1146/annurev.marine.010908.163834.

Duhamel, S., Björkman, K. M., van Wambeke, F., Moutin, T., and Karl, D. M. (2011). Characterization of alkaline phosphatase activity in the north and south pacific subtropical gyres: implications for phosphorus cycling. *Limnol. Oceanogr.* 56, 1244–1254. doi:10.4319/lo.2011.56.4.1244.

Dutkiewicz, S., Morris, J. J., Follows, M. J., Scott, J., Levitan, O., Dyhrman, S. T., et al. (2015). Impact of ocean acidification on the structure of future phytoplankton communities. *Nat. Clim. Chang.* 5, 1002–1006. doi:10.1038/nclimate2722.

Dyhrman, S. T., and Haley, S. T. (2006). Phosphorus scavenging in the unicellular marine diazotroph *Crocosphaera watsonii. Appl. Environ. Microbiol.* doi:10.1128/AEM.72.2.1452-1458.2006.

Echeveste, P., Agustí, S., and Dachs, J. (2010). Cell size dependent toxicity thresholds of polycyclic aromatic hydrocarbons to natural and cultured phytoplankton populations. *Environ. Pollut.* 158, 299–307. doi:10.1016/j.envpol.2009.07.006.

Eichner, M., Kranz, S. A., and Rost, B. (2014a). Combined effects of different CO_2 levels and N sources on the diazotrophic cyanobacterium *Trichodesmium*. *Physiol. Plant.* 152, 316–330. doi:10.1111/ppl.12172.

Eichner, M., Rost, B., and Kranz, S. A. (2014b). Diversity of ocean acidification effects on marine N_2 fixers. *J. Exp. Mar. Bio. Ecol.* 457, 199–207. doi:10.1016/j.jembe.2014.04.015.

Erni-cassola, G., Zadjelovic, V., Gibson, M. I., and Christie-oleza, J. A. (2019). Distribution of plastic polymer types in the marine environment; a meta- analysis. *J. Hazard. Mater.* 369, 691–698. doi:10.1016/j.jhazmat.2019.02.067.

Etheridge, D. M., Steele, L. P., Langenfelds, R. L., Francey, R. J., Barnola, J. M., and Morgan, V. I. (1996). Natural and anthropogenic changes in atmospheric CO_2 over the last 1000 years from air in Antarctic ice and firn. *J. Geophys. Res. Atmos.* doi:10.1029/95JD03410.

Everaert, G., Van Cauwenberghe, L., De Rijcke, M., Koelmans, A. A., Mees, J., Vandegehuchte, M., et al. (2018). Risk assessment of microplastics in the ocean: Modelling approach and first conclusions. *Environ. Pollut.* 242, 1930–1938. doi:10.1016/j.envpol.2018.07.069.

Falkowski, P. G. (1997). Evolution of the nitrogen cycle and its influence on the biological sequestration of CO_2 in the ocean. *Nature* 387, 272–275. doi:10.1038/387272a0.

Fernández-Juárez, V., Bennasar-Figueras, A., Tovar-Sanchez, A., and Agawin, N. S. R. (2019). The role of iron in the P-acquisition mechanisms of the unicellular N_2 -fixing cyanobacteria *Halothece* sp., found in association with the Mediterranean seagrass *Posidonia oceanica*. *Front. Microbiol.* 10, 1–22. doi:10.3389/fmicb.2019.01903.

Fernández-Juárez, V., Bennasar-Figueras, A., Sureda-Gomila, A., Ramis-Munar, G., and Agawin, N. S. R. (2020). Differential effects of varying concentrations of phosphorus, iron, and nitrogen in N_2-fixing cyanobacteria. *Front. Microbiol.* 11, 1–19. doi:10.3389/fmicb.2020.541558.

Fernández-Juárez, V., López-Alforja, X., Frank-Comas, A., Echeveste, P., Bennasar-Figueras, A., Ramis-Munar, G., Gomila, R. M., and Agawin, N. S. R. (2021). " The good , the bad and the double-sword" Effects of microplastics and their organic additives in marine bacteria. *Front. Microbiol.* 11, 1–12. doi:10.3389/fmicb.2020.581118.

Ferrat, L., Pergent-Martini, C., and Roméo, M. (2003). Assessment of the use of biomarkers in aquatic plants for the evaluation of environmental quality: application to seagrasses. *Aquat. Toxicol.* 65, 187–204. doi:10.1016/S0166-445X(03)00133-4.

Fillat, M. F. (2014). The fur (ferric uptake regulator) superfamily: diversity and versatility of key transcriptional regulators. *Arch. Biochem. Biophys.* 546, 41–52. doi:10.1016/j.abb.2014.01.029.

Finn, R. D., Coggill, P., Eberhardt, R. Y., Eddy, S. R., Mistry, J., Mitchell, A. L., et al. (2016). The Pfam protein families database: towards a more sustainable future. *Nucleic Acids Res.* 44, D279–D285. doi:10.1093/nar/gkv1344.

Flecha, S., Pérez, F. F., García-Lafuente, J., Sammartino, S., Ríos, A. F., and Huertas, I. E. (2015). Trends of pH decrease in the Mediterranean Sea through high frequency observational data: Indication of ocean acidification in the basin. *Sci. Rep.* 5, 1–8. doi:10.1038/srep16770.

Flombaum, P., Gallegos, J. L., Gordillo, R. A., Rincon, J., Zabala, L. L., Jiao, N., et al. (2013). Present and future global distributions of the marine Cyanobacteria *Prochlorococcus* and *Synechococcus*. *Proc. Natl. Acad. Sci.* 110, 9824–9829. doi:10.1073/pnas.1307701110.

Fredriksson, C., and Bergman, B. (1997). Ultrastructural characterisation of cells specialised for nitrogen fixation in a non-heterocystous cyanobacterium, *Trichodesmium* spp. *Protoplasma* 197, 76–85. doi:10.1007/BF01279886.

Friedlingstein, P., O'Sullivan, M., Jones, M. W., Andrew, R. M., Hauck, J., Olsen, A., Peters, G. P., Peters, W., Pongratz, J., Sitch, S., Le Quéré, C., Canadell, J. G., Ciais, P., Jackson, R. B., Alin, S., Aragão, L. E. O. C., Arneth, A., Arora, V., Bates, N. R., Becker, M., Benoit-Cattin, A., Bittig, H. C., Bopp, L., Bultan, S., Chandra, N., Chevallier, F., Chini, L. P., Evans, W., Florentie, L., Forster, P. M., Gasser, T., Gehlen, M., Gilfillan, D., Gkritzalis, T., Gregor, L., Gruber, N., Harris, I., Hartung, K., Haverd, V., Houghton, R. A., Ilyina, T., Jain, A. K., Joetzjer, E., Kadono, K., Kato, E., Kitidis, V., Korsbakken, J. I., Landschützer, P., Lefèvre, N., Lenton, A., Lienert, S., Liu, Z., Lombardozzi, D., Marland, G., Metzl, N., Munro, D. R., Nabel, J. E. M. S., Nakaoka, S.-I., Niwa, Y., O'Brien, K., Ono, T., Palmer, P. I., Pierrot, D., Poulter, B., Resplandy, L., Robertson, E., Rödenbeck, C., Schwinger, J., Séférian, R., Skjelvan, I., Smith, A. J. P., Sutton, A. J., Tanhua, T., Tans, P. P., Tian, H., Tilbrook, B., van der Werf, G., Vuichard, N., Walker, A. P., Wanninkhof, R., Watson, A. J., Willis, D., Wiltshire, A. J., Yuan, W., Yue, X., and Zaehle, S. (2020).

Global Carbon Budget, Earth Syst. Sci. Data, 12, 3269–3340, https://doi.org/10.5194/essd-12-3269-2020, 2020.

Fu, F. X., Zhang, Y., Bell, P. R. F., and Hutchins, D. A. (2005). Phosphate uptake and growth kinetics of *Trichodesmium* (Cyanobacteria) isolates from the North Atlantic Ocean and the Great Barrier Reef, Australia. *J. Phycol.* 41, 62–73. doi:10.1111/j.1529-8817.2005.04063.x.

Fu, F. X., Warner, M. E., Zhang, Y., Feng, Y., and Hutchins, D. A. (2007). Effects of increased temperature and CO_2 on photosynthesis, growth, and elemental ratios in marine *Synechococcus* and *Prochlorococcus* (Cyanobacteria). *J. Phycol.* 43, 485–496. doi:10.1111/j.1529-8817.2007.00355.x.

Fu, F. X., Mulholland, M. R., Garcia, N. S., Beck, A., Bernhardt, P. W., Warner, M. E., Sañudo-Wilhelmy, S. A, and Hutchins., D. A (2008). Interactions between changing pCO_2, N_2 fixation, and Fe limitation in the marine unicellular cyanobacterium *Crocosphaera*. *Limnol. Oceanogr.* 53, 2472–2484. doi:10.4319/lo.2008.53.6.2472.

Fu, F. X., Yu, E., Garcia, N. S., Gale, J., Luo, Y., Webb, E. A., and Hutchins D. A. (2014). Differing responses of marine N_2 fixers to warming and consequences for future diazotroph community structure. *Aquat. Microb. Ecol.* 72, 33–46. doi:10.3354/ame01683.

Gallo, F., Fossi, C., Weber, R., Santillo, D., Sousa, J., Ingram, I., et al. (2018). Marine litter plastics and microplastics and their toxic chemicals components: the need for urgent preventive measures. *Environ. Sci. Eur.* 30. doi:10.1186/s12302-018-0139-z.

Garcia, N. S., Fu, F. X., Breene, C. L., Bernhardt, P. W., Mulholland, M. R., Sohm, J. A., et al. (2011). Interactive effects of irradiance and CO_2 on CO_2 fixation and N_2 fixation in the diazotroph *Trichodesmium erythraeum* (cyanobacteria). *J. Phycol.* 47, 1292–1303. doi:10.1111/j.1529-8817.2011.01078.x.

Garcia, N. S., Fu, F. X., Breene, C. L., Yu, E. K., Bernhardt, P. W., Mulholland, M. R., et al. (2013a). Combined effects of CO_2 and light on large and small isolates of the unicellular N_2-fixing cyanobacterium *Crocosphaera* watsonii from the western tropical Atlantic Ocean. *Eur. J. Phycol.* 48, 128–139. doi:10.1080/09670262.2013.773383.

Garcia, N. S., Fu, F. X., and Hutchins, D. A. (2013b). Colimitation of the unicellular photosynthetic diazotroph *Crocosphaera watsonii* by phosphorus, light, and carbon dioxide. *Limnol. Oceanogr.* 58, 1501–1512. doi:10.4319/lo.2013.58.4.1501.

Garcia, N. S., Fu, F., Sedwick, P. N., and Hutchins, D. A. (2015). Iron deficiency increases growth and nitrogen-fixation rates of phosphorus-deficient marine cyanobacteria. *ISME J.* 9, 238–245. doi:10.1038/ismej.2014.104.

García, M. J. L. (2015). Recent warming in the balearic sea and Spanish Mediterranean coast. Towards an earlier and longer summer. *Atmosfera* 28, 149–160. doi:10.20937/atm.2015.28.03.01.

Gardner, S. G., Johns, K. D., Tanner, R., and McCleary, W. R. (2014). The PhoU protein from *Escherichia coli* interacts with PhoR, PstB, and metals to form a phosphate-signaling complex at the membrane. *J. Bacteriol.* 196, 1741–1752. doi:10.1128/JB.00029-14.

Ge, C., Chai, Y., Wang, H., and Kan, M. (2017). Ocean acidification: one potential driver of phosphorus eutrophication. *Mar. Pollut. Bull.* 115, 149–153. doi:10.1016/j.marpolbul.2016.12.016.

Geider, R. J., and La Roche, J. (2002). Redfield revisited: variability of C:N:P in marine microalgae and its biochemical basis. *Eur. J. Phycol.* 37, 1–17. doi:10.1017/S0967026201003456.

Ghaffar, S., Stevenson, R. J., and Khan, Z. (2017). Effect of phosphorus stress on *Microcystis aeruginosa* growth and phosphorus uptake. *PLoS One* 12. doi:10.1371/journal.pone.0174349.

Giner-Lamia, J., Robles-Rengel, R., Hernández-Prieto, M. A., Isabel Muro-Pastor, M., Florencio, F. J., and Futschik, M. E. (2017). Identification of the direct regulon of NtcA during early acclimation to nitrogen starvation in the cyanobacterium *Synechocystis* sp. PCC 6803. *Nucleic Acids Res.* 45, 11800–11820. doi:10.1093/nar/gkx860.

Golosova, O., Henderson, R., Vaskin, Y., Gabrielian, A., Grekhov, G., Nagarajan, V., et al. (2014). Unipro UGENE NGS pipelines and components for variant calling, RNA-seq and ChIP-seq data analyses. *PeerJ* 2, e644. doi:10.7717/peerj.644.

Großkopf, T., and Soyer, O. S. (2014). Synthetic microbial communities. *Curr. Opin. Microbiol.* 18, 72–77. doi:10.1016/j.mib.2014.02.002.

Guillard, R. R. L. (1973). Division rate. *Handb. of phycological methods (Stein, J.R., Ed. Cambridge Univ. Press. Cambridge*, 289–311. doi:10.1016/S0927-0507(07)15025-8.

Gurevich, A., Saveliev, V., Vyahhi, N., and Tesler, G. (2013). QUAST: Quality assessment tool for genome assemblies. *Bioinformatics*.

doi:10.1093/bioinformatics/btt086.

Gutiérrez, J. L., Jones, C. G., Byers, J. E., Arkema, K. K., Berkenbusch, K., Commito, A., et al. (2012). 'Physical ecosystem engineers and the functioning of estuaries and coasts'. *Treatise on Estuarine and Coastal Science* doi:10.1016/B978-0-12-374711-2.00705-1.

Haft, D. H., DiCuccio, M., Badretdin, A., Brover, V., Chetvernin, V., O'Neill, K., et al. (2018). RefSeq: An update on prokaryotic genome annotation and curation. *Nucleic Acids Res.* doi:10.1093/nar/gkx1068.

Hahladakis, J. N., Velis, C. A., Weber, R., Iacovidou, E., and Purnell, P. (2018). An overview of chemical additives present in plastics: Migration, release, fate and environmental impact during their use, disposal and recycling. *J. Hazard. Mater.* 344, 179–199. doi:10.1016/j.jhazmat.2017.10.014.

Hansen, H. P., and Koroleff, F. (2007). "Determination of nutrients" in *Method of seawater analysis*. eds. K. Grasshoff, K. Kremling, and M. Ehrhardt. doi: 10.1002/9783527613984.ch10

Haramaty, L., Quigg, A., Berman-Frank, I., Finkel, Z. V., and Irwin, A. J. (2007). Nitrogen-fixation strategies and Fe requirements in cyanobacteria. *Limnol. Oceanogr.* 52, 2260–2269. doi:10.4319/lo.2007.52.5.2260.

Harpole, W. S., Ngai, J. T., Cleland, E. E., Seabloom, E. W., Borer, E. T., Bracken, M. E. S., et al. (2011). Nutrient co-limitation of primary producer communities. *Ecol. Lett.* 14, 852–862. doi:10.1111/j.1461-0248.2011.01651.x.

Harrison, Jesse P.; Sapp, Melanie; Schratzberger, Michaela; Osborn, A. M. (2011). Interactions between micro-organisms and metronidazole. *J. Antimicrob. Chemother.* 10, 84–87. doi:10.1093/jac/10.2.84.

Hartmann, N. B., Hüffer, T., Thompson, R. C., Hassellöv, M., Verschoor, A., Daugaard, A. E., et al. (2019). Are we speaking the same language? recommendations for a definition and categorization framework for plastic debris. *Environ. Sci. Technol.* 53, 1039–1047. doi:10.1021/acs.est.8b05297.

Hassenteufel, W., Jagitsch, R., and Kocz, F. . (1963). Impregnation of glass surfacae against sortion of phospahate traces. *Limnol. Oceanogr.* 8, 152–156.

Hauksson, J. B., Andrésson, Ó. S., and Ásgeirsson, B. (2000). Heat-labile bacterial alkaline phosphatase from a marine Vibrio sp. *Enzyme Microb. Technol.* 27, 66–73. doi:10.1016/S0141-0229(00)00152-6.

He, Z., Xiong, J., Kent, A. D., Deng, Y., Xue, K., Wang, G., et al. (2014). Distinct responses of soil microbial communities to elevated CO_2 and O_3 in a soybean agro-ecosystem. *ISME J.* 8, 714–726. doi:10.1038/ismej.2013.177.

Hedges, L. V., Gurevitch, J., and Curtis, P. S. (1999). The meta-analysis of response ratios in experimental ecology. Ecology 80, 1150–1156. doi: 10.1890/0012-9658(1999)080[1150:tmaorr]2.0.co;2

Hellweger, F. L., Huang, Y., and Luo, H. (2018). Carbon limitation drives GC content evolution of a marine bacterium in an individual-based genome-scale model. *ISME J.* 12, 1180–1187. doi:10.1038/s41396-017-0023-7.

Hemminga, M. A., and Duarte, C. M. (2002). Book Reviews. *Limnol. Ocean.* 55, 193–196. doi:10.1348/000711002159653.

Hennon, G. M., Morris, J. J., Haley, S. T., Zinser, E. R., Durrant, A. R., Entwistle, E., et al. (2017). The impact of elevated CO_2 on *Prochlorococcus* and microbial interactions with a 'helper' bacterium *Alteromonas*. *ISME J.* 12, 520–531. doi:10.1038/ismej.2017.189.

Hermabessiere, L., Dehaut, A., Paul-Pont, I., Lacroix, C., Jezequel, R., Soudant, P., et al. (2017). Occurrence and effects of plastic additives on marine environments and organisms: A review. *Chemosphere*. doi:10.1016/j.chemosphere.2017.05.096.

Hernández, I., Niell, F. X., and Whitton, B. A. (2002). Phosphatase activity of benthic marine algae. An overview. *J. Appl. Phycol.* 14, 475–487. doi:10.1023/A:1022370526665.

Herrero, A., and Flores, E. (2008). The cyanobacteria: Molecular biology, genomics, and evolution. Wymondham, UK: Caister Academic Press.

Hillebrand, H., Dürselen, C. D., Kirschtel, D., Pollingher, U., and Zohary, T. (1999). Biovolume calculation for pelagic and benthic microalgae. *J. Phycol.* 35, 403–424. doi:10.1046/j.1529-8817.1999.3520403.x.

Hoegh-Guldberg, O., and Bruno, J. F. (2010). The impact of climate change on the world's marine ecosystems. *Science (80-.).* 328, 1523–1528. doi:10.1126/science.1189930.

Hoffman, B. M., Lukoyanov, D., Yang, Z.-Y., Dean, D. R., and Seefeldt, L. C. (2014). Mechanism of nitrogen fixation by nitrogenase: the next stage. *Chem. Rev.* 114, 4041–4062. doi:10.1021/cr400641x.

Hong, H., Shen R., and Zhang, F. (2017). The complex effects of ocean acidification on the prominent N_2-fixing cyanobacterium *Trichodesmium*. *Science (80-.).* 357, 527–531. doi:10.1126/science.aao0067.

Huang, B. (2009). MetaPocket : A meta approach to improve protein ligand binding site Prediction. 13, 325–330.

Huerta-Cepas, J., Szklarczyk, D., Heller, D., Hernández-Plaza, A., Forslund, S. K., Cook, H., et al. (2018). eggNOG 5.0: a hierarchical, functionally and phylogenetically annotated orthology resource based on 5090 organisms and 2502 viruses. *Nucleic Acids Res.* 47, 309–314. doi:10.1093/nar/gky1085.

Hutchins, D. A., Fu, F. X., Zhang, Y., Warner, M. E., Feng, Y., Portune, K., Bernhardt, P. W, and Mulholland, M. R. (2007). CO_2 control of *Trichodesmium* N_2 fixation, photosynthesis, growth rates, and elemental ratios: Implications for past, present, and future ocean biogeochemistry. *Limnol. Oceanogr.* 52, 1293–1304. doi:10.4319/lo.2007.52.4.1293.

Ibacache-Quiroga, C., Ojeda, J., Espinoza-Vergara, G., Olivero, P., Cuellar, M., and Dinamarca, M. A. (2013). The hydrocarbon-degrading marine bacterium *Cobetia* sp. strain MM1IDA2H-1 produces a biosurfactant that interferes with quorum sensing of fish pathogens by signal hijacking. *Microb. Biotechnol.* 6, 394–405. doi:10.1111/1751-7915.12016.

IPCC. Climate Change 2014: Impacts, Adaptation, and Vulnerability. Part A: global and sectoral aspects. contribution of working group ii to the fifth assessment report of the intergovernmental panel on climate change 1132 (Cambridge University Press, 2014).

Ivleva, N. B., and Golden, S.S. (2007). Protein extraction, fractionation, and purification from cyanobacteria. Methods Mol. Biol. 362, 365-73. doi: 10.1007/978-1-59745-257-1_26

Jacq, V. (2014). Response of the unicellular diazotrophic Cyanobacterium *Crocosphaera watsonii* to iron limitation. *PLoS One* 9. doi:10.1371/journal.pone.0086749.

Jaén-Luchoro, D., Aliaga-Lozano, F., Gomila, R. M., Gomila, M., Salvà-Serra, F., Lalucat, J., et al. (2017). First insights into a type II toxin-antitoxin system from the clinical isolate *Mycobacterium* sp. MHSD3, similar to epsilon/zeta systems. *PLoS One* 12, 1–20. doi:10.1371/journal.pone.0189459.

Jaén-Luchoro, D., Gonzales-Siles, L., Karlsson, R., Svensson-Stadler, L., Molin, K., Cardew, S., et al. (2020). *Corynebacterium sanguinis* sp. nov., a clinical and

environmental associated *Corynebacterium*. *Syst. Appl. Microbiol.* 43, 126039. doi:10.1016/j.syapm.2019.126039.

Jensen, B. B., and Cox, R. P. (1983). Direct measurements of steady-state kinetics of cyanobacterial N_2 uptake by membrane-leak mass spectrometry and comparisons between nitrogen fixation and acetylene reduction. *Appl. Environ. Microbiol.* 45, 1331–1337.

Jiang, H. B., Fu, F. X., Rivero-Calle, S., Levine, N. M., Sañudo-Wilhelmy, S. A., Qu, P. P., Wang, X. W., Pinedo-Gonzalez, P., Zhu, Z., and Hutchins D. A. (2018). Ocean warming alleviates iron limitation of marine nitrogen fixation. *Nat. Clim. Chang.* 8, 709–712. doi:10.1038/s41558-018-0216-8.

Jiang, L. Q., Carter, B. R., Feely, R. A., Lauvset, S. K., and Olsen, A. (2019). Surface ocean pH and buffer capacity: past, present and future. *Sci. Rep.* 9, 1–11. doi:10.1038/s41598-019-55039-4.

Joint, I., Doney, S. C., and Karl, D. M. (2011). Will ocean acidification affect marine microbes. *ISME J.* 5, 1–7. doi:10.1038/ismej.2010.79.

Kadam, P. C., and Boone, D. R. (1996). Influence of pH on ammonia accumulation and toxicity in halophilic, methylotrophic methanogens. *Appl. Environ. Microbiol.* 62, 4486–4492. doi:10.1128/aem.62.12.4486-4492.1996.

Kageyama, H., Tripathi, K., Rai, A. K., Cha-Um, S., Waditee-Sirisattha, R., and Takabe, T. (2011). An alkaline phosphatase/phosphodiesterase, PhoD, induced by salt stress and secreted out of the cells of *Aphanothece halophytica*, a halotolerant cyanobacterium. *Appl. Environ. Microbiol.* 77, 5178–5183. doi:10.1128/AEM.00667-11.

Kane, I.A., Clare, M.A., Miramontes, E., Wogelius, R., Rothwell, J.J., Garreau, P., et al. (2020). Seafloor microplastic hotspots controlled by deep-sea circulation. *Science* 5899:aba5899. doi: 10.1126/science.aba5899

Kaushik, M. S., Singh, P., Tiwari, B., and Mishra, A. K. (2016). Ferric Uptake Regulator (FUR) protein: properties and implications in cyanobacteria. *Ann. Microbiol.* 66, 61–75. doi:10.1007/s13213-015-1134-x.

Kawai, F. (2010). The biochemistry and molecular biology of xenobiotic polymer degradation by Microorganisms. *Biosci. Biotechnol. Biochem.* 74, 1743–1759. doi:10.1271/bbb.100394.

Kennedy, E. J. (2014). Biological Drug Products: Development and Strategies . Edited by Wei Wang and Manmohan Singh . *ChemMedChem*.

doi:10.1002/cmdc.201402432.

Kim, H., Choo, Y. J., Song, J., Lee, J. S., Lee, K. C., and Cho, J. C. (2007). *Marinobacterium litorale* sp. nov. in the order *Oceanospirillales*. *Int. J. Syst. Evol. Microbiol.* 57, 1659–1662. doi:10.1099/ijs.0.64892-0.

Kim, J. M., Lee, K., Shin, K., Kang, J. H., Lee, H. W., Kim, M., et al. (2006). The effect of seawater CO_2 concentration on growth of a natural phytoplankton assemblage in a controlled mesocosm experiment. *Limnol. Oceanogr.* 51, 1629–1636. doi:10.4319/lo.2006.51.4.1629.

Kim, M. S., Roh, S. W., and Bae, J. W. (2010). *Cobetia crustatorum* sp. nov., a novel slightly halophilic bacterium isolated from traditional fermented seafood in Korea. *Int. J. Syst. Evol. Microbiol.* 60, 620–626. doi:10.1099/ijs.0.008847-0.

Klotz, A., Georg, J., Bučinská, L., Watanabe, S., Reimann, V., Januszewski, W., et al. (2016). Awakening of a dormant cyanobacterium from nitrogen chlorosis reveals a genetically determined Program. *Cell Press* 26, 2862–2872. doi:10.1016/j.cub.2016.08.054.

Klotz, A., Reinhold, E., Doello, S., and Forchhammer, K. (2015). Nitrogen Starvation Acclimation in *Synechococcus elongatus*: Redox-Control and the Role of Nitrate Reduction as an Electron Sink. *Life* 5, 888–904. doi:10.3390/life5010888.

Knapp, A. N. (2012). The sensitivity of marine N2 fixation to dissolved inorganic nitrogen. *Front. Microbiol.* 3, 1–14. doi:10.3389/fmicb.2012.00374.

Kornberg, A. (1995). Inorganic polyphosphate: Toward making a forgotten polymer unforgettable. *J. Bacteriol.* 177, 491–496. doi:10.1128/jb.177.3.491-496.1995.

Kranz, S. A., Sültemeyer, D., Richter, K. U., and Rost, B. (2009). Carbon acquisition by Trichodesmium: the effect of pCO_2 and diurnal changes. *Limnol. Oceanogr.* 54, 548–559. doi:10.4319/lo.2009.54.2.0548.

Kranz, S. A., Eichner, M., and Rost, B. (2011). Interactions between CCM and N_2 fixation in *Trichodesmium*. *Photosynth. Res.* 109, 73–84. doi:10.1007/s11120-010-9611-3.

Kranzler, C., Rudolf, M., Keren, N., and Schleiff, E. (2013). *Iron in Cyanobacteria*. doi:10.1016/B978-0-12-394313-2.00003-2.

Kranzler, C., Lis, H., Finkel, O. M., Schmetterer, G., Shaked, Y., and Keren, N. (2014). Coordinated transporter activity shapes high-affinity iron acquisition in cyanobacteria. *ISME J.* 8, 409–417. doi:10.1038/ismej.2013.161.

Krauk, J. M., Villareal, T. A., Sohm, J. A., Montoya, J. P., and Capone, D. G. (2006). Plasticity of N:P ratios in laboratory and field populations of *Trichodesmium* spp. *Aquat. Microb. Ecol.* 42, 243–253. doi:10.3354/ame042243.

Krause, E., Wichels, A., Giménez, L., Lunau, M., Schilhabel, M. B., and Gerdts, G. (2012). Small changes in ph have direct effects on marine bacterial community composition: a microcosm approach. *PLoS One* 7. doi:10.1371/journal.pone.0047035.

Kretz, C. B., Bell, D. W., Lomas, D. A., Lomas, M. W., and Martiny, A. C. (2015). Influence of growth rate on the physiological response of marine *Synechococcus* to phosphate limitation. *Front. Microbiol.* 6, 6–11. doi:10.3389/fmicb.2015.00085.

Kühn, S., Bravo Rebolledo, E. L., and Van Franeker, J. A. (2015). 'Deleterious effects of litter on marine life', in *Marine Anthropogenic Litter* doi:10.1007/978-3-319-16510-3_4.

Kumar, S., Stecher, G., and Tamura, K. (2016). MEGA7: molecular evolutionary genetics analysis version 7.0 for Bigger Datasets. *Mol. Biol. Evol.* doi:10.1093/molbev/msw054.

Kuo, J. (2005). A revision of the genus *Heterozostera* (*Zosteraceae*). *Aquat. Bot.* doi:10.1016/j.aquabot.2004.10.005.

Küpper, H., Šetlík, I., Seibert, S., Prášil, O., Šetlikova, E., Strittmatter, M., et al. (2008). Iron limitation in the marine cyanobacterium *Trichodesmium* reveals new insights into regulation of photosynthesis and nitrogen fixation. *New Phytol.* 179, 784–798. doi:10.1111/j.1469-8137.2008.02497.x.

Kustka, A. B., Sañudo-Wilhelmy, S. A., Carpenter, E. J., Capone, D., Burns, J., and Sunda, W. G. (2004). Iron requirements for dinitrogen- and ammonium-supported growth in cultures of *Trichodesmium* (IMS 101): Comparison with nitrogen fixation rates and iron:carbon ratios of field populations. *Limnol. Oceanogr.* 49, 1224. doi:10.4319/lo.2004.49.4.1224.

Kuznecova, J., Šulčius, S., Vogts, A., Voss, M., Jürgens, K., and Šimoliūnas, E. (2020). Nitrogen flow in diazotrophic cyanobacterium *Aphanizomenon flos-aquae* is altered by cyanophage Infection. *Front. Microbiol.* 11, 1–14. doi:10.3389/fmicb.2020.02010.

Kuznetsov, S. I., Dubinina, G. A., and Lapteva, N. A. (1979). Biology of oligotrophic bacteria. *Annu. Rev. Microbiol.* 33, 377–387. doi:10.1146/annurev.mi.33.100179.002113.

Lagus, A., Suomela, J., Weithoff, G., Heikkilä, K., Helminen, H., and Sipura, J. (2004). Species-specific differences in phytoplankton responses to N and P enrichments and the N:P ratio in the Archipelago Sea, northern Baltic Sea. *J. Plankton Res.* 26, 779–798. doi:10.1093/plankt/fbh070.

Latifi, A., Jeanjean, R., Lemeille, S., Havaux, M., and Zhang, C. C. (2005). Iron starvation leads to oxidative stress in *Anabaena* sp. strain PCC 7120. *J. Bacteriol.* doi:10.1128/JB.187.18.6596-6598.2005.

Latifi, A., Ruiz, M., and Zhang, C. C. (2009). Oxidative stress in cyanobacteria. *FEMS Microbiol. Rev.* 33, 258–278. doi:10.1111/j.1574-6976.2008.00134.x.

Lau, C. K. Y., Krewulak, K. D., and Vogel, H. J. (2016). Bacterial ferrous iron transport: The Feo system. *FEMS Microbiol. Rev.* 40, 273–298. doi:10.1093/femsre/fuv049.

Lazzari, P., Solidoro, C., Salon, S., and Bolzon, G. (2016). Spatial variability of phosphate and nitrate in the Mediterranean Sea: a modeling approach. *Deep. Res. Part I Oceanogr. Res. Pap.* 108, 39–52. doi:10.1016/j.dsr.2015.12.006.

Lee, S. J., Park, Y. S., Kim, S. J., Lee, B. J., and Suh, S. W. (2014). Crystal structure of PhoU from *Pseudomonas aeruginosa*, a negative regulator of the Pho regulon. *J. Struct. Biol.* 188, 22–29. doi:10.1016/j.jsb.2014.08.010.

Lejeusne, C., Chevaldonné, P., Pergent-Martini, C., Boudouresque, C. F., and Pérez, T. (2010). Climate change effects on a miniature ocean: the highly diverse, highly impacted Mediterranean Sea. *Trends Ecol. Evol.* 25, 250–260. doi:10.1016/j.tree.2009.10.009.

Lesser, M. P. (2006). Oxidative stress in marine environments: biochemistry and physiological ecology. *Annu. Rev. Physiol.* 68, 253–278. doi:10.1146/annurev.physiol.68.040104.110001.

Levitan, O., Rosenberg, G., Setlik, I., Setlikova, E., Grigel, J., Klepetar, J., Prasil, O. and Berman-Frank, I. (2007). Elevated CO_2 enhances nitrogen fixation and growth in the marine cyanobacterium *Trichodesmium*. *Glob. Chang. Biol.* 13, 531–538. doi:10.1111/j.1365-2486.2006.01314.x.

Li, W. K. W., McLaughlin, F. A., Lovejoy, C., and Carmack, E. C. (2009). Smallest algae thrive as the arctic ocean freshens. *Science (80-.).* 326, 539. doi:10.1126/science.1179798.

Li, P., Liu, W., and Gao, K. (2013). Effects of temperature, pH, and UV radiation on alkaline phosphatase activity in the terrestrial cyanobacterium *Nostoc flagelliforme*. *J. Appl. Phycol.* 25, 1031–1038. doi:10.1007/s10811-012-9936-8.

Li, Z., Natarajan, P., Ye, Y., Hrabe, T., and Godzik, A. (2014). POSA: A user-driven, interactive multiple protein structure alignment server. *Nucleic Acids Res.* 42. doi:10.1093/nar/gku394.

Litchman, E., Edwards, K. F., Klausmeier, C. A., and Thomas, M. K. (2012). Phytoplankton niches, traits and eco-evolutionary responses to global environmental change. *Mar. Ecol. Prog. Ser.* 470, 235–248. doi:10.3354/meps09912.

Liu, W., Au, D. W. T., Anderson, D. M., Lam, P. K. S., and Wu, R. S. S. (2007). Effects of nutrients, salinity, pH and light:dark cycle on the production of reactive oxygen species in the alga *Chattonella marina*. *J. Exp. Mar. Bio. Ecol.* 346, 76–86. doi:10.1016/j.jembe.2007.03.007.

Llacer, J. L., Espinosa, J., Castells, M. A., Contreras, A., Forchhammer, K., and Rubio, V. (2010). Structural basis for the regulation of NtcA-dependent transcription by proteins PipX and PII. *Proc. Natl. Acad. Sci.* 107, 15397–15402. doi:10.1073/pnas.1007015107.

López-Gomollón, S., Hernández, J. A., Wolk, C. P., Peleato, M. L., and Fillat, M. F. (2007). Expression of furA is modulated by NtcA and strongly enhanced in heterocysts of *Anabaena* sp. PCC 7120. *Microbiology* 153, 42–50. doi:10.1099/mic.0.2006/000091-0.

Lubin, E. A., Fiebig, A., Laub, M. T., Henry, J. T., and Crosson, S. (2015). Identification of the PhoB regulon and role of phou in the phosphate starvation response of *Caulobacter crescentus*. *J. Bacteriol.* 198, 187–200. doi:10.1128/jb.00658-15.

Luo, H., Benner, R., Long, R. A., and Hu, J. (2009). Subcellular localization of marine bacterial alkaline phosphatases. *Proc. Natl. Acad. Sci.* 106, 21219–21223. doi:10.1073/pnas.0907586106.

Machado, M. C., Vimbela, G. V., Silva-Oliveira, T. T., Bose, A., and Tripathi, A. (2020). The response of *Synechococcus* sp. PCC 7002 to micro-/nano polyethylene particles - Investigation of a key anthropogenic stressor. *PLoS One* 15, 1–14. doi:10.1371/journal.pone.0232745.

Mackey, K. R. M., Mioni, C. E., Ryan, J. P., and Paytan, A. (2012). Phosphorus cycling in the red tide incubator region of Monterey Bay in response to upwelling. *Front. Microbiol.* 3, 1–14. doi:10.3389/fmicb.2012.00033.

Mahowald, N. M., Hamilton, D. S., Mackey, K. R. M., Moore, J. K., Baker, A. R., Scanza, R. A., et al. (2018). Aerosol trace metal leaching and impacts on marine microorganisms. *Nat. Commun.* 9. doi:10.1038/s41467-018-04970-7.

Maity, S., and Pramanick, K. (2020). Perspectives and challenges of micro/nanoplastics-induced toxicity with special reference to phytotoxicity. *Glob. Chang. Biol.* 26, 3241–3250. doi:10.1111/gcb.15074.

Manhart, J. R., and Wong, P. P. (1980). Nitrate effect on nitrogen fixation (acetylene reduction): activities of legume root nodules induced by rhizobia with varied nitrate reductase activities. *Plant Physiol.* 65, 502–505. doi:10.1104/pp.65.3.502.

Marañón, E., Lorenzo, M. P., Cermeño, P., and Mouriño-Carballido, B. (2018). Nutrient limitation suppresses the temperature dependence of phytoplankton metabolic rates. *ISME J.* 12, 1836–1845. doi:10.1038/s41396-018-0105-1.

Marmur, J. (1961). A procedure for the isolation of deoxyribonucleic acid from micro-organisms. *J. Mol. Biol.* doi:10.1016/S0022-2836(61)80047-8.

Martínez-Crego, B., Romero, J., and Alcoverro, T. (2006). The use of surface alkaline phosphatase activity in the seagrass *Posidonia oceanica* as a biomarker of eutrophication. *Mar. Ecol.* 27, 381–387. doi:10.1111/j.1439-0485.2006.00101.x.

Meier-Kolthoff, J. P., Auch, A. F., Klenk, H. P., and Göker, M. (2013). Genome sequence-based species delimitation with confidence intervals and improved distance functions. *BMC Bioinformatics*. doi:10.1186/1471-2105-14-60.

Mills, M. M., Ridame, C., Davey, M., La Roche, J., and Geider, R. J. (2004). Iron and phosphorus co-limit nitrogen fixation in the eastern tropical North Atlantic. *Nature*, 232–294. doi:10.1038/nature02550.

Monod, J. (1949). The growth of bacterial cultures. *Annu. Rev. Microbiol.* doi:10.1146/annurev.mi.03.100149.002103.

Montecino, V., and Lange, C. B. (2009). The Humboldt Current System: Ecosystem components and processes, fisheries, and sediment studies. *Prog. Oceanogr.* doi:10.1016/j.pocean.2009.07.041.

Moore, C. M., Mills, M. M., Langlois, R., Milne, A., Achterberg, E. P., La Roche, J., et al. (2008). Relative influence of nitrogen and phosphorus availability on phytoplankton physiology and productivity in the oligotrophic sub-tropical North Atlantic Ocean. *Limnol. Oceanogr.* 53, 291–305. doi:10.4319/lo.2008.53.1.0291.

Moore, C. M, Mills, M. M., Achterberg, E. P., Geider, R. J., Laroche, J., Lucas, M. I., et al. (2009). Large-scale distribution of Atlantic nitrogen fixation controlled by iron availability. *Nat. Geosci.*, 867–871.

Moore, C. M., Mills, M. M., Arrigo, K. R., Berman-Frank, I., Bopp, L., Boyd, P. W., et al. (2013). Processes and patterns of oceanic nutrient limitation. *Nat. Geosci.*, 701–710. doi:10.1038/ngeo1765.

Moore, J. K., Doney, S. C., Glover, D. M., and Fung, I. Y. (2001). Iron cycling and nutrient-limitation patterns in surface waters of the world ocean. *Deep. Res. Part II Top. Stud. Oceanogr.* 49, 463–507. doi:10.1016/S0967-0645(01)00109-6.

Morris, J. J., R. Kirkegaard, M. J. Szul, Z. I. Johnson, and E. R. Zinser. 2008. Facilitation of robust growth of *Prochlorococcus* colonies and dilute liquid cultures by 'helper' heterotrophic bacteria. Appl. Environ. Microbiol. doi:10.1128/AEM.02479-07

Millero, F. J., Woosey, R., Ditrolio, B., and Water J. (2009). Effect of ocean acidification on the speciation of metals in seawater. *Oceanography* 22, 72–85. doi:10.5670/oceanog.2009.98

Mus, F., Alleman, A. B., Pence, N., Seefeldt, L. C., and Peters, J. W. (2018). Exploring the alternatives of biological nitrogen fixation. *Metallomics* 10, 523–538. doi:10.1039/c8mt00038g.

Naik, R. K., Naik, M. M., D'Costa, P. M., and Shaikh, F. (2019). Microplastics in ballast water as an emerging source and vector for harmful chemicals, antibiotics, metals, bacterial pathogens and HAB species: A potential risk to the marine environment and human health. *Mar. Pollut. Bull.* 149, 110525. doi:10.1016/j.marpolbul.2019.110525.

Nelms, S. E., Galloway, T. S., Godley, B. J., Jarvis, D. S., and Lindeque, P. K. (2018). Investigating microplastic trophic transfer in marine top predators. *Environ. Pollut.* 238, 999–1007. doi:10.1016/j.envpol.2018.02.016.

Nelson, D. C., Waterbury, J. B., and Jannasch, H. W. (1982). Nitrogen fixation and nitrate utilization by marien and freshwater Beggiatoa. *Mar. Biol.*, 172–177.

Ng, T. S., Chew, S. Y., Rangasamy, P., Mohd Desa, M. N., Sandai, D., Chong, P. P., et al. (2015). SNF3 as high affinity glucose sensor and its function in supporting the viability of *Candida glabrata* under glucose-limited environment. *Front. Microbiol.* 6, 1–12. doi:10.3389/fmicb.2015.01334.

Nielsen, L. T., Hallegraeff, G. M., Wright, S. W., and Hansen, P. J. (2012). Effects of experimental seawater acidification on an estuarine plankton community. *Aquat. Microb. Ecol.* 65, 271–285. doi:10.3354/ame01554.

Noinaj, N., Guillier, M., Barnard, T. J., and Buchanan, S. K. (2010). TonB-Dependent transporters: tegulation, structure, and function. *Annu. Rev. Microbiol.* 64, 43–60. doi:10.1146/annurev.micro.112408.134247.

Noskova, Y., Likhatskaya, G., Terentieva, N., Son, O., Tekutyeva, L., and Balabanova, L. (2019). A novel alkaline phosphatase/phosphodiesterase, CamPhoD, from marine bacterium *Cobetia amphilecti* KMM 296. *Mar. Drugs* 17, 1–20. doi:10.3390/md17120657.

Novichkov, P. S., Kazakov, A. E., Ravcheev, D. A., Leyn, S. A., Kovaleva, G. Y., Sutormin, R. A., et al. (2013). RegPrecise 3.0 - A resource for genome-scale exploration of transcriptional regulation in bacteria. *BMC Genomics* 14, 1. doi:10.1186/1471-2164-14-745.

Oberbeckmann, S., Loeder, M. G. J., Gerdts, G., and Osborn, M. A. (2014). Spatial and seasonal variation in diversity and structure of microbial biofilms on marine plastics in Northern European waters. *FEMS Microbiol. Ecol.* 90, 478–492. doi:10.1111/1574-6941.12409.

Ogonowski, M., Motiei, A., Ininbergs, K., Hell, E., Gerdes, Z., Udekwu, K. I., et al. (2018). Evidence for selective bacterial community structuring on microplastics. *Environ. Microbiol.* 20, 2796–2808. doi:10.1111/1462-2920.14120.

Ohta, T., Kawabata, T., Nishikawa, K., Tani, A., Kimbara, K., and Kawai, F. (2006). Analysis of amino acid residues involved in catalysis of polyethylene glycol dehydrogenase from *Sphingopyxis terrae,* using three-dimensional molecular modeling-based kinetic characterization of mutants. *Appl. Environ. Microbiol.* 72, 4388–4396. doi:10.1128/AEM.02174-05.

Oliver, A. E., Newbold, L. K., Whiteley, A. S., and van der Gast, C. J. (2014). Marine bacterial communities are resistant to elevated carbon dioxide levels. *Environ. Microbiol. Rep.* 6, 574–582. doi:10.1111/1758-2229.12159.

Pade, N., and Hagemann, M. (2015). Salt acclimation of cyanobacteria and their application in biotechnology. *Life* 5, 25–49. doi:10.3390/life5010025.

Pagels, F., Guedes, A. C., Amaro, H. M., Kijjoa, A., and Vasconcelos, V. (2019). Phycobiliproteins from cyanobacteria: Chemistry and biotechnological applications. *Biotechnol. Adv.* 37, 422–443. doi:10.1016/j.biotechadv.2019.02.010.

Palmiéri, J., Orr, J. C., Dutay, J. C., Béranger, K., Schneider, A., Beuvier, J., et al. (2015). Simulated anthropogenic CO_2 storage and acidification of the Mediterranean Sea. *Biogeosciences* 12, 781–802. doi:10.5194/bg-12-781-2015.

Paul-Pont, I., Tallec, K., Gonzalez-Fernandez, C., Lambert, C., Vincent, D., Mazurais, D., et al. (2018). Constraints and priorities for conducting experimental exposures of marine organisms to microplastics. *Front. Mar. Sci.* 5, 1–22. doi:10.3389/fmars.2018.00252.

Perry, C. J., and Dennison, W. C. (1999). Microbial nutrient cycling in seagrass sediment. *J. Aust. Geol. Geophys.* 17, 227–231.

Pham, D. N., and Burgess, B. K. (1993). Nitrogenase Reactivity: Effects of pH on substrate reduction and CO inhibition. *Biochemistry* 32, 13725–13731. doi:10.1021/bi00212a043.

Piccardo, M., Provenza, F., Grazioli, E., Cavallo, A., Terlizzi, A., and Renzi, M. (2020). PET microplastics toxicity on marine key species is influenced by pH, particle size and food variations. *Sci. Total Environ.* 715, 136947. doi:10.1016/j.scitotenv.2020.136947.

Picossi, S., Flores, E., and Herrero, A. (2014). ChIP analysis unravels an exceptionally wide distribution of DNA binding sites for the NtcA transcription factor in a heterocyst-forming cyanobacterium. *BMC Genomics* 15. doi:10.1186/1471-2164-15-22.

Pomeroy, L. R., and Wiebe, W. J. (2001). Temperature and substrates as interactive limiting factors for marine heterotrophic bacteria. *Aquat. Microb. Ecol.* 23, 187–204. doi:10.3354/ame023187.

Porra, R. J., Thompson, W. A., and P.E., K. (1989). Determination of accurate extinction coefficients and simultaneous equations for assayin chlorophylls a and b extracted with four different solvents. *Biochim. Biophys. Acta* 975, 384–394.

Powley, H. R., Cappellen, P. Van, and Krom, M. D. (2017a). Nutrient cycling in the Mediterranean Sea: the key to understanding how the unique marine ecosystem functions and responds to anthropogenic pressures. *Mediterr. Identities - Environ. Soc. Cult.* doi:10.5772/intechopen.70878.

Powley, H. R., Krom, M. D., and Van Cappellen, P. (2017b). Understanding the unique biogeochemistry of the Mediterranean Sea: Insights from a coupled phosphorus and nitrogen model. *Global Biogeochem. Cycles* 31, 1010–1031. doi:10.1002/2017GB005648.

Puxty, R. J., Millard, A. D., Evans, D. J., and Scanlan, D. J. (2015). Shedding new light on viral photosynthesis. *Photosynth. Res.* 126, 71–97. doi:10.1007/s11120-014-0057-x.

Puxty, R. J., Evans, D. J., Millard, A. D., and Scanlan, D. J. (2018). Energy limitation of cyanophage development: implications for marine carbon cycling. *ISME J.* 12, 1273–1286. doi:10.1038/s41396-017-0043-3.

Quigg, A., Irwin, A. J., and Finkel, Z. V. (2011). Evolutionary inheritance of elemental stoichiometry in phytoplankton. in *Proceedings of the Royal Society B: Biological Sciences* doi:10.1098/rspb.2010.1356.

Radwan, S., Mahmoud, H., Khanafer, M., Al-Habib, A., and Al-Hasan, R. (2010). Identities of epilithic hydrocarbon-utilizing diazotrophic bacteria from the Arabian Gulf coasts, and their potential for oil bioremediation without nitrogen supplementation. *Microb. Ecol.* 60, 354–363. doi:10.1007/s00248-010-9702-x.

Rae, B. D., Long, B. M., Badger, M. R., and Price, G. D. (2013). Functions, compositions, and evolution of the two types of carboxysomes: polyhedral microcompartments that facilitate CO_2 fixation in cyanobacteria and some proteobacteria. *Microbiol. Mol. Biol. Rev.* 77, 357–379. doi:10.1128/mmbr.00061-12.

Raupach, M. R., Marland, G., Ciais, P., Le Quéré, C., Canadell, J. G., Klepper, G., et al. (2007). Global and regional drivers of accelerating CO_2 emissions. *Proc. Natl. Acad. Sci. U. S. A.* 104, 10288–10293. doi:10.1073/pnas.0700609104.

Reay, D. S., Nedwell, D. B., Priddle, J., and Ellis-Evans, J. C. (1999). Temperature dependence of inorganic nitrogen uptake: reduced affinity for nitrate at suboptimal temperatures in both algae and bacteria. *Appl. Environ. Microbiol.* 65, 2577–2584. doi:10.1128/aem.65.6.2577-2584.1999.

Reddy, K. J., Haskell, J. B., Sherman, D. M., and Sherman, L. A. (1993). Unicellular, aerobic nitrogen-fixing cyanobacteria of the genus *Cyanothece*. *J. Bacteriol.* 175, 1284–1292. doi:10.1128/jb.175.5.1284-1292.1993.

Reddy, M. S., Shaik Basha, Adimurthy, S., and Ramachandraiah, G. (2006). Description of the small plastics fragments in marine sediments along the Alang-Sosiya ship-breaking yard, India. *Estuar. Coast. Shelf Sci.* doi:10.1016/j.ecss.2006.03.018.

Redfield, A. C. (1934). On the proportions of organic derivatives in sea water and their relation to the composition of plankton. *James Johnstone Meml. Vol. Univ. Press Liverpool*, 176–192.

Reisser, J., Slat, B., Noble, K., Plessis, K., Epp, M., Proietti, M., et al. (2015). The vertical distribution of buoyant plastics at sea: an observational study in the North Atlantic Gyre. 1249–1256. doi:10.5194/bg-12-1249-2015.

Renn, C. E. (1937). Bacteria and the phophorus cycle in the sea. *Biol. Bull.* 72, 190–195.

Richaud, C., Zabulon, G., Joder, A., Thomas, J., and Zabulon, R. (2001). Nitrogen or sulfur starvation differentially affects phycobilisome degradation and expression of the *nblA* gene in *Synechocystis* Strain PCC 6803. *J. Bacteriol.* 183, 2989–2994. doi:10.1128/JB.183.10.2989.

Richter, M., Rosselló-Móra, R., Oliver Glöckner, F., and Peplies, J. (2016). JSpeciesWS: A web server for prokaryotic species circumscription based on pairwise genome comparison. *Bioinformatics*. doi:10.1093/bioinformatics/btv681.

Ridame, C., Le Moal, M., Guieu, C., Ternon, E., Biegala, I. C., L'Helguen, S., et al. (2011). Nutrient control of N_2 fixation in the oligotrophic Mediterranean Sea and the impact of Saharan dust events. *Biogeosciences* 8, 2773–2783. doi:10.5194/bg-8-2773-2011.

Rippka, R., Deruelles, J., and Waterbury, J. B. (1979). Generic assignments, strain histories and properties of pure cultures of cyanobacteria. *J. Gen. Microbiol.* 111, 1–61. doi:10.1099/00221287-111-1-1.

Roche, D. B., Buenavista, M. T., and McGuffin, L. J. (2013). The FunFOLD2 server for the prediction of protein-ligand interactions. *Nucleic Acids Res.* 41, 303–307. doi:10.1093/nar/gkt498.

Rochman, C. M., Hentschel, B. T., and The, S. J. (2014). Long-term sorption of metals is similar among plastic types: Implications for plastic debris in aquatic environments. *PLoS One* 9. doi:10.1371/journal.pone.0085433.

Rodriguez, F., Lillington, J., Johnson, S., Timmel, C. R., Lea, S. M., and Berks, B. C. (2014). Crystal structure of the Bacillus subtilis phosphodiesterase PhoD reveals an iron and calcium-containing active site. *J. Biol. Chem.* 289, 30889–30899. doi:10.1074/jbc.M114.604892.

Romano, S., Bondarev, V., Kölling, M., Dittmar, T., and Schulz-Vogt, H. N. (2017). Phosphate limitation triggers the dissolution of precipitated iron by the marine bacterium *Pseudovibrio* sp. FO-BEG1. *Front. Microbiol.* 8, 1–11. doi:10.3389/fmicb.2017.00364.

Romera-Castillo, C., Pinto, M., Langer, T. M., Álvarez-Salgado, X. A., and Herndl, G. J. (2018). Dissolved organic carbon leaching from plastics stimulates microbial activity in the ocean. *Nat. Commun.* 9. doi:10.1038/s41467-018-03798-5.

Rosa, L. T., Dix, S. R., Rafferty, J. B., and Kelly, D. J. (2019). A new mechanism for high-affinity Uptake of C4-dicarboxylates in bacteria revealed by the structure of *Rhodopseudomonas palustris* MatC (RPA3494), a periplasmic binding protein of

the Tripartite Tricarboxylate Transporter (TTT) Family. *J. Mol. Biol.* 431, 351–367. doi:10.1016/j.jmb.2018.11.016.

Rubio, L., Marcos, R., and Hernández, A. (2020). Potential adverse health effects of ingested micro- and nanoplastics on humans. Lessons learned from in vivo and in vitro mammalian models. *J. Toxicol. Environ. Heal. - Part B Crit. Rev.* doi:10.1080/10937404.2019.1700598.

Sabine, C. L., Feely, R. A., Gruber, N., Key, R. M., Lee, K., Bullister, J. L., et al. (2004). The oceanic sink for anthropogenic CO_2. *Science (80-.).* doi:10.1126/science.1097403.

Salvà Serra, F., Svensson-Stadler, L., Busquets, A., Jaén-Luchoro, D., Karlsson, R., et al. (2018). A protocol for extraction and purification of high-quality and quantity bacterial DNA applicable for genome sequencing: a modified version of the Marmur procedure. *Protoc. Exch.* doi:10.1038/protex.2018.084.

Samperio-Ramos, G., Santana Casiano, J. M., and González Dávila, M. (2016). Effect of ocean warming and acidification on the Fe(II) oxidation rate in oligotrophic and eutrophic natural waters. *Biogeochemistry* 128, 19–34. doi:10.1007/s10533-016-0192-x.

Sandh, G., Xu, L., and Bergman, B. (2012). Diazocyte development in the marine diazotrophic cyanobacterium *Trichodesmium*. *Microbiology* 158, 345–352. doi:10.1099/mic.0.051268-0.

Santelices, B. (1980). Phytogeographic characterization of the temperate coast of Pacific South America. *Phycologia*. doi:10.2216/i0031-8884-19-1-1.1.

Santos-Beneit, F. (2015). The Pho regulon: A huge regulatory network in bacteria. *Front. Microbiol.* 6, 1–13. doi:10.3389/fmicb.2015.00402.

Santruckova, H., Bird, M. I., Elhottová, D., Novák, J., Picek, T., Šimek, M., et al. (2005). Heterotrophic fixation of CO_2 in soil. *Microb. Ecol.* 49, 218–225. doi:10.1007/s00248-004-0164-x.

Sañudo-Wilhelmy, S. A., Kustka, A. B., Gobler, C. J., Hutchins, D. A., Yang, M., Lwiza, K., et al. (2001). Phosphorus limitation of nitrogen fixation by *Trichodesmium* in the central Atlantic Ocean. *Nature* 411, 66–69. doi:10.1038/35075041.

Sanz-Sáez, I., Salazar, G., Sánchez, P., Lara, E., Royo-Llonch, M., Sà, E. L., et al. (2020). Diversity and distribution of marine heterotrophic bacteria from a large culture collection. *BMC Microbiol.* 20, 1–16. doi:10.1186/s12866-020-01884-7.

Sarker, I., Moore, L. R., Paulsen, I. T., and Tetu, S. G. (2020). Assessing the toxicity of leachates from weathered plastics on photosynthetic marine bacteria *Prochlorococcus*. *Front. Mar. Sci.* 7, 1–14. doi:10.3389/fmars.2020.571929.

Sarmento, H., Montoya, J. M., Vázquez-Domínguez, E., Vaqué, D., and Gasol, J. M. (2010). Warming effects on marine microbial food web processes: How far can we go when it comes to predictions? *Philos. Trans. R. Soc. B Biol. Sci.* 365, 2137–2149. doi:10.1098/rstb.2010.0045.

Sarthou, G., and Jeandel, C. (2001). Seasonal variations of iron concentrations in the Ligurian Sea and iron budget in the Western Mediterranean Sea. *Mar. Chem.* 74, 115–129. doi:10.1016/S0304-4203(00)00119-5.

Schabhüttl, S., Hingsamer, P., Weigelhofer, G., Hein, T., Weigert, A., and Striebel, M. (2013). Temperature and species richness effects in phytoplankton communities. *Oecologia* 171, 527–536. doi:10.1007/s00442-012-2419-4.

Schubert, E., Mengel, K., and Schubert, S. (1990). Soil pH and calcium effect on nitrogen fixation and growth of board bean. *Agron. J.* 82, 969–972. doi:10.2134/agronj1990.00021962008200050026x.

Schut, F., Prins, R. A., and Gottschal, J. C. (1997). Oligotrophy and pelagic marine bacteria: Facts and fiction. *Aquat. Microb. Ecol.* doi:10.3354/ame012177.

Schwarz, R., and Forchhammer, K. (2005). Acclimation of unicellular cyanobacteria to macronutrient deficiency: Emergence of a complex network of cellular responses. *Microbiology* 151, 2503–2514. doi:10.1099/mic.0.27883-0.

Schwarzenbach, R. P., Gschwend, P. M., and Imboden, D. M. (2002). *Environmental Organic Chemistry*. doi:10.1002/0471649643.

Sebastian, M., and Ammerman, J. W. (2009). The alkaline phosphatase PhoX is more widely distributed in marine bacteria than the classical PhoA. *ISME J.* 3, 563–572. doi:10.1038/ismej.2009.10.

Sebastian, M., and Ammerman, J. W. (2011). Role of the phosphatase PhoX in the phosphorus metabolism of the marine bacterium *Ruegeria pomeroyi* DSS-3. *Environ. Microbiol. Rep.* 3, 535–542. doi:10.1111/j.1758-2229.2011.00253.x.

Seeley, M. E., Song, B., Passie, R., and Hale, R. C. (2020). Microplastics affect sedimentary microbial communities and nitrogen cycling. *Nat. Commun.* 11, 1–10. doi:10.1038/s41467-020-16235-3.

Shi, D., Kranz, S. A., Kim, J. M., and Morel, F. M. M. (2012). Ocean acidification slows nitrogen fixation and growth in the dominant diazotroph *Trichodesmium* under low-iron conditions. *Proc. Natl. Acad. Sci. U. S. A.* 109. doi:10.1073/pnas.1216012109.

Shi, D., Xu, Y., Hopkinson, B. M., and Morel, F. M. M. (2010). Effect of ocean acidification on iron availability to marine phytoplankton. *Science (80-.).* 327, 676–679. doi:10.1126/science.1183517.

Shiozaki, T., Ijichi, M., Kodama, T., Takeda, S., Furuya, K., Ijichi, M., et al. (2014). Heterotrophic bacteria as major nitrogen fixers in the euphotic zone of the Indian Ocean. *Global Biogeochem. Cycles*, 1096–1110. doi:10.1002/2014GB004886.Received.

Smith, T. M., York, P. H., Broitman, B. R., Thiel, M., Hays, G. C., van Sebille, E., et al. (2018). Rare long-distance dispersal of a marine angiosperm across the Pacific Ocean. *Glob. Ecol. Biogeogr.* 27, 487–496. doi:10.1111/geb.12713.

Sobiechowska-Sasim, M., Stoń-Egiert, J., and Kosakowska, A. (2014). Quantitative analysis of extracted phycobilin pigments in cyanobacteria—an assessment of spectrophotometric and spectrofluorometric methods. *J. Appl. Phycol.* 26, 2065–2074. doi:10.1007/s10811-014-0244-3.

Sohm, J. A., Webb, E. A., and Capone, D. G. (2011). Emerging patterns of marine nitrogen fixation. *Nat. Rev. Microbiol.* 9, 499–508. doi:10.1038/nrmicro2594.

Spona-Friedl, M., Braun, A., Huber, C., Eisenreich, W., Griebler, C., Kappler, A., et al. (2020). Substrate-dependent CO_2 fixation in heterotrophic bacteria revealed by stable isotope labelling. *FEMS Microbiol. Ecol.* doi:10.1093/femsec/fiaa080.

Stal, L. J. (1988). Acetylene reduction technique for assay of nitrogenase. *Methods Enzymol.* 167, 474–484.

Statham, P. J., and Hart, V. (2005). Dissolved iron in the Cretan Sea (eastern Mediterranean). *Limnol. Oceanogr.* 50, 1142–1148. doi:10.4319/lo.2005.50.4.1142.

Striebel, M., Schabhüttl, S., Hodapp, D., Hingsamer, P., and Hillebrand, H. (2016). Phytoplankton responses to temperature increases are constrained by abiotic conditions and community composition. *Oecologia* 182, 815–827. doi:10.1007/s00442-016-3693-3.

Su, Z., Olman, V., and Xu, Y. (2007). Computational prediction of Pho regulons in cyanobacteria. *BMC Genomics* 8, 1–12. doi:10.1186/1471-2164-8-156.

Suaria, G., Avio, C. G., Mineo, A., Lattin, G. L., Magaldi, M. G., Belmonte, G., et al. (2016). The Mediterranean Plastic Soup: synthetic polymers in Mediterranean surface waters. *Sci. Rep.*, 1–10. doi:10.1038/srep37551.

Sunda, W., and Huntsman, S. (2015). High iron requirement for growth, photosynthesis, and low-light acclimation in the coastal cyanobacterium Synechococcus bacillaris. *Front. Microbiol.* 6, 1–13. doi:10.3389/fmicb.2015.00561.

Sureda, A., Natalotto, A., Álvarez, E., and Deudero, S. (2013). Increased antioxidant response and capability to produce ROS in hemocytes of *Pinna nobilis* L. exposed to anthropogenic activity. *Environ. Pollut.* 181, 321–324. doi:10.1016/j.envpol.2013.06.029.

Tandeau de Marsac, N., and Houmard, J. (1993). Adaptation of cyanobacteria to environmental stimuli: new steps towards molecular mechanisms. *FEMS Microbiol. Lett.* 104, 119–189. doi:10.1016/0378-1097(93)90506-W.

Tanhua, T., Hainbucher, D., Schroeder, K., Cardin, V., Álvarez, M., and Civitarese, G. (2013). The Mediterranean Sea system: a review and an introduction to the special issue. *Ocean Sci.* 9, 789–803. doi:10.5194/os-9-789-2013.

Tatusova, T., Dicuccio, M., Badretdin, A., Chetvernin, V., Nawrocki, E. P., Zaslavsky, L., et al. (2016). NCBI prokaryotic genome annotation pipeline. *Nucleic Acids Res.* doi:10.1093/nar/gkw569.

Teira, E., Fernández, A., Álvarez-Salgado, X. A., García-Martín, E. E., Serret, P., and Sobrino, C. (2012). Response of two marine bacterial isolates to high CO_2 concentration. *Mar. Ecol. Prog. Ser.* 453, 27–36. doi:10.3354/meps09644.

Tetu, S. G., Sarker, I., Schrameyer, V., Pickford, R., Elbourne, L. D. H., Moore, L. R., et al. (2019). Plastic leachates impair growth and oxygen production in *Prochlorococcus*, the ocean's most abundant photosynthetic bacteria. *Commun. Biol.* 2, 184. doi:10.1038/s42003-019-0410-x.

Thackeray, S. J., Jones, I. D., and Maberly, S. C. (2008). Long-term change in the phenology of spring phytoplankton: Species-specific responses to nutrient enrichment and climatic change. *J. Ecol.* 96, 523–535. doi:10.1111/j.1365-2745.2008.01355.x.

The UniProt Consortium (2014). UniProt: a hub for protein information. *Nucleic Acids Res.* 43, D204-12. doi:10.1093/nar/gku989.

Thiel, M., Macaya, E.C., Acuña, E., Arntz, W.E., Bastias, H., Brokordt, K., Camus, P. A., Castilla, J.C., Castro, L.R., Cortés, M., Dumont, C.P., Escribano, R., Fernández,

M., Gajardo, J.A., Gaymer, C.F., Gomez, I., González, A.E., González, H.E., Haye, P. A., Illanes, J.-E., Iriarte, J.L., Lancellotti, D.A., Luna-Jorquera, G., Luxoro, C., Manríquez, P.H., Marín, V., Muñoz, P., Navarrete, S.A., Perez, E., Poulin, E., Sellanes, J., Sepúlveda, H.H., Stotz, W., Tala, F., Thomas, A., Vargas, C.A., V., et al. (2007). the Humboldt Current System of Northern and Central Chile oceanographic processes, ecological interactions and socioeconomic feedback. *Oceanogr. Mar. Biol.*, 195–344.

Thingstad, T. F., Krom, M. D., Mantoura, R. F. C., Flaten, C. A. F., Groom, S., Herut, B., et al. (2005). Nature of phosphorus limitation in the ultraoligotrophic eastern Mediterranean. *Science (80-.).* 309, 1068–1071. doi:10.1126/science.1112632.

Thomas, M. K., Aranguren-Gassis, M., Kremer, C. T., Gould, M. R., Anderson, K., Klausmeier, C. A., et al. (2017). Temperature–nutrient interactions exacerbate sensitivity to warming in phytoplankton. *Glob. Chang. Biol.* 23, 3269–3280. doi:10.1111/gcb.13641.

Tiwari, B., Singh, S., Kaushik, M. S., and Mishra, A. K. (2015). Regulation of organophosphate metabolism in cyanobacteria. A review. *Microbiology* 84, 291–302. doi:10.1134/S0026261715030200.

Toepel, J., Welsh, E., Summerfield, T. C., Pakrasi, H. B., and Sherman, L. A. (2008). Differential transcriptional analysis of the cyanobacterium *Cyanothece* sp. strain ATCC 51142 during light-dark and continuous-light growth. *J. Bacteriol.* 190, 3904–3913. doi:10.1128/JB.00206-08.

Tortell, P. D., Maldonado, M. T., and Price, N. M. (1996). The role of heterotrophic bacteria in iron-limited ocean ecosystems. *Nature*. doi:10.1038/383330a0.

Tripathi, K., Sharma, N. K., Kageyama, H., Takabe, T., and Rai, A. K. (2013). Physiological, biochemical and molecular responses of the halophilic cyanobacterium *Aphanothece* halophytica to Pi-deficiency. *Eur. J. Phycol.* 48, 461–473. doi:10.1080/09670262.2013.859303.

Troncoso, V. A., Daneri, G., Cuevas, L. A., Jacob, B., and Montero, P. (2003). Bacterial carbon flow in the Humboldt Current System off Chile. *Mar. Ecol. Prog. Ser.* 250, 1–12. doi:10.3354/meps250001.

Turk-Kubo, K. A., Achilles, K. M., Serros, T. R. C., Ochiai, M., Montoya, J. P., and Zehr, J. P. (2012). Nitrogenase (*nifH*) gene expression in diazotrophic cyanobacteria in the Tropical North Atlantic in response to nutrient amendments. *Front. Microbiol.* 3, 1–17. doi:10.3389/fmicb.2012.00386.

Tuson, H. H., and Weibel, D. B. (2013). Bacteria-surface interactions. *Soft Matter* 9, 4368–4380. doi:10.1039/c3sm27705d.

Twiner, M. J. (2000). Possible physiological mechanisms for production of hydrogen peroxide by the ichthyotoxic flagellate *Heterosigma akashiwo*. *J. Plankton Res.* 22, 1961–1975. doi:10.1093/plankt/22.10.1961.

Ugarelli, K., Chakrabarti, S., Laas, P., and Stingl, U. (2017). The seagrass holobiont and its microbiome. *Microorganisms* 5, 81. doi:10.3390/microorganisms5040081.

Urbanek, A. K., Rymowicz, W., and Mirończuk, A. M. (2018). Degradation of plastics and plastic-degrading bacteria in cold marine habitats. *Appl. Microbiol. Biotechnol.* 102, 7669–7678. doi:10.1007/s00253-018-9195-y.

Vassallo, P., Paoli, C., Rovere, A., Montefalcone, M., Morri, C., and Bianchi, C. N. (2013). The value of the seagrass *Posidonia oceanica*: A natural capital assessment. *Mar. Pollut. Bull.* 75, 157–167. doi:10.1016/j.marpolbul.2013.07.044.

Wang, J., Zhang, M. Y., Chen, T., Zhu, Y., Teng, Y., Luo, Y. M., et al. (2015). Isolation and identification of a di-(2-ethylhexyl) phthalate-degrading bacterium and its role in the bioremediation of a contaminated soil. *Pedosphere* 25, 202–211. doi:10.1016/S1002-0160(15)60005-4.

Wang, L., and Zheng, B. (2008). Toxic effects of fluoranthene and copper on marine diatom *Phaeodactylum tricornutum*. *J. Environ. Sci.* 20, 1363–1372. doi:10.1016/S1001-0742(08)62234-2.

Wannicke, N., Endres, S., Engel, A., Grossart, H.-P., Nausch, M., Unger, J., and Voss, M (2012). Response of *Nodularia spumigena* to pCO_2- Part 1: growth, production and nitrogen cycling. *Biogeosciences* 9, 2973–2988. doi:10.5194/bg-9-2973-2012.

Ward, B. A., Dutkiewicz, S., Moore, C. M., and Follows, M. J. (2013). Iron, phosphorus, and nitrogen supply ratios define the biogeography of nitrogen fixation. *Limnol. Oceanogr.* 58, 2059–2075. doi:10.4319/lo.2013.58.6.2059.

Wattam, A. R., Davis, J. J., Assaf, R., Boisvert, S., Brettin, T., Bun, C., et al. (2017). Improvements to PATRIC, the all-bacterial bioinformatics database and analysis resource center. *Nucleic Acids Res.* 45, D535–D542. doi:10.1093/nar/gkw1017.

Weidberg, N., Ospina-Alvarez, A., Bonicelli, J., Barahona, M., Aiken, C. M., Broitman, B. R., et al. (2020). Spatial shifts in productivity of the coastal ocean over the past two decades induced by migration of the Pacific Anticyclone and Bakun's effect in the Humboldt Upwelling Ecosystem. *Glob. Planet. Change* 193, 103259. doi:10.1016/j.gloplacha.2020.103259.

Whitton, B. A. ed. (2012). *The Biotechnology of Cyanobacteria II: Their Diverisity in Space and Time,*.

Wick, R. R., Judd, L. M., Gorrie, C. L., and Holt, K. E. (2017). Unicycler: Resolving bacterial genome assemblies from short and long sequencing reads. *PLoS Comput. Biol.* doi:10.1371/journal.pcbi.1005595.

Widdel, F. (2010). Theory and Measurement of Bacterial Growth. Bremen: University Bremen.

Widder, S., Allen, R. J., Pfeiffer, T., Curtis, T. P., Wiuf, C., Sloan, W. T., et al. (2016). Challenges in microbial ecology: building predictive understanding of community function and dynamics. *ISME J.* 10, 2557–2568. doi:10.1038/ismej.2016.45.

Wrightson, L., and Tagliabue, A. (2020). Quantifying the impact of climate change on marine diazotrophy: insights from earth system models. *Front. Mar. Sci.* 7, 1–9. doi:10.3389/fmars.2020.00635.

Yang, M., Zhao, W., and Xie, X. (2014). Effects of nitrogen, phosphorus, iron and silicon on growth of five species of marine benthic diatoms. *Acta Ecol. Sin.* 34, 311–319. doi:10.1016/j.chnaes.2014.10.003.

Yong, S. C., Roversi, P., Lillington, J., Rodriguez, F., Krehenbrink, M., Zeldin, O. B., et al. (2014). A complex iron-calcium cofactor catalyzing phosphotransfer chemistry. *Science (80-.).* 345, 1170–1173. doi:10.1126/science.1254237.

Yoshida, N., Inaba, S., and Takagi, H. (2014). Utilization of atmospheric ammonia by an extremely oligotrophic bacterium, *Rhodococcus erythropolis* N9T-4. *J. Biosci. Bioeng.* 117, 28–32. doi:10.1016/j.jbiosc.2013.06.005.

Yu Plisova, E., Balabanova, L. A., Ivanova, E. P., Kozhemyako, V. B., Mikhailov, V. V., Agafonova, E. V., et al. (2005). A highly active alkaline phosphatase from the marine bacterium *Cobetia*. *Mar. Biotechnol.* 7, 173–178. doi:10.1007/s10126-004-3022-4.

Yu, T., and Chen, Y. (2019). Effects of elevated carbon dioxide on environmental microbes and its mechanisms: A review. *Sci. Total Environ.* 655, 865–879. doi:10.1016/j.scitotenv.2018.11.301.

Yuan, Z. C., Zaheer, R., Morton, R., and Finan, T. M. (2006). Genome prediction of PhoB regulated promoters in *Sinorhizobium meliloti* and twelve proteobacteria. *Nucleic Acids Res.* 34, 2686–2697. doi:10.1093/nar/gkl365.

Zehr, J. P. (2011). Nitrogen fixation by marine cyanobacteria. *Trends Microbiol.* 19, 162–173. doi:10.1016/j.tim.2010.12.004.

Zehr, J. P., and Capone, D. G. (2020). Changing perspectives in marine nitrogen fixation. *Science (80-.).* 368. doi:10.1126/science.aay9514.

Zeng, Y. F., Ko, T. P., Lai, H. L., Cheng, Y. S., Wu, T. H., Ma, Y., et al. (2011). Crystal structures of *Bacillus* alkaline phytase in complex with divalent metal ions and inositol hexasulfate. *J. Mol. Biol.* 409, 214–224. doi:10.1016/j.jmb.2011.03.063.

Zettler, E. R., Mincer, T. J., and Amaral-Zettler, L. A. (2013). Life in the 'plastisphere': microbial communities on plastic marine debris. *Environ. Sci. Technol.* 47, 7137–7146. doi:10.1021/es401288x.

Zhang, A., Carroll, A. L., and Atsumi, S. (2017). Carbon recycling by cyanobacteria: Improving CO_2 fixation through chemical production. *FEMS Microbiol. Lett.* 364, 1–7. doi:10.1093/femsle/fnx165.

Zhang, Y. (2008). I-TASSER server for protein 3D structure prediction. *BMC Bioinformatics* 9, 40. doi:10.1186/1471-2105-9-40.

Zhang, Y., Burris, R. H., Ludden, P. W., and Roberts, G. P. (1997). Regulation of nitrogen fixation in *Azospirillum brasilens*e. *FEMS Microbiol. Lett.* 152, 195–204. doi:10.1016/S0378-1097(97)00187-0.

Zoete, V., and Michielin, O. (2011). SwissDock , a protein-small molecule docking web service based on EADock DSS. *Nucleic Acids Res.* 39, 270–277. doi:10.1093/nar/gkr366.